Distribution Agreement

In presenting this thesis or dissertation as a partial fulfillment of the requirements for an advanced degree from Emory University, I hereby grant to Emory University and its agents the non-exclusive license to archive, make accessible, and display my thesis or dissertation in whole or in part in all forms of media, now or hereafter known, including display on the world wide web. I understand that I may select some access restrictions as part of the online submission of this thesis or dissertation. I retain all ownership rights to the copyright of the thesis or dissertation. I also retain the right to use in future works (such as articles or books) all or part of this thesis or dissertation.

Signature:

_____ _____

Christian M. Wallen Date

The Coordination Chemistry of Hydrogen Peroxide

By

Christian M. Wallen
Doctor of Philosophy

Chemistry

_____

Christopher C. Scarborough
Advisor

_____

Simon B. Blakey
Committee Member

_____

Lanny S. Liebeskind
Committee Member

Accepted:

_____

Lisa A. Tedesco, Ph.D.
Dean of the James T. Laney School of Graduate Studies

_____

Date

The Coordination Chemistry of Hydrogen Peroxide

By

Christian M. Wallen
Bachelor of Science, Union University, 2008

Advisor: Christopher C. Scarborough, Ph.D.

An abstract of
A dissertation submitted to the Faculty of the
James T. Laney School of Graduate Studies of Emory University
in partial fulfillment of the requirements for the degree of
Doctor of Philosophy
in Chemistry
2016

Abstract

The Coordination Chemistry of Hydrogen Peroxide

By Christian M. Wallen

Hydrogen peroxide is generally hailed as a green oxidant, since it produces water as the sole stoichiometric byproduct and it has a high oxidative efficiency. It can be safely manufactured on scale and is used in the epoxidation of propylene and in the delignification of wood pulp for paper production. Since hydrogen peroxide has relatively low oxidative power, it usually requires activation by a transition metal catalyst. These catalytic systems typically generate M–OOH, M=O, M–O–M, or •OH species, which have limitations in oxidative scope and selectivity. Metal hydrogen peroxide adducts have been kinetically and computationally implicated as active intermediates in oxidative mechanisms but have previously never been observed experimentally. The work herein describes the first observed M(H_2O_2) adducts with transition metals, explores the thermodynamics of their formation, and investigates their stability to disproportionation. The information gained in this work could ultimately set the stage for the development of novel oxidative methodologies employing hydrogen peroxide as the sole stoichiometric oxidant.

The first part of this work describes the formation of a Zn(H_2O_2) adduct with a sulfonamido ligand. Computational evidence suggests that hydrogen bonding acceptors stabilize binding of hydrogen peroxide to metal ions so a ligand was prepared with an open metal coordination site surrounded by sulfonyl groups, which serve as strong hydrogen bond acceptors. This ligand successfully stabilizes binding of H_2O_2 and the first crystal structure of an M(H_2O_2) adduct was obtained. In the third chapter, the binding of H_2O_2 to a redox-active metal (Co) is observed spectroscopically and the first binding constant for H_2O_2 bound to a metal ion was measured. In the next chapter, the sulfonamido ligand electronics were further explored through the preparation of heterotrimetallic complexes bearing a novel alkyl sulfonamido ligand, which demonstrates increased electron density on the sulfonyl groups. The final chapter further explores the formation of M(H_2O_2) adducts with redox-active metals (Co, Ni, and Cu) on sulfonamido ligands, establishing the influence of changing counterion, ligand electronics, and metal identity on binding strengths and decay kinetics.

The Coordination Chemistry of Hydrogen Peroxide

By

Christian M. Wallen
Bachelor of Science, Union University, 2008

Advisor: Christopher C. Scarborough, Ph.D.

A dissertation submitted to the Faculty of the
James T. Laney School of Graduate Studies of Emory University
in partial fulfillment of the requirements for the degree of
Doctor of Philosophy
in Chemistry
2016

Acknowledgements

Many people realize that earning a PhD is a significant achievement. Few people realize, however, that earning a PhD is not accomplished simply by long hours of strenuous toiling by a determined individual. The process of earning a PhD certainly requires toil and struggle, but it also requires input from numerous other individuals, from all walks of life. These individuals offer support in a variety of ways: voicing much-needed encouragement and emotional support during a particularly rough season, providing sought-after knowledge and training, lending aid that requires unique technical skills, offering positive feedback, and especially giving constructive criticism. I am not able to recount them all, but I would be remiss not to extend my sincerest appreciation to a few of the individuals who played a significant role in my graduate studies.

First, my advisor, Chris Scarborough, who taught me most of what I know about chemistry. His scientific curiosity knows no bounds and is simultaneously inspiring and amusing. Chris has also taught me about professionalism, a dying virtue in higher academia, and about the importance of living a life that is satisfying. He has been excellent mentor in every sense of the word and I am sure his influence has shaped me more than I can currently comprehend.

I would like to thank my dissertation committee, Dr. Lanny Liebeskind and Dr. Simon Blakey, for giving me the opportunity to pursue and continue my graduate studies at Emory. Their scientific knowledge, feedback, and constructive criticism was crucial to my success in graduate school.

Also, Dr. John Bacsa, for collecting countless data sets on my crystal samples and for teaching me about the beautiful science of crystallography.

My college professors: Dr. Johnston, Dr. Henrie, Dr. Salazar, Dr. Ward, Dr. Guilaran, Dr. Nettles, Dr. Moss, Dr. Dawson, and many more, who taught me about chemistry, physics, and math and inspired me with their character and friendship.

I would also like to thank my colleagues in the Scarborough Group, Tom Pickel, Robert Harris, Michelle Leidy, and Dan Liu for being great colleagues and friends and for putting up with all my puns and "dad jokes".

I would not be here without the influence and support of my family, especially my grandfather "Papa", who struck the spark of curiosity in me that grew into the burning desire to understand, my mom, who devoted her life to giving knowledge and wisdom to all 8 of her children, and my dad, who taught me the value of self-discipline with respect to the mind, emotions, and work ethic.

And most importantly, I owe a debt of gratitude to my lovely wife Rebecca, who has been a constant ray of sunshine during the past four years. She encourages me to work hard and strive for excellence. She patiently listens to me talk about my struggles in research and genuinely seeks to understand and help in any way she can, even when the conversation goes well beyond her understanding of chemistry. Being married to a graduate student in chemistry is not easy, but Rebecca navigated it with a smile and a laugh. I truly do not deserve her and I know that I never will.

Table of Contents

List of Figures

Chapter 1

Chapter 2

Chapter 3

Chapter 5

List of Tables

Chapter 1

Chapter 2

Chapter 3

Chapter 4

Chapter 5

List of Schemes

Chapter 1

List of Compounds

Abbreviation	Formula	Structure
H_3Ts_3tren	$N(CH_2CH_2NHTs)_3$	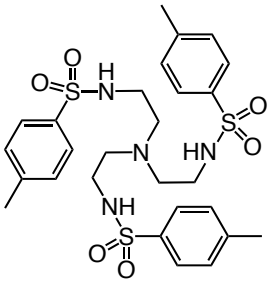
2-1(OH$_2$)	[^{n}Bu$_4$N][(Ts$_3$tren)Zn^{II}(OH$_2$)]	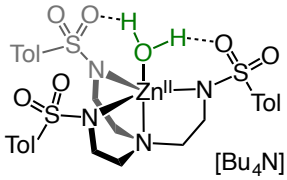
2-1	[^{n}Bu$_4$N][(Ts$_3$tren)Zn^{II})]	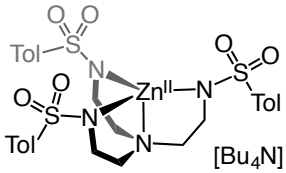
2-1(N$_2$H$_4$)	[^{n}Bu$_4$N][(Ts$_3$tren)Zn^{II}(N$_2$H$_4$)]	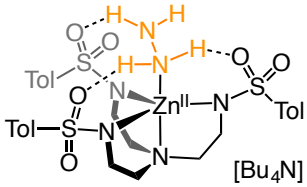
2-1(NH$_2$OH)	[^{n}Bu$_4$N][(Ts$_3$tren)Zn^{II}(NH$_2$OH)]	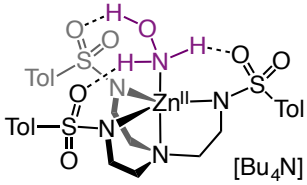
2-1(H$_2$O$_2$)	[^{n}Bu$_4$N][(Ts$_3$tren)Zn^{II}(H$_2$O$_2$)]	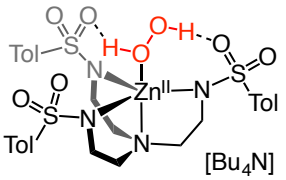

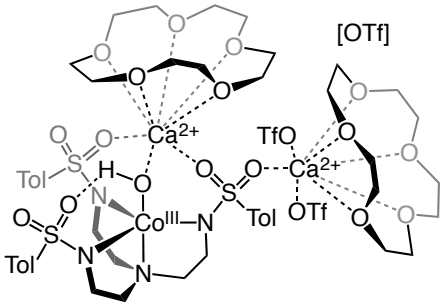

3-2 ..... $[(Ts_3tren)Co^{III}(\mu\text{-}OH)Ca^{2+}(15\text{-crown-}5)][(OTf)_2Ca^{2+}(15\text{-crown-}5)][OTf]$

$[^{tBu}PhPPh_3][Br]$ ..$[^{3,5\text{-}tBu}PhPPh_3][Br]$ .....

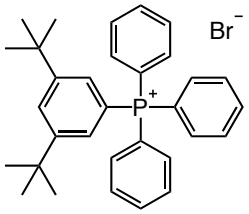

3-1^{P}(OH$_2$).....$[^{tBu}PhPPh_3][(Ts_3tren)Co^{II}(H_2O)]$ .....

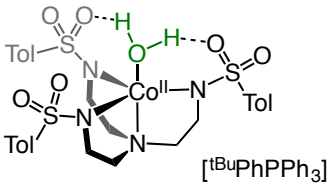

3-1^{P} .....$[^{tBu}PhPPh_3][(Ts_3tren)Co^{II}]$.....

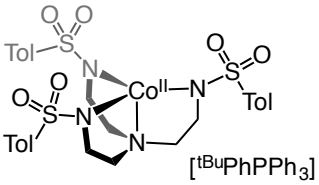

4-1 .....$[Ca^{2+}][(Ts_3tren)Co^{II})]_2$ .....

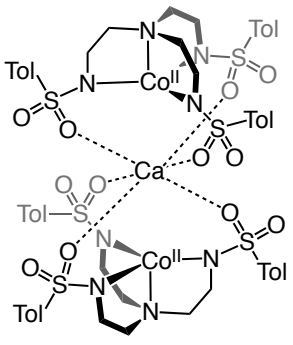

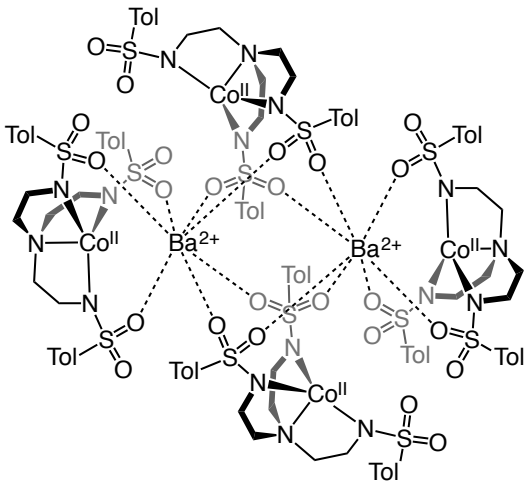

4-3 .....$[Ba^{2+}]_2[(Ts_3tren)Co^{II})]_4$ .....

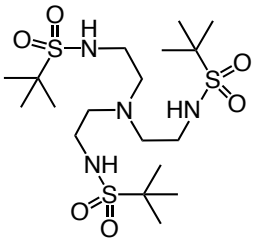

H_3Bus_3tren .....$N(CH_2CH_2NHSO_2tBu)_3$ .....

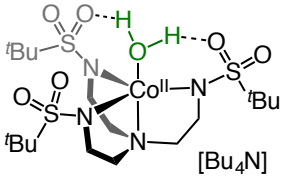

4-4(OH$_2$) .....$[^nBu_4N][(Bus_3tren)Co^{II}(OH_2)]$ .....

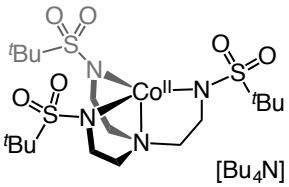

4-4 .....$[^nBu_4N][(Bus_3tren)Co^{II})]$ .....

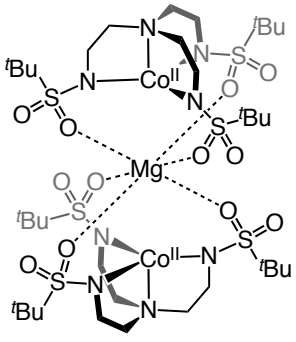

4-5^{Mg} .....$[Mg^{2+}][(Bus_3tren)Co^{II})]_2$ .....

Chapter 1
Hydrogen Peroxide: Production, Application, and Reactivity with Transition Metals

1.1 Industry of Hydrogen Peroxide

1.1.1 Hydrogen Peroxide: A Stoichiometric Oxidant with Immense Industrial Potential

Hydrogen peroxide is generally hailed as a green oxidant, since it produces water as the sole stoichiometric byproduct and it has high oxidative efficiency.[1] It can be safely manufactured on scale and is used in the epoxidation of propylene and in the delignification of wood pulp for paper production.[1] Since hydrogen peroxide has relatively low oxidative power, it usually requires activation by a transition metal catalyst. These catalytic systems typically generate M–OOH, M=O, M–O–M, or •OH species, which have limitations in oxidative scope and selectivity. Metal hydrogen peroxide adducts have been kinetically and computationally implicated as active intermediates in oxidative mechanisms but have previously never been observed experimentally. This work establishes the existence of M(H_2O_2) adducts, explores the thermodynamics of their formation, and investigates their stability to disproportionation. This information could ultimately set the stage for the development of novel oxidative methodologies employing hydrogen peroxide as the sole stoichiometric oxidant.

1.1.2 Hydrogen Peroxide Versus Other Common Oxidants

Table 1-1 compares the oxidative efficiency of common oxidants and their respective oxidative synthetic precursors. While oxygen is ideal in terms of oxidative efficiency, using oxygen on an industrial scale requires special precautions to avoid explosive mixtures.[2-3] Peracids such peracetic acid and meta-chloroperoxybenzoic acid (mCPBA) are strong oxidants but their instability necessitates dilution with associated acid to avoid explosive mixtures. Additionally, they are manufactured from hydrogen peroxide, which increases

their economic footprint. Tert-butyl hydroperoxide is made by autoxidation of isobutane, making it inexpensive, but disposal of the tert-butanol byproduct increases the associated expense. Urea hydrogen peroxide (UHP), sodium perborate, and sodium percarbonate are all solids that contain hydrogen peroxide, which makes them easier and safer to transport but decreases their efficiency. Oxone® (trademarked by DuPont) is a triple-salt mixture containing the peroxymonosulfate ion, which is a powerful oxidant, but explosive in nature. While many of these oxidants are used in the chemical industry, hydrogen peroxide remains one of the most desirable oxidants due to the ease of handling, high oxidative efficiency, and water being the sole byproduct.

Table 1-1. List of common oxidants.

Oxidant	Efficiency[a]	Precursor[b]	Byproduct
O_2	50%, 100%[d]	--	H_2O
H_2O_2	47%	O_2	H_2O
$MeCO_3H$	21%	H_2O_2	$MeCO_2H$
tBuOOH	18%	O_2	tBuOH
urea–H_2O_2[c]	17%	H_2O_2	urea, H_2O
sodium perborate[c]	16%	H_2O_2	borax
sodium percarbonate[c]	15%	H_2O_2	sodium carbonate
mCPBA	9%	H_2O_2	mCBA[e]
Oxone®	5%	H_2O_2	$KHSO_4$

[a]Mass percent of atoms capable of performing oxidations. [b]Synthetic precursor with oxidative abilities. [c]Releases molecular hydrogen peroxide in aqueous solutions. [d]In some systems both atoms of oxygen are used productively. [e]Meta-chlorobenzoic acid.

1.1.3 Production of Hydrogen Peroxide: Anthraquinone Process

There are several methods for production of hydrogen peroxide, but over 95% of the world's supply of hydrogen peroxide is produced by the Anthraquinone Process.[4] This

process consists of four main stages: hydrogenation of anthraquinone, oxidation of anthraquinol, extraction of hydrogen peroxide, and purification/concentration of hydrogen peroxide (Scheme 1-1).

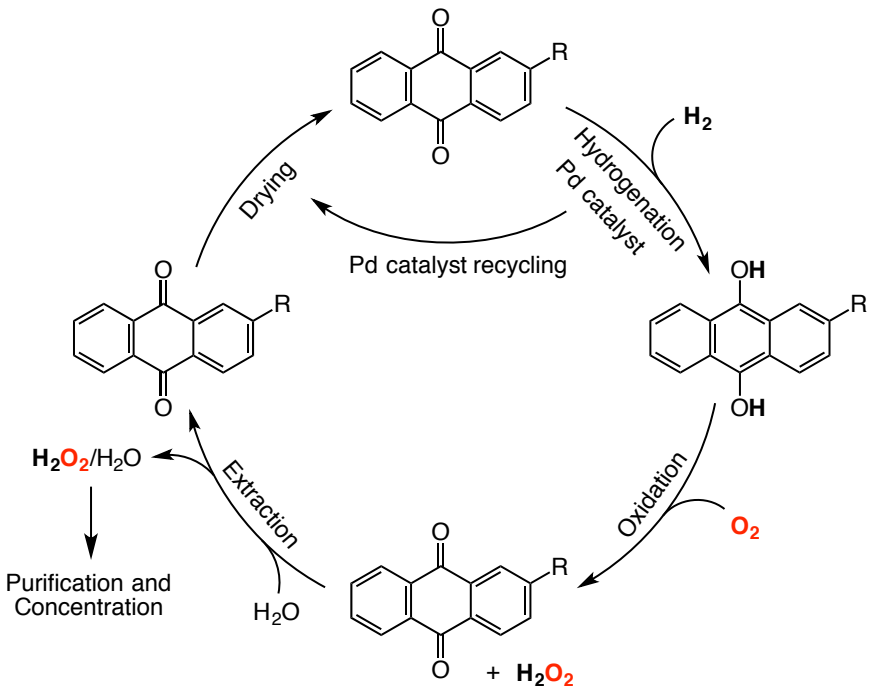

Scheme 1-1. Simplified representation of the Anthraquinone Process. R = Et, or H.

During the first stage, the working solution, which consists of an alkyl-substituted anthraquinone (usually 2-ethylanthraquinone) a polar organic solvent, and a non-polar aromatic organic solvent, is reduced using hydrogen gas and a solid-supported palladium catalyst.[4] After reaching about 60% reduction to anthraquinol, the solid catalyst is filtered away from the working solution to be recycled for later use.[4] The introduction of air to the reduced working solution leads to autoxidation of the anthraquinol, forming hydrogen peroxide and regenerating the anthraquinone. The hydrogen peroxide is then separated from the working solution by an extraction process which involves water passing through a countercurrent column. The working solution containing the anthraquinone is then dried for reuse in the next cycle. The total yield of the oxidation and extraction processes is

typically 95%.[4] The aqueous extraction solution contains between 25 and 45% hydrogen peroxide, as well as small amounts of organic solvent. This solution is purified and concentrated via distillation. Commercial grades of hydrogen peroxide are 30%, 50%, and sometimes 70% (v/v) in water. Although pure hydrogen peroxide is rather stable, even small amounts of metal contaminants can rapidly disproportionate hydrogen peroxide, releasing oxygen, water, and heat. Therefore, solutions of hydrogen peroxide are typically stabilized with small amounts of Sn(IV) or phosphates.[1] Solutions of hydrogen peroxide at concentrations higher than 68% (by volume) are still considered unsafe, since the heat generated by complete decomposition of peroxide at those concentrations is enough to vaporize all of the water in the solution.

1.1.4 Applications for Hydrogen Peroxide

In 2005, the global production of (pure) hydrogen peroxide was 2.2 billion kilograms and was growing at 4% per year.[4-6] About 50% of this amount is used in the delignification of wood pulp for the paper industry and 10% of is consumed in the bleaching of fabrics in the textile industry.[5] This demand is increasing as other bleaching agents, such sodium hypochlorite and sodium hydrosulfite, are becoming less popular due to their toxicity, corrosiveness, and negative environmental impact.[6] About 20% of hydrogen peroxide consumption is in the manufacture of sodium perborate and percarbonate salts for use in detergents.[7] These detergents produce hydrogen peroxide when dissolved in water, creating a solution that can remove stains and brighten colors, while hypochlorite-based detergents can lead to loss of color or yellowing of fabric.[4, 6] Another significant application of hydrogen peroxide is in water purification, which accounts for 10% of global consumption.[7] The advantages are obvious, since hydrogen peroxide has relatively low

toxicity and deoxygenation yields only water. Hydrogen peroxide treatment has been shown to effectively remove toxic and harmful chemicals, such as cyanide, thiocyanate, nitrite, chloride, hypochlorite, and H_2S from water supplies.[1, 4, 6] The remaining 5% of hydrogen peroxide is used in a number of other processes, including electronics etching and oxidation of hydrocarbons such as propylene to propylene oxide, a process which is expected to grow significantly in upcoming years.[7-8]

1.1.5 Hydrogen Peroxide Activation with Transition Metals

Hydrogen peroxide is used in a number of chemical syntheses on the industrial and laboratory scale, but many of these processes require the use of metal catalysts to "activate" hydrogen peroxide.[1, 5, 8-13] As shown in Figure 1-1, activation of hydrogen peroxide can be accomplished through a variety of oxidatively active intermediates. Each of the species in Figure 1-1 will be discussed in detail in the following sections of this chapter. Some of the active intermediates in these mechanisms are widely accepted (a-d) while others are supported only by computational evidence (e-g). Metal hydrogen peroxide adducts (g) fall in the latter category as they have never been experimentally observed, but have been proposed to be active intermediates based on kinetic and theoretical data. Failed attempts to observe hydrogen peroxide coordination to open sites on a metal have led multiple authors to conclude that hydrogen peroxide is a very poor ligand for transition metals,[14-15] but the computational evidence on $M(H_2O_2)$ adducts strongly suggests that hydrogen bonding interactions could be used to stabilize this otherwise weak interaction.[16-17] In fact, hydrogen bonding plays a key role in many of the oxidative species shown in Figure 1-1, which will be demonstrated in the following sections, and is vital to the formation and observation of $M(H_2O_2)$ adducts, as will be seen in the following chapters of this work.

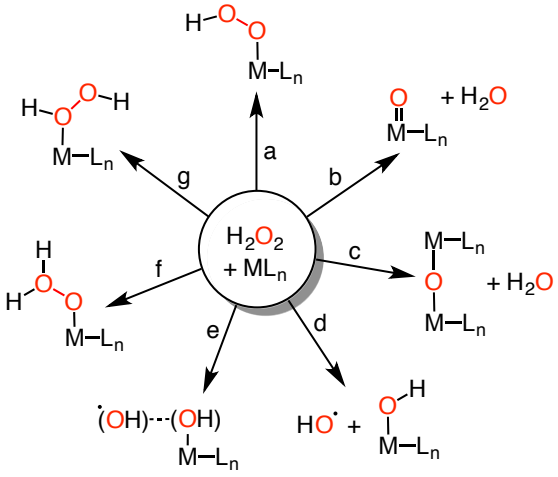

Figure 1-1. Possible intermediates for activation of hydrogen peroxide with a transition metal: (a) metal hydroperoxo; (b) terminal metal oxo; (c) bridging metal oxo; (d) Fenton chemistry; (e) tethered hydroxyl radical; (f) M–OOH$_2$ complex, (g) M(H_2O_2) adduct (this work). Well-established intermediates: a-d. Theoretically implied intermediates: e-g.

1.2 Established Mechanisms for Hydrogen Peroxide Activation

1.2.1 Propylene Oxide, the HPPO Process, and M–OOH Intermediates

One significant application of hydrogen peroxide in chemical synthesis is the production of propylene oxide. In 2010, the global production of propylene oxide was 7.5 billion kg.[8] Propylene oxide is largely produced using a chlorohydrin process, which involves oxidation with hypochlorous acid (generated from chlorine and water) followed by dehydrochlorination with sodium or calcium hydroxide (Scheme 1-2).[18] The use of chlorine reagents and significant formation of salt byproducts in this process have prompted many scientists to look for green alternative routes over many years, but the chlorohydrin route has remained the primary process.[8, 18] More recently, an improved process known as the HPPO (Hydrogen Peroxide to Propylene Oxide) process has emerged and is gradually replacing the chlorohydrin route.[4, 8] The HPPO process involves direct formation of

propylene oxide from propylene using hydrogen peroxide and TS-1, a titanosilicate catalyst (Scheme 1-2).[8]

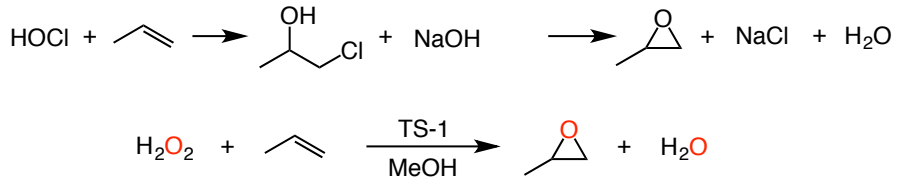

Scheme 1-2. Industrial formation of propylene oxide using the chlorohydrin route (above) and the HPPO process (below).

The mechanism of the HPPO process is believed to involve deprotonation of hydrogen peroxide by a siloxy group, forming a Ti–OOH species (Scheme 1-3).[8] A solvent molecule (methanol) also coordinates to titanium and hydrogen bonds to the coordinated hydroperoxide ligand. This hydrogen bonding interaction facilitates formation of water during the epoxidation of propylene in the following mechanistic step.

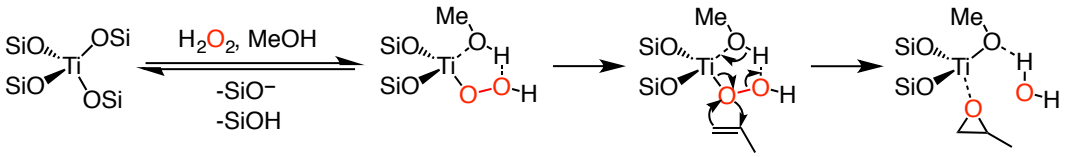

Scheme 1-3. Mechanism for propylene oxidation in HPPO process. Red oxygen atoms are derived from hydrogen peroxide.

A similar mechanism is thought to occur in the classic Sharpless oxidation, where the active intermediate is believed to be a side-on Ti–OO^{t}Bu complex,[19-20] and another computational report has suggested that Baeyer-Villager oxidations catalyzed by titanium and tin with hydrogen peroxide may involve M-OOH intermediates.[12] For all three of these mechanisms, hydrogen bonding interactions play an important role in the formation and reactivity of these intermediates.

1.2.2 Activation Via Metal Oxo Intermediates

Among the most versatile oxidants in biology are the cytochrome P450 enzymes, which oxidize a variety of substrates via an Fe^{IV}(porphyrin) complex known as Compound 1 (Figure 1-2).[21] In the accepted biological mechanism, Compound 1 is formed aerobically through multiple reduction and protonation steps, but it can also be formed by exogenous hydrogen peroxide through the "shunt" pathway (Figure 1-2).[21]

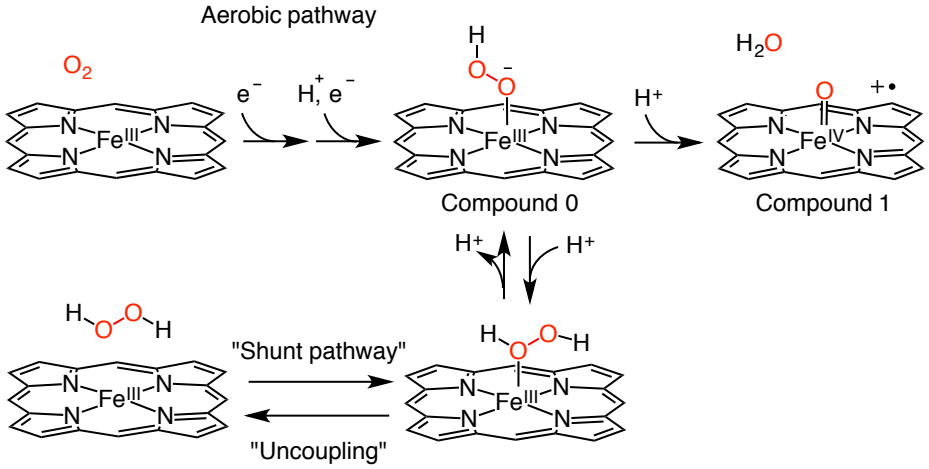

Figure 1-2. Formation of Compound 1 via aerobic and shunt pathways.

The formation and reactivity of synthetic iron oxo compounds from oxygen and hydrogen peroxide has been studied extensively by Que, who has demonstrated that iron oxo complexes are powerful oxidants, but are typically unselective and, therefore, difficult to use in productive catalysis.[22-24] For certain applications of hydrogen peroxide, however, selectivity is less of a major concern. For example, the majority of hydrogen peroxide is used in bleaching process (i.e. wood pulp, textiles, stain removal), which require oxidation of a wide variety of unsaturated organic chromophores.[1, 5, 9] In order to perform this task effectively, hydrogen peroxide must either be heated to high temperatures or activated with

a metal catalyst, often manganese.[5, 9] The mechanisms by which these catalysts oxidize lignin and other organic chromophores are not completely understood, but there are many proposed active species, some of which are shown in Figure 1-3.[5, 9, 13, 25] Two common ligands for manganese in bleaching processes, 1,4,7-trimethyl-1,4,7-triazacyclononane (Me_3tacn) ligand and 1,2-bis(4,7-dimethyl-1,4,7-triazacylonone-1-yl)ethane (Me_4dtne), are also shown Figure 1-3).[5, 9] All of these intermediates involve electrophilic oxidation through a terminal metal oxo or bridging metal oxo species derived from hydrogen peroxide (b and c, Figure 1-1).

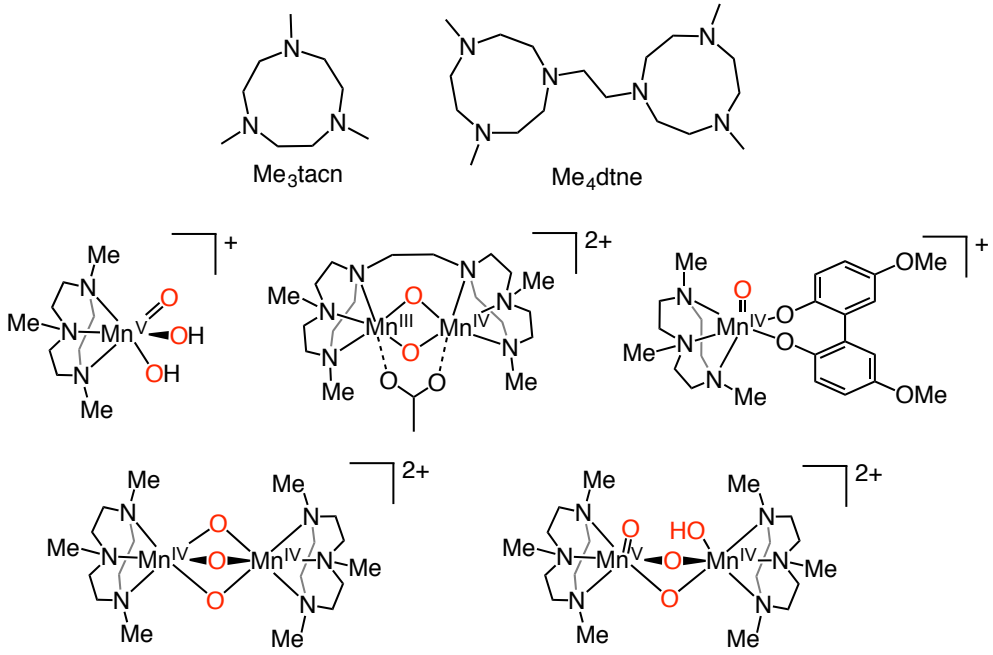

Figure 1-3. Top: two ligands commonly used for manganese bleaching catalysts. Middle and bottom: Proposed active intermediates for oxidation with H_2O_2 and Mn catalysts. Red oxygen atoms are derived from H_2O_2.

Even though metal oxo complexes are often unselective oxidants, they can still be used productively in catalysis. In two examples from Lau, a manganese nitrido complex[11] and osmium nitrido complex[26] are able to oxidize alkanes using hydrogen peroxide to form

terminal metal oxo complexes (b, Figure 1-1). The two mechanisms are quite similar so only the calculated mechanism for the osmium nitrido complex is shown in Scheme 1-4.[11, 26] The calculated mechanism suggests initial formation of an $Os^{VI}(H_2O_2)$ adduct, which engages in hydrogen bonding interactions with acetic acid, followed by proton transfer to form an Os^{VI}–OOH_2 intermediate.[26] Water is released and the metal is oxidized to produce an Os^{VIII}=O intermediate.[26] This metal oxo then abstracts an H-atom from cyclohexane to initiate alkane oxidation.[26] Again, we see that hydrogen bonding plays an important role in stabilizing the $M(H_2O_2)$ adduct and the following oxidative stops.

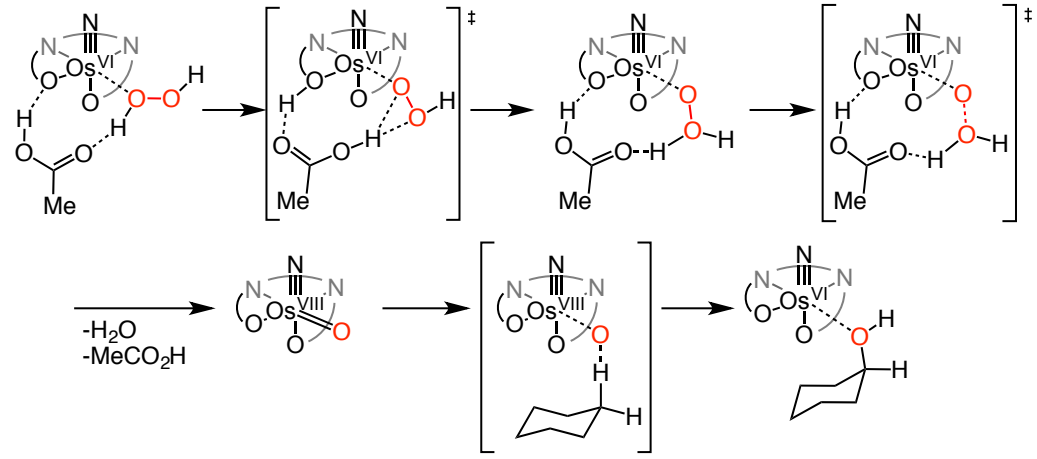

Scheme 1-4. Calculated intermediates and transition states (in brackets) in a calulated mechanism for oxidation of cyclohexane by a nitrido osmium salen complex and H_2O_2.[26]

1.2.3 Fenton Chemistry and Hydroxyl Radicals

The hydroxyl radical is a powerful oxidant, second only to elemental fluorine in oxidizing power.[1] Hydroxyl radicals can be generated by homolysis of hydrogen peroxide using UV-light or a metal catalyst (d, Figure 1-1).[1] Fenton first reported the use of iron(II) and hydrogen peroxide to generate hydroxyl radicals for oxidation of tartaric acid in 1894.[27] Using iron(II) and hydrogen peroxide to generate hydroxyl radicals is now known as

Fenton chemistry and is used extensively in water purification.[28-29] Some important reactions of the thermal Fenton systems for treatment of organic contaminants in wastewater are shown in Scheme 1-5. Iron(II) ions are oxidized by hydrogen peroxide to form iron(III) ions, hydroxide ions, and hydroxyl radicals (*a*, Scheme 1-5). The hydroxyl radicals can react with more hydrogen peroxide in solution, forming hydroperoxide radicals which unproductively disproportionate into water and oxygen (*b-c*, Scheme 1-5). Alternatively, the hydroxyl radicals can also productively oxidize organic compounds, attacking C–H, N–H, O–H, and C=C bonds (*d-f*, Scheme 1-5). Given enough reagent, organic matter can be oxidized completely to CO_2, and H_2O, and inorganic acids (if heteroatoms were present).[29]

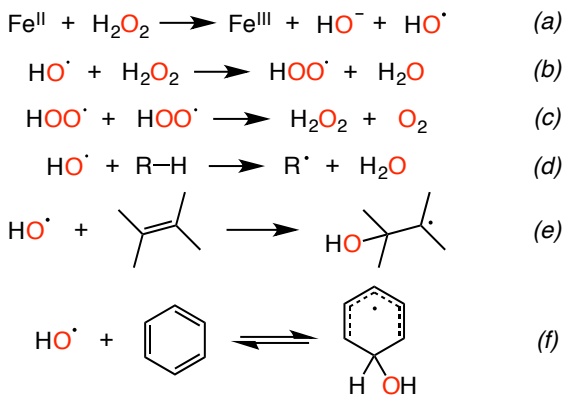

Scheme 1-5. Important reactions in Fenton systems for oxidizing organic components in wastewater. Red oxygen atoms derived from hydrogen peroxide.

Iron is not the only metal that can generate hydroxyl radicals from hydrogen peroxide. Using experimental and theoretical methods, Shul'pin reported an oxovanadium complex which reacts with hydrogen peroxide to form hydroxyl and hydroperoxyl radicals, which can oxidize cyclohexane to cyclohexyl hydroperoxide in the presence of pyrazine-2-carboxylic acid.[30] The reported mechanism for the generation of hydroxyl and

hydroperoxyl radicals is shown in Scheme 1-6. In the calculated mechanism, water molecules are shown to assist in proton transfer through hydrogen bonding interactions.[30] Similar mechanism have been calculated for rhenium systems.[31]

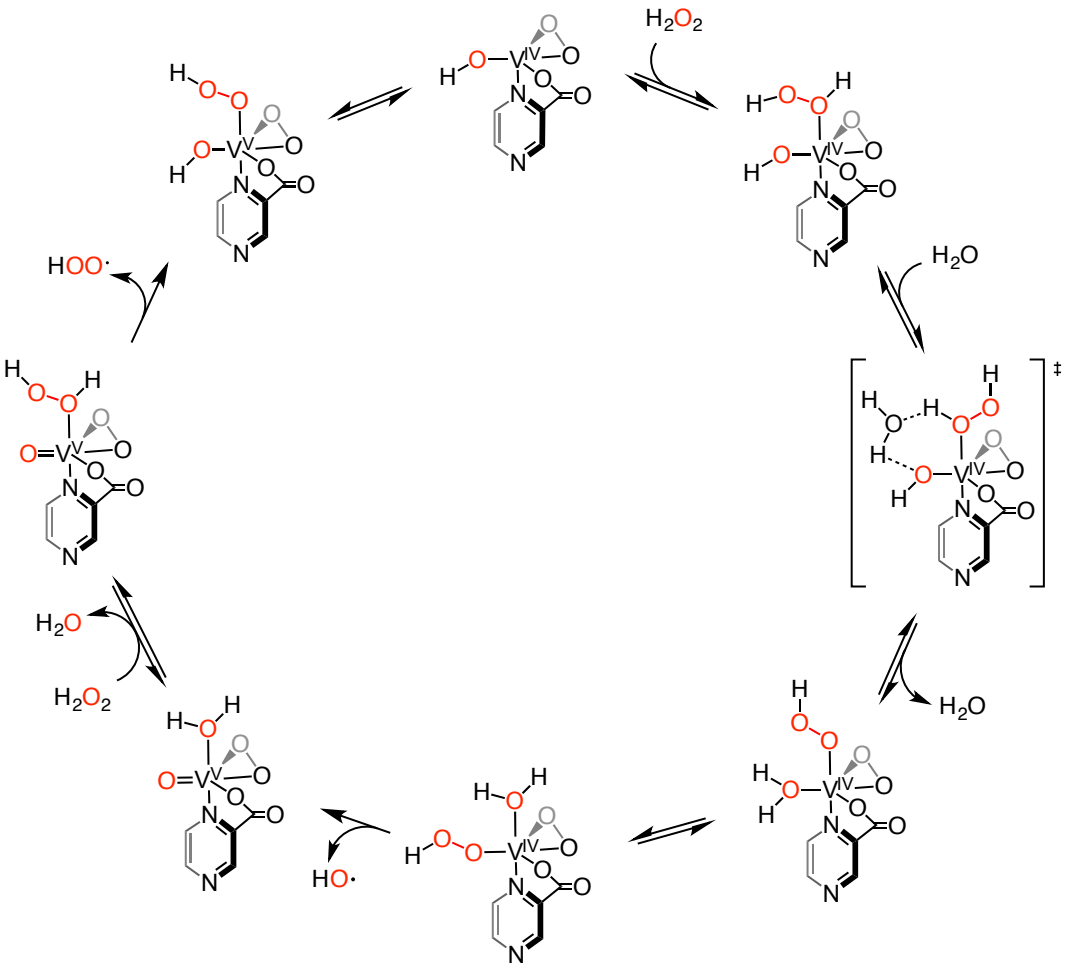

Scheme 1-6. Generation of hydroxyl and hydroperoxyl radicals from hydrogen peroxide with oxovanadium complexes and pyrazine-2-carboxylic acid.[30] Calculated transition state showing example of proton transfer assisted by water in brackets.

1.3 Theoretical Hydrogen Peroxide Activation Mechanisms

1.3.1 Tethered HO• Radicals

Because hydroxyl radicals are such a powerful oxidant, selectivity is often a challenge in Fenton reactions. However, it is theoretically possible to use hydrogen bonding interactions to guide reactions with hydroxyl radicals (e, Figure 1-1). While this has never been experimentally observed, studies have shown this is possible. Stahl has reported an aerobic oxidation of hydroquinone with a cobalt salophen ligand.[32] In this oxidation, one equivalent of O_2 is able to oxidize two equivalents of hydroquinone to para-quinone.[32] The calculated mechanism suggests that O_2 binds to the cobalt complex, and after oxidizing the first equivalent of hydroquinone, forms a Co(H_2O_2) adduct, which binds to the second equivalent of hydroquinone and a solvent molecule (methanol) through hydrogen bonding interactions (Scheme 1-7).[32] After homolysis of the O–O bond, forming a Co^{III}–OH and •OH, these hydrogen bonding interactions keep the hydroxyl radical in close proximity to the metal and substrate, allowing for H-atom transfer and release of water (Scheme 1-7).[32] The Co^{III}–OH complex is then able to oxidize the semiquinone species to form water and the second equivalent of para-quinone.[32]

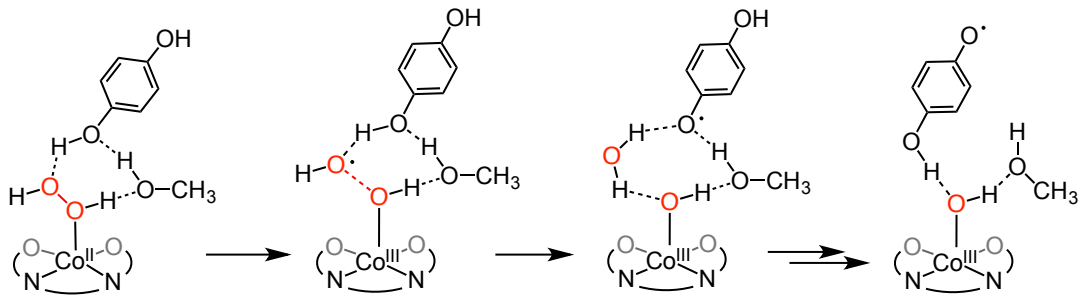

Scheme 1-7. Calculated intermediates in aerobic oxidation of hydroquinone by Co(salophen) catalyst.[32]

Another example of hydrogen bonds being used to control hydroxyl radical reactivity was reported by Shaik in 2016, in a theoretical study investigating the reactivity of H_2O_2-dependent cytochrome P450 enzyme ($P450_{SP\alpha}$).[17] The calculated mechanism suggests that an $Fe^{III}(H_2O_2)$ complex forms and is stabilized by hydrogen bonding interactions with enzyme residues and water molecules.[17] These hydrogen bonding interactions facilitate homolysis of the O–O bond, forming a tethered hydroxyl radical, which then goes on to oxidize the complex to form Compound 1 (Scheme 1-8), which is the generally accepted active species for substrate oxidation in cytochrome P450 enzymes.[17] It should be noted that if this situation were altered such that the metal ion and ligand platform were resistant to oxidation, the tethered hydroxyl radical could be expected to react productively with a nearby substrate molecule, as observed with cobalt.[32]

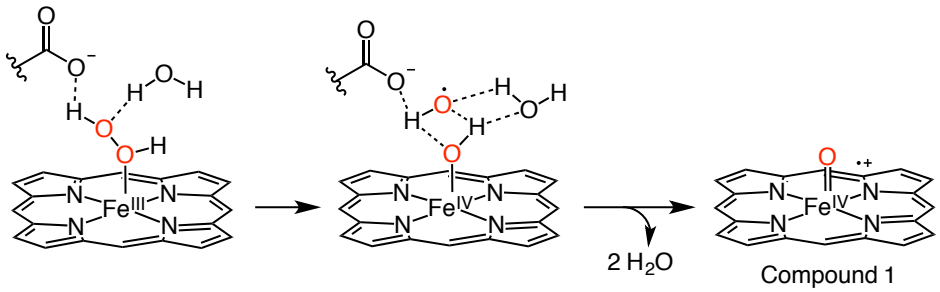

Scheme 1-8. Formation of Compound 1 from $Fe^{III}(H_2O_2)$ adduct stabilized by hydrogen bonding interactions.[17]

1.3.2 Activation through M-OOH_2 Intermediates

Another oxidative species in H_2O_2-activation that has been theoretically implicated, but never observed experimentally, is the M-OOH_2 adduct (f, Figure 1-1), the tautomer form of $M(H_2O_2)$. Lau reports the use of a manganese nitride complex in the epoxidation of alkenes and oxidation of alcohols.[33] According to DFT calculations, a $Mn^{V}(H_2O_2)$ adduct

engages in hydrogen bonds with acetic acid molecules, which facilitate proton transfer to form a Mn^{V}–OOH_2 complex which is the oxidative intermediate for alkene epoxidation (Scheme 1-9).

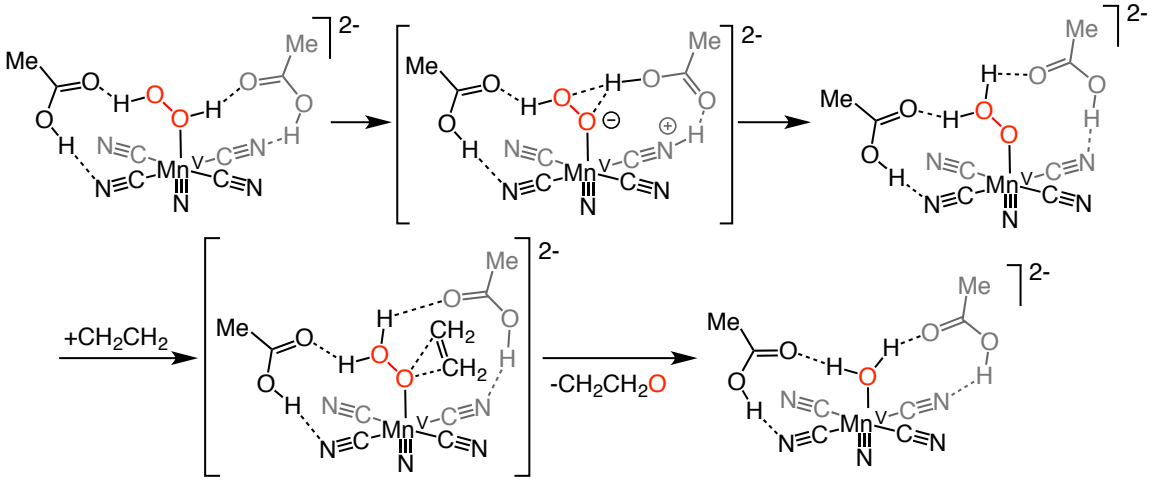

Scheme 1-9. Calculated intermediates and transition states (in brackets) showing possible mechanism for epoxidation of alkenes using Mn^{V} catalyst and H_2O_2.[33]

1.4 Theoretical Support For M(H_2O_2) Adducts

1.4.1 M(H_2O_2) Intermediates in Cytochrome P450cam enzymes

The last species in Figure 1-1 is the M(H_2O_2) adduct, which, as we have discussed, has been supported by extensive calculations but not observed experimentally. Many have assumed that M(H_2O_2) adducts would not be observable if formed, but would instead rapidly decompose via oxidation of the metal or via disproportionation of peroxide into water and oxygen. Nevertheless, Coon and coworkers proposed the existence of Fe(H_2O_2) intermediates as an active "second oxidant" for mutant Cytochrome P450cam enzymes (P450cam), in addition to Compound 1, in order to explain their unique reactivity profile.[34-37] In the generally accepted mechanism for oxidation with Cytochrome P450 enzymes, an Fe^{III}–OOH porphyrin complex (Compound 0, Scheme 1-10) is protonated on the distal

oxygen atom, which forms water and an Fe^{IV}=O porphyrin-radical species (Compound 1, Scheme 1-10), which is able to oxidize a variety of substrates.[35] In the P450cam enzymes, the protein residue which facilitates protonation of the distal oxygen atom is removed, effectively shutting down formation of Compound 1 through that pathway (top, Scheme 1-10).[34] This leaves only the pathway for protonation of the proximal oxygen, forming the $Fe(H_2O_2)$ adduct (bottom, Scheme 1-10), which was thought to be a "second oxidant" responsible for the different reactivity profile for P450cam enzymes.[34, 37]

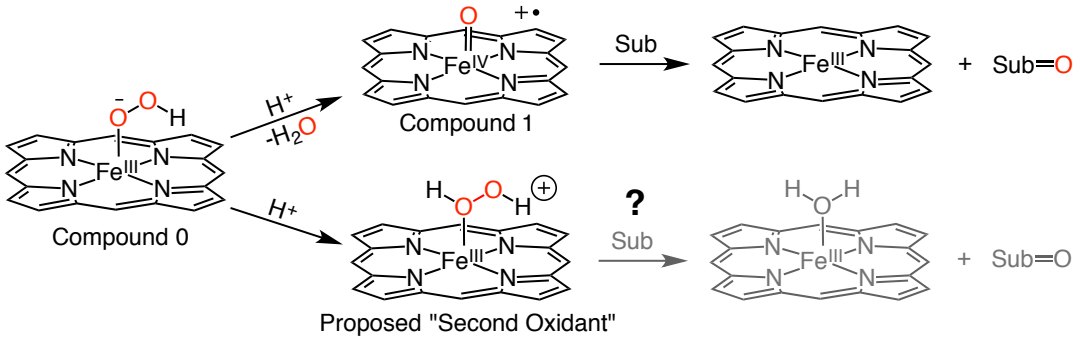

Scheme 1-10. Formation of Compound 1 (top) and Fe(H_2O_2) adduct (below) via protonation of Compound 0.

While it is generally accepted that H_2O_2 can be formed by Cytochrome P450 enzymes, it is usually assumed to immediately release after forming, since it is often observed as a byproduct (the "uncoupling" mechanism).[21, 35, 38-39] Therefore, the ability of an $Fe^{III}(H_2O_2)$ species to participate in substrate oxidization was called into question by Shaik and others.[40] Furthermore, in 2008 Mayer attempted to form a $Ga(H_2O_2)$ adduct supported by tetraphenylporphyrin (Scheme 1-11). This Ga^{III}(porphyrin) complex is electronically similar to Fe^{III}(porphyrin) complexes, except that Ga^{III} is inert to oxidation by H_2O_2. After adding anhydrous hydrogen peroxide in CD_2Cl_2, no evidence was found for any interaction between H_2O_2 and Ga^{III}.[14] From this report, it was generally concluded that H_2O_2 is a poor

ligand for transition metals.[41-43] The crucial problem with Mayer's system, however, is the absence of any opportunity for hydrogen bonding intramolecularly or with solvent.

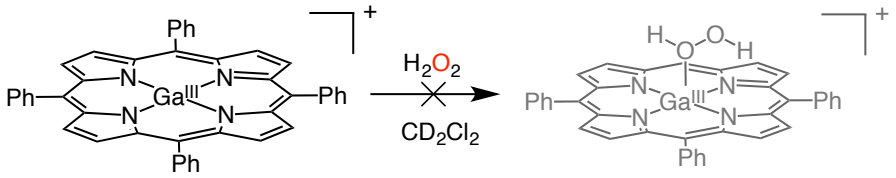

Scheme 1-11. Hydrogen peroxide does not coordinate to gallium tetraphenylporphyrin complexes.[14]

Shaik later reported new computational evidence, in 2015, that supported formation of an $Fe(H_2O_2)$ adduct in mutant cytochrome P450 enzymes when stabilized by hydrogen bonding interactions with a protein residue in the enzyme active site (Scheme 1-12).[16] In addition to the hydrogen bonds, the adduct is trapped by steric pressure from the substrate in the active-site pocket, leading to homolysis of the O–O bond. The hydroxyl radical is stabilized by hydrogen bond interactions with the protein residue and the newly formed Fe^{IV}–OH species, ultimately leading to formation of water and Compound 1, which then oxidizes the substrate (Scheme 1-12).[16] As discussed earlier, Shaik reported a very similar mechanism in 2016 for $P450_{SP\alpha}$ enzymes (Section 1.3.1, Scheme 1-8).[17] It is possible in both cases that the tethered hydroxyl radical could have instead oxidized the substrate, if the metal and ligand were altered to be more resistant to oxidation.

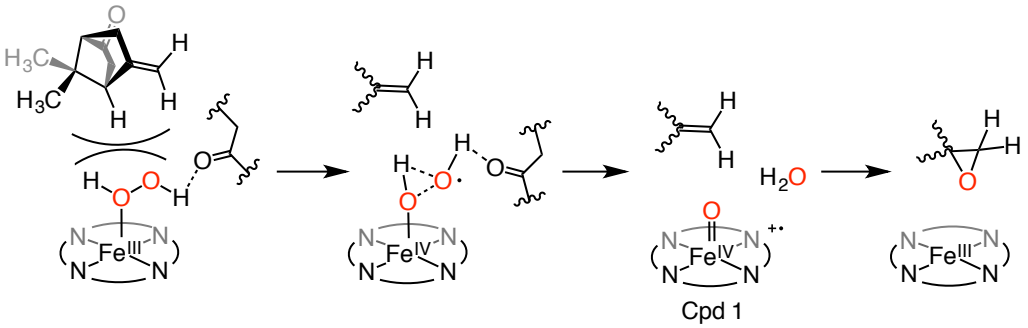

Scheme 1-12. Calculated mechanism for alternate formation of Compound 1 from $Fe^{III}(H_2O_2)$ adduct and subsequent substrate oxidation.[16]

1.4.2 The $M(H_2O_2)$ Adduct

The tethered hydroxyl radical species and the M–OOH_2 species (e and f, Figure 1-1) could serve as powerful intermediate for oxidation of saturated and unsaturated hydrocarbons. It is important to note that many of the oxidative species discussed thus far, including the M–OOH_2 and tethered •OH species, began as $M(H_2O_2)$ adducts stabilized by hydrogen bonding. Furthermore, it is possible that $M(H_2O_2)$ adducts themselves could be oxidatively active (g, Figure 1-1). In fact, $M(H_2O_2)$ adducts would likely be more electrophilic than analogous M–OOH species, due to the presence of an extra proton. This extra proton could also help to stabilize the leaving group after oxidation of substrate (i.e. $M–OH^- + H^+ \rightarrow M–OH_2$). Also, since hydrogen peroxide is neutral, $M(H_2O_2)$ systems do not require deprotonation before activation, thus eliminating the need for stoichiometric or catalytic base, although intramolecular hydrogen bonding interactions could greatly help to facilitate proton transfer. For these reasons, establishing the existence of $M(H_2O_2)$ adducts and investigating their stability is of vital importance in understanding mechanisms of hydrogen peroxide activation and developing novel methodologies with hydrogen peroxide as the sole stoichiometric oxidant.

1.5 References

1. Jones, C. W., *Applications of of Hydrogen Peroxide and Derivatives*. Royal Society: Cambridge, U.K., 1999.

2. Osterberg, P. M.; Niemeier, J. K.; Welch, C. J.; Hawkins, J. M.; Martinelli, J. R.; Johnson, T. E.; Root, T. W.; Stahl, S. S., Experimental Limiting Oxygen Concentrations for Nine Organic Solvents at Temperatures and Pressures Relevant to Aerobic Oxidations in the Pharmaceutical Industry. *Organic Process Research & Development* **2015,** *19* (11), 1537-1543.

3. Caron, S.; Dugger, R. W.; Ruggeri, S. G.; Ragan, J. A.; Ripin, D. H. B., Large-Scale Oxidations in the Pharmaceutical Industry. *Chem. Rev.* **2006,** *106* (7), 2943-2989.

4. Campos-Martin, J. M.; Blanco-Brieva, G.; Fierro, J. L. G., Hydrogen Peroxide Synthesis: An Outlook beyond the Anthraquinone Process. *Angew. Chem. Int. Ed.* **2006,** *45* (42), 6962-6984.

5. Hage, R.; Lienke, A., Applications of Transition-Metal Catalysts to Textile and Wood-Pulp Bleaching. *Angew. Chem. Int. Ed.* **2006,** *45* (2), 206-222.

6. Samanta, C., Direct synthesis of hydrogen peroxide from hydrogen and oxygen: An overview of recent developments in the process. *Applied Catalysis A: General* **2008,** *350* (2), 133-149.

7. Hydrogen Peroxide. http://www.essentialchemicalindustry.org/chemicals/hydrogen-peroxide.html (accessed November 19, 2016).

8. Russo, V.; Tesser, R.; Santacesaria, E.; Di Serio, M., Chemical and Technical Aspects of Propene Oxide Production via Hydrogen Peroxide (HPPO Process). *Ind. Eng. Chem. Res.* **2013,** *52* (3), 1168-1178.

9. Hage, R.; de Boer, J. W.; Gaulard, F.; Maaijen, K., Chapter Three - Manganese and Iron Bleaching and Oxidation Catalysts. In *Adv. Inorg. Chem.*, Rudi van, E.; Colin, D. H., Eds. Academic Press: 2013; Vol. Volume 65, pp 85-116.

10. da Silva, J. A. L.; da Silva, J. J. R. F.; Pombeiro, A. J. L., Oxovanadium complexes in catalytic oxidations. *Coord. Chem. Rev.* **2011,** *255* (19–20), 2232-2248.

11. Ma, L.; Pan, Y.; Man, W.-L.; Kwong, H.-K.; Lam, W. W. Y.; Chen, G.; Lau, K.-C.; Lau, T.-C., Highly Efficient Alkane Oxidation Catalyzed by [MnV(N)(CN)4]2–. Evidence for [MnVII(N)(O)(CN)4]2– as an Active Intermediate. *J. Am. Chem. Soc.* **2014,** *136* (21), 7680-7687.

12. Sever, R. R.; Root, T. W., Comparison of Epoxidation and Baeyer–Villiger Reaction Pathways for Ti(IV)–H2O2 and Sn(IV)–H2O2. *The Journal of Physical Chemistry B* **2003,** *107* (38), 10521-10530.

13. Oszajca, M.; Franke, A.; Brindell, M.; Stochel, G.; van Eldik, R., Redox cycling in the activation of peroxides by iron porphyrin and manganese complexes. 'Catching' catalytic active intermediates. *Coord. Chem. Rev.* **2016,** *306, Part 2*, 483-509.

14. DiPasquale, A. G.; Mayer, J. M., Hydrogen Peroxide: A Poor Ligand to Gallium Tetraphenylporphyrin. *J. Am. Chem. Soc.* **2008,** *130* (6), 1812-1813.

15. Mirza, S. A.; Bocquet, B.; Robyr, C.; Thomi, S.; Williams, A. F., Reactivity of the Coordinated Hydroperoxo Ligand. *Inorg. Chem.* **1996,** *35* (5), 1332-1337.

16. Wang, B.; Li, C.; Dubey, K. D.; Shaik, S., Quantum Mechanical/Molecular Mechanical Calculated Reactivity Networks Reveal How Cytochrome P450cam and Its T252A Mutant Select Their Oxidation Pathways. *J. Am. Chem. Soc.* **2015,** *137* (23), 7379-7390.

17. Ramanan, R.; Dubey, K. D.; Wang, B.; Mandal, D.; Shaik, S., Emergence of Function in P450-Proteins: A Combined Quantum Mechanical/Molecular Mechanical and Molecular Dynamics Study of the Reactive Species in the H2O2-Dependent Cytochrome P450SP α and Its Regio- and Enantioselective Hydroxylation of Fatty Acids. *J. Am. Chem. Soc.* **2016,** *138* (21), 6786-6797.

18. Wittcoff, H. A.; Reuben, B. G.; Plotkin, J. S., *Industrial Organic Chemicals*. Third Edition ed.; John Wiley & Sons, Inc: Hoboken, New Jersey, 2013.

19. Katsuki, T.; Sharpless, K. B., The first practical method for asymmetric epoxidation. *J. Am. Chem. Soc.* **1980,** *102* (18), 5974-5976.

20. Gao, Y.; Klunder, J. M.; Hanson, R. M.; Masamune, H.; Ko, S. Y.; Sharpless, K. B., Catalytic asymmetric epoxidation and kinetic resolution: modified procedures including in situ derivatization. *J. Am. Chem. Soc.* **1987,** *109* (19), 5765-5780.

21. Shaik, S.; Kumar, D.; de Visser, S. P.; Altun, A.; Thiel, W., Theoretical Perspective on the Structure and Mechanism of Cytochrome P450 Enzymes. *Chem. Rev.* **2005,** *105* (6), 2279-2328.

22. McDonald, A. R.; Que Jr, L., High-valent nonheme iron-oxo complexes: Synthesis, structure, and spectroscopy. *Coord. Chem. Rev.* **2013,** *257* (2), 414-428.

23. Oloo, W. N.; Que, L., Bioinspired Nonheme Iron Catalysts for C–H and C=C Bond Oxidation: Insights into the Nature of the Metal-Based Oxidants. *Acc. Chem. Res.* **2015,** *48* (9), 2612-2621.

24. Puri, M.; Que, L., Toward the Synthesis of More Reactive S = 2 Non-Heme Oxoiron(IV) Complexes. *Acc. Chem. Res.* **2015,** *48* (8), 2443-2452.

25. C. Gilbert, B.; W. J. Kamp, N.; R. Lindsay Smith, J.; Oakes, J., Electrospray mass spectrometry evidence for an oxo-manganese(V) species generated during the reaction of

manganese triazacyclononane complexes with H2O2 and 4-methoxyphenol in aqueous solution. *Journal of the Chemical Society, Perkin Transactions 2* **1998,** (9), 1841-1844.

26. Chen, M.; Pan, Y.; Kwong, H.-K.; Zeng, R. J.; Lau, K.-C.; Lau, T.-C., Catalytic oxidation of alkanes by a (salen)osmium(vi) nitrido complex using H2O2 as the terminal oxidant. *Chem. Commun.* **2015,** *51* (71), 13686-13689.

27. Fenton, H. J. H., LXXIII.-Oxidation of tartaric acid in presence of iron. *Journal of the Chemical Society, Transactions* **1894,** *65* (0), 899-910.

28. Neyens, E.; Baeyens, J., A review of classic Fenton's peroxidation as an advanced oxidation technique. *Journal of Hazardous Materials* **2003,** *98* (1–3), 33-50.

29. Pignatello, J. J.; Oliveros, E.; MacKay, A., Advanced Oxidation Processes for Organic Contaminant Destruction Based on the Fenton Reaction and Related Chemistry. *Critical Reviews in Environmental Science and Technology* **2006,** *36* (1), 1-84.

30. Kirillova, M. V.; Kuznetsov, M. L.; Romakh, V. B.; Shul'pina, L. S.; Fraústo da Silva, J. J. R.; Pombeiro, A. J. L.; Shul'pin, G. B., Mechanism of oxidations with H2O2 catalyzed by vanadate anion or oxovanadium(V) triethanolaminate (vanadatrane) in combination with pyrazine-2-carboxylic acid (PCA): Kinetic and DFT studies. *Journal of Catalysis* **2009,** *267* (2), 140-157.

31. Kuznetsov, M. L.; Pombeiro, A. J. L., Radical Formation in the [MeReO3]-Catalyzed Aqueous Peroxidative Oxidation of Alkanes: A Theoretical Mechanistic Study. *Inorg. Chem.* **2009,** *48* (1), 307-318.

32. Anson, C. W.; Ghosh, S.; Hammes-Schiffer, S.; Stahl, S. S., Co(salophen)-Catalyzed Aerobic Oxidation of p-Hydroquinone: Mechanism and Implications for Aerobic Oxidation Catalysis. *J. Am. Chem. Soc.* **2016,** *138* (12), 4186-4193.

33. Kwong, H.-K.; Lo, P.-K.; Lau, K.-C.; Lau, T.-C., Epoxidation of alkenes and oxidation of alcohols with hydrogen peroxide catalyzed by a manganese(v) nitrido complex. *Chem. Commun.* **2011,** *47* (14), 4273-4275.

34. Chandrasena, R. E. P.; Vatsis, K. P.; Coon, M. J.; Hollenberg, P. F.; Newcomb, M., Hydroxylation by the Hydroperoxy-Iron Species in Cytochrome P450 Enzymes. *J. Am. Chem. Soc.* **2004,** *126* (1), 115-126.

35. Coon, M. J., Cytochrome P450: nature's most versatile biological catalyst. *Annu Rev Pharmacol Toxicol* **2005,** *45* (1), 1-25.

36. Newcomb, M.; Toy, P. H., Hypersensitive Radical Probes and the Mechanisms of Cytochrome P450-Catalyzed Hydroxylation Reactions. *Acc. Chem. Res.* **2000,** *33* (7), 449-455.

37. Sheng, X.; Zhang, H.; Hollenberg, P. F.; Newcomb, M., Kinetic Isotope Effects in Hydroxylation Reactions Effected by Cytochrome P450 Compounds I Implicate Multiple Electrophilic Oxidants for P450-Catalyzed Oxidations. *Biochemistry* **2009,** *48* (7), 1620-1627.

38. Denisov, I. G.; Makris, T. M.; Sligar, S. G.; Schlichting, I., Structure and Chemistry of Cytochrome P450. *Chem. Rev.* **2005,** *105* (6), 2253-2278.

39. Ortiz de Montellano, P. R., *Cytochrome P450: Structure, Mechanism, and Biochemistry*. Kluwer/Plenum: New York, 2005.

40. Li, C.; Zhang, L.; Zhang, C.; Hirao, H.; Wu, W.; Shaik, S., Which Oxidant Is Really Responsible for Sulfur Oxidation by Cytochrome P450? *Angew. Chem. Int. Ed.* **2007,** *46* (43), 8168-8170.

41. Medvedev, A. G.; Mikhaylov, A. A.; Churakov, A. V.; Vener, M. V.; Tripol'skaya, T. A.; Cohen, S.; Lev, O.; Prikhodchenko, P. V., Potassium, Cesium, and Ammonium Peroxogermanates with Inorganic Hexanuclear Peroxo Bridged Germanium Anion Isolated from Aqueous Solution. *Inorg. Chem.* **2015,** *54* (16), 8058-8065.

42. Mikhaylov, A. A.; Medvedev, A. G.; Churakov, A. V.; Grishanov, D. A.; Prikhodchenko, P. V.; Lev, O., Peroxide Coordination of Tellurium in Aqueous Solutions. *Chem. Eur. J.* **2016**, 2980–2986.

43. Wolanov, Y.; Shurki, A.; Prikhodchenko, P. V.; Tripolskaya, T. A.; Novotortsev, V. M.; Pedahzur, R.; Lev, O., Aqueous stability of alumina and silica perhydrate hydrogels: experiments and computations. *Dalton Trans.* **2014,** *43* (44), 16614-16625.

Chapter 2

A Hydrogen Peroxide Complex of Zinc

Adapted from: Wallen, C. M.; Bacsa, J.; Scarborough, C. C., Hydrogen Peroxide Complex of Zinc. *J. Am. Chem. Soc.* **2015,** *137* (46), 14606-14609.

2.1 Abstract

Metal(H_2O_2) complexes have been implicated in kinetic and computational studies but have never been observed. Accordingly, H_2O_2 has been described as a very weak ligand. In this chapter, we report the first metal(H_2O_2) adduct, which is made possible by incorporating intramolecular hydrogen-bonding interactions with bound H_2O_2. This $Zn^{II}(H_2O_2)$ complex decays in solution by a second-order process that is slow enough to enable characterization of this species by X-ray crystallography. The work herein speaks to the existence of metal(H_2O_2) intermediates in chemistry and biology, and opens the door to exploration of these species in oxidation catalysis.

2.2 Introduction

2.2.1 Hydrogen peroxide and M(H_2O_2) adducts

Hydrogen peroxide is a readily accessible and "green" oxidant,[1-2] with major industrial applications including bleaching of raw cotton and wood pulp, textile bleaching,[3-4] and propylene epoxidation.[5] These industrial processes are improved by the use of metal catalysts that activate H_2O_2. Remarkably, metal(H_2O_2) adducts that may be important intermediates in H_2O_2 activation have never been observed, although they have been kinetically implicated.[6-9] In cytochromes P450, an $Fe^{III}(H_2O_2)$ adduct may be the "second oxidant" or a precursor to the second oxidant (Figure 2-1a), and is likely the source of free H_2O_2 formed via "uncoupling."[10-13] The intermediacy of $Fe^{III}(H_2O_2)$ complexes in cytochromes P450 has been contentious, and Mayer demonstrated that related (porphyrin)Ga^{III} complexes do not interact with H_2O_2 in anhydrous CH_2Cl_2 solutions despite the availability of open coordination sites on Ga^{III} and a strong interaction between

Ga^{III} and added H_2O (Figure 2-1C).[14-15] However, a recent computational study by Shaik supported H_2O_2 coordination in cytochromes P450, not as the "second oxidant" but as an alternative route to the reactive Fe^{IV}(oxo) species (Compound 1, Figure 2-1A),[16] where hydrogen bonding between the coordinated H_2O_2 ligand and the surrounding environment was critical to the accessibility and longevity of this $Fe^{III}(H_2O_2)$ species (Figure 2-1B). Related computational studies of M/H_2O_2 oxidation catalysts (M = Mn, Os) also implicate the intermediacy of $M(H_2O_2)$ adducts that benefit from intramolecular hydrogen bonding involving bound H_2O_2.[17-19] Herein, we report the first coordination compound of H_2O_2, a $Zn^{II}(H_2O_2)$ species that features hydrogen bonding between bound H_2O_2 and the ancillary ligand.

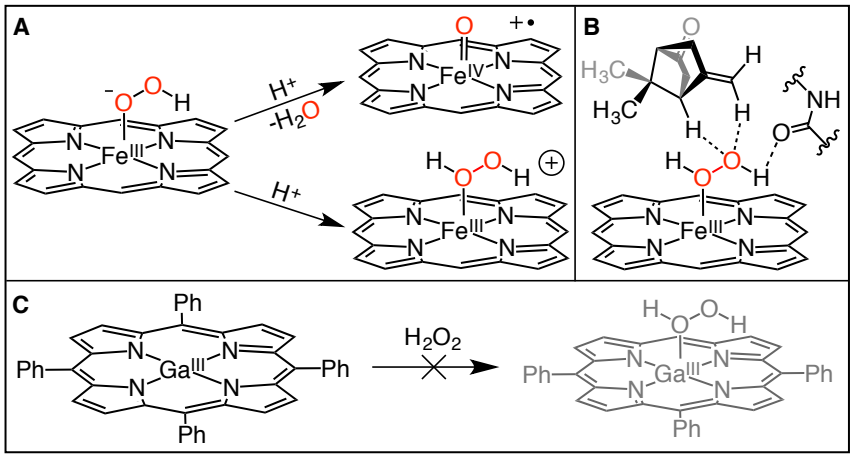

Figure 2-1. (A) Proposed $Fe^{III}(H_2O_2)$ adduct in cytochromes P450.[10-13] (B) Shaik's computed $Fe^{III}(H_2O_2)$ adduct demonstrating the importance of second-sphere hydrogen-bonding interactions with bound H_2O_2 for preventing "uncoupling."[16] (C) Demonstration by Mayer that H_2O_2 is a very poor ligand for Ga^{III}.[14]

Ligands that engage in second-sphere hydrogen bonding have been utilized extensively by Borovik, with highlights including the sole report of a high-spin Fe^{III}(oxo) species stabilized by intramolecular hydrogen-bond donors[20] and O_2 activation at Co^{II} centers that was dependent on the presence and number of second-sphere hydrogen-bond donors.[21] Recognizing the higher acidity of H_2O_2 compared to H_2O and the corresponding demonstration by Prikhodchenko that H_2O_2 is a more effective hydrogen-bond donor than H_2O,[22-25] we targeted ligands that would provide second-sphere hydrogen-bond acceptors. We were particularly attracted by trianionic trisulfonamido derivatives of tren (tren = tris(2-aminoethyl)amine) that have been demonstrated by Borovik to provide an electron-rich coordination environment well suited for hydrogen bonding with H_2O and HO^- ligands.[26-33] Reasoning that diamagnetic metals would enable the study of metal(H_2O_2) interactions by ^{1}H NMR spectroscopy, we targeted Zn^{II} complexes supported by trisulfonamido derivatives of tren.

2.2.2 Designing a Ligand Platform

Based on the computational evidence that hydrogen bonding is essential for stabilizing the otherwise weak binding of hydrogen peroxide to transition metals, we pursued a ligand platform that included hydrogen bond acceptors in a secondary coordination sphere. Electron-rich carbonyl groups, such as amidates or ureates, could serve as hydrogen bond acceptors, but they provide little flexibility. Ideally, the ligand framework would provide freedom for the adduct to find the most stable orientation. Therefore, we looked to groups containing electron-rich sp^3-hybridized oxygen atoms, such as sulfonyl or phosphoryl groups. Also, since these adducts are not expected to be very stable, we wished to provide steric protection for the H_2O_2 moiety. With these requirements in mind, we decided to use

a tripodal sulfonamido ligand used extensively by Borovik (Figure 2-2).[44-50] The six sulfonyl oxygen atoms surrounding the open coordination site on the metal center should provide plenty of hydrogen bonding opportunities while also maintaining flexibility. Furthermore, the sulfonyl groups form an electron-rich belt which should discourage the approach of nucleophiles to the electrophilic bound hydrogen peroxide.

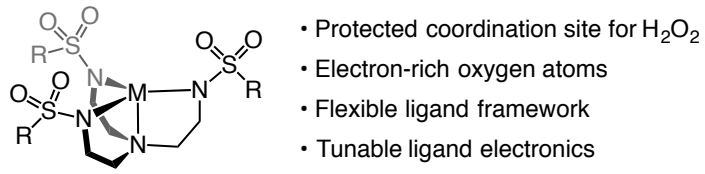

Figure 2-2. Sulfomido complex design for stabilizing M(H_2O_2) species.

2.3 Results and Discussion

2.3.1 Synthesis of Complexes

Combining H_3Ts_3tren, KH, and $ZnCl_2$ in DMF, followed by addition of [^{n}Bu$_4$N][Br] and H_2O, provides access to [^{n}Bu$_4$N][(Ts_3tren)Zn^{II}(OH_2)] in 92% crystalline yield (**2-1(OH_2)**, Scheme 2-1). X-ray crystallographic characterization of **2-1(OH_2)** shows hydrogen-bonding interactions between the bound H_2O protons and the sulfonyl oxygens (Figure 2-3) similar to what Borovik observed with other metals.[26-33] Displacement of water from **2-1(OH_2)** was readily accomplished with both hydrazine and hydroxylamine, which are structurally analogous to H_2O_2 (Scheme 2-1). The X-ray crystal structures of **2-1(N_2H_4)** and **2-1(NH_2OH)** also exhibit second-sphere hydrogen bonding interactions, in these cases demonstrating hydrogen bonding with the terminal ZH group (Figure 2-3). While crystallographically characterized metal–(N_2H_4) complexes are abundant, we are aware of

only five other metal–(NH_2OH) species that have been crystallographically characterized.[34-38]

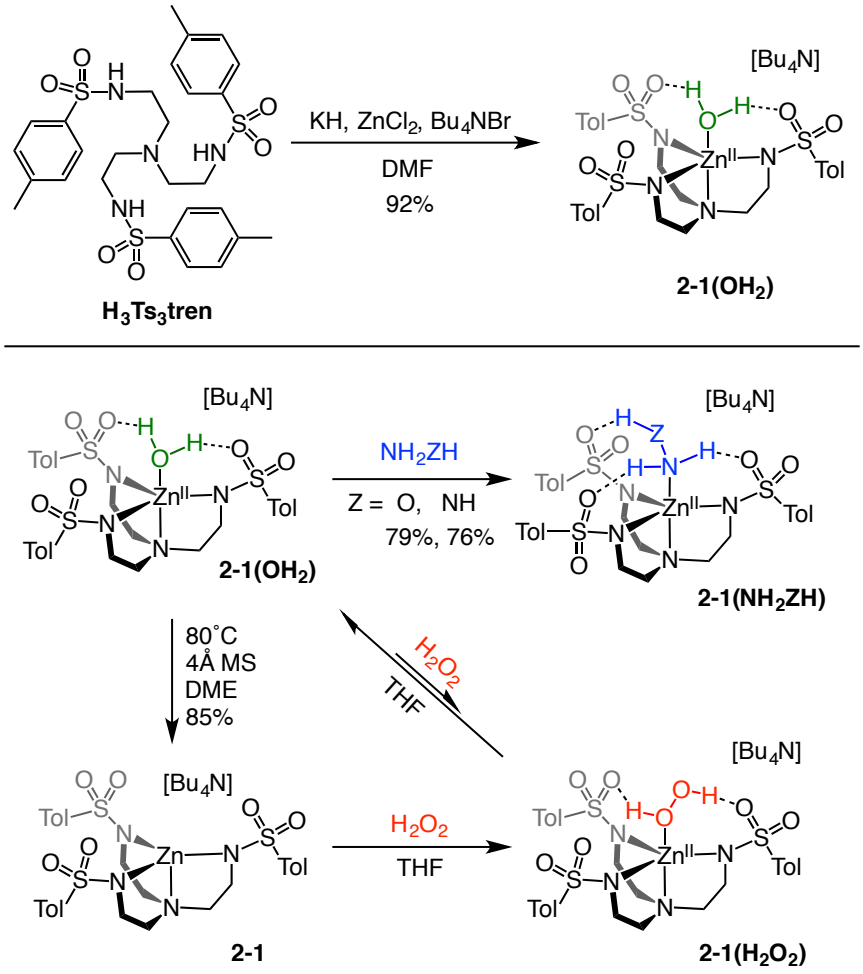

Scheme 2-1. Synthesis of compounds examined. Yields of crystalline products shown.

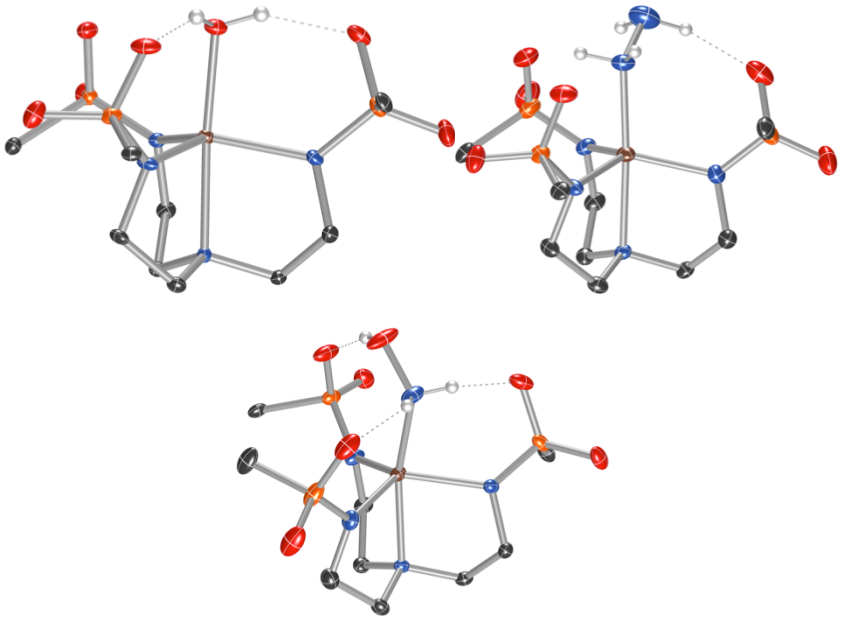

Figure 2-3. X-ray crystal structures of the anions in ***2-1(OH$_2$)*** *(left),* ***2-1(N$_2$H$_4$)*** *(middle), and* ***2-1(NH$_2$OH)*** *(right), highlighting intramolecular hydrogen bonding. Aryl groups truncated for clarity.*

2.3.2 Anhydrous Solutions of Hydrogen Peroxide

One inherent challenge of trying to observe M(H_2O_2) adducts is water. Water is often an excellent ligand for metals and is also very capable of forming hydrogen bonds. In contrast, hydrogen peroxide is known to be a weak ligand for metals,[14-15] which means it probably will not be able to competitively bind in the presence of water. Since most commercial sources of hydrogen peroxide are aqueous, obtaining anhydrous solutions of hydrogen peroxide is a challenge. Prikhodchenko has reported the preparation of solid "perhydrates" which consist of hydrogen peroxide co-crystalized with an amino acid such as L-serine and glycine.[51] By stirring the serine hydrogen peroxide with organic solvents it is possible to extract the hydrogen peroxide from these crystalline adducts to obtain anhydrous solutions of hydrogen peroxide.[52] If the solvent has a relatively low boiling point, the hydrogen

peroxide can be concentrated under vacuum to over 99% purity.[52] The disadvantage of this approach is that the serine perhydrate must be prepared from a ≥70% aqueous hydrogen peroxide solution. Since it is difficult to purchase a solution at this concentration for laboratory work, it must be prepared by concentrating a 50% aqueous solution under vacuum.[52] Alternatively, the co-crystallized adduct of hydrogen peroxide and urea is readily available. By simply stirring this solid in anhydrous solvent, we found that solutions of hydrogen peroxide with <5% H_2O relative to H_2O_2 are readily accessible at concentrations up to 500mM in tetrahydrofuran (THF) and THF-d_8.

2.3.3 Safety note

With regard to the safety concerns many might have for solutions of hydrogen peroxide in organic solvent, it should be noted that hydrogen peroxide is inherently stable and is produced in organic solution during the anthraquinone process (Section 1.1.2).[1] Care should always be taken with H_2O_2 solutions and complexes, but as long as these solutions are made at reasonably low concentrations and kept free from metal salt contamination, there should be no cause for concern.

2.3.4 ^{1}H-NMR of Zinc Complex with H_2O_2

We next turned to exploring coordination of H_2O_2 to Zn^{II}. Addition of this solution of H_2O_2 (1 equivalent) to a THF-d_8 solution of **2-1(OH$_2$)** resulted in a 0.72 ppm upfield shift of bound water towards the free-H_2O resonance of 2.54 ppm with concomitant 0.05 ppm downfield shift of the H_2O_2 resonance away from free H_2O_2 (9.40 ppm) (Figure 2-15). This was the first indication that H_2O_2 interacts with **2-1(OH$_2$)** and reveals that K_{eq} for H_2O displacement by H_2O_2 is less than unity (Scheme 2-1). This contrasts the observation that

both N_2H_4 and NH_2OH quantitatively displace H_2O from **2-1(OH$_2$)**, and is consistent with H_2O_2 being the weakest ligand of this series.

Encouraged by the interaction of H_2O_2 with **2-1(OH$_2$)** in THF-d_8, we turned to dehydration of **2-1(OH$_2$)** to probe coordination of H_2O_2 to **2-1** in the absence of H_2O. Formation of anhydrous **2-1** was accomplished by heating **2-1(OH$_2$)** in glyme to 80 ºC overnight in the presence of 4Å molecular sieves, followed by precipitation with pentane. Dehydration was verified by the disappearance of any resonance associated with bound or free H_2O by ^{1}H NMR spectroscopy. Addition of one equivalent of anhydrous H_2O_2 to **2-1** in THF-d_8 resulted in a 0.45 ppm downfield shift of the H_2O_2 proton resonances, consistent with interaction between H_2O_2 and **2-1** to form **2-1(H$_2$O$_2$)**, although the nature of the interaction (coordination, hydrogen bonding, electrostatic interaction) could not be established from these data (Figure 2-4). Importantly, no interaction between H_2O_2 and H_3Ts_3tren or between H_2O_2 and $ZnCl_2$ in THF-d_8 is observed by ^{1}H NMR spectroscopy (Figure 2-10, Table 2-1). The H_2O_2 proton resonance in **2-1(H$_2$O$_2$)** shifts linearly downfield with decreasing temperature with a slope that is steeper than that of free H_2O_2 or that of bound H_2O in **2-1(OH$_2$)** (Figure 2-14). This large temperature dependence is indicative of strong intramolecular hydrogen bonding in **2-1(H$_2$O$_2$)**.[39-41] At room temperature, **2-1(H$_2$O$_2$)** decomposes in solution to **2-1(OH$_2$)** by a second order pathway ($k = 3.8 \times 10^{-3}$ M^{-1} s^{-1}, Figure 2-9).

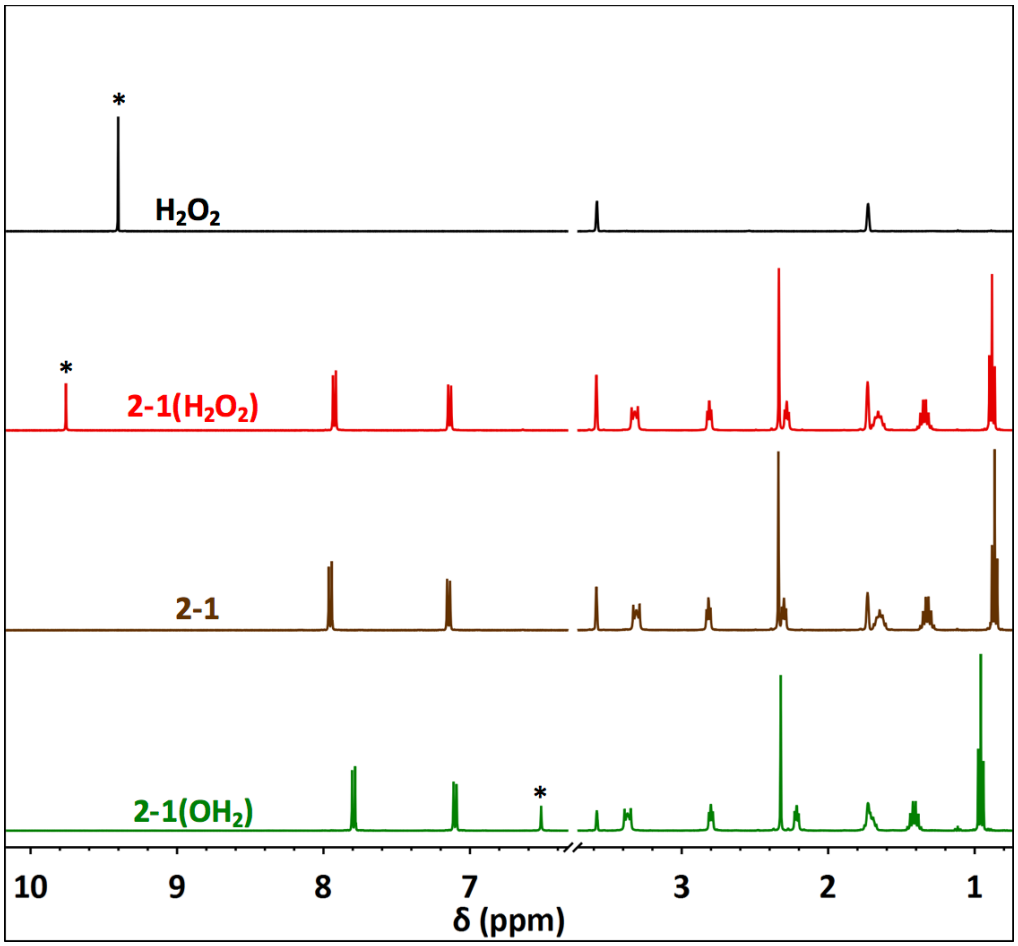

Figure 2-4. From top to bottom, ^{1}H NMR spectra (THF-d_8) of H_2O_2, ***2-1(H_2O_2)****,* ***2-1****, and* ***2-1(OH_2)****. Free (top) and bound H_2O_2 (second from top) and bound H_2O positions (bottom) are marked with an asterisk. Free H_2O in THF-d_8 appears at 2.54 ppm.*

Table 2-1. Shift of hydrogen peroxide proton signal in THF-d_8.

Sample	Signal (ppm)	Shift from free position (ppm)
H_2O_2	9.391	--
$ZnCl_2 + H_2O_2$	9.386	-0.005
$H_3Ts_3tren + H_2O_2$	9.399	0.008
2-1(OH$_2$) + H_2O_2	9.455	0.064
1 + H_2O_2	9.854	0.463

2.3.5 Solid-state Characterization of Zn(H_2O_2) Adduct

Precipitation of **2-1(H_2O_2)** and re-dissolution in THF-d_8 indicated the presence of a 1:1 mixture of **2-1(OH$_2$)** and **2-1(H_2O_2)** in the solid state. This solid was explored by thermogravimetric analysis (TGA) to probe the strength of the H_2O_2 interaction with **2-1** in the solid state by comparison to crystalline and powdered samples of **2-1(OH$_2$)** (Figure 2-5). These data show that H_2O_2 is the first ligand to be lost upon heating solid samples of **2-1(OH$_2$)**/**2-1(H_2O_2)** because there is a lower-temperature mass-loss event than observed in powdered samples of **2-1(OH$_2$)**. Therefore, in both the solid state and in solution, H_2O_2 is a weaker ligand than H_2O for **2-1**.

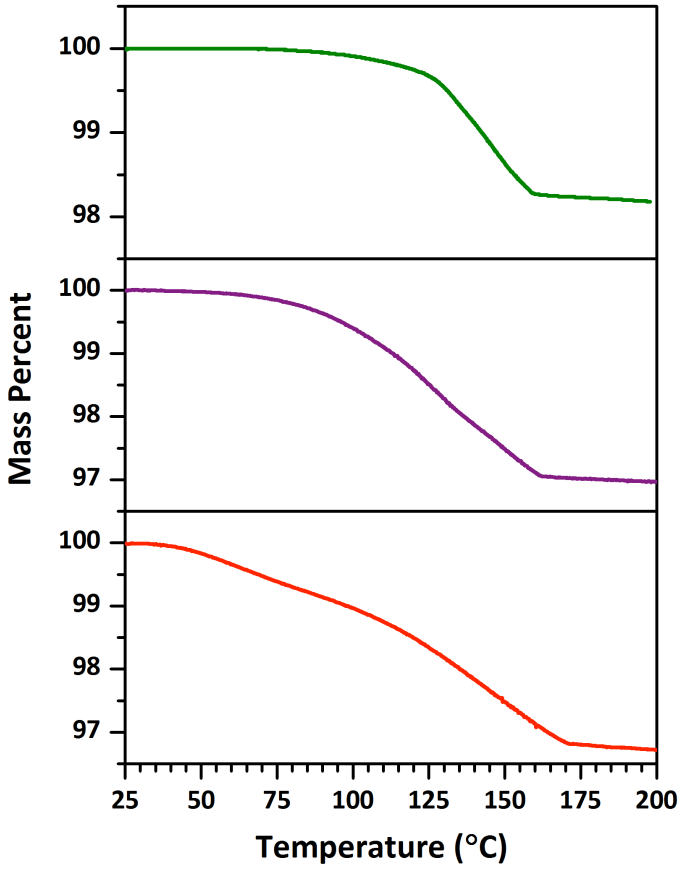

Figure 2-5. TGA traces of crystalline ***2-1(OH$_2$)*** *(top), powdered* ***2-1(OH$_2$)*** *(middle), and powdered 1:1 mixture of* ***2-1(H$_2$O$_2$)*** *and* ***2-1(OH$_2$)*** *(bottom). Mass loss experimental/theoretical: 0.74mg/0.82mg (top), 0.67mg/0.63mg (middle), 0.70mg/0.82mg (bottom).*

2.3.6 First Crystal Structure of M(H$_2$O$_2$) Adduct

Encouraged by the isolation of solid samples containing **2-1(H$_2$O$_2$)** despite the bimolecular decay pathway of this species, we explored whether crystalline samples of **2-1(H$_2$O$_2$)** could be obtained. Rapid crystallization of **2-1(H$_2$O$_2$)** from THF with MTBE provided crystals with varying amounts of bound H_2O and H_2O_2, with the best crystal examined having a 50:50 disorder of **2-1(H$_2$O$_2$)** (Figure 2-6) and **2-1(H$_2$O$_2$)**, each refined as a distinct

component. The H_2O_2 and H_2O ligands share the same apical position. The electron density of **2-1(OH_2)**/**2-1(H_2O_2)** (see Appendix 2) unambiguously establishes the presence of a bent H_2O_2 ligand coordinated to Zn^{II}. **2-1(H_2O_2)** is the first structurally characterized H_2O_2 coordination compound. H_2O_2 coordination to Zn^{II} is analogous to coordination of N_2H_4 and NH_2OH, where intramolecular hydrogen bonding between both H_2O_2 protons and the sulfonyl oxygens is observed in the solid state. The Zn–O bond lengths of **2-1(OH_2)** and **2-1(H_2O_2)** (2.185(10) Å and 2.171(10) Å, respectively) fall within 1σ of one another, consistent with formation of a direct Zn–O bond in each case. The O–O bond length in **2-1(H_2O_2)** is 1.445(14) Å, indicative of an O–O single bond.

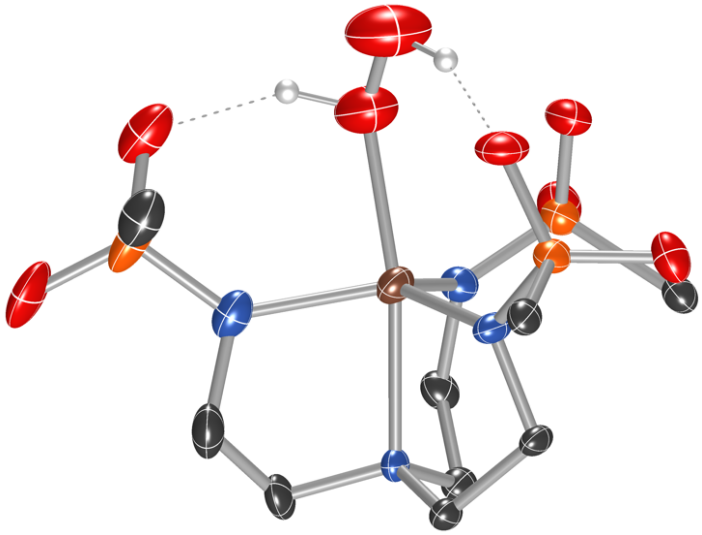

*Figure 2-6. X-ray crystal structure of the anion in **2-1(H_2O_2)** from a 1:1 crystal of **2-1(OH_2)**: **2-1(H_2O_2)**. Aryl groups truncated for clarity.*

2.3.7 Competitive Binding by H_2O and H_2O_2

While H_2O_2 has been described as a very poor ligand,[14, 42] H_2O is a common ligand in coordination chemistry. Both of these ligands can engage in hydrogen bonding, so we probed the extent to which coordination of H_2O to **2-1** was favored over coordination of

H_2O_2. As described above, addition of one equivalent of H_2O_2 to **2-1(OH$_2$)** in THF-d_8 results in a 0.05 ppm downfield shift of H_2O_2 from its uncoordinated position with a concomitant 0.72 ppm upfield shift of H_2O from its coordinated position (Figure 2-15), enabling us to measure the equilibrium constant for H_2O vs. H_2O_2 coordination to **2-1** by comparing these exchange-averaged chemical shifts to their corresponding free and bound shifts (see Section 2.5.5 for details; exchange of H_2O and H_2O_2 is fast on the NMR timescale even at –100 ºC, Figure 2-15). We calculate that $K_{eq} = 37$ ($\Delta G^\circ = -2.1$ kcal/mol) in favor of H_2O coordination to **1** over H_2O_2.

$$K_{eq} = \frac{[\mathbf{2-1(OH_2)}][\mathbf{H_2O_2}]}{[\mathbf{2-1(H_2O_2)}][\mathbf{H_2O}]} \approx 37$$

H_2O remains a better ligand than H_2O_2 even with supporting ligands that facilitate second-sphere hydrogen-bonding interactions, but the preference is not particularly stark: the ratio of bound H_2O to bound H_2O_2 at equal concentrations of these two species and **2-1** is ~6:1.

2.4 Conclusions

We have demonstrated the first H_2O_2 coordination complex, where the M–(H_2O_2) interaction is facilitated by second-sphere hydrogen-bonding interactions. Coordination of H_2O_2 speaks to the viability of metal(H_2O_2) adducts as intermediates in catalysis,[6-9, 17-19] particularly in reference to the "second oxidant" in cytochromes P450.[10-13, 16] Furthermore, an understanding of how to facilitate formation of metal(H_2O_2) adducts opens a new pathway for exploring H_2O_2 activation for substrate oxidation reactions and eventual methodologies using H_2O_2 as the sole stoichiometric oxidant.

2.5 Experimental

2.5.1 Materials and Methods

All room temperature ^{1}H-NMR and ^{13}C-NMR spectra were obtained on a 400MHz instrument and referenced to residual solvent. Low-temperature NMR experiments were conducted on a 600MHz NMR spectrometer and referenced to residual solvent. IR spectra were obtained using a Nicolet 380 FT-IR with Smart Orbit Diamond ATR attachment. X-ray crystallography data was collected and analyzed by the Emory University Department of Chemistry X-Ray Crystallography Center. Elemental analyses were performed by Atlantic Microlabs in Norcross, GA. All reactions sensitive to air and/or moisture were carried out in an MBraun UNIlab glovebox under nitrogen atmosphere. Solvents for use in the glovebox were degassed by evacuation and purging with nitrogen and dried using 3Å molecular sieves. Anhydrous tetrahydrofuran was prepared in the glovebox by storing over 3Å molecular sieves for several days and then filtering through a column of activated alumina to remove trace water and peroxides. THF-d_8 was purchased from Cambridge Isotope Laboratories and dried using 3Å molecular sieves. Reagents were purchased from Sigma-Aldrich, Fisher Scientific, Acros Organics, or Strem Chemicals and used without further purification.

2.5.2 Extraction of H_2O_2 in THF

Urea hydrogen peroxide was stirred in anhydrous THF for 30min. The solution was filtered through celite and cooled to –40 ˚C for several hours to crystalize dissolved urea. The solution was filtered through celite again to remove urea crystals. Iodometric titration was used to determine the peroxide concentration in this solution. The same procedure was used

to extract hydrogen peroxide into THF-d_8. 1H NMR spectroscopy was used to ensure that the solution contained <5% water.

2.5.3 Syntheses

H_3Ts_3tren

Ligand precursor was synthesized according to a modified literature procedure.[43] A solution of p-toluenesulfonyl chloride (11.64g, 0.061mol) dissolved in 100mL of diethyl ether was added to a solution of triethylamine (8.4mL, 0.060mol) and tris(2-aminoethyl)amine (2.9mL, 0.019mol) in 80mL of deionized water. The reaction mixture was stirred vigorously for 14hrs. The white solid was filtered from the reaction mixture, washed with water (100mL) and diethyl ether (300mL). Drying under vacuum yielded pure product (11.0g, 93% yield). Characterization data agreed with published material.[43] ^{1}H NMR (400 MHz, $CDCl_3$): δ 7.77 (d, 6H, J=8.3Hz, Ar-H), 7.26 (d, 6Hf, J=8.3Hz), 5.85 (t, 3H), 2.89 (m, 6H), 2.45 (m, 6H), 2.39 (s, 9H); ^{13}C NMR (100 Hz, $CDCl_3$): δ 143.8, 137.2, 130.2, 127.6, 54.5, 41.2, 22.0.

Synthesis and Characterization of $Bu_4N[Ts_3trenZn–OH_2]$ {2-1(OH_2)}

In a glovebox, $ZnCl_2$ (1.16g, 8.54mmol) was added to a stirring solution of H_3Ts_3tren (5.20g, 8.54mmol) in 15mL of DMF. Potassium hydride (1.06g, 26.48mmol) was added carefully and the mixture was stirred overnight. The solution was removed from the glovebox and tetrabutylammonium bromide (2.67g, 8.54mmol) was added. The mixture was diluted with water (200mL) and DCM (200mL). The organic layer was separated and washed with more water (200mL) then brine (200mL). The organic layer was then dried with Na_2SO_4, filtered, and concentrated under reduced pressure. Addition of ether into this concentrated solution resulted in formation of colorless crystals (7.29g, 92% yield). ^{1}H

NMR (400 MHz, $CDCl_3$): δ 7.79 (d, 6H, J=8.2Hz), 7.12 (d, 6H, J=8.2Hz), 6.63 (br s, 2H), 3.27 (m, 8H), 2.88 (t, 6H, J=5.4Hz), 2.33 (s, 9H), 2.29 (t, 6H, J=5.5Hz), 1.64 (m, 8H), 1.40 (m, 8H), 0.96 (t, 12H, J=7.3Hz). ^{13}C NMR (100 Hz, $CDCl_3$): δ 142.0, 140.1, 129.1, 127.2, 58.7, 52.5, 42.1, 24.1, 21.4, 19.8, 13.9. Anal. calcd (found) for ($C_{43}H_{71}N_5O_7S_3Zn$): C, 55.44 (55.65); H, 7.68 (7.70); N, 7.52 (7.42). IR (FT-ATR, cm^{-1}): 3296, 2961, 2873, 1598, 1494, 1466, 1382, 1351, 1270, 1240, 1158, 1128, 1103, 1077, 1046, 974, 930, 871, 846, 812, 738, 710, 657, 595, 549.

Synthesis and Characterization of Bu_4N[Ts_3trenZn–N_2H_4] {2-1(N_2H_4)}

Hydrazine solution (220μL, 1.0M in THF, 0.22mmol) and 1–OH_2 (102mg, 0.11mmol) was added to 0.5mL of DCM. Vapor diffusion of diethyl ether into this solution produced colorless crystals (72mg, 76% yield). ^1H NMR (400 MHz, $CDCl_3$): δ 7.83 (d, 6H, J=8.1Hz), 7.15 (d, 6H, J=8.1Hz), 4.86 (br s, 2H), 4.10 (br s, 2H), 3.28 (m, 8H), 2.86 (t, 6H, J=5.3Hz), 2.35 (s, 9H), 2.27 (t, 6H, J=5.3Hz), 1.63 (m, 8H), 1.41 (m, 8H), 0.97 (t, 12H, J=7.3Hz). ^{13}C NMR (100 Hz, $CDCl_3$): δ 142.8, 140.0, 129.0, 127.0, 58.4, 42.6, 24.1, 21.5, 19.8, 13.9. IR (FT-ATR, cm^{-1}): 3260, 3329, 3295, 2955, 2874, 1598, 1537, 1493, 1467, 1382, 1351, 1285, 1245, 1243, 1129, 1098, 1079, 1045, 984, 971, 930, 870, 846, 813, 794, 739, 710, 659, 592, 548. Anal. calcd (found) for ($C_{43}H_{72}N_7O_6S_3Zn$): C, 54.67 (54.86); H, 7.68 (7.81); N, 10.38 (10.17).

Synthesis and Characterization of Bu_4N[Ts_3trenZn–NH_2OH] {2-1(NH_2OH)}

Hydroxylamine solution (42mg, 0.63mmol, 50wt% in H_2O) was diluted with 1mL of 1:1 THF and MeOH, and added to 1–OH_2 (118mg, 0.127mmol). This solution was stirred until everything dissolves and then filtered through celite. Vapor diffusion of diethyl ether into this solution yielded colorless crystals (88 mg, 79% yield). ^1H NMR (400 MHz, $CDCl_3$): δ

8.33 (br s, 1H), 7.79 (d, 6H, J=8.1Hz), 7.18 (br s, 2H), 7.12 (d, 6H, J=8.1Hz), 3.25 (m, 8H), 2.81 (t, 6H, J=5.2Hz), 2.33 (s, 9H), 2.22 (t, 6H, J=5.2Hz), 1.61 (m, 8H), 1.41 (m, 8H), 0.96 (t, 12H, J=7.8Hz). ^{13}C NMR (100 Hz, $CDCl_3$): δ 142.8, 140.0, 129.0, 127.0, 58.54, 54.6, 42.7, 24.1, 21.4, 19.8, 13.9. IR (FT-ATR, cm^{-1}): 3289, 2963, 2874, 1598, 1494, 1466, 1383, 1352, 1286, 1245, 1129, 1097, 1079, 1045, 970, 932, 871, 846, 812, 793, 738, 696, 659, 591, 547. Anal. calcd (found) for ($C_{43}H_{72}N_6O_7S_3Zn$): C, 54.56 (54.81); H, 7.67 (7.46); N, 8.88 (9.00).

Synthesis and Characterization of Bu_4N[Ts_3trenZn] {2-1}

In the glovebox, **2-1(OH_2)** (347mg) was dissolved in 1,2-dimethoxyethane (5mL) and 4Å molecular sieves were added. The vessel was sealed and heated to 80˚C overnight. Pentane was added to precipitate the Bu_4N[Ts_3trenZn] complex (288mg, 85% yield). ^{1}H NMR (400 MHz, $CDCl_3$): δ 8.01 (d, 6H, J=8.1Hz), 7.21 (d, 6H, J=8.1Hz), 3.14 (m, 8H), 2.92 (t, 6H, J=5.5Hz), 2.43 (t, 6H, J=5.5Hz), 2.35 (s, 9H), 1.49 (m, 8H), 1.17 (m, 8H), 0.76 (t, 12H, J=7.8Hz); ^{13}C NMR (100 Hz, $CDCl_3$): δ 142.0, 140.1, 129.1, 127.2, 58.66, 52.5, 42.1, 24.1, 21.4, 19.8, 13.9.

Crystallization of Bu_4N[Ts_3trenZn–H_2O_2] {2-1(H_2O_2)}

In the glovebox, **2-1** was dissolved in THF and 1 molar equivalent of hydrogen peroxide solution in THF was added. Layering of this solution under *tert*-butyl methyl ether at room temperature yielded colorless crystals. ^{1}H NMR of a sample of crystals indicated the presence of 44% Zn–H_2O_2 complex and 58% Zn–OH_2 complex. A single crystal was selected and mounted on the diffractometer.

2.5.4 NMR Experiments

^{1}H-NMR of 1-H_2O_2 decay in THF-d_8

In a glovebox, 19.2mg of **2-1** and one molar equivalent of hydrogen peroxide (152μL of 138mM solution in THF-d_8) were added to a J. Young NMR tube and diluted with THF-d_8 to 11mM. The sample was analyzed over the course of 14hrs at 20˚C. Spectra were taken every 21.7 minutes; taking 8 scans with a relaxation delay of 30sec.

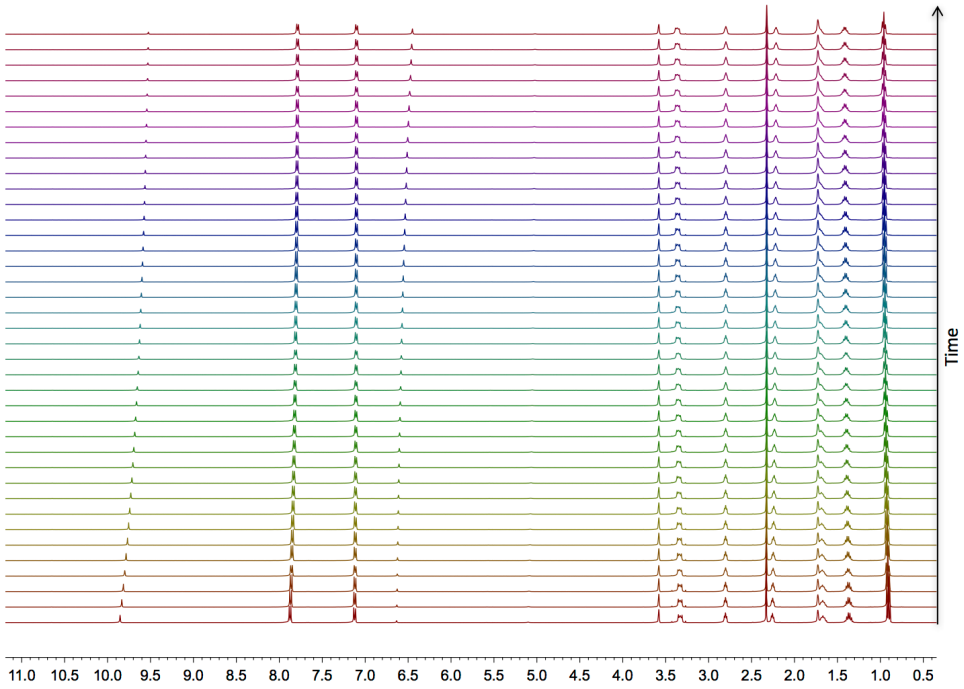

*Figure 2-7. ^{1}H-NMR of **2-1(H_2O_2)** decay into **2-1(OH_2)** in THF-d_8.*

Decay of H_2O_2 in THF-d_8

In the glovebox, 280μL of 138mM solution in THF-d_8 was added to J. Young tube and diluted with THF-d_8 to 22mM. The sample was analyzed over the course of 14hrs at 20˚C. Spectra were taken every 21.7 minutes; taking 8 scans with a relaxation delay of 30sec.

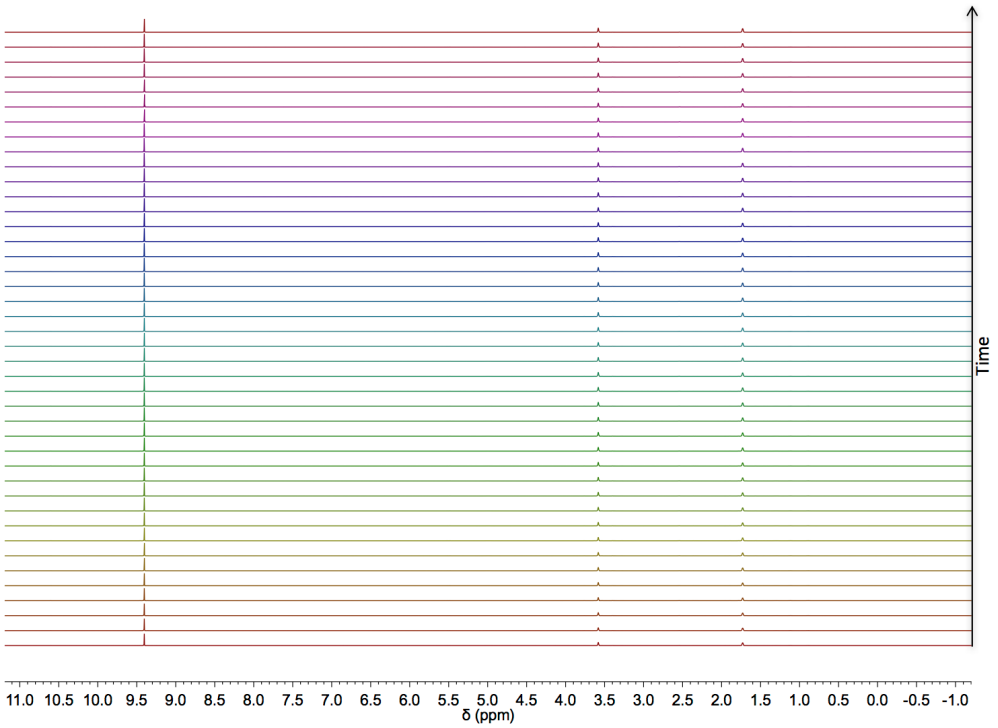

Figure 2-8. ^{1}H-NMR of H_2O_2 decay in THF-d_8.

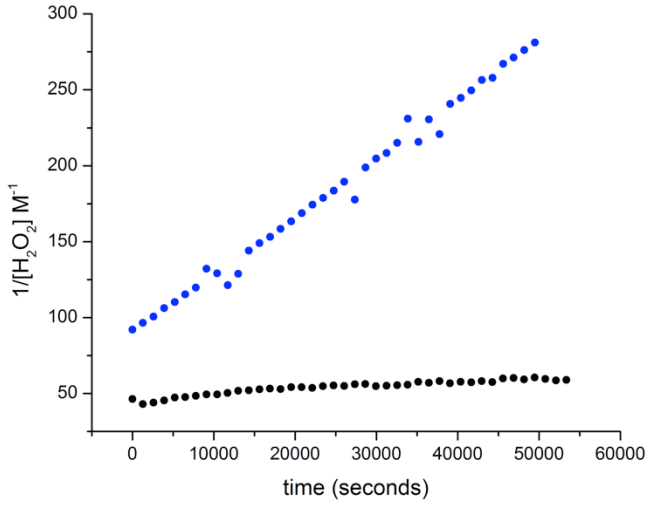

*Figure 2-9. Second-order decay of **2-1(H_2O_2)** (blue) with k = 3.8x10^{-3} M^{-1} s^{-1} and H_2O_2 (black) with k = 2.7x10^{-4} M^{-1} s^{-1}.*

^{1}H-NMR of H_2O_2 with H_3Ts_3tren and $ZnCl_2$ in THF-d_8

In a glovebox, H_3Ts_3tren (14mg) and H_2O_2 (171μL of 138mM solution) was dissolved in THF-d_8. Similarly, $ZnCl_2$ (6.41mg) and H_2O_2 (70μL of 671mM solution) were dissolved in THF-d_8. A ^{1}H-NMR spectrum was collected for each sample to determine the position of the H_2O_2 resonance.

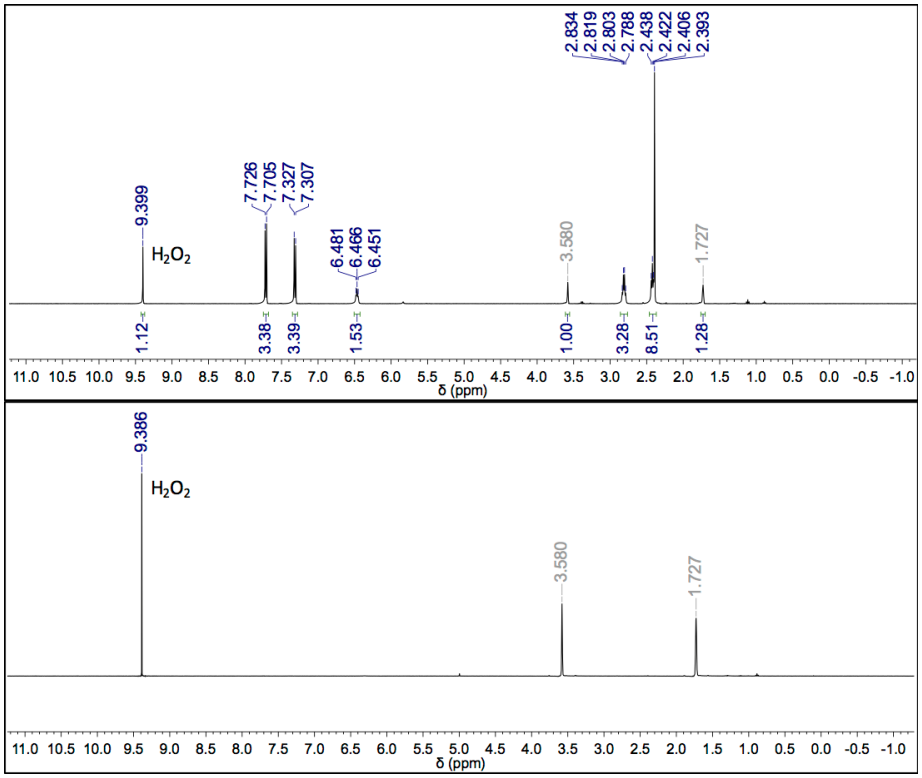

Figure 2-10. ^{1}H-NMR of H_2O_2 with H_3Ts_3tren (above) and $ZnCl_2$ (below), showing negligible shift of H_2O_2 resonance.

Low-temperature investigation of 2-1(H_2O_2) in THF-d_8

In the glovebox, 20.9mg of **2-1** and H_2O_2 (86μL of 266mM solution in THF-d_8) were added to a J. Young NMR tube and diluted with THF-d_8 to 19mM. Spectra were taken at the following temperatures: 293, 253, 243, 233, 223, 213, 208, 203, 198, 193, 188, 183, 178, and 173K. Each spectrum comprised of 8 scans with a relaxation delay of 30sec. Close-up spectra of upfield and downfield regions provided in NMR Spectra section.

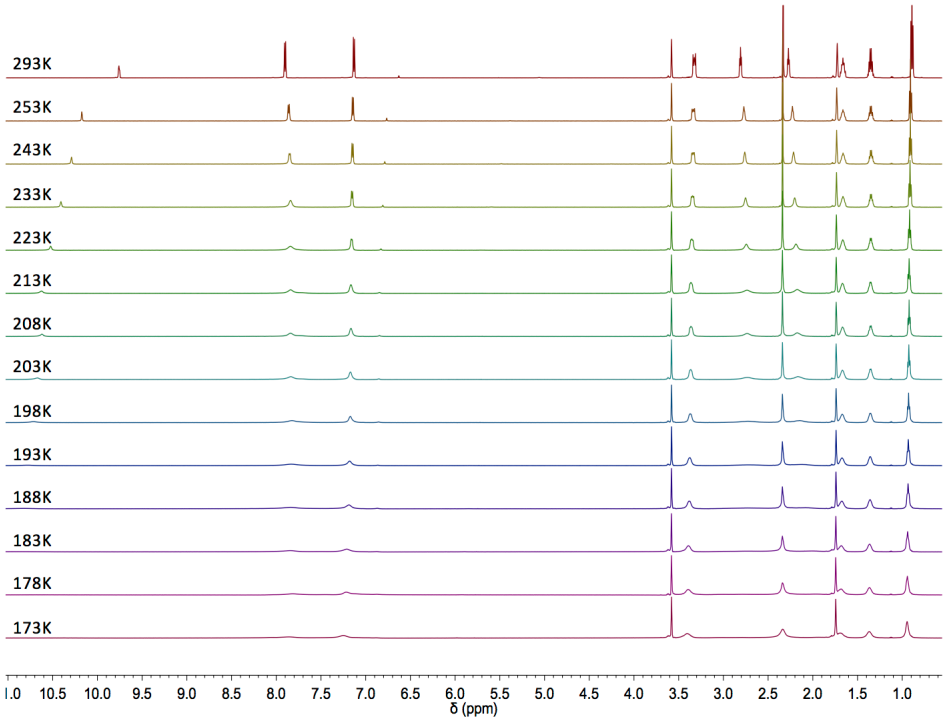

Figure 2-11. Variable Temperature ^{1}H-NMR of ***2-1(H_2O_2)*** *in THF-d_8.*

Low-temperature investigation of H_2O_2 in THF-d_8

In the glovebox, 90μL of 266mM solution of hydrogen peroxide in THF-d_8 was added to a J. Young NMR tube and diluted with THF-d_8 to 46mM. The tube was sealed and the sample placed in the instrument. Spectra were taken at the following temperatures: 293, 223, 213, 203, 193, and 183K. Each spectrum comprised of 8 scans with a relaxation delay of 30sec. Close-up spectra of upfield and downfield regions provided in NMR Spectra section.

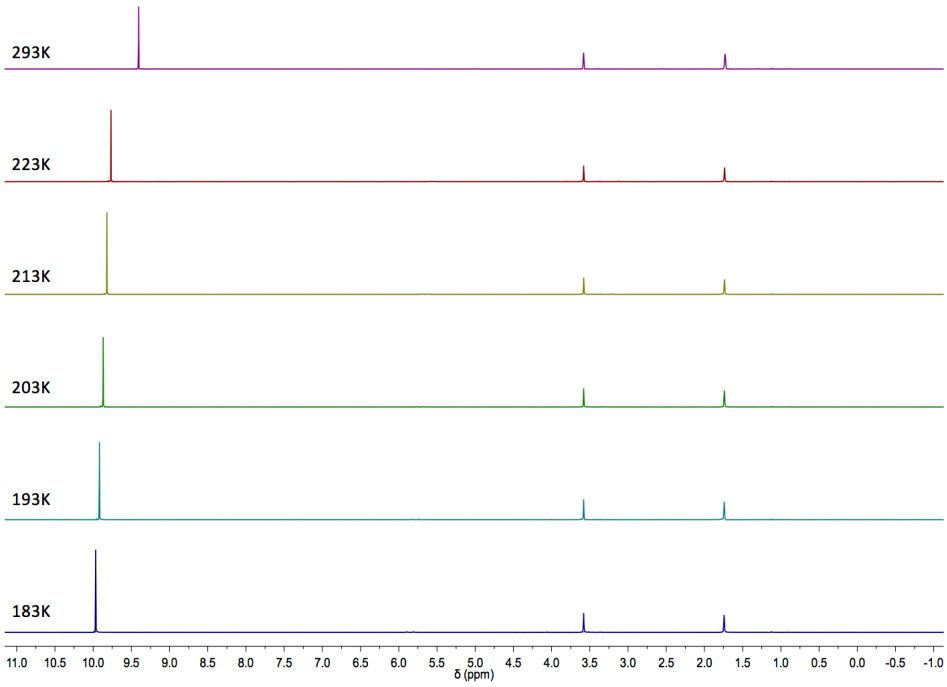

Figure 2-12. Variable Temperature ^{1}H-NMR of H_2O_2 in THF-d_8.

Low-temperature investigation of 2-1(OH_2) and 2-1 in THF-d_8

In the glovebox, a sample of **2-1(OH_2)** was partially dehydrated by heating under vacuum. A portion (18.8mg) of this solid was dissolved in THF-d_8 and placed in a J. Young tube. Room temperature NMR indicated the presence of 30% water bound to Zn. Spectra were taken at the following temperatures: 223, 213, 208, 203, 198, 193, 188, 183, 178, and 173K. Each spectrum comprised of 8 scans with a relaxation delay of 30sec.

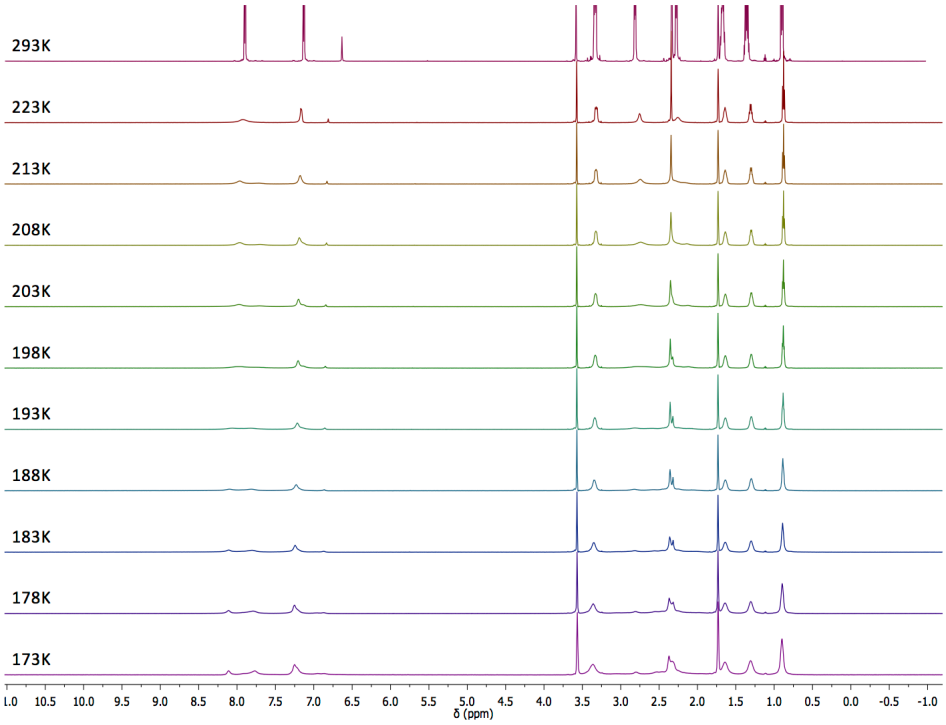

*Figure 2-13. Variable Temperature ^{1}H-NMR of **2-1(OH_2)** in THF-d_8.*

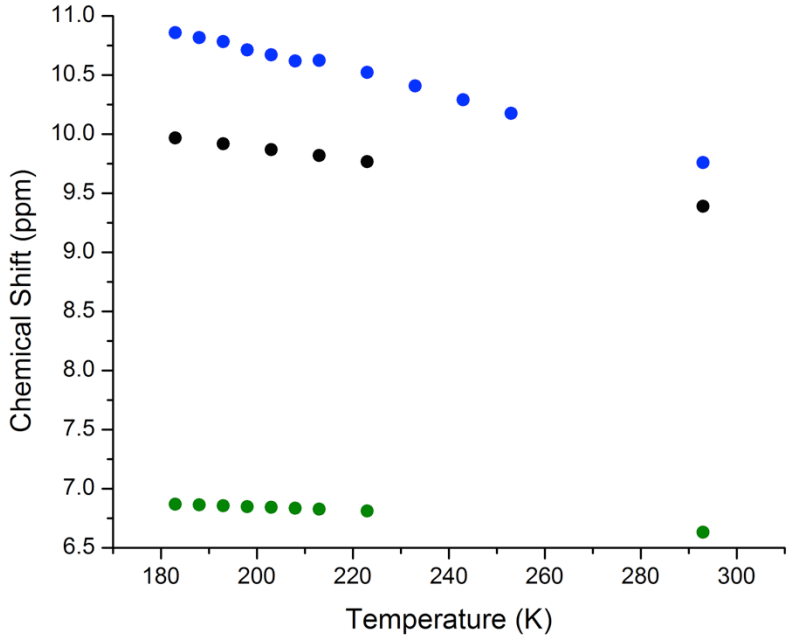

Figure 2-14. Temperature dependence of chemical shift of proton signal for bound peroxide (blue), free peroxide (black), and bound water (green).

Competition of peroxide and water binding to zinc complex

In the glovebox, 23.0mg of **2-1(OH$_2$)** and 1 molar equivalent of hydrogen peroxide (36μL of 700mM solution in THF-d$_8$) was added to a J. Young tube with THF-d$_8$. A spectrum was taken at room temperature (8 scans, relaxation delay = 30s).

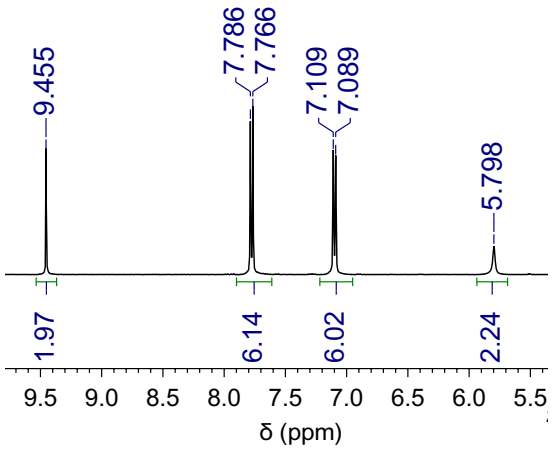

*Figure 2-15. ^{1}H-NMR of **2-1(OH$_2$)** and **2-1(H$_2$O$_2$)** equilibrium measurement in THF-d$_8$.*

2.5.5 Equilibrium Calculation

In the competition spectrum mentioned above, the integration of the sulfonamidate ligand was set to 1 equivalent and the integration and position of both the water signals and the peroxide signals were used with the following equations to calculate K_{eq} for the competitive binding:

$$(I_{Exp})(S_{Exp}) = (I_{Bound})(S_{Bound}) + (I_{Free})(S_{Free})$$

$$(I_{Exp}) = (I_{Bound}) + (I_{Free})$$

where I_{Exp} and S_{Exp} are the integration and chemical shift, respectively, of the ligand (water or peroxide) measured in the competition spectrum, S_{Free} and S_{Bound} are the chemical shifts of the ligand in its free position and when it is bound to the zinc complex, respectively, and I_{Bound} and I_{Free} are the calculated equivalents of ligand bound to the zinc complex and free in solution, respectively. These values are then used in the following equations:

$$K_{eq} = \frac{[I_{BoundPeroxide}][I_{FreeWater}]}{[I_{BoundWater}][I_{FreePeroxide}]}$$

$$\Delta G = -RTlnK_{eq}$$

to obtain the unitless equilibrium constant and free energy difference between peroxide complex and aqua complex. The measured and calculated values are listed in the table below.

*Table 2-2. Calculated values for **2-1(OH_2)** and **2-1(H_2O_2)** equilibrium THF-d_8.*

	H_2O_2	H_2O
S_{Free}	9.404	2.460
S_{Bound}	9.854	6.514
S_{Exp}	9.455	5.798
I_{Exp}	0.985	1.120
I_{Bound}	0.111	0.922
I_{Free}	0.874	0.198
% bound	0.113	0.823
% free	0.887	0.177

2.5.6 Gravimetric Analysis

Data collected on a PerkinElmer STA-6000. Samples were loaded into platinum crucible and analyzed with the following temperature method: hold at 25˚C for 1 minute, heat at 5˚C/min to 250˚C, hold at 250˚C for 1 minute.

Preparation of 2-1(OH_2) samples

Crystalline **2-1(OH_2)** was crushed to a powder and 42mg loaded into the crucible. Additionally, **2-1(OH_2)** was dissolved in THF and then precipitated with pentane. After allowing the white solid to fully precipitate, the supernatant was decanted and the solid was dried briefly under vacuum. A portion of this solid was dissolved in $CDCl_3$ and 1H-NMR was used to determine the amounts of water and solvent in the solid. A crucible was loaded with 30mg of this solid for data collection.

Preparation of 2-1(H_2O_2) sample

In the glovebox, **2-1** was dissolved in THF and 1 molar equivalent of hydrogen peroxide solution in THF was added. Pentane was added to this solution to precipitate white solid. After allowing the white solid to full precipitate, the supernatant was decanted and the solid

was dried briefly under vacuum. A portion of this solid was dissolved in $CDCl_3$ and ^{1}H-NMR was used to determine the relative amounts of water and peroxide in the solid. A crucible was loaded with 23mg of this solid for data collection.

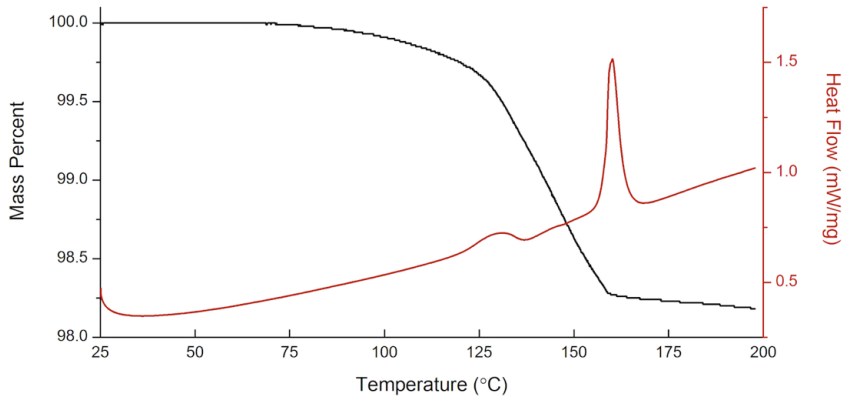

Figure 2-16. TGA (black) and DSC (red) of ***2-1(OH$_2$)*** *crystalline material.*

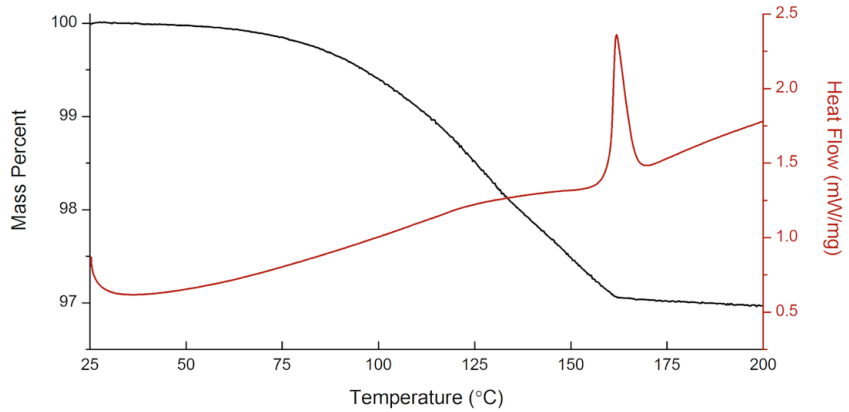

Figure 2-17. TGA (black) and DSC (red) of ***2-1(OH$_2$)*** *precipitated material.*

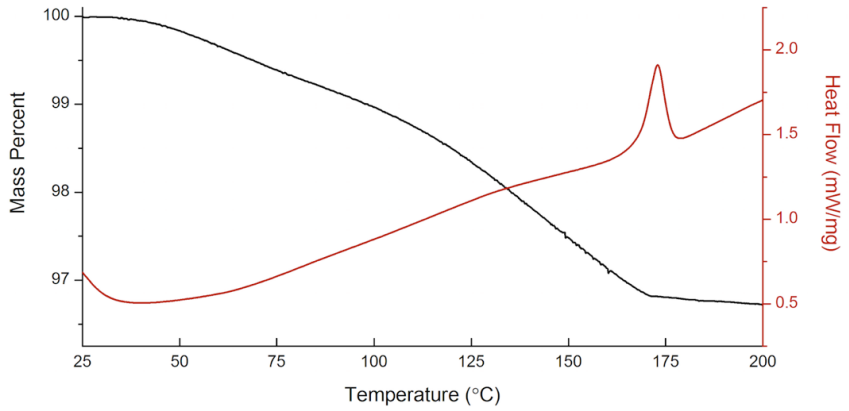

Figure 2-18. TGA (black) and DSC (red) of ***2-1(OH$_2$)*** *and* ***2-1(H$_2$O$_2$)*** *precipitated mixture.*

2.5.7 IR Spectra

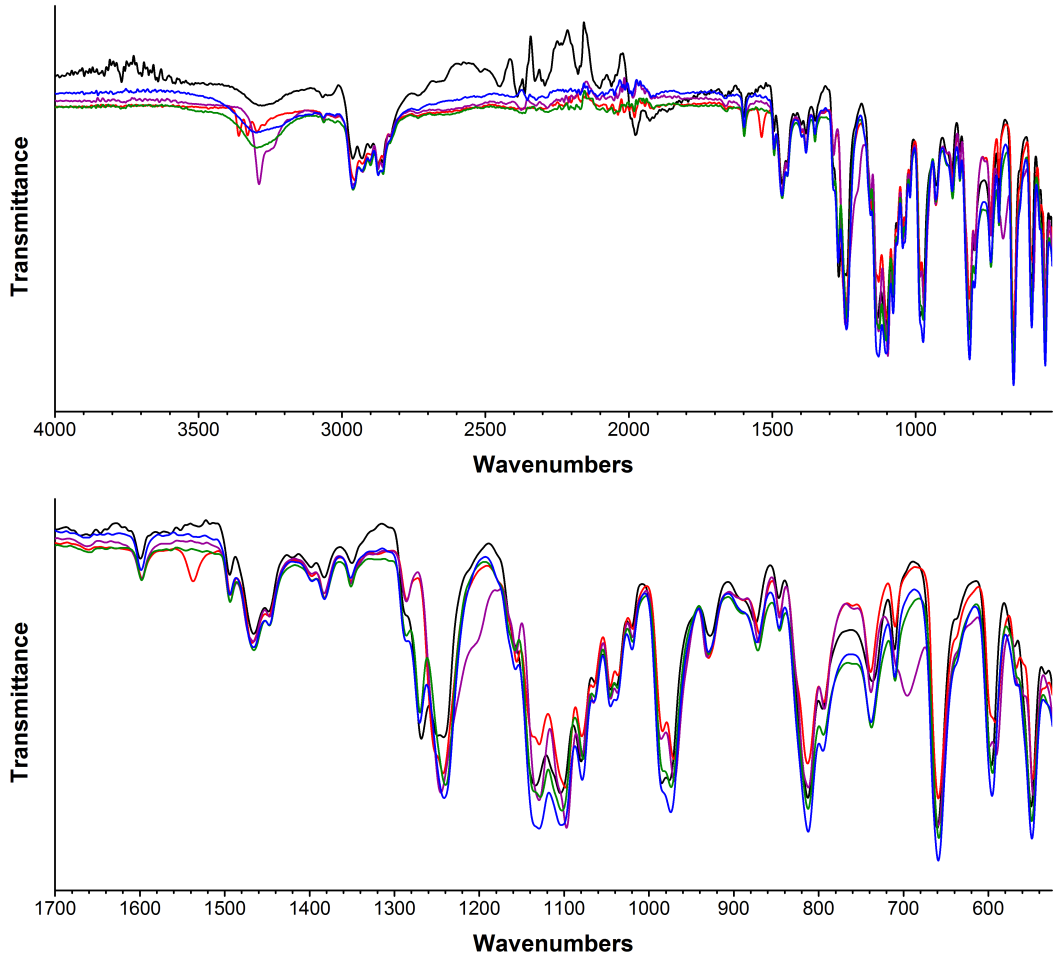

Figure 2-19. IR Spectra of 1 (—), 1-OH_2 (—), 1-H_2O_2/1-OH_2 (—) (mixed solid), 1-N_2H_4 (—), and 1-NH_2OH (—) (top), with an expansion showing the region where O–O, N–O, and N–N stretches should be, if observable (bottom).

2.6 References

1. Jones, C. W., *Applications of of Hydrogen Peroxide and Derivatives*. Royal Society: Cambridge, U.K., 1999.

2. Lancaster, M., *Green Chemistry*. Royal Society: Cambridge, U.K., 2002.

3. Hage, R.; Lienke, A., Applications of Transition-Metal Catalysts to Textile and Wood-Pulp Bleaching. *Angew. Chem. Int. Ed.* **2006,** *45* (2), 206-222.

4. Hage, R.; de Boer, J. W.; Gaulard, F.; Maaijen, K., Chapter Three - Manganese and Iron Bleaching and Oxidation Catalysts. In *Adv. Inorg. Chem.*, Rudi van, E.; Colin, D. H., Eds. Academic Press: 2013; Vol. Volume 65, pp 85-116.

5. Russo, V.; Tesser, R.; Santacesaria, E.; Di Serio, M., Chemical and Technical Aspects of Propene Oxide Production via Hydrogen Peroxide (HPPO Process). *Ind. Eng. Chem. Res.* **2013,** *52* (3), 1168-1178.

6. Mirza, S. A.; Bocquet, B.; Robyr, C.; Thomi, S.; Williams, A. F., Reactivity of the Coordinated Hydroperoxo Ligand. *Inorg. Chem.* **1996,** *35* (5), 1332-1337.

7. Wolak, M.; van Eldik, R., Mechanistic studies on peroxide activation by a water-soluble iron(III)-porphyrin: implications for O-O bond activation in aqueous and nonaqueous solvents. *Chemistry* **2007,** *13* (17), 4873-83.

8. Theodoridis, A.; Maigut, J.; Puchta, R.; Kudrik, E. V.; van Eldik, R., Novel Iron(III) Porphyrazine Complex. Complex Speciation and Reactions with NO and H2O2. *Inorg. Chem.* **2008,** *47* (8), 2994-3013.

9. Afanasiev, P.; Kudrik, E. V.; Millet, J.-M. M.; Bouchu, D.; Sorokin, A. B., High-valent diiron species generated from N-bridged diiron phthalocyanine and H2O2. *Dalton Trans.* **2011,** *40* (3), 701-710.

10. Coon, M. J., Cytochrome P450: nature's most versatile biological catalyst. *Annu Rev Pharmacol Toxicol* **2005,** *45* (1), 1-25.

11. Denisov, I. G.; Makris, T. M.; Sligar, S. G.; Schlichting, I., Structure and Chemistry of Cytochrome P450. *Chem. Rev.* **2005,** *105* (6), 2253-2278.

12. Shaik, S.; Kumar, D.; de Visser, S. P.; Altun, A.; Thiel, W., Theoretical Perspective on the Structure and Mechanism of Cytochrome P450 Enzymes. *Chem. Rev.* **2005,** *105* (6), 2279-2328.

13. Ortiz de Montellano, P. R., *Cytochrome P450: Structure, Mechanism, and Biochemistry*. Kluwer/Plenum: New York, 2005.

14. DiPasquale, A. G.; Mayer, J. M., Hydrogen Peroxide: A Poor Ligand to Gallium Tetraphenylporphyrin. *J. Am. Chem. Soc.* **2008,** *130* (6), 1812-1813.

15. Lithium oxalate monoperhydrate may contain an interaction between lithium ions and the oxygens of hydrogen peroxide in the solid state: Pedersen, B. F. *Acta Chem. Scand.* **1969**, *23*, 1871-1877.

16. Wang, B.; Li, C.; Dubey, K. D.; Shaik, S., Quantum Mechanical/Molecular Mechanical Calculated Reactivity Networks Reveal How Cytochrome P450cam and Its T252A Mutant Select Their Oxidation Pathways. *J. Am. Chem. Soc.* **2015,** *137* (23), 7379-7390.

17. Kwong, H.-K.; Lo, P.-K.; Lau, K.-C.; Lau, T.-C., Epoxidation of alkenes and oxidation of alcohols with hydrogen peroxide catalyzed by a manganese(v) nitrido complex. *Chem. Commun.* **2011,** *47* (14), 4273-4275.

18. Ma, L.; Pan, Y.; Man, W.-L.; Kwong, H.-K.; Lam, W. W. Y.; Chen, G.; Lau, K.-C.; Lau, T.-C., Highly Efficient Alkane Oxidation Catalyzed by [MnV(N)(CN)4]2–. Evidence for [MnVII(N)(O)(CN)4]2– as an Active Intermediate. *J. Am. Chem. Soc.* **2014,** *136* (21), 7680-7687.

19. Chen, M.; Pan, Y.; Kwong, H.-K.; Zeng, R. J.; Lau, K.-C.; Lau, T.-C., Catalytic oxidation of alkanes by a (salen)osmium(vi) nitrido complex using H2O2 as the terminal oxidant. *Chem. Commun.* **2015,** *51* (71), 13686-13689.

20. MacBeth, C. E.; Golombek, A. P.; Young, V. G.; Yang, C.; Kuczera, K.; Hendrich, M. P.; Borovik, A. S., O2 Activation by Nonheme Iron Complexes: A Monomeric Fe(III)-Oxo Complex Derived From O2. *Science* **2000,** *289* (5481), 938-941.

21. Lucas, R. L.; Zart, M. K.; Murkerjee, J.; Sorrell, T. N.; Powell, D. R.; Borovik, A. S., A Modular Approach toward Regulating the Secondary Coordination Sphere of Metal Ions:

Differential Dioxygen Activation Assisted by Intramolecular Hydrogen Bonds. *J. Am. Chem. Soc.* **2006,** *128* (48), 15476-15489.

22. Wolanov, Y.; Shurki, A.; Prikhodchenko, P. V.; Tripolskaya, T. A.; Novotortsev, V. M.; Pedahzur, R.; Lev, O., Aqueous stability of alumina and silica perhydrate hydrogels: experiments and computations. *Dalton Trans.* **2014,** *43* (44), 16614-16625.

23. Churakov, A. V.; Prikhodchenko, P. V.; Howard, J. A. K.; Lev, O., Glycine and l-serine crystalline perhydrates. *Chem. Commun.* **2009,** (28), 4224-4226.

24. Prikhodchenko, P. V.; Medvedev, A. G.; Tripol'skaya, T. A.; Churakov, A. V.; Wolanov, Y.; Howard, J. A. K.; Lev, O., Crystal structures of natural amino acid perhydrates. *CrystEngComm* **2011,** *13* (7), 2399-2407.

25. Vener, M. V.; Medvedev, A. G.; Churakov, A. V.; Prikhodchenko, P. V.; Tripol'skaya, T. A.; Lev, O., H-Bond Network in Amino Acid Cocrystals with H2O or H2O2. The DFT Study of Serine–H2O and Serine–H2O2. *J. Phys. Chem. A* **2011,** *115* (46), 13657-13663.

26. Park, Y. J.; Ziller, J. W.; Borovik, A. S., The effects of redox-inactive metal ions on the activation of dioxygen: isolation and characterization of a heterobimetallic complex containing a Mn(III)-(mu-OH)-Ca(II) core. *J. Am. Chem. Soc.* **2011,** *133* (24), 9258-61.

27. Lacy, D. C.; Park, Y. J.; Ziller, J. W.; Yano, J.; Borovik, A. S., Assembly and Properties of Heterobimetallic CoII/III/CaII Complexes with Aquo and Hydroxo Ligands. *J. Am. Chem. Soc.* **2012,** *134* (42), 17526-17535.

28. Park, Y. J.; Cook, S. A.; Sickerman, N. S.; Sano, Y.; Ziller, J. W.; Borovik, A. S., Heterobimetallic Complexes with MIII-(μ-OH)-MII Cores (MIII = Fe, Mn, Ga; MII = Ca, Sr, and Ba): Structural, Kinetic, and Redox Properties. *Chem Sci* **2013,** *4* (2), 717-726.

29. Sano, Y.; Weitz, A. C.; Ziller, J. W.; Hendrich, M. P.; Borovik, A. S., Unsymmetrical Bimetallic Complexes with MII–(μ-OH)–MIII Cores (MIIMIII = FeIIFeIII, MnIIFeIII, MnIIMnIII): Structural, Magnetic, and Redox Properties. *Inorg. Chem.* **2013,** *52* (18), 10229-10231.

30. Sickerman, N. S.; Henry, R. M.; Ziller, J. W.; Borovik, A. S., Preparation and structural properties of InIII–OH complexes. *Polyhedron* **2013,** *58*, 65-70.

31. Cook, S. A.; Ziller, J. W.; Borovik, A. S., Iron(II) Complexes Supported by Sulfonamido Tripodal Ligands: Endogenous versus Exogenous Substrate Oxidation. *Inorg. Chem.* **2014,** *53* (20), 11029-11035.

32. Sickerman, N. S.; Peterson, S. M.; Ziller, J. W.; Borovik, A. S., Synthesis, structure and reactivity of FeII/III-NH3 complexes bearing a tripodal sulfonamido ligand. *Chem. Commun.* **2014,** *50* (19), 2515-2517.

33. Lau, N.; Ziller, J. W.; Borovik, A. S., Sulfonamido tripods: Tuning redox potentials via ligand modifications. *Polyhedron* **2015,** *85*, 777-782.

34. Engelhardt, L.; Newman, P.; Raston, C.; White, A., Crystal structure of Hexakis(hydroxylamine-N)nickel(II) sulphate. *Aust. J. Chem.* **1974,** *27* (3), 503-507.

35. Southern, J. S.; Hillhouse, G. L.; Rheingold, A. L., Preparation of a Nitroxyl (HNO) Complex of Rhenium by Selective Oxidation of Coordinated Hydroxylamine. *J. Am. Chem. Soc.* **1997,** *119* (50), 12406-12407.

36. Zheng, H.; Leung, W.-H.; Chim, J. L. C.; Lai, W.; Lam, C.-H.; Williams, I. D.; Wong, W.-T., Heterobimetallic μ-nitrido complexes containing ruthenium(II) dithiocarbamate. *Inorg. Chim. Acta* **2000,** *306* (2), 184-192.

37. Matsukawa, S.; Kuwata, S.; Ishii, Y.; Hidai, M., Coordination behaviour of (diaryl disulfide)-bridged dinuclear thiairidaindan cores: ligand substitution by isocyanides, CO, hydrazines and hydroxylamine, and related reactions. *J. Chem. Soc., Dalton Trans.* **2002,** (13), 2737-2746.

38. Chardon, E.; Dahm, G.; Guichard, G.; Bellemin-Laponnaz, S., Exploring Nitrogen Ligand Diversity in trans-N-Heterocyclic Carbene–Amine Platinum Complexes : Synthesis, Characterization, and Application to Fluorescence. *Chem. Asian J.* **2013,** *8* (6), 1232-1242.

39. Muller, N.; Reiter, R. C., Temperature Dependence of Chemical Shifts of Protons in Hydrogen Bonds. *J. Chem. Phys.* **1965,** *42* (9), 3265-3269.

40. Schaefer, T.; Kotowycz, G., Temperature dependence of chemical shifts of protons in hydrogen bonds. Experimental evidence on an intramolecular hydrogen bond. *Can. J. Chem.* **1968,** *46* (17), 2865-2868.

41. Garcia-Viloca, M.; Gelabert, R.; González-Lafont, À.; Moreno, M.; Lluch, J. M., Temperature Dependence of Proton NMR Chemical Shift As a Criterion To Identify Low-Barrier Hydrogen Bonds. *J. Am. Chem. Soc.* **1998,** *120* (39), 10203-10209.

42. Medvedev, A. G.; Mikhaylov, A. A.; Churakov, A. V.; Vener, M. V.; Tripol'skaya, T. A.; Cohen, S.; Lev, O.; Prikhodchenko, P. V., Potassium, Cesium, and Ammonium Peroxogermanates with Inorganic Hexanuclear Peroxo Bridged Germanium Anion Isolated from Aqueous Solution. *Inorg. Chem.* **2015,** *54* (16), 8058-8065.

43. Motekaitis, R. J.; Martell, A. E.; Murase, I., Cascade halide binding by multiprotonated 7,19,30-trioxa-1,4,10,13,16,22,27,33-octaazabicyclo[11.11.11]pentatriacontane (BISTREN) and copper(II) BISTREN cryptates. *Inorg. Chem.* **1986,** *25* (7), 938-944.

Chapter 3

Hydrogen Peroxide Coordination to Cobalt(II) Facilitated by Second-Sphere Hydrogen Bonding

Adapted from: Wallen, C. M.; Palatinus, L.; Bacsa, J.; Scarborough, C. C., Hydrogen Peroxide Coordination to Cobalt(II) Facilitated by Second-Sphere Hydrogen Bonding. *Angew. Chem. Int. Ed.* **2016,** *55* (39), 11902-11906.

3.1 Abstract

$M(H_2O_2)$ adducts have been postulated as intermediates in biological and industrial processes; however, only one observable $M(H_2O_2)$ adduct has been reported, where M is redox-inactive zinc. In this chapter, direct solution-phase detection of a $M(H_2O_2)$ adduct with a redox-active metal, cobalt(II), is described. This $Co^{II}(H_2O_2)$ compound is made observable by incorporating second-sphere hydrogen-bonding interactions between bound H_2O_2 and the supporting ligand, a trianionic trisulfonamido ligand. Thermodynamics of H_2O_2 binding and decay kinetics of the $Co^{II}(H_2O_2)$ species are described, as well as the reaction of this $Co^{II}(H_2O_2)$ species with Group II cations.

3.2 Introduction

3.2.1 $M(H_2O_2)$ Adducts With Redox-Active Metals

H_2O_2 is an attractive and green industrial oxidant that is readily prepared from H_2 and O_2.[1-2] Applications of H_2O_2 include bleaching of cotton and wood pulp[3-4] and oxygenation of propylene to propylene oxide.[5] Oxidations by H_2O_2 often employ metal catalysts, possibly involving $M(H_2O_2)$ intermediates, as such adducts have been computationally[6-9] and kinetically[10-13] implicated. An $Fe^{III}(H_2O_2)$ species has been proposed in cytochromes P450 as or en route to the ill-defined "second oxidant," the key intermediate in a minor oxidation pathway typically overshadowed by the canonical pathway proceeding through Compound 1.[14-17] A computational study by Shaik[18] predicted that longevity of $Fe^{III}(H_2O_2)$ adducts in cytochromes P450 is increased when hydrogen-bonding interactions are present between bound H_2O_2 and basic moieties in the active-site pocket (**A**, Figure 3-1). In 2015, we reported the first $M(H_2O_2)$ adduct, a Zn^{II} species (**2-1(H_2O_2)**), Figure 3-1) made observable

by incorporating second-sphere hydrogen-bonding interactions between H_2O_2 and a trianionic trisulfonamido ancillary ligand.[19] Given the presence of a redox-active metal in the putative $Fe^{III}(H_2O_2)$ species in cytochromes P450, we became interested in studying the viability of coordination of H_2O_2 to redox-active metals. Herein, we detail the first observable $M(H_2O_2)$ adduct bearing a redox-active metal.

The rate of H_2O_2 disproportionation into O_2 and H_2O is accelerated by the presence of redox-active metals,[1] so we anticipated that analogs of **2-1(H_2O_2)** incorporating redox-active metals would be shorter lived. We chose to explore a Co^{II} analog of **2-1(H_2O_2)**, as a $Co^{II}(H_2O_2)$ species (**B**, Figure 3-1) had recently been computationally implicated as reactive for oxidation of hydroquinone to benzoquinone.[9] As described below, our observed $Co^{II}(H_2O_2)$ species is shorter lived than **2-1(H_2O_2)**, but its accessibility corroborates the existence of $M(H_2O_2)$ adducts with redox-active metals and provides a platform for developing catalysts for oxidation reactions with H_2O_2.

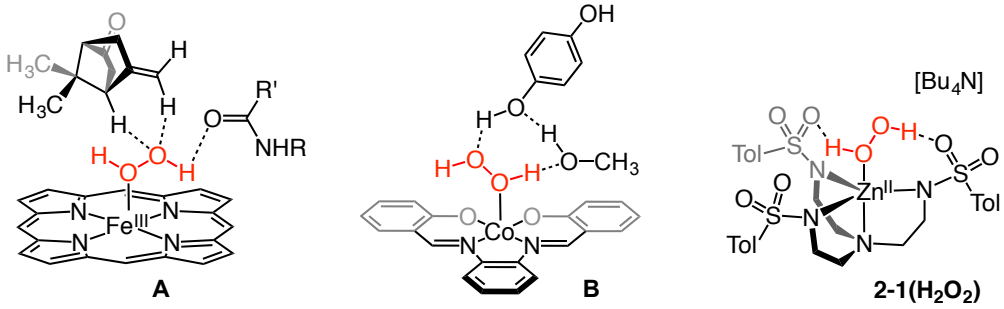

Figure 3-1. Computed structure[18] demonstrating the importance of hydrogen bonding in an $Fe^{III}(H_2O_2)$ species in cytochromes P450 (A); a calculated $Co(H_2O_2)$ intermediate in aerobic hydroquinone oxidation (B);[9] and the first H_2O_2 coordination compound (C).[19]

3.3 Results and Discussion

3.3.1 Synthesis of Cobalt Complexes

Combining H_3Ts_3tren with $Co^{II}Cl_2$ and KH in DMF, followed by addition of $^nBu_4NBr$ and aqueous workup provided $[^nBu_4N][(Ts_3tren)Co^{II}(OH_2)]$ (**3-1(OH$_2$)**in 77% crystalline yield (Scheme 3-1). The H_2O ligand in **3-1(OH$_2$)** is readily displaced by NH_2OH, N_2H_4, or NH_3 to afford **3-1(NH$_2$OH), 3-1(N$_2$H$_4$)**, and **3-1(NH$_3$)**. X-ray crystallographic characterization of these species revealed the presence of hydrogen-bonding interactions between the sulfonyl oxygens and the axial-ligand protons (Figure 3-2), including the protons of the distal heteroatom in N_2H_4 and NH_2OH. **3-1** and **3-1(OH$_2$)** are differentiated by electronic absorption spectroscopy; however, **3-1(OH$_2$)** is not distinguishable from its 5-coordinate nitrogenous analogs by this technique except by band intensity, where complexes with axial nitrogen ligands show more intense d-d transitions than **3-1(OH$_2$)** (Figure 3-3).

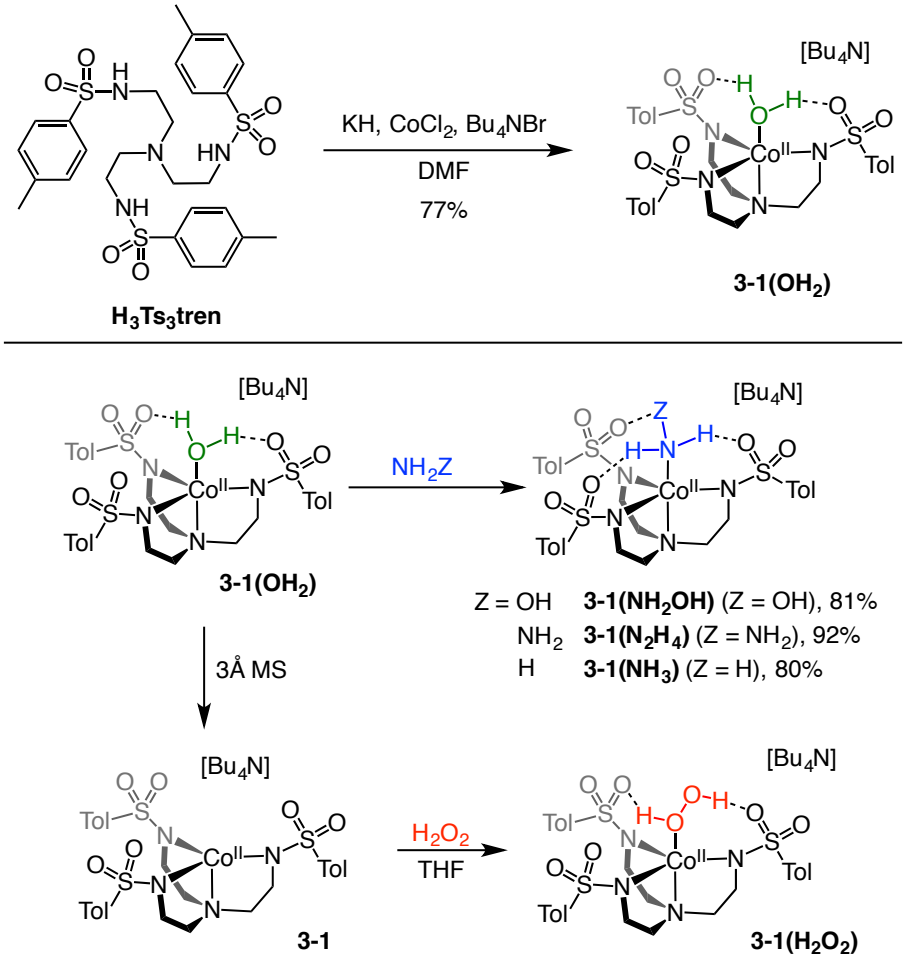

*Scheme 3-1. Synthesis of **3-1** and **3-1(L)**. Yields are of crystalline product.*

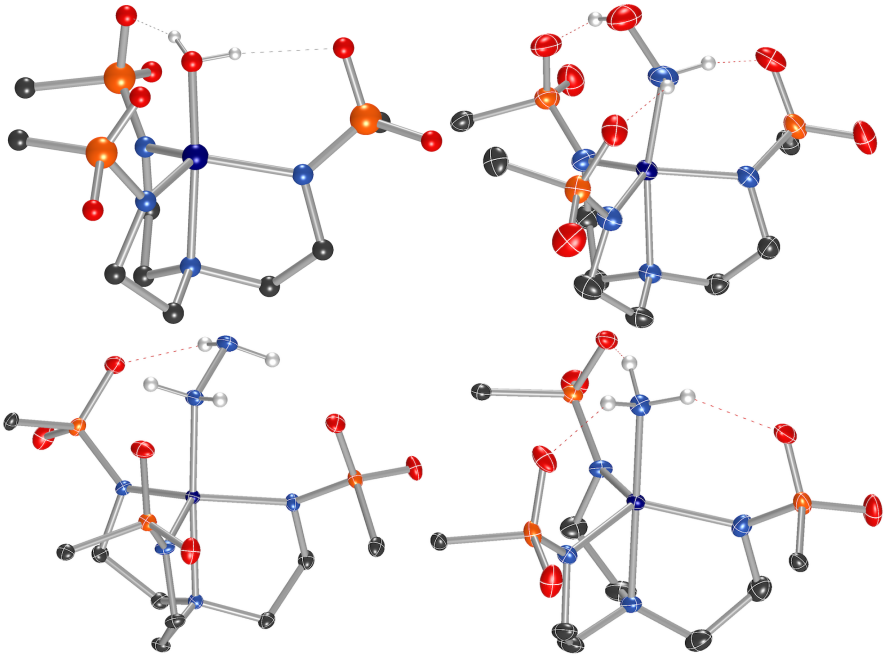

Figure 3-2. X-ray crystal structures of the anions in ***3-1(OH$_2$)*** *(top left),* ***3-1(NH$_2$OH)*** *(top right),* ***3-1(N$_2$H$_4$)*** *(bottom left), and* ***3-1(NH$_3$)*** *(bottom right) demonstrating intramolecular hydrogen bonding with the axial ligand ([^{n}Bu$_4$N]$^+$ ions omitted). Tolyl groups of the trianionic ligand are truncated for clarity. Only hydrogens from the axial ligands are shown.* ***3-1(OH$_2$)****, which is very similar to a complex reported by Borovik[20], is an incommensurately modulated structure and is therefore represented as a ball-and-stick model.*

3.3.2 Spectroscopic Observation of a Co(H$_2$O$_2$) Adduct

Previously, we reported a method for accessing anhydrous H_2O_2 in THF.[19] Although we have not encountered problems with such solutions, they should be handled with care, as formation of radicals and/or organic peroxides is possible, particularly upon heating or irradiation. Addition of anhydrous H_2O_2 in THF to **3-1(OH$_2$)** did not result in any notable changes in the electronic absorption spectrum, and addition of H_2O_2 to **3-1** provided an absorption spectrum of a five-coordinate Co^{II} species that was indistinguishable from **3-1(OH$_2$)** (Figure 3-3). Despite the redox potential of **3-1(OH$_2$)** (+78 mV vs. Fc/Fc$^+$ in

CH_2Cl_2, Section 3.5.7) no cobalt oxidation products were spectroscopically observable on addition of H_2O_2 to **3-1** or **3-1(OH$_2$)**.[21] Generation of 5-coordinate Co^{II} on addition of H_2O_2 to **3-1** is consistent either with formation of **3-1(H_2O_2)** or formation of **3-1(OH$_2$)** following immediate H_2O_2 disproportionation by Co^{II}. Distinguishing between these possibilities required a method of directly detecting H_2O_2 in these **3-1**/H_2O_2 solutions. Despite the paramagnetic nature of the complexes studied, ^{1}H NMR spectroscopy proved a viable technique for studying coordination of H_2O_2 to **3-1** (Figure 3-4).

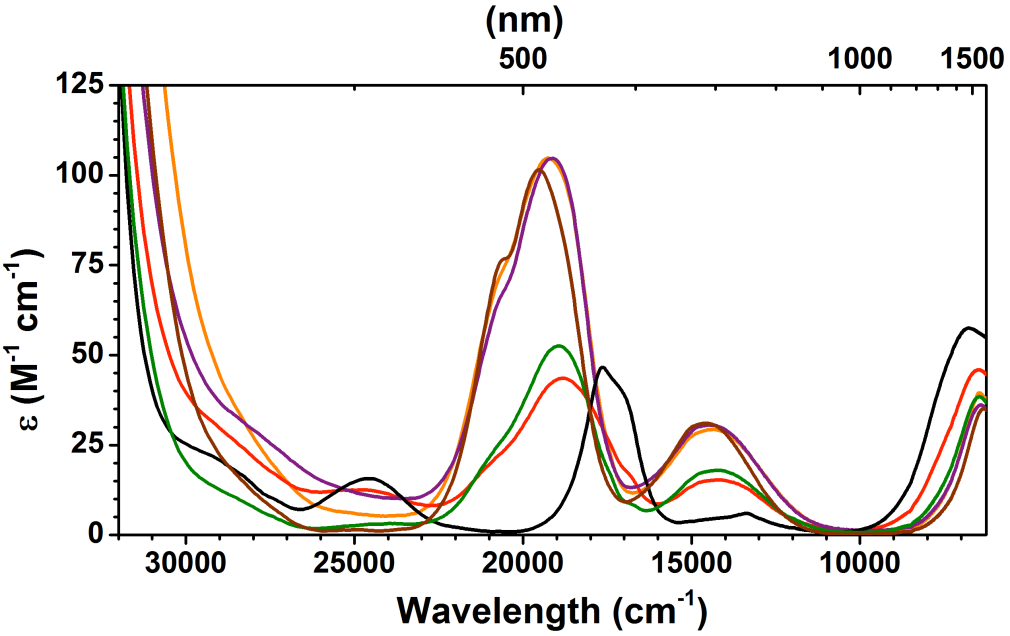

Figure 3-3. Electronic absorption spectra in THF: ***3-1*** *(–),* ***3-1(OH$_2$)*** *(–),* ***3-1(H_2O_2)*** *(–),* ***3-1(NH_3)*** *(–),* ***3-1(N_2H_4)*** *(–), and* ***3-1(NH_2OH)*** *(–).*

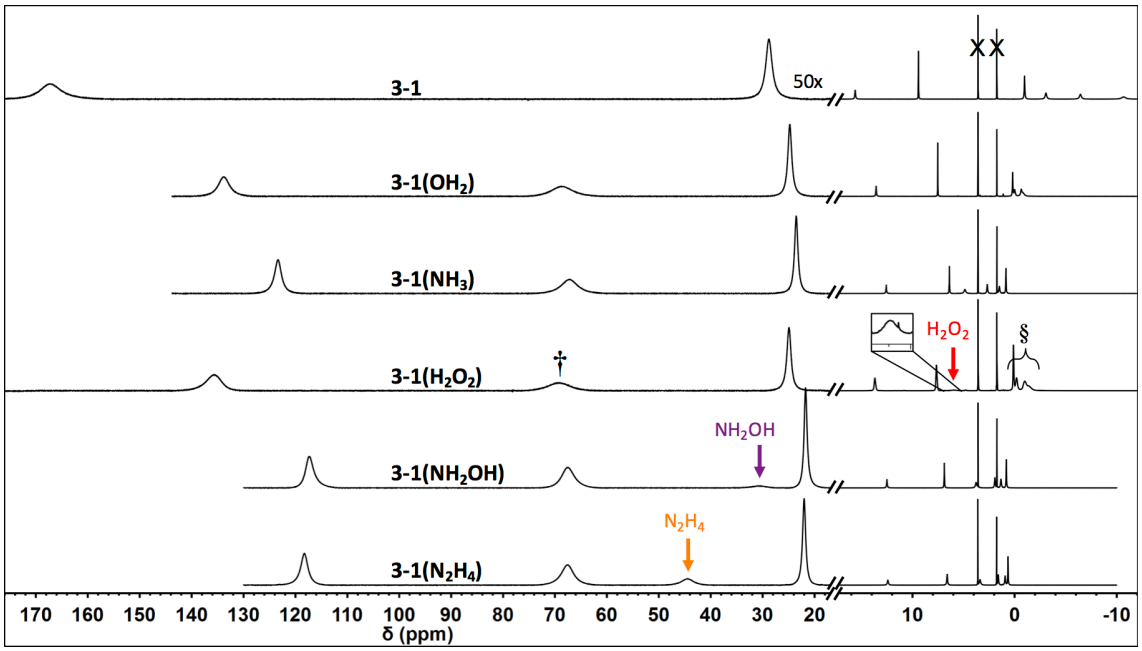

Figure 3-4. ^{1}H-NMR spectra (THF-d_8) of cobalt complexes scaled to show resonances for visible axial ligands (N_2H_4, NH_2OH, and H_2O_2), the presence of alkyl bridge signal in 5-coordinate complexes (†), and positions of [^{n}Bu$_4$N]$^+$ resonances (§), which are dependent on the number of second-sphere hydrogen bonds (O···H = 0, 2, 3). Residual THF-d_8 signals indicated by X.

^{1}H NMR resonances associated with **3-1(L)** were assigned by comparing spectra of related complexes, including [^{tBu}ArPPh$_3$][(Ts$_3$tren)Co^{II}] (**3-1^P**) a complex analogous to **3-1**, containing an asymmetrically substituted aryl phosphonium counterion, [^{tBu}ArPPh$_3$]$^+$ in place of the [^{n}Bu$_4$N]$^+$ ion (Section 3.3.4). All 5-coordinate **3-1(L)** species show a –CH$_2$– resonance near 65 ppm, and the presence of this signal in a solution containing H_2O_2 and **3-1** (†, Figure 3-4) corroborates the electronic absorption data (Figure 3-3) revealing a 5-coordinate Co^{II} ion. The positions of the [^{n}Bu$_4$N]$^+$ proton resonances are affected by the presence of axial ligands on cobalt. In the ^{1}H NMR spectrum of **3-1**, the [^{n}Bu$_4$N]$^+$ signals are spaced between 1 and –11 ppm, where the large paramagnetic shifting is consistent with interaction between this cation and the cobalt complex in solution, likely through

hydrogen bonding between the alpha-hydrogens on $[^{n}Bu_4N]^+$ and the sulfonyl oxygens as seen in the solid state. For derivatives of **3-1(L)** with three second-sphere hydrogen bonds (**3-1(NH$_2$OH)**, **3-1(NH$_3$)**, and **3-1(N$_2$H$_4$)**) the $[^{n}Bu_4N]^+$ signals are less paramagnetically shifted (0 to 5 ppm), consistent with axial coordination disrupting hydrogen bonding between the ions in solution. For **3-1(OH$_2$)**, which only contains two second-sphere hydrogen bonds, the $[^{n}Bu_4N]^+$ resonances overlap between 1 and –1 ppm. When anhydrous H_2O_2 is combined with **3-1**, the $[^{n}Bu_4N]^+$ proton resonances appear between 1 and –2 ppm, similar to **3-1(OH$_2$)** (§, Figure 3-4). These data suggest that the axial ligand in a solution of **3-1** and anhydrous H_2O_2 is diprotic, which could be explained by binding of H_2O or H_2O_2. For complexes **3-1(OH$_2$)** and **3-1(NH$_3$)**, the proton resonances corresponding to the axial ligand are not observable by ^{1}H NMR spectroscopy, even upon addition of excess ligand (Figure 3-10). However, ^{1}H NMR spectra of **3-1(N$_2$H$_4$)** and **3-1(NH$_2$OH)** show signals at 44 ppm and 30 ppm, respectively, corresponding to the axial-ligand protons (Figure 3-4). The spectrum of a solution of **3-1** and anhydrous H_2O_2 contains a broad signal at 5.9 ppm (Figure 3-4). Over time, this signal shifts to 8.8 ppm (closer to free H_2O_2 at 9.4 ppm) and decreases in intensity following a first-order pathway with a half-life of 353 ± 33 seconds (Figure 3-5). This shifted H_2O_2 resonance is the first direct evidence that H_2O_2 is binding to Co^{II} in **3-1**, as the ^{1}H NMR and electronic spectra demonstrate that Co^{II} is five-coordinate under these conditions. The decay product of **3-1(H$_2$O$_2$)** was identified as **3-1(OH$_2$)** by crystallization of the bulk material. The shifting H_2O_2 resonance throughout decay of **3-1(H$_2$O$_2$)** points to an equilibrium between free and bound H_2O_2 that is perturbed by H_2O formed upon H_2O_2 disproportionation, leading us to examine the equilibrium constants of binding H_2O_2 and H_2O to **3-1**.

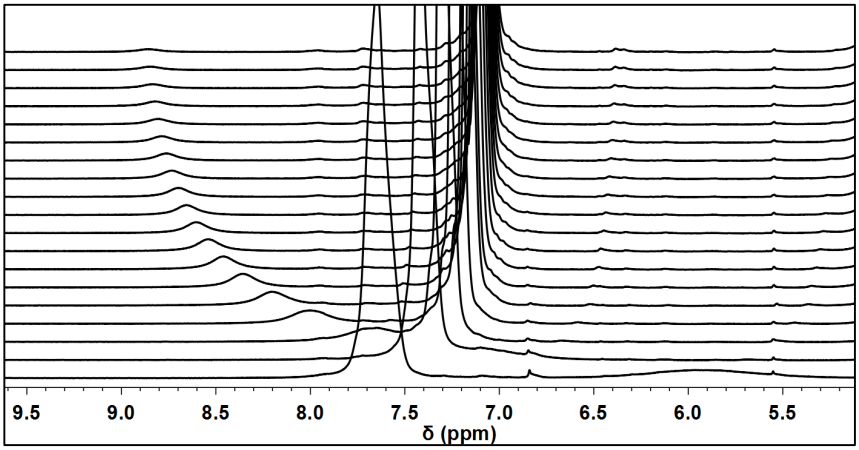

Figure 3-5. Room-temperature decay of ***3-1(H$_2$O$_2$)*** *measured by ^{1}H NMR spectroscopy (THF-d_8). The H_2O_2 resonance shifts from 5.9 ppm to 8.8 ppm. The decay product was confirmed by X-ray crystallography to be* ***3-1(OH$_2$)****. The tall signal at 7.7 ppm shifting to 7.1 ppm is a methyl group on the sulfonamidate ligand.*

To probe whether H_2O_2 binding is perturbed by the presence of H_2O, H_2O_2 was added to **3-1(OH$_2$)** and its decay monitored by ^{1}H NMR spectroscopy. Initially, the H_2O_2 resonance appears at 8.8 ppm (c.f. 5.9 ppm in the absence of H_2O) and then shifts toward 9.1 ppm ($t_{½}$ = 1190 ± 10 s). When H_2O_2 is added to **3-1(NH$_3$)**, the H_2O_2 resonance remains at 9.5 ppm and decays with a half-life of 13700 ± 200 s. These data are consistent with H_2O_2 disproportionation occurring upon coordination to **3-1**, and with H_2O_2 being a weaker ligand for **3-1** than H_2O or NH_3, consistent with descriptions of H_2O_2 as a very poor ligand.[22-24] The first-order decay of **3-1(H$_2$O$_2$)** contrasts the second-order decay mechanism of **2-1(H$_2$O$_2$)**, which bears the same ligand and counterion, and at the same starting concentration has a half-life of 10^4 s.[19] This comparison suggests that the redox-active nature of M has a dramatic effect on the stability of M(H_2O_2) species.

3.3.3 Binding Constants Measured by Photometric Titrations

We sought to quantify binding affinities of **3-1** for H_2O and H_2O_2. H_2O_2 has been described as a poor ligand[22-26] such that its coordination to metals was not unambiguously detected until 2015.[19] Prikhodchenko demonstrated that H_2O_2 is a more effective hydrogen-bond donor than H_2O, clarifying the importance of second-sphere hydrogen bonding in H_2O_2 coordination.[26-29] Owing to the short lifetime of **3-1(H_2O_2)**, we turned to photometric titrations using electronic absorption spectroscopy to determine the binding constants for H_2O and H_2O_2 to **3-1** at –70 ºC, as **3-1(H_2O_2)** does not detectably decay within one hour at temperatures below –40 ºC by NMR spectroscopy. Titration of **3-1** with H_2O or anhydrous H_2O_2 in THF at –70 ºC afforded the curves shown in Figure 3-6, from which K_{eq} values for coordination of H_2O_2 and H_2O to **3-1** are derived: 31.3 ± 0.2 M^{-1} and 31,600 ± 12,600 M^{-1} at –70 ºC, respectively. These data also establish a preference for binding of **3-1** to H_2O over H_2O_2, where K_{eq} for displacing H_2O_2 in **3-1(H_2O_2)** by H_2O at –70˚C is 1010 ± 400 (ΔG = –2.8 kcal/mol). To our knowledge, this is the first H_2O_2/metal binding constant measured.

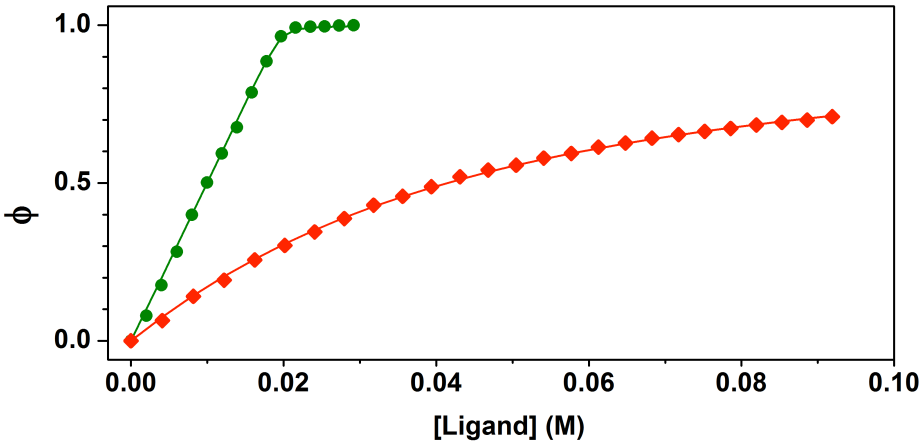

*Figure 3-6 Photometric titrations of **3-1** with H_2O (•) and H_2O_2 (◆) in THF at –70 °C. Data are plotted as fractional saturation vs. concentration of ligand (H_2O or H_2O_2). The curves, which are non-linear fits to the data, enable calculation of K_{eq} (3.16 ± 1.26 × 10^4 M^{-1} for H_2O and 31.3 ± 0.2 M^{-1} for H_2O_2).*

3.3.4 Reactivity with Group II Metals

Finally, we probed the reactivity of **3-1(H_2O_2)**. Borovik reported that a species closely related to **3-1** is inert to PhIO, but upon addition of Group II ions, oxidation of the Co^{II} center by PhIO affords an isolable $Co^{III}(\mu\text{-OH})Ca^{2+}$ species.[20] This transformation may involve a transient Co^{IV} intermediate, as redox-inert cations are known to facilitate two-electron oxidation of Co^{II} to Co^{IV}.[30-31] We probed whether Group II ions could similarly promote cobalt oxidation and H_2O_2 O–O cleavage in **3-1(H_2O_2)**. Addition of $M(OTf)_2$ (M = Ca^{2+}, Sr^{2+} or Ba^{2+}) to **3-1(H_2O_2)** resulted in rapid conversion to intensely green products, each with nearly identical electronic absorption spectra. The spectroscopic properties of these green species did not satisfactorily agree with Borovik's report of a red-brown $Co^{III}(\mu\text{-OH})Ca^{2+}$ species;[20] however, combination of (15-crown-5)$Ca(OTf)_2$ and **3-1(H_2O_2)** afforded X–ray-quality crystals of a $Co^{III}(\mu\text{-OH})Ca^{2+}$ complex (**3-2**, Scheme 3-2, Figure 3-7), demonstrating Group II ion-induced oxidation of Co^{II} to Co^{III} by H_2O_2. The oxidation

potential of **3-1(OH$_2$)** is +78 mV vs. Fc/Fc$^+$ in CH_2Cl_2 (Section 3.3.7), so the oxidative stability of the Co^{II} ion in **3-1(H$_2$O$_2$)** suggests that one-electron redox processes involving **3-1(H$_2$O$_2$)** are not preferred. We expect that the Group II ions are brought into close proximity with coordinated H_2O_2 in **3-1(H$_2$O$_2$)**, as we and Borovik[20, 32] have shown that such sulfonyl oxygens bind Group II metal ions without significantly impacting the electronic properties of Co^{II}. We hypothesize that the Group II ion-induced oxidative conversion of **3-1(H$_2$O$_2$)** to **3-2** may involve a transient Co^{IV}(oxo)/Ca^{2+}(OH$_2$), Co^{IV}(OH)/Ca^{2+}(OH), or Co^{III}–(OH)---(•OH) species that rapidly reacts with a hydrogen-atom donor, likely THF, to afford the observed Co^{III} species **3-2**. Rapid decomposition of Co^{IV} has been demonstrated in the instability of related Co^{IV}(oxo)[20, 30-31] and Co^{IV}(nitrido)[33] species. Regardless of mechanism, the Group II ion-induced conversion of **3-1(H$_2$O$_2$)** into **3-2** provides a new approach to H_2O_2 activation involving coordination to one metal and activation by a second metal. We are currently exploring this dual-activation pathway of H_2O_2 for use in oxidation catalysis.

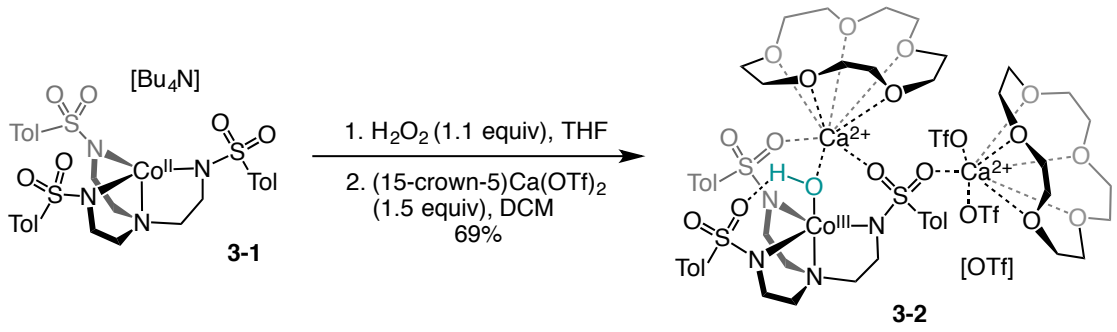

*Scheme 3-2. Reaction of **3-1(H$_2$O$_2$)** with Ca^{2+} to form **3-2**. Yield of cyrstalline product, based on limiting Ca^{2+}.*

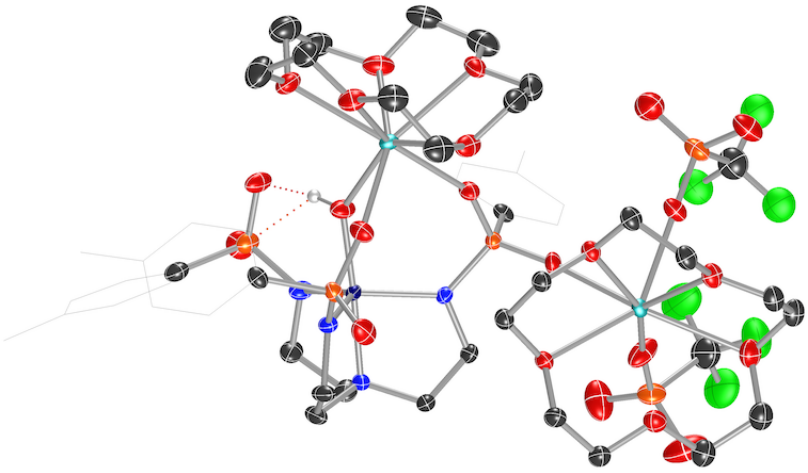

Figure 3-7. The crystal structure of ***3-2****. Hydrogen atoms not on axial ligand have been omitted. Lattice THF molecule and unbound triflate counterion have been removed, and sulfonamidate ligand arms truncated for clarity.*

3.4 Conclusions

In summary, we have obtained the first direct evidence for formation of a $M(H_2O_2)$ complex with a redox-active metal. Mixing **3-1** and anhydrous H_2O_2 results in coordination of an axial ligand to cobalt(II) at temperatures where H_2O_2 is not disproportionated by **3-2**, and low-temperature photometric titration of **3-1** with H_2O_2 or H_2O, as well as decay kinetics of **3-1(H_2O_2)** in the presence of H_2O, reveal that H_2O_2 is a weaker ligand for the Co^{II} center in **3-1** than H_2O. **3-1(H_2O_2)** is stable to oxidation of the Co^{II} center, but addition of (15-crown-5)$Ca(OTf)_2$ induces oxidation to afford the $Co^{III}(\mu\text{-OH})Ca^{2+}$ complex **3-2**. Activation of coordinated H_2O_2 by a secondary metal is a novel approach to developing oxidation reactions with H_2O_2, and our efforts on expanding the coordination chemistry of H_2O_2 and exploiting the reactivity of $M(H_2O_2)$ adducts are on-going.

3.5 Experimental

3.5.1 Materials and Methods

Elemental analyses were performed by Atlantic Microlabs in Norcross, GA. IR spectra were obtained using a Nicolet 380 FT-IR with Smart Orbit Diamond ATR attachment. Mass spectrometric analysis was collected at the Emory University Mass Spectrometry Center using electrospray ionization on a Thermo Finnigan LTQ-FTMS instrument. Crystal diffraction data collected by Emory University Department of Chemistry X-Ray Crystallography Center. NMR data collected on a 400MHz or 500MHz instrument and referenced to residual solvent peaks or external standard (Ph_3PO for ^{31}P). Magnetic susceptibility was measured with Evan's method on a 500MHz NMR spectrometer. All reactions sensitive to air and/or moisture were carried out in an MBraun UNIlab glovebox under a nitrogen atmosphere. Solvents for use in the glovebox were degassed by evacuation and purging with nitrogen (three or more cycles) and dried using 3Å molecular sieves. Anhydrous THF (HPLC grade, inhibitor-free) was degassed, brought into the glovebox, and stored over molecular sieves for at least two days before filtering through activated alumina. Reagents were purchased from Sigma-Aldrich, Oakwood Chemicals, or Strem Chemicals and used without further purification. Preparation of 15-crown-5•$Ca(OTf)_2$ adduct,[34] 15-crown-5•$Sr(OTf)_2$ adduct,[35] and anhydrous solutions of H_2O_2/THF have been previously reported (section 2.3.3). A more accurate quantification of H_2O_2 in H_2O_2/THF solutions is described below.

3.5.2 Quantification of hydrogen peroxide in THF

A 2% titanium(IV) oxysulfate solution was prepared by dissolving 12.5g of $TiOSO_4$ in 500mL of 2M H_2SO_4. A solution of 30% H_2O_2 was diluted to ~1M H_2O_2 with water. Three aliquots were taken from this stock solution and diluted tenfold. The absorbance at 240nm was measured for each aliquot to obtain the concentration of hydrogen peroxide ($\varepsilon_{240} = 43.6$ M^{-1} cm^{-1}). This stock solution and the titanium oxysulfate solutions was used to make six solutions in 250mL volumetric flasks containing 20mL titanium oxysulfate solution, 300μL of THF, and various concentrations of hydrogen peroxide (50mM - 1M). The absorbance at 407nm was measured (pertitanic acid) and a standard curve was generated. To determine the concentration of hydrogen peroxide in THF solutions, three 300μL aliquots of THF solution were each added to a 250mL volumetric flask with 20mL titanium oxysulfate solution and diluted with water. The absorbance values at 407nm were averaged and used to calculate concentration of hydrogen peroxide. For solutions in the 1-3M H_2O_2 window, only 100μL of the H_2O_2/THF solution was used instead of 300μL.

3.5.3 Syntheses

[^{n}Bu$_4$N][(Ts$_3$tren)Co^{II}(OH$_2$)] {3-1(OH$_2$)}

In a two-neck flask, H_3Ts_3tren (8.56g, 14.1mmol) and $CoCl_2$ (1.83g, 14.1mmol) were stirred in 40 mL DMA under nitrogen. KH (1.75g, 43.6mmol) was added in portions carefully, which causes the solution to change from blue to purple. After stirring overnight, Bu_4NBr (4.53g, 14.1mmol) was added with a few drops of methanol to quench any residual hydride base. The reaction mixture was diluted with CH_2Cl_2 (200 mL) and washed with water (3×200 mL) and brine (200 mL). The organic layer was dried with Na_2SO_4, filtered and concentrated under rotary evaporation. Addition of diethyl ether afforded purple

crystals product (9.99g, 77% yield). Anal. calcd (found) for ($C_{43}H_{71}CoN_5O_7S_3$) C, 55.82 (55.88); H, 7.74 (7.67); N, 7.57 (7.50). UV-Vis (TFE, ε in $M^{-1}cm^{-1}$): 222 (7,220), 528 (44) and 1571 (36). IR (FT-ATR, cm^{-1}): 3293 (ν_{OH}), 3058, 2959, 2894, 2854, 1586, 1483, 1465, 1442, 1367, 1350, 1290, 1275, 1240, 1129, 1105, 1080, 1042, 1019, 970, 932, 871, 813, 753, 727, 709, 692, 663, 598, 569, 548, 530. ESMS: Exact mass calcd for $C_{27}H_{33}CoN_4O_6S_3^-$ [ML^-], 664.08997. Found: 664.08929 (Δ = 1.0 ppm). Magnetic susceptibility (Evan's method, $CDCl_3$): $\mu_{obs} = 3.46\ \mu_B$.

[^{n}Bu$_4$N][(Ts$_3$tren)Co^{II})] {3-1}

In a glovebox, **3-1(OH$_2$)** was dissolved in dichloromethane with 3Å molecular sieves. After sitting overnight the solution was filtered through celite and layered under ether. Blue crystals were formed which were suitable for analysis by X-ray crystallography. UV-Vis (CH_2Cl_2, ε in $M^{-1}cm^{-1}$): 248sh (14,100), 270sh (11,800), 408 (17), 567 (51), 746 (7) and 1483 (59). Magnetic susceptibility (Evan's method, $CDCl_3$): $\mu_{obs} = 4.29\ \mu_B$.

[^{n}Bu$_4$N][(Ts$_3$tren)Co^{II}(N$_2$H$_4$)] {3-1(N$_2$H$_4$)}

Hydrazine solution (563μL, 1.0M in THF, 0.56mmol) was added to [^{n}Bu$_4$N][(Ts$_3$tren)Co^{II}(OH$_2$)] (**3-1(OH$_2$)**) (104mg, 0.11mmol) and mixed until dissolved. Vapor diffusion of diethyl ether into this solution produced purple crystals suitable for XRD (97 mg, 92% yield). ^{1}H NMR (500 MHz, THF-d_8) δ 122 – 115 (bs, 6H, NCH_2), 72 – 64 (bs, 6H, NCH_2), 48 – 41 (bs, 2H, NH_2), 23 – 21 (bs, 6H, Ar-H), 12.4 (s, 6H, Ar-H), 6.6 (s, 9H, Ar-CH_3), 3.4 (s, 8H, Bu_4N^+), 1.6 (s, 8H, Bu_4N^+), 0.9 (s, 8H, Bu_4N^+), 0.7 (s, 12H, Bu_4N^+). Anal. calcd (found) for ($C_{43}H_{73}CoN_7O_6S_3$): C, 54.99 (55.09); H, 7.83 (7.79); N, 10.44 (10.28). UV-Vis (THF, ε in $M^{-1}cm^{-1}$): 519 (105), 697 (29) and 1545 (40). IR (FT-ATR, cm^{-1}): 3360 (ν_{NH}), 3332 (ν_{NH}), 2956, 2855, 1598, 1538, 1493, 1468, 1382, 1350,

1246, 1153, 1130, 1094, 1080, 1041, 967, 933, 869, 846, 811, 793, 740, 710, 660, 595, 570, 549. FTMS (NSI): m/z^- = 664.08967, calcd: 664.08997 (ML_1^-), Δ = 0.5 ppm.

[^{n}Bu$_4$N][(Ts$_3$tren)Co^{II}(NH$_2$OH)] {3-1(NH$_2$OH)}

Hydroxylamine solution (15mg, 0.23mmol, 50wt% in H_2O) was diluted with 0.5mL of MeOH, and added to a solution of **3-1(OH$_2$)** (105mg, 0.11mmol) in 0.5mL DCM. This solution was mixed thoroughly and filtered through celite. Vapor diffusion of diethyl ether into this solution yielded a mixture of purple crystals and dark amorphous powder. The mixture was washed repeatedly with ether, each time allowing the crystals to settle before pulling off the supernatant with a pipet. The leftover purple crystals were suitable for XRD (86mg, 81% yield). ^{1}H NMR (500 MHz, THF-d_8) δ 121 – 113 (bs, 6H, NCH_2), 72 – 63 (bs, 6H, NCH_2), 33 – 28 (bs, 2H, OH), 23 – 21 (bs, 6H, Ar-H), 12.5 (s, 6H, Ar-H), 6.9 (s, 9H, Ar-CH_3), 3.8 (s, 8H, Bu_4N^+), 1.9 (s, 8H, Bu_4N^+), 1.3 (s, 8H, Bu_4N^+), 0.8 (s, 12H, Bu_4N^+). Anal. calcd (found) for ($C_{43}H_{72}CoN_6O_7S_3$) C, 54.93 (55.23); H, 7.72 (7.94); N, 8.94 (8.68). UV-Vis (THF, ε in $M^{-1}cm^{-1}$): 523 (105), 697 (31) and 1545 (36). IR (FT-ATR, cm^{-1}): 3299 (ν_{NH}), 2957, 1598, 1466, 1383, 1351, 1246, 1153, 1129, 1092, 1037, 966, 935, 870, 846, 812, 793, 740, 710, 689, 659, 594, 569, 548. FTMS (NSI): m/z^- $C_{27}H_{36}CoN_5O_7S_3^-$, 697.11719. Calcd: 697.11143 ($L_1ML_2^-$), Δ = 8 ppm.

[^{n}Bu$_4$N][(Ts$_3$tren)Co^{II}(NH$_3$)] {3-1(NH$_3$)}

Nitrogen gas was bubbled through a solution of NH_4OH and the evolved gas was bubbled through a solution of **3-1(OH$_2$)** in 8mL of DCM for 15 minutes. Diethyl ether was added to this solution to afford purple crystals (183mg, 80% yield). ^{1}H NMR (500 MHz, THF-d_8) δ 127 – 120 (bs, 6H, NCH_2), 72 – 62 (bs, 6H, NCH_2), 33 – 28 (bs, 2H, OH), 26 – 21 (bs, 6H, Ar-H), 12.6 (s, 6H, Ar-H), 6.4 (s, 9H, Ar-CH_3), 4.9 (s, 8H, Bu_4N^+), 2.7 (s, 8H, Bu_4N^+),

1.5 (s, 8H, Bu_4N^+), 0.9 (s, 12H, Bu_4N^+). Anal. calcd (found) for ($C_{43}H_{72}CoN_6O_7S_3$) C, 55.88 (55.62); H, 7.85 (7.90); N, 9.09 (8.87). UV-Vis (THF, ε in $M^{-1}cm^{-1}$): 512 (102), 686 (31) and 1582 (35). IR (FT-ATR, cm^{-1}): 3362 (ν_{NH}), 2960, 2870, 1599, 1491, 1464, 1381, 1350, 1241, 1127, 1097, 1079, 1041, 1019, 970, 935, 872, 813, 740, 710, 662, 596, 551. FTMS (NSI): m/z^- = 681.11757, calcd: 681.11652 ($L_1ML_2^-$), Δ = 2 ppm.

[(Ts_3tren)Co^{III}(OH)($Ca(OTf)_2$•15-crown-5)$_2$][OTf] {3-2}

In a glovebox, **3-1** (121mg, 0.13mmol) and hydrogen peroxide solution (395μL, 0.15mmol, 382mM in THF) were mixed in 1mL THF. (15-crown-5)$Ca(OTF)_2$ (112mg, 0.20mmol) dissolved in 1mL of DCM was added to the blue-violet solution, which immediately turned dark green and bubbled. This mixture was removed from the glovebox. Vapor diffusion of diethyl ether into the green solution produced dark green crystals. We note that stoichiometric ratios of 15-crown-5•$Ca(OTF)_2$ adduct and **3-1** gave material that was difficult to purify, so substoichiometric (15-crown-5)$Ca(OTF)_2$ was employed. (122mg, 69% yield, based on limiting calcium adduct). Elemental analysis indicated 50% loss of lattice THF. Anal. calcd (found) for ($C_{104}H_{156}Ca_4Co_2F_{18}N_8O_{53}S_{12}$) C, 37.05 (37.09); H, 4.66 (4.67); N, 3.32 (3.26). UV-Vis (THF, ε in $M^{-1}cm^{-1}$): 430 (3,600), 706 (530). IR (FT-ATR, cm^{-1}): 3427 (ν_{OH}), 2922, 2853, 1600, 1461, 1377, 1358, 1300, 1240, 1147, 1081, 1028, 972, 950, 872, 822, 753, 709, 669, 636, 608, 572, 553.

[^{tBu}ArPPh$_3$]Br {3-3}

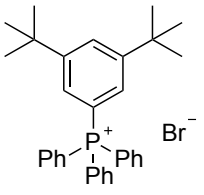

The phosphonium bromide salt was synthesized following literature methods.[36] 1-Bromo-3,5-di-tert-butylbenzene (9.93g, 36.88mmol), triphenylphosphine (10.16g, 38.73mmol, 1.05eq), nickel(II) bromide (3mol%, 240mg, 1.1mmol), and ethylene glycol (12.3mL) were added to a 25mL pressure

flask with a stir bar. The flask was sealed and heated to 150˚C. After stirring 6hrs, the flask was allowed to cool. The mixture was diluted with dichloromethane (400mL) and washed with water (3x300mL) and brine. The organic layer was dried with magnesium sulfate, filtered, and concentrated via rotary evaporation. Diethyl ether was added to precipitate a white solid, which was collected via filtration and dried under high-vacuum. (16.06g, 83% yield). ^{1}H NMR (400 MHz, $CDCl_3$): δ 7.96-7.90 (m, 3H), 7.85 (q, 1H, J=1.6Hz), 7.84-7.78 (m, 6H), 7.64-7.56 (m, 6H), 7.30 (d, 1H, J=1.7Hz), 7.27 (d, 1H, J=1.7Hz), 1.25 (s, 18H); ^{13}C NMR (100 Hz, DMSO-d6): δ 154.0 (d, J=12Hz), 136.1, 134.4 (d, J=10Hz), 131.0 (d, J=12Hz), 130.2, 128.5 (d, J=11Hz), 118.3, 117.4, 35.5, 31.2; ^{31}P ($CDCl_3$, 162Hz) δ 23.33.

[^{tBu}ArPPh$_3$][(Ts$_3$tren)Co^{II}(H$_2$O)] {3-1^{P}(OH$_2$)}

In a glovebox, H_3Ts_3tren (1.5g, 2.48mmol) and $CoCl_2$ (323mg, 2.48mmol) was dissolved in 10mL of dimethylacetamide. Potassium hydride (309mg, 7.70mmol) was added slowly while stirring. The reaction was stirred overnight and **3-3** (543mg, 2.48mmol) was added in 4mL of methanol. The mixture was removed from the glovebox and diluted with 5mL of diethyl ether. This mixture was dropped into 1L of diethyl ether and allowed to settle for 30min. The solution was filtered and the filtrate washed with dichloromethane. The filtrate and rinsate were combined and then diluted with 1L of pentane and allowed to settle for 1hr. The pink solid was collected by filtration and dissolved in acetone. The cloudy purple mixture was filtered through celite and concentrated via rotary evaporation. Diffusion of diethyl ether into this solution afforded purple crystals suitable for XRD (0.827g, 29% yield). ^{1}H NMR (500 MHz, THF-d_8) δ 156 – 144 (bs, 6H, NCH_2), 83 – 68 (bs, 6H, NCH_2), 28 – 25 (bs, 6H, Ar-H), 14.5 (s, 6H, Ar-H), 8.6 (s, 9H, Ar-CH_3), 8 – 6 (m, $^{tBu}ArPPh_3^+$), 2.1 (s, $^{tBu}ArPPh_3^+$), 1.0 (s, 5H, $^{tBu}ArPPh_3^+$). Anal. calcd (found) for

($C_{59}H_{71}CoN_4O_7PS_3$): C, 62.47 (62.48); H, 6.31 (6.27); N, 4.94 (5.01). UV-Vis (THF, ε, in $M^{-1}cm^{-1}$): 528 (59), 686 (21) and 1582 (37). IR (FT-ATR, cm^{-1}): 3307 (ν_{OH}), 2956, 2863, 1594, 1466, 1438, 1395, 1363, 1247, 1136, 1107, 1079, 1042, 971, 931, 878, 815, 750, 724, 691, 631, 599. 580, 547, 528. FTMS (NSI): m/z^- = 664.09052, calcd: 664.08997 (ML_1^-), Δ = 0.8 ppm. m/z^+ = 451.25485, calcd: 451.25491 ($^{tBu}PhPPh_3^+$), Δ = 0.1 ppm.

[^{tBu}ArPPh$_3$][(Ts$_3$tren)Co^{II}] {3-1^P}

3-1^P(OH$_2$) (621mg) was dissolved in THF and treated with 3Å molecular sieves overnight at 60˚C. The solution was filtered and the product crystallized by the addition of ether and pentane (437mg, 72% yield). ^{1}H NMR (500 MHz, THF-d_8) δ 166 – 153 (bs, 6H, NCH_2), 80 – 65 (bs, 6H, NCH_2), 28 – 21 (bs, 6H, Ar-H), 14.7 (s, 6H, Ar-H), 9.0 (s, 9H, Ar-CH_3), 7.2 (s, 1H, $^{tBu}ArPPh_3^+$), 5.2 (s, 2H, $^{tBu}ArPPh_3^+$), 2.5 (s, 5H, $^{tBu}ArPPh_3^+$), 1.1 (s, 5H, $^{tBu}ArPPh_3^+$), 0.6 (s, 18H, $^{tBu}ArPPh_3^+$).

(15-crown-5)Ba(OTf)$_2$

In a glovebox, $Ba(OTf)_2$ (0.955g, 2.19mmol) and 15-crown-5 ether (0.488g, 2.21mmol) was stirred in acetonitrile at 80˚C for 2hrs and then cooled to room temperature. After filtering the solution was concentrated under vacuum and diethyl ether was added to precipitate adduct. Product washed with more ether and dried under vacuum (1.22g, 85% yield). Anal. calcd (found) for ($C_{12}H_{20}CaF_6O_{11}S_2$): $C_{12}H_{20}CaF_6O_{11}S_2$: C, 21.98 (22.11); H, 3.07 (2.89).

Additional formation of "Co^{III}–OH"

Solutions of equimolar **3-1** and (15-crown-5)M$(OTf)_2$ (M= Sr, Ba) in THF were prepared. Additionally, **4-1** (see Chapter 4) was dissolved in a THF/MeOH mixture. Hydrogen peroxide solution in THF was added (1.1 equivalents) to each of the three cobalt solutions,

which all immediately turned dark green. The solutions were filtered and the absorption spectra collected.

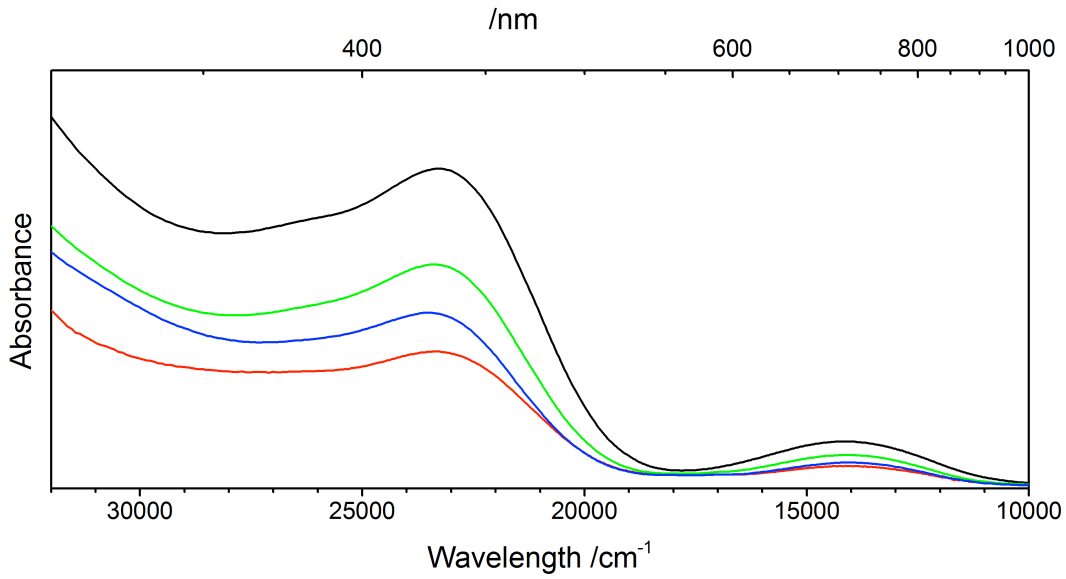

Figure 3-8. Absorption data for ***3-2*** *(—) and "Co^{III}-OH" species generated with Sr (—) and Ba (—) and heterotrimetallic complex* ***4-1*** *(—).*

3.5.4 Paramagnetic NMR Experiments

^{1}H NMR of paramagnetic species taken in THF-d_8 at 25-30mM (acquisition time = 0.5sec; relaxation delay = 0.6sec). A spectral window of 300ppm to –100ppm was scanned initially to find all paramagnetically shifted signals and then narrowed to improve baseline integrity while still including all peaks. All spectra were adjusted with a manual multireference point baseline correction in MNova software to allow for signal integration.

Signal Assignments

The ^{1}H-NMR spectra of **3-1** and **3-1(OH$_2$)** are compared with **3-1^P**, **3-1^P(OH$_2$)**, **4-4(OH$_2$)**, and **4-4** in order to assign signals to specific proton environments. See Chapter 4 for full characterization of **4-4** and **4-4(OH$_2$)**.

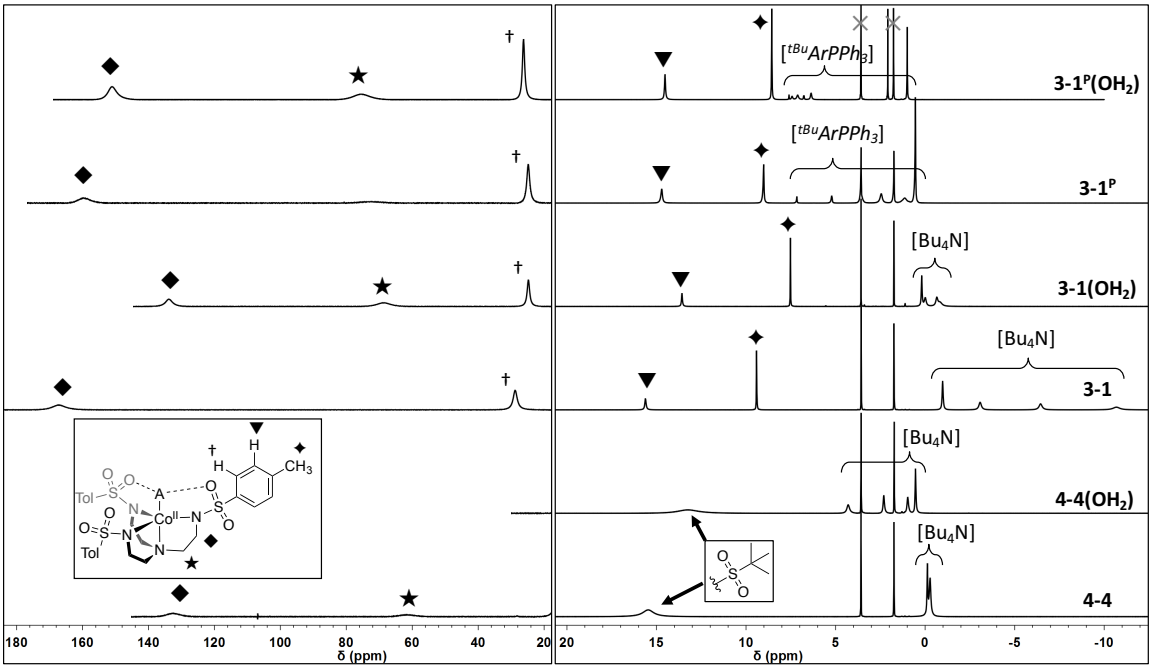

Figure 3-9. [1]H-NMR of cobalt complexes showing signal assignments to proton environments on the ligand and counterion. Spectra split and intensities scaled to allow paramagnetically broadened peaks to be seen more clearly. Solvent indicated with (X)

Addition of excess water to 3-1

In a glovebox, a solution of **3-1** in THF-d_8 was sealed in an NMR tube with a rubber septum. The ^{1}H-NMR spectrum was taken and 1 equivalent of H_2O in THF-d_8 was added via gastight syringe. The spectrum was taken again and this process repeated until a total of 5 equivalents had been added.

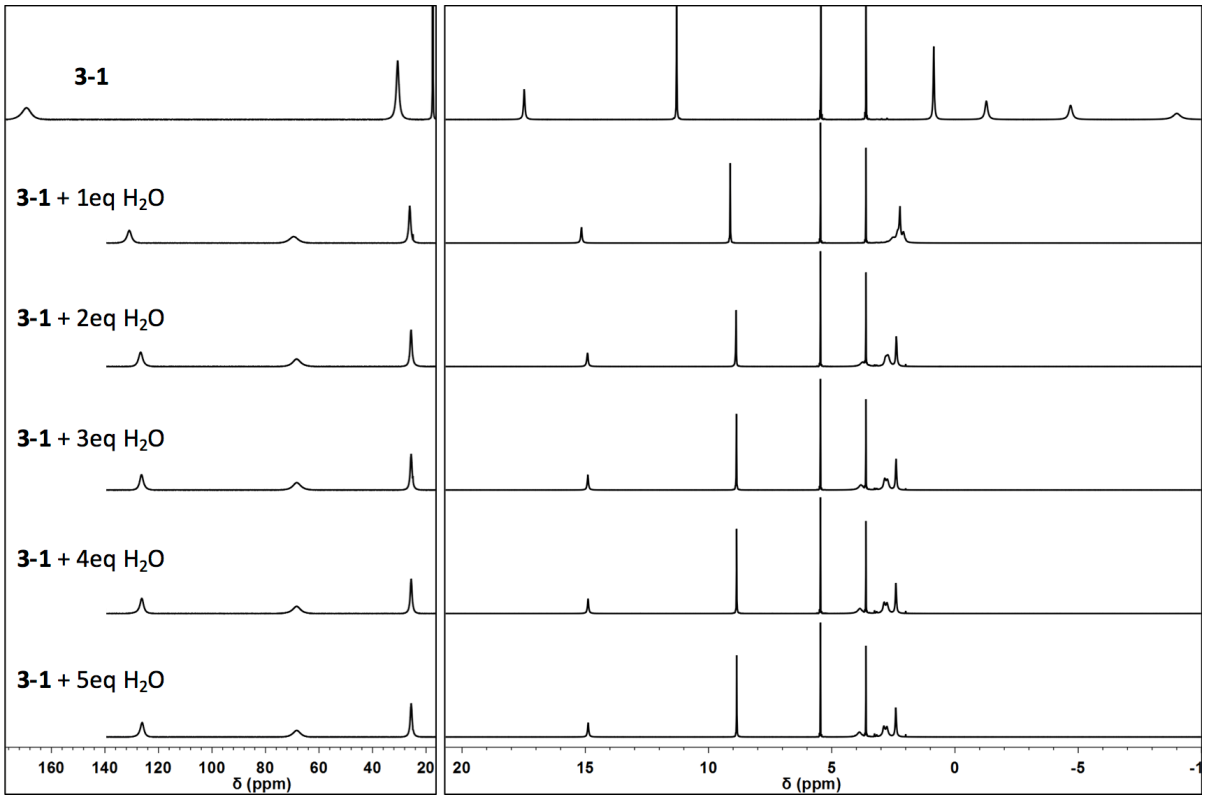

*Figure 3-10. ^{1}H-NMR of **3-1** titrated with water in THF-d_8. Spectra split and intensities scaled to allow paramagnetically broadened peaks to be seen more clearly.*

3.5.5 NMR decay experiments

In a glovebox, an NMR was charged with 15-20mg of complex in 600μL THF-d_8 and fitted with a septum closure. After setting up the experiment with this sample, a solution of hydrogen peroxide in THF-d_8 was added to the NMR tube via gastight syringe. Spectrum were taken over a period of time lasting at least three half-lives. For the selected spectra, the baseline was adjusted and the integration of the H_2O_2 peak was plotted versus time. The data was fit to first-order decay using Origin.

3-1(H_2O_2) Decay

3-1 (16.5mg) was dissolved in 500μL of THF-d_8 and 111μL of 163.5mM H_2O_2 in THF-d_8 solution added. Due to an overlap of the H_2O_2 peak with a solvent peak during the first

4min, a number of spectrum were chosen for analysis after the initial 4 min, extending over a period of 3 half-lives.

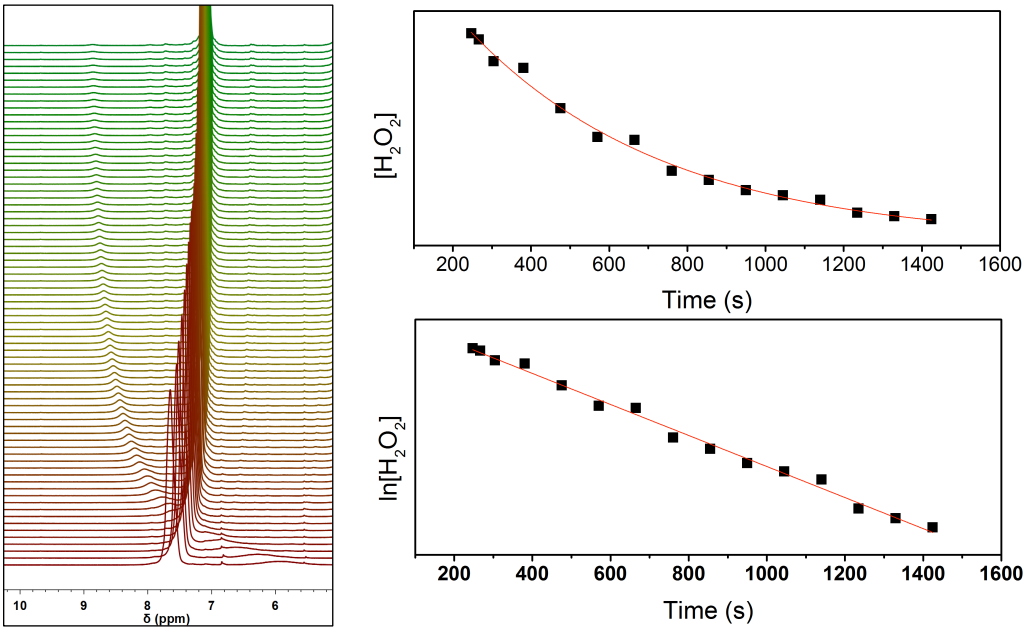

Figure 3-11. Decay of ***3-1(H$_2$O$_2$)*** *(left), exponential curve fit (top right), and linear fit (bottom right).*

3-1(OH_2) + H_2O_2 Decay

3-1(OH_2) (16.5mg) was dissolved in 600μL of THF-d_8 and 148μL of 121mM H_2O_2 in THF-d_8 solution added.

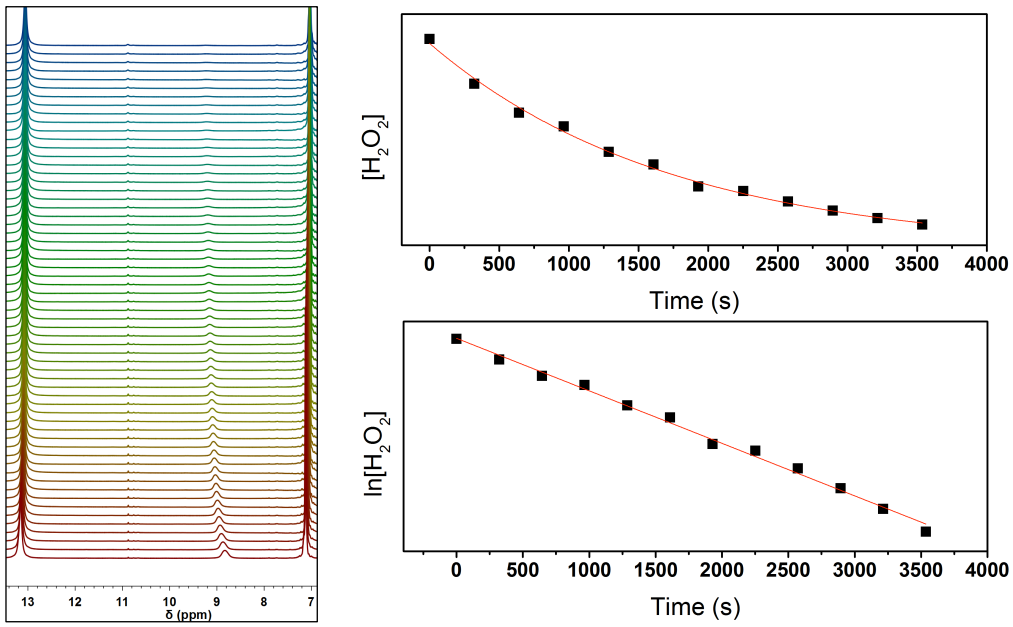

*Figure 3-12. Decay of H_2O_2 with **3-1(OH_2)** (left), exponential curve fit (top right), and linear fit (bottom right).*

3-1(NH_3) + H_2O_2 Decay

1–NH_3 (16.17mg) was dissolved in 500μL of THF-d_8 and 152μL of 121mM H_2O_2 in THF-d_8 solution added.

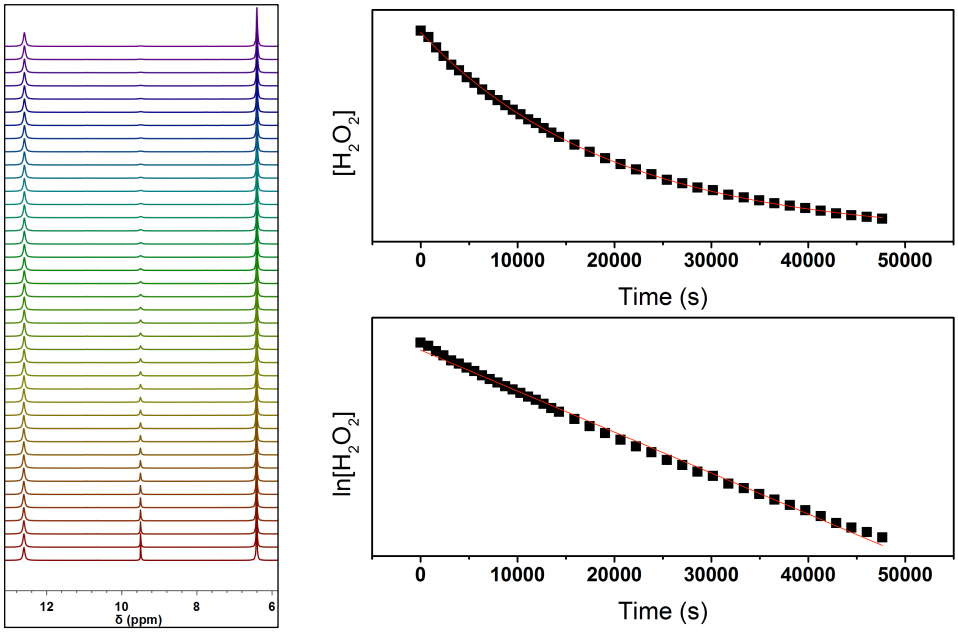

*Figure 3-13. Decay of H_2O_2 with **3-1(NH_3)** (left), exponential curve fit (top right), and linear fit (bottom right).*

Table 3-1. Exponential decay fit parameters.

Complex	$t_{1/2}$ **(s)**	$\mathbf{R^2}$
3-1(H_2O_2)	353 ± 33	0.99238
3-1(OH_2) + H_2O_2	1190 ± 100	0.99511
3-1(NH_3) + H_2O_2	13700 ± 200	0.99968

3.5.6 Photometric Titrations

Electronic Absorption of 3-1(H_2O_2) at –70˚C

An anhydrous H_2O_2/THF solution was concentrated under vacuum to 1.62M H_2O_2. Using a UNISOKU CoolSpeK UV USP-203 cryostat attachment, a cuvette containing 2.5mL of this solution was cooled to –70˚C. A balloon of nitrogen attached to a long needle was used to equilibrate the pressure inside the cuvette as it was cooled. Using a syringe, 1.0mL of a 69.0mM solution of **3-1** in THF was added and the solution stirred for several minutes at –70C before scanning the solution. The solution was scanned every 2 minutes to insure that adequate mixing had occurred. The molar ratio of cobalt complex to hydrogen peroxide adduct was 1:60.

Titrations of Water and Hydrogen Peroxide

Using a UNISOKU CoolSpeK UV USP-203 cryostat attachment, a cuvette containing a solution of 20mM **3-1** in anhydrous THF and closed with a septum cap was cooled to –70˚C. A balloon of nitrogen attached to a long needle was used to equilibrate the pressure inside the cuvette as it was cooled. A solution of ligand (H_2O or H_2O_2) in THF was added via gastight syringe incrementally. After each addition of ligand, the solution was stirred for ~30sec before a spectrum was taken. The first spectrum was subtracted from the last spectrum to find the point of greatest change. For the H_2O titration, the absorbance values at 522nm were normalized from 0 to 1 and plotted versus concentration of ligand. For the H_2O_2 titration, the fractional occupation was calculated by normalizing the absorbance values at 525nm against the absorbance of the saturated spectrum at 525nm, which was calculated using the molar absorptivity measured in the above experiment. Origin was used to model both sets of data to the following equation[37]:

$$\phi = \frac{[\mathrm{Co}] + [\mathrm{L}] + {}^{1}/_{\mathrm{K}} - \sqrt{\left([\mathrm{Co}] + [L] + {}^{1}/_{\mathrm{K}}\right)^{2} - 4[\mathrm{Co}][\mathrm{L}]}}{2[\mathrm{Co}]}$$

where ϕ is the fractional occupation represented by the normalized absorbance values, [L] is the concentration of ligand for each data point, [Co] is the concentration of cobalt complex for each data point, and K is the binding constant.

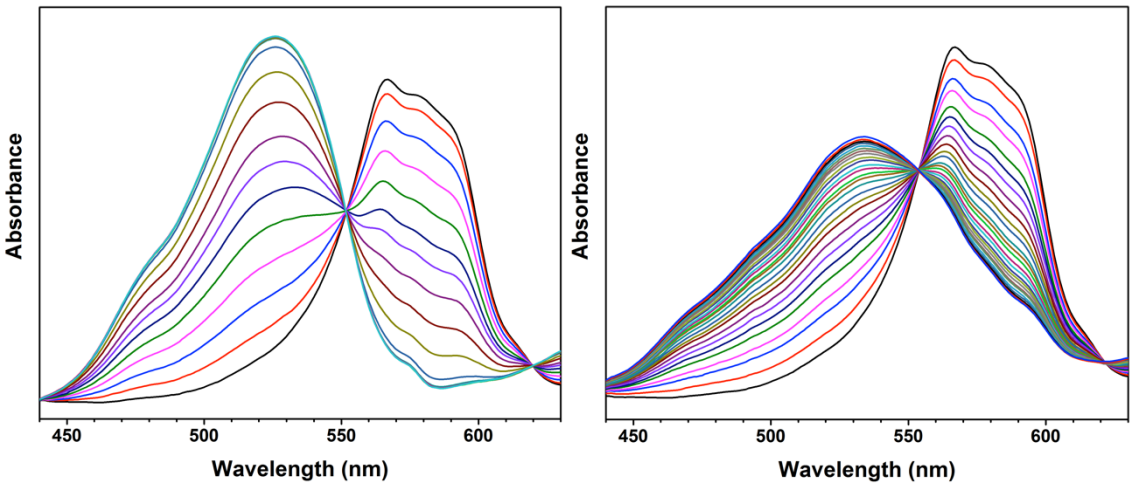

*Figure 3-14. UV-Vis traces of titrations of **3-1** with water (left) and hydrogen peroxide (right).*

Table 3-2. Parameters for fitting photometric titration data.

Ligand	K (M^{-1})	R^2
H_2O	31600 ± 12600	0.99904
H_2O_2	31.3 ± 0.2	0.99946

3.5.7 Electrochemistry

Cyclic voltammetric experiments were conducted in dichloromethane with 0.1M tetrabutylammonium hexafluorophosphate as supporting electrolyte and a glassy carbon

working electrode. The reference electrode solution was made with $Ag(NO_3)$ in acetonitrile. The potential window was scanned at 0.1 V/s.

Table 3-3. Electrochemical data. Scan rate = 100 mV/s with [^{n}Bu$_4$N][PF$_6$] as the supporting electrolyte. All values vs. Fc/Fc$^+$. See Figure 4-5 for electrochemical traces.

	E_{anodic} (mV)	$E_{cathodic}$ (mV)	$E_{½}$ (mV)
3-1(OH$_2$)	+125	+30	+78

3.5.8 Crystallographic Information

Note regarding structure of complex 3-1(OH$_2$) (CCDC 1447760)

Complex **3-1(OH$_2$)** is incommensurately modulated and requires special interpretation. Here we report a description of the structure.

The diffraction pattern of **3-1(OH$_2$)** could be indexed with a monoclinic cell with parameters 14.4100(9) 14.8474(9) 22.0905(14) 90 103.7287(15) 90. A closer analysis of the diffraction pattern revealed the presence of additional spots at positions h±α, k, l±γ with α =-0.18654 and γ=0.30978. The analysis of the diffraction symmetry and systematic absences indicated a superspace group $P2_1/n(a0g)0s$ (a non-standard setting of P2/b(ab0)00, number 14.1.2.1 in [38]). The structure was solved in (3+1)D superspace using the program Superflip.[39] The symmetry analysis of the solution[40] confirmed the estimated superspace group. The analysis of the solution revealed a predominantly occupational character of the modulation. The complex anion **3-1(OH$_2$)** adopts two conformations, which differ predominantly in the position of two tolyl groups (Fig. S4). These conformations differ also in the orientation of the H_2O molecule, and differ in the

intramolecular hydrogen bonding scheme. The $[^{n}Bu_4N]^+$ cation reacts to the conformational changes of the **3-1(OH_2)** anion by a conformational change in one of the butyl chains.

The occupational modulation is harmonic. This means that at each position of the anion in **3-1(OH_2)** both conformations are present with certain probability, but the probability of each conformation at certain position in the crystal is given by a harmonic modulation wave. Such a structure is extremely complicated to represent and to analyze. Therefore we deposit only the average structure, where both conformations superpose. Such a structure allows the understanding of the connectivity and hydrogen-bonding scheme. It has to be born in mind, however, that it is only an approximation and the true structure is not disordered in the way suggested by the average structure.

3.6 References

1. Jones, C. W., *Applications of of Hydrogen Peroxide and Derivatives*. Royal Society: Cambridge, U.K., 1999.

2. Lancaster, M., *Green Chemistry*. Royal Society: Cambridge, U.K., 2002.

3. Hage, R.; de Boer, J. W.; Gaulard, F.; Maaijen, K., Chapter Three - Manganese and Iron Bleaching and Oxidation Catalysts. In *Adv. Inorg. Chem.*, Rudi van, E.; Colin, D. H., Eds. Academic Press: 2013; Vol. Volume 65, pp 85-116.

4. Hage, R.; Lienke, A., Applications of Transition-Metal Catalysts to Textile and Wood-Pulp Bleaching. *Angew. Chem. Int. Ed.* **2006,** *45* (2), 206-222.

5. Russo, V.; Tesser, R.; Santacesaria, E.; Di Serio, M., Chemical and Technical Aspects of Propene Oxide Production via Hydrogen Peroxide (HPPO Process). *Ind. Eng. Chem. Res.* **2013,** *52* (3), 1168-1178.

6. Chen, M.; Pan, Y.; Kwong, H.-K.; Zeng, R. J.; Lau, K.-C.; Lau, T.-C., Catalytic oxidation of alkanes by a (salen)osmium(vi) nitrido complex using H2O2 as the terminal oxidant. *Chem. Commun.* **2015,** *51* (71), 13686-13689.

7. Kwong, H.-K.; Lo, P.-K.; Lau, K.-C.; Lau, T.-C., Epoxidation of alkenes and oxidation of alcohols with hydrogen peroxide catalyzed by a manganese(v) nitrido complex. *Chem. Commun.* **2011,** *47* (14), 4273-4275.

8. Ma, L.; Pan, Y.; Man, W.-L.; Kwong, H.-K.; Lam, W. W. Y.; Chen, G.; Lau, K.-C.; Lau, T.-C., Highly Efficient Alkane Oxidation Catalyzed by [MnV(N)(CN)4]2–. Evidence for [MnVII(N)(O)(CN)4]2– as an Active Intermediate. *J. Am. Chem. Soc.* **2014,** *136* (21), 7680-7687.

9. Anson, C. W.; Ghosh, S.; Hammes-Schiffer, S.; Stahl, S. S., Co(salophen)-Catalyzed Aerobic Oxidation of p-Hydroquinone: Mechanism and Implications for Aerobic Oxidation Catalysis. *J. Am. Chem. Soc.* **2016,** *138* (12), 4186-4193.

10. Afanasiev, P.; Kudrik, E. V.; Millet, J.-M. M.; Bouchu, D.; Sorokin, A. B., High-valent diiron species generated from N-bridged diiron phthalocyanine and H2O2. *Dalton Trans.* **2011,** *40* (3), 701-710.

11. Mirza, S. A.; Bocquet, B.; Robyr, C.; Thomi, S.; Williams, A. F., Reactivity of the Coordinated Hydroperoxo Ligand. *Inorg. Chem.* **1996,** *35* (5), 1332-1337.

12. Theodoridis, A.; Maigut, J.; Puchta, R.; Kudrik, E. V.; van Eldik, R., Novel Iron(III) Porphyrazine Complex. Complex Speciation and Reactions with NO and H2O2. *Inorg. Chem.* **2008,** *47* (8), 2994-3013.

13. Wolak, M.; van Eldik, R., Mechanistic studies on peroxide activation by a water-soluble iron(III)-porphyrin: implications for O-O bond activation in aqueous and nonaqueous solvents. *Chemistry* **2007,** *13* (17), 4873-83.

14. Coon, M. J., Cytochrome P450: nature's most versatile biological catalyst. *Annu Rev Pharmacol Toxicol* **2005,** *45* (1), 1-25.

15. Denisov, I. G.; Makris, T. M.; Sligar, S. G.; Schlichting, I., Structure and Chemistry of Cytochrome P450. *Chem. Rev.* **2005,** *105* (6), 2253-2278.

16. Ortiz de Montellano, P. R., *Cytochrome P450: Structure, Mechanism, and Biochemistry*. Kluwer/Plenum: New York, 2005.

17. Shaik, S.; Kumar, D.; de Visser, S. P.; Altun, A.; Thiel, W., Theoretical Perspective on the Structure and Mechanism of Cytochrome P450 Enzymes. *Chem. Rev.* **2005,** *105* (6), 2279-2328.

18. Wang, B.; Li, C.; Dubey, K. D.; Shaik, S., Quantum Mechanical/Molecular Mechanical Calculated Reactivity Networks Reveal How Cytochrome P450cam and Its T252A Mutant Select Their Oxidation Pathways. *J. Am. Chem. Soc.* **2015,** *137* (23), 7379-7390.

19. Wallen, C. M.; Bacsa, J.; Scarborough, C. C., Hydrogen Peroxide Complex of Zinc. *J. Am. Chem. Soc.* **2015,** *137* (46), 14606-14609.

20. Lacy, D. C.; Park, Y. J.; Ziller, J. W.; Yano, J.; Borovik, A. S., Assembly and Properties of Heterobimetallic CoII/III/CaII Complexes with Aquo and Hydroxo Ligands. *J. Am. Chem. Soc.* **2012,** *134* (42), 17526-17535.

21. Since related CoIII species display intense electronic transitions in the visible region,[31] the presence of >0.1% CoIII would be visible by electron absorption spectroscopy in solutions of 1 and H2O2.

22. DiPasquale, A. G.; Mayer, J. M., Hydrogen Peroxide: A Poor Ligand to Gallium Tetraphenylporphyrin. *J. Am. Chem. Soc.* **2008,** *130* (6), 1812-1813.

23. Medvedev, A. G.; Mikhaylov, A. A.; Churakov, A. V.; Vener, M. V.; Tripol'skaya, T. A.; Cohen, S.; Lev, O.; Prikhodchenko, P. V., Potassium, Cesium, and Ammonium Peroxogermanates with Inorganic Hexanuclear Peroxo Bridged Germanium Anion Isolated from Aqueous Solution. *Inorg. Chem.* **2015,** *54* (16), 8058-8065.

24. Mikhaylov, A. A.; Medvedev, A. G.; Churakov, A. V.; Grishanov, D. A.; Prikhodchenko, P. V.; Lev, O., Peroxide Coordination of Tellurium in Aqueous Solutions. *Chem. Eur. J.* **2016**, 2980–2986.

25. Churakov, A. V.; Sladkevich, S.; Lev, O.; Tripol'skaya, T. A.; Prikhodchenko, P. V., Cesium Hydroperoxostannate: First Complete Structural Characterization of a Homoleptic Hydroperoxocomplex. *Inorg. Chem.* **2010,** *49* (11), 4762-4764.

26. Wolanov, Y.; Shurki, A.; Prikhodchenko, P. V.; Tripolskaya, T. A.; Novotortsev, V. M.; Pedahzur, R.; Lev, O., Aqueous stability of alumina and silica perhydrate hydrogels: experiments and computations. *Dalton Trans.* **2014,** *43* (44), 16614-16625.

27. Churakov, A. V.; Prikhodchenko, P. V.; Howard, J. A. K.; Lev, O., Glycine and l-serine crystalline perhydrates. *Chem. Commun.* **2009,** (28), 4224-4226.

28. Prikhodchenko, P. V.; Medvedev, A. G.; Tripol'skaya, T. A.; Churakov, A. V.; Wolanov, Y.; Howard, J. A. K.; Lev, O., Crystal structures of natural amino acid perhydrates. *CrystEngComm* **2011,** *13* (7), 2399-2407.

29. Vener, M. V.; Medvedev, A. G.; Churakov, A. V.; Prikhodchenko, P. V.; Tripol'skaya, T. A.; Lev, O., H-Bond Network in Amino Acid Cocrystals with H2O or H2O2. The DFT Study of Serine–H2O and Serine–H2O2. *J. Phys. Chem. A* **2011,** *115* (46), 13657-13663.

30. Hong, S.; Pfaff, F. F.; Kwon, E.; Wang, Y.; Seo, M.-S.; Bill, E.; Ray, K.; Nam, W., Spectroscopic Capture and Reactivity of a Low-Spin Cobalt(IV)-Oxo Complex Stabilized by Binding Redox-Inactive Metal Ions. *Angew. Chem. Int. Ed.* **2014,** *53* (39), 10403-10407.

31. Pfaff, F. F.; Kundu, S.; Risch, M.; Pandian, S.; Heims, F.; Pryjomska-Ray, I.; Haack, P.; Metzinger, R.; Bill, E.; Dau, H.; Comba, P.; Ray, K., An Oxocobalt(IV) Complex Stabilized by Lewis Acid Interactions with Scandium(III) Ions. *Angew. Chem. Int. Ed.* **2011,** *50* (7), 1711-1715.

32. Cook, S. A.; Borovik, A. S., Molecular Designs for Controlling the Local Environments around Metal Ions. *Acc. Chem. Res.* **2015,** *48* (8), 2407-2414.

33. Zolnhofer, E. M.; Käß, M.; Khusniyarov, M. M.; Heinemann, F. W.; Maron, L.; van Gastel, M.; Bill, E.; Meyer, K., An Intermediate Cobalt(IV) Nitrido Complex and its N-Migratory Insertion Product. *J. Am. Chem. Soc.* **2014,** *136* (42), 15072-15078.

34. Park, Y. J.; Ziller, J. W.; Borovik, A. S., The effects of redox-inactive metal ions on the activation of dioxygen: isolation and characterization of a heterobimetallic complex containing a Mn(III)-(mu-OH)-Ca(II) core. *J. Am. Chem. Soc.* **2011,** *133* (24), 9258-61.

35. Park, Y. J.; Cook, S. A.; Sickerman, N. S.; Sano, Y.; Ziller, J. W.; Borovik, A. S., Heterobimetallic Complexes with MIII-(μ-OH)-MII Cores (MIII = Fe, Mn, Ga; MII = Ca, Sr, and Ba): Structural, Kinetic, and Redox Properties. *Chem Sci* **2013,** *4* (2), 717-726.

36. Marcoux, D.; Charette, A. B., Nickel-Catalyzed Synthesis of Phosphonium Salts from Aryl Halides and Triphenylphosphine. *Advanced Synthesis & Catalysis* **2008,** *350* (18), 2967-2974.

37. Cooper, A., Thermodynamics and interactions. In *Biophysical Chemistry*, The Royal Society of Chemistry: 2004; Vol. 16, pp 99-122.

38. Palatinus, L.; Chapuis, G., SUPERFLIP - a computer program for the solution of crystal structures by charge flipping in arbitrary dimensions. *Journal of Applied Crystallography* **2007,** *40* (4), 786-790.

39. Palatinus, L.; van der Lee, A., Symmetry determination following structure solution in P1. *Journal of Applied Crystallography* **2008,** *41* (6), 975-984.

40. Stokes, H. T.; Campbell, B. J.; van Smaalen, S., Generation of (3 + d)-dimensional superspace groups for describing the symmetry of modulated crystalline structures. *Acta Crystallographica Section A* **2011,** *67* (1), 45-55.

Chapter 4

Heterotrimetallic Sandwich Complexes Supported by Sulfonamido Ligands

Published in part in: Wallen, C. M.; Wielizcko, M.; Bacsa, J.; Scarborough, C. C., Heterotrimetallic sandwich complexes supported by sulfonamido ligands. *Inorg. Chem. Front.* **2016,** *3* (1), 142-149.

4.1 Abstract

The only observed $M(H_2O_2)$ adducts are supported by aryl-sulfonamido ligands that are able to stabilize the otherwise weak binding of hydrogen peroxide to transition metals. In this chapter, we report the synthesis of a novel alkyl-sulfonamido ligand bearing *tert*-butyl groups and its complexes of cobalt. The increased electron density of the sulfonyl oxygen atoms is demonstrated by the formation of well-defined isostructural heterotrimetallic sandwich complexes where two anionic $[LCo^{II}]^-$ fragments are bridged by a Group II metal ion (Mg^{2+}, Ca^{2+}, Sr^{2+}, or Ba^{2+}). Solution studies on these novel sandwich complexes by cyclic voltammetry and electronic absorption spectroscopy indicate that these structures are not dramatically altered in solution, opening the door to the exploration of reactivity at Co^{II} that is modified by Group II ions.

4.2 Introduction

4.2.1 $M(H_2O_2)$ Adducts with Sulfonamido Ligands

H_2O_2 is generally hailed as an attractive and green industrial oxidant due to its high oxidative efficiency and having only water as its sole stoichiometric byproduct.[1] It is used in a variety of chemical processes including bleaching of cotton and wood pulp and oxygenation of propylene to propylene oxide, which often involve activation with metal catalysts.[1-5] Hydrogen peroxide is known to be a weak ligand for metals,[6-7] but calculations suggest that H_2O_2 binding can be facilitated by intramolecular hydrogen bonding.[8-12] $M(H_2O_2)$ adducts have been implicated computationally[10-13] and kinetically[7, 14-16] in oxidative mechanisms with hydrogen peroxide, but only two examples have ever been observed experimentally (Chapters 2 and 3).[17-18] In both of these complexes, binding of

hydrogen peroxide is facilitated by hydrogen bonding interactions with sulfonyl groups on the supporting ligand (Figure 4-1). Therefore, the binding of hydrogen peroxide could be strengthened by increasing the electron density of the sulfonyl groups. This chapter describes our successful attempt to synthesize an alkyl-sulfonamidate ligand, as well as a demonstration of the increased donating ability of the sulfonyl oxygen atoms through their interactions with Group II metal ions.

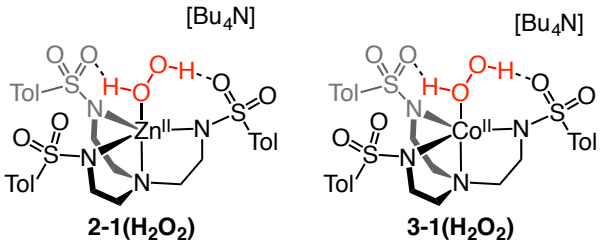

Figure 4-1. Experimentally observed $M(H_2O_2)$ adducts.

4.2.2 Heterometallic Complexes with Group II Ions

The properties and reactivity of transition metals can be dramatically modified by the presence of second-sphere redox-inactive metals. This is most notably seen in the oxygen-evolving complex (OEC) of photosystem II,[19] where second-sphere calcium or strontium[20-21] is required for the formation of O_2 from water at the manganese cluster. Synthetic models of the OEC[22] have corroborated the importance of the redox-inert ion by demonstrating a dependence of the redox potentials[23-25] and reactivity[26-28] of manganese clusters on the identity of the redox-inert ion. The effects of second-sphere redox-inert metals have been demonstrated in other systems as well, for example by affecting the properties and reactivity of metal–oxo[29-39] and metal–peroxo[40-44] species, by altering the rate of O_2 activation by Mn^{II} and Fe^{II},[45-47] by controlling the accessibility and reactivity of copper-nitrene species,[48-50] by changing the reactivity of a Cu^{III}–OH species,[51] and by modulating

the water-oxidation reactivity of cobalt and manganese oxides.[52-53] Clearly, redox-inert metals can have a profound effect on the properties and reactivity of nearby transition metals. Borovik has demonstrated that redox-inert ions may be brought into close proximity to transition- and main-group metals coordinated by sulfonamido ligands, due to the electron-rich nature of the sulfonyl oxygens.[45-47, 54-58] Our demonstration that second-sphere Group II ions in cobalt sulfonamidate complexes promotes reactivity with hydrogen peroxide has prompted us to further explore the interactions between redox-inactive ions and sulfonamidate complexes. While heterometallic systems that involve either a 1:1 ratio of redox-active and redox-inert metal ions[29-36, 38-51] or the interaction of a redox-inert metal ion with a cluster of redox-active metals[22-28, 37] are common, we targeted systems with a 2:1 ratio of redox-active and redox-inert metal ions that could be well suited for splitting symmetric small molecules (e.g. H_2O_2). In particular, we have been targeting systems where the redox-active metal ion maintains an open coordination site, as the availability of this site would form the focus of reactivity studies. Since previous work by Borovik[45-47, 54-58] and our group focused on aryl sulfonamido ligands, we also sought to probe the behaviour of a more electron-rich alkyl sulfonamido analog. In this chapter, we describe the assembly of heterotrimetallic (Co^{II}_2M) sandwich complexes (M = Mg^{2+}, Ca^{2+}, Sr^{2+}, or Ba^{2+}) supported by a new sulfonamido ligand that feature open axial coordination sites on each Co^{II} ion.

4.3 Results and Discussion

4.3.1 Complexation of Aryl-Sulfonamidate Complexes with Group II Metals

We reasoned that heterotrimetallic sandwich compounds would be accessible from the $[(Ts_3tren)Co^{II}]^-$ unit found in **3-1(L)** complexes (see Chapter 3). $[Ts_3tren]^{3-}$ is smaller than the R = mesityl derivative employed by Borovik in the synthesis of heterobimetallic cobalt complexes,[54] and we reasoned that this diminished size might be important for assembly of heterotrimetallic systems. Heating $Ca(OTf)_2$ and **3-1** in methanol/glyme to 85˚C provided a novel sandwich compound that crystallized upon cooling (Scheme 4-1, Figure 4-2), wherein two $[(Ts_3tren)Co^{II})]^-$ units are bonded to Ca^{2+} through one sulfonyl oxygen of each ligand arm to afford the sandwich compound $[Ca^{2+}][(Ts_3tren)Co^{II})]_2$ (**4-1**), a species that is octahedral at Ca^{2+} and trigonal monopyramidal at the two Co^{II} ions. Attempts to prepare structurally related species using $Mg(OTf)_2$ and $Sr(OTf)_2$ were unsuccessful, but we were able to crystallize the partially hydrated polymeric Sr^{2+}-containing heterometallic complex $[Sr^{2+}][(Ts_3tren)Co^{II})]_2(H_2O)_{1.5}$ (**4-2**) (Scheme 4-1, Figure 4-2). A two-step procedure employing $Ba(OTf)_2$ and molecular sieves afforded crystalline $[Ba^{2+}]_2[(Ts_3tren)Co^{II})]_4$ (**4-3**) (Scheme 4-1, Figure 4-2), which features two seven-coordinate Ba^{2+} ions bridging four $[(Ts_3tren)Co^{II}]$ units.

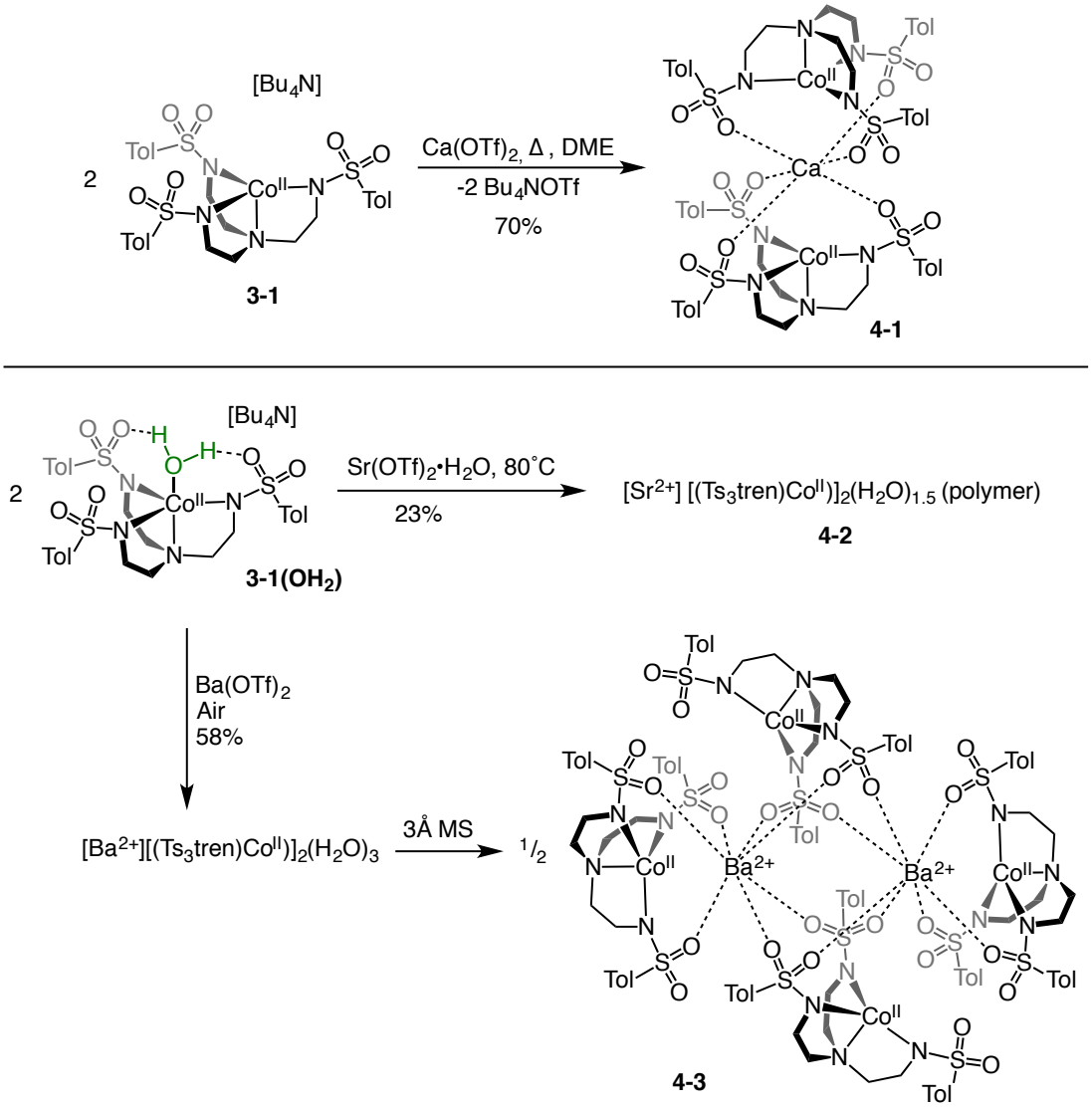

*Scheme 4-1. Synthesis of heterometallic complexes **4-1**, **4-2**, and **4-3**. Yields shown are of cyrstalline product.*

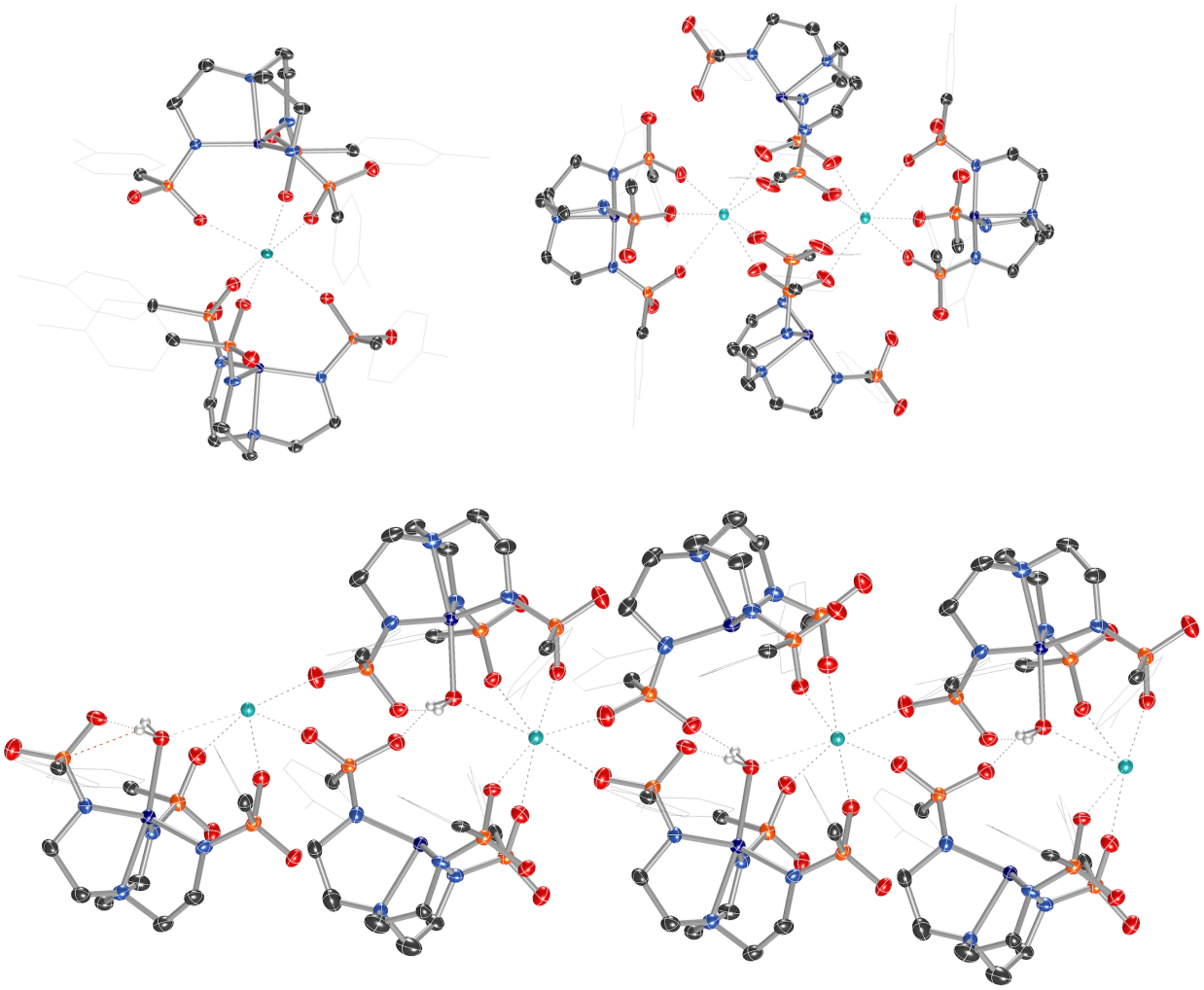

*Figure 4-2. Solid-state molecular structures of **4-1** (top left), **4-3** (top right), and polymeric **4-2** (bottom). Only axial ligand protons are shown. Sulfonamido ligand arms have been reduced for clarity. Lattice water molecule in **4-2** not shown.*

4.3.2 Synthesis of Complexes With Novel Alkyl-Sulfonamido Ligand

The difficulties in obtaining isostructural heterometallic complexes with aryl sulfonamido complexes led us to explore alkylsulfonyl groups that would provide more electron-rich oxygen donors than the arylsulfonyl ligands in **4-1**. This reasoning is supported by the higher acidity of $PhSO_2NH_2$ than $CH_3SO_2NH_2$ (pK_a = 16.1 vs. 17.5, respectively).[59-60]

Ms_3H_3tren[61] was not targeted owing to its water solubility; instead, we targeted (^{t}BuSO$_2$NHCH$_2$CH$_2$)$_3$N (H_3Bus_3tren, Bus = busyl). Bus_3H_3tren had not been reported, and accessing this ligand in an analogous manner to H_3Ts_3tren is not feasible because ^{t}BuSO$_2$Cl is not an effective sulfonyl transfer agent (^{t}BuSO$_2$Cl decomposes into isobutylene, SO_2, and HCl on addition to amines).[62-64] However, busyl amides are accessible from amine sulfinylation with ^{t}BuSOCl[65-66] followed by oxygen-atom transfer to sulfur with *m*-CPBA.[67] We accessed H_3Bus_3tren from commercially available ^{t}BuSS^{t}Bu over four steps in 21% overall yield (Scheme 4-2). This ligand was metallated analogously to H_3Ts_3tren, providing crystalline [^{n}Bu$_4$N][(Bus_3tren)Co^{II}(OH$_2$)] (**4-4(OH$_2$)**) in 47% yield (Scheme 4-2, Figure 4-3). As with **3-1(OH$_2$)**, **4-4(OH$_2$)** could be readily dehydrated with 3Å molecular sieves to afford the crystalline four-coordinate complex **4-4** (Figure 4-3).

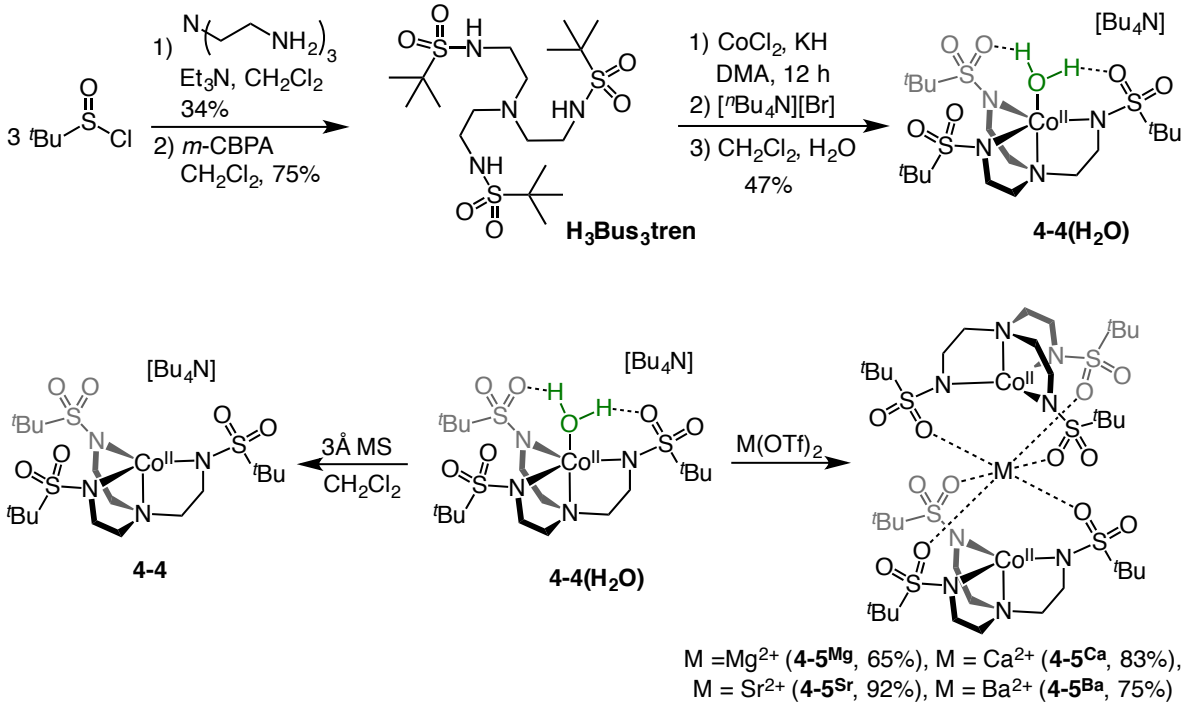

*Scheme 4-2. Synthesis **4-4(OH$_2$)**, **4-4**, **4-5^{Mg}**, **4-5^{Ca}**, **4-5^{Sr}**, and **4-5^{Ba}**. Yields are of crystalline products.*

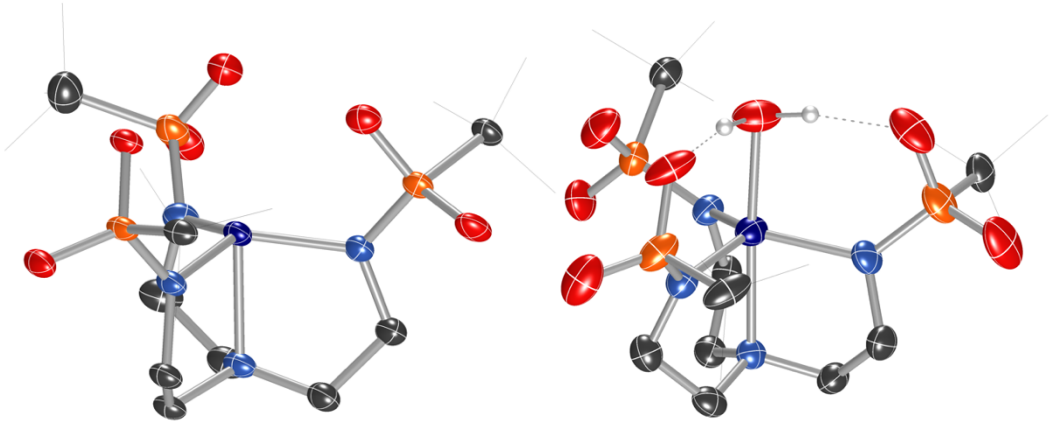

Figure 4-3. Solid-state molecular structures of the anions in ***4-4*** *(left) and* ***4-4(OH$_2$)*** *(right).*

Addition of M(OTf)$_2$ to **4-4** with heat provided crystalline samples of **4-5^{M}**, where M = Mg, Ca, Sr, and Ba (Scheme 4-2, Figure 4-4). In contrast to compounds containing [(Ts$_3$tren)Co^{II})]$^-$, the Group II ion in each of these species is octahedral, and each member of the series is isostructural: the redox-inert metal ion is bound symmetrically by one sulfonyl oxygen of each busyl group. The ability to access this isostructural series that was inaccessible with [(Ts$_3$tren)Co^{II})]$^-$ may at least partially result from the increased electron density of the sulfonyl oxygens of busyl vs. tosyl groups. Table 4-1 highlights relevant crystallographic distances. The Co–N$_{ax}$ distance is sensitive to the coordination number at cobalt, where this bond in species containing [(Bus$_3$tren)Co^{II})]$^-$ elongates by ~0.1 Å upon coordination of H$_2$O. Differences between the Co–N$_{ax}$ distances for all four-coordinate species containing [(Bus$_3$tren)Co^{II})]$^-$ are within 3σ. The Co–N$_{eq}$ bond lengths are sensitive to the coordination number of cobalt, but to a lesser extent than the Co–N$_{ax}$ distance. No clear trends in Co–N bond lengths are observed for the **4-5^{M}** series; however, the Co---M distance increases monotonically with increasing size of the Group II ion.

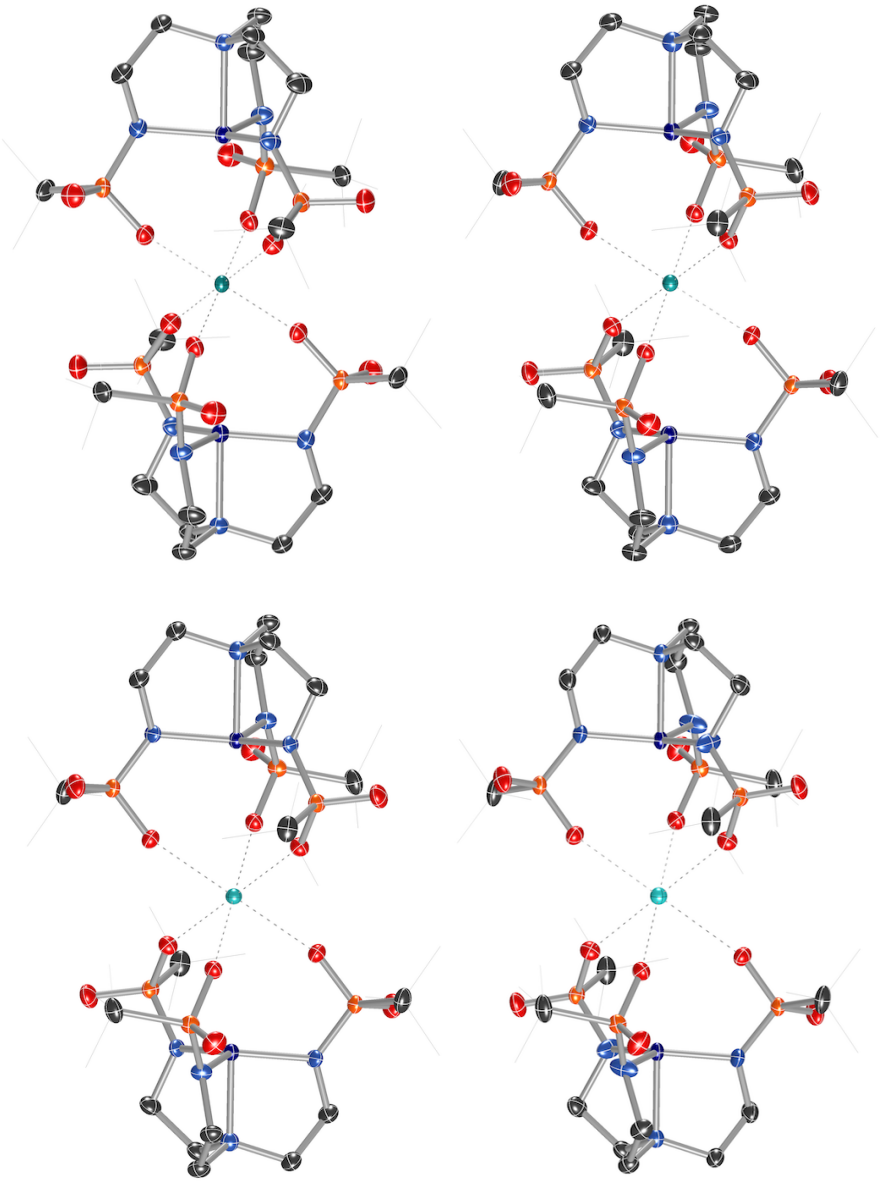

Figure 4-4. From left to right, solid-state molecular structures of ***4-5***^{Mg}, ***4-5***^{Ca}, ***4-5***^{Sr}, *and* ***4-5***^{Ba}.

*Table 4-1. Crystallographic distances for compounds containing [**2**]⁻.*

Compound	Co–N_{ax} [a]	Co–N_{eq} [b]	Co–OH_2	Co---M
4-4(OH_2)	2.246(3) Å	2.038(3) Å, 2.014(3) Å, 2.030(3) Å	2.134(3) Å	---
4-4	2.109(6) Å	1.933(5) Å, 1.937(6) Å, 1.991(6) Å	---	---
4-5^{Mg}	2.1069(10) Å	1.9440(7) Å	---	3.4101(9) Å
4-5^{Ca}	2.0951(19) Å	1.9344(11) Å	---	3.5485(11) Å
4-5^{Sr}	2.087(3) Å	1.965(6) Å	---	3.6411(10) Å
4-5^{Ba}	2.087(5) Å	1.942(3) Å	---	3.7490(7) Å

*[a] Scan rate = 100 mV/s with [$^{n}Bu_4N$][PF_6] as the supporting electrolyte. All values vs. Fc/Fc^+. See **Error! Reference source not found.** for electrochemical traces. [b] Features of aqua complexes consistently appear as minor impurities, likely arising from adventitious H_2O in the experimental setup. [c] The return oxidation wave of **3-1** is not discernible. [d] Electrochemically irreversible, but cycling current does not result in changes to the voltammogram (chemically reversible). [e] Multiple oxidation events. [f] Position of final (lowest-potential) reduction wave.*

4.3.3 Electrochemistry of Trimetallic Complexes

We next explored the Co^{II}/Co^{III} redox couple of **3-1(OH_2)**, **4-4(OH_2)**, **3-1**, and **4-4** in CH_2Cl_2 using cyclic voltammetry to probe the effect of coordination number and ligand identity on redox potential as a benchmark for probing the members of the **4-5^{M}** series (**Error! Reference source not found.**). Borovik recently demonstrated that the Fe^{II}/Fe^{III} redox couple in $[Me_4N][((ArSO_2))_3tren)Fe^{II}(OH_2)]$ is sensitive to the electronic properties of the aryl group,[55] so we wanted to probe the extent to which the Co^{II}/Co^{III} couple is sensitive to the nature of the sulfonyl substituent (*p*-tolyl vs. *tert*-butyl). The

electrochemical data are summarized in Table 4-2. Both species containing $[(Bus_3tren)Co^{II})]^-$ are more easily oxidized than the corresponding $[(Ts_3tren)Co^{II})]^-$ species, where the onset of oxidation was shifted by –30 and –60 mV for the respective hydrated and anhydrous $[(Bus_3tren)Co^{II})]^-$ species compared to the $[(Ts_3tren)Co^{II})]^-$ species in CH_2Cl_2, consistent with busyl amides being more electron rich than tosyl amides. Furthermore, the onset of oxidation for the four-coordinate species **3-1** and **4-4** were shifted by +270 and +240 mV from the corresponding hydrated species, revealing a strong dependence of the Co^{II}/Co^{III} couple on coordination number.[68] These data clearly demonstrate the stronger donor strength of $[Bus_3tren]^{3-}$ compared to $[Ts_3tren]^{3-}$, and also provide a benchmark for electrochemical studies of the members of the **4-5^{M}** series.

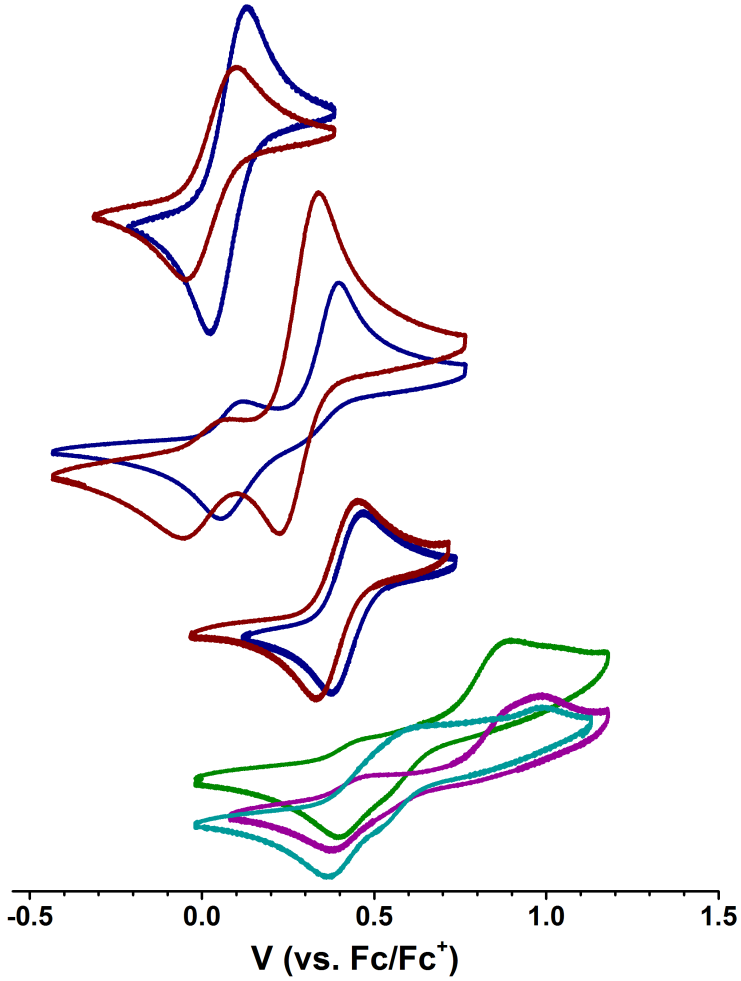

Figure 4-5. Electrochemical data. Top: Cyclic voltammograms of ***3-1(OH$_2$)*** *(—) and* ***4-4(OH$_2$)*** *(—) in CH_2Cl_2. Second from top:* ***3-1*** *(—) and* ***4-4*** *(—) in CH_2Cl_2 (smaller features are from hydrated forms derived from adventitious water in the experimental setup). Second from bottom:* ***3-1(OH$_2$)*** *(—) and* ***4-4(OH$_2$)*** *(—) in TFE.Bottom:* ***4-5^{Ca}*** *(—),* ***4-5^{Sr}*** *(—), and* ***4-5^{Ba}*** *(—) in TFE. Scan rate = 100 mV/s.*

Table 4-2. Electrochemical data.[a]

Compound	Solvent	E_{anodic} (mV)	$E_{cathodic}$ (mV)	$E_{½}$ (mV)
3-1(OH_2)	CH_2Cl_2 (TFE)	+125 (+465)	+30 (+380)	+78 (+422)
3-1[b]	CH_2Cl_2	+395	---[c]	*irr.*[d]
4-4(OH_2)	CH_2Cl_2 (TFE)	+95 (+450)	–40 (+335)	+28 (+392)
4-4[b]	CH_2Cl_2	+335	+230	+282
4-5^{Ca}	TFE	*multiple*[e]	+405[f]	*irr.*[d]
4-5^{Sr}	TFE	*multiple*[e]	+385[f]	*irr.*[d]
4-5^{Ba}	TFE	*multiple*[e]	+370[f]	*irr.*[d]

[a] *Scan rate = 100 mV/s with [^{n}Bu$_4$N][PF_6] as the supporting electrolyte. All values vs. Fc/Fc$^+$. See* ***Error! Reference source not found.*** *for electrochemical traces.* [b] *Features of aqua complexes consistently appear as minor impurities, likely arising from adventitious H_2O in the experimental setup.* [c] *The return oxidation wave of* ***3-1*** *is not discernible.* [d] *Electrochemically irreversible, but cycling current does not result in changes to the voltammogram (chemically reversible).* [e] *Multiple oxidation events.* [f] *Position of final (lowest-potential) reduction wave.*

We next interrogated how the position of the Co^{II}/Co^{III} redox couple was affected by the presence and identity of a second-sphere Group II ion by examining the electrochemical properties of the members of the **4-5^{M}** series (M = Ca, Sr, and Ba).[69] These species are not soluble in CH_2Cl_2, but they are soluble in 2,2,2-trifluoroethanol (TFE). We therefore examined the electrochemical behavior of **3-1(OH_2)** and **4-4(OH_2)** in TFE to benchmark the **4-5^{M}** data. We were unable to measure the electrochemical properties of **3-1** and **4-4** in TFE because UV-vis indicated that these complexes were always 5-coordinate in TFE and

electrochemical studies of these compounds in TFE provided data that matched the hydrated species, indicating either that these species bind residual water in the TFE despite distillation from $MgSO_4$ or that TFE occupies the fifth coordination site on Co^{II} in these compounds. Nevertheless, all **4-5^{M}** species explored maintained a four-coordinate geometry at cobalt by absorption spectroscopy (Figure 4-6), suggesting that these species remain intact in solution to the extent that they prevent coordination of H_2O or TFE to the Co^{II} ions. As seen in Table 4-2, solvent has a strong effect on the position of the Co^{II}/Co^{III} redox couple in **4-4(OH$_2$)** (+28 mV in CH_2Cl_2 and +390 mV in TFE), likely reflecting hydrogen bonding between TFE and the sulfonyl oxygens that pulls electron density away from the anionic nitrogen donors. The cyclic voltammograms of the members of the **4-5^{M}** series are distinct from the voltammogram of **4-4(OH$_2$)** even in the presence of a large excess of $[^{n}Bu_4N]^+$, suggesting that these **4-5^{M}** species are not ionized in TFE. The voltammograms of **4-5^{M}** species are complicated by the presence of multiple oxidation events, which is consistent with the **M2$_2$** species remaining intact in solution. However, the final return reduction events of **4-5^{Ca}**, **4-5^{Sr}**, and **4-5^{Ba}** (Table 4-2) approach the position of the return reduction event of **4-4(OH$_2$)** in TFE, where **4-5^{Ba}** is the closest and **4-5^{Ca}** is the furthest of this series. This suggests that (1) the identity of the metal ion affects the potential of the return reduction event indicating that these redox-inert metal ions remain in close contact to the $[(Bus_3tren)Co^{II})]^-$ ions throughout the electrochemical event, and (2) electrochemical oxidation results in occupation of the fifth coordination site on the electrophilic four-coordinate Co^{III} centers either by water or TFE. Electrochemical cycling experiments indicate that the overall processes are all chemically reversible, so the complexity of the oxidation events likely reflects reversible and oxidation-state-dependent

occupation of the fifth coordination site on cobalt, although mixed valency and partial disruption of M---OS interactions may also play a role. From these data, we see that the interactions between the M^{2+} ion and the $[(Bus_3tren)Co^{II})]^-$ units are still present in solution, although it is unclear whether these interactions are the same as in the solid-state structures.

4.3.4 Absorption Spectroscopy of Trimetallic Complexes

We next turned to electronic absorption spectroscopy to probe the extent to which the Co^{II} ions in the **4-5^{M}** series remain four-coordinate in solution. **4-4** and **4-4(OH$_2$)** are clearly distinguishable by their electronic absorption profiles in CH_2Cl_2 (Figure 4-6), most notably by the presence of a transition of the anhydrous species at 414 nm that is absent in the hydrated species, providing a benchmark for assessing the coordination number of the cobalt ions in the members of the **4-5^{M}** series in solution. As described above, **4-5^{Ca}**, **4-5^{Sr}**, and **4-5^{Ba}** are all soluble in TFE but are insoluble in CH_2Cl_2. Consistent with our electrochemical studies, dissolution of **4-4** in TFE furnishes an absorption spectrum that is indistinguishable from the absorption spectrum of **4-4(OH$_2$)** in TFE, suggesting that **4-4** is binding either residual water from the TFE or TFE itself in the fifth coordination site of Co^{II}. However, the positions of the peaks of **4-4(OH$_2$)** are nearly solvent independent (no solvatochromism), giving us confidence in our ability to distinguish between the spectra of four- and five-coordinate Co^{II} species in both CH_2Cl_2 and TFE.

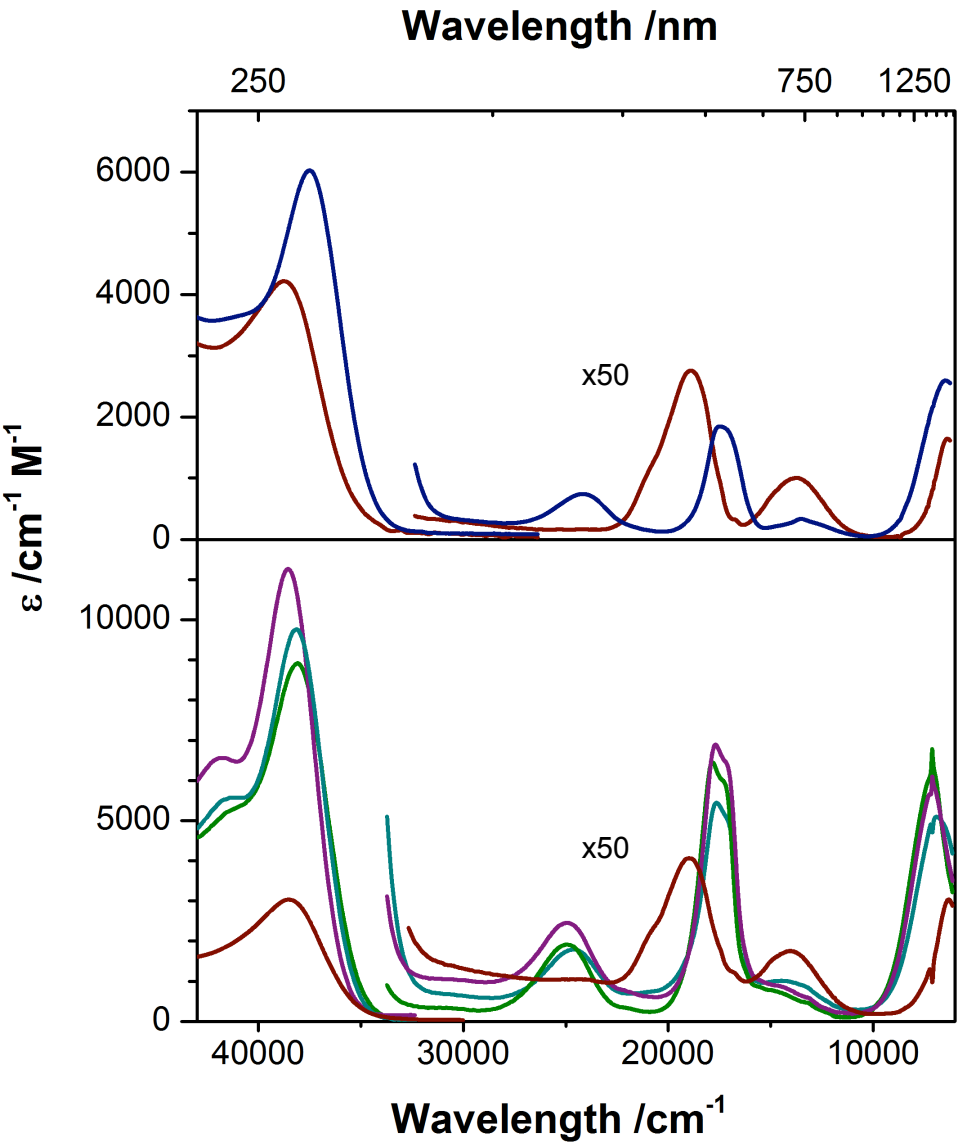

Figure 4-6. Electronic absorption spectra of ***4-4*** *(—) and* ***4-4(OH$_2$)*** *(—) in CH_2Cl_2 (top); and* ***4-4(OH$_2$)*** *(—),* ***4-5^{Ca}*** *(—),* ***4-5^{Sr}*** *(—), and* ***4-5^{Ba}*** *(—) in TFE (bottom).*

All three soluble members of the **4-5^{M}** series give nearly identical electronic absorption spectra in TFE, and these spectra clearly align with the spectrum of **4-4** in CH_2Cl_2, including the presence of a transition around 400 nm, indicating that four-coordinate Co^{II} centers are present in each sandwich complex even though no efforts were made to dry the TFE and the samples were prepared open to air. Given our inability to obtain spectra of **4-**

4 in TFE, the presence of four-coordinate Co^{II} ions in the members of the **4-5^{M}** series indicates that $[(Bus_3tren)Co^{II})]^-$ binds preferentially to the Group II ions examined instead of water, and that these interactions between $[(Bus_3tren)Co^{II})]^-$ and M^{2+} prevent H_2O or TFE coordination at Co^{II}. Furthermore, the positions of the d-d bands are largely unaffected by the identity of the countercation ($[^nBu_4N]^+$, Ca^{2+}, Sr^{2+}, or Ba^{2+}), even though the electrochemical properties of $[(Bus_3tren)Co^{II})]^-$ are affected by the identity of the counteraction (Figure 4-5, Table 4-2). Taken together, the electrochemical and electronic absorption data reveal that **4-5^{M}** species are not ionized in solution, but retain four coordinate Co^{II} ions and interactions between the Group II ions and $[(Bus_3tren)Co^{II})]^-$ even in wet TFE.

4.3.4 Hydration Stability of Trimetallic Complexes

In an effort to quantify the extent to which the **4-5^{M}** and **4-1** species remain intact in solutions containing H_2O, we explored the hydration reactivity of the four-coordinate Co^{II} ions in samples of **4-5^{M}** and **Ca1$_2$** in dried TFE by titrating H_2O and measuring the change in absorption profile consistent with conversion from four- to five-coordinate Co^{II} (Section 4.5.4). Figure 4-7 shows the decay of four-coordinate Co^{II} upon titration with H_2O, and we have verified that the product in each case corresponds to five-coordinate Co^{II} derived from hydration of the Co^{II} ion. As shown in Figure 4-7, there is a strong dependence of the extent of hydration of **4-5^{M}** and **4-1** on the identity of both the redox-inert metal ion and the ligand (aryl- vs. alkylsulfonamide). Both **4-5^{Ca}** and **4-5^{Sr}** contain essentially all four-coordinate Co^{II} ions in dried TFE, whereas both **4-5^{Ba}** and **4-1** contain both four- and five-coordinate Co^{II} ions in dried TFE. The extent of hydration in the **4-5^{M}** series is strongly dependent on the nature of M, where hydration of **4-5^{Ca}** is most difficult (half of the Co^{II} ions are five-

coordinate when 209 equivalents of H_2O are added), followed by hydration of **4-5^{Sr}** (half of the Co^{II} ions are five-coordinate when 116 equivalents of H_2O are added), and **4-5^{Ba}** is already a mixture of four- and five-coordinate Co^{II} species in the absence of added H_2O, consistent with Ca^{2+} having the strongest interaction with the sulfonyl oxygens and Ba^{2+} having the weakest. While the extent of hydration is dependent on the identity of the redox-inert metal ion in the **4-5^{M}** series, the starkest difference in hydration is derived from changing the ligand from an arylsulfonamide ligand in **4-1** ($[Ts_3tren]^{3-}$) to an alkylsulfonamide ligand in **4-5^{Ca}** ($[Bus_3tren]^{3-}$), where hydration of **4-1** occurs much more readily than hydration of **4-5^{Ca}**. This is consistent with the solid-state behavior of members of **4-1** and the **4-5^{M}** series, where isostructural members of the **4-5^{M}** series were accessible for M = Mg^{2+}, Ca^{2+}, Sr^{2+} and Ba^{2+}, whereas with $[(Ts_3tren)Co^{II})]^-$ anions, the only accessible sandwich compound was **4-1**. The relative ease of hydration of **4-1** and **4-5^{Ca}** is also a clear indication that the alkylsulfonyl oxygens are more electron rich than arylsulfonyl oxygens, and accordingly bind Ca^{2+} more tightly. Taken together, the solid-state, solution-phase, and redox behavior of Co^{II} ions in complexes of $[(Ts_3tren)Co^{II})]^-$ and $[(Bus_3tren)Co^{II})]^-$ reveal that $[Bus_3tren]^{3-}$ is a significantly improved ligand for interactions with second-sphere redox-inert metal ions than $[Ts_3tren]^{3-}$.

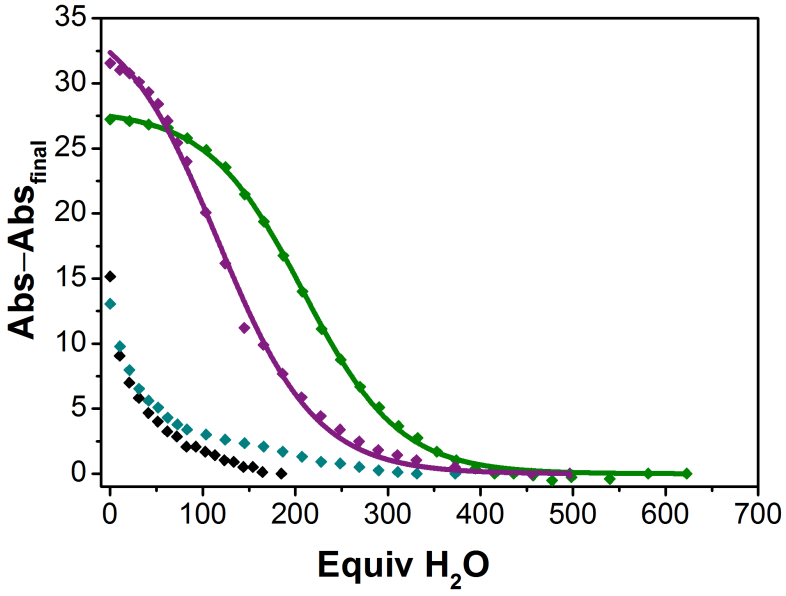

*Figure 4-7. Decay of four-coordinate Co^{II} ions in **4-5^{Ca}** (◆), **4-5^{Sr}** (◆), **4-5^{Ba}** (◆) and **Ca1$_2$** (◆) into five-coordinate Co^{II} in TFE with added water. Abs–Abs$_{final}$ represents the absorption of **4-5^{Ca}** at 401 nm, **4-5^{Sr}** at 401 nm, **4-5^{Ba}** at 406 nm, and **4-1** at 406 nm as a function of added equivalents of H_2O, with the final absorption value for each species subtracted from each point. The curves for **4-5^{Ca}** and **4-5^{Sr}** are fits to the data using sigmoidal logistic functions (see Section 4.5.4).*

4.4 Conclusions

We have detailed the synthesis of novel heterotrimetallic sandwich complexes involving two Co^{II} ions bridged by redox-inert metal ions (Mg^{2+}, Ca^{2+}, Sr^{2+}, and Ba^{2+}). These **4-5^{M}** assemblies, which are made readily accessible by the new ligand $[Bus_3tren]^{3-}$, are isostructural across the entire series. Furthermore, electrochemical and electronic absorption studies indicate that **4-5^{Ca}**, **4-5^{Sr}**, and **4-5^{Ba}** retain interactions between the Group II ions and $[(Bus_3tren)Co^{II})]^{-}$ in solution. The solid-state, solution-phase, and redox behavior of members of the **4-5^{M}** series compared to related complexes derived from $[(Ts_3tren)Co^{II})]^{-}$ demonstrates the improved properties of alkylsulfonamide ($[Bus_3tren]^{3-}$)

vs. arylsulfonamides ($[Ts_3tren]^{3-}$) ligands for formation of discrete heterotrimetallic sandwich complexes. These results highlight the rational design of complex heterotrimetallic clusters with significant solution integrity, and open the door to the exploration of the effect of Group II ions on reactivity at the open coordination site of Co^{II} in these systems. Furthermore, these results demonstrate the increased electron density of the sulfonyl oxygen atoms on the novel alkyl-sulfonamido ligand $[Bus_3tren]^{3-}$. Metal complexes of this ligand should increase the binding strength of protic ligands such as H_2O_2.

4.5 Experimental

4.5.1 Materials and Methods

Elemental analyses were performed by Atlantic Microlabs in Norcross, GA. IR spectra were obtained using a Nicolet 380 FT-IR with Smart Orbit Diamond ATR attachment. All room temperature ^{1}H-NMR and ^{13}C-NMR spectra were obtained on a 400MHz or 500MHz instrument and referenced to residual solvent. Mass spectrometric analysis was collected by Emory University Mass Spectrometry Center using electrospray ionization on a Thermo Finnigan LTQ-FTMS instrument. Magnetic susceptibility was measured with Evan's method on a 500MHz NMR spectrometer. X-ray crystallographic data was collected and analyzed by the Emory University Department of Chemistry X-Ray Crystallography Center. All reactions sensitive to air and/or moisture were carried out in an MBraun UNIlab glovebox under a nitrogen atmosphere. Solvents for use in the glovebox were degassed by evacuation and purging with nitrogen and dried using 3Å molecular sieves. Reagents were purchased from Sigma-Aldrich, Fisher Scientific, Acros Organics, Oakwood Chemicals, or Strem Chemicals and used without further purification. 15-crown-5•$Mg(OTf)_2$[70] was

synthesized using previously published methods. *tert*-butyl *tert*-butanethiosulfinate was synthesized according literature procedure[71] with the following change: after drying the solution of thiosulfinate in dichloromethane with sodium sulfate, the solvent was removed under vacuum. This thiosulfinate was then used to make *tert*-butylsulfinyl chloride according to another published procedure.[65]

4.5.2 Syntheses

$[Ca^{2+}][(Ts_3tren)Co^{II})]_2$ {4-1}

Under nitrogen, **3-1(OH_2)** (2.05g, 2.2mmol) was dissolved in 10 mL glyme with a few drops of methanol and dried overnight with 3Å molecular sieves. This solution was filtered into a vial and $Ca(OTf)_2$ (488mg, 1.4mmol) in methanol was added. The tightly-capped vial was heated to 85°C, while periodically releasing pressure manually as blue crystals formed and the supernatant lightened. When most of the color of the solution had bleached, the supernatant was decanted and the crystals washed with glyme and ether. The crystals were then dried under vacuum. A few crystals taken from the mixture after washing with ether and before drying were found suitable for analysis by X-ray crystallography (1.06g, 70% yield). Anal. calcd (found) for ($C_{54}H_{66}CaCo_2N_8O_{12}S_6$): C, 47.36 (47.21); H, 4.86 (4.97); N, 8.18 (8.04). UV–vis (TFE, ε in $M^{-1}cm^{-1}$): 222 (58,800), 406 (25), 561 (89), 700 (26) and 1439 (94). IR (FT-ATR, cm^{-1}): 2903, 2858, 1560, 1496, 1446, 1400, 1342, 1253, 1116, 1081, 1035, 972, 916, 868, 810, 735, 708, 664, 606, 549. ESMS: Exact mass calcd for $C_{27}H_{35}CaCoN_4O_7S_3^+$ [$ML^- + H_2O + Ca^{2+}$], 722.06203. Found: 722.06202 (Δ = 0.01 ppm). Exact mass calcd for $C_{27}H_{37}CaCoN_4O_8S_3^+$ [$ML^- + 2H_2O + Ca^{2+}$], 740.07259. Found: 740.07259 (Δ = 0.0 ppm). Magnetic susceptibility (Evan's method, TFE-d_3): μ_{obs} = 5.82 μ_B.

$[Sr^{2+}]$ $[(Ts_3tren)Co^{II})]_2(H_2O)_{1.5}$ {4-2}

3-1(OH_2) (85mg, 0.092mmol) and Sr(OTf)•H_2O (18mg, 0.046mmol) were mixed in 2 mL of acetone and evaporated to dryness. The pink residue was dissolved in 2 mL of acetonitrile with minimal methanol and heated to 80˚C overnight. The purple crystals were washed with dichloromethane, acetonitrile, and ether and dried under vacuum to yield purple crystalline product (15mg, 23% yield). Anal. calcd (found) for ($C_{54}H_{69}Co_2N_8O_{13.5}S_6Sr$): C, 44.92 (44.54); H, 4.82 (4.76); N, 7.76 (7.74). UV–vis (TFE, ε in $M^{-1}cm^{-1}$): 222 (52,900), 411 (26), 561 (91), 690 (20) and 1421 (107). IR (FT-ATR, cm^{-1}): 2911, 2856, 1600, 1496, 1446, 1398, 1246, 1126, 1079, 1040, 1020, 979, 928, 873, 811, 734, 708, 663, 601, 580, 549. ESMS: Exact mass calcd for $C_{27}H_{33}CoN_4O_6S_3^-$ [ML^-], 664.08997. Found: 664.08670 (Δ = 4.9 ppm).

$[Ba^{2+}][(Ts_3tren)Co^{II})]_2$•$3H_2O$

3-1(OH_2) (493mg, 0.53mmol) and $Ba(OTf)_2$ (116mg, 0.27mmol) were dissolved separately in acetone. The barium-containing solution was added to the cobalt solution and solution left open to air. A pink powder precipitated from solution, which was collected by filtration, washed with cold acetone and ether, and dried on the filter to afford pink BaCoTs•$(H_2O)_3$ (235mg, 58%). Anal. Calcd for $C_{54}H_{66}BaCo_2N_8O_{12}S_6$: C, 42.65 (42.36); H, 4.77 (4.69); N, 7.37 (7.24). UV–vis (TFE, ε in $M^{-1}cm^{-1}$): 222 (56,400), 404 (29), 563 (103), 694 (18) and 1391 (103). IR (FT-ATR, cm^{-1}): 3514 (ν_{OH}), 2954, 2904, 2856, 1599, 1495, 1447, 1399, 1352, 1246, 1220, 1207, 1139, 1115, 1073, 1038, 970, 933, 879, 812, 742, 708, 661, 600. ESMS: Exact mass calcd for $C_{18}H_{39}CoN_4O_6S_3^-$ [ML^-], 664.08997 (Δ =). Found: 664.08997 (Δ = 0.0 ppm). Magnetic susceptibility (Evan's method, TFE-d_3): μ_{obs} = 6.03 μ_B.

$[Ba^{2+}]_2[(Ts_3tren)Co^{II})]_4Ba1_2•3H_2O$ {4-3}

In a glovebox, $[Ba^{2+}][(Ts_3tren)Co^{II})]_2•3H_2O$ was dissolved in dichloromethane and dehydrated using 3Å molecular sieves. After sitting overnight the solution was filtered through celite and layered under ether, forming blue X-ray quality crystals.

H_3Bus_3tren

An oven-dried 250 mL flask was charged with a dry stir bar, cooled under vaccum, and filled with 100 mL of anhydrous dichloromethane under nitrogen. To this flask, *tert*-butyl sulfinyl chloride (33.7g, 240mmol) was added via cannula at –78˚C. Tris(2-aminoethyl)amine (H_6tren) (11.6 mL, 77mmol) and triethylamine (35.6 mL, 255mmol) were mixed in anhydrous dichloromethane (40 mL) in a separate dry flask under nitrogen and added to the reaction vessel via cannula. After addition, the flask was stirred overnight under nitrogen and allowed to slowly warm to room temperature. The organic mixture was then washed with saturated aqueous sodium bicarbonate solution (3×200 mL), brine (200 mL), and dried over magnesium sulfate. The drying agent was filtered away and the filtrate concentrated via rotary evaporation. Pentane was added to precipitate the sulfinamide product. Yield: 34%. The proton NMR spectrum of this product indicates asymmetry consistent with the presence of three chiral sulfur centers in the same molecule, where the relative stereochemistry at each sulfur is random. Mass spectrometry of the precipitated product indicated the correct mass (ESMS: Exact mass calcd for $C_{18}H_{43}N_4O_3S_3^+$ [M + H], 459.24918. Found: 459.24877 (Δ = 0.9 ppm)) and this product was used in the next step without further purification. The crude mixture can be recrystallized with dichloromethane and pentane to afford a crystalline isomer(s) with a complex but well-defined splitting pattern (see page S8). The trisulfinamide product (4.9g, 10.6mmol) was stirred in 40 mL

dichloromethane at 0˚C open to the air. To this stirred solution, 3-chloroperbenzoic acid (*m*-CPBA, 10.7g, 77% mixture, 48mmol active oxidant) was added carefully to control bubbling. The reaction was stirred for 5 minutes and was quenched with 40% aqueous sodium bisulfite solution and stirred for another 5 minutes. This mixture was extracted with dichloromethane and the organic layer was washed with aqueous sodium bicarbonate (2×100 mL), brine (100 mL), and dried over magnesium sulfate. The drying agent was filtered away and the filtrate concentrated to dryness under rotary evaporation. Drying further under vacuum yielded an off-white solid (4.0g, 75% yield). IR (FT-ATR, cm^{-1}): 3262 (ν_{NH}), 2944, 2811, 1455, 1431, 1398, 1367, 1292, 1207, 1110, 1078, 1050, 1028, 950, 927, 894, 825, 814, 793, 732, 662, 565. δH(500 MHz; CDCl3) 1.39 (27 H, s, tBu), 2.59 (6 H, t, NCH_2), 3.27 (6 H, s, $BusNCH_2$) and 5.7 (3 H, t, NH). δC(125 MHz; CDCl3) 24.2, 42.0, 55.0, 60.0. ESMS: Exact mass calcd for $C_{18}H_{43}N_4O_6S_3^+$ [M + H], 507.23392. Found: 507.23400 (Δ = 0.2 ppm).

[^{n}Bu$_4$N][(Bus$_3$tren)Co^{II}(OH$_2$)] {4-4(OH$_2$)}

In a schlenck flask, H_3Bus_3tren (5.27g, 10.4mmol) and $CoCl_2$ (1.35g, 10.4mmol) were stirred in 40 mL DMA under nitrogen. KH (1.29g, 32.2mmol) was added in portions carefully to keep bubbling to a minimum, and the solution turned from blue to turquoise. After stirring overnight, the solution had turned purple, and Bu_4NBr (3.36g, 10.4mmol) was added with a few drops of methanol to quench any residual hydride base. The reaction mixture was diluted with CH_2Cl_2 (200 mL), and washed with water (3×200 mL) and brine (200 mL). The organic layer was dried with Na_2SO_4, filtered and concentrated under rotary evaporation. Addition of diethyl ether afforded purple flaky product (4.0g, 47% yield). Vapor diffusion of ether into a CH_2Cl_2 solution of the product afforded flaky purple crystals

suitable for X-ray diffraction analysis. Anal. calcd (found) for ($C_{34}H_{77}CoN_5O_7S_3$): C, 49.61 (49.88); H, 9.43 (9.44); N, 8.51 (8.29). UV–vis (TFE, ε in $M^{-1}cm^{-1}$): 260 (3,070), 527 (47) and 1587 (31). IR (FT-ATR, cm^{-1}): 3332 (ν_{OH}), 2960, 2874, 1479, 1455, 1386, 1358, 1277, 1229, 1161, 1121, 1105, 1079, 1063, 1038, 971, 959, 922, 887, 858, 813, 799, 737, 667, 590, 542. ESMS: Exact mass calcd for $C_{18}H_{39}CoN_4O_6S_3^-$ [ML^-], 562.13692. Found: 562.13708 (Δ = 0.3 ppm). Exact mass calcd for $C_{52}H_{114}Co_2N_9O_{12}S_6^-$ [$2ML^- + Bu_4N^+$], 1366.55807. Found: 1366.55703 (Δ = 0.8 ppm). Exact mass calcd for $C_{18}H_{39}CoN_4O_6S_3^-$ [$ML^- + Bu_4N^+ + H_2O - e^-$], 822.43116. Found: 822.43413 (Δ = 3.6 ppm). Exact mass calcd for $C_{50}H_{111}CoN_6O_6S_3^+$ [$ML^- + 2Bu_4N^+$], 1046.70537. Found: 1046.70848 (Δ = 3.0 ppm). Magnetic susceptibility (Evan's method, $CDCl_3$): $\mu_{obs} = 4.12\ \mu_B$.

[^{n}Bu$_4$N][(Bus$_3$tren)Co^{II}] {4-4}

In a glovebox, **4-4(OH$_2$)** was dissolved in dichloromethane with 3Å molecular sieves. After sitting overnight the solution was filtered through celite and layered under ether. Blue crystals were formed which were suitable for X-ray diffraction analysis. UV–vis (CH_2Cl_2, ε in $M^{-1}cm^{-1}$): 267 (6,030), 414 (15), 571 (37), 741 (7) and 1543 (52). Magnetic susceptibility (Evan's method, $CDCl_3$): $\mu_{obs} = 4.40\ \mu_B$.

[Mg^{2+}][(Bus$_3$tren)Co^{II})]$_2$ {4-5^{Mg}}

4-4(OH$_2$) (72mg, 0.088mmol) and 15-crown-5 $Mg(OTf)_2$ adduct (24mg, 0.044mmol) were stirred in acetonitrile at 65°C. Crystals slowly formed as the solution lightened in color. When the solution stopped lightening, the supernatant was decanted from the crystals and the crystals were washed with dichloromethane and dried under vacuum to yield blue crystalline product. Although these crystals were found to be insoluble in traditional organic solvents, some of the crystals were found to be suitable for X-ray diffraction

analysis (33mg, 65% yield). Anal. Calcd for $C_{36}H_{78}MgCo_2N_8O_{12}S_6$: C, 37.61 (37.91); H, 6.84 (6.93); N, 9.75 (9.76). IR (FT-ATR, cm^{-1}): 2909, 2865, 1478, 1461, 1393, 1365, 1333, 1274, 1244, 1224, 1141, 1080, 1032, 964, 913, 857, 816, 805, 726, 669, 614, 559, 542.

$[Ca^{2+}][(Bus_3tren)Co^{II})]_2$ {4-5^{Ca}}

4-4(OH_2) (478mg, 0.58mmol) was dissolved in 120 mL methanol at 60˚C, and $Ca(OTf)_2$ (98mg, 0.29mmol) was dissolved separately in 5 mL methanol at 60˚C. The calcium solution was added dropwise into the cobalt solution without stirring. The reaction solution was maintained at 60˚C, promoting formation of crystals concomitant bleaching of the supernatant. When the solution stopped losing color, the supernatant was decanted and the remaining blue crystals were washed with ether and dried under vacuum. Before drying, some blue crystals were examined by X-ray crystallography. If the methanol solution was too concentrated or too cool, a blue powder came out of solution. This powder has the same composition as the crystalline samples as shown by elemental analysis (280mg, 83% yield). Anal. Calcd for $C_{36}H_{78}CaCo_2N_8O_{12}S_6$: C, 47.4 (47.5); H, 4.9 (4.75); N, 8.2 (8.05). UV–vis (TFE, ε in $M^{-1}cm^{-1}$): 240 (6,560), 260 (11,200), 401 (38), 560 (129) and 1405 (136). IR (FT-ATR, cm^{-1}): 2906, 2864, 1479, 1393, 1363, 1335, 1272, 1244, 1227, 1133, 1075, 1032, 966, 914, 860, 815, 727, 673, 611, 561. ESMS: Exact mass calcd for $C_{18}H_{41}CaCoN_4O_7S_3^+$ [$ML^- + H_2O + Ca^{2+}$], 620.10898. Found: 620.10939 (Δ = 0.7 ppm). Magnetic susceptibility (Evan's method, TFE-d_3): μ_{obs} = 6.18 μ_B.

$[Sr^{2+}][(Bus_3tren)Co^{II})]_2$ {4-5^{Sr}}

4-4(OH_2) (119mg, 0.15mmol) and $Sr(OTf)_2 \bullet H_2O$ (29mg, 0.07mmol) were dissolved separately in acetone, and these solutions were mixed. A blue powder formed, which was allowed to settle. This blue powder was triturated with methanol and ether, and then dried

under vacuum. Vapor diffusion of ether into a solution of this solid in dichloromethane and methanol afforded X-ray quality crystals (81mg, 92% yield). Anal. Calcd for $C_{36}H_{78}Co_2N_8O_{12}S_6Sr$: C, 35.65 (35.65); H, 6.48 (6.43); N, 9.24 (9.12). UV–vis (TFE, ε in $M^{-1}cm^{-1}$): 240sh (5,550), 262 (9,760), 401 (49), 565 (138) and 1405 (122). IR (FT-ATR, cm^{-1}): 2966, 2901, 2864, 1470, 1455, 1392, 1363, 1335, 1272, 1229, 1129, 1072, 1033, 965, 918, 861, 815, 739, 728, 675, 666, 607, 594, 563. ESMS: Exact mass calcd for $C_{18}H_{39}CoN_4O_6S_3Sr^+$ [$ML^- + Sr^{2+}$], 650.04144. Found: 650.04186 (Δ = 0.6 ppm). Exact mass calcd for $C_{18}H_{41}CoN_4O_7S_3Sr^+$ [$ML^- + H_2O + Sr^{2+}$], 668.05200. Found: 668.05233 (Δ = 0.5 ppm). Magnetic susceptibility (Evan's method, TFE-d_3): $\mu_{obs} = 6.12\ \mu_B$.

$[Ba^{2+}][(Bus_3tren)Co^{II})]_2$ {4-5^{Ba}}

4-4(OH_2) (97.0mg, 0.12mmol) and $Ba(OTf)_2$ (25.7mg, 0.06mmol) were dissolved in acetone and heated to 65˚C until supernatant stopped lightening and blue crystals stopped forming. The supernatant was decanted away, and the crystals were washed with ether and dried under vacuum to yield blue crystalline product. Vapor diffusion of ether into a solution of **4-5**^{Ba} in dichloromethane and methanol yielded crystals suitable for X-ray crystallography (57.0 mg, 75%yield). Anal. calcd for $C_{108}H_{138}Co_4N_{16}O_{27}S_{12}Sr_2$: C, 44.92 (44.54); H, 4.82 (4.76); N, 7.76 (7.74). UV–vis (TFE, ε in $M^{-1}cm^{-1}$): 241 (5,220), 263 (8,930), 406 (36), 567 (109) and 1446 (102). IR (FT-ATR, cm^{-1}): 2967, 2900, 2859, 1471, 1393, 1363, 1233, 1123, 1070, 1040, 966, 924, 862, 814, 739, 665, 593, 563. ESMS: Exact mass calcd for $C_{18}H_{39}CoN_4O_6S_3^-$ [ML^-], 562.13692. Found: 562.13584 (Δ = 1.9 ppm). Magnetic susceptibility (Evan's method, TFE-d_3): $\mu_{obs} = 6.10\ \mu_B$.

4.5.3 Electrochemistry

Cyclic voltammetric experiments were conducted in trifluoroethanol (TFE) or dichloromethane with 0.1M tetrabutylammonium hexafluorophosphate as supporting electrolyte and a glassy carbon working electrode. The reference electrode solution was made with $Ag(PF_6)$ in TFE or $Ag(NO_3)$ in acetonitrile for the dichloromethane solutions. For **3-1** and **4-4**, the experiments were performed inside a glovebox using anhydrous dichloromethane. The potential window was scanned at 0.1 V/s.

4.5.4 Water Titrations

Trifluoroethanol (TFE) was freshly distilled from calcium sulfate and sodium carbonate under nitrogen and degassed prior to use. Sandwich complexes were weighed out in a glovebox, dissolved in TFE and diluted to 5mL in volumetric flasks. A gas-tight syringe was used to dispense 3.5mL of each solution into a quartz cuvette fitted with a septum cap. Water was added to the cuvette in 5μL, 10μL, or 20μL increments from a gas-tight syringe. Each solution was scanned initially and inverted several times after each addition of water. For each complex, four wavelengths were chosen for data workup. For each wavelength, the smallest absorbance value was subtracted from the series of data points and these values were divided by the concentration of the sandwich complex in solution. These data were plotted versus equivalents of water added. The curves for **4-5**^{Ca} and **4-5**^{Sr} were fit to a sigmoidal logistic functions using Origin (below). The data for **4-1** and **4-5**^{Ba} could not be reasonably modeled.

$$y = \frac{a}{1 + e^{-k(x-c)}}$$

Table 4-3. Fitting parameters for ***4-5***^{Ca} *and* ***4-5***^{Sr}.

	a		c		k		Statistics	
	Value	**Error**	**Value**	**Error**	**Value**	**Error**	**Reduced Chi-Sqr**	**Adj. R-Square**
4-5^{Ca}	27.95	0.18	208.71	1.30	-0.01927	.00037	0.08362	0.99931
4-5^{Sr}	35.99	0.90	115.94	3.79	-0.01887	.00081	0.40771	0.99738

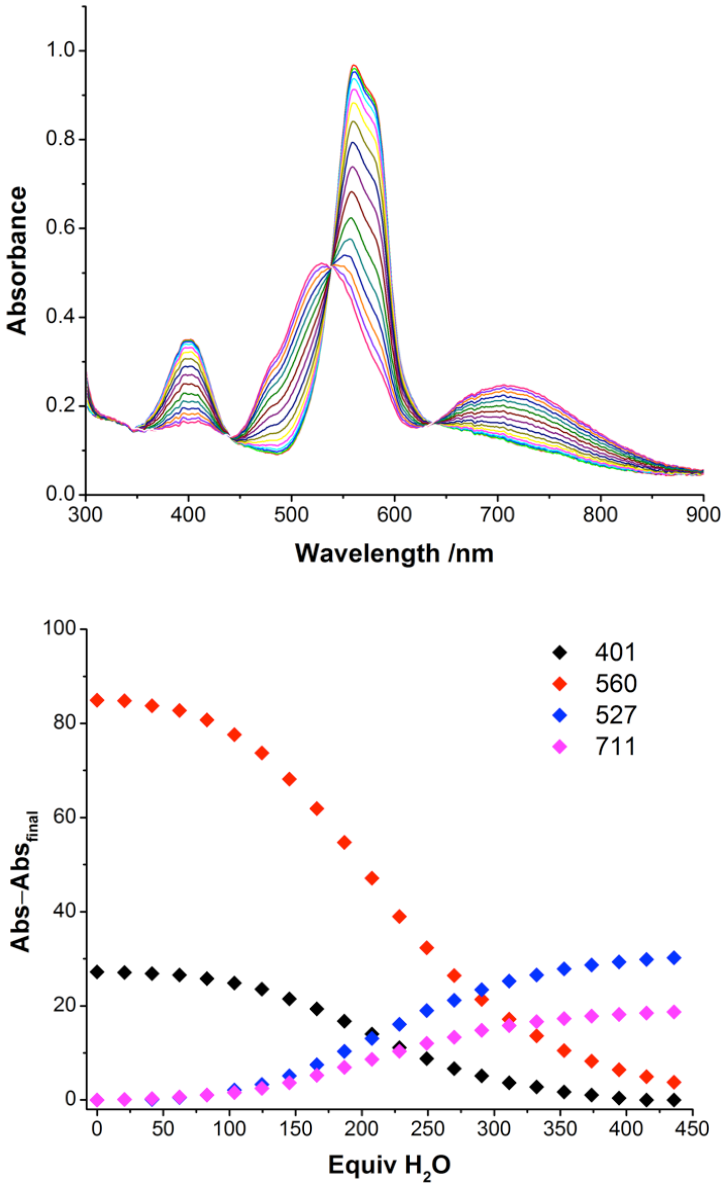

Figure 4-8. Titration of water with ***4-5***^{Ca} *UV-Vis traces (left) and titration curves (right).*

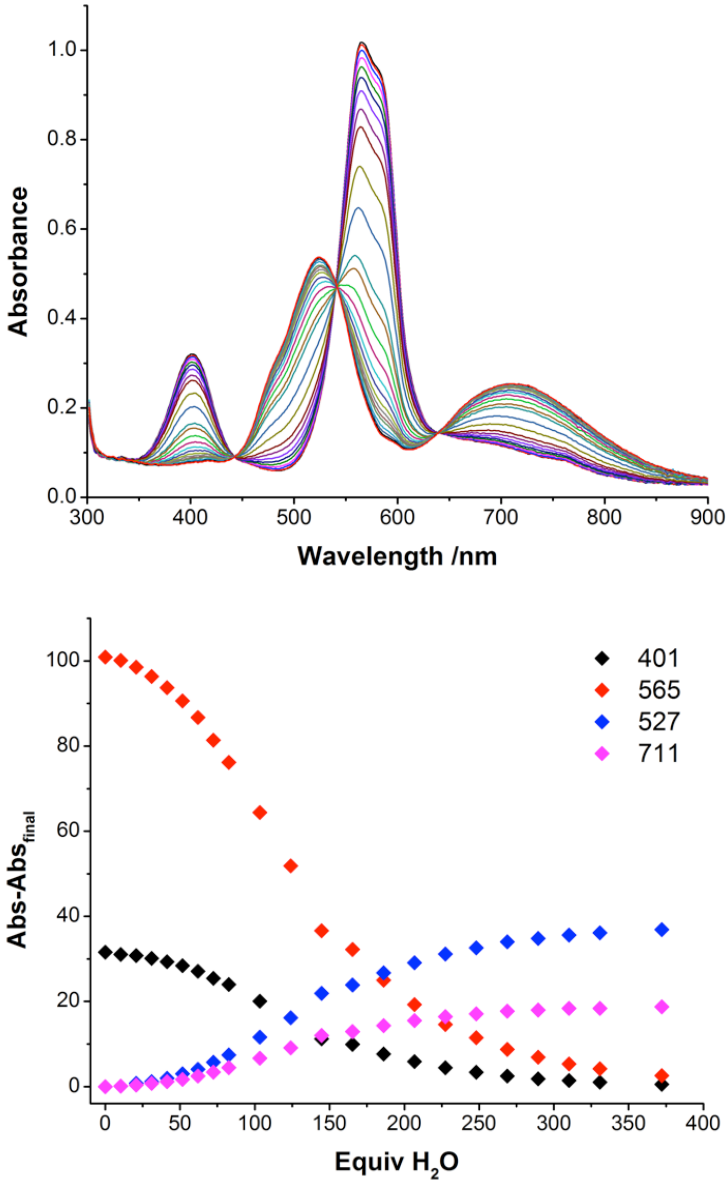

Figure 4-9. Titration of water with ***4-5***^{Sr} *UV-Vis traces (left) and titration curves (right).*

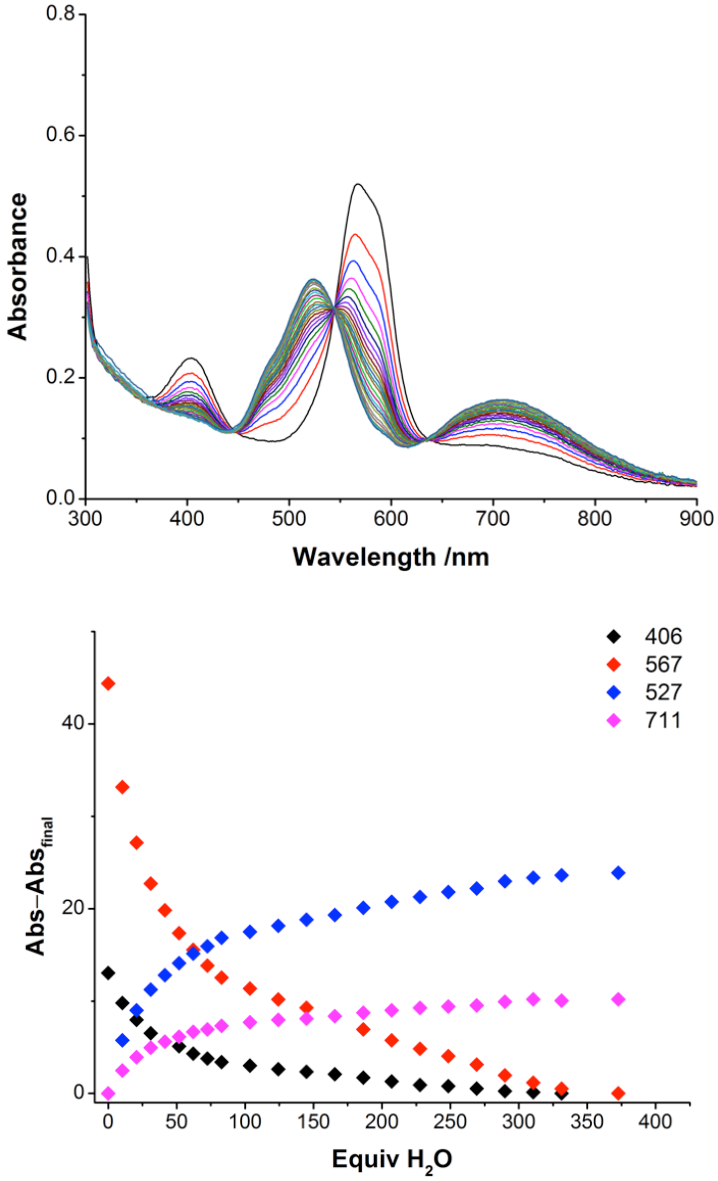

Figure 4-10. Titration of water with ***4-5***^{Ba} *UV-Vis traces (left) and titration curves (right).*

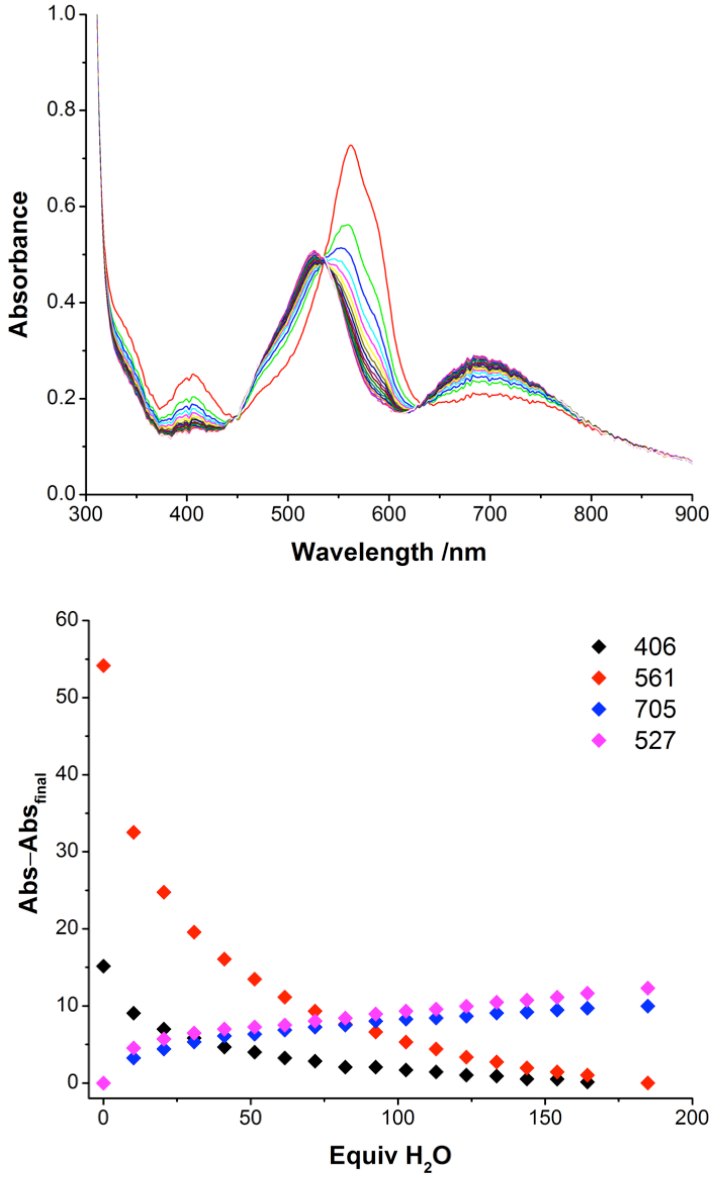

*Figure 4-11. Titration of water with **4-1** UV-Vis traces (left) and titration curves (right).*

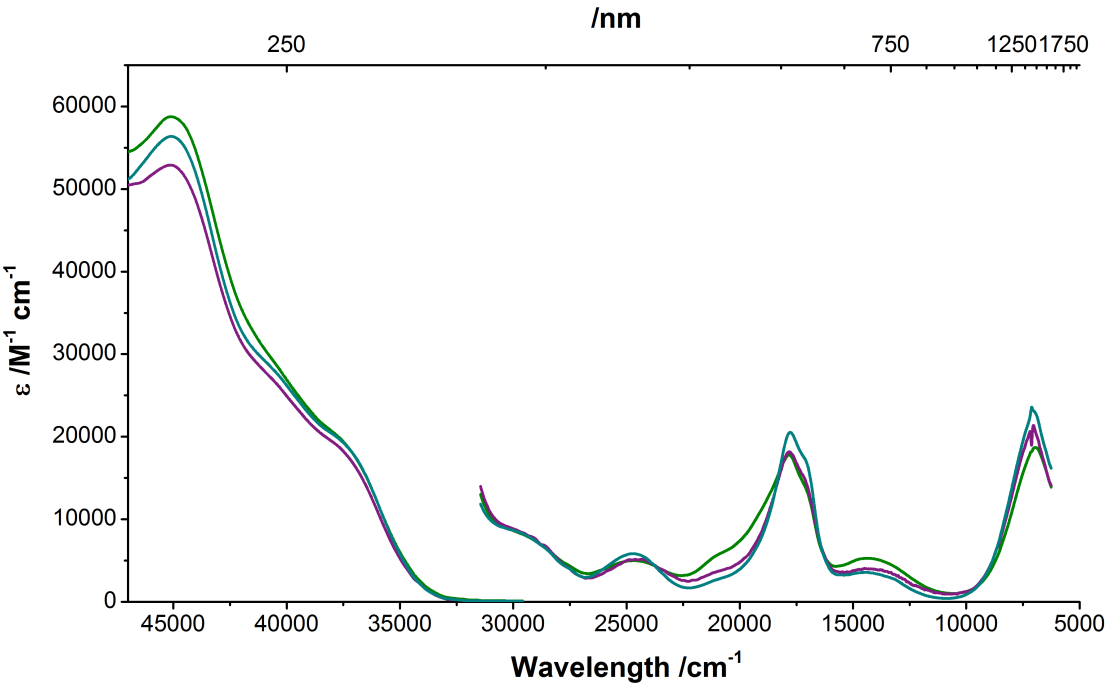

Figure 4-12. Absorption spectra of ***CaI_2*** *(—),* ***$SrI_2 \bullet (OH_2)_{1.5}$*** *(—), and* ***$BaI_2 \bullet (OH_2)_3$*** *(—) in trifluoroethanol.*

4.6 References

1. Jones, C. W., *Applications of of Hydrogen Peroxide and Derivatives*. Royal Society: Cambridge, U.K., 1999.

2. Lancaster, M., *Green Chemistry*. Royal Society: Cambridge, U.K., 2002.

3. Hage, R.; de Boer, J. W.; Gaulard, F.; Maaijen, K., Chapter Three - Manganese and Iron Bleaching and Oxidation Catalysts. In *Adv. Inorg. Chem.*, Rudi van, E.; Colin, D. H., Eds. Academic Press: 2013; Vol. Volume 65, pp 85-116.

4. Hage, R.; Lienke, A., Applications of Transition-Metal Catalysts to Textile and Wood-Pulp Bleaching. *Angew. Chem. Int. Ed.* **2006,** *45* (2), 206-222.

5. Russo, V.; Tesser, R.; Santacesaria, E.; Di Serio, M., Chemical and Technical Aspects of Propene Oxide Production via Hydrogen Peroxide (HPPO Process). *Ind. Eng. Chem. Res.* **2013,** *52* (3), 1168-1178.

6. DiPasquale, A. G.; Mayer, J. M., Hydrogen Peroxide: A Poor Ligand to Gallium Tetraphenylporphyrin. *J. Am. Chem. Soc.* **2008,** *130* (6), 1812-1813.

7. Mirza, S. A.; Bocquet, B.; Robyr, C.; Thomi, S.; Williams, A. F., Reactivity of the Coordinated Hydroperoxo Ligand. *Inorg. Chem.* **1996,** *35* (5), 1332-1337.

8. Wang, B.; Li, C.; Dubey, K. D.; Shaik, S., Quantum Mechanical/Molecular Mechanical Calculated Reactivity Networks Reveal How Cytochrome P450cam and Its T252A Mutant Select Their Oxidation Pathways. *J. Am. Chem. Soc.* **2015,** *137* (23), 7379-7390.

9. Ramanan, R.; Dubey, K. D.; Wang, B.; Mandal, D.; Shaik, S., Emergence of Function in P450-Proteins: A Combined Quantum Mechanical/Molecular Mechanical and Molecular Dynamics Study of the Reactive Species in the H2O2-Dependent Cytochrome P450SPα and Its Regio- and Enantioselective Hydroxylation of Fatty Acids. *J. Am. Chem. Soc.* **2016,** *138* (21), 6786-6797.

10. Anson, C. W.; Ghosh, S.; Hammes-Schiffer, S.; Stahl, S. S., Co(salophen)-Catalyzed Aerobic Oxidation of p-Hydroquinone: Mechanism and Implications for Aerobic Oxidation Catalysis. *J. Am. Chem. Soc.* **2016,** *138* (12), 4186-4193.

11. Chen, M.; Pan, Y.; Kwong, H.-K.; Zeng, R. J.; Lau, K.-C.; Lau, T.-C., Catalytic oxidation of alkanes by a (salen)osmium(vi) nitrido complex using H2O2 as the terminal oxidant. *Chem. Commun.* **2015,** *51* (71), 13686-13689.

12. Kwong, H.-K.; Lo, P.-K.; Lau, K.-C.; Lau, T.-C., Epoxidation of alkenes and oxidation of alcohols with hydrogen peroxide catalyzed by a manganese(v) nitrido complex. *Chem. Commun.* **2011,** *47* (14), 4273-4275.

13. Ma, L.; Pan, Y.; Man, W.-L.; Kwong, H.-K.; Lam, W. W. Y.; Chen, G.; Lau, K.-C.; Lau, T.-C., Highly Efficient Alkane Oxidation Catalyzed by [MnV(N)(CN)4]2–. Evidence for [MnVII(N)(O)(CN)4]2– as an Active Intermediate. *J. Am. Chem. Soc.* **2014,** *136* (21), 7680-7687.

14. Afanasiev, P.; Kudrik, E. V.; Millet, J.-M. M.; Bouchu, D.; Sorokin, A. B., High-valent diiron species generated from N-bridged diiron phthalocyanine and H2O2. *Dalton Trans*. **2011,** *40* (3), 701-710.

15. Theodoridis, A.; Maigut, J.; Puchta, R.; Kudrik, E. V.; van Eldik, R., Novel Iron(III) Porphyrazine Complex. Complex Speciation and Reactions with NO and H2O2. *Inorg. Chem*. **2008,** *47* (8), 2994-3013.

16. Wolak, M.; van Eldik, R., Mechanistic studies on peroxide activation by a water-soluble iron(III)-porphyrin: implications for O-O bond activation in aqueous and nonaqueous solvents. *Chemistry* **2007,** *13* (17), 4873-83.

17. Wallen, C. M.; Bacsa, J.; Scarborough, C. C., Hydrogen Peroxide Complex of Zinc. *J. Am. Chem. Soc*. **2015,** *137* (46), 14606-14609.

18. Wallen, C. M.; Palatinus, L.; Bacsa, J.; Scarborough, C. C., Hydrogen Peroxide Coordination to Cobalt(II) Facilitated by Second-Sphere Hydrogen Bonding. *Angew. Chem. Int. Ed*. **2016,** *55* (39), 11902-11906.

19. McEvoy, J. P.; Brudvig, G. W., Water-Splitting Chemistry of Photosystem II. *Chem. Rev*. **2006,** *106* (11), 4455-4483.

20. Cox, N.; Rapatskiy, L.; Su, J.-H.; Pantazis, D. A.; Sugiura, M.; Kulik, L.; Dorlet, P.; Rutherford, A. W.; Neese, F.; Boussac, A.; Lubitz, W.; Messinger, J., Effect of Ca2+/Sr2+ Substitution on the Electronic Structure of the Oxygen-Evolving Complex of Photosystem II: A Combined Multifrequency EPR, 55Mn-ENDOR, and DFT Study of the S2 State. *J. Am. Chem. Soc*. **2011,** *133* (10), 3635-3648.

21. Pushkar, Y.; Yano, J.; Sauer, K.; Boussac, A.; Yachandra, V. K., Structural changes in the Mn4Ca cluster and the mechanism of photosynthetic water splitting. *Proc. Natl. Acad. Sci*. **2008,** *105* (6), 1879-1884.

22. Mukhopadhyay, S.; Mandal, S. K.; Bhaduri, S.; Armstrong, W. H., Manganese Clusters with Relevance to Photosystem II. *Chem. Rev*. **2004,** *104* (9), 3981-4026.

23. Kanady, J. S.; Tsui, E. Y.; Day, M. W.; Agapie, T., A Synthetic Model of the Mn3Ca Subsite of the Oxygen-Evolving Complex in Photosystem II. *Science* **2011,** *333* (6043), 733-736.

24. Tsui, E. Y.; Agapie, T., Reduction potentials of heterometallic manganese–oxido cubane complexes modulated by redox-inactive metals. *Proc. Natl. Acad. Sci.* **2013,** *110* (25), 10084-10088.

25. Tsui, E. Y.; Tran, R.; Yano, J.; Agapie, T., Redox-inactive metals modulate the reduction potential in heterometallic manganese–oxido clusters. *Nat. Chem.* **2013,** *5* (4), 293-299.

26. Nayak, S.; Nayek, H. P.; Dehnen, S.; Powell, A. K.; Reedijk, J., Trigonal propeller-shaped [MnIII3MIINa] complexes (M = Mn, Ca): structural and functional models for the dioxygen evolving centre of PSII. *Dalton Trans.* **2011,** *40* (12), 2699-2702.

27. Kanady, J. S.; Mendoza-Cortes, J. L.; Tsui, E. Y.; Nielsen, R. J.; Goddard, W. A.; Agapie, T., Oxygen Atom Transfer and Oxidative Water Incorporation in Cuboidal Mn3MOn Complexes Based on Synthetic, Isotopic Labeling, and Computational Studies. *J. Am. Chem. Soc.* **2013,** *135* (3), 1073-1082.

28. Kanady, J. S.; Lin, P.-H.; Carsch, K. M.; Nielsen, R. J.; Takase, M. K.; Goddard, W. A.; Agapie, T., Toward Models for the Full Oxygen-Evolving Complex of Photosystem II by Ligand Coordination To Lower the Symmetry of the Mn3CaO4 Cubane: Demonstration That Electronic Effects Facilitate Binding of a Fifth Metal. *J. Am. Chem. Soc.* **2014,** *136* (41), 14373-14376.

29. Miller, C. G.; Gordon-Wylie, S. W.; Horwitz, C. P.; Strazisar, S. A.; Peraino, D. K.; Clark, G. R.; Weintraub, S. T.; Collins, T. J., A Method for Driving O-Atom Transfer: Secondary Ion Binding to a Tetraamide Macrocyclic Ligand. *J. Am. Chem. Soc.* **1998,** *120* (44), 11540-11541.

30. Fukuzumi, S.; Morimoto, Y.; Kotani, H.; Naumov, P.; Lee, Y.-M.; Nam, W., Crystal structure of a metal ion-bound oxoiron(IV) complex and implications for biological electron transfer. *Nat. Chem.* **2010,** *2* (9), 756-759.

31. Morimoto, Y.; Kotani, H.; Park, J.; Lee, Y.-M.; Nam, W.; Fukuzumi, S., Metal Ion-Coupled Electron Transfer of a Nonheme Oxoiron(IV) Complex: Remarkable Enhancement of Electron-Transfer Rates by Sc3+. *J. Am. Chem. Soc.* **2011,** *133* (3), 403-405.

32. Park, J.; Morimoto, Y.; Lee, Y.-M.; Nam, W.; Fukuzumi, S., Metal Ion Effect on the Switch of Mechanism from Direct Oxygen Transfer to Metal Ion-Coupled Electron Transfer in the Sulfoxidation of Thioanisoles by a Non-Heme Iron(IV)–Oxo Complex. *J. Am. Chem. Soc.* **2011,** *133* (14), 5236-5239.

33. Park, J.; Morimoto, Y.; Lee, Y.-M.; You, Y.; Nam, W.; Fukuzumi, S., Scandium Ion-Enhanced Oxidative Dimerization and N-Demethylation of N,N-Dimethylanilines by a Non-Heme Iron(IV)-Oxo Complex. *Inorg. Chem.* **2011,** *50* (22), 11612-11622.

34. Pfaff, F. F.; Kundu, S.; Risch, M.; Pandian, S.; Heims, F.; Pryjomska-Ray, I.; Haack, P.; Metzinger, R.; Bill, E.; Dau, H.; Comba, P.; Ray, K., An Oxocobalt(IV) Complex Stabilized by Lewis Acid Interactions with Scandium(III) Ions. *Angew. Chem. Int. Ed.* **2011,** *50* (7), 1711-1715.

35. Leeladee, P.; Baglia, R. A.; Prokop, K. A.; Latifi, R.; de Visser, S. P.; Goldberg, D. P., Valence Tautomerism in a High-Valent Manganese–Oxo Porphyrinoid Complex Induced by a Lewis Acid. *J. Am. Chem. Soc.* **2012,** *134* (25), 10397-10400.

36. Chen, J.; Lee, Y.-M.; Davis, K. M.; Wu, X.; Seo, M. S.; Cho, K.-B.; Yoon, H.; Park, Y. J.; Fukuzumi, S.; Pushkar, Y. N.; Nam, W., A Mononuclear Non-Heme Manganese(IV)–Oxo Complex Binding Redox-Inactive Metal Ions. *J. Am. Chem. Soc.* **2013,** *135* (17), 6388-6391.

37. Herbert, D. E.; Lionetti, D.; Rittle, J.; Agapie, T., Heterometallic Triiron-Oxo/Hydroxo Clusters: Effect of Redox-Inactive Metals. *J. Am. Chem. Soc.* **2013,** *135* (51), 19075-19078.

38. Yoon, H.; Lee, Y.-M.; Wu, X.; Cho, K.-B.; Sarangi, R.; Nam, W.; Fukuzumi, S., Enhanced Electron-Transfer Reactivity of Nonheme Manganese(IV)–Oxo Complexes by Binding Scandium Ions. *J. Am. Chem. Soc.* **2013,** *135* (24), 9186-9194.

39. Hong, S.; Pfaff, F. F.; Kwon, E.; Wang, Y.; Seo, M.-S.; Bill, E.; Ray, K.; Nam, W., Spectroscopic Capture and Reactivity of a Low-Spin Cobalt(IV)-Oxo Complex Stabilized by Binding Redox-Inactive Metal Ions. *Angew. Chem. Int. Ed.* **2014,** *53* (39), 10403-10407.

40. Yao, S.; Xiong, Y.; Vogt, M.; Grützmacher, H.; Herwig, C.; Limberg, C.; Driess, M., O O Bond Activation in Heterobimetallic Peroxides: Synthesis of the Peroxide [LNi(μ,η2:η2-O2)K] and its Conversion into a Bis(μ-Hydroxo) Nickel Zinc Complex. *Angew. Chem. Int. Ed.* **2009,** *48* (43), 8107-8110.

41. Lee, Y.-M.; Bang, S.; Kim, Y. M.; Cho, J.; Hong, S.; Nomura, T.; Ogura, T.; Troeppner, O.; Ivanovic-Burmazovic, I.; Sarangi, R.; Fukuzumi, S.; Nam, W., A mononuclear nonheme iron(iii)-peroxo complex binding redox-inactive metal ions. *Chem. Sci.* **2013,** *4* (10), 3917-3923.

42. Li, F.; Van Heuvelen, K. M.; Meier, K. K.; Münck, E.; Que, L., Sc3+-Triggered Oxoiron(IV) Formation from O2 and its Non-Heme Iron(II) Precursor via a Sc3+–Peroxo–Fe3+ Intermediate. *J. Am. Chem. Soc.* **2013,** *135* (28), 10198-10201.

43. Bang, S.; Lee, Y.-M.; Hong, S.; Cho, K.-B.; Nishida, Y.; Seo, M. S.; Sarangi, R.; Fukuzumi, S.; Nam, W., Redox-inactive metal ions modulate the reactivity and oxygen release of mononuclear non-haem iron(III)–peroxo complexes. *Nat. Chem.* **2014,** *6* (10), 934-940.

44. Lee, Y.-M.; Bang, S.; Yoon, H.; Bae, S. H.; Hong, S.; Cho, K.-B.; Sarangi, R.; Fukuzumi, S.; Nam, W., Tuning the Redox Properties of a Nonheme Iron(III)–Peroxo Complex Binding Redox-Inactive Zinc Ions by Water Molecules. *Chem. Eur. J.* **2015,** *21* (30), 10676-10680.

45. Park, Y. J.; Ziller, J. W.; Borovik, A. S., The effects of redox-inactive metal ions on the activation of dioxygen: isolation and characterization of a heterobimetallic complex containing a Mn(III)-(mu-OH)-Ca(II) core. *J. Am. Chem. Soc.* **2011,** *133* (24), 9258-61.

46. Park, Y. J.; Cook, S. A.; Sickerman, N. S.; Sano, Y.; Ziller, J. W.; Borovik, A. S., Heterobimetallic Complexes with MIII-(*μ*-OH)-MII Cores (MIII = Fe, Mn, Ga; MII = Ca, Sr, and Ba): Structural, Kinetic, and Redox Properties. *Chem Sci* **2013,** *4* (2), 717-726.

47. Cook, S. A.; Ziller, J. W.; Borovik, A. S., Iron(II) Complexes Supported by Sulfonamido Tripodal Ligands: Endogenous versus Exogenous Substrate Oxidation. *Inorg. Chem.* **2014,** *53* (20), 11029-11035.

48. Kundu, S.; Miceli, E.; Farquhar, E.; Pfaff, F. F.; Kuhlmann, U.; Hildebrandt, P.; Braun, B.; Greco, C.; Ray, K., Lewis Acid Trapping of an Elusive Copper–Tosylnitrene Intermediate Using Scandium Triflate. *J. Am. Chem. Soc.* **2012,** *134* (36), 14710-14713.

49. Abram, S.-L.; Monte-Perez, I.; Pfaff, F. F.; Farquhar, E. R.; Ray, K., Evidence of two-state reactivity in alkane hydroxylation by Lewis-acid bound copper-nitrene complexes. *Chem. Commun.* **2014,** *50* (69), 9852-9854.

50. Monte-Pérez, I.; Kundu, S.; Ray, K., An Open-Shell Spin Singlet Copper-Nitrene Intermediate Binding Redox-innocent Metal Ions: Influence of the Lewis Acidity of the Metal Ions on Spectroscopic and Reactivity Properties. *Z. Anorg. Allg. Chem.* **2015,** *641* (1), 78-82.

51. Halvagar, M. R.; Tolman, W. B., Isolation of a 2-Hydroxytetrahydrofuran Complex from Copper-Promoted Hydroxylation of THF. *Inorg. Chem.* **2013,** *52* (15), 8306-8308.

52. Risch, M.; Klingan, K.; Ringleb, F.; Chernev, P.; Zaharieva, I.; Fischer, A.; Dau, H., Water Oxidation by Electrodeposited Cobalt Oxides—Role of Anions and Redox-Inert Cations in Structure and Function of the Amorphous Catalyst. *ChemSusChem* **2012,** *5* (3), 542-549.

53. Wiechen, M.; Zaharieva, I.; Dau, H.; Kurz, P., Layered manganese oxides for water-oxidation: alkaline earth cations influence catalytic activity in a photosystem II-like fashion. *Chem. Sci.* **2012,** *3* (7), 2330-2339.

54. Lacy, D. C.; Park, Y. J.; Ziller, J. W.; Yano, J.; Borovik, A. S., Assembly and Properties of Heterobimetallic CoII/III/CaII Complexes with Aquo and Hydroxo Ligands. *J. Am. Chem. Soc.* **2012,** *134* (42), 17526-17535.

55. Lau, N.; Ziller, J. W.; Borovik, A. S., Sulfonamido tripods: Tuning redox potentials via ligand modifications. *Polyhedron* **2015,** *85*, 777-782.

56. Sano, Y.; Weitz, A. C.; Ziller, J. W.; Hendrich, M. P.; Borovik, A. S., Unsymmetrical Bimetallic Complexes with MII–(μ-OH)–MIII Cores (MIIMIII = FeIIFeIII, MnIIFeIII, MnIIMnIII): Structural, Magnetic, and Redox Properties. *Inorg. Chem.* **2013,** *52* (18), 10229-10231.

57. Sickerman, N. S.; Henry, R. M.; Ziller, J. W.; Borovik, A. S., Preparation and structural properties of InIII–OH complexes. *Polyhedron* **2013,** *58*, 65-70.

58. Cook, S. A.; Borovik, A. S., Molecular Designs for Controlling the Local Environments around Metal Ions. *Acc. Chem. Res.* **2015,** *48* (8), 2407-2414.

59. Bordwell, F. G.; Algrim, D., Nitrogen acids. 1. Carboxamides and sulfonamides. *J. Org. Chem.* **1976,** *41* (14), 2507-2508.

60. Bordwell, F. G.; Fried, H. E.; Hughes, D. L.; Lynch, T. Y.; Satish, A. V.; Whang, Y. E., Acidities of carboxamides, hydroxamic acids, carbohydrazides, benzenesulfonamides, and benzenesulfonohydrazides in DMSO solution. *J. Org. Chem.* **1990,** *55* (10), 3330-3336.

61. Schwarz, A. D.; Herbert, K. R.; Paniagua, C.; Mountford, P., Ligand Variations in New Sulfonamide-Supported Group 4 Ring-Opening Polymerization Catalysts. *Organometallics* **2010,** *29* (18), 4171-4188.

62. Aller, R. T. v.; Scott, R. B.; Brockelbank, E. L., A Study of Aliphatic Sulfonyl Compounds. VIII. The Thermal Decomposition of Trimethylmethanesulfonyl Chloride1. *J. Org. Chem.* **1966,** *31* (7), 2357-2365.

63. Asinger, F.; Laue, P.; Fell, B.; Gubelt, G., Untersuchungen zum Probelem des tetriären Butansulfochlorids. *Chem. Ber.* **1967,** *100* (5), 1696-1700.

64. King, J. F.; Lam, J. Y. L.; Dave, V., tert-Butyl Cation Formation in the Hydrolysis of 2-Methyl-2-propanesulfonyl Chloride, the Simplest Tertiary Alkanesulfonyl Chloride. *J. Org. Chem.* **1995,** *60* (9), 2831-2834.

65. Gontcharov, A. V.; Liu, H.; Sharpless, K. B., tert-Butylsulfonamide. A New Nitrogen Source for Catalytic Aminohydroxylation and Aziridination of Olefins. *Org. Lett.* **1999,** *1* (5), 783-786.

66. Netscher, T.; Prinzbach, H., Sterically Crowded Sulfonate Esters: Nobel Leaving Groups with Hindered S–O Cleavage. *Synthesis* **1987,** (8), 683-688.

67. Sun, P.; Weinreb, S. M.; Shang, M., tert-Butylsulfonyl (Bus), a New Protecting Group for Amines. *J. Org. Chem.* **1997,** *62* (24), 8604-8608.

68. Onset of oxidation is used here instead of E½ because some events are electrochemically irreversible. Each of these electrochemical events may be cycled without changes to the voltammogram, demonstrating chemical reversibility.

69. 4-4Mg is not sufficiently soluble for study by CV or electronic absorption spectroscopy.

70. Sanchez, E. R.; Gessel, M. C.; Groy, T. L.; Caudle, M. T., Interaction of Biotin with Mg–O Bonds: Bifunctional Binding and Recognition of Biotin and Related Ligands by the Mg(15-crown-5)2+ Unit. *J. Am. Chem. Soc.* **2002,** *124* (9), 1933-1940.

71. Netscher, T.; Prinzbach, H., Sterically Crowded Sulfonate Esters: Novel Leaving Groups with Hindered S-O Cleavage. *Synthesis* **1987,** *1987* (08), 683-688.

Chapter 5

Coordination of Hydrogen Peroxide with Late Transition Metal Sulfonamido Complexes

5.1 Abstract

Adducts of hydrogen peroxide and transition metals have been implicated as intermediates in a number of biological and industrial processes, but have only recently been observed. Therefore, knowledge of how hydrogen peroxide interacts with transition metals is extremely limited. Herein, we report the synthesis of H_2O_2 complexes of cobalt, nickel, and copper supported by sulfonamido ligands with second-sphere hydrogen bonding. Binding constant and decay kinetics are reported for four new $M(H_2O_2)$ adducts.

5.2 Introduction

5.2.1 $M(H_2O_2)$ Adducts As Reactive Intermediates

Hydrogen peroxide is an attractive oxidant because of its low toxicity, high oxidative efficiency and benign byproducts.[1] Large-scale applications of hydrogen peroxide include the bleaching of wood pulp and textiles and the epoxidation of propylene, processes which involve activation of hydrogen peroxide with metal catalysts.[2-4] The nature of the interaction between the metal ion and hydrogen peroxide in these systems is not thoroughly understood, but a number of chemical species have been proposed as intermediates in computational[5-8] and kinetic[9-12] studies. Furthermore, $M(H_2O_2)$ adducts have been computationally implicated to act as secondary reactive intermediates in a variety of cytochrome P450 enzymes.[13-18] In a calculated mechanism for cytochrome P450cam enzymes, an $Fe^{III}(H_2O_2)$ adduct is stabilized by a hydrogen bond accepting protein residue and prevented from "uncoupling" (loss of H_2O_2 by decomplexation) by steric pressure from the substrate (**A**, Figure 5-1), ultimately forming Compound 1, which is the generally

accepted active oxidant in cytochrome P450 enzymes.[17-18] In another example, cobalt salophen complexes are shown to aerobically oxidize hydroquinone and a $Co^{II}(H_2O_2)$ adduct, stabilized by hydrogen bonding to the hydroquinone substrate and solvent molecule (**B**, Figure 5-1), is calculated as an active intermediate.[8] Both of these species react by one-electron reduction of bound H_2O_2 by the metal center to afford M^{n+1}–OH hydrogen bonded to a hydroxyl radical. For **A**, this leads to HAT from the Fe^{IV}-OH made accessible by the redox activity of the porphyrin ligand, whereas with **B**, the Co^{III}-OH complex is not susceptible to further oxidation, allowing the tethered •OH to react directly with the substrate. Hydroxyl radicals are potent, albeit unselective, oxidants, and we remain intrigued by accessing selective •OH chemistry by such a mechanism. To reach this long-term goal, we set out to explore H_2O_2 coordination to divalent metal centers with electrochemically accessible trivalent oxidation states.

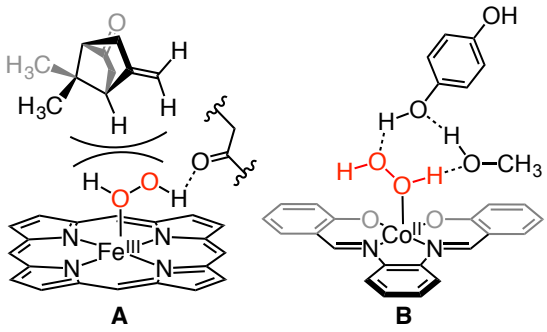

*Figure 5-1. Calculated $Fe^{III}(H_2O_2)$ intermediate in formation of Compound 1 from in Cytochrome P450cam enzyme (**A**).[18] Calculated $Co^{II}(H_2O_2)$ adduct in aerobic oxidation of hydroquinone by cobalt salophen complexes (**B**).[8]*

5.2.2 Previously Reported $M(H_2O_2)$ Adducts

Despite the many theoretical examples, $M(H_2O_2)$ adducts were not experimentally observed until recently. In 2015, we published characterization of the first $Zn(H_2O_2)$ adduct

(**2-1(H_2O_2)**, Figure 5-2), which included lifetime measurements and the first crystal structure with hydrogen peroxide bound to a metal ion.[19] In 2016, we reported the first observable M(H_2O_2) adduct with a redox-active metal, Co^{II} (**3-1(H_2O_2)**, Figure 5-2), along with lifetime measurements and the first measured binding constant for hydrogen peroxide and a transition metal.[20] Both of these complexes are supported by aryl-sulfonamido ligands, which are able to stabilize the otherwise weak M(H_2O_2) interaction through second-sphere hydrogen bonding (Chapters 2 and 3). Our development of the novel alkyl-sulfonamido ligand $[Bus_3tren]^{3-}$ and our work with cobalt complexes of this ligand (Chapter 4, **4-4(OH_2)**, Figure 5-2) has prompted us to investigate the binding strength and decay kinetics of Co(H_2O_2) adducts supported by the more electron-rich alkyl-sulfonamido ligands. Additionally, there is crystallographic and spectroscopic evidence that hydrogen bonding interactions between the NCH_2R groups in the $[Bu_4N]^+$ counterion and the O(=S) groups interfere with the binding of protic axial ligands such as H_2O_2 (Chapters 2 and 3); therefore, we have developed a novel non-coordinating solubilized tetra-aryl phosphonium cation that does not engage in hydrogen bonding. Since our work with M(H_2O_2) adducts thus far has been with cobalt and zinc, we wanted to connect these studies by expanding to copper and nickel complexes as well. This chapter contains our investigation of binding strength and decay kinetics with M(H_2O_2) adducts of Co, Ni, and Cu, using both aryl- and alkyl-sulfonamido ligands and both ammonium and phosphonium non-coordinating cations. It is our belief that information on these M(H_2O_2) adducts will be vital in understanding the viability and behavior of M(H_2O_2) intermediates in biological and industrial oxidation mechanisms, and will illuminate the path to development of novel oxidative methodologies employing H_2O_2 as the sole stoichiometric oxidant.

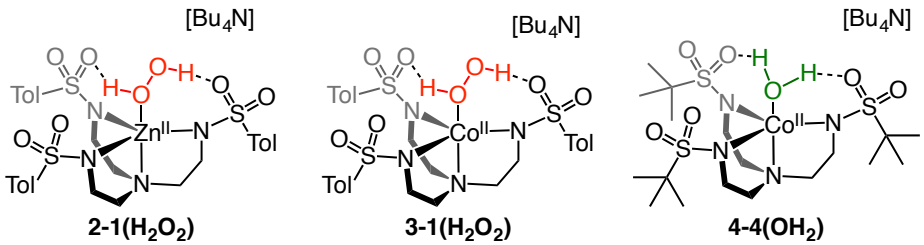

Figure 5-2. Previously reported sulfonamidate complexes interacting with hydrogen peroxide and aqua ligands through second-sphere hydrogen bonding interactions.

5.3 Results and Discussion

5.3.1 Synthesis of Sulfonamido Complex with Phosphonium Counterion

The preparation of **3-1^{P}(OH$_2$)** and **3-1^{P}** has been presented in previous chapters; however, their synthesis will be discussed here in depth. In Chapter 2 and 3, ^{1}H-NMR spectroscopy of 4-coordinate complexes **2-1** and **3-1** indicated a noticeable shift in the resonances of the $[Bu_4N]^+$ ion upon addition of H_2O or H_2O_2. Crystallographic data of **2-1(OH$_2$)** suggests that the NCH_2R groups in the $[Bu_4N]^+$ counterion are engaged in weak hydrogen bonding with the sulfonyl groups on the sulfonamido ligand. The solid-state and solution-state data suggested to us that the binding of H_2O_2 to the sulfonamido complexes might be disrupted in part by the $[Bu_4N]^+$ counterion. In the search for non-coordinating cations that would not disrupt hydrogen bond interactions of bonded H_2O_2 with sulfonamido ligands, the Scarborough group devised an asymmetrically substituted tetra-aryl phosphonium ion $[^{tBu}ArPPh_3]^+$ (Scheme 5-1). In 2008, Charette published a nickel-catalyzed coupling of triphenylphosphine and aryl halides for the preparation of a wide-variety of asymmetric tetra-aryl phosphonium salts, $[ArPPh_3]X$ ($X = Cl^-, Br^-, I^-, {}^-OTf$).[21] By using this procedure, we were able to synthesize a novel tetra-aryl phosphonium from 1-bromo-3,5-di-tert-butylbenzene and triphenylphosphine (Scheme 5-1). The inclusion of *tert*-butyl groups

serve to increase the solubility of the phosphonium ion without adding any acidic protons that might engage in hydrogen bonding interactions with the sulfonamido ligand.

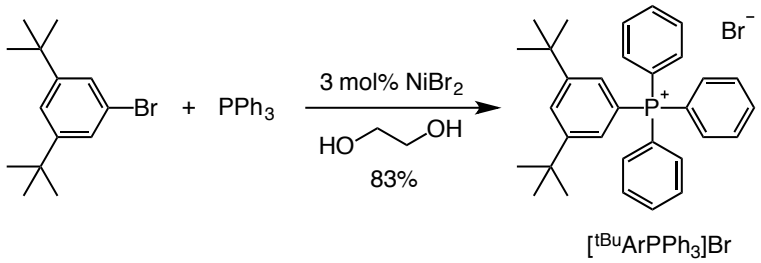

Scheme 5-1. Synthesis of novel asymetric arylphosphonium cation.

With this new cation in hand, we were able to synthesize crystalline $[^{tBu}ArPPh_3][(Ts_3tren)Co^{II}(H_2O)]$ (**3-1^{P}(OH$_2$)**, Scheme 5-2, Figure 5-3), which can be dehydrated at room temperature with 3Å molecular sieves to produce $[^{tBu}ArPPh_3][(Ts_3tren)Co^{II}]$ (**3-1^{P}**, Scheme 5-2).

5.3.1 Synthesis of Sulfonamido Complexes with Copper and Nickel

To further explore the effect of redox-active metal ions in the formation of $M(H_2O_2)$ adducts, we pursued sulfonamido complexes of nickel and copper. For these complexes, the $[Bu_4N]^+$ counterion was used, because of their ease of preparation and so that we could make a direct comparison to **2-1(H$_2$O$_2$)** and **3-1(H$_2$O$_2$)**. Preparation of sulfonamido complexes with copper and nickel from H_3Ts_3tren was performed with very good yields (Scheme 5-2). Crystals of $[^{n}Bu_4N][(Ts_3tren)Ni^{II}(OH_2)]$ **(5-1(OH$_2$))** and $[^{n}Bu_4N][(Ts_3tren)Cu^{II}(OH_2)]$ **(5-2(OH$_2$))** were obtained by diffusion of diethyl ether into a solution of the metal complex in DCM and their solid-state structures are shown in Figure 5-3. The green complex **5-1(OH$_2$)** was dehydrated by heating in THF to 60˚C for several days in the presence of 3Å molecular sieves, periodically monitoring via absorption spectroscopy. After filtration of the molecular sieves, the orange 4-coordinate complex

[^{n}Bu$_4$N][(Ts$_3$tren)Ni^{II}] (**5-1**) was crystallized by addition of diethyl ether and pentane. The need for heat to dehydrate the nickel complexes stands in contrast to the complete dehydration of analogous cobalt complexes at room temperature with 3Å molecular sieves (Chapter 3). Furthermore, only partial dehydration of the copper complex **5-2(OH$_2$)** was achieved after several days of treatment with molecular sieves at 60˚C. Further attempts to completely dehydrate this complex were unsuccessful. These observations suggest stronger binding of H$_2$O in **5-1(OH$_2$)** and **5-2(OH$_2$)** than in **3-1(OH$_2$)**.

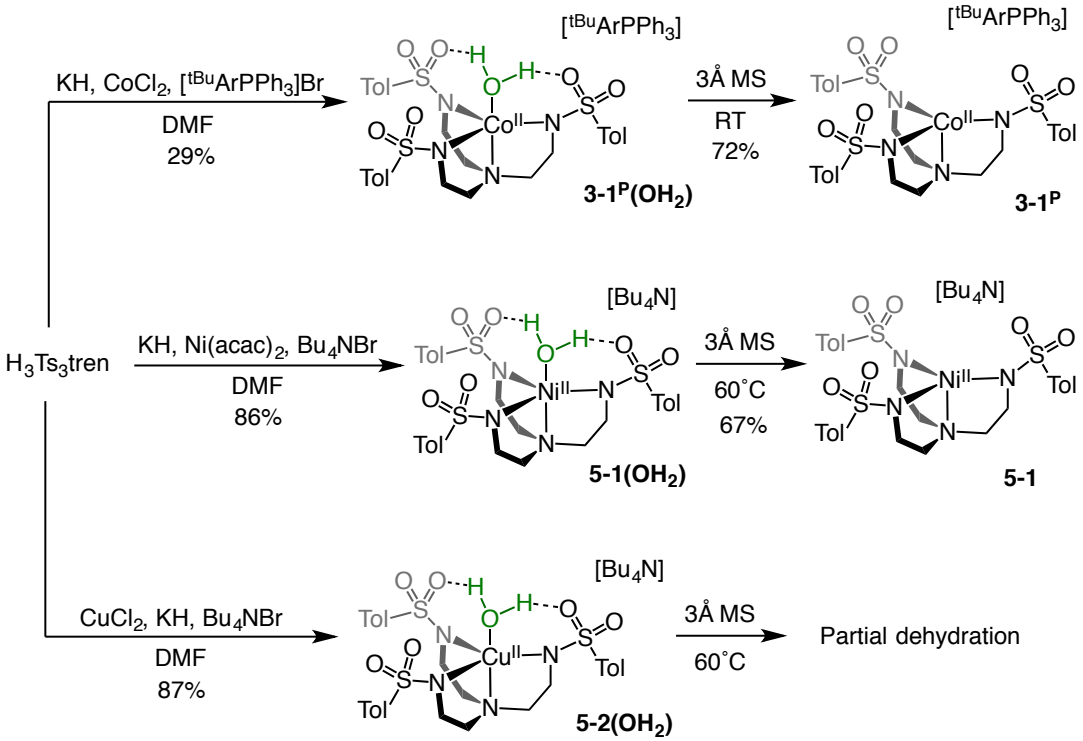

Scheme 5-2. Synthesis of new metal sulfanamido complexes. Yields of crystalline product are shown.

The preparation of a Co^{II} complex with the electron-rich [Bus$_3$tren]$^{3-}$ ligand, which will also be explored in this study, has been presented in Chapter 4 (**4-4(OH$_2$)** and **4-4**).

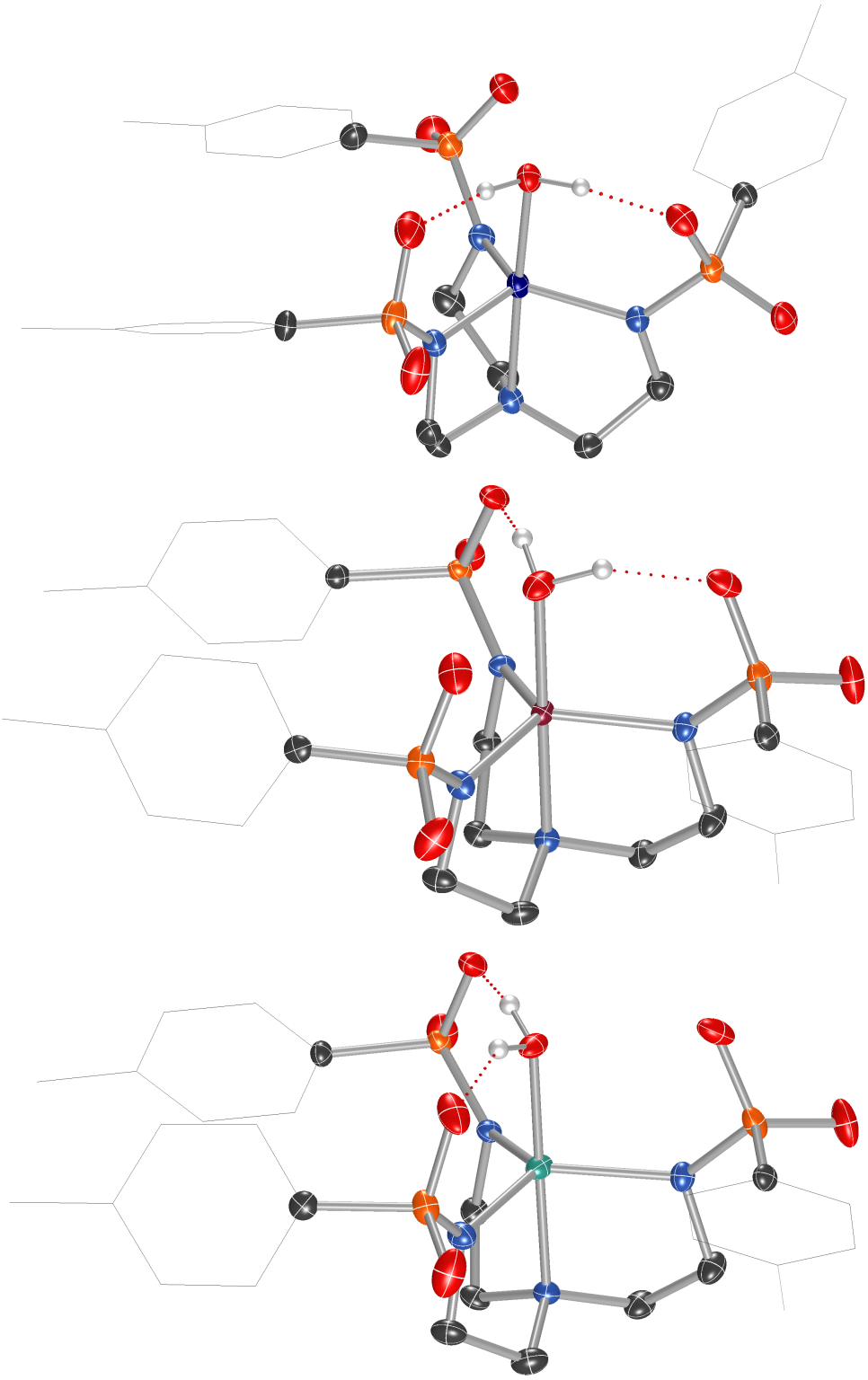

Figure 5-3. Solid-state structures of the anions in ***3-1^{P}(OH$_2$)*** *(top),* ***5-1(OH$_2$)*** *(middle), and* ***5-2(OH$_2$)*** *(bottom). Ligand arms have been truncated and hydrogen atoms on carbon have been omitted for clarity.*

5.3.2 Measuring Binding Constants

As described above, the nickel and copper complexes (**5-1(OH_2)** and **5-2(OH_2)**) are more difficult to dehydrate than the analogous cobalt complex (**3-1(OH_2)**). This prompted us to measure the binding constants for both water and hydrogen peroxide to each of the sulfonamido complexes, in order to determine the effect of changing the counterion, ligand electronics, and metal ion. Photometric titrations with water were performed at room temperature in THF. However, since we have demonstrated that **3-1(H_2O_2)** is short-lived at room temperature (Chapter 3), titrations with H_2O_2 were performed at –70°C for **3-1**, **3-1^P**, **4-4**, and **5-1** in THF. For each titration, water or H_2O_2 was added incrementally to a solution of 4-coordinate complex in THF. The differences in absorbance at two wavelengths, one decreasing in intensity and one increasing in intensity, were measured, normalized, and averaged to correct for any inconsistencies in ligand addition. The titration curve for each complex was modelled mathematically to determine the binding constant (K_{eq}) for each ligand-complex pair, which are shown in Table 5-1. Experimental details and titration curves are shown in Section 5.5.4. Unfortunately, the difficulty in accessing anhydrous **5-2** rendered titrations with either water or peroxide impossible under our experimental conditions.

*Table 5-1. Binding constants for binding of water and H_2O_2 to Co^{II} in **3-1**, **3-1^P**, **4-4**.*

	3-1	**3-1^P**	**4-4**
H_2O	2660 ± 360	5760 ± 1260	45100 ± 9230
H_2O_2	34.4 ± 1.50	78.7 ± 5.90	17000 ± 4050

Discussion of changes in counterion.

The use of the phosphonium cation $[^{tBu}ArPPh_3]^+$ in place of the ammonium cation $[^nBu_4N]^+$ results in approximately doubling the binding strength for both water and peroxide. This supports the theory that $[^nBu_4N]^+$ can disrupt hydrogen bonding interactions between a protic axial ligand and the O=(S) groups on the sulfonamidate ligand.

Discussion of changes in ligand electronics.

Since the alkyl-sulfonamido complex **4-4** possesses a more electron-rich ligand than **3-1**, we expect **4-4** to have stronger hydrogen bonding interactions and, therefore, bind protic axial ligands more strongly. Interestingly, the use of the alkylsulfonamidate ($[Bus_3tren]^{3-}$) on cobalt (**4-4**) in place of the arylsulfonamidate ligand ($[Ts_3tren]^{3-}$) on cobalt (**3-1**) increases the binding strength for an aqua ligand by a factor of 17, but increases the binding strength for H_2O_2 by a factor of 500 (Table 5-1). Previous studies by Prikhodchenko have shown H_2O_2 to be a superior hydrogen-bond donor compared to water[22-25] and our recent work has demonstrated that the O=(S) groups on the $[Bus_3tren]^{3-}$ ligand are more electron-rich than those on $[Ts_3tren]^{3-}$ (Chapter 4). Therefore, it seems that these two effects work together to disproportionately strengthen the interaction between **4-4** and H_2O_2. This observation is of particular importance with respect to the future development of catalytic systems. Since hydrogen peroxide is typically used as an aqueous solution, and water is a byproduct of oxidation by hydrogen peroxide, the binding of hydrogen peroxide will often be in competition with binding of water to the catalyst. The ability to bias the equilibrium of competitive binding could greatly improve catalytic systems using hydrogen peroxide as a stoichiometric oxidant.

Discussion of changes in metal ion.

The titration curves for **5-1** with water and peroxide were too sharp to mathematically calculate a reasonable value for K_{eq}. This is due to an important limitation in measuring binding constants using titration methods. As K_{eq} increases, the mathematically modeled curve relies on an increasingly smaller portion of data, which in turn increases the uncertainty of the mathematical fit (Section 5.5.4, Figure 5-9). However, the lower limits for K_{eq} can be estimated by comparing simulated titration curves with experimental data. Using this approach, we estimated that the K_{eq} values for binding of water and H_2O_2 to Ni^{II} in **5-1** are both above 200,000 M^{-1} (see Section 5.5.4); much greater than those for the cobalt complex **3-1** (2660 ± 360 and 34.4 ± 1.50, respectively), consistent with observation that **5-1(OH$_2$)** is difficult to dehydrate.

Summary of binding constant data.

Using photometric titrations we measured the binding constants for binding of water or hydrogen peroxide to the metal ion in a series of 4-coordinate metal sulfonamidate complexes. From these experiments, we have observed the following: weak hydrogen bonding by non-coordinating counterions affect binding of protic ligands to a small but non-insignificant degree; increasing electron density on the sulfonamido ligand strengthens binding of protic ligands, affecting the stronger hydrogen bond donor (H_2O_2) more than the weaker hydrogen bond donor (H_2O); but the greatest influence on the binding strength of protic ligands is the identity of the transition metal ion.

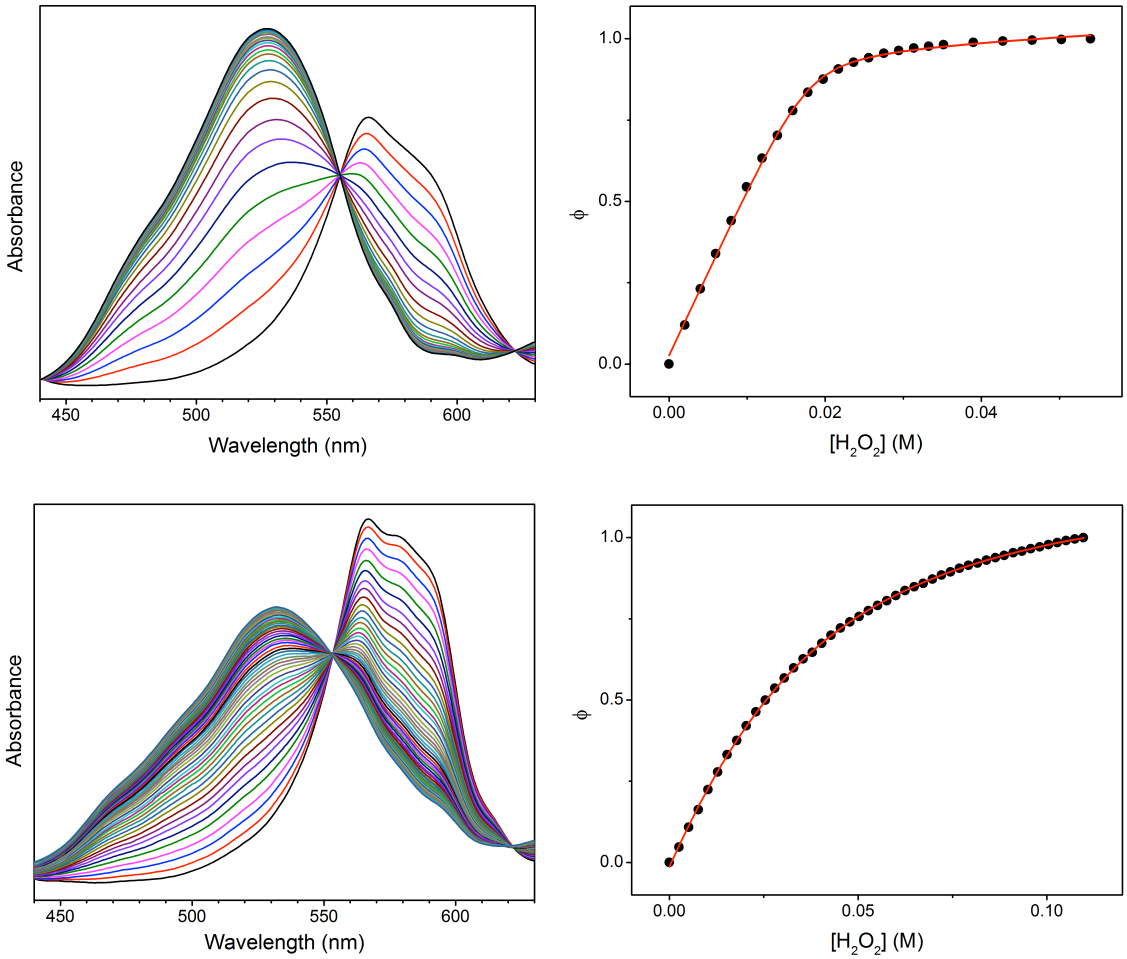

Figure 5-4. Sample photometric titration data. Absorption traces (left) and titration curves with mathematical fits (right). Top: ***3-1*** *and water at room temperature. Bottom:* ***3-1*** *and H_2O_2 at –70°C. Titration curves for* ***3-1^P***, ***4-4***, *and* ***5-1*** *with water and H_2O are shown in Figure 5-8.*

5.3.3 Lifetime Measurements

We sought to measure the decay kinetics for the decay of bound H_2O_2 into water and oxygen for complexes **3-1(H_2O_2)**, **3-1^P(H_2O_2)**, **4-4(H_2O_2)**, and **5-1(H_2O_2)**. In Chapter 3, decay of **3-1(H_2O_2)** could be monitored using ^{1}H NMR. Unfortunately, this technique could not be used for the related nickel (**5-1**) and copper (**5-2**) complexes, due to paramagnetic broadening that completely obscured the H_2O_2 signal. Therefore, an alternate method of

detecting H_2O_2 decay had to be employed. Since the decay of **3-1(H_2O_2)** to **3-1(OH_2)** had been observed to produce O_2 gas, we reasoned that the decay of bound H_2O_2 into H_2O would directly correlate to an increase in pressure in a closed system. Thus, we decided to monitor headspace pressure above a sample of M(H_2O_2) as a means of measuring decay kinetics. When we monitored the headspace pressure above a sample of **3-1** and H_2O_2 in anhydrous THF, we observed an initial increase in pressure followed by a slow decrease in pressure back to the initial pressure. This led us to conclude that the oxygen being produced by disproportionation was being consumed in autoxidation of THF. We sought to avoid this problem by changing the solvent to acetonitrile, which is not susceptible to autoxidation.

Preparation of H_2O_2 solutions in acetonitrile.

In our previous work, anhydrous solutions of H_2O_2 were made in THF by extraction from the urea hydrogen peroxide adduct (Section 2.5). Since THF is not compatible with the experimental setup, we needed to find a way to obtain anhydrous H_2O_2 in acetonitrile. We discovered that anhydrous solutions of H_2O_2 in diethyl ether were also accessible by stirring the urea hydrogen peroxide adduct in anhydrous diethyl ether and filtering away the solid (Section 5.5.2). Cooling this solution crystallizes any dissolved urea, which can be filtered away. By adding this H_2O_2/ether solution to anhydrous acetonitrile and then removing the diethyl ether under vacuum, we obtained anhydrous solutions of H_2O_2 in acetonitrile (Section 5.5.2).

Decay of M(H_2O_2) adducts in acetonitrile.

With these solutions in hand, we were able to generate **3-1(H_2O_2)**, **3-1^p(H_2O_2)**, **4-4(H_2O_2)**, and **5-1(H_2O_2)** in acetonitrile by combining one equivalent of H_2O_2 with anhydrous **3-1**, **3-**

1^{P}, **4-4**, and **5-1**. For each experiment, the 4-coordinate complex was stirred in acetonitrile at 25˚C in a sealed system. One equivalent of H_2O_2 in acetonitrile was added and the headspace pressure was measured over time using a digital manometer. The pressure data were then fit to an inverse exponential decay function and the excellence of the fit demonstrated that decay of bound H_2O_2 in each case follows first-order kinetics. The manometric data and mathematical fits are shown in Figure 5-5 and the calculated half-life values for each complex are shown in Table 5-2. Since anhydrous **5-2** is not accessible, we estimated the half-life of **5-2(H_2O_2)** by treating a red solid consisting of an unknown ratio of **5-2(OH_2)** and **5-2** with approximately one equivalent of hydrogen peroxide and measuring the solution manometrically, which should give an upper estimate of the lifetime of **5-2(OH_2)**, since protic ligands such as H_2O or NH_3 increase the lifetime of M(H_2O_2) adducts through competitive displacement of H_2O_2 (Chapter 3).

Table 5-2. Decay rates for M(H_2O_2) adduct.

	3-1(H_2O_2)	**3-1^{P}(H_2O_2)**	**4-4(H_2O_2)**	**5-1(H_2O_2)**	**5-2(H_2O_2)[a]**
$t_{1/2}$ **(sec)**	173.5 ± 0.6	283.2 ± 2.6	66.2 ± 0.7	576.4 ± 5.2	53.4 ± 1.0
$\mathbf{R^2}$	0.99959	0.99913	0.99960	0.99606	0.99932

[a]*Mixture of **5-2(H_2O_2)** and **5-2(OH_2)**. Pressure data and mathematical modelling presented in Section 5.5.4.*

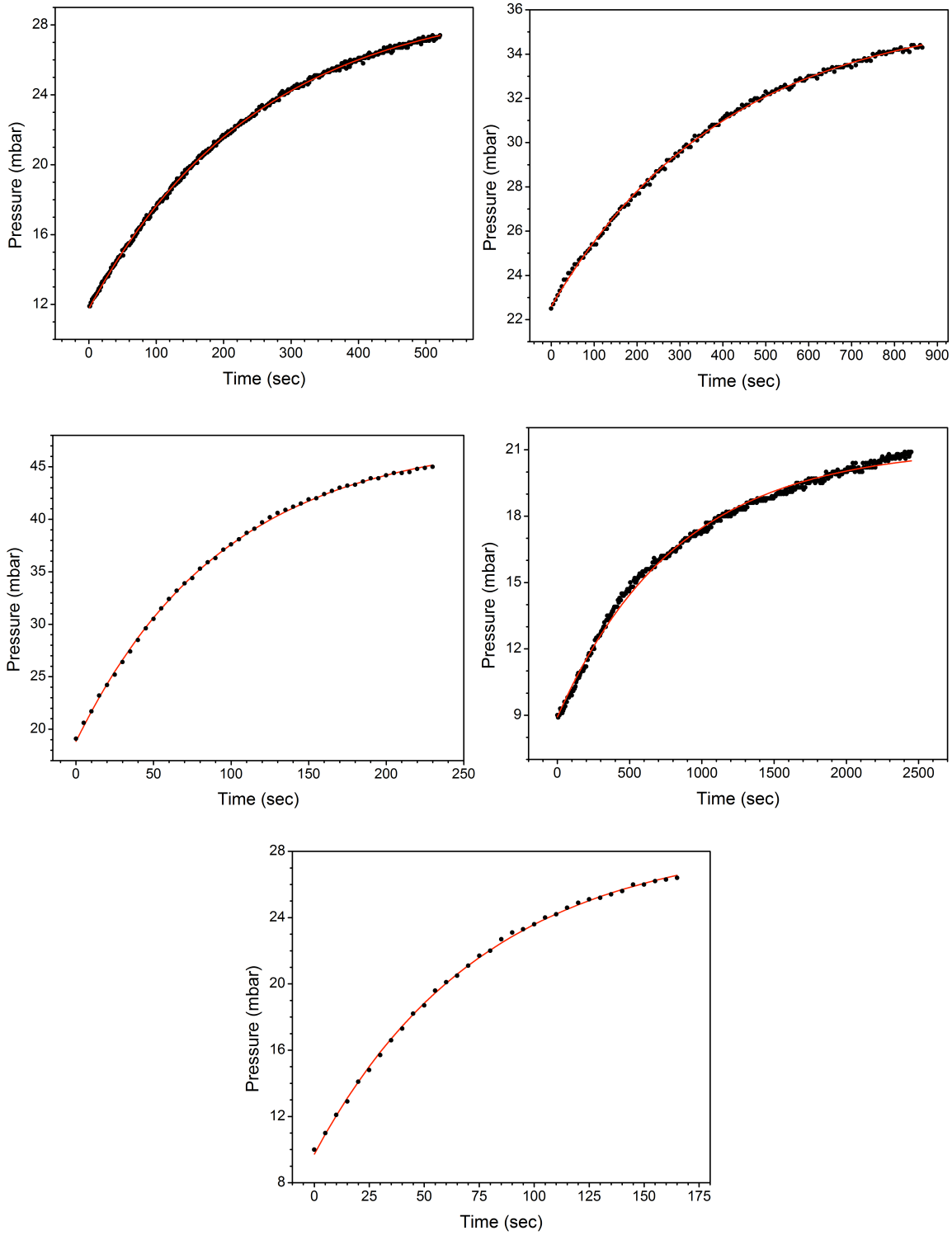

Figure 5-5. Pressure measurements for ***3-1(H_2O_2)*** *(top left),* ***3-1^P(H_2O_2)*** *(top right),* ***4-4(H_2O_2)*** *(middle left),* ***5-1(H_2O_2)*** *(middle right), and the mixture of* ***5-2/5-2(H_2O_2)*** *(bottom).*

Discussion of decay kinetics of Co(H_2O_2) adducts.

The half-life of **3-1(H_2O_2)** in acetonitrile is 173.5 ± 0.6 sec, which is shorter than the half-life reported for decay in THF-d_8 (353 ± 33 sec, Chapter 3). In acetonitrile, the half-life of **4-4(H_2O_2)** is 66.2 ± 0.7 sec, 2.6 times shorter than **3-1(H_2O_2)** in acetonitrile. Since K_{eq} for binding of H_2O_2 to the metal ion in **4-4(H_2O_2)** is higher than in **3-1(H_2O_2)**, the faster decay of H_2O_2 in **4-4(H_2O_2)** is consistent with stronger binding of H_2O_2 leading to shorter lifetimes. The half-life of **3-1^p(H_2O_2)** is 283.2 ± 2.6, 1.6 times *slower* than that of **3-1(H_2O_2)** in acetonitrile. Since the binding of H_2O_2 in **3-1^p(H_2O_2)** is stronger than in **3-1(H_2O_2)** these data are not consistent with the theory that larger K_{eq} values lead to shorter lifetimes.

Discussion of decay kinetics of nickel and copper M(H_2O_2) adducts.

The nickel complex **5-1(H_2O_2)**, which displayed the highest binding constant, has a significantly *longer* half-life (576.4sec), 3.3 times longer than that of **3-1(H_2O_2)**. These data are also not consistent with the theory that larger K_{eq} values lead to shorter lifetimes. The sample containing the mixture of **5-2(H_2O_2)** and **5-2(OH_2)** has the shortest half-life (53.4sec). We have noted that competing protic ligands such as H_2O increase the half-life of M(H_2O_2) adducts (Chapter 3), so it is likely that the decay rate of pure **5-2(H_2O_2)** is even faster than what we observed. Since we were not able to calculate a K_{eq} for H_2O_2 binding to **5-2**, it is impossible to correlate these two factors. From these data, we see that decay rates for M(H_2O_2) adducts do not directly correlate to the strength of H_2O_2 binding to the metal. We next probed whether lifetimes of the M(H_2O_2) adducts could be related to the accessibility of other metal oxidation states.

5.3.4 Electrochemical Experiments

In an attempt to gain insights into the unexpected decay rates of the $M(H_2O_2)$ adducts, we decided to measure the M^{II}/M^{III} oxidation potentials for the series of $M(OH_2)$ complexes. We considered that there might be a correlation between the M^{II}/M^{III} oxidation couple and the decay rates of the respective $M(H_2O_2)$ adducts. Redox potentials for **3-1(OH_2)** and **4-4(OH_2)** in THF have been reported in Chapter 4, but are repeated here for discussion. Cyclic voltammetry experiments with electrochemical cycling were performed on **3-1(OH_2)**, **5-1(OH_2)**, and **5-2(OH_2)** in CH_2Cl_2 (

Table 5-3) and externally referenced to Fc/Fc^+. In the case of **3-1^P(OH_2)**, a phosphonium supporting electrolyte, $[^{tBu}ArPPh_3]PF_6$, was used instead of $[^nBu_4N]PF_6$ in order to avoid negating the non-coordinating nature of the $[^{tBu}ArPPh_3]^+$ counterion.

Discussion on electrochemical properties for Co(OH_2) complexes.

The three cobalt complexes (**3-1(OH_2)**, **3-1^P(OH_2)**, and **4-4(OH_2)**) all have very similar oxidation potentials in CH_2Cl_2 (Figure 5-6). The $Co^{II/III}$ redox couple $E_{½}$ for **3-1^P(OH_2)** (+63mV) is shifted negative from that of **3-1(OH_2)** (+78mV) by just 15mV, indicating that the counterion identity has very little impact on the redox potential of these complexes. Similarly, the sulfonamido ligand electronics seem to have only a slightly larger effect on the cobalt redox potential, since the $Co^{II/III}$ redox couple for **4-4(OH_2)** (+28mV) is only 50mV negative from that of **3-1(OH_2)**. Electrochemical cycling for the cobalt complexes indicate the chemical reversibility of each Co^{II}/Co^{III} redox event.

Discussion on electrochemical properties for nickel and copper M(OH_2) complexes.

The cyclic voltammogram for the nickel complex **5-1(OH_2)** shows an oxidation event at +517mV with a decreased intensity of the return reduction wave (Figure 5-6), but the

M^{II}/M^{III} redox event is still chemically reversible. Similarly, the M^{II}/M^{III} oxidation event for the copper complex **5-2(OH_2)** at +620mV has no return reduction wave (Figure 5-6), but is still chemically reversible. Since the M^{II}/M^{III} redox couple for **5-2(OH_2)** could not be compared with those of the other complexes, the M^{II}/M^{III} oxidation potential was compared to those of the other complexes (

Table 5-3). Moving to the right on the first row of transition metals results in positively shifted M^{II}/M^{III} oxidation potentials. The oxidation of **5-1(OH_2)** occurs approximately 400mV more positive than that of **3-1(OH_2)** (+125mV) and the oxidation of **5-2(OH_2)** occurs approximately 500mV more positive than oxidation of **3-1(OH_2)**.

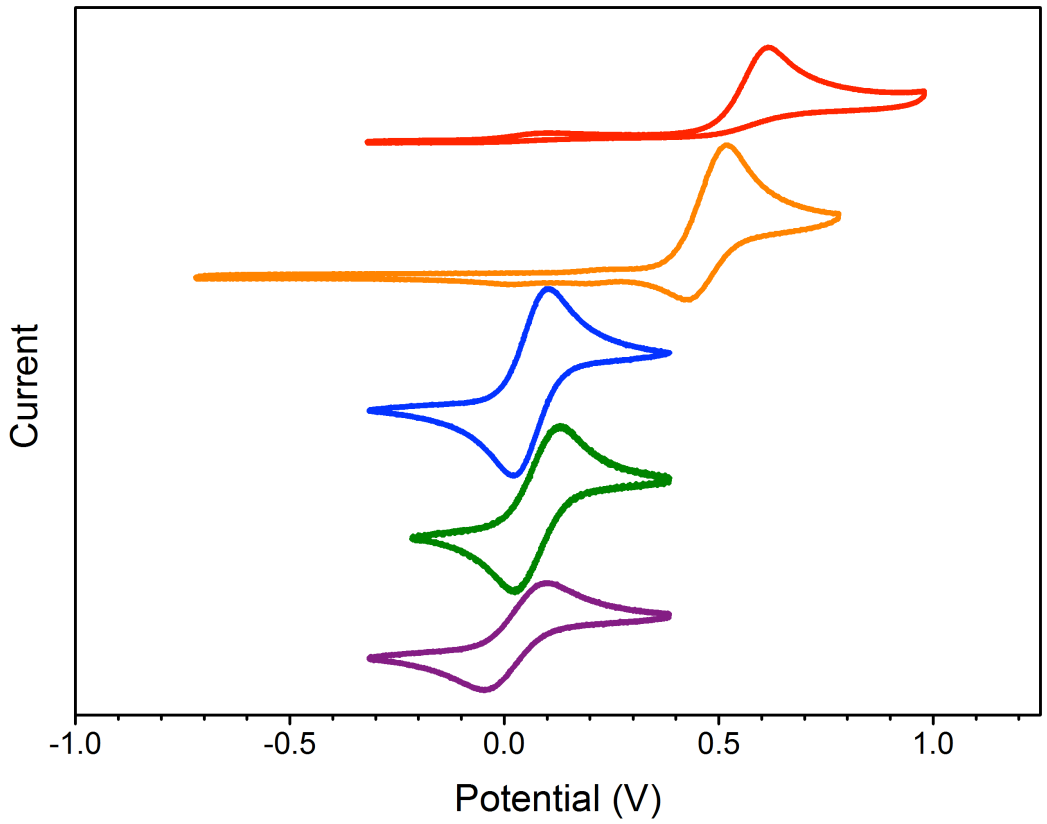

*Figure 5-6. Cyclic Voltammograms for **3-1(OH_2)** (—), **3-1^P(OH_2)** (—), **4-4(OH_2)** (—), **5-1(OH_2)** (—), **5-2(OH_2)** (—). Potential is referenced to Fc/Fc^+.*

Table 5-3. Electrochemical data.[a]

	E_{anodic} (mV)	$E_{cathodic}$ (mV)	$E_{½}$ (mV)
3-1(OH_2)	+125	+30	+78
3-1^p(OH_2)	+105	+21	+63
4-4(OH_2)	+95	–40	+28
5-1(OH_2)	+517	+420[d]	+469
5-2(OH_2)	+620	---[c]	---

[a]Scan rate = 100 mV/s with [^{n}Bu$_4$N][PF_6] as the supporting electrolyte (unless otherwise noted). All values vs. Fc/Fc$^+$. See Figure 5-6 for electrochemical traces. Data for ***3-1(OH_2)*** *and* ***4-4(OH_2)*** *is reported previously (Chapter 4) and included here for convenience. [b][^{tBu}ArPPh$_3$][PF_6] used as the supporting electrolyte. [c]The return oxidation wave of* ***5-2(OH_2)*** *is not discernible. [d]Electrochemically irreversible, but cycling current does not result in changes to the voltammogram (chemically reversible).*

5.3.5 Comparison of Electrochemical, Manometric, and Photometric Titration Data

The decay kinetics of the M(H_2O_2) adducts do not display a direct correlation to the electrochemical data for the corresponding M(OH_2) complexes. Figure 5-7 summarizes the three sets of data presented in this chapter. The copper complex **5-2(OH_2)** has the most positive M^{II}/M^{III} oxidation potential (620mV) and the corresponding **5-2(H_2O_2)** adduct has the *shortest* half-life (>53.4 ± 1.0 sec). The nickel complex **5-1(OH_2)** has the second most

positive M^{II}/M^{III} oxidation potential (517mV) but the corresponding **5-1(H_2O_2)** adduct has the *longest* half-life (576.4 ± 5.2 sec). Additionally, the strength of H_2O_2 binding to the metal ion in the M(H_2O_2) adducts do not correlate to their half-life values. The nickel complex **5-1(H_2O_2)** has the longest half-life and the highest measured binding constant for H_2O_2 to a metal ion, while the cobalt complex bearing the electron-rich $[Bus_3tren]^{3-}$ ligand (**4-4(H_2O_2)**) has the second highest measured binding constant for H_2O_2 to cobalt and the second shortest half-life, behind the copper complex (**5-2(H_2O_2)**). As seen in Chapter 1, the mechanisms for decay of M(H_2O_2) adducts are ill-defined and poorly understood, so the lack of a simple correlation between data sets is not problematic.

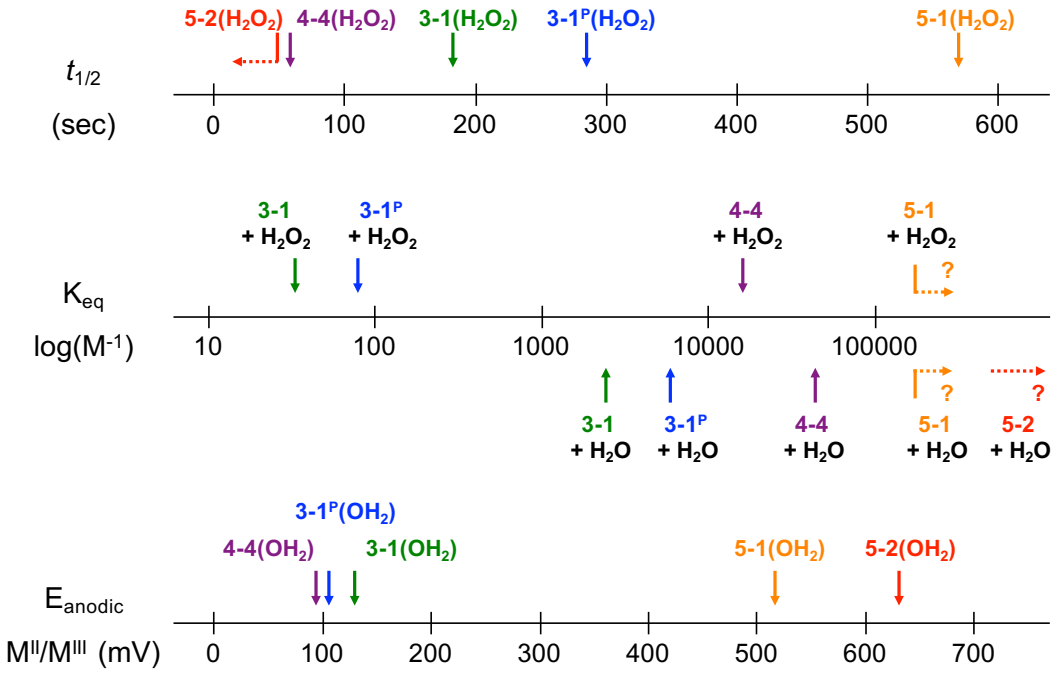

Figure 5-7. Linear scales for half-life vaues (top), binding constants (middle), and M^{II}/M^{III} oxidation potentials (bottom) for metal sulfonamidate complexes.

Complexity of $M(H_2O_2)$ decay.

These data indicate that the decay kinetics for $M^{II}(H_2O_2)$ adducts with sulfonamido complexes do not depend directly on the strength of H_2O_2 binding to the metal ion. However, there are two components that contribute to strength of binding for water and hydrogen peroxide to metal sulfonamido complexes: M–O bond strength and hydrogen bonding between the sulfonyl groups and protic ligand. The binding data in Table 5-1 suggest that these two components can have varying influence on total binding strength. It is possible that these two factors also influence the decay of $M(H_2O_2)$ adducts to varying degrees. For example, the computational evidence discussed in Chapter 1 suggests that hydrogen bonding interactions have a dramatic effect on the reactivity of $M(H_2O_2)$ adducts. One possible step in the decay mechanism of $M(H_2O_2)$ adducts with sulfonamido ligands is shown in Scheme 5-3. In this example, it can be seen how the accessibility of M^{III}, M–O bond strength, electron density of the ligand "R" group, and the hydrogen bonding donating ability of the Y–H group could all directly affect the stabilization of the tethered •OH species. The relative effect for each of these factors is impossible to determine without extensive data on decay kinetics for $M(H_2O_2)$ adducts. Investigation into the mechanism of $M(H_2O_2)$ decay is ongoing in the Scarborough group.

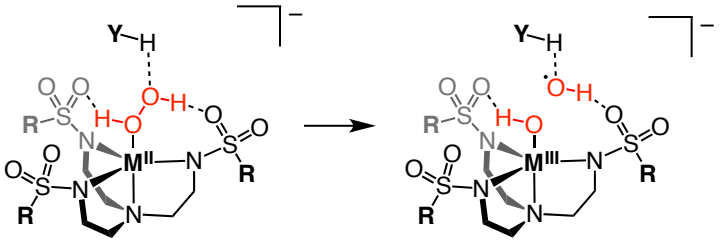

Scheme 5-3. Possible step in the decay of $M(H_2O_2)$ supported by sulfonamido ligands.

Discussion of individual observations.

Regardless of decay mechanism, the data discussed in this chapter demonstrate important individual effects of changing ligand electronics, counterion, and metal identity on the lifetime of $M(H_2O_2)$ adducts and binding strength of hydrogen peroxide. First, the use of the novel phosphonium cation $[^{tBu}ArPPh_3]^+$ strengthens the binding of hydrogen peroxide to cobalt sulfonamido complexes. Secondly, the K_{eq} values for protic ligands binding to the cobalt complex (**4-4**) bearing the alkyl-sulfonamido ligand $[Bus_3tren]^{3-}$ demonstrate that increased ligand electron density on the sulfonyl groups strengthens the binding of hydrogen peroxide to a greater extent than the binding of water to the metal ion. Additionally, the nickel complex **5-1(H_2O_2)** displayed the longest lifetime known for $M(H_2O_2)$ adducts with redox-active metals and the highest binding constant measured for hydrogen peroxide to a metal ion. Finally, the decreased accessibility of higher metal oxidation states (M^{III}) with nickel and copper complexes could be important in avoiding formation of unselective M^{IV}=O species (see Chapter 1). These observations will be useful in developing future catalytic reactions with hydrogen peroxide as the sole stoichiometric oxidant.

5.4 Conclusions

In summary, a series of metal-sulfonamido complexes were synthesized that engage in second-sphere hydrogen bonding with water and hydrogen peroxide. Binding constants for both water and hydrogen peroxide with metal-sulfonamido complexes further support the concept that hydrogen bonding is vital to stabilize $M(H_2O_2)$ adducts. We have demonstrated that the placement of strong hydrogen bonding acceptors could be used as a strategy to bias a metal complex to preferentially bind hydrogen peroxide in the presence

of water. This information is of particular importance with respect to catalytic systems, as hydrogen peroxide will have to compete with water in catalytic systems using aqueous sources of hydrogen peroxide. The titration data also demonstrate that the binding of hydrogen peroxide to the anionic sulfonamido complexes can be hindered by cations with hydrogen bond donors, such as ammonium ions. However, the binding of hydrogen peroxide is most significantly affected by the identity of the metal ion. We have provided evidence that $M(H_2O_2)$ adducts are accessible with nickel and copper, which were previously unknown, opening the door to further explore the reactivity of $M(H_2O_2)$ adducts with redox-active metals. Decay kinetics were obtained for $M(H_2O_2)$ adducts with cobalt, nickel and copper, but no direct correlation between either H_2O_2 binding strength or M^{II}/M^{III} redox potentials was observed. A nickel complex of hydrogen peroxide (**5-1(H_2O_2)**) displayed both the highest measured K_{eq} for hydrogen peroxide binding to a metal ion and the longest half-life for a $M(H_2O_2)$ adduct with redox active metal. The decreased accessibility of Ni^{III} relative to Co^{III} suggests a promising opportunity to explore the reactivity of $Ni(H_2O_2)$ adducts that are less susceptible to oxidation of the metal center. In short, the data presented in this chapter provide vital knowledge in understanding the characteristics and stability of hydrogen peroxide adducts with redox-active transition metals and serve as an excellent foundation of knowledge for future development of novel catalytic systems.

5.5 Experimental

5.5.1 Materials and Methods

Elemental analyses were performed by Atlantic Microlabs in Norcross, GA. IR spectra were obtained using a Nicolet 380 FT-IR with Smart Orbit Diamond ATR attachment.

Mass spectrometric analysis was collected at the Emory University Mass Spectrometry Center using electrospray ionization on a Thermo Finnigan LTQ-FTMS instrument. Thermogravimetric data collected on a PerkinElmer STA-6000. Digital manometer manufactured by Sper Scientific. Crystal diffraction data collected by Emory University Department of Chemistry X-Ray Crystallography Center. NMR data collected on a 400MHz or 500MHz instrument and referenced to residual solvent peaks. All reactions sensitive to air and/or moisture were carried out in an MBraun UNIlab glovebox under a nitrogen atmosphere. Solvents for use in the glovebox were degassed by sparging with nitrogen and dried using activated 3Å molecular sieves. Anhydrous THF (HPLC grade, inhibitor-free) was degassed, brought into the glovebox, and stored over molecular sieves for at least two days before filtering through activated alumina. Reagents were purchased from Sigma-Aldrich, Oakwood Chemicals, or Strem Chemicals and used without further purification.

5.5.2 Syntheses

[^{n}Bu$_4$N][(Ts$_3$tren)Ni^{II}(OH$_2$)] {5-1(OH$_2$)}

In a glovebox, H_3Ts_3tren (607mg, 0.997mmol) was dissolved in dimethylformamide and stirred while slowly adding potassium hydride (124mg, 3.09mol). After stirring for approximately 1 hour material starts to precipitate from the solution. Ni(acac)$_2$ (256mg, 0.997mmol) was added and the solution stirred for 3 hours. The solution was removed from the glovebox and Bu_4NBr (322mg, 0.997mmol) was added. The solution was diluted with water and extracted with dichloromethane. The organic layer was washed with DI water (2x), brine, and then dried with Na_2SO_4. The green solution was filtered and concentrated via rotary evaporation. The viscous solution was diluted with a little dichloromethane and

crystallized via vapor diffusion with diethyl ether to afford large dark green crystals (790mg, 86%). Anal. calcd (found) for ($C_{43}H_{69}N_5NiO_6S_3$): C, 55.84 (56.08); H, 7.74 (7.81); N, 7.57 (7.59). λ_{max}, nm (ε, $M^{-1}\,cm^{-1}$): 426 (107), 487 (40) and 710 (57). IR (cm^{-1}): 3273, 2959, 2860, 1599, 1490, 1464, 1381, 1349, 1233, 1112, 1077, 1036, 974, 933, 876, 812, 740, 710, 661, 597, 551. FTMS (NSI): *m/z*– = 663.09245, calcd: 663.09212 (ML_1^-), Δ = 0.5 ppm; *m/z*– = 681.10298, calcd: 681.10268 ($^{tBu}PhPPh_3^+$), Δ = 0.4 ppm.

[^{n}Bu$_4$N][(Ts$_3$tren)Ni^{II}] {5-1}

In a glovebox, **5-1(OH$_2$)** (564mg) was dissolved in THF at 60°C and treated with 3Å molecular sieves. After heating for three days the orange solution was filtered through celite and ether was added to yield orange crystals (370mg, 67%). λ_{max}, nm (ε, $M^{-1}\,cm^{-1}$): 466 (46), 716 (13).

[^{n}Bu$_4$N][(Ts$_3$tren)Cu^{II}(OH$_2$)] {5-2(OH$_2$)}

In a glovebox, H_3Ts_3tren (575mg, 0.945mmol) was dissolved in dimethylformamide and stirred while slowly adding potassium hydride (117mg, 2.93mol). After stirring for approximately 10 minutes $CuCl_2$ (128mg, 0.945mmol) was added and the solution stirred overnight. The solution was removed from the glovebox and Bu_4NBr (305mg, 0.945mmol) was added. The solution was diluted with water and extracted with dichloromethane. The organic layer was washed with DI water (2x), brine, and then dried with Na_2SO_4. The green solution was filtered and concentrated via rotary evaporation. The residue was dissolve in dichloromethane and crystallized via vapor diffusion with diethyl ether to afford large green crystals (762mg, 87%). Anal. calcd (found) for ($C_{43}H_{71}CuN_5O_7S_3$): C, 55.55 (55.66); H, 7.70 (7.65); N, 7.53 (7.57). λ_{max}, nm (ε, $M^{-1}\,cm^{-1}$): 1084 (247). IR (cm^{-1}): 3182, 2960, 2860, 1599, 1490, 1381, 1348, 1260, 1226, 1139, 1115, 1074, 1034, 992, 973, 929, 879,

813, 742, 710, 661, 597, 551. FTMS (NSI): *m/z*– = 668.08655, calcd: 668.08637 ($ML1^-$), $\Delta = 0.3$ ppm.

[^{tBu}ArPPh$_3$][PF$_6$]

Dissolve [^{tBu}ArPPh$_3$][Br] (2.18g, 4.1mmol) in DCM. Dissolve NH_4PF_6 (1.62g, 9.95mmol, 2.4eq) in DI water. Combine each solution and stir vigorously for 10min before allowing layers to separate. Remove the organic layer and wash aqueous layer with DCM. Combine organic layers and dry with Na_2SO_4. Filter and concentrate via rotary evaporation. Dry thoroughly under vacuum to yield white powder (2.22g, 91%). Anal. calcd (found) for ($C_{32}H_{36}F_6P_2$): C, 64.43 (64.56); H, 6.08 (6.05).

Extraction of H_2O_2 in diethyl ether

In a glovebox, urea hydrogen peroxide was stirred in anhydrous diethyl ether for several hours. After allowing the urea solid to settle, the solution was decanted and stored at -35˚C overnight. The solution was filtered through celite and concentrated under vacuum. The concentration of H_2O_2 can be determined periodically using a pertitanic acid assay (Section 3.5). After reaching the desired concentration, the solution was stored at -35˚C. Occasionally, additional white solid forms in these solutions, which can be filtered over celite.

Preparation of H_2O_2 in Acetonitrile

An amount of H_2O_2 in diethyl ether is added to anhydrous acetonitrile. The diethyl ether is then removed under vacuum. A pertitanic acid assay can be used to determine the concentration of H_2O_2 in these solutions. The same procedure can be used to obtain H_2O_2 solutions in MeCN-d_3 and nitromethane. ^{1}H NMR spectroscopy was used to ensure that the solution contained <5% water.

5.5.3 Photometric Titrations of Water and Hydrogen Peroxide

Using a UNISOKU CoolSpeK UV USP-203 cryostat attachment, a tall cuvette containing a solution of 4-coordinate metal-sulfonamidate complex (20mM) in anhydrous THF and closed with a septum cap was cooled to –70˚C. A balloon of nitrogen attached to a needle was used to equilibrate the pressure inside the cuvette as it cooled. A solution of ligand (H_2O or H_2O_2) in THF was added via gastight syringe incrementally. After each addition of ligand, the solution was stirred for 1min before a spectrum was taken. The absorbance values at two wavelengths (one with increasing intensity and one with decreasing intensity) were each normalized from 0 to 1 and then averaged to obtain values for fractional occupation. Origin was used to model each set of data to the following equation: where ϕ is the fractional occupation represented by the normalized absorbance values, [L] is the concentration of ligand for each data point, [Co] is the concentration of cobalt complex for each data point, K is the binding constant.

$$\phi = \frac{[\mathrm{Co}]+([\mathrm{L}]+\rho)+\frac{1}{K}-\sqrt{\left([\mathrm{Co}]+([\mathrm{L}]+\rho)+\frac{1}{K}\right)^2-4[\mathrm{Co}]([\mathrm{L}]+\rho)}}{2[\mathrm{Co}]} + ([\mathrm{L}]+\rho)\times m + b \quad \text{(Eq. 5-1)}$$

In order to improve the mathematical fit in case of error, several parameters were added to the published equation. The parameter *m* and *b* are vertical scaling and shift factors. The parameter ρ is a horizontal shift factor, which allows the fit to account for the presence of 5-coordinate metal-sulfonamidate complex prior to addition of water or H_2O_2. These fitting factors allow the equation to most closely model the sharpness of the titration curve, which determines the value of the binding constant, K_{eq}.

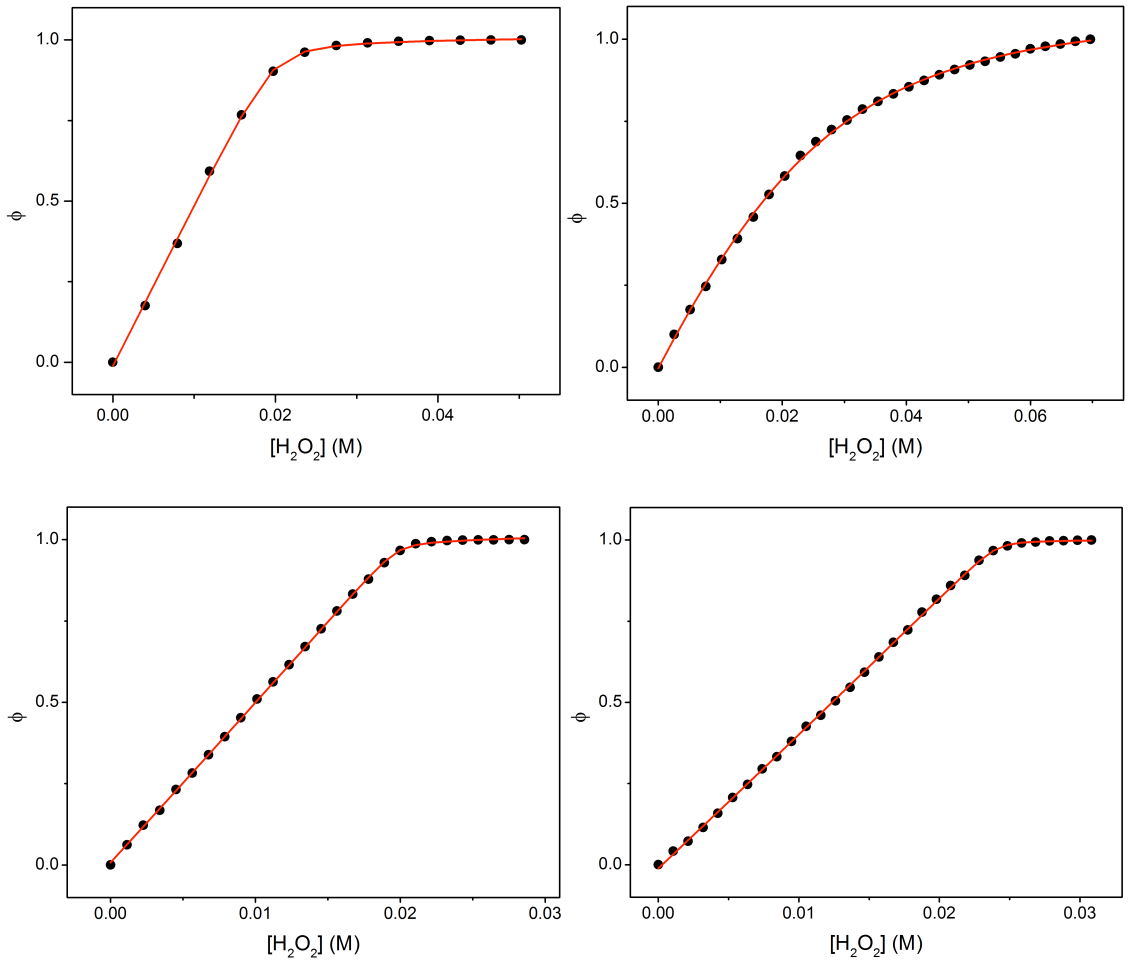

Figure 5-8. Titration curveswith mathematical fits for: ***3-1***^{P} *and* H_2O *(top left);* ***3-1***^{P} *and* H_2O_2 *(top right);* ***4-4*** *and* H_2O *(bottom left);* ***4-4*** *and* H_2O_2 *(bottom right).*

Modeling data for titrations with 5-1.

Titration curves for **5-1** were simulated using Equation 5-1 for both water and peroxide. As K_{eq} increases, the curve approaches a sharp angle and the usable data to model the curve decreases. Figure 5-9 and Figure 5-10 show there is almost no discernible difference for values K_{eq} at or above 1,000,000 M^{-1}. Fitting values above 100,000 M^{-1} relies on only a few points of data, greatly increasing the uncertainty of the mathematical fit. Therefore, simulated curves were compared with the experimental titration curves to estimate the magnitude of K_{eq} for **5-1** binding to water and H_2O_2 (Figure 5-11). Only values above 200,000 M^{-1} appear to fit the experimental titration curves.

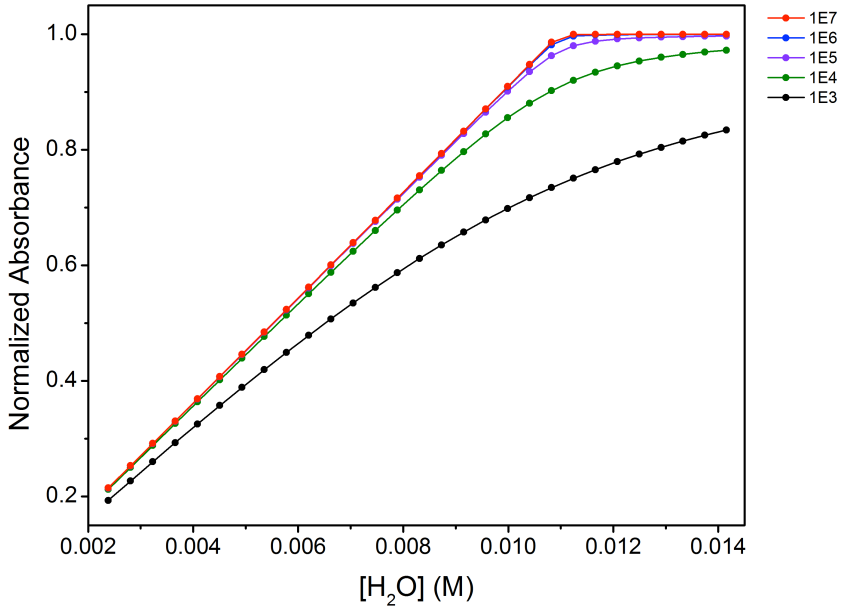

*Figure 5-9. Simulated titration curves for **5-1** binding with water/H_2O_2 with different magnitudes for K_{eq}.*

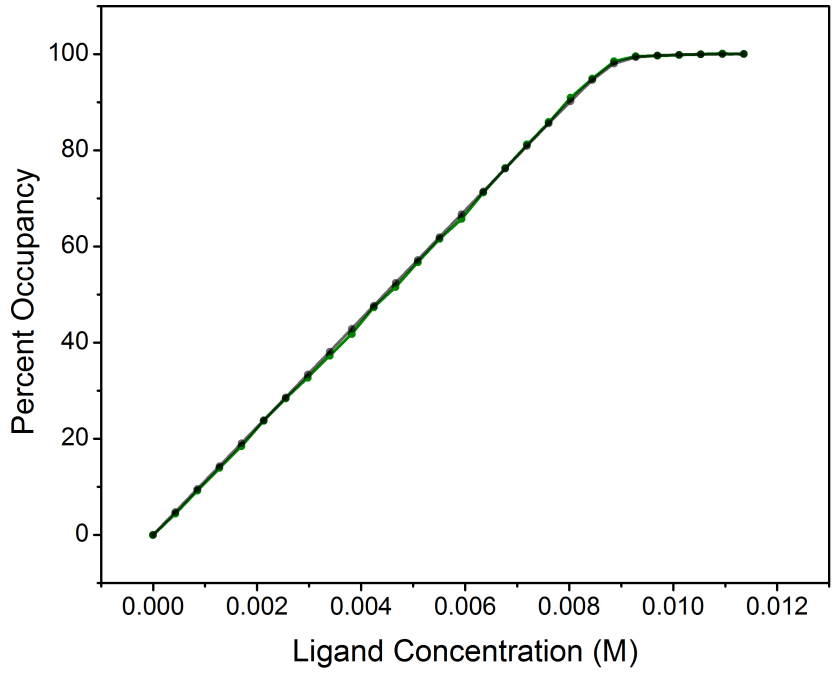

Figure 5-10. Simulated curves (gray) with experimental titration curves for water with ***5-1*** *and* K_{eq}*=200,000* M^{-1}.

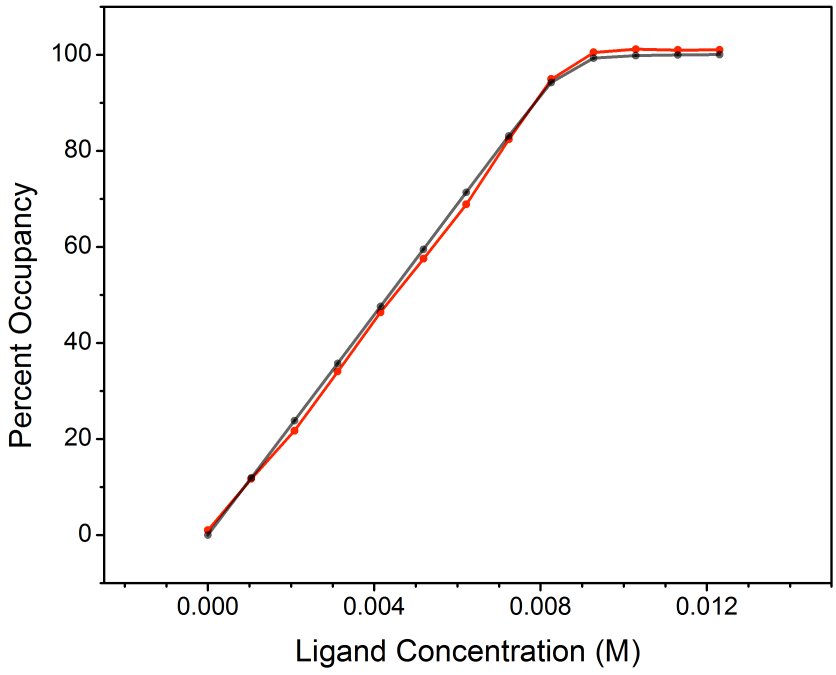

Figure 5-11. Simulated curves (gray) with experimental titration curves for H_2O_2 *with* ***5-1*** *and* K_{eq}*=200,000* M^{-1}.

5.5.4 Manometric decay experiments

Experimental setup

In a glovebox, approximately 150mg of each complex is dissolved in 48mL of anhydrous acetonitrile in a 100mL Schlenk flask fitted with a stir bar and sealed with a well-greased hose adapter with glass stopcock. A fresh rubber septum is placed on the flask's hose adapter and both glass stopcock are closed. One equivalent of H_2O_2 in acetonitrile is drawn into a gas-tight syringe fitted with a long needle. This needle is inserted into the septa on the Schlenk flask, but not into the solution. This apparatus is removed from the glovebox and stirred in a large water bath gently stirred at 25˚C. The hose adapter is secured tightly to the flask using rubber bands and the plastic hose for the manometer attached tightly to the hose adapter. A balloon of dry oxygen fitted with a needle is placed into the septum. Both stopcocks are opened and the atmosphere purged with approximately 1L of oxygen gas. This is to ensure that the solution is saturated with dissolved oxygen. After the purge, the plastic hose is attached to the digital manometer, sealing the system. The system is allowed to equilibrate for at least 15min. The digital manometer begins taking pressure readings immediately prior to injection of peroxide. The long needle of the gas-tight syringe (still in the septa) is inserted through the stopcock opening and into the reaction solution. The peroxide is injected, the needle removed, and the glass stopcock closed in rapid succession. The system is allowed to stir gently in the 25˚C water bath for approximately 1hr before pressure readings are concluded. Experimental setup shown in Figure 5-12.

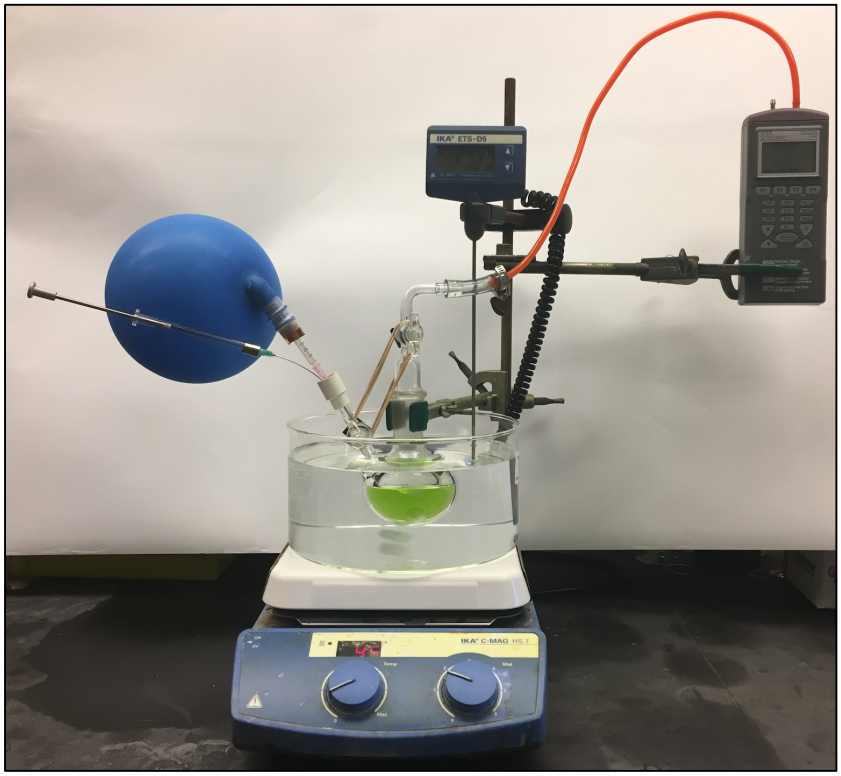

Figure 5-12. Manometric experiment setup for ***5-1(H_2O_2)*** *before injection of* H_2O_2.

Data workup

To process the raw data, the initial data points (pre-injection and injection) are removed. An early portion of the data is modeled using the following exponential function in Origin:

$$P = C - Ae^{-t/\tau}$$

where P is pressure, C and A are fitting parameters (such that $P_0 = C - A$), and τ is the time constant. The half-life of the corresponding exponential decay can be determined using the equation: $T_{1/2} = \tau \cdot \ln(2)$. After calculating an initial half-life, the data set was adjusted to include at least three half-lives. The fitting process was repeated using the adjusted set of data.

Table 5-4. Fitting parameters for manometric experiments.

	3-1(H_2O_2)	**3-1^P(H_2O_2)**	**4-4(H_2O_2)**	**5-1(H_2O_2)**	**5-2(H_2O_2)**
C	29.62 ± 0.03	36.03 ± 0.05	47.77 ± 0.11	21.14 ± 0.03	28.79 ± 0.14
A	17.86 ± 0.02	13.43 ± 0.04	28.94 ± 0.10	12.22 ± 0.04	19.06 ± 0.12
τ	250.29 ± 0.92	408.56 ± 3.71	95.57 ± 1.02	831.53 ± 7.47	76.97 ± 1.38
R^2	0.99959	0.99913	0.9996	0.99606	0.99932
$T_{1/2}$ (sec)	173.5 ± 0.6	283.2 ± 2.6	66.2 ± 0.7	576.4 ± 5.2	53.4 ± 1.0

5.5.5 Cyclic Voltammetry

Cyclic voltammetry experiments were run in dichloromethane with 0.1M tetrabutylammonium hexafluorophosphate or [^{tBu}ArPPh$_3$][PF_6] hexafluorophosphate (for **3-1^P(OH_2)**) as supporting electrolyte and using a glassy carbon working electrode. The reference electrode solution was made with Ag(NO_3) and supporting electrolyte in acetonitrile. Ferrocene was used as an external reference before and after the sample runs. The potential window was scanned at 0.1 V/s.

5.6 References

1. Jones, C. W., *Applications of of Hydrogen Peroxide and Derivatives*. Royal Society: Cambridge, U.K., 1999.

2. Hage, R.; de Boer, J. W.; Gaulard, F.; Maaijen, K., Chapter Three - Manganese and Iron Bleaching and Oxidation Catalysts. In *Adv. Inorg. Chem.*, Rudi van, E.; Colin, D. H., Eds. Academic Press: 2013; Vol. Volume 65, pp 85-116.

3. Hage, R.; Lienke, A., Applications of Transition-Metal Catalysts to Textile and Wood-Pulp Bleaching. *Angew. Chem. Int. Ed.* **2006,** *45* (2), 206-222.

4. Russo, V.; Tesser, R.; Santacesaria, E.; Di Serio, M., Chemical and Technical Aspects of Propene Oxide Production via Hydrogen Peroxide (HPPO Process). *Ind. Eng. Chem. Res.* **2013,** *52* (3), 1168-1178.

5. Chen, M.; Pan, Y.; Kwong, H.-K.; Zeng, R. J.; Lau, K.-C.; Lau, T.-C., Catalytic oxidation of alkanes by a (salen)osmium(vi) nitrido complex using H2O2 as the terminal oxidant. *Chem. Commun.* **2015,** *51* (71), 13686-13689.

6. Kwong, H.-K.; Lo, P.-K.; Lau, K.-C.; Lau, T.-C., Epoxidation of alkenes and oxidation of alcohols with hydrogen peroxide catalyzed by a manganese(v) nitrido complex. *Chem. Commun.* **2011,** *47* (14), 4273-4275.

7. Ma, L.; Pan, Y.; Man, W.-L.; Kwong, H.-K.; Lam, W. W. Y.; Chen, G.; Lau, K.-C.; Lau, T.-C., Highly Efficient Alkane Oxidation Catalyzed by [MnV(N)(CN)4]2–. Evidence for [MnVII(N)(O)(CN)4]2– as an Active Intermediate. *J. Am. Chem. Soc.* **2014,** *136* (21), 7680-7687.

8. Anson, C. W.; Ghosh, S.; Hammes-Schiffer, S.; Stahl, S. S., Co(salophen)-Catalyzed Aerobic Oxidation of p-Hydroquinone: Mechanism and Implications for Aerobic Oxidation Catalysis. *J. Am. Chem. Soc.* **2016,** *138* (12), 4186-4193.

9. Afanasiev, P.; Kudrik, E. V.; Millet, J.-M. M.; Bouchu, D.; Sorokin, A. B., High-valent diiron species generated from N-bridged diiron phthalocyanine and H2O2. *Dalton Trans.* **2011,** *40* (3), 701-710.

10. Mirza, S. A.; Bocquet, B.; Robyr, C.; Thomi, S.; Williams, A. F., Reactivity of the Coordinated Hydroperoxo Ligand. *Inorg. Chem.* **1996,** *35* (5), 1332-1337.

11. Theodoridis, A.; Maigut, J.; Puchta, R.; Kudrik, E. V.; van Eldik, R., Novel Iron(III) Porphyrazine Complex. Complex Speciation and Reactions with NO and H2O2. *Inorg. Chem.* **2008,** *47* (8), 2994-3013.

12. Wolak, M.; van Eldik, R., Mechanistic studies on peroxide activation by a water-soluble iron(III)-porphyrin: implications for O-O bond activation in aqueous and nonaqueous solvents. *Chemistry* **2007,** *13* (17), 4873-83.

13. Chandrasena, R. E. P.; Vatsis, K. P.; Coon, M. J.; Hollenberg, P. F.; Newcomb, M., Hydroxylation by the Hydroperoxy-Iron Species in Cytochrome P450 Enzymes. *J. Am. Chem. Soc.* **2004,** *126* (1), 115-126.

14. Coon, M. J., Cytochrome P450: nature's most versatile biological catalyst. *Annu Rev Pharmacol Toxicol* **2005,** *45* (1), 1-25.

15. Newcomb, M.; Toy, P. H., Hypersensitive Radical Probes and the Mechanisms of Cytochrome P450-Catalyzed Hydroxylation Reactions. *Acc. Chem. Res.* **2000,** *33* (7), 449-455.

16. Sheng, X.; Zhang, H.; Hollenberg, P. F.; Newcomb, M., Kinetic Isotope Effects in Hydroxylation Reactions Effected by Cytochrome P450 Compounds I Implicate Multiple Electrophilic Oxidants for P450-Catalyzed Oxidations. *Biochemistry* **2009,** *48* (7), 1620-1627.

17. Ramanan, R.; Dubey, K. D.; Wang, B.; Mandal, D.; Shaik, S., Emergence of Function in P450-Proteins: A Combined Quantum Mechanical/Molecular Mechanical and Molecular Dynamics Study of the Reactive Species in the H2O2-Dependent Cytochrome P450SPα and Its Regio- and Enantioselective Hydroxylation of Fatty Acids. *J. Am. Chem. Soc.* **2016,** *138* (21), 6786-6797.

18. Wang, B.; Li, C.; Dubey, K. D.; Shaik, S., Quantum Mechanical/Molecular Mechanical Calculated Reactivity Networks Reveal How Cytochrome P450cam and Its T252A Mutant Select Their Oxidation Pathways. *J. Am. Chem. Soc.* **2015,** *137* (23), 7379-7390.

19. Wallen, C. M.; Bacsa, J.; Scarborough, C. C., Hydrogen Peroxide Complex of Zinc. *J. Am. Chem. Soc.* **2015,** *137* (46), 14606-14609.

20. Wallen, C. M.; Palatinus, L.; Bacsa, J.; Scarborough, C. C., Hydrogen Peroxide Coordination to Cobalt(II) Facilitated by Second-Sphere Hydrogen Bonding. *Angew. Chem. Int. Ed.* **2016,** *55* (39), 11902-11906.

21. Marcoux, D.; Charette, A. B., Nickel-Catalyzed Synthesis of Phosphonium Salts from Aryl Halides and Triphenylphosphine. *Advanced Synthesis & Catalysis* **2008,** *350* (18), 2967-2974.

22. Churakov, A. V.; Prikhodchenko, P. V.; Howard, J. A. K.; Lev, O., Glycine and l-serine crystalline perhydrates. *Chem. Commun.* **2009,** (28), 4224-4226.

23. Prikhodchenko, P. V.; Medvedev, A. G.; Tripol'skaya, T. A.; Churakov, A. V.; Wolanov, Y.; Howard, J. A. K.; Lev, O., Crystal structures of natural amino acid perhydrates. *CrystEngComm* **2011,** *13* (7), 2399-2407.

24. Vener, M. V.; Medvedev, A. G.; Churakov, A. V.; Prikhodchenko, P. V.; Tripol'skaya, T. A.; Lev, O., H-Bond Network in Amino Acid Cocrystals with H2O or H2O2. The DFT Study of Serine–H2O and Serine–H2O2. *J. Phys. Chem. A* **2011,** *115* (46), 13657-13663.

25. Wolanov, Y.; Shurki, A.; Prikhodchenko, P. V.; Tripolskaya, T. A.; Novotortsev, V. M.; Pedahzur, R.; Lev, O., Aqueous stability of alumina and silica perhydrate hydrogels: experiments and computations. *Dalton Trans.* **2014,** *43* (44), 16614-16625.

Appendix 1. NMR Characterization Data

Chapter 2

Symbol Key (Chapter 2 only)

* - diethyl ether
◆ – DCM
†- 1,2-dimethoxyethane
⅄- urea
• - THF
★ – Environmental interference
7.26 - Residual NMR solvent

H_2O_2 (extracted from urea adduct)
^1H, THF-d_8 400MHz

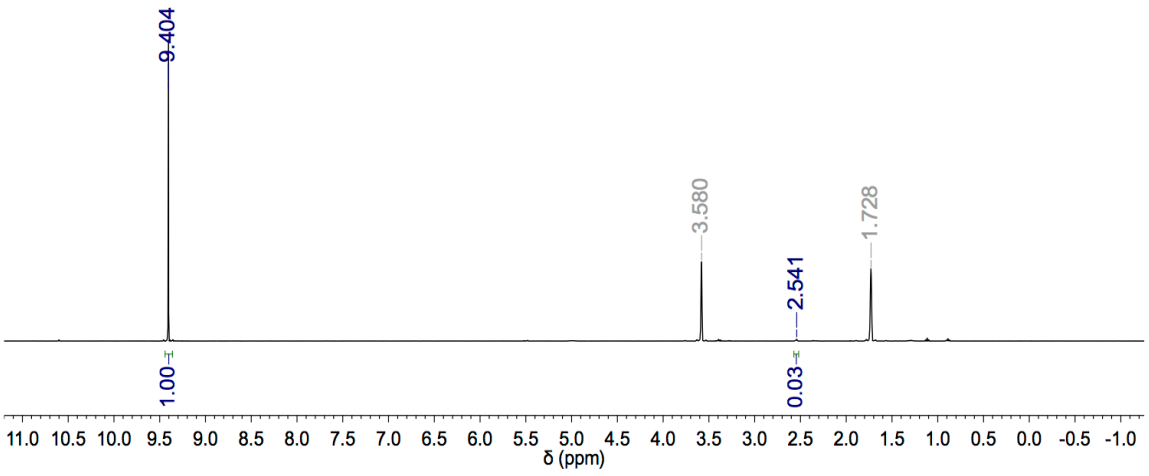

H_2O_2 (with water)
^1H, THF-d_8 400MHz

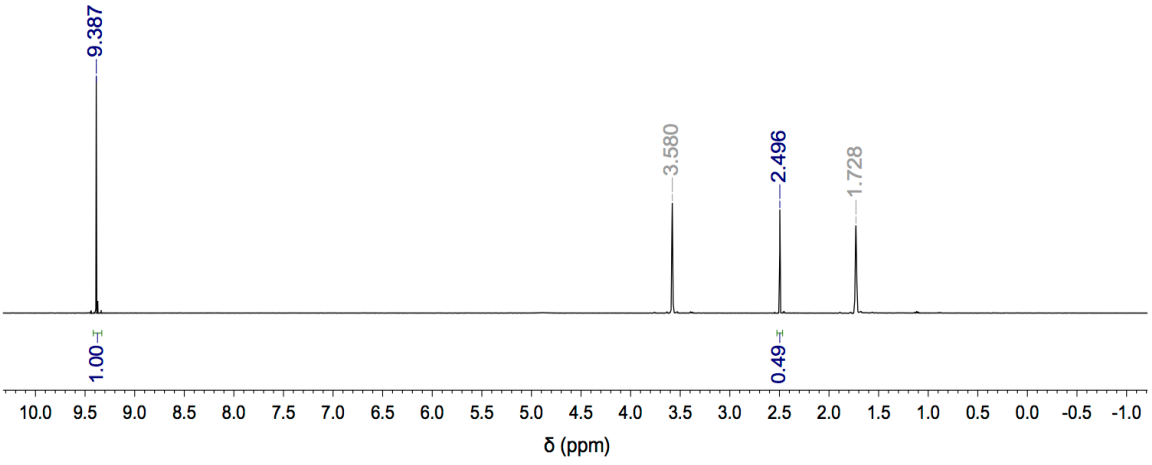

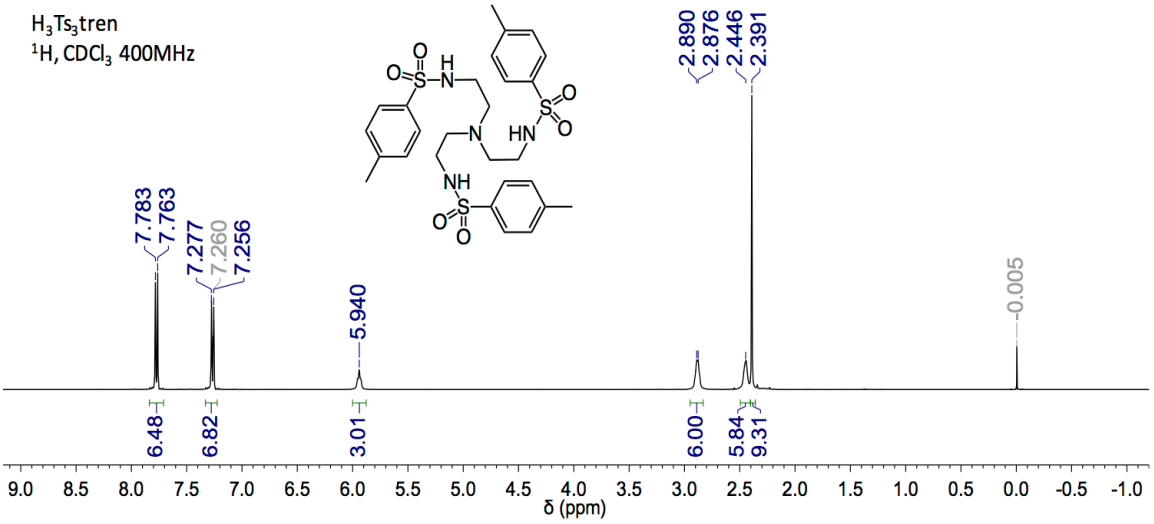
H3Ts3tren
1H, CDCl3 400MHz
7.783
7.763
7.277
7.260
7.256
5.940
2.890
2.876
2.446
2.391
0.005
6.48
6.82
3.01
6.00
5.84
9.31
δ (ppm)

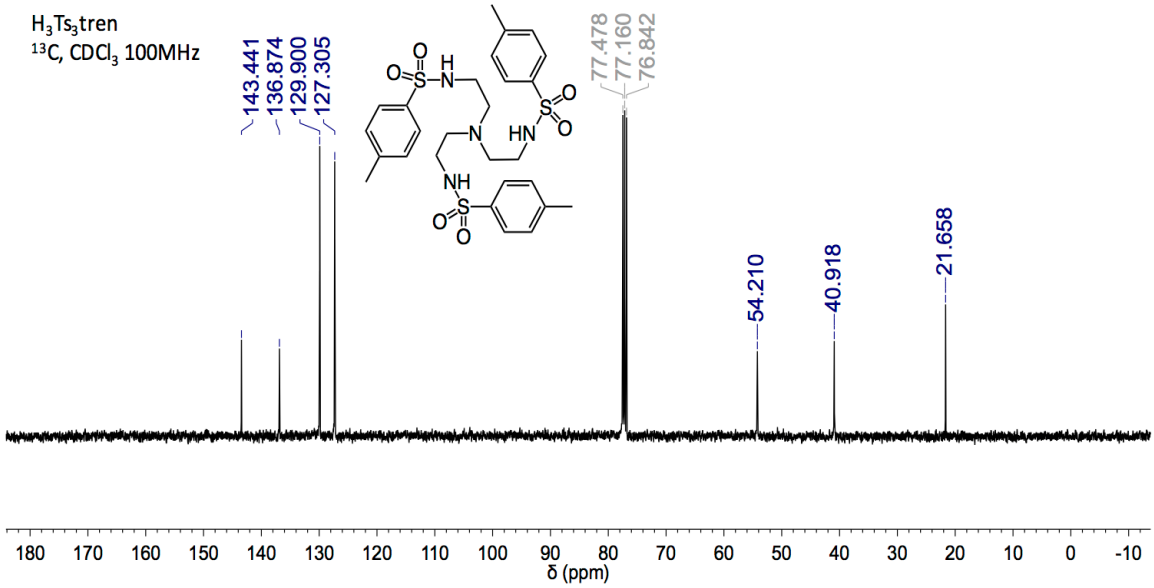
H3Ts3tren
13C, CDCl3 100MHz
143.441
136.874
129.900
127.305
77.478
77.160
76.842
54.210
40.918
21.658
δ (ppm)

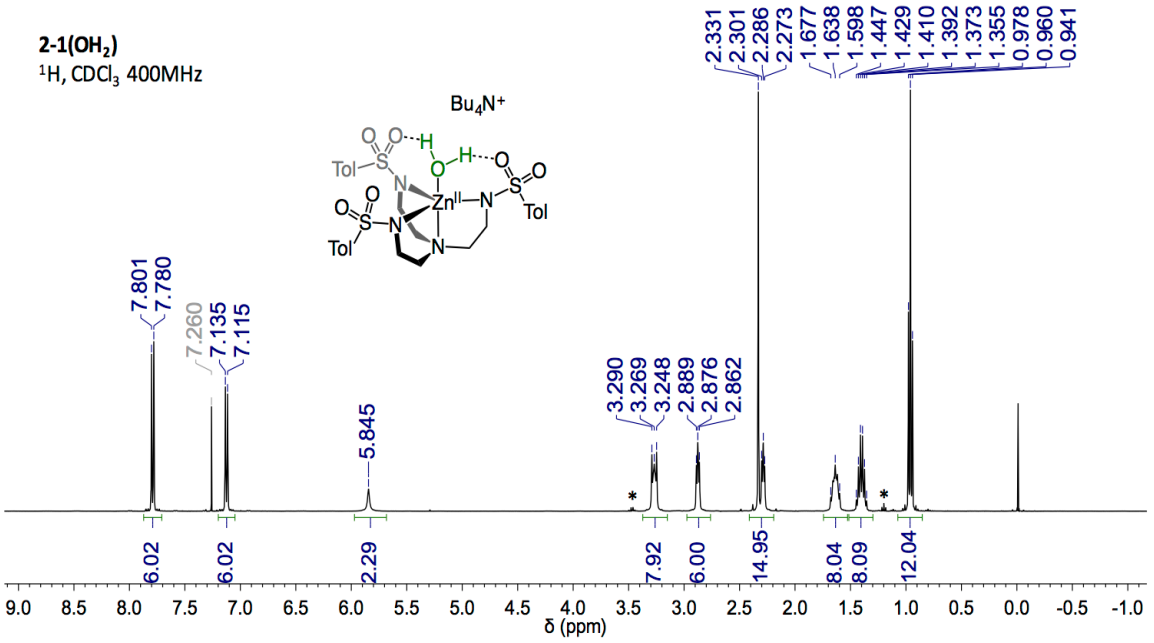
2-1(OH2)
1H, CDCl3 400MHz
Bu4N+
Tol
Zn
7.801
7.780
7.260
7.135
7.115
5.845
3.290
3.269
3.248
2.889
2.876
2.862
2.331
2.301
2.286
2.273
1.677
1.638
1.598
1.447
1.429
1.410
1.392
1.373
1.355
0.978
0.960
0.941
6.02
6.02
2.29
7.92
6.00
14.95
8.04
8.09
12.04
δ (ppm)

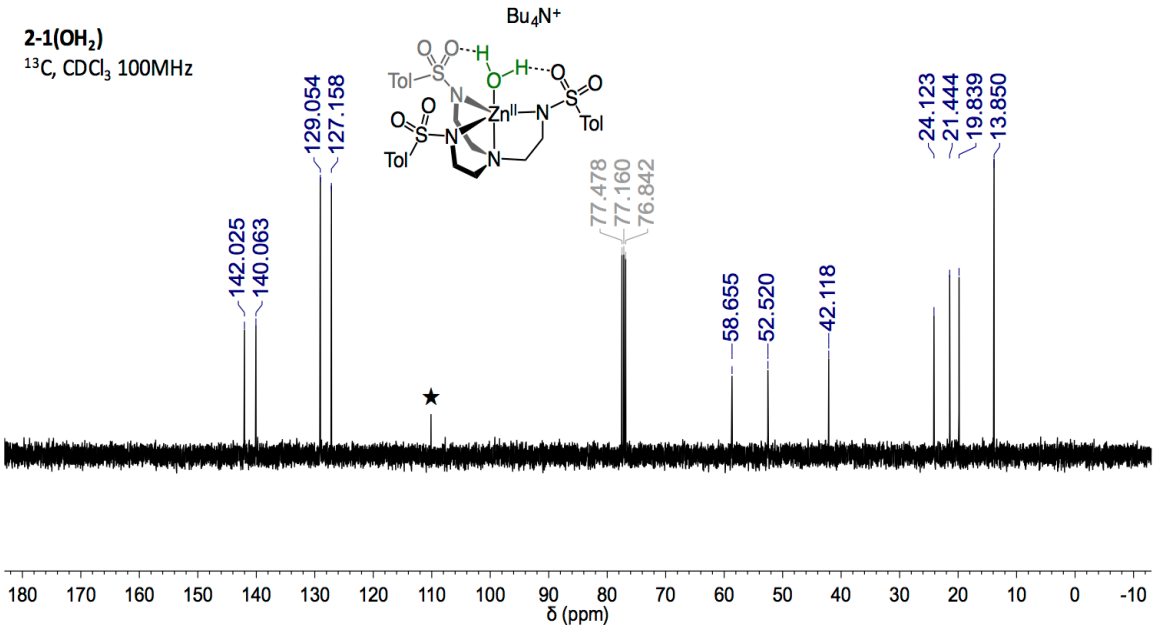
2-1(OH2)
13C, CDCl3 100MHz
Bu4N+
Tol
Zn
129.054
127.158
142.025
140.063
77.478
77.160
76.842
58.655
52.520
42.118
24.123
21.444
19.839
13.850
δ (ppm)

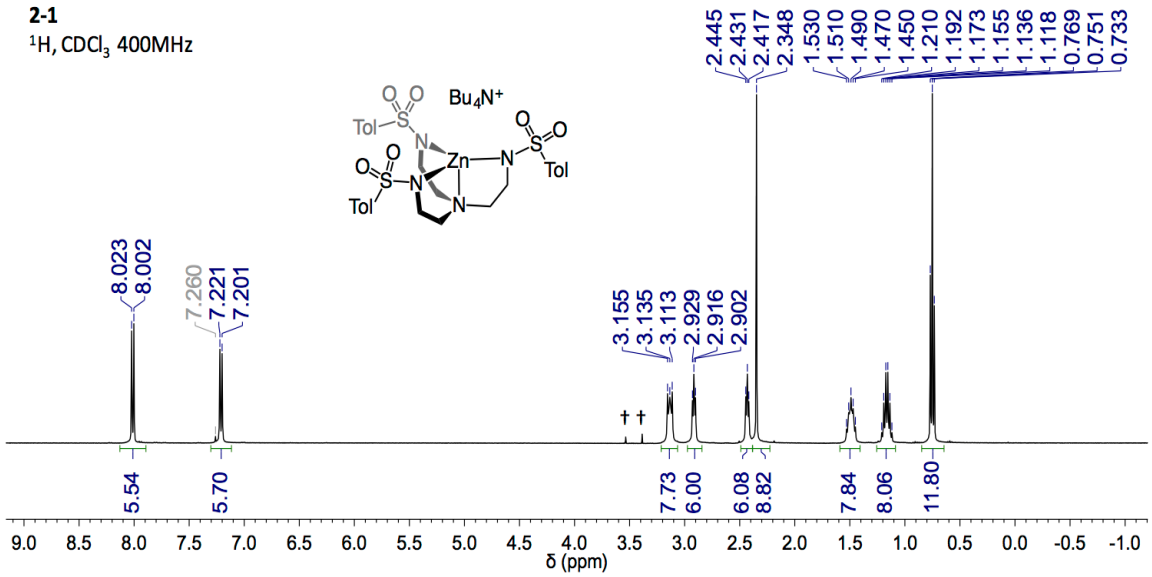
2-1
^{1}H, CDCl$_3$ 400MHz
Bu$_4$N$^+$
Tol
Zn
N
O
S
8.023
8.002
7.260
7.221
7.201
3.155
3.135
3.113
2.929
2.916
2.902
2.445
2.431
2.417
2.348
1.530
1.510
1.490
1.470
1.450
1.210
1.192
1.173
1.155
1.136
1.118
0.769
0.751
0.733
5.54
5.70
7.73
6.00
6.08
8.82
7.84
8.06
11.80
δ (ppm)

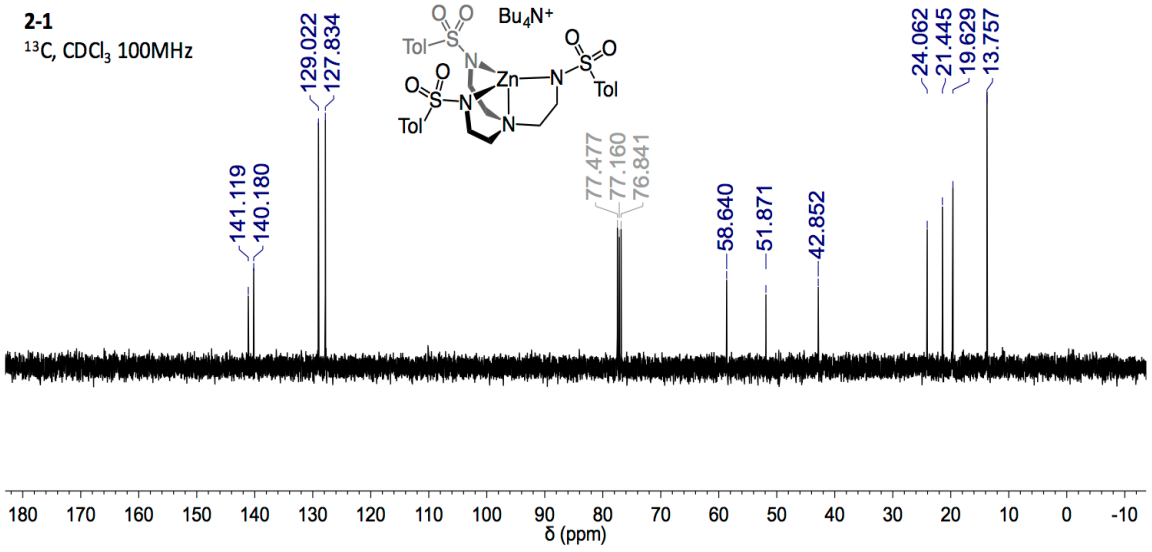
2-1
^{13}C, CDCl$_3$ 100MHz
Bu$_4$N$^+$
Tol
Zn
N
O
S
129.022
127.834
141.119
140.180
77.477
77.160
76.841
58.640
51.871
42.852
24.062
21.445
19.629
13.757
δ (ppm)

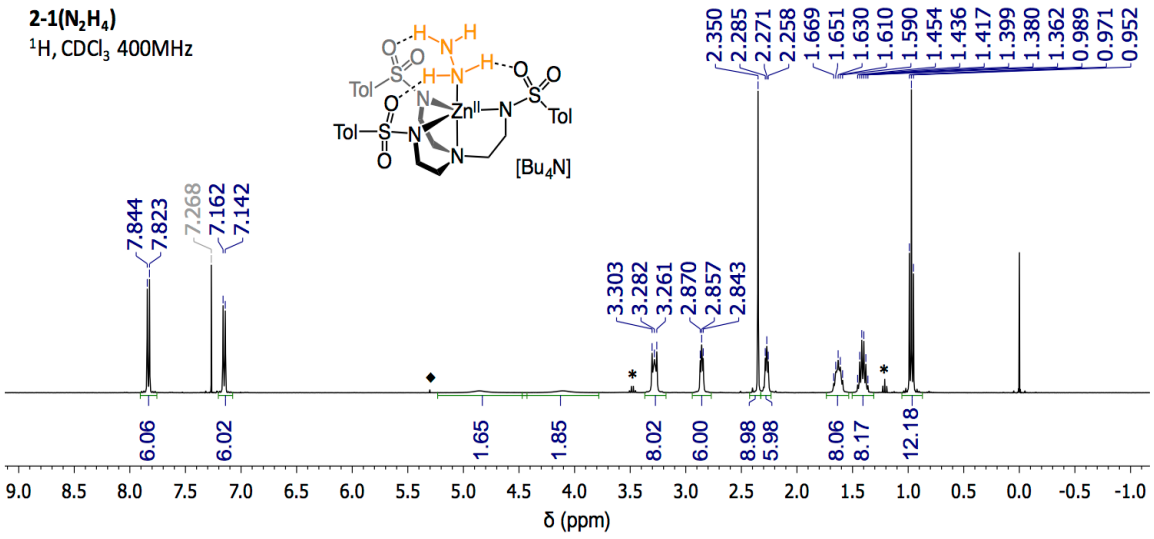
2-1(N2H4)
1H, CDCl3 400MHz
[Bu4N]
7.844
7.823
7.268
7.162
7.142
3.303
3.282
3.261
2.870
2.857
2.843
2.350
2.285
2.271
2.258
1.669
1.651
1.630
1.610
1.590
1.454
1.436
1.417
1.399
1.380
1.362
0.989
0.971
0.952
6.06
6.02
1.65
1.85
8.02
6.00
8.98
5.98
8.06
8.17
12.18
δ (ppm)

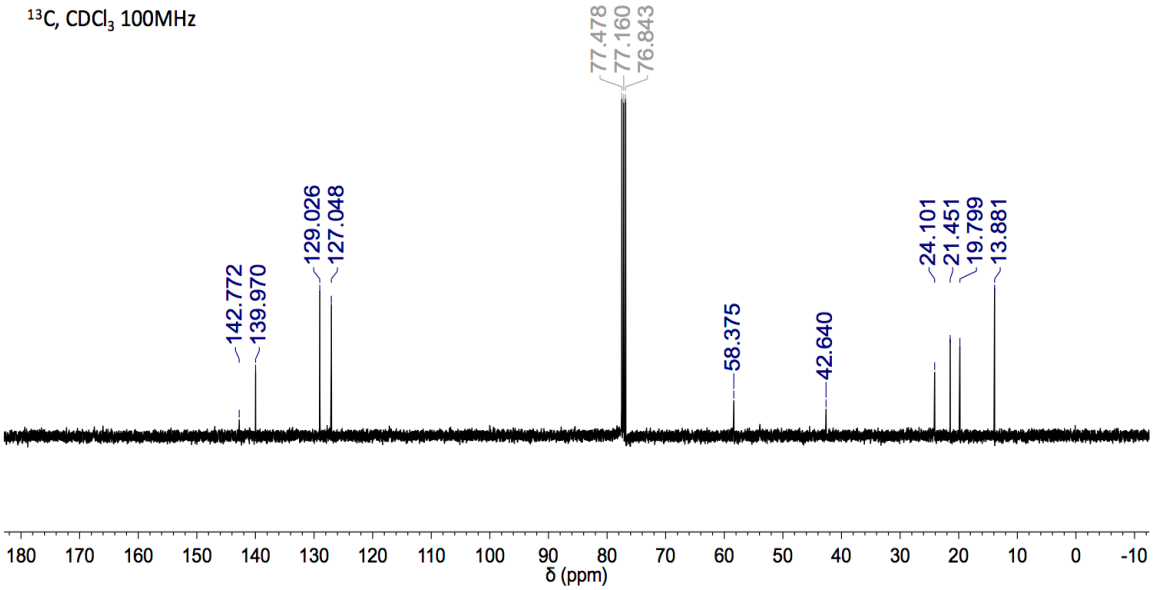
13C, CDCl3 100MHz
77.478
77.160
76.843
142.772
139.970
129.026
127.048
58.375
42.640
24.101
21.451
19.799
13.881
δ (ppm)

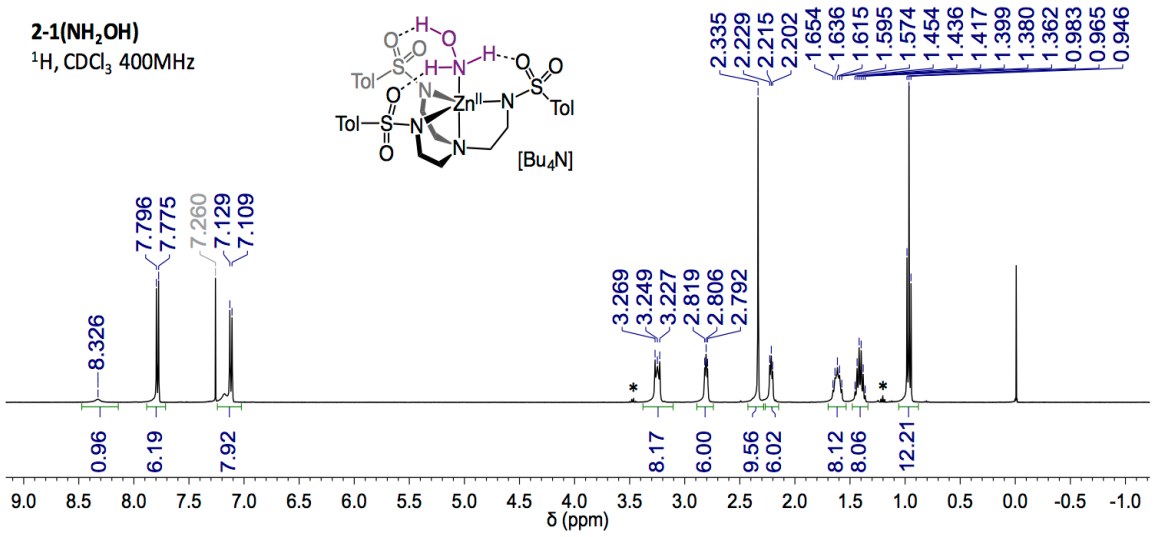
2-1(NH2OH)
1H, CDCl3 400MHz
[Bu4N]
δ (ppm)

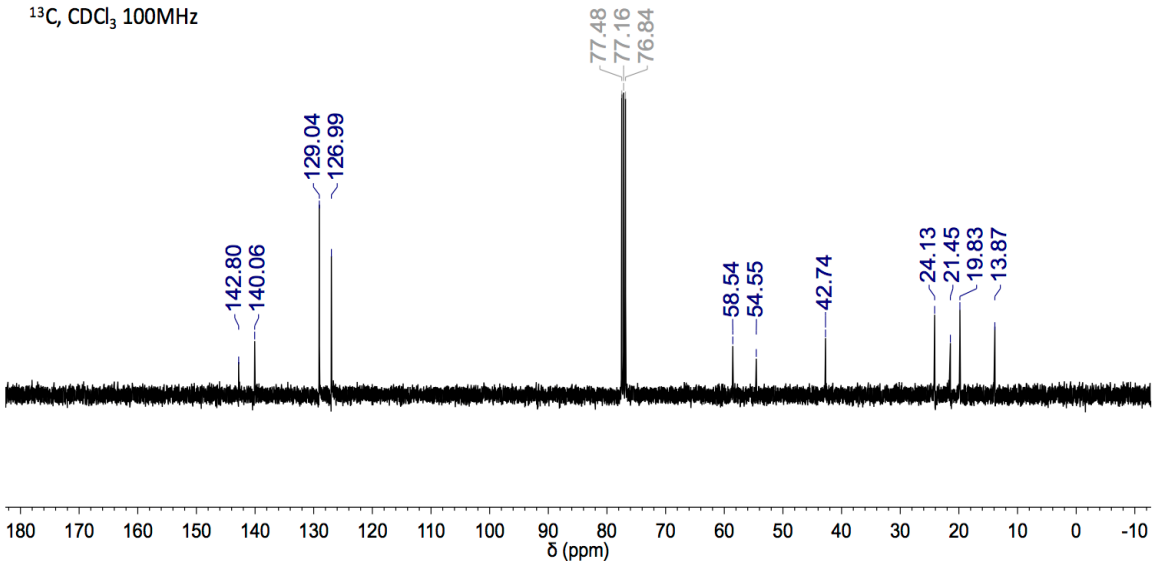
13C, CDCl3 100MHz
δ (ppm)

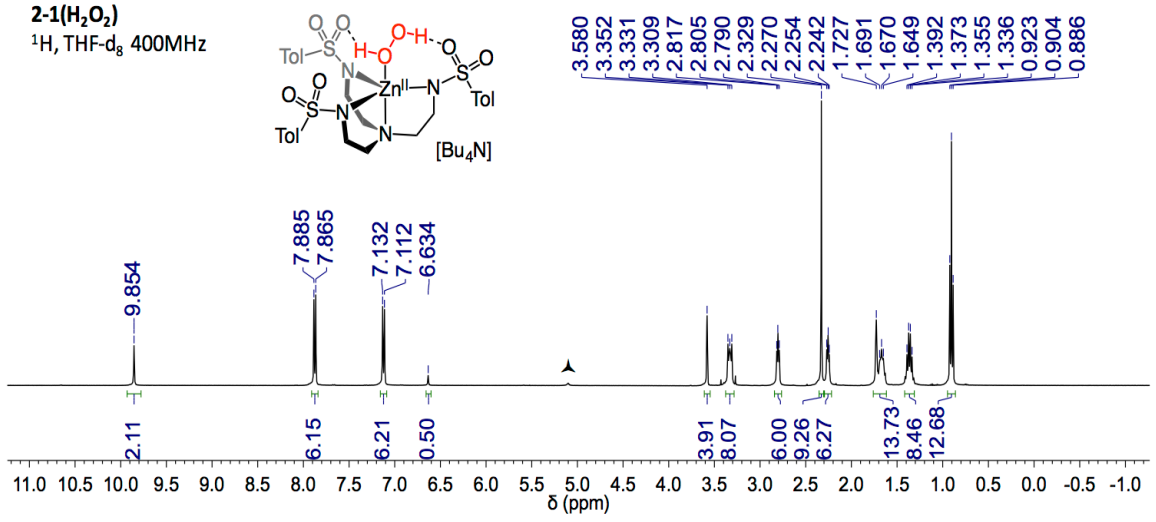
2-1(H2O2)
1H, THF-d8 400MHz
[Bu4N]
δ (ppm)

Chapter 3

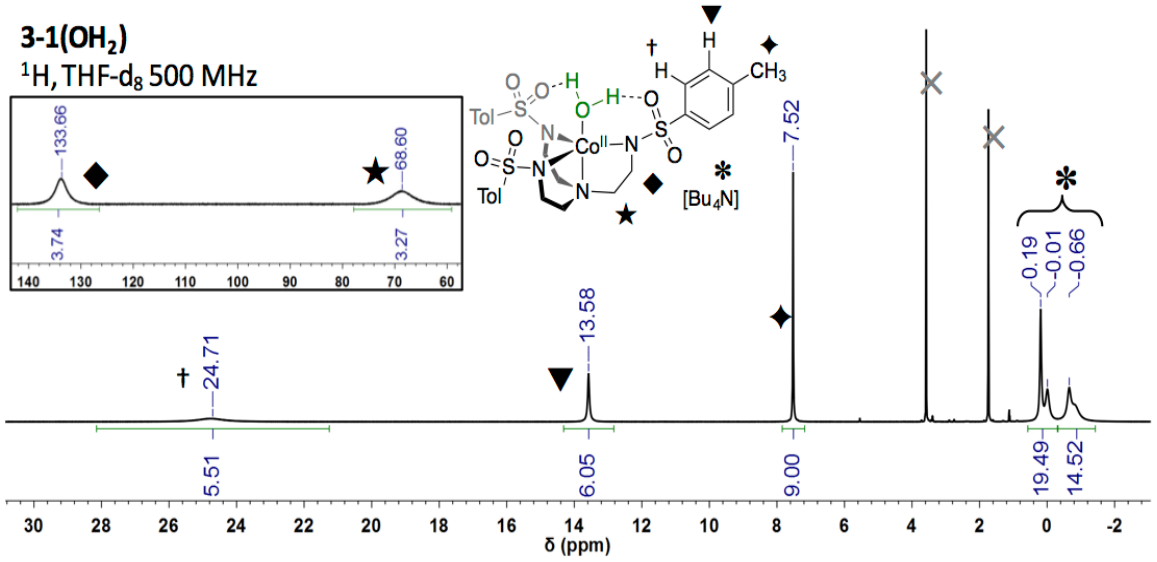

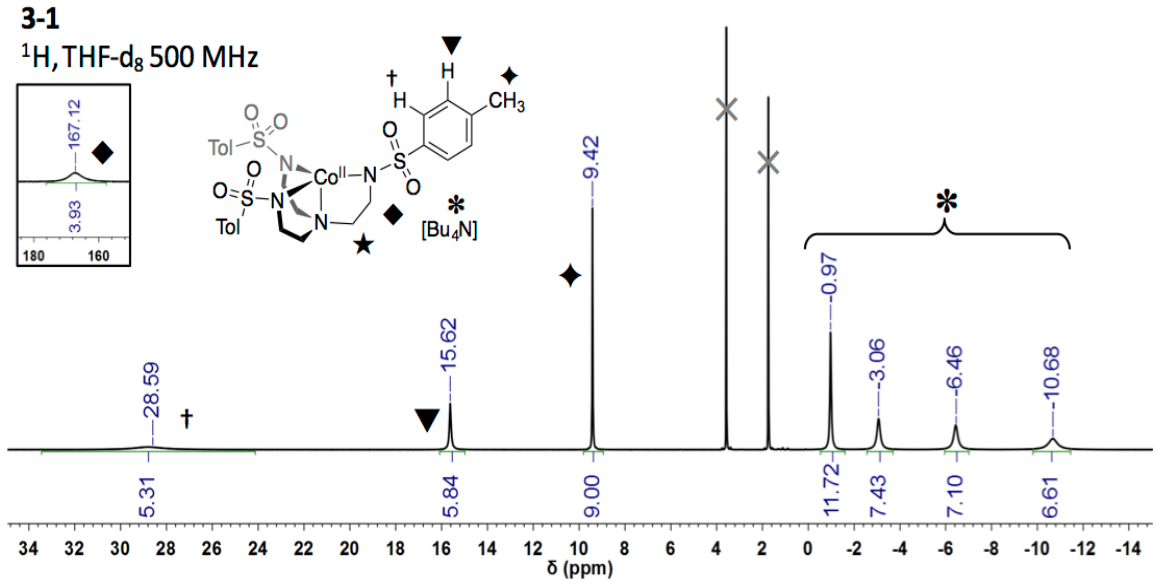

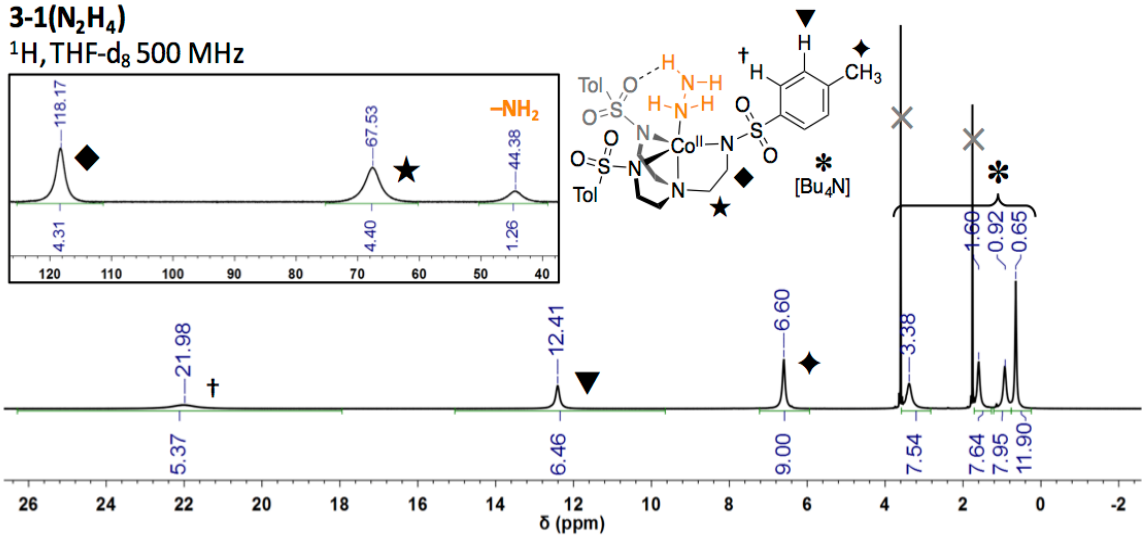
3-1(N2H4)
1H, THF-d8 500 MHz
–NH2
δ (ppm)

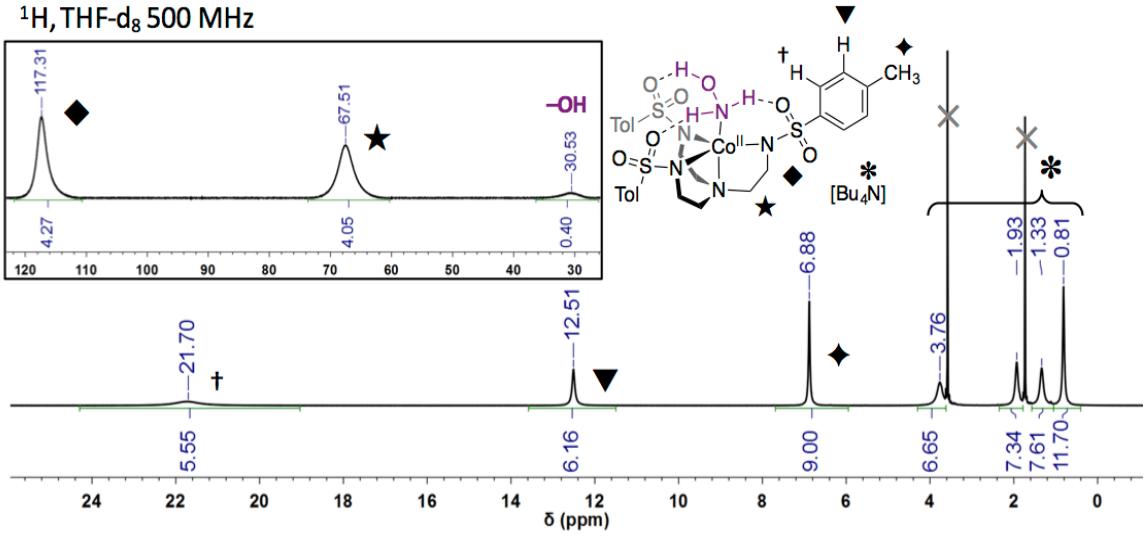
3-1(NH2OH)
1H, THF-d8 500 MHz
–OH
δ (ppm)

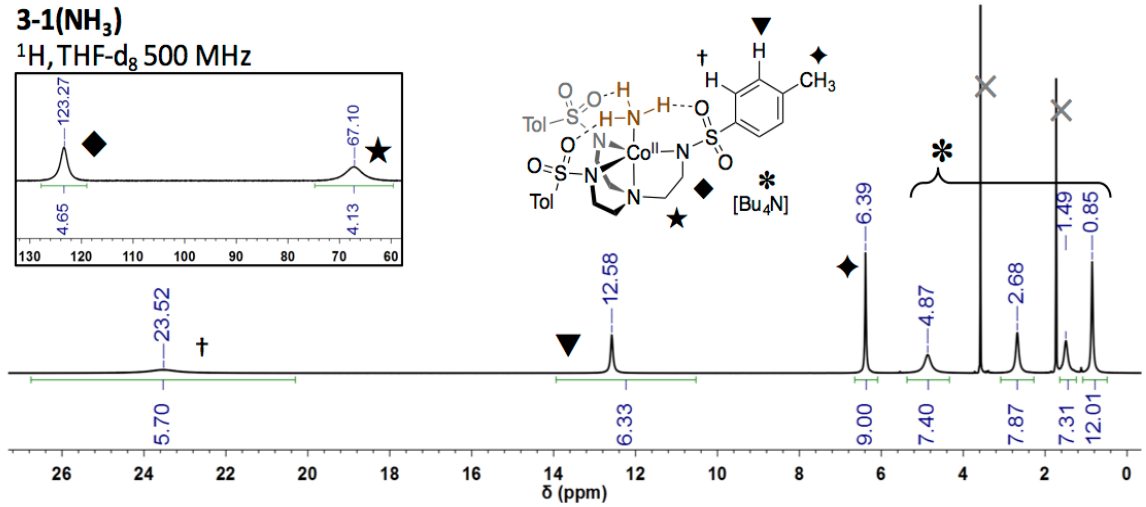
3-1(NH3)
1H, THF-d8 500 MHz
δ (ppm)

Chapter 4

Trisulfinamide crystals, ^{1}H
400MHz, $CDCl_3$

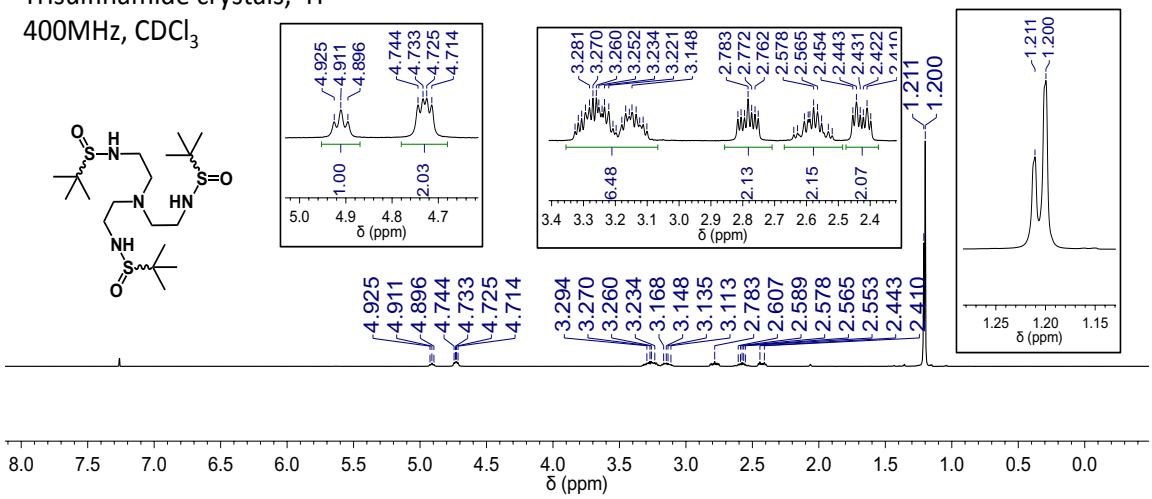

H_3Bus_3tren, ^{1}H
500MHz, $CDCl_3$

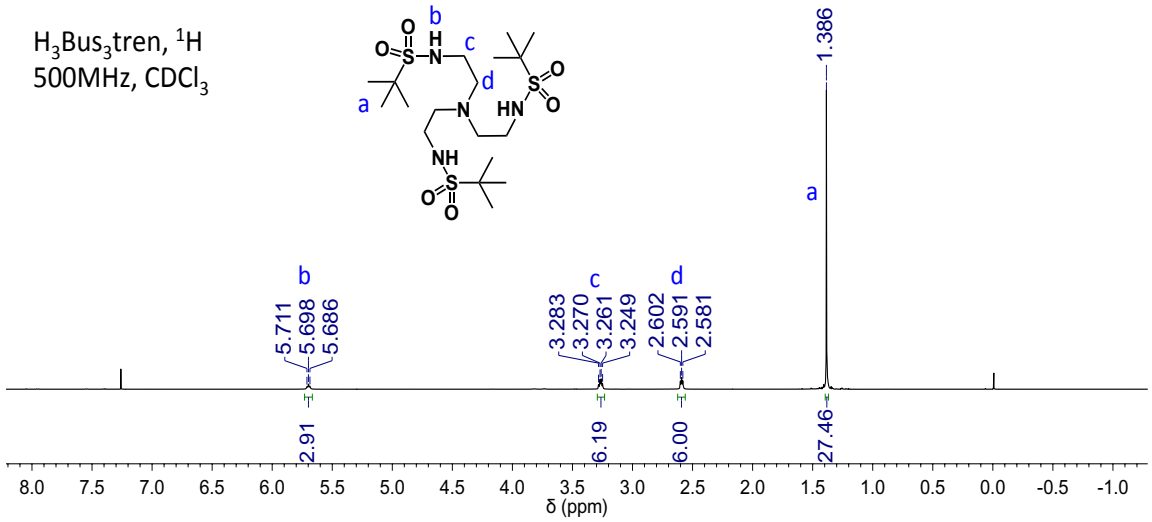

H_3Bus_3tren, ^{13}C
125MHz, $CDCl_3$

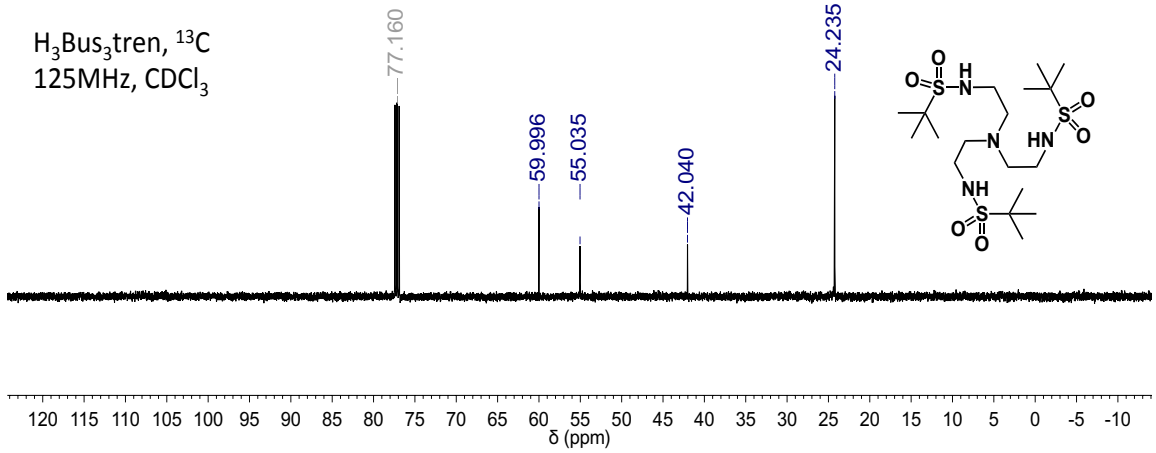

Appendix 2. Crystallography Data

2-1(OH_2)

Submitted by: **Christian Wallen**
Emory University
Solved by: **Marika Wieliczko**
Sample ID: **CMW 04-057 BuZnTsAq**

EMORY UNIVERSITY | X-ray Crystallography Center

Crystal Data and Experimental[1-5]

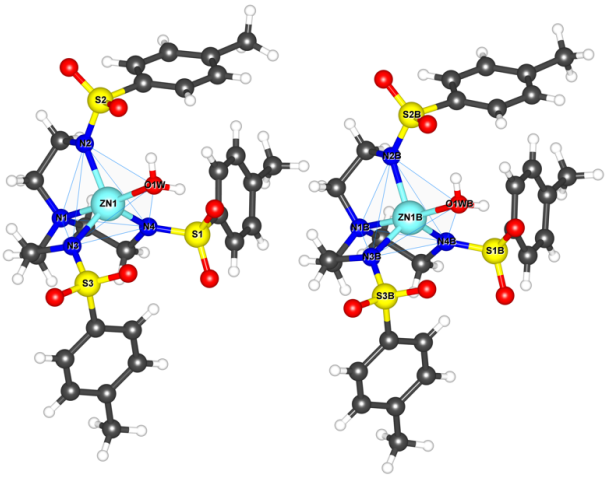

Experimental. Single clear colourless prism-shaped crystals of (**CMW04-057BuZnTsAq**) were recrystallised from a mixture of DCM and diethyl ether by vapor diffusion. A suitable crystal (0.59×0.42×0.16) was selected and mounted on a loop with paratone oil on a Bruker APEX-II CCD diffractometer. The crystal was cooled to T = 100(2) K during the data collection. The structure was solved with **Superflip** (L. Palatinus & G. Chapuis, 2007) using the Charge Flipping algorithm and by using **Olex2** (Dolomanov et al., 2009) as the graphical interface. The model was refined with version of **ShelXL-97** (Sheldrick, 2008) using Least Squares minimisation.

Crystal Data. $C_{43}H_{71}N_5O_7S_3Zn$, M_r = 931.59, triclinic, P-1 (No. 2), a = 13.4908(18) Å, b = 18.694(3) Å, c = 19.366(3) Å, α = 98.2422(18)°, β = 92.1817(19)°, γ = 108.3957(18)°, V = 4568.7(11) Å^3, T = 100(2) K, Z = 4, Z' = 2, μ(MoK_α) = 0.728, 73265 reflections measured, 22779 unique (R_{int} = 0.0364) which were used in all calculations. The final wR_2 was 0.1204 (all data) and R_1 was 0.0431 (I > 2(I)).

Compound	**CMW04-057BuZnTsAq**
Formula	$C_{43}H_{71}N_5O_7S_3Zn$
$D_{calc.}$/ g cm^{-3}	1.354
μ/mm^{-1}	0.728
Formula Weight	931.59
Colour	clear colourless
Shape	prism
Max Size/mm	0.59
Mid Size/mm	0.42
Min Size/mm	0.16
T/K	100(2)
Crystal System	triclinic
Space Group	P-1
a/Å	13.4908(18)
b/Å	18.694(3)
c/Å	19.366(3)
α/°	98.2422(18)
β/°	92.1817(19)
γ/°	108.3957(18)
V/Å^3	4568.7(11)
Z	4
Z'	2
Θ_{min}/°	1.597
Θ_{max}/°	28.435
Measured Refl.	73265
Independent Refl.	22779
Reflections Used	17786
R_{int}	0.0364
Parameters	1079
Restraints	0
Largest Peak	1.299
Deepest Hole	-0.435
GooF	1.045
wR_2 (all data)	0.1204
wR_2	0.1087
R_1 (all data)	0.0588
R_1	0.0431
CCDC Number	1429660

Structure Quality Indicators

Refinement: Shift 0.005 | Max Peak 1.3 | Min Peak -0.4 | GooF 1.045

A clear colourless prism-shaped crystal with dimensions 0.59×0.42×0.16 mm-1 was mounted on a loop with paratone oil. Data were collected using a Bruker APEX-II CCD diffractometer equipped with an Oxford Cryosystems low-temperature apparatus operating at T = 100(2) K.

Data were measured using ϕ and ω scans with a narrow frame width using MoK_α radiation (fine-focus sealed tube, 45 kV, 35 mA). The total number of runs and images was based on the strategy calculation from the program **APEXII** (Bruker, 2014). The maximum resolution achieved was Θ = 28.43°.

Unit cell indexing was performed by using the **APEXII** (Bruker, 2014) software and refined using **SAINT** (Bruker, V8.34A, 2013) on 9792 reflections, 13% of the observed reflections. Data reduction, scaling and absorption corrections were performed using **SAINT** (Bruker, V8.34A, 2013) and **SADABS-2014/5** (Bruker,2014) (for scaling/absorption correction), wR_2(int) was 0.1135 before and 0.0459 after correction. The ratio of minimum to maximum transmission is 0.8348. The $\lambda/2$ correction factor is 0.00150.. The final completeness is 100.00 out to 28.435 in Θ. The absorption coefficient (μ) of this material is 0.728 mm^{-1} and the minimum and maximum transmissions are 0.6225 and 0.7457.

The structure was solved with **Superflip** (L. Palatinus & G. Chapuis, 2007) using the Charge Flipping solution method and by using **Olex2** (Dolomanov et al., 2009) as the graphical interface. The structure was refined by Least Squares using version of **ShelXL-97** (Sheldrick, 2008). All non-hydrogen atoms were refined anisotropically. Hydrogen atom positions were calculated geometrically and refined using the riding model. The value of Z' is 2. This means that there are two independent molecules in the asymmetric unit.

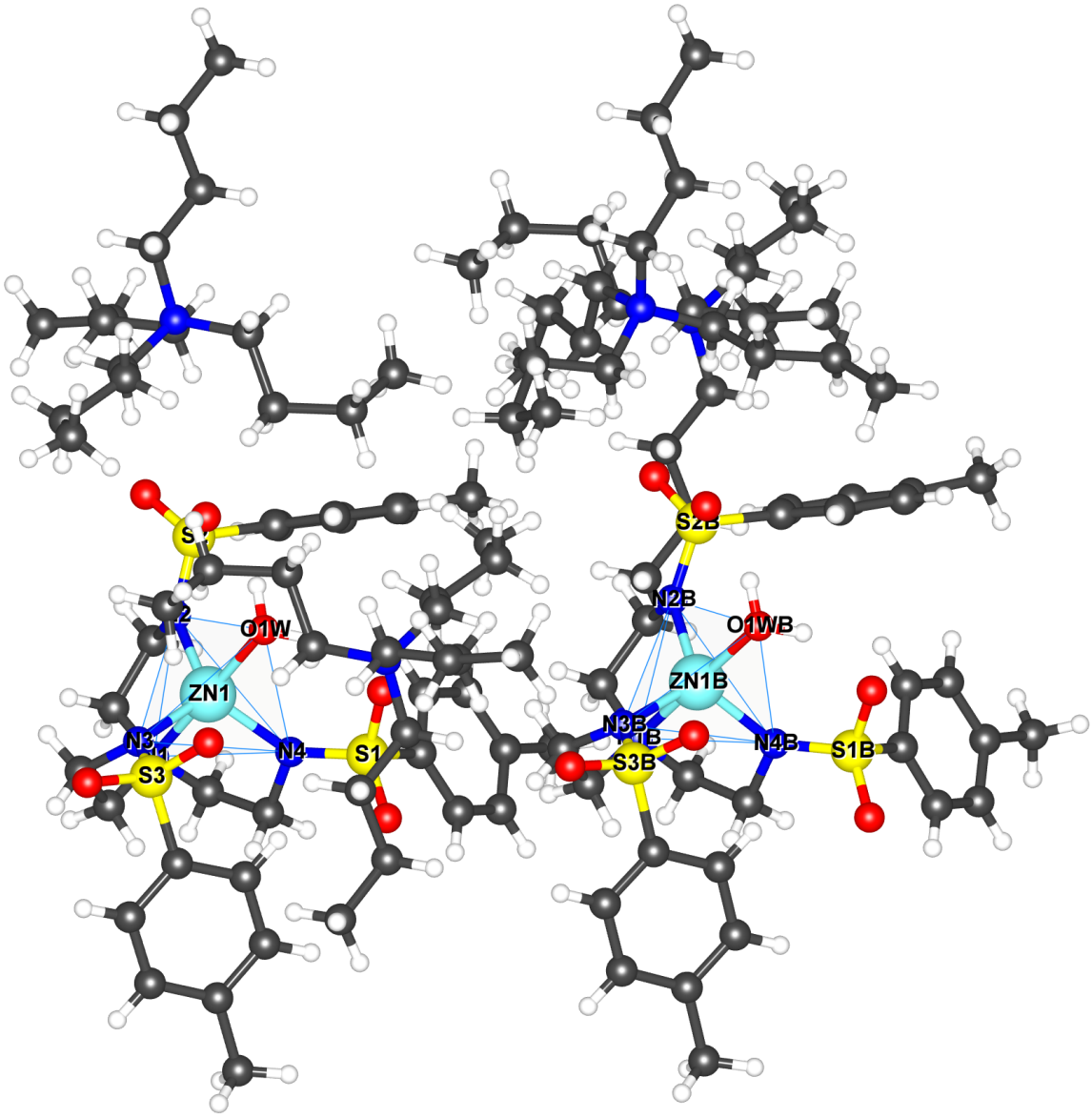

Figure 1: Plot of the asymmetric unit

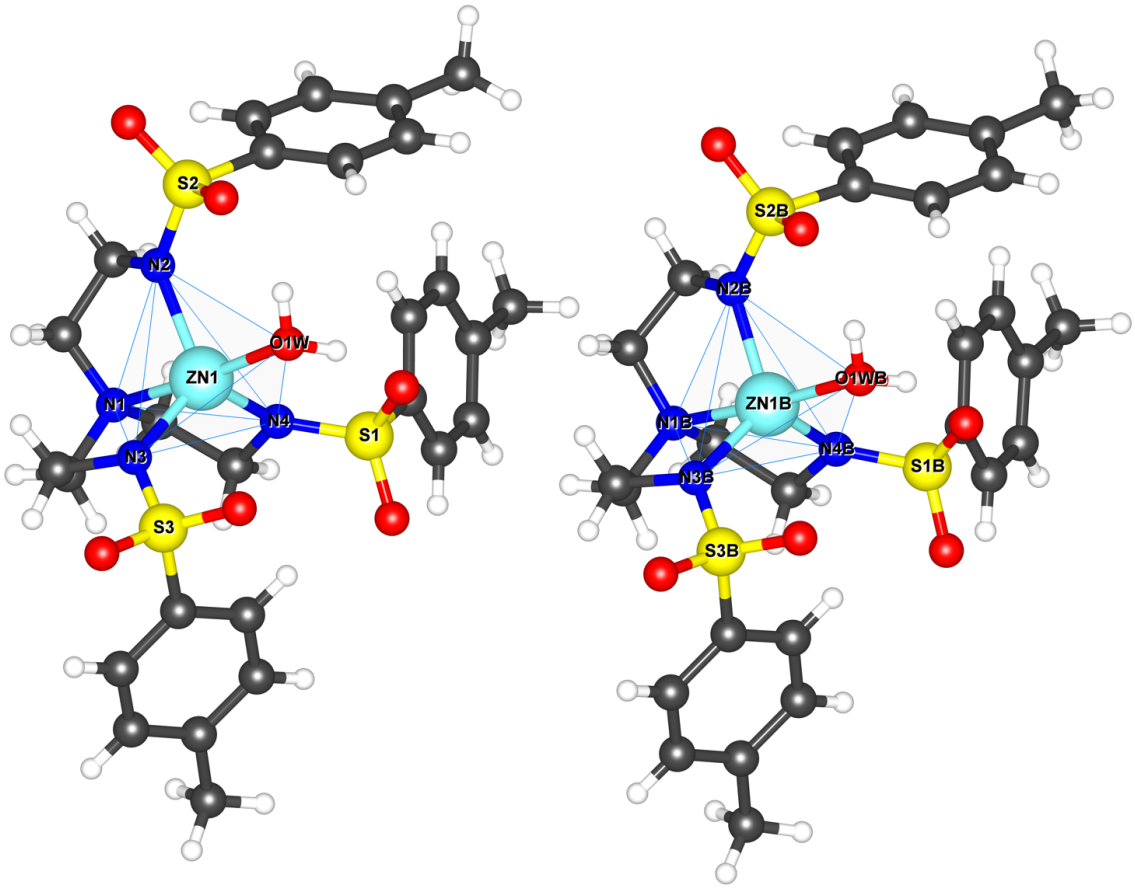

Figure 2: The two independent ZnLAq molecules.

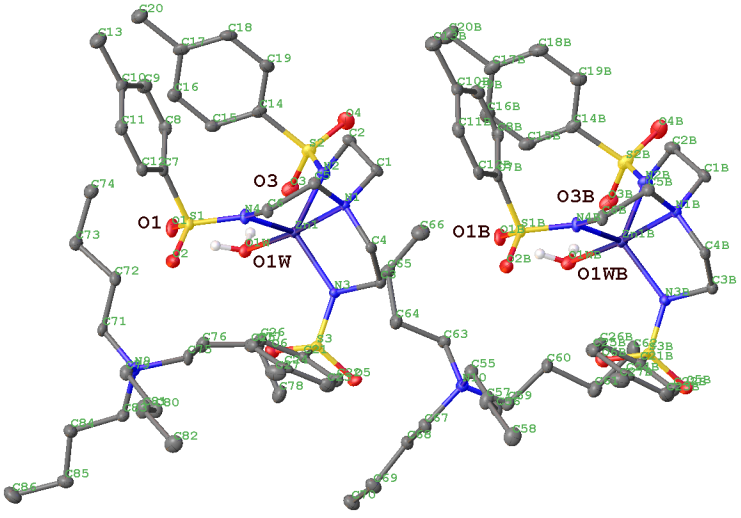

Figure 3: The following hydrogen bonding interactions with a maximum D-D distance of 2.9 Å and a minimum angle of 120 ˚ are present in **CMW04_057BuZnTsAq**: O1W-O1 =2.695 Å, O1W-O3 =2.712 Å, O1WB-O1B =2.689 Å, O1WB-O3B =2.731 Å.

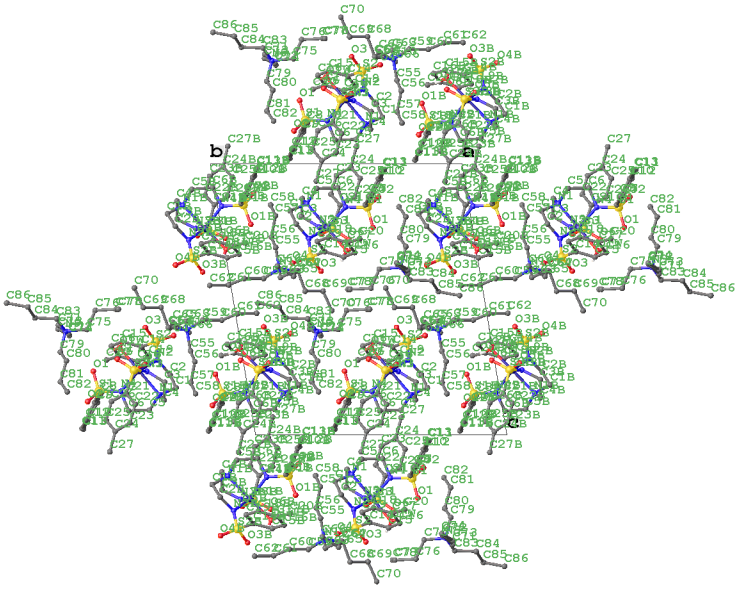

Figure 4: Packing diagram of CMW04_057BuZnTsAq.

Data Plots: Diffraction Data

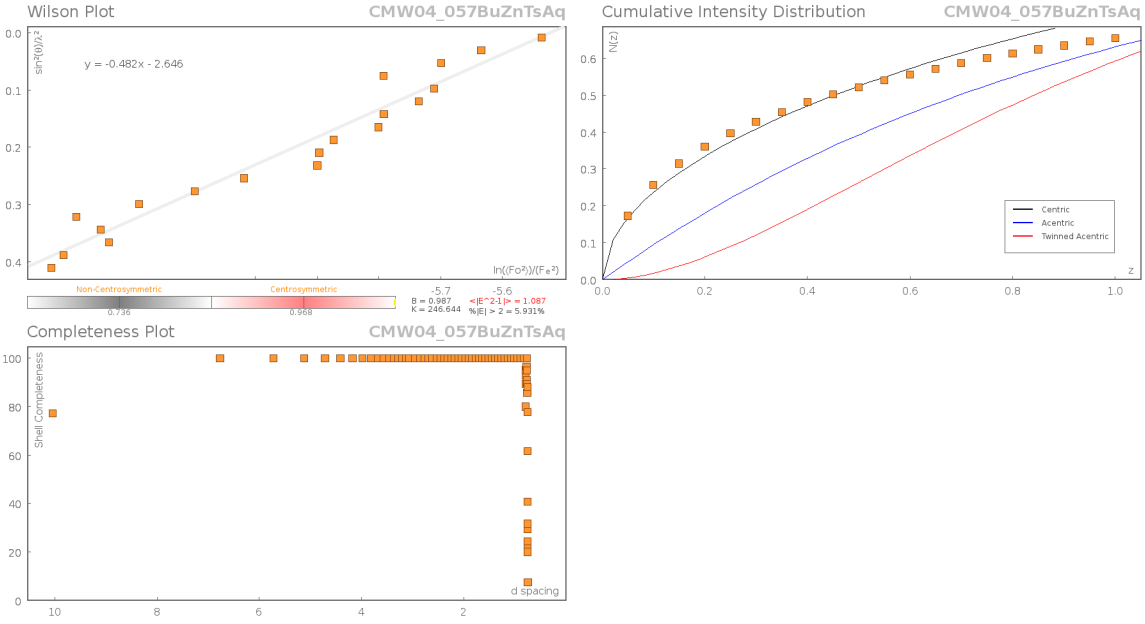

Data Plots: Refinement and Data

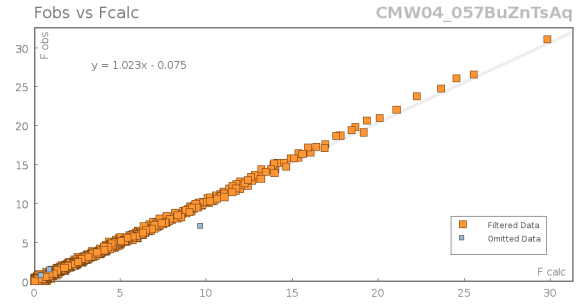

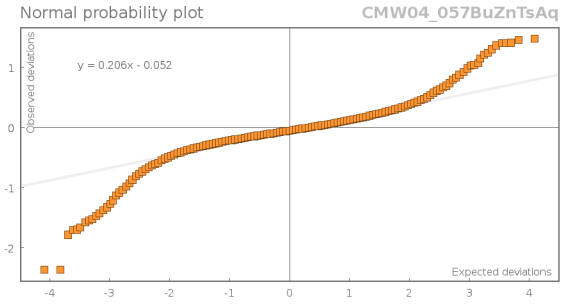

Reflection Statistics

Total reflections (after filtering)	73274	Unique reflections	22779
Completeness	0.99	Mean I/σ	15.05
hklsub>max</sub> collected	(18, 24, 25)	hklsub>min</sub> collected	(-18, -24, -25)
hkl_{max} used	(18, 24, 25)	hkl_{min} used	(-18, -24, 0)
Lim d_{max} collected	100.0	Lim d_{min} collected	0.36
d_{max} used	12.75	d_{min} used	0.75
Friedel pairs	17513	Friedel pairs merged	1
Inconsistent equivalents	0	R_{int}	0.0364
R_{sigma}	0.0398	Intensity transformed	0
Omitted reflections	0	Omitted by user (OMIT hkl)	9
Multiplicity	(15940, 16863, 6360, 1132)	Maximum mulitplicity	8
Removed systematic absences	0	Filtered off (Shel/OMIT)	0

Images of the Crystal on the Diffractometer

Table 1: Fractional Atomic Coordinates (×10⁴) and Equivalent Isotropic Displacement Parameters (Å²×10³) for **CMW04_057BuZnTsAq**. U_{eq} is defined as 1/3 of the trace of the orthogonalised U_{ij}.

Atom	x	y	z	U_{eq}
Zn1	297.5(2)	5781.6(2)	2363.5(2)	9.43(6)
Zn1B	284.6(2)	10645.2(2)	2378.3(2)	10.66(6)
S3	-2173.2(3)	5587.7(3)	2386.0(2)	10.12(9)
S1	185.0(4)	4050.4(3)	1613.0(2)	13.3(1)
S1B	185.2(4)	8962.3(3)	1521.7(2)	12.78(10)
S3B	-2152.4(3)	10532.3(3)	2398.5(2)	12.65(10)
S2	2435.6(4)	6644.8(3)	3436.5(2)	13.84(10)
S2B	2381.6(4)	11347.5(3)	3483.7(2)	15.92(10)
O1B	265.3(11)	8802.2(8)	2230.3(7)	19.2(3)
O1	319.2(12)	3960.8(8)	2343.0(7)	21.1(3)
O5B	-2787.4(11)	10999.8(8)	2643.7(8)	18.9(3)
O2B	-739.8(11)	8473.9(8)	1077.9(8)	19.7(3)
O5	-2827.1(10)	6054.2(8)	2598.0(7)	14.9(3)
O3	1756.6(11)	6316.9(9)	3957.1(7)	18.4(3)
O2	-767.8(11)	3535.3(8)	1219.9(8)	21.6(3)

Atom	x	y	z	U_{eq}
O1W	143.4(10)	5169.8(8)	3209.3(7)	15.1(3)
O1WB	43.0(11)	9945.4(9)	3158.0(7)	17.6(3)
O4	3182.1(11)	7399.4(9)	3662.2(8)	22.8(3)
O3B	1657.3(11)	11034.9(9)	3985.9(7)	21.5(3)
O6	-2176(1)	4997.3(8)	2788.6(7)	15.8(3)
O6B	-2200.3(11)	9892.8(8)	2748.4(7)	18.3(3)
O4B	3196.4(12)	12064.4(9)	3733.9(8)	24.4(3)
N4	368.8(13)	4919.3(9)	1595.7(8)	12.8(3)
N4B	365.1(12)	9837.8(9)	1562.8(8)	12.6(3)
N3B	-967.6(12)	11023.7(9)	2388.6(8)	12.1(3)
N2B	1725.7(12)	11379.8(10)	2810.1(8)	14.3(3)
N2	1727.2(12)	6590.4(9)	2758.8(8)	12.6(3)
N1	627.1(11)	6432.9(9)	1471.3(8)	9.0(3)
N1B	692.2(12)	11380.1(9)	1534.6(8)	10.6(3)
N3	-1007.0(11)	6095.2(9)	2338.2(8)	10.1(3)
N10	-2472.3(12)	7959.7(9)	3869.7(8)	12.8(3)
N9	-2307.9(12)	3120.8(9)	3816.9(8)	12.7(3)
C68	-3487.4(14)	7077.6(11)	4698.8(10)	14.7(4)
C73	434.7(15)	2844.1(12)	3899.7(11)	18.1(4)
C65	68.5(15)	7441.6(12)	4150.1(11)	18.8(4)
C20B	4876.9(18)	9154.9(14)	2920.4(13)	29.6(5)
C24B	-3361.5(15)	9522.1(12)	107.3(11)	17.7(4)
C72	-374.8(15)	3219.0(11)	3719.9(10)	14.7(4)
C3B	-787.7(14)	11698.1(11)	2038.2(10)	13.9(4)
C23	-3644.3(15)	5074.6(12)	432(1)	18.1(4)
C7	1214.9(14)	3813.0(11)	1192.2(10)	12.0(4)
C75	-2007.5(15)	3985.0(11)	3885.8(10)	14.6(4)
C64	-1094.2(15)	7280.8(12)	3934.8(11)	18.2(4)
C24	-3388.7(14)	4441.2(12)	123.6(10)	16.9(4)
C84	-3543.3(16)	1990.4(12)	4314.2(12)	20.9(4)
C78	-2518.0(16)	5370.8(13)	4633.5(11)	21.7(4)
C10	2830.5(15)	3423.9(12)	546.9(10)	15.4(4)
C7B	1255.7(14)	8772.1(11)	1110.8(10)	12.1(4)
C21B	-2661.1(14)	10134.0(11)	1513.3(10)	13.8(4)
C61	-2281.4(16)	10079.3(12)	4469.9(11)	19.3(4)
C3	-888.2(14)	6729.0(11)	1936.1(10)	12.5(4)
C21	-2700.2(14)	5122.6(11)	1519.6(10)	11.9(4)
C57	-3405.7(17)	7765.2(13)	1918.6(10)	19.6(4)
C10B	2913.8(15)	8415.1(12)	494.8(10)	16.3(4)
C1	1497.2(14)	7143.1(11)	1729.2(9)	12.3(4)
C20	5062.5(16)	4562.6(13)	2759.2(12)	22.6(5)
C85	-4518.8(15)	1779.1(12)	4716.6(11)	18.3(4)
C18	4670.2(14)	5791.6(12)	2701.2(11)	18.5(4)
C4	-345.7(13)	6586.8(11)	1280.6(9)	11.2(4)
C4B	-247.4(14)	11587.4(11)	1371.7(10)	12.1(4)
C56	-3348.9(15)	8066.7(11)	2701.5(10)	14.5(4)
C5B	961.5(14)	10916.7(11)	937.2(9)	12.9(4)
C5	915.1(14)	5941.0(11)	904.1(9)	12.1(4)
C25	-2789.9(15)	4148.6(12)	535.1(11)	18.2(4)
C80	-3552.5(15)	2959.4(12)	2725.3(10)	16.9(4)
C66	814.1(17)	8020.7(13)	3774.0(11)	23.7(5)
C8B	2258.3(15)	9054.7(11)	1461.4(10)	15.5(4)
C13B	3796.5(17)	8190.1(13)	177.2(12)	24.3(5)
C14	3203.8(14)	6036.9(12)	3242(1)	14.1(4)
C23B	-3654.8(15)	10120.8(12)	455.7(11)	19.7(4)
C70	-4591.0(16)	6147.9(13)	5419.7(11)	21.7(4)
C17	4407.0(14)	5073.0(12)	2906.5(10)	16.7(4)

Atom	x	y	z	U_{eq}
C9B	3073.3(15)	8871.4(12)	1152.0(11)	17.9(4)
C19	4081.2(14)	6268.2(12)	2866.6(10)	17.2(4)
C8	2238.6(15)	4115.1(11)	1510.9(10)	15.9(4)
C67	-3344.9(15)	7234.8(11)	3957.9(10)	14.8(4)
C77	-1442.0(15)	5277.3(11)	4631.0(11)	18.3(4)
C11B	1917.8(15)	8156.0(11)	143.3(10)	16.0(4)
C13	3690.2(17)	3189.3(14)	202.3(12)	24.3(5)
C9	3030.9(15)	3914.3(12)	1183.0(11)	18.7(4)
C69	-4447.5(15)	6368.9(12)	4695.5(11)	19.0(4)
C11	1808.1(15)	3138.2(11)	229.9(10)	15.3(4)
C6B	305.4(15)	10080.9(11)	872.4(9)	13.4(4)
C27	-3745.3(17)	4088.9(14)	-633.4(11)	24.9(5)
C55	-2413.4(15)	7962.9(12)	3086.2(10)	14.8(4)
C22B	-3314.5(15)	10424.5(12)	1152.4(11)	17.9(4)
C1B	1595.9(14)	12051.2(11)	1839.6(10)	14.5(4)
C63	-1423.0(14)	7971.3(11)	4188.9(10)	14.2(4)
C79	-2641.0(15)	2777.3(12)	3051.6(10)	15.4(4)
C59	-2724.6(15)	8652.1(11)	4234.4(10)	15.3(4)
C19B	3995.5(15)	10899.2(13)	2955.5(11)	19.6(4)
C14B	3071.0(15)	10681.8(12)	3284.3(10)	15.6(4)
C12	1006.2(15)	3333.9(11)	549.9(10)	13.5(4)
C26	-2443.1(14)	4484.1(11)	1226.2(10)	14.8(4)
C71	-1391.8(14)	2876.9(11)	4049.4(10)	13.8(4)
C82	-4643.7(17)	2788.6(13)	1583.7(11)	23.4(5)
C22	-3312.3(14)	5413.9(12)	1120.2(10)	15.0(4)
C74	1494.3(15)	3247.2(12)	3655.9(11)	18.7(4)
C81	-3782.7(17)	2583.6(13)	1954.7(11)	21.3(4)
C18B	4564.9(16)	10399.3(13)	2825.5(11)	22.3(5)
C62	-1417.5(18)	10840.1(12)	4485.6(12)	25.3(5)
C16	3522.0(15)	4851.2(12)	3275.7(10)	17.1(4)
C27B	-3720.0(17)	9205.3(14)	-653.8(11)	24.3(5)
C15	2924.6(15)	5321.0(12)	3440(1)	16.6(4)
C25B	-2718.0(15)	9231.4(12)	481.2(11)	18.5(4)
C15B	2717.0(15)	9959.3(13)	3465(1)	18.9(4)
C12B	1092.0(15)	8334.7(11)	448(1)	13.8(4)
C83	-3184.1(15)	2841.5(11)	4281.5(10)	15.1(4)
C6	281.1(15)	5106.0(11)	885.0(9)	12.3(4)
C2	2288.8(14)	6994.0(11)	2216.8(10)	13.8(4)
C17B	4227.1(15)	9681.1(13)	3023.9(11)	20.2(4)
C16B	3296.2(16)	9464.6(13)	3338.9(11)	21.2(4)
C26B	-2363.2(15)	9534.1(12)	1177.5(11)	16.7(4)
C58	-4319.1(17)	7883.4(13)	1514.6(11)	22.9(5)
C60	-1877.6(15)	9414.4(11)	4233.1(10)	15.4(4)
C2B	2334.7(15)	11819.3(12)	2303.9(10)	16.7(4)
C76	-1490.5(16)	4441.4(11)	4592.6(10)	17.1(4)
C86	-4799.7(18)	963.5(13)	4862.5(13)	27.4(5)

Table 2: Anisotropic Displacement Parameters (×10^4) **CMW04_057BuZnTsAq**. The anisotropic displacement factor exponent takes the form: $-2\pi^2[h^2a^{*2} \times U_{11} + \ldots + 2hka^* \times b^* \times U_{12}]$

Atom	U_{11}	U_{22}	U_{33}	U_{23}	U_{13}	U_{12}
Zn1	10.14(10)	11.52(11)	7.27(10)	2.35(8)	0.94(7)	4.02(8)
Zn1B	12.38(10)	12.69(12)	7.46(11)	1.59(8)	0.82(7)	4.86(8)
S3	9.30(19)	11.4(2)	9.7(2)	1.80(17)	1.42(15)	3.18(16)
S1	16.3(2)	11.0(2)	14.6(2)	4.48(18)	4.25(17)	5.76(18)
S1B	15.3(2)	10.0(2)	13.7(2)	2.65(17)	1.95(17)	4.62(17)

Atom	U_{11}	U_{22}	U_{33}	U_{23}	U_{13}	U_{12}
S3B	12.5(2)	13.0(2)	13.0(2)	2.31(17)	3.45(16)	4.60(17)
S2	13.8(2)	17.1(2)	10.0(2)	0.53(18)	-3.17(16)	5.29(18)
S2B	16.4(2)	21.9(3)	9.7(2)	-2.55(18)	-3.03(17)	9.29(19)
O1B	28.3(8)	16.3(7)	17.8(7)	9.4(6)	6.9(6)	10.6(6)
O1	34.0(8)	18.8(8)	17.5(7)	10.7(6)	9.4(6)	14.3(7)
O5B	16.3(7)	18.3(8)	22.5(8)	0.4(6)	6.3(6)	7.0(6)
O2B	15.2(7)	13.2(7)	28.2(8)	-1.1(6)	-0.1(6)	3.4(6)
O5	12.3(6)	16.4(7)	15.7(7)	-0.8(5)	3.1(5)	5.8(5)
O3	20.5(7)	27.9(8)	9.6(7)	2.7(6)	1.0(5)	11.9(6)
O2	15.5(7)	15.5(7)	32.9(9)	2.2(6)	4.0(6)	4.4(6)
O1W	17.6(7)	18.2(7)	13.2(7)	7.5(6)	3.4(5)	8.6(6)
O1WB	19.4(7)	23.4(8)	14.2(7)	7.5(6)	5.0(5)	10.6(6)
O4	21.6(7)	21.1(8)	20.8(8)	-1.8(6)	-8.9(6)	3.6(6)
O3B	24.0(7)	35.8(9)	9.9(7)	2.9(6)	1.9(5)	17.3(7)
O6	15.1(6)	17.1(7)	15.2(7)	7.0(6)	2.2(5)	3.5(5)
O6B	19.6(7)	17.3(7)	18.6(7)	8.0(6)	5.7(5)	4.1(6)
O4B	25.4(8)	22.7(8)	21.6(8)	-6.7(6)	-11.1(6)	8.9(7)
N4	21.1(8)	11.6(8)	7.7(7)	3.7(6)	2.5(6)	7.1(7)
N4B	20.6(8)	9.9(8)	8.3(7)	2.2(6)	1.3(6)	6.2(6)
N3B	12.9(7)	11.9(8)	12.3(8)	3.2(6)	2.9(6)	4.4(6)
N2B	13.6(7)	18.4(9)	9.4(8)	0.9(6)	-1.6(6)	4.3(6)
N2	12.7(7)	15.5(8)	9.3(7)	3.5(6)	-0.9(6)	4.0(6)
N1	8.7(7)	8.7(7)	9.1(7)	1.2(6)	0.1(5)	2.4(6)
N1B	11.6(7)	10.5(8)	9.1(7)	1.2(6)	0.3(5)	2.9(6)
N3	10.4(7)	11.0(8)	9.6(7)	3.3(6)	1.8(5)	3.8(6)
N10	13.9(7)	13.7(8)	10.6(8)	0.4(6)	1.1(6)	5.0(6)
N9	17.3(8)	11.9(8)	11.4(8)	3.6(6)	1.1(6)	7.2(6)
C68	15.4(9)	12.8(10)	15.6(9)	3.3(7)	0.2(7)	3.8(7)
C73	19.3(10)	18.2(10)	19.9(10)	7.8(8)	3.5(8)	8.0(8)
C65	17.4(9)	19.9(11)	20.9(10)	3.2(8)	0.4(8)	8.7(8)
C20B	28.5(12)	34.8(14)	30.9(13)	0.1(11)	-0.5(9)	20.4(11)
C24B	11.4(8)	18.2(10)	18.7(10)	2.4(8)	1.7(7)	-1.7(7)
C72	19.4(9)	12.8(10)	13.5(9)	4.5(7)	3.4(7)	6.1(8)
C3B	13.9(8)	10.5(9)	17.1(9)	2.3(7)	2.0(7)	3.8(7)
C23	15.0(9)	21.5(11)	16.3(10)	3.9(8)	-3.3(7)	4.2(8)
C7	15.4(9)	10.8(9)	12.0(9)	5.0(7)	2.9(7)	5.9(7)
C75	20.0(9)	10.3(9)	14.9(9)	3.2(7)	-0.2(7)	6.5(7)
C64	19.1(9)	13.9(10)	22(1)	1.2(8)	1.6(8)	6.8(8)
C24	10.4(8)	19.6(11)	14.6(9)	1.0(8)	2.2(7)	-2.9(7)
C84	17.1(9)	16.7(11)	30.4(12)	7.5(9)	7.3(8)	5.5(8)
C78	26.0(11)	19.3(11)	22.2(11)	1.0(9)	1.0(8)	11.9(9)
C10	18.5(9)	15.8(10)	15.0(9)	6.6(8)	2.9(7)	8.0(8)
C7B	16.0(9)	8.2(9)	12.1(9)	2.7(7)	0.1(7)	3.7(7)
C21B	11.5(8)	12.5(9)	15.8(9)	3.0(7)	1.6(7)	1.4(7)
C61	23.7(10)	18.6(11)	16.9(10)	0.9(8)	1.9(8)	9.9(8)
C3	12.7(8)	11.9(9)	14.5(9)	3.4(7)	1.8(7)	5.6(7)
C21	10.6(8)	11.2(9)	12.5(9)	2.0(7)	1.0(6)	1.4(7)
C57	30.0(11)	20.2(11)	12.0(9)	1.5(8)	0.9(8)	13.5(9)
C10B	18.8(9)	14.6(10)	18.1(10)	7.4(8)	5.9(7)	6.3(8)
C1	12.5(8)	11.8(9)	10.6(9)	4.0(7)	0.5(6)	0.4(7)
C20	18.5(10)	25.0(12)	25.6(11)	1.8(9)	2.0(8)	10.1(9)
C85	14.6(9)	20.9(11)	17.5(10)	2.8(8)	2.3(7)	3.3(8)
C18	9.6(8)	26.8(12)	18.8(10)	6.9(8)	1.7(7)	4.1(8)
C4	11.1(8)	11.5(9)	11.5(9)	4.5(7)	0.0(6)	3.5(7)
C4B	14.4(8)	10.2(9)	12.2(9)	3.8(7)	0.2(7)	3.9(7)
C56	19.6(9)	12.3(9)	11.4(9)	2.7(7)	1.9(7)	4.6(8)
C5B	15.4(9)	14.7(10)	9.3(9)	1.8(7)	2.7(7)	5.7(7)

Atom	U_{11}	U_{22}	U_{33}	U_{23}	U_{13}	U_{12}
C5	14.3(8)	14.3(9)	8.7(9)	2.2(7)	2.7(6)	5.5(7)
C25	15.9(9)	14.1(10)	21.3(10)	-3.9(8)	3.0(8)	3.3(8)
C80	19.3(9)	15.3(10)	14.2(9)	-1.9(8)	-1.6(7)	5.4(8)
C66	23.4(11)	29.7(13)	19.7(11)	5.5(9)	5.9(8)	10.0(9)
C8B	20.2(9)	11.1(9)	13.6(9)	-0.5(7)	-1.4(7)	4.4(8)
C13B	21.7(10)	26.1(12)	27.8(12)	5.7(9)	7.7(9)	10.5(9)
C14	11.4(8)	19.7(10)	11.6(9)	2.0(7)	-3.2(7)	6.3(7)
C23B	15.1(9)	20.0(11)	23.1(11)	6.8(9)	-2.8(8)	3.5(8)
C70	20.2(10)	21.2(11)	22.4(11)	8.9(9)	3.0(8)	2.3(8)
C17	11.0(8)	24.0(11)	14.2(9)	1.2(8)	-3.0(7)	6.0(8)
C9B	15.0(9)	17(1)	19.8(10)	4.0(8)	-0.9(7)	2.3(8)
C19	12.7(9)	18.8(10)	19.5(10)	6.4(8)	-1.7(7)	2.8(8)
C8	19.6(9)	13.1(10)	12.7(9)	-1.0(7)	-2.6(7)	3.8(8)
C67	16.4(9)	12.6(10)	14.1(9)	1.4(7)	1.4(7)	3.0(7)
C77	19.3(9)	13.3(10)	20.9(10)	-1.4(8)	3.8(8)	4.8(8)
C11B	22.4(10)	12.9(10)	12.0(9)	1.8(7)	1.1(7)	4.9(8)
C13	24.1(11)	27.6(12)	26.0(12)	5.9(9)	7.0(9)	13.8(9)
C9	15.6(9)	19.6(11)	18.9(10)	1.1(8)	-3.7(7)	4.5(8)
C69	17.1(9)	19.3(11)	17.4(10)	4.9(8)	-1.6(7)	0.9(8)
C11	20.9(9)	14.3(10)	11.2(9)	1.5(7)	-0.1(7)	6.8(8)
C6B	21.3(9)	13.0(9)	7.1(8)	1.1(7)	0.9(7)	7.5(8)
C27	20.8(10)	31.4(13)	16.1(10)	-2.9(9)	-0.1(8)	2.8(9)
C55	18.0(9)	15.6(10)	10.9(9)	1.8(7)	3.9(7)	5.7(8)
C22B	16.5(9)	15.8(10)	22.2(11)	2.2(8)	1.7(8)	6.8(8)
C1B	14.4(9)	11.6(9)	14.1(9)	1.2(7)	1.2(7)	0.0(7)
C63	12.7(8)	14(1)	14.8(9)	0.7(7)	0.1(7)	3.8(7)
C79	21.3(9)	14.8(10)	10.8(9)	1.8(7)	1.4(7)	7.1(8)
C59	17.5(9)	15.6(10)	13.8(9)	0.3(7)	2.4(7)	7.6(8)
C19B	15.5(9)	23.7(11)	19.2(10)	3.7(8)	1.0(7)	6.0(8)
C14B	15.3(9)	21.3(11)	10.3(9)	-2.6(8)	-3.4(7)	9.0(8)
C12	15.5(9)	11.0(9)	13.4(9)	2.7(7)	-1.2(7)	3.6(7)
C26	13.4(8)	12.7(9)	18.4(10)	2.0(8)	1.0(7)	4.5(7)
C71	16.2(9)	12.0(9)	16.4(9)	5.2(7)	2.0(7)	7.5(7)
C82	24.3(11)	25.7(12)	17.7(10)	-3.0(9)	-3.0(8)	8.0(9)
C22	15.0(9)	14.7(10)	15.7(10)	1.2(8)	0.6(7)	5.9(7)
C74	19.0(9)	18.8(11)	19.2(10)	2.2(8)	2.7(8)	7.9(8)
C81	28.2(11)	18.6(11)	16.2(10)	-2.3(8)	-3.9(8)	9.1(9)
C18B	14.5(9)	31.1(13)	19.9(11)	0.4(9)	2.4(8)	7.0(9)
C62	32.8(12)	14.7(11)	27.2(12)	0.1(9)	-3.0(9)	8.1(9)
C16	14.9(9)	18.9(10)	18(1)	6.5(8)	-0.8(7)	5.0(8)
C27B	20.7(10)	29.5(13)	18.2(11)	0.4(9)	1.0(8)	3.4(9)
C15	12.6(9)	23.2(11)	15.9(10)	7.5(8)	2.5(7)	6.4(8)
C25B	16.6(9)	15.4(10)	21.6(11)	-0.8(8)	3.1(8)	4.2(8)
C15B	14.9(9)	27.2(12)	15.7(10)	3.9(8)	0.4(7)	8.2(8)
C12B	16.9(9)	9.8(9)	13.9(9)	3.5(7)	-1.1(7)	2.9(7)
C83	15.3(9)	16.4(10)	16.3(10)	5.0(8)	4.5(7)	7.6(8)
C6	18.3(9)	12.1(9)	6.8(8)	1.4(7)	0.3(7)	5.5(7)
C2	10.7(8)	15.8(10)	12.9(9)	3.7(7)	0.1(7)	0.9(7)
C17B	17.1(9)	25.9(12)	18.1(10)	-1.8(8)	-3.0(8)	10.8(9)
C16B	20.9(10)	21.8(11)	22.1(11)	5.3(9)	-1.6(8)	8.5(9)
C26B	15.7(9)	15.7(10)	19.6(10)	2.1(8)	1.1(7)	6.8(8)
C58	30.0(11)	26.8(12)	12.5(10)	1.2(8)	-1.1(8)	11.2(9)
C60	19.3(9)	12(1)	16.3(10)	2.3(7)	3.2(7)	6.7(8)
C2B	13.4(9)	19.6(11)	14.7(9)	1.4(8)	1.1(7)	2.7(8)
C76	20.1(9)	16.7(10)	15.8(10)	0.2(8)	-2.1(7)	9.3(8)
C86	25.1(11)	23.9(12)	30.3(12)	9.2(10)	7.7(9)	1.4(9)

Table 3: Bond Lengths in Å for **CMW04_057BuZnTsAq**.

Atom	Atom	Length/Å
Zn1	O1W	2.1089(13)
Zn1	N4	2.0592(16)
Zn1	N2	2.0755(16)
Zn1	N1	2.2327(15)
Zn1	N3	2.0239(15)
Zn1B	O1WB	2.1054(14)
Zn1B	N4B	2.0536(16)
Zn1B	N3B	2.0268(16)
Zn1B	N2B	2.0560(16)
Zn1B	N1B	2.2571(16)
S3	O5	1.4554(14)
S3	O6	1.4391(14)
S3	N3	1.5742(15)
S3	C21	1.7825(19)
S1	O1	1.4585(15)
S1	O2	1.4468(15)
S1	N4	1.5695(17)
S1	C7	1.7786(19)
S1B	O1B	1.4530(15)
S1B	O2B	1.4505(14)
S1B	N4B	1.5667(17)
S1B	C7B	1.7820(19)
S3B	O5B	1.4518(14)
S3B	O6B	1.4421(15)
S3B	N3B	1.5746(16)
S3B	C21B	1.785(2)
S2	O3	1.4575(14)
S2	O4	1.4450(15)
S2	N2	1.5657(16)
S2	C14	1.777(2)
S2B	O3B	1.4550(15)
S2B	O4B	1.4431(16)
S2B	N2B	1.5673(16)
S2B	C14B	1.784(2)
N4	C6	1.477(2)
N4B	C6B	1.480(2)
N3B	C3B	1.474(2)
N2B	C2B	1.476(2)
N2	C2	1.474(2)
N1	C1	1.474(2)
N1	C4	1.474(2)
N1	C5	1.474(2)
N1B	C4B	1.473(2)
N1B	C5B	1.471(2)
N1B	C1B	1.475(2)
N3	C3	1.480(2)
N10	C67	1.525(2)
N10	C55	1.523(2)
N10	C63	1.516(2)
N10	C59	1.525(2)
N9	C75	1.521(2)
N9	C79	1.518(2)
N9	C71	1.520(2)
N9	C83	1.518(2)
C68	C67	1.513(3)
C68	C69	1.532(3)
C73	C72	1.526(3)
C73	C74	1.519(3)
C65	C64	1.530(3)
C65	C66	1.520(3)
C20B	C17B	1.509(3)
C24B	C23B	1.396(3)
C24B	C27B	1.507(3)
C24B	C25B	1.391(3)
C72	C71	1.526(3)
C3B	C4B	1.527(3)
C23	C24	1.396(3)
C23	C22	1.383(3)
C7	C8	1.396(3)
C7	C12	1.387(3)
C75	C76	1.518(3)
C64	C63	1.517(3)
C24	C25	1.393(3)
C24	C27	1.511(3)
C84	C85	1.528(3)
C84	C83	1.521(3)
C78	C77	1.516(3)
C10	C13	1.510(3)
C10	C9	1.388(3)
C10	C11	1.393(3)
C7B	C8B	1.395(3)
C7B	C12B	1.389(3)
C21B	C22B	1.387(3)
C21B	C26B	1.392(3)
C61	C62	1.523(3)
C61	C60	1.528(3)
C3	C4	1.522(2)
C21	C26	1.396(3)
C21	C22	1.390(3)
C57	C56	1.530(3)
C57	C58	1.526(3)
C10B	C13B	1.507(3)
C10B	C9B	1.395(3)
C10B	C11B	1.389(3)
C1	C2	1.515(3)
C20	C17	1.499(3)
C85	C86	1.522(3)
C18	C17	1.397(3)
C18	C19	1.383(3)
C56	C55	1.520(3)
C5B	C6B	1.518(3)
C5	C6	1.519(3)
C25	C26	1.389(3)
C80	C79	1.515(3)
C80	C81	1.531(3)
C8B	C9B	1.384(3)
C14	C19	1.396(3)
C14	C15	1.386(3)
C23B	C22B	1.386(3)
C70	C69	1.521(3)

Atom	Atom	Length/Å
C17	C16	1.395(3)
C8	C9	1.387(3)
C77	C76	1.534(3)
C11B	C12B	1.389(3)
C11	C12	1.387(3)
C1B	C2B	1.519(3)
C59	C60	1.520(3)
C19B	C14B	1.393(3)
C19B	C18B	1.388(3)
C14B	C15B	1.384(3)
C82	C81	1.520(3)
C18B	C17B	1.390(3)
C16	C15	1.381(3)
C25B	C26B	1.389(3)
C15B	C16B	1.390(3)
C17B	C16B	1.386(3)

Table 4: Bond Angles in ° for **CMW04_057BuZnTsAq**.

Atom	Atom	Atom	Angle/°
O1W	Zn1	N1	174.29(5)
N4	Zn1	O1W	97.49(6)
N4	Zn1	N2	115.64(6)
N4	Zn1	N1	80.86(6)
N2	Zn1	O1W	95.57(6)
N2	Zn1	N1	80.34(6)
N3	Zn1	O1W	103.80(6)
N3	Zn1	N4	117.75(6)
N3	Zn1	N2	119.39(6)
N3	Zn1	N1	81.75(6)
O1WB	Zn1B	N1B	174.61(5)
N4B	Zn1B	O1WB	97.33(6)
N4B	Zn1B	N2B	113.72(7)
N4B	Zn1B	N1B	80.33(6)
N3B	Zn1B	O1WB	103.85(6)
N3B	Zn1B	N4B	119.49(6)
N3B	Zn1B	N2B	119.22(7)
N3B	Zn1B	N1B	81.50(6)
N2B	Zn1B	O1WB	96.17(6)
N2B	Zn1B	N1B	80.47(6)
O5	S3	N3	111.49(8)
O5	S3	C21	104.53(8)
O6	S3	O5	117.03(8)
O6	S3	N3	109.16(8)
O6	S3	C21	106.81(9)
N3	S3	C21	107.19(8)
O1	S1	N4	107.73(9)
O1	S1	C7	106.26(9)
O2	S1	O1	115.53(9)
O2	S1	N4	114.59(9)
O2	S1	C7	104.79(9)
N4	S1	C7	107.29(9)
O1B	S1B	N4B	108.41(8)
O1B	S1B	C7B	106.09(9)
O2B	S1B	O1B	115.77(9)
O2B	S1B	N4B	114.08(9)
O2B	S1B	C7B	104.71(9)
N4B	S1B	C7B	107.08(9)
O5B	S3B	N3B	112.04(9)
O5B	S3B	C21B	104.91(9)
O6B	S3B	O5B	117.08(9)
O6B	S3B	N3B	108.66(9)
O6B	S3B	C21B	105.99(9)
N3B	S3B	C21B	107.52(9)
O3	S2	N2	108.12(8)
O3	S2	C14	105.28(9)
O4	S2	O3	116.29(9)
O4	S2	N2	113.00(9)
O4	S2	C14	105.35(9)
N2	S2	C14	108.24(9)
O3B	S2B	N2B	108.33(9)
O3B	S2B	C14B	105.11(9)
O4B	S2B	O3B	116.57(9)
O4B	S2B	N2B	112.16(9)
O4B	S2B	C14B	104.27(9)
N2B	S2B	C14B	109.99(9)
S1	N4	Zn1	130.89(9)
C6	N4	Zn1	112.35(12)
C6	N4	S1	114.24(12)
S1B	N4B	Zn1B	130.94(9)
C6B	N4B	Zn1B	112.79(12)
C6B	N4B	S1B	114.08(12)
S3B	N3B	Zn1B	127.00(10)
C3B	N3B	Zn1B	111.76(11)
C3B	N3B	S3B	115.16(12)
S2B	N2B	Zn1B	128.54(10)
C2B	N2B	Zn1B	113.02(12)
C2B	N2B	S2B	115.21(13)
S2	N2	Zn1	129.44(9)
C2	N2	Zn1	112.64(11)
C2	N2	S2	114.45(12)
C1	N1	Zn1	106.76(10)
C1	N1	C4	111.84(15)
C4	N1	Zn1	106.32(10)
C5	N1	Zn1	106.58(11)
C5	N1	C1	112.15(14)
C5	N1	C4	112.68(14)
C4B	N1B	Zn1B	105.95(11)
C4B	N1B	C1B	112.32(15)
C5B	N1B	Zn1B	106.89(11)
C5B	N1B	C4B	113.05(14)
C5B	N1B	C1B	111.94(14)
C1B	N1B	Zn1B	106.10(11)
S3	N3	Zn1	127.99(9)
C3	N3	Zn1	111.57(11)

Atom	Atom	Atom	Angle/°
C3	N3	S3	114.90(12)
C55	N10	C67	107.23(14)
C55	N10	C59	111.84(15)
C63	N10	C67	111.27(15)
C63	N10	C55	108.82(14)
C63	N10	C59	108.68(14)
C59	N10	C67	109.03(14)
C79	N9	C75	108.31(14)
C79	N9	C71	108.23(14)
C79	N9	C83	111.90(15)
C71	N9	C75	111.75(14)
C83	N9	C75	108.67(14)
C83	N9	C71	108.02(14)
C67	C68	C69	109.44(16)
C74	C73	C72	111.25(16)
C66	C65	C64	114.45(18)
C23B	C24B	C27B	121.05(19)
C25B	C24B	C23B	118.04(19)
C25B	C24B	C27B	120.9(2)
C71	C72	C73	110.70(16)
N3B	C3B	C4B	109.78(15)
C22	C23	C24	121.94(19)
C8	C7	S1	119.59(15)
C12	C7	S1	120.35(14)
C12	C7	C8	120.06(17)
C76	C75	N9	116.24(16)
C63	C64	C65	110.69(16)
C23	C24	C27	120.94(19)
C25	C24	C23	117.83(18)
C25	C24	C27	121.2(2)
C83	C84	C85	109.96(17)
C9	C10	C13	121.39(18)
C9	C10	C11	118.69(18)
C11	C10	C13	119.92(18)
C8B	C7B	S1B	119.79(15)
C12B	C7B	S1B	120.24(14)
C12B	C7B	C8B	119.97(18)
C22B	C21B	S3B	121.45(16)
C22B	C21B	C26B	119.90(18)
C26B	C21B	S3B	118.61(15)
C62	C61	C60	110.51(17)
N3	C3	C4	109.35(15)
C26	C21	S3	119.38(14)
C22	C21	S3	120.77(15)
C22	C21	C26	119.74(18)
C58	C57	C56	111.45(17)
C9B	C10B	C13B	120.85(19)
C11B	C10B	C13B	120.38(19)
C11B	C10B	C9B	118.75(18)
N1	C1	C2	110.68(15)
C86	C85	C84	111.52(18)
C19	C18	C17	121.08(18)
N1	C4	C3	109.79(14)
N1B	C4B	C3B	109.75(15)
C55	C56	C57	110.23(16)

Atom	Atom	Atom	Angle/°
N1B	C5B	C6B	111.06(15)
N1	C5	C6	110.97(14)
C26	C25	C24	121.11(19)
C79	C80	C81	109.61(16)
C9B	C8B	C7B	119.26(18)
C19	C14	S2	120.06(16)
C15	C14	S2	120.74(15)
C15	C14	C19	119.17(18)
C22B	C23B	C24B	121.46(19)
C18	C17	C20	121.83(18)
C16	C17	C20	120.58(19)
C16	C17	C18	117.56(19)
C8B	C9B	C10B	121.33(18)
C18	C19	C14	120.36(19)
C9	C8	C7	118.98(18)
C68	C67	N10	116.51(15)
C78	C77	C76	112.55(17)
C10B	C11B	C12B	120.53(18)
C8	C9	C10	121.60(18)
C70	C69	C68	112.05(16)
C12	C11	C10	120.48(18)
N4B	C6B	C5B	108.72(15)
C56	C55	N10	115.62(15)
C23B	C22B	C21B	119.63(19)
N1B	C1B	C2B	110.52(16)
N10	C63	C64	115.83(16)
C80	C79	N9	115.87(16)
C60	C59	N10	114.62(15)
C18B	C19B	C14B	120.0(2)
C19B	C14B	S2B	119.41(17)
C15B	C14B	S2B	121.18(15)
C15B	C14B	C19B	119.39(19)
C11	C12	C7	120.17(17)
C25	C26	C21	119.89(18)
N9	C71	C72	115.21(15)
C23	C22	C21	119.47(19)
C82	C81	C80	112.20(18)
C19B	C18B	C17B	120.74(19)
C15	C16	C17	121.83(19)
C16	C15	C14	119.99(18)
C26B	C25B	C24B	121.16(19)
C14B	C15B	C16B	120.22(19)
C7B	C12B	C11B	120.11(18)
N9	C83	C84	116.11(16)
N4	C6	C5	108.38(15)
N2	C2	C1	108.51(14)
C18B	C17B	C20B	120.78(19)
C16B	C17B	C20B	120.4(2)
C16B	C17B	C18B	118.8(2)
C17B	C16B	C15B	120.8(2)
C25B	C26B	C21B	119.81(19)
C59	C60	C61	110.97(16)
N2B	C2B	C1B	108.81(15)
C75	C76	C77	110.03(16)

Table 5: Hydrogen Fractional Atomic Coordinates (×10⁴) and Equivalent Isotropic Displacement Parameters (Å²×10³) for **CMW04_057BuZnTsAq**. U_{eq} is defined as 1/3 of the trace of the orthogonalised U_{ij}.

Atom	x	y	z	U_{eq}
H1WA	645	5414	3549	23
H1WB	189	4710	3070	23
H1WC	468	10183	3538	26
H1WD	170	9516	3006	26
H68A	-3585	7523	4995	18
H68B	-2854	6992	4897	18
H73A	508	2860	4413	22
H73B	189	2301	3673	22
H65A	202	7629	4661	23
H65B	226	6956	4059	23
H20D	4743	8885	2436	44
H20E	4688	8783	3242	44
H20F	5622	9455	3015	44
H72A	-91	3775	3894	18
H72B	-520	3143	3205	18
H3BA	-344	12160	2358	17
H3BB	-1466	11771	1920	17
H23	-4059	5279	161	22
H75A	-1525	4154	3525	18
H75B	-2649	4114	3780	18
H64A	-1223	7152	3418	22
H64B	-1521	6837	4136	22
H84A	-2975	1860	4550	25
H84B	-3704	1695	3834	25
H78A	-2892	5173	4167	33
H78B	-2442	5913	4759	33
H78C	-2916	5086	4977	33
H61A	-2883	10048	4144	23
H61B	-2528	10045	4943	23
H3A	-467	7219	2228	15
H3B	-1586	6763	1804	15
H57A	-2741	8033	1731	24
H57B	-3490	7213	1851	24
H1A	1218	7527	1981	15
H1B	1846	7352	1327	15
H20A	5308	4595	2291	34
H20B	4641	4034	2781	34
H20C	5667	4725	3109	34
H85A	-4392	2135	5166	22
H85B	-5116	1834	4441	22
H18	5263	5955	2444	22
H4A	-819	6145	953	13
H4B	-178	7040	1043	13
H4BA	-737	11178	1021	15
H4BB	-44	12066	1170	15
H56A	-3283	8615	2771	17
H56B	-4002	7788	2895	17
H5BA	1714	10969	1000	15
H5BB	842	11107	501	15

Atom	x	y	z	U_{eq}
H5A	1672	6009	977	15
H5B	787	6095	449	15
H25	-2616	3712	340	22
H80A	-3379	3520	2761	20
H80B	-4181	2767	2980	20
H66A	1539	8066	3917	36
H66B	713	8518	3896	36
H66C	672	7851	3267	36
H8B	2380	9369	1908	19
H13D	4468	8578	361	36
H13E	3712	8150	-333	36
H13F	3784	7696	297	36
H23B	-4097	10325	210	24
H70A	-4620	6587	5752	33
H70B	-4000	5991	5570	33
H70C	-5246	5723	5404	33
H9B	3755	9060	1392	21
H19	4275	6756	2724	21
H8	2390	4453	1946	19
H67A	-4014	7262	3755	18
H67B	-3208	6794	3679	18
H77A	-1008	5583	5062	22
H77B	-1097	5479	4225	22
H11B	1800	7854	-309	19
H13A	4374	3551	401	37
H13B	3612	3190	-303	37
H13C	3643	2675	285	37
H9	3728	4117	1399	22
H69A	-5082	6471	4523	23
H69B	-4368	5936	4369	23
H11	1659	2807	-209	18
H6BA	-432	10011	719	16
H6BB	573	9767	519	16
H27A	-4481	4049	-731	37
H27B	-3676	3578	-722	37
H27C	-3311	4411	-939	37
H55A	-1775	8379	3017	18
H55B	-2332	7474	2868	18
H22B	-3528	10829	1381	21
H1BA	1344	12435	2119	17
H1BB	1976	12287	1459	17
H63A	-1445	8020	4703	17
H63B	-877	8433	4091	17
H79A	-2030	2957	2779	18
H79B	-2829	2215	3006	18
H59A	-3385	8665	4003	18
H59B	-2847	8588	4726	18
H19B	4236	11390	2820	23
H12	312	3139	328	16
H26	-2032	4279	1499	18
H71A	-1599	2313	3937	17
H71B	-1254	3020	4565	17
H82A	-4773	2530	1096	35

Atom	x	y	z	U_{eq}
H82B	-4426	3343	1596	35
H82C	-5288	2625	1820	35
H22	-3501	5843	1318	18
H74A	1409	3280	3158	28
H74B	1973	2959	3725	28
H74C	1784	3763	3927	28
H81A	-3135	2748	1713	26
H81B	-3996	2022	1926	26
H18B	5192	10550	2599	27
H62A	-819	10867	4803	38
H62B	-1683	11260	4651	38
H62C	-1195	10883	4013	38
H16	3325	4363	3418	20
H27D	-4438	9205	-751	36
H27E	-3700	8681	-758	36
H27F	-3254	9524	-947	36
H15	2323	5153	3689	20
H25B	-2518	8819	256	22
H15B	2076	9801	3676	23
H12B	414	8157	203	17
H83A	-3796	2974	4115	18
H83B	-2950	3125	4763	18
H6A	-463	5015	732	15
H6B	553	4777	550	15
H2A	2658	6679	1950	17
H2B	2816	7484	2438	17
H16B	3051	8972	3470	25
H26B	-1919	9332	1424	20
H58A	-4976	7632	1709	34
H58B	-4355	7663	1020	34
H58C	-4214	8432	1555	34
H60A	-1649	9442	3755	19
H60B	-1263	9455	4551	19
H2BA	2680	11503	2014	20
H2BB	2885	12280	2557	20
H76A	-772	4416	4661	21
H76B	-1896	4220	4970	21
H86A	-4916	610	4419	41
H86B	-5440	841	5107	41
H86C	-4224	914	5156	41

2-1(N_2H_4)

EMORY UNIVERSITY | X-ray Crystallography Center

Submitted by: **Christian Wallen**

Solved by: **John Bacsa**

Sample ID: **CMW04-088BuZnTsN2H4**

Crystal Data and Experimental

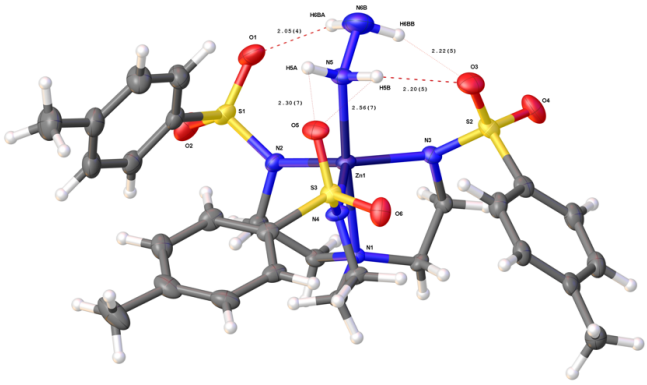

Experimental. Single colourless needle-shaped crystals of (**CMW04-088BuZnTsN2H4**) were recrystallised from a mixture of DCM and ethanol by vapor diffusion. A suitable crystal (0.56×0.20×0.15) mm was selected and mounted on a loop with paratone oil on a Bruker APEX-II CCD diffractometer. The crystal was cooled to T = 100(2) K during data collection. The structure was solved with the **ShelXT-2014/4** (Sheldrick, 2015) structure solution program in the space group P1 (#1) using combined Patterson, direct and dual-space recycling methods (which confirmed the space group to be P-1 (#2)) using **Olex2** (Dolomanov et al., 2009). The structure was refined with version 2014/7 of **ShelXL** (Sheldrick, 2008) using Least Squares minimisation.

Crystal Data. $C_{43}H_{73}N_7O_6S_3Zn$, M_r = 945.63, triclinic, P-1 (No. 2), a = 9.117(2) Å, b = 13.492(3) Å, c = 20.272(4) Å, α = 97.526(3)°, β = 96.225(3)°, γ = 109.087(3)°, V = 2305.5(9) Å^3, T = 100(2) K, Z = 2, Z' = 1, μ(MoK$_\alpha$) = 0.722, 33079 reflections measured, 10558 unique (R_{int}# = 0.0497) which were used in all calculations. The final wR_2 was 0.1793 (all data) and R_1 was 0.0713 (I > 2(I)).

Compound	**CMW04-088BuZnTsN2H4**
Formula	$C_{43}H_{73}N_7O_6S_3Zn$
$D_{calc.}$/ g cm^{-3}	1.362
μ/mm^{-1}	0.722
Formula Weight	945.63
Colour	colourless
Shape	needle
Max Size/mm	0.56
Mid Size/mm	0.20
Min Size/mm	0.15
T/K	100(2)
Crystal System	triclinic
Space Group	P-1
a/Å	9.117(2)
b/Å	13.492(3)
c/Å	20.272(4)
α/°	97.526(3)
β/°	96.225(3)
γ/°	109.087(3)
V/Å^3	2305.5(9)
Z	2
Z'	1
Θ_{min}/°	1.760
Θ_{max}/°	27.484
Measured Refl.	33079
Independent Refl.	10558
Reflections I >2sigma(I)	8173
R_{int}	0.0497
Parameters	636
Restraints	319
Largest Peak	1.452
Deepest Hole	-1.004
GooF	1.042
wR_2 (all data)	0.1793
wR_2	0.1624
R_1 (all data)	0.0954
R_1	0.0713
CCDC Number	1429661

Structure Quality Indicators

Reflections:	d min	0.77	I/σ	13.2	Rint	4.97%	complete 100%
Refinement:	Shift	0.000	Max Peak	1.4	Min Peak	-1.0	GooF 1.042

Experimental Extended. A colourless needle-shaped crystal with dimensions 0.56×0.20×0.15 mm was mounted on a loop with paratone oil. Data were collected using a Bruker APEX-II CCD diffractometer equipped with an Oxford Cryosystems low-temperature apparatus operating at $T = 100(2)$ K.

Data were measured using ω scans with MoK$_\alpha$ radiation (fine-focus sealed tube, 45 kV, 35 mA). The total number of runs and images was based on the strategy calculation from the program **APEX2** (Bruker, 2014). The maximum resolution achieved was $\Theta = 27.484°$.

Unit cell indexing was performed by using the **APEX2** (Bruker, 2014) software and refined using **SAINT** (Bruker, V8.34A, 2013) on 9800 reflections, 30% of the observed reflections. Data reduction, scaling and absorption corrections were performed using **SAINT** (Bruker, V8.34A, 2013) and **SADABS-2014/5** (Bruker, 2014) was used for absorption correction. The Ratio of minimum to maximum transmission is 0.8574. The $\lambda/2$ correction factor is 0.00150. The final completeness is 99.8% out to 27.484 in Θ. The absorption coefficient (μ) of this material is 0.722 mm^{-1} and the minimum and maximum transmissions are 0.6393 and 0.7456.

The structure was solved with **ShelXT-2014/4** (Sheldrick, 2015) in the in the space group P1 (#1) using combined Patterson, direct and dual-space recycling methods (which confirmed the space group to be P-1 (#2)) and by using **Olex2** (Dolomanov et al., 2009) as the graphical interface. The structure was refined by Least Squares using version 2014/7 of **ShelXL** (Sheldrick, 2008). All non-hydrogen atoms were refined anisotropically. Hydrogen atom positions were calculated geometrically and refined using the riding model.

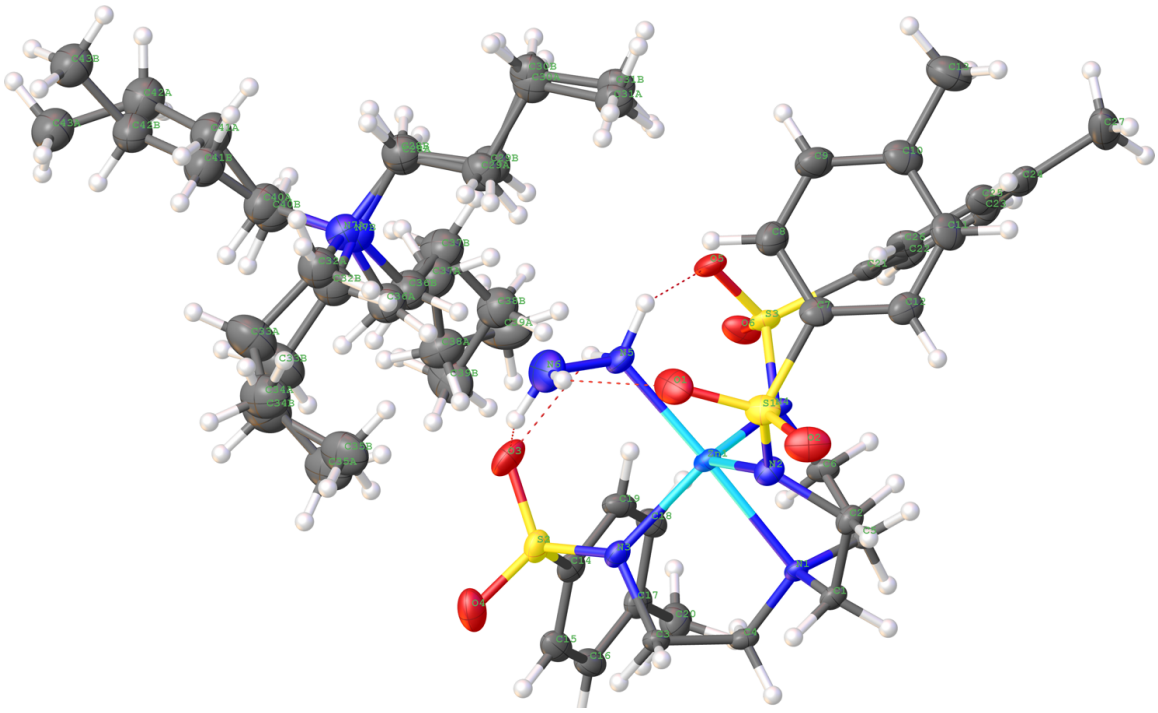

Figure 1: Plot of the asymmetric unit.

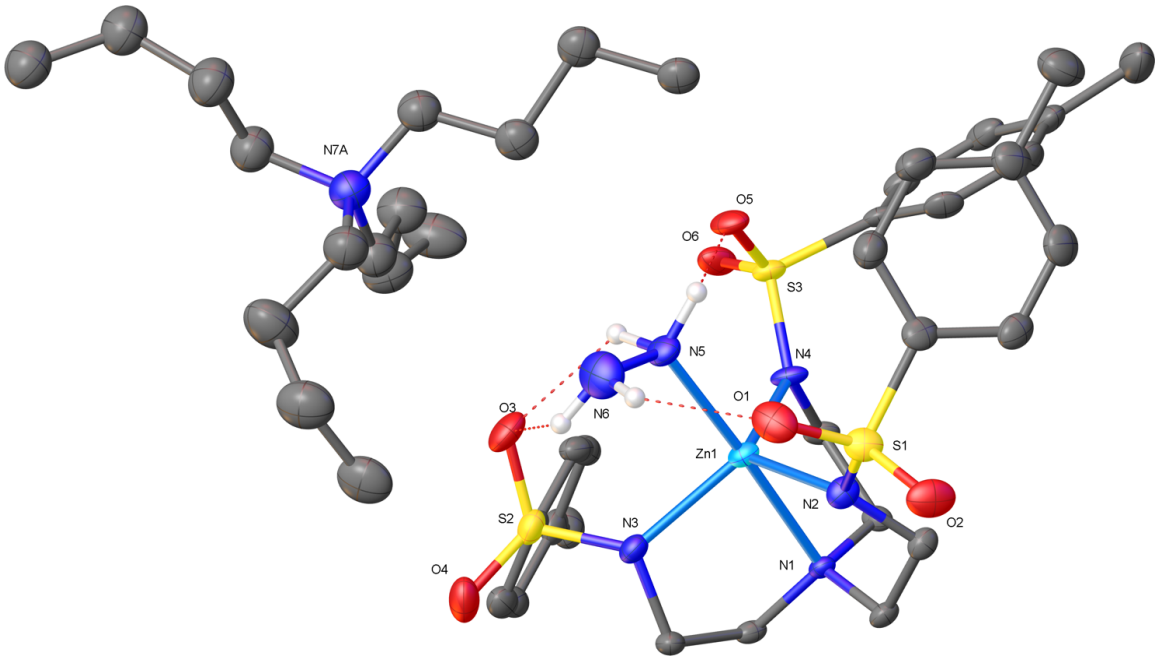

Figure 2: Plot of the asymmetric unit with one component of the disorder and H atoms (except H bonded H atoms) removed for clarity.

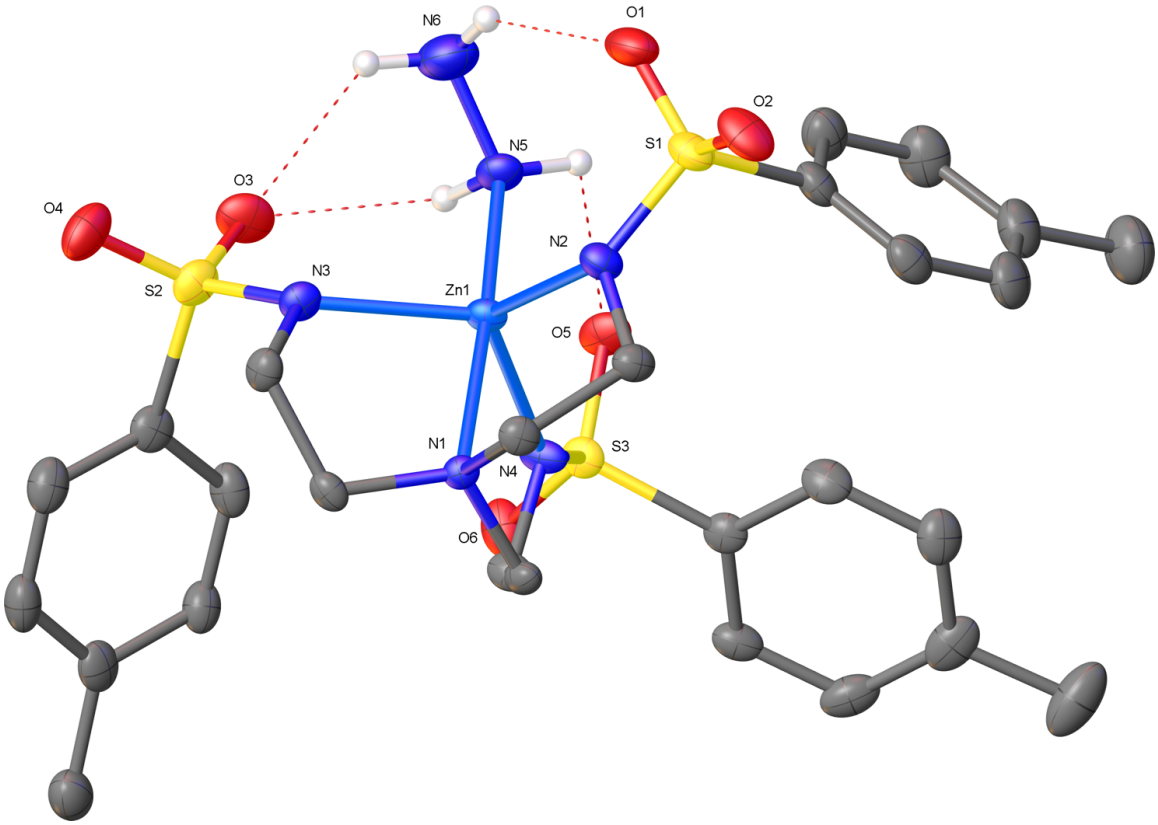

Figure 3:

Plot of the anionic part of the asymmetric unit.

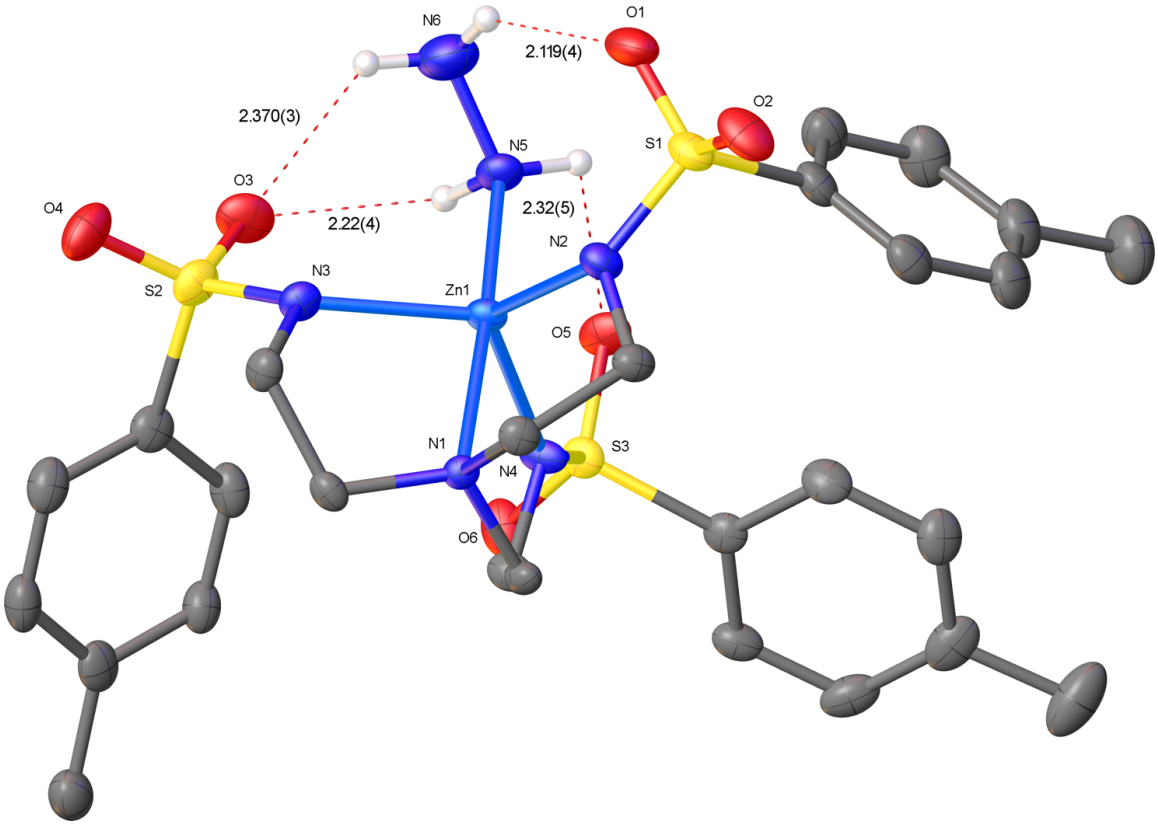

Figure 4:

Plot of the anionic part of the asymmetric unit with h-bond distances.

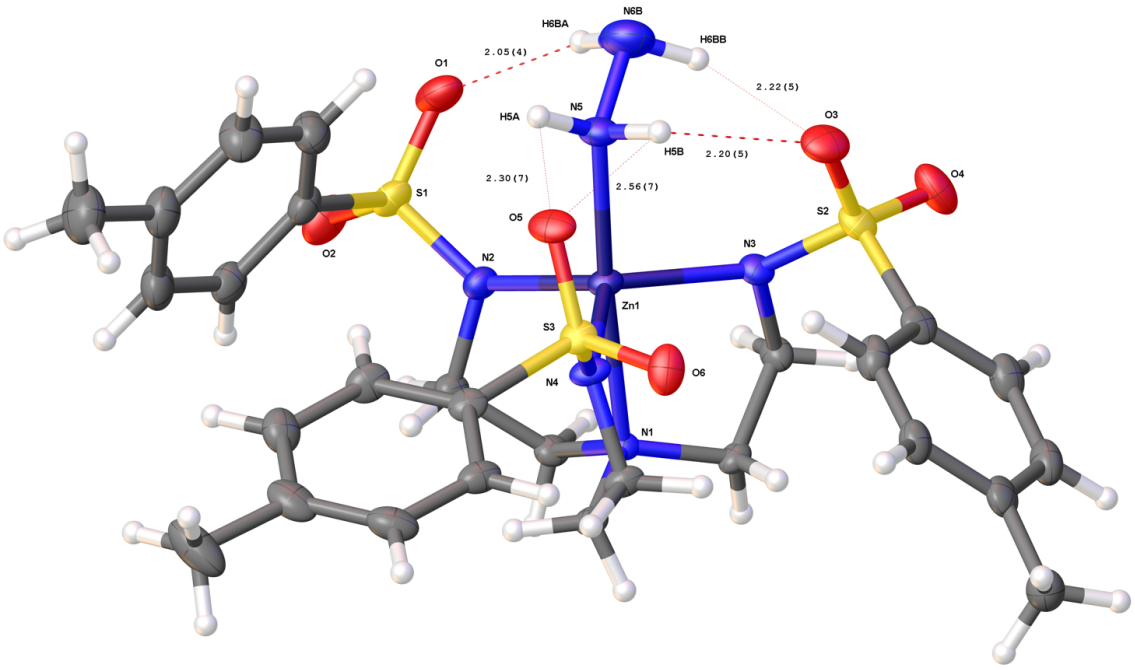

Figure 5: Plot of a second view of the anionic part of the asymmetric unit with h-bond distances.

Data Plots: Diffraction Data

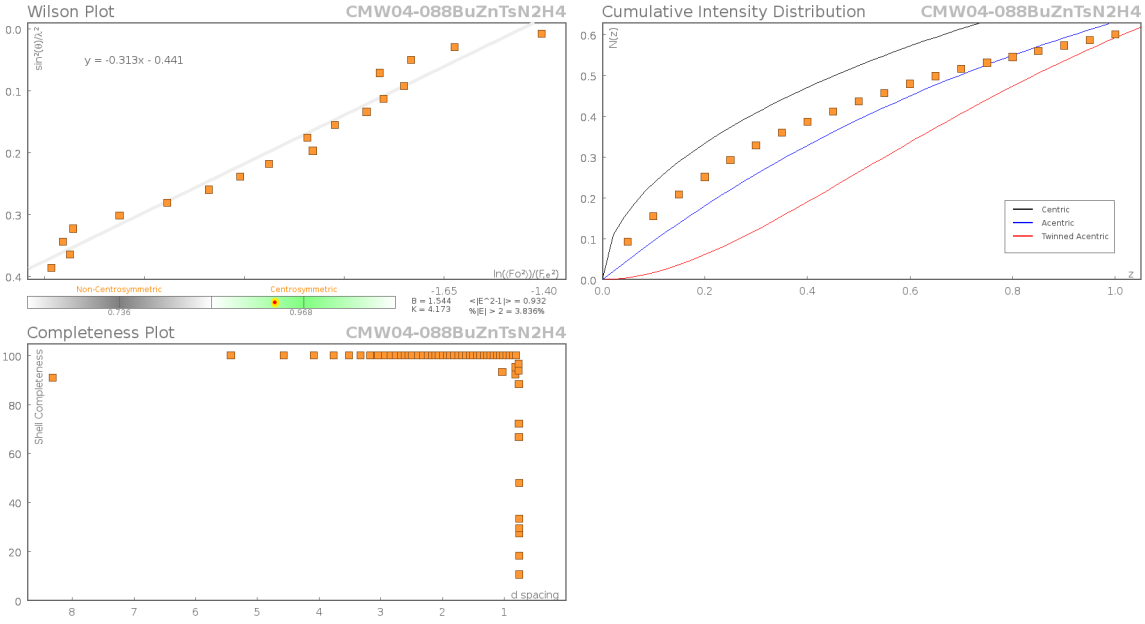

Data Plots: Refinement and Data

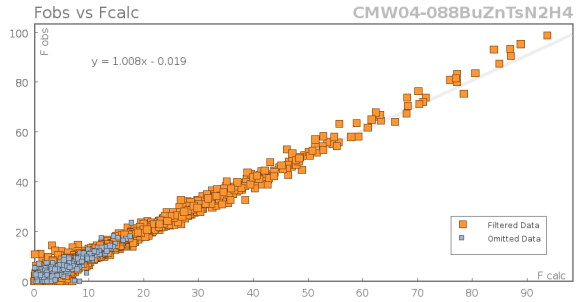

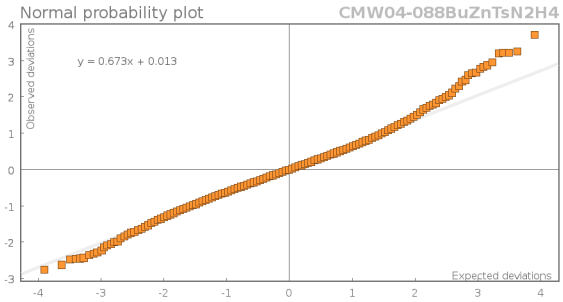

Reflection Statistics

Total reflections (after filtering)	33114	Unique reflections	10558
Completeness	0.998	Mean I/σ	13.23
hklsub>max</sub> collected	(11, 17, 26)	hklsub>min</sub> collected	(-11, -17, -26)
hkl_{max} used	(11, 17, 26)	hkl_{min} used	(-11, -17, 0)
Lim d_{max} collected	20.0	Lim d_{min} collected	0.77
d_{max} used	11.57	d_{min} used	0.77
Friedel pairs	10157	Friedel pairs merged	1
Inconsistent equivalents	0	R_{int}	0.0497
R_{sigma}	0.0547	Intensity transformed	0
Omitted reflections	0	Omitted by user (OMIT hkl)	35
Multiplicity	(10105, 9472, 1269, 250, 1)	Maximum mulitplicity	9
Removed systematic absences	0	Filtered off (Shel/OMIT)	747

Images of the Crystal on the Diffractometer

Table 1: Fractional Atomic Coordinates (×10^4) and Equivalent Isotropic Displacement Parameters (Å^2×10^3) for **CMW04-088BuZnTsN2H4**. U_{eq} is defined as 1/3 of of the trace of the orthogonalised U_{ij}.

Atom	x	y	z	U_{eq}
N7A	890(11)	-2351(7)	3930(4)	36.1(7)
C28A	172(13)	-1498(9)	3891(7)	38.8(9)
C29A	1270(20)	-441(12)	3810(20)	36.3(18)
C30A	330(30)	373(15)	3830(30)	35.7(11)
C31A	1410(30)	1419(14)	3700(30)	31.9(15)
C32A	2275(15)	-1979(9)	4500(5)	43.9(11)
C33A	3030(17)	-2780(12)	4671(11)	61.3(16)
C34A	4784(15)	-2209(19)	4961(8)	57(3)
C35A	5890(20)	-1990(20)	4458(11)	50.9(19)
C36A	1448(12)	-2642(12)	3276(5)	40.9(11)
C37A	390(20)	-2798(18)	2653(5)	46.8(13)

Atom	x	y	z	U_{eq}
C38A	660(20)	-3495(14)	2066(6)	45(4)
C39A	-180(30)	-3470(20)	1393(6)	60(6)
C40A	-342(16)	-3356(7)	4062(6)	44.1(10)
C41A	-1100(20)	-3289(10)	4664(7)	49.9(14)
C42A	-2527(15)	-4259(13)	4673(9)	51(2)
C43A	-2370(20)	-5099(12)	5060(10)	49.3(15)
N7B	881(5)	-2318(3)	3836(2)	36.1(7)
C28B	196(7)	-1445(4)	3940(3)	38.8(9)
C29B	1057(9)	-444(6)	3708(6)	36.3(18)
C30B	194(13)	391(7)	3868(10)	35.7(11)
C31B	1132(11)	1427(6)	3681(10)	31.9(15)
C32B	2418(7)	-2021(4)	4314(3)	43.9(11)
C33B	3213(9)	-2844(6)	4331(5)	61.3(16)
C34B	4782(8)	-2382(8)	4821(5)	60(2)
C35B	6091(9)	-1542(7)	4604(4)	50.9(19)
C36B	1183(7)	-2525(5)	3116(2)	40.9(11)
C37B	-135(10)	-2748(7)	2581(3)	46.8(13)
C38B	262(9)	-2901(5)	1878(3)	42.5(15)
C39B	617(11)	-3901(6)	1686(4)	51.5(19)
C40B	-276(7)	-3350(4)	3972(3)	44.1(10)
C41B	-657(9)	-3408(5)	4656(4)	49.9(14)
C42B	-2018(9)	-4396(5)	4706(4)	47.5(17)
C43B	-2798(9)	-4434(6)	5318(4)	49.3(15)
Zn1	6334.9(5)	728.0(3)	2309.7(2)	17.10(12)
S1	8062.5(12)	2993.7(8)	3351.1(5)	24.9(2)
S2	5887.2(12)	-1781.5(8)	2360.8(5)	25.0(2)
S3	2911.1(10)	467.0(8)	1434.3(5)	19.0(2)
O1	7553(4)	2403(3)	3880.3(15)	35.5(7)
O2	9543(4)	3879(3)	3522.6(16)	35.7(8)
O4	6741(4)	-2410(2)	2631.8(17)	36.4(8)
O5	2514(3)	591(2)	2102.8(15)	26.7(6)
O6	1944(3)	-507(2)	980.3(16)	28.8(7)
N1	7871(3)	895(2)	1500.0(15)	14.2(6)
N2	8034(4)	2192(3)	2713.5(16)	21.4(7)
O3	4562(4)	-1728(3)	2681.4(16)	33.7(7)
N3	6967(4)	-616(3)	2340.2(16)	19.9(7)
N4	4723(4)	667(3)	1496.2(15)	18.8(7)
N5	4841(4)	470(3)	3038.1(17)	23.9(7)
N6	5343(5)	241(3)	3669(2)	44.3(10)
C1	9314(4)	1810(3)	1777.5(19)	18.2(7)
C2	8931(5)	2672(3)	2205.2(19)	20.7(8)
C3	8360(4)	-537(3)	2006(2)	19.6(8)
C4	8183(4)	-111(3)	1357.9(19)	17.6(7)
C5	6989(4)	1102(3)	910.7(18)	17.9(7)
C6	5238(4)	488(3)	872.1(19)	20.0(8)
C7	6625(5)	3597(3)	3164(2)	25.2(9)
C8	5186(6)	3264(4)	3384(2)	32.5(10)
C9	4122(6)	3767(4)	3259(3)	36.5(11)
C10	4454(6)	4610(3)	2914(3)	34.5(10)
C11	5887(6)	4927(3)	2681(2)	33.3(10)
C12	6961(5)	4422(3)	2800(2)	28.0(9)
C13	3292(6)	5173(4)	2793(3)	45.4(13)
C14	5096(4)	-2436(3)	1513(2)	22.5(8)
C15	5707(5)	-3141(3)	1188(2)	27.8(9)
C16	5146(5)	-3565(3)	512(2)	29.1(9)
C17	3980(5)	-3312(3)	150(2)	26.3(9)
C18	3368(5)	-2611(3)	489(2)	24.7(8)

Atom	x	y	z	U_{eq}
C19	3921(5)	-2167(3)	1162(2)	25.8(9)
C20	3392(6)	-3767(4)	-588(2)	33.3(10)
C21	2566(4)	1507(3)	1060.8(19)	18.8(7)
C22	1642(4)	1289(3)	436(2)	22.6(8)
C23	1270(5)	2082(4)	167(2)	29.2(9)
C24	1846(5)	3115(4)	514(2)	31.4(10)
C25	2841(5)	3346(3)	1131(2)	28.2(9)
C26	3198(4)	2549(3)	1406(2)	24.1(8)
C27	1393(6)	3982(5)	239(3)	49.9(15)

Table 2: Anisotropic Displacement Parameters (×10^4) **CMW04-088BuZnTsN2H4**. The anisotropic displacement factor exponent takes the form: -2PI^2[a*^2 × U_{11} + ... 2hka*× b*× U_{12}]

Atom	U_{11}	U_{22}	U_{33}	U_{23}	U_{13}	U_{12}
N7A	34.7(13)	37.4(13)	36.0(14)	6(1)	6.9(11)	12.1(10)
C28A	38.0(17)	40.4(13)	38(2)	4.9(12)	6.4(15)	13.9(12)
C29A	32(2)	40.3(14)	33(5)	4.7(17)	-1(3)	11.4(15)
C30A	30(2)	38.8(15)	34(3)	5.1(14)	-1.7(19)	9.1(14)
C31A	25(4)	37.4(16)	31(3)	3.5(14)	-2(4)	10.0(17)
C32A	40.7(15)	45.4(18)	44.8(19)	9.0(14)	4.1(14)	14.5(13)
C33A	57(2)	60(2)	70(3)	9.1(19)	-3.3(18)	29.2(17)
C34A	55(2)	73(7)	45(4)	7(4)	1(2)	29(2)
C35A	51(2)	65(4)	38(4)	5(3)	-6(2)	28(2)
C36A	44(2)	40(2)	38.9(14)	6.8(12)	8.7(13)	14.9(16)
C37A	48(3)	54(3)	38.6(16)	5.8(14)	7.0(15)	19(2)
C38A	39(7)	54(8)	40(3)	3(3)	7(3)	14(7)
C39A	62(12)	86(14)	40(3)	0(3)	5(3)	43(12)
C40A	44.6(16)	41.4(14)	45.4(16)	8.2(12)	10.3(13)	12.3(12)
C41A	52(2)	48.9(18)	48.6(16)	11.4(12)	14.0(14)	15.1(13)
C42A	51(2)	50(2)	50(3)	11.1(18)	10.9(16)	14.6(14)
C43A	49(3)	49(2)	48(3)	10(2)	12(2)	14(2)
N7B	34.7(13)	37.4(13)	36.0(14)	6(1)	6.9(11)	12.1(10)
C28B	38.0(17)	40.4(13)	38(2)	4.9(12)	6.4(15)	13.9(12)
C29B	32(2)	40.3(14)	33(5)	4.7(17)	-1(3)	11.4(15)
C30B	30(2)	38.8(15)	34(3)	5.1(14)	-1.7(19)	9.1(14)
C31B	25(4)	37.4(16)	31(3)	3.5(14)	-2(4)	10.0(17)
C32B	40.7(15)	45.4(18)	44.8(19)	9.0(14)	4.1(14)	14.5(13)
C33B	57(2)	60(2)	70(3)	9.1(19)	-3.3(18)	29.2(17)
C34B	52(2)	71(4)	62(4)	15(3)	1(2)	28(2)
C35B	51(2)	65(4)	38(4)	5(3)	-6(2)	28(2)
C36B	44(2)	40(2)	38.9(14)	6.8(12)	8.7(13)	14.9(16)
C37B	48(3)	54(3)	38.6(16)	5.8(14)	7.0(15)	19(2)
C38B	43(4)	49(3)	35(2)	6.4(17)	5.3(19)	16(3)
C39B	66(5)	60(4)	31(3)	4(2)	-3(3)	31(4)
C40B	44.6(16)	41.4(14)	45.4(16)	8.2(12)	10.3(13)	12.3(12)
C41B	52(2)	48.9(18)	48.6(16)	11.4(12)	14.0(14)	15.1(13)
C42B	53(3)	43(3)	52(3)	13(2)	18(2)	19(2)
C43B	49(3)	49(2)	48(3)	10(2)	12(2)	14(2)
Zn1	13.3(2)	22.3(2)	15.2(2)	2.91(16)	4.60(16)	5.10(17)
S1	25.1(5)	28.1(5)	18.7(5)	-3.3(4)	0.3(4)	9.3(4)
S2	21.7(5)	22.3(5)	29.4(5)	10.6(4)	6.4(4)	2.4(4)
S3	10.4(4)	24.3(5)	22.8(5)	3.2(4)	4.5(3)	6.4(4)
O1	46(2)	45.3(19)	19.7(15)	1.6(13)	4.6(14)	23.8(16)
O2	26.5(16)	35.9(18)	34.1(17)	-11.7(14)	-3.6(13)	6.3(14)
O4	34.3(18)	27.1(16)	44.4(19)	16.7(14)	0.1(15)	4.0(14)
O5	19.3(14)	41.4(17)	27.0(15)	12.0(13)	12.2(12)	15.5(13)

Atom	U_{11}	U_{22}	U_{33}	U_{23}	U_{13}	U_{12}
O6	14.9(14)	23.8(15)	43.6(18)	-0.2(13)	-1.3(13)	5.6(11)
N1	9.4(14)	17.1(14)	15.8(14)	3.8(11)	2.9(11)	3.6(11)
N2	21.3(17)	21.3(16)	18.4(16)	-0.1(13)	3.4(13)	4.6(13)
O3	27.7(16)	34.9(17)	34.2(17)	9.4(14)	15.0(14)	0.8(13)
N3	16.2(16)	21.7(16)	21.5(16)	6.7(13)	6.1(13)	4.1(13)
N4	9.8(14)	31.4(17)	15.4(15)	1.1(13)	2.8(12)	8.2(13)
N5	23.4(17)	30.6(18)	20.6(16)	8.0(13)	9.9(13)	10.1(15)
N6	54(3)	55(3)	29.6(19)	14.2(18)	10.1(18)	23(2)
C1	12.0(17)	19.7(18)	21.0(18)	3.9(14)	4.6(14)	2.1(14)
C2	19.6(19)	20.2(18)	19.1(18)	2.6(14)	3.7(15)	2.9(15)
C3	15.1(18)	20.9(18)	26(2)	6.8(15)	6.6(15)	8.6(15)
C4	12.5(17)	18.4(17)	20.8(18)	-0.5(14)	5.2(14)	4.5(14)
C5	19.5(18)	23.0(18)	15.4(17)	4.3(14)	5.6(14)	11.7(15)
C6	10.9(17)	28(2)	19.8(18)	0.6(15)	0.0(14)	7.3(15)
C7	26(2)	20.6(19)	26(2)	-4.6(15)	5.0(17)	7.0(16)
C8	34(2)	26(2)	39(3)	7.5(18)	13(2)	8.8(19)
C9	25(2)	34(2)	51(3)	7(2)	13(2)	8.6(19)
C10	33(2)	23(2)	44(3)	-2.0(19)	3(2)	9.0(19)
C11	36(3)	18(2)	42(3)	1.3(18)	5(2)	6.2(18)
C12	25(2)	20.8(19)	32(2)	-2.0(17)	7.0(18)	2.0(16)
C13	40(3)	40(3)	61(4)	5(2)	6(3)	21(2)
C14	14.3(18)	19.4(18)	30(2)	6.4(16)	4.4(16)	-0.6(15)
C15	18(2)	21.2(19)	42(3)	8.3(18)	3.4(18)	4.3(16)
C16	26(2)	19.7(19)	45(3)	8.0(18)	12.3(19)	10.0(17)
C17	25(2)	15.9(18)	35(2)	6.6(16)	9.3(18)	1.9(16)
C18	18.2(19)	18.7(18)	36(2)	5.5(16)	3.0(17)	5.5(15)
C19	17.1(19)	21.4(19)	40(2)	3.6(17)	8.5(17)	7.4(16)
C20	41(3)	25(2)	35(2)	6.6(18)	11(2)	12(2)
C21	8.8(15)	25.3(18)	22.0(18)	3.3(14)	4.5(13)	5.2(14)
C22	13.8(18)	29(2)	19.7(19)	-0.4(15)	3.7(15)	1.8(15)
C23	17(2)	45(3)	26(2)	15.3(19)	5.3(16)	6.6(18)
C24	17(2)	40(3)	42(3)	21(2)	11.2(18)	8.5(18)
C25	18(2)	22(2)	42(3)	6.5(18)	6.7(18)	2.5(16)
C26	11.0(17)	31(2)	25(2)	-0.3(16)	-2.1(15)	4.9(16)
C27	30(3)	52(3)	77(4)	41(3)	12(3)	14(2)

Table 3: Bond Lengths in Å for **CMW04-088BuZnTsN2H4**.

Atom	Atom	Length/Å
N7A	C28A	1.504(4)
N7A	C32A	1.517(4)
N7A	C36A	1.520(4)
N7A	C40A	1.528(4)
C28A	C29A	1.488(7)
C29A	C30A	1.592(8)
C30A	C31A	1.501(5)
C32A	C33A	1.515(4)
C33A	C34A	1.539(10)
C34A	C35A	1.504(6)
C36A	C37A	1.452(9)
C37A	C38A	1.512(9)
C38A	C39A	1.500(5)
C40A	C41A	1.472(8)
C41A	C42A	1.519(5)
C42A	C43A	1.497(5)
N7B	C28B	1.506(4)

Atom	Atom	Length/Å
N7B	C32B	1.516(4)
N7B	C36B	1.521(4)
N7B	C40B	1.526(4)
C28B	C29B	1.489(7)
C29B	C30B	1.592(8)
C30B	C31B	1.501(5)
C32B	C33B	1.513(5)
C33B	C34B	1.539(10)
C34B	C35B	1.505(6)
C36B	C37B	1.453(9)
C37B	C38B	1.512(9)
C38B	C39B	1.500(6)
C40B	C41B	1.471(8)
C41B	C42B	1.519(4)
C42B	C43B	1.496(6)
Zn1	N1	2.258(3)
Zn1	N2	2.067(3)
Zn1	N3	2.080(3)

Atom	Atom	Length/Å
Zn1	N4	2.060(3)
Zn1	N5	2.102(3)
S1	O1	1.446(3)
S1	O2	1.451(3)
S1	N2	1.565(3)
S1	C7	1.788(4)
S2	O4	1.444(3)
S2	O3	1.450(3)
S2	N3	1.568(3)
S2	C14	1.781(4)
S3	O5	1.443(3)
S3	O6	1.449(3)
S3	N4	1.573(3)
S3	C21	1.776(4)
N1	C1	1.472(4)
N1	C4	1.475(5)
N1	C5	1.476(5)
N2	C2	1.470(5)
N3	C3	1.484(5)
N4	C6	1.415(5)
N5	N6	1.418(5)
C1	C2	1.514(5)
C3	C4	1.514(5)
C5	C6	1.527(5)
C7	C8	1.384(6)
C7	C12	1.385(6)
C8	C9	1.374(7)
C9	C10	1.380(7)
C10	C11	1.391(7)
C10	C13	1.509(7)
C11	C12	1.382(6)
C14	C15	1.382(6)
C14	C19	1.395(6)
C15	C16	1.386(6)
C16	C17	1.384(6)
C17	C18	1.392(6)
C17	C20	1.508(6)
C18	C19	1.382(6)
C21	C22	1.382(5)
C21	C26	1.387(6)
C22	C23	1.380(6)
C23	C24	1.378(7)
C24	C25	1.397(6)
C24	C27	1.512(6)
C25	C26	1.386(6)

Table 4: Bond Angles in ° for **CMW04-088BuZnTsN2H4**.

Atom	Atom	Atom	Angle/°
C28A	N7A	C32A	110.1(3)
C28A	N7A	C36A	111.8(4)
C28A	N7A	C40A	109.3(3)
C32A	N7A	C36A	108.8(3)
C32A	N7A	C40A	108.9(3)
C36A	N7A	C40A	107.9(3)
C29A	C28A	N7A	115.5(4)
C28A	C29A	C30A	108.5(5)
C31A	C30A	C29A	108.5(5)
C33A	C32A	N7A	117.7(5)
C32A	C33A	C34A	110.2(6)
C35A	C34A	C33A	116.5(7)
C37A	C36A	N7A	117.1(5)
C36A	C37A	C38A	114.1(6)
C39A	C38A	C37A	114.5(6)
C41A	C40A	N7A	119.0(4)
C40A	C41A	C42A	114.5(5)
C43A	C42A	C41A	119.9(6)
C28B	N7B	C32B	110.1(3)
C28B	N7B	C36B	111.6(4)
C28B	N7B	C40B	109.4(3)
C32B	N7B	C36B	108.8(3)
C32B	N7B	C40B	109.2(3)
C36B	N7B	C40B	107.7(3)
C29B	C28B	N7B	115.3(4)
C28B	C29B	C30B	108.5(5)
C31B	C30B	C29B	108.5(5)
C33B	C32B	N7B	117.9(4)
C32B	C33B	C34B	110.3(6)
C35B	C34B	C33B	116.4(7)
C37B	C36B	N7B	116.9(5)
C36B	C37B	C38B	114.2(6)
C39B	C38B	C37B	114.4(5)
C41B	C40B	N7B	119.2(4)
C40B	C41B	C42B	114.4(5)
C43B	C42B	C41B	120.0(6)
N2	Zn1	N1	80.08(12)
N2	Zn1	N3	117.35(13)
N2	Zn1	N5	103.37(14)
N3	Zn1	N1	80.35(12)
N3	Zn1	N5	97.02(13)
N4	Zn1	N1	80.14(11)
N4	Zn1	N2	117.31(13)
N4	Zn1	N3	116.81(13)
N4	Zn1	N5	98.99(13)
N5	Zn1	N1	176.40(13)
O1	S1	O2	116.7(2)
O1	S1	N2	108.79(19)
O1	S1	C7	105.4(2)
O2	S1	N2	111.92(19)
O2	S1	C7	104.5(2)
N2	S1	C7	109.06(19)
O4	S2	O3	115.9(2)
O4	S2	N3	113.16(18)
O4	S2	C14	105.1(2)
O3	S2	N3	108.25(18)
O3	S2	C14	106.28(19)

Atom	Atom	Atom	Angle/°
N3	S2	C14	107.59(18)
O5	S3	O6	115.74(19)
O5	S3	N4	108.76(17)
O5	S3	C21	106.10(18)
O6	S3	N4	113.49(17)
O6	S3	C21	104.96(18)
N4	S3	C21	107.12(17)
C1	N1	Zn1	106.3(2)
C1	N1	C4	112.3(3)
C1	N1	C5	111.3(3)
C4	N1	Zn1	107.1(2)
C4	N1	C5	112.6(3)
C5	N1	Zn1	106.8(2)
S1	N2	Zn1	128.2(2)
C2	N2	Zn1	112.1(2)
C2	N2	S1	115.2(3)
S2	N3	Zn1	128.42(19)
C3	N3	Zn1	110.9(2)
C3	N3	S2	114.8(3)
S3	N4	Zn1	130.58(18)
C6	N4	Zn1	112.8(2)
C6	N4	S3	114.1(2)
N6	N5	Zn1	120.7(3)
N1	C1	C2	110.4(3)
N2	C2	C1	108.2(3)
N3	C3	C4	109.6(3)
N1	C4	C3	109.6(3)
N1	C5	C6	109.0(3)
N4	C6	C5	111.8(3)
C8	C7	S1	121.2(3)

Atom	Atom	Atom	Angle/°
C8	C7	C12	119.2(4)
C12	C7	S1	119.5(3)
C9	C8	C7	120.3(4)
C8	C9	C10	121.3(4)
C9	C10	C11	118.2(4)
C9	C10	C13	120.9(5)
C11	C10	C13	121.0(5)
C12	C11	C10	121.0(4)
C11	C12	C7	119.9(4)
C15	C14	S2	121.0(3)
C15	C14	C19	120.0(4)
C19	C14	S2	118.8(3)
C14	C15	C16	119.2(4)
C17	C16	C15	122.1(4)
C16	C17	C18	117.8(4)
C16	C17	C20	121.7(4)
C18	C17	C20	120.5(4)
C19	C18	C17	121.2(4)
C18	C19	C14	119.7(4)
C22	C21	S3	120.9(3)
C22	C21	C26	119.3(4)
C26	C21	S3	119.8(3)
C23	C22	C21	121.1(4)
C24	C23	C22	120.2(4)
C23	C24	C25	118.8(4)
C23	C24	C27	120.7(5)
C25	C24	C27	120.5(5)
C26	C25	C24	121.1(4)
C25	C26	C21	119.4(4)

Table 5: Hydrogen Fractional Atomic Coordinates (×10^4) and Equivalent Isotropic Displacement Parameters (Å^2×10^3) for **CMW04-088BuZnTsN2H4**. U_{eq} is defined as 1/3 of of the trace of the orthogonalised U_{ij}.

Atom	x	y	z	U_{eq}
H28A	-702	-1750	3505	47
H28B	-286	-1404	4306	47
H29A	1672	-503	3383	44
H29B	2171	-182	4187	44
H30A	-608	91	3472	43
H30B	-12	470	4269	43
H31A	1514	1363	3226	48
H31B	2444	1600	3978	48
H31C	967	1976	3829	48
H32A	3098	-1366	4388	53
H32B	1925	-1713	4911	53
H33A	2919	-3301	4260	74
H33B	2489	-3174	5006	74
H34A	4901	-1523	5244	68
H34B	5113	-2647	5261	68
H35A	5356	-2407	4014	76
H35B	6811	-2179	4601	76
H35C	6238	-1226	4431	76

Atom	x	y	z	U_{eq}
H36A	2448	-2072	3257	49
H36B	1683	-3305	3293	49
H37A	497	-2094	2530	56
H37B	-709	-3124	2732	56
H38A	1804	-3266	2053	54
H38B	318	-4239	2146	54
H39A	187	-3849	1035	90
H39B	51	-2729	1332	90
H39C	-1311	-3817	1371	90
H40A	-1184	-3625	3664	53
H40B	161	-3901	4087	53
H41A	-1420	-2653	4696	60
H41B	-314	-3185	5069	60
H42A	-3330	-3998	4849	61
H42B	-2958	-4611	4198	61
H43A	-2297	-5699	4750	74
H43B	-3283	-5349	5285	74
H43C	-1410	-4801	5398	74
H28C	-902	-1720	3701	47
H28D	161	-1272	4427	47
H29C	1066	-592	3217	44
H29D	2159	-151	3943	44
H30C	-882	121	3606	43
H30D	114	498	4354	43
H31D	1358	1295	3223	48
H31E	2121	1753	3998	48
H31F	527	1909	3701	48
H32C	3169	-1375	4199	53
H32D	2224	-1823	4776	53
H33C	3409	-3064	3873	74
H33D	2515	-3481	4476	74
H34C	4579	-2074	5258	72
H34D	5150	-2977	4900	72
H35D	6210	-1795	4144	76
H35E	7074	-1397	4910	76
H35F	5841	-887	4616	76
H36C	2046	-1894	3047	49
H36D	1562	-3135	3069	49
H37C	-545	-2152	2632	56
H37D	-985	-3399	2632	56
H38C	-633	-2911	1550	51
H38D	1185	-2282	1843	51
H39D	662	-4014	1202	77
H39E	-212	-4509	1789	77
H39F	1631	-3834	1941	77
H40C	-1275	-3514	3663	53
H40D	141	-3927	3844	53
H41C	-913	-2770	4822	60
H41D	288	-3386	4958	60
H42C	-2841	-4524	4311	57
H42D	-1637	-5006	4655	57
H43D	-3695	-5101	5254	74
H43E	-3168	-3828	5390	74
H43F	-2044	-4396	5712	74
H5	4260(50)	960(30)	3100(30)	52(17)
H5A	4050(40)	-224(19)	2840(30)	56(17)
H1A	9828	2099	1404	22

Atom	x	y	z	U_{eq}
H1B	10056	1575	2055	22
H2A	9913	3252	2429	25
H2B	8301	2977	1919	25
H3A	8458	-1249	1905	23
H3B	9325	-55	2310	23
H4A	9158	14	1158	21
H4B	7304	-641	1030	21
H5B	7351	872	493	21
H5C	7175	1875	955	21
H6C	4629	710	522	24
H6D	5034	-283	737	24
H8	4932	2685	3622	39
H9	3139	3530	3413	44
H11	6131	5499	2437	40
H12	7929	4641	2633	34
H13A	3861	5934	2814	68
H13B	2611	5082	3139	68
H13C	2648	4869	2347	68
H15	6502	-3332	1425	33
H16	5575	-4044	289	35
H18	2555	-2434	254	30
H19	3502	-1680	1383	31
H20A	2262	-3896	-686	50
H20B	3580	-4440	-697	50
H20C	3951	-3261	-859	50
H22	1256	583	188	27
H23	614	1914	-259	35
H25	3279	4060	1366	34
H26	3871	2715	1828	29
H27A	314	3905	303	75
H27B	1461	3921	-243	75
H27C	2111	4680	478	75
H6A	5721	-325	3618	60
H6B	6172	817	3925	60

Table 6: Hydrogen Bond information for **CMW04-088BuZnTsN2H4**.

D	H	A	d(D-H)/Å	d(H-A)/Å	d(D-A)/Å	D-H-A/deg
N5	H5	O5	0.973(5)	2.32(5)	2.749(5)	106(4)
N5	H5A	O3	0.974(5)	2.22(4)	2.878(5)	124(4)
C2	H2A	O2	0.99	2.37	2.835(5)	108.1
C3	H3A	O4	0.99	2.56	2.997(5)	106.4
C8	H8	O1	0.95	2.55	2.915(6)	103.0
C12	H12	O2	0.95	2.72	2.981(6)	96.8
C15	H15	O4	0.95	2.55	2.909(6)	102.8
C19	H19	O3	0.95	2.72	3.015(6)	98.8
C22	H22	O6	0.95	2.48	2.870(5)	104.7
C26	H26	O5	0.95	2.88	3.074(5)	92.6
N6	H6A	O3	0.93	2.37	2.938(5)	119.0
N6	H6B	O1	0.93	2.12	2.897(6)	140.2

2-1(NH_2OH)

EMORY UNIVERSITY | X-ray Crystallography Center

Submitted by: **Christian Wallen**

Solved by: **John Bacsa**

Sample ID: **CMW04_BuTsNH2OH**

Crystal Data and Experimental

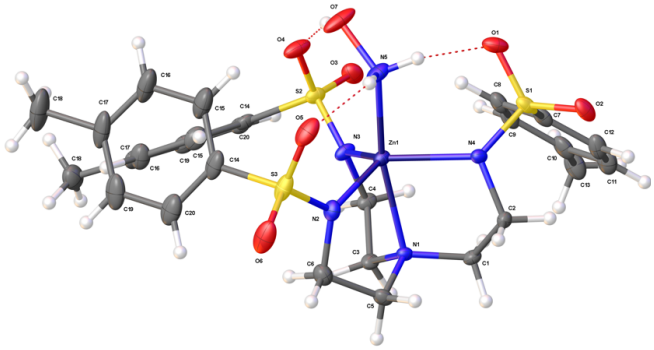

Experimental. Single colourless prism-shaped crystals of (**CMW04-BuTsNH2OH**) were recrystallised from a mixture of THF and diethyl ether by vapor diffusion. A suitable crystal (0.63×0.28×0.20 mm) was selected and mounted on a loop with paratone oil on a Bruker APEX-II CCD diffractometer. The crystal was cooled to T = 100(2) K during the data collection. The structure was solved with **Superflip** (L. Palatinus & G. Chapuis, 2007) using the Charge Flipping solution method and by using **Olex2** (Dolomanov et al., 2009) as the graphical interface. The model was refined with version of **ShelXL-97** (Sheldrick, 2008) using Least Squares minimisation.

Crystal Data. $C_{43}H_{72}N_6O_7S_3Zn$, M_r = 946.61, triclinic, P-1 (No. 2), a = 13.579(2) Å, b = 18.615(3) Å, c = 20.015(4) Å, α = 90.555(2)°, β = 100.310(2)°, γ = 110.958(2)°, V = 4633.2(14) Å^3, T = 100(2) K, Z = 4, Z' = 2, μ(MoK$_\alpha$) = 0.720, 77125 reflections measured, 21226 unique (R_{int} = 0.0402) which were used in all calculations. The final wR_2 was 0.1356 (all data) and R_1 was 0.0541 (I > 2(I)).

Compound	**CMW04-BuTsNH2OH**
Formula	$C_{43}H_{72}N_6O_7S_3Zn$
$D_{calc.}$/ g cm^{-3}	1.357
μ/mm^{-1}	0.720
Formula Weight	946.61
Colour	colourless
Shape	prism
Max Size/mm	0.63
Mid Size/mm	0.28
Min Size/mm	0.20
T/K	100(2)
Crystal System	triclinic
Space Group	P-1
a/Å	13.579(2)
b/Å	18.615(3)
c/Å	20.015(4)
α/°	90.555(2)
β/°	100.310(2)
γ/°	110.958(2)
V/Å^3	4633.2(14)
Z	4
Z'	2
Θ_{min}/°	1.504
Θ_{max}/°	27.484
Measured Refl.	77125
Independent Refl.	21226
Reflections Used	16159
R_{int}	0.0402
Parameters	1335
Restraints	606
Largest Peak	1.174
Deepest Hole	-0.417
GooF	1.057
wR_2 (all data)	0.1356
wR_2	0.1162
R_1 (all data)	0.0795
R_1	0.0541
CCDC Number	1429662

Structure Quality Indicators

Refinement: Shift -0.002 | Max Peak 1.2 | Min Peak -0.4 | GooF 1.057

A colourless prism-shaped crystal with dimensions 0.63×0.28×0.20 mm was mounted on a loop with paratone oil. Data were collected using a Bruker APEX-II CCD diffractometer equipped with an Oxford Cryosystems low-temperature apparatus operating at T = 100(2) K.

Data were measured using ω scans with a narrow frame width using MoK_α radiation (sealed tube, 45 kV, 35 mA). The total number of runs and images was based on the strategy calculation from the program **APEX2** (Bruker, 2014). The maximum resolution achieved was Θ = 27.484°.

Unit cell indexing was performed by using the **APEX2** (Bruker, 2014) software and refined using **SAINT** (Bruker, V8.34A, 2013) on 9762 reflections, 13% of the observed reflections. Data reduction, scaling and absorption corrections were performed using **SAINT** (Bruker, V8.34A, 2013) and SADABS-2014/5 (Bruker,2014/5) was used for absorption correction.wR_2(int) was 0.1626 before and 0.0570 after correction.The Ratio of minimum to maximum transmission is 0.8518. The $\lambda/2$ correction factor is 0.00150. The final completeness is 99.9% out to 27.484° in Θ. The absorption coefficient (μ) of this material is 0.720 mm^{-1} and the minimum and maximum transmissions are 0.6355 and 0.7461.

The structure was solved with **Superflip** (L. Palatinus & G. Chapuis, 2007) in the space group P-1 (# 2) by Charge Flipping using the Charge Flipping solution method and by using **Olex2** (Dolomanov et al., 2009) as the graphical interface. The structure was refined by Least Squares using version of **ShelXL-97** (Sheldrick, 2008). All non-hydrogen atoms were refined anisotropically. Hydrogen atom positions were calculated geometrically and refined using the riding model.

The value of Z' is 2. This means that there are two independent molecules in the asymmetric unit. There is considerable disorder in the crystal structure. The disorder was modeled using SAME commands to restrain the 1-2 and 1-3 interatomic distances within tolyl and NEt_4 groups to be similar.

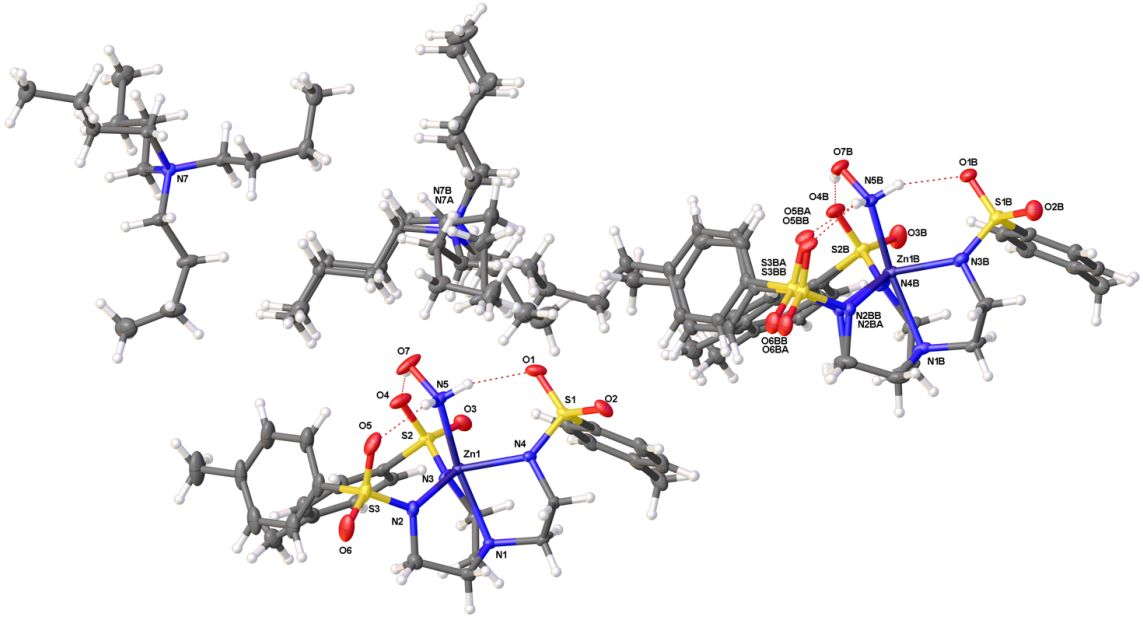

Figure 1: Plot of the asymmetric unit

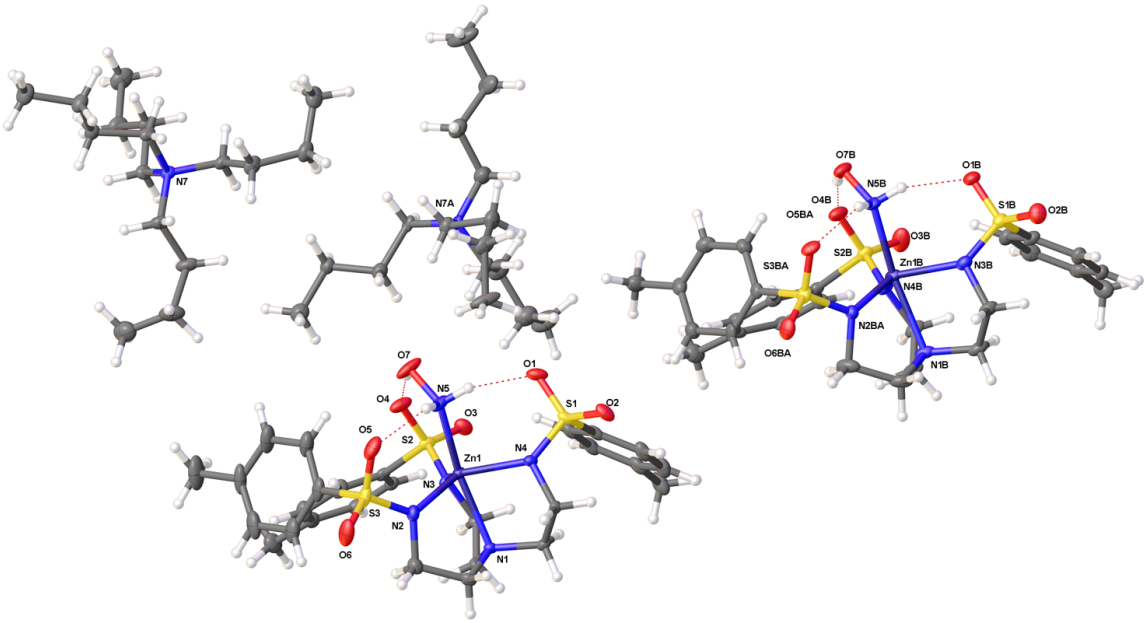

Figure 2: Plot of the asymmetric unit showing one component of the disorder only

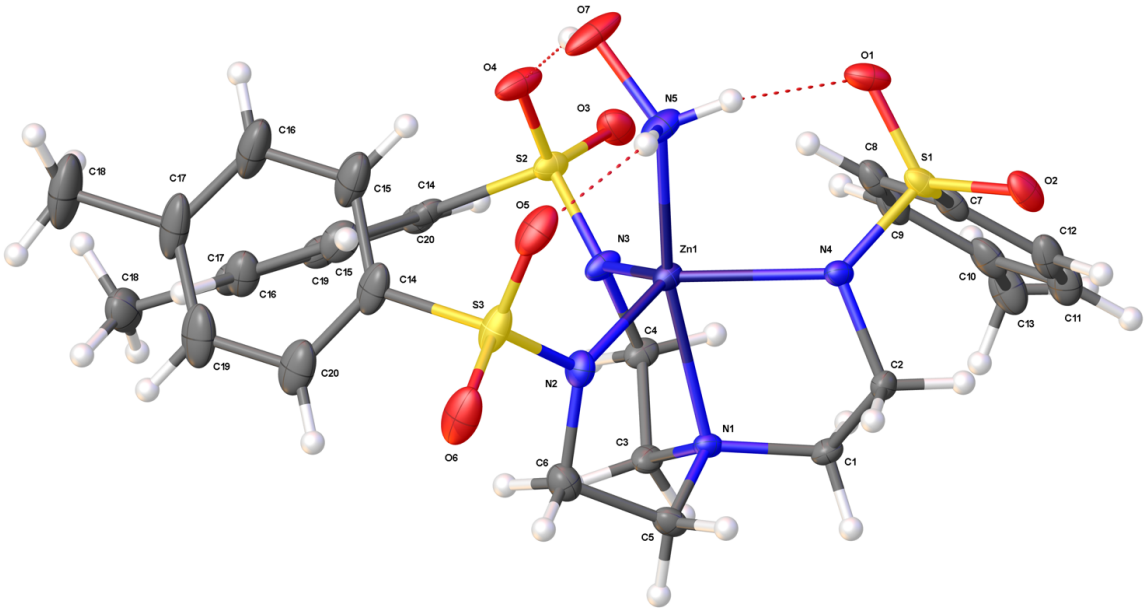

Figure 3: Plot of one of two symmetry independent [ZnR] anions.

Data Plots: Diffraction Data

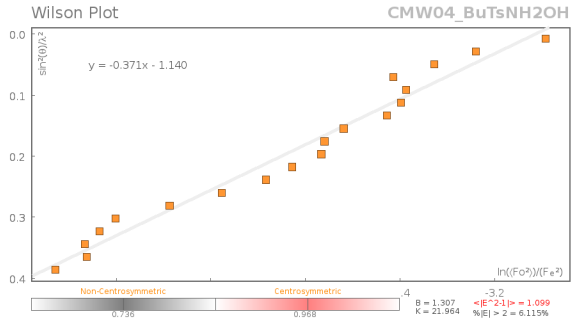

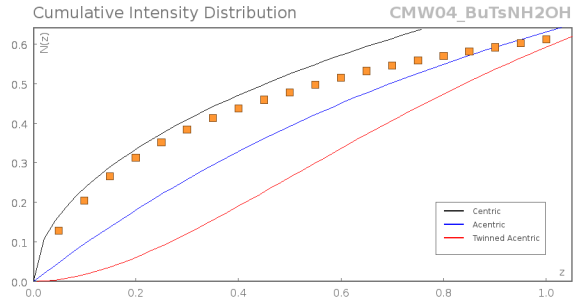

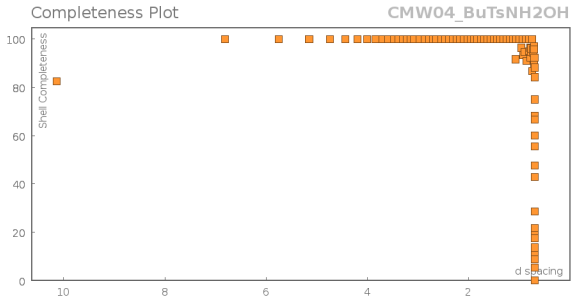

Data Plots: Refinement and Data

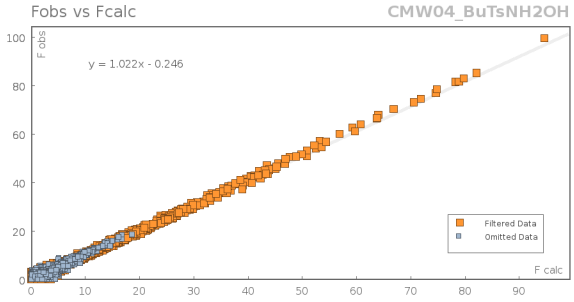

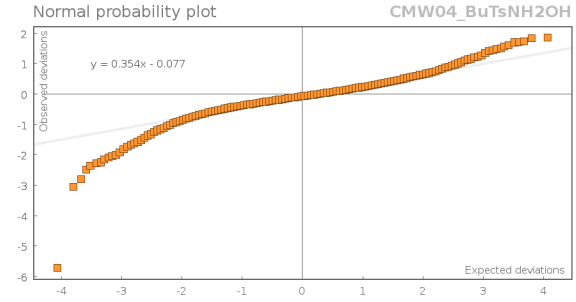

Reflection Statistics

Total reflections (after filtering)	77126	Unique reflections	21226
Completeness	0.999	Mean I/σ	15.03
hklsub>max</sub> collected	(19, 26, 28)	hklsub>min</sub> collected	(-19, -26, -28)
hkl_{max} used	(17, 24, 25)	hkl_{min} used	(-17, -24, 0)
Lim d_{max} collected	20.0	Lim d_{min} collected	0.77
d_{max} used	13.54	d_{min} used	0.77
Friedel pairs	25804	Friedel pairs merged	1
Inconsistent equivalents	0	R_{int}	0.0402
R_{sigma}	0.0382	Intensity transformed	0
Omitted reflections	0	Omitted by user (OMIT hkl)	1
Multiplicity	(21271, 26911, 5225, 683, 368)	Maximum mulitplicity	10
Removed systematic absences	0	Filtered off (Shel/OMIT)	18214

Table 1: Fractional Atomic Coordinates (×10⁴) and Equivalent Isotropic Displacement Parameters (Å²×10³) for **CMW04_BuTsNH2OH**. U_{eq} is defined as 1/3 of the trace of the orthogonalised U_{ij}.

Atom	x	y	z	U_{eq}
Zn1	6027.1(2)	5517.1(2)	2304.0(2)	12.86(8)
S1	4586.0(5)	6633.2(4)	2312.7(3)	15.94(14)
S2	4193.6(5)	3892.6(4)	1528.8(3)	16.43(14)
S3	8026.3(6)	5261.2(4)	3342.8(4)	24.20(17)
O1	3981.1(16)	6038.7(12)	2701.4(11)	23.5(5)
O2	4731.5(16)	7419.2(12)	2521.8(11)	22.8(5)
O3	3207.2(16)	3891.0(12)	1114.2(11)	24.0(5)
O4	4134.8(18)	3696.1(12)	2225.9(11)	26.5(5)
O5	7504.6(19)	5359.3(12)	3889.1(11)	29.4(5)
O6	9190.5(19)	5535.9(13)	3502.5(13)	35.3(6)
O7	4763(2)	4550.1(13)	3401.1(11)	35.6(6)
N2	7596.7(19)	5611.9(13)	2694.5(12)	18.3(5)
N1	6825.5(17)	6069.5(12)	1451.0(11)	12.6(4)
N3	5184.0(19)	4665.9(13)	1542.1(11)	16.1(5)
N5	5434(2)	5283.9(14)	3215.9(12)	22.5(5)
N4	5680.0(18)	6533.3(12)	2289.8(11)	13.4(4)
C7	3835(2)	6461.9(16)	1464.5(15)	18.2(6)
C8	3358(2)	5712.3(17)	1156.5(15)	19.6(6)
C12	3811(2)	7080.4(17)	1083.4(16)	23.0(6)
C1	6492(2)	6725.9(15)	1273.9(13)	14.7(5)
C2	6392(2)	7115.2(15)	1917.9(13)	13.9(5)
C3	6458(2)	5461.9(15)	887.3(13)	15.4(5)
C10	2834(2)	6194.7(18)	86.4(16)	23.5(6)
C4	5304(2)	4933.7(15)	860.5(13)	15.8(5)
C11	3312(2)	6939.5(18)	400.4(17)	25.5(7)
C6	8255(2)	5744.5(17)	2163.2(15)	21.7(6)
C13	2315(3)	6059(2)	-659.3(16)	28.5(7)
C5	7994(2)	6322.7(16)	1708.2(14)	17.5(6)
C9	2857(2)	5585.3(17)	479.9(16)	22.3(6)
Zn1B	913.4(2)	10371.4(2)	2337.0(2)	15.63(8)
S1B	-508.8(6)	11492.9(4)	2343.9(3)	17.99(14)
S2B	-844.5(6)	8796.9(4)	1461.2(4)	18.34(15)
S3BA	2872(7)	10191(2)	3419(4)	17.8(5)
S3BB	2819(7)	10028(2)	3437(4)	17.8(5)
O1B	-1155.8(17)	10868.8(12)	2686.5(10)	22.5(4)
O2B	-365.8(18)	12263.4(12)	2590.7(11)	26.4(5)
O3B	-1805.0(18)	8791.6(13)	1014.4(13)	34.1(6)
O4B	-971.4(18)	8556.5(12)	2136.8(11)	25.5(5)
O5BA	2354(14)	10262(10)	3936(11)	20.4(17)
O5BB	2188(14)	10141(10)	3964(11)	20.4(17)
O6BA	4020(12)	10500(5)	3612(8)	25.5(14)
O6BB	3988(12)	10293(5)	3632(8)	25.5(14)
O7B	-475.6(18)	9308.2(12)	3355.4(11)	25.1(5)
N1B	1812.5(19)	10985.2(14)	1518.5(11)	19.1(5)
N2BA	2444(10)	10536(5)	2763(5)	15.4(11)
N2BB	2465(10)	10386(5)	2768(5)	15.4(11)
N3B	584.0(19)	11388.2(13)	2338.0(12)	18.1(5)
N4B	127.1(19)	9583.6(13)	1524.7(11)	17.0(5)
N5B	214(2)	10058.1(14)	3213.2(12)	20.2(5)
C2B	3159(2)	10605(2)	2257.6(15)	27.6(7)
C3B	1502(2)	11659.0(17)	1364.7(14)	22.2(6)
C4B	1346(2)	12002.1(17)	2015.1(15)	21.8(6)
C5B	1474(2)	10415.7(17)	931.0(14)	22.5(6)
C1B	2966(2)	11212.5(19)	1813.4(15)	25.4(6)
C6B	300(2)	9897.5(17)	861.6(14)	20.7(6)
C7B	-1213(2)	11374.3(17)	1487.0(14)	19.6(6)
C8B	-1703(2)	10633.8(17)	1154.3(16)	23.5(6)

Atom	x	y	z	U_{eq}
C9B	-2200(2)	10540.7(18)	477.2(16)	24.5(6)
C10B	-2218(2)	11173.0(18)	112.3(15)	21.8(6)
C11B	-1720(2)	11904.9(17)	452.6(15)	20.7(6)
C12B	-1225(2)	12009.5(17)	1134.9(15)	20.9(6)
C13B	-2745(3)	11072(2)	-633.7(16)	28.7(7)
N7	3285.2(18)	962.5(13)	6090.1(11)	14.3(5)
C28	4444(2)	1302.3(17)	5982.3(14)	20.2(6)
C29	4574(2)	1538.9(19)	5261.7(15)	26.2(7)
C30	5743(3)	1780(2)	5190.6(18)	34.6(8)
C31	6068(3)	1114(2)	5080.6(19)	38.1(8)
C32	2745(2)	173.2(15)	5700.7(14)	16.6(5)
C33	1593(2)	-254.0(16)	5771.1(15)	18.6(6)
C34	1150(3)	-1057.8(17)	5408.4(16)	26.2(7)
C35	-4(3)	-1488.8(19)	5467.0(18)	33.6(8)
C36	2660(2)	1472.4(16)	5830.3(14)	18.5(6)
C37	3153(2)	2302.2(16)	6136.7(15)	22.9(6)
C38	2435(3)	2753.1(17)	5870.1(16)	25.2(7)
C39	1435(3)	2565.6(19)	6175.9(17)	30.4(7)
C40	3299(2)	917.2(15)	6852.5(13)	16.1(5)
C41	3715(2)	327.3(16)	7196.8(14)	18.6(6)
C42	3994(3)	538.4(17)	7963.0(15)	23.8(6)
C43	4316(3)	-58.6(18)	8371.9(16)	28.9(7)
N7A	1692(3)	4171.5(19)	3939(2)	16.0(14)
C21A	1926(4)	4524(2)	3282(2)	20.0(11)
C22A	1161(5)	4129(4)	2640(3)	37.0(15)
C23A	1561(5)	4534(4)	2038(3)	38.7(15)
C24A	799(5)	4255(4)	1374(3)	44.1(18)
C25A	2573(4)	4630(2)	4530(2)	21.7(11)
C26A	2627(4)	5447(3)	4691(3)	26.1(12)
C27A	3757(4)	5961(3)	5041(3)	25.9(12)
C28A	4576(7)	6163(7)	4580(6)	36(3)
C29A	602(4)	4151(3)	4049(2)	27.9(11)
C30A	246(4)	3833(3)	4696(2)	27.5(10)
C31A	-876(7)	3839(5)	4707(5)	35(2)
C32A	-1314(5)	3451(5)	5304(3)	49(2)
C33A	1648(4)	3334(2)	3883(2)	16.4(9)
C34A	2646(5)	3251(3)	3710(5)	20.6(10)
C35A	2656(5)	2438(3)	3818(6)	20(1)
C36A	3686(9)	2388(6)	3676(11)	27(3)
N7B	1780(3)	4106(2)	3773(3)	17.4(18)
C21B	1349(5)	4019(3)	3018(3)	28.5(17)
C22B	1258(6)	4710(3)	2682(3)	24.2(15)
C23B	801(6)	4494(3)	1931(3)	28.7(16)
C24B	635(6)	5131(4)	1539(3)	28.8(16)
C25B	2847(4)	4782(3)	3947(2)	20.1(14)
C26B	3401(5)	4900(4)	4695(3)	25.7(15)
C27B	4543(4)	5487(4)	4794(3)	28.0(16)
C28B	4617(9)	6296(6)	4628(10)	46(5)
C29B	980(4)	4224(3)	4166(3)	27.9(11)
C30B	15(4)	3524(3)	4239(3)	27.5(10)
C31B	-674(9)	3752(5)	4665(7)	23(3)
C32B	-1557(5)	3059(4)	4835(4)	30.5(17)
C33B	1947(5)	3355(3)	3980(3)	16.4(9)
C34B	2888(7)	3243(4)	3748(6)	20.6(10)
C35B	2885(7)	2426(4)	3850(7)	20(1)
C36B	3889(11)	2359(6)	3680(11)	20(3)
C14_1	-430(9)	8052(6)	1095(5)	15.4(7)

Atom	x	y	z	U_{eq}
C15_1	377(11)	7868(7)	1496(5)	19.5(9)
C16_1	648(6)	7268(4)	1273(3)	19.6(15)
C17_1	119(5)	6842(3)	654(2)	18.8(14)
C18_1	374(5)	6160(3)	437(3)	31.1(15)
C19_1	-667(5)	7046(3)	248(2)	17.7(15)
C20_1	-944(8)	7647(5)	466(4)	18.4(16)
C14_2	-527(9)	8125(6)	1062(4)	15.4(7)
C15_2	280(11)	7880(8)	1377(5)	19.5(9)
C16_2	477(6)	7296(4)	1055(3)	18.0(15)
C17_2	-128(5)	6946(3)	422(2)	14.0(13)
C18_2	67(5)	6291(3)	88(3)	24.7(13)
C19_2	-904(5)	7218(3)	99(3)	14.2(13)
C20_2	-1108(8)	7802(5)	417(4)	12.6(13)
C14_3	2511(7)	9181(2)	3228(5)	16.3(9)
C15_3	1612(10)	8645(3)	3413(9)	21.4(10)
C16_3	1380(9)	7863(3)	3280(9)	24(2)
C17_3	2033(6)	7604(2)	2959(5)	21.2(17)
C18_3	1811(8)	6752(2)	2854(6)	30(2)
C19_3	2931(5)	8147(3)	2774(4)	22.3(10)
C20_3	3167(7)	8931(3)	2903(6)	20.1(16)
C14_4	2396(7)	9008(2)	3269(5)	16.3(9)
C15_4	1462(9)	8509(3)	3446(10)	21.4(10)
C16_4	1188(9)	7718(3)	3340(9)	19.9(17)
C17_4	1836(6)	7414(2)	3059(5)	19.3(16)
C18_4	1548(7)	6553(2)	2965(6)	27.2(19)
C19_4	2725(5)	7921(3)	2837(4)	22.3(10)
C20_4	3019(7)	8714(3)	2953(6)	20.8(16)
C14_5	4477.7(19)	3146.9(13)	1138.6(11)	15.4(5)
C15_5	5295(2)	2918.8(14)	1464.2(12)	22.4(6)
C16_5	5483(2)	2315.4(15)	1168.1(14)	25.4(7)
C17_5	4870(2)	1936.2(13)	545.5(13)	20.5(6)
C18_5	5056(3)	1262.9(15)	238.5(16)	29.4(7)
C19_5	4067(2)	2181.5(13)	217.3(11)	18.3(6)
C20_5	3870.8(19)	2783.0(14)	511.0(11)	15.8(5)
C14_6	7611(2)	4242.7(12)	3163.1(15)	27.6(7)
C15_6	6723(2)	3742.4(14)	3386.5(17)	35.5(8)
C16_6	6462(2)	2951.5(14)	3292.5(18)	40.9(9)
C17_6	7068(2)	2649.5(13)	2965.8(17)	38.8(9)
C18_6	6812(3)	1790.1(14)	2898(2)	52.0(12)
C19_6	7923(2)	3156.6(14)	2712.5(16)	37.0(8)
C20_6	8197(2)	3949.3(14)	2811.0(16)	32.5(8)

Table 2: Anisotropic Displacement Parameters ($\times 10^4$) **CMW04_BuTsNH2OH**. The anisotropic displacement factor exponent takes the form: $-2\pi^2[h^2a^{*2} \times U_{11} + \ldots + 2hka^* \times b^* \times U_{12}]$

Atom	U_{11}	U_{22}	U_{33}	U_{23}	U_{13}	U_{12}
Zn1	15.27(15)	11.21(15)	10.30(14)	0.18(11)	2.42(11)	2.73(12)
S1	11.8(3)	16.9(3)	17.7(3)	-5.7(2)	3.2(2)	3.6(2)
S2	17.8(3)	11.7(3)	16.2(3)	-1.7(2)	5.4(3)	0.1(2)
S3	25.8(4)	15.6(3)	23.9(4)	3.3(3)	-9.1(3)	5.5(3)
O1	17.2(10)	26.9(11)	22.8(11)	-3.9(9)	9.7(8)	1.1(9)
O2	17.4(10)	21(1)	28.9(11)	-11.9(9)	1.7(8)	7.2(8)
O3	16.5(10)	19.7(10)	33.1(12)	-2.8(9)	5.2(9)	3.2(8)
O4	36.5(13)	15.7(10)	19.7(11)	-0.6(8)	13.3(9)	-3.2(9)
O5	40.0(13)	21.2(11)	18.2(10)	4.5(8)	-4.9(9)	5.7(10)
O6	26.3(12)	24.3(12)	43.3(14)	5.3(10)	-15.8(10)	5.7(10)

Atom	U_{11}	U_{22}	U_{33}	U_{23}	U_{13}	U_{12}
O7	56.2(16)	18.2(11)	17.1(11)	3.8(9)	11.5(11)	-6.9(11)
N2	19.9(12)	17.8(12)	17.8(12)	2.8(9)	0.5(9)	9.1(10)
N1	11.4(10)	11.7(10)	13.6(10)	-0.1(8)	4.4(8)	2.2(8)
N3	20.8(12)	10.6(10)	11.6(11)	-0.6(8)	3.7(9)	-0.7(9)
N5	32.7(14)	16.7(12)	14.3(11)	3.8(9)	7.4(10)	3.1(10)
N4	13.2(11)	11.7(10)	14.9(11)	-0.4(8)	5.1(9)	2.8(8)
C7	8.2(12)	21.9(14)	22.8(14)	-5.6(11)	-0.8(10)	5.6(11)
C8	14.1(13)	20.3(14)	25.0(15)	-5.1(11)	1.1(11)	8.5(11)
C12	15.3(14)	18.4(14)	32.3(17)	-6.4(12)	-3.5(12)	6.9(11)
C1	14.6(13)	14.4(12)	13.7(12)	3.4(10)	3.9(10)	3(1)
C2	15.1(13)	11.1(12)	15.7(12)	1.6(10)	3.6(10)	4.7(10)
C3	19.2(13)	15.1(13)	12.5(12)	0.6(10)	6.1(10)	5.6(11)
C10	13.9(13)	29.6(16)	27.7(16)	-6.1(13)	-1.0(12)	11.4(12)
C4	19.3(13)	14.9(13)	10.0(12)	-1.1(10)	2.7(10)	2.8(10)
C11	18.7(15)	24.9(15)	31.9(17)	-1.0(13)	-3.2(12)	10.8(12)
C6	19.4(14)	22.5(15)	24.1(15)	-0.3(12)	2.9(12)	9.6(12)
C13	25.8(16)	34.0(18)	26.7(16)	-7.2(13)	-5.0(13)	17.3(14)
C5	11.5(12)	18.7(13)	20.9(14)	-1.1(11)	3.8(10)	3.7(10)
C9	15.9(14)	20.1(14)	29.8(16)	-8.7(12)	0.7(12)	7.3(11)
Zn1B	14.46(16)	19.78(17)	8.99(15)	1.07(12)	1.61(11)	2.24(12)
S1B	20.1(3)	16.5(3)	15.1(3)	1.7(3)	2.7(3)	4.3(3)
S2B	15.1(3)	16.5(3)	18.5(3)	2.3(3)	1.7(3)	0.6(3)
S3BA	19.7(7)	16.9(13)	12.6(4)	-1.1(13)	-4.3(4)	5.1(15)
S3BB	19.7(7)	16.9(13)	12.6(4)	-1.1(13)	-4.3(4)	5.1(15)
O1B	23.6(11)	24.9(11)	20.4(10)	7.5(8)	9.8(8)	7.7(9)
O2B	30.3(12)	22.1(11)	23.4(11)	-4.0(9)	-1.2(9)	8.7(9)
O3B	18.7(11)	25.9(12)	46.4(15)	6.3(10)	-8.5(10)	1.6(9)
O4B	31.1(12)	18.1(10)	26.3(11)	4.1(9)	15.1(9)	3.1(9)
O5BA	23(4)	23(4)	9.1(15)	1(3)	2(2)	1(3)
O5BB	23(4)	23(4)	9.1(15)	1(3)	2(2)	1(3)
O6BA	22.2(13)	24(4)	23.6(13)	2(3)	-9(1)	7(3)
O6BB	22.2(13)	24(4)	23.6(13)	2(3)	-9(1)	7(3)
O7B	34.7(12)	19.2(10)	22.8(11)	7.4(8)	15.6(10)	6.6(9)
N1B	16.5(11)	21.6(11)	10.9(10)	-2.1(8)	2.8(8)	-2.9(9)
N2BA	15.7(11)	17(2)	14.1(10)	0.6(13)	1.3(8)	6.9(15)
N2BB	15.7(11)	17(2)	14.1(10)	0.6(13)	1.3(8)	6.9(15)
N3B	17.6(11)	17.6(11)	15.2(11)	2.3(9)	2.7(9)	2.1(9)
N4B	17.9(11)	15.3(11)	11.5(10)	1.5(8)	1.0(9)	-0.5(9)
N5B	23.0(13)	24.7(13)	14.3(11)	6.4(10)	8.1(10)	8(1)
C2B	15.1(13)	46.2(18)	17.4(13)	-1.6(12)	3.7(11)	6.2(13)
C3B	23.4(14)	20.5(13)	13.8(12)	1.9(10)	4.2(11)	-2.9(11)
C4B	22.5(14)	17.6(13)	18.0(13)	1.3(10)	4.7(11)	-1.8(11)
C5B	26.9(15)	22.7(14)	10.9(12)	0.2(10)	5.3(10)	-0.2(11)
C1B	14.8(13)	36.2(16)	17.6(13)	-4.7(12)	5.4(10)	-0.8(11)
C6B	23.9(14)	19.5(13)	10.4(12)	0.7(10)	-0.2(10)	-0.5(11)
C7B	17.5(14)	22.5(14)	15.4(13)	4.5(11)	2.3(11)	3.7(11)
C8B	24.0(15)	17.8(14)	24.5(15)	5.0(12)	4.2(12)	2.8(12)
C9B	21.4(15)	22.7(15)	23.6(15)	-4.8(12)	1.5(12)	2.9(12)
C10B	13.6(13)	31.0(16)	19.5(14)	2.9(12)	2.6(11)	7.0(12)
C11B	18.5(14)	22.8(14)	23.2(15)	8.0(12)	5.3(11)	9.6(12)
C12B	17.5(14)	16.6(14)	24.7(15)	2.4(11)	1.0(11)	3.2(11)
C13B	25.2(16)	40.0(19)	19.8(15)	-0.2(13)	-0.4(12)	13.0(14)
N7	13.9(11)	14.4(11)	9.8(10)	-2.6(8)	-0.5(8)	0.7(9)
C28	15.3(13)	22.7(14)	16.3(13)	-2.1(11)	4.0(11)	-0.8(11)
C29	22.0(15)	29.0(16)	19.2(15)	-0.5(12)	7.9(12)	-2.5(13)
C30	24.8(17)	39(2)	31.6(18)	-2.1(15)	11.4(14)	-1.3(14)
C31	27.9(18)	48(2)	35.6(19)	4.9(16)	2.8(15)	11.7(16)

Atom	U_{11}	U_{22}	U_{33}	U_{23}	U_{13}	U_{12}
C32	18.3(13)	13.9(13)	15.3(13)	-4(1)	2.6(10)	3.6(11)
C33	17.5(14)	14.5(13)	19.1(14)	-2(1)	3.6(11)	0.4(11)
C34	28.2(16)	16.3(14)	26.8(16)	-5.8(12)	3.1(13)	0.7(12)
C35	36.0(19)	20.7(16)	28.7(17)	-3.4(13)	0.1(14)	-4.6(14)
C36	20.9(14)	14.8(13)	17.3(13)	3(1)	5.5(11)	2.7(11)
C37	25.6(15)	13.9(13)	21.3(14)	-1.6(11)	-0.5(12)	0.4(11)
C38	31.1(17)	15.0(14)	24.0(15)	1.6(11)	-1.0(13)	4.8(12)
C39	42(2)	24.3(16)	25.5(16)	-3.0(13)	1.3(14)	15.1(15)
C40	20.1(14)	12.7(12)	12.4(12)	-1.6(10)	3.9(10)	2(1)
C41	19.7(14)	15.6(13)	18.2(14)	1.4(10)	2.6(11)	4.1(11)
C42	31.0(17)	20.3(14)	16.8(14)	1.7(11)	1.2(12)	7.3(13)
C43	34.0(18)	24.9(16)	21.8(15)	1.9(12)	-3.2(13)	7.6(14)
N7A	18(3)	14(2)	13(2)	5.2(17)	-0.8(18)	3.8(19)
C21A	16(2)	17(2)	26(2)	10.7(19)	3.0(18)	5.2(18)
C22A	36(2)	38(2)	32(2)	8.0(17)	5.0(17)	8.6(16)
C23A	40(2)	39(2)	35(2)	7.4(16)	10.0(17)	9.6(16)
C24A	43(4)	50(4)	24(3)	6(3)	2(3)	1(3)
C25A	22.1(18)	17.3(17)	21.6(18)	-0.2(14)	0.1(14)	4.5(14)
C26A	29(3)	17(3)	31(3)	2(2)	3(2)	8(2)
C27A	31(3)	14(2)	23(3)	-3(2)	3(2)	-2(2)
C28A	42(6)	28(4)	18(5)	-7(4)	14(4)	-17(3)
C29A	27(2)	26.3(15)	29.9(16)	7.9(12)	6.7(15)	8.6(15)
C30A	26(2)	25(2)	24.3(19)	4.6(16)	-0.2(17)	3.9(18)
C31A	26(4)	49(5)	28(4)	16(4)	2(3)	14(4)
C32A	27(3)	72(5)	22(3)	17(3)	-2(3)	-9(3)
C33A	15.4(19)	13.6(12)	13.9(14)	3.6(10)	-5.5(14)	1.7(12)
C34A	22(2)	16.6(12)	19.9(14)	1.4(10)	2.3(18)	4.2(12)
C35A	22(2)	18.6(12)	18.6(14)	3.7(10)	2.1(18)	6.9(12)
C36A	28(4)	24(4)	24(4)	0(3)	2(3)	5(3)
N7B	18(4)	13(3)	18(3)	-4(2)	4(3)	2(3)
C21B	34(4)	17(3)	24(4)	-7(3)	-3(3)	2(3)
C22B	24(3)	20(3)	26(3)	-3(2)	2(3)	7(3)
C23B	26(4)	34(4)	25(3)	-3(3)	10(3)	8(3)
C24B	17(3)	30(4)	32(4)	-8(3)	5(3)	1(3)
C25B	19(2)	19(2)	21(2)	0.5(15)	4.0(15)	5.0(15)
C26B	31(4)	17(3)	22(3)	4(2)	3(3)	1(3)
C27B	30(4)	29(4)	17(3)	-1(3)	3(3)	2(3)
C28B	65(10)	22(5)	33(8)	2(4)	-11(6)	5(5)
C29B	27(2)	26.3(15)	29.9(16)	7.9(12)	6.7(15)	8.6(15)
C30B	26(2)	25(2)	24.3(19)	4.6(16)	-0.2(17)	3.9(18)
C31B	23(3)	23(3)	22(3)	3.9(18)	4.3(19)	7.4(19)
C32B	30(4)	32(4)	28(4)	7(3)	9(3)	8(3)
C33B	15.4(19)	13.6(12)	13.9(14)	3.6(10)	-5.5(14)	1.7(12)
C34B	22(2)	16.6(12)	19.9(14)	1.4(10)	2.3(18)	4.2(12)
C35B	22(2)	18.6(12)	18.6(14)	3.7(10)	2.1(18)	6.9(12)
C36B	18(5)	24(5)	11(4)	-2(3)	2(5)	-2(3)
C14_1	14.9(14)	13.7(15)	14.8(12)	1.5(11)	3.9(10)	1.5(9)
C15_1	17(2)	17.1(13)	18(3)	1(2)	-0.5(17)	-0.2(12)
C16_1	16(3)	22(3)	18(4)	5(3)	1(3)	4(2)
C17_1	11(3)	25(3)	20(3)	4(3)	6(3)	5(2)
C18_1	30(4)	26(3)	36(4)	-4(3)	8(3)	9(3)
C19_1	23(4)	23(4)	8(3)	4(3)	4(3)	9(3)
C20_1	12(4)	22(5)	16(3)	1(3)	-2(2)	3(3)
C14_2	14.9(14)	13.7(15)	14.8(12)	1.5(11)	3.9(10)	1.5(9)
C15_2	17(2)	17.1(13)	18(3)	1(2)	-0.5(17)	-0.2(12)
C16_2	15(3)	20(3)	16(3)	3(2)	-2(2)	4(2)
C17_2	12(3)	15(3)	14(3)	4(2)	1(2)	4(2)

Atom	U_{11}	U_{22}	U_{33}	U_{23}	U_{13}	U_{12}
C18_2	23(3)	23(3)	30(4)	-3(3)	6(3)	10(3)
C19_2	14(3)	14(3)	12(3)	1(2)	-1(2)	5(2)
C20_2	10(3)	13(3)	14(2)	1(2)	2.9(19)	3(2)
C14_3	17.3(14)	17.0(17)	13.8(13)	0.8(16)	-2(1)	7.5(14)
C15_3	20(3)	23(2)	22.5(19)	0(3)	4.3(19)	10(2)
C16_3	19(5)	25(4)	20(4)	0(4)	2(4)	1(3)
C17_3	25(4)	24(4)	16(4)	2(3)	1(3)	13(3)
C18_3	27(5)	27(4)	38(5)	4(4)	13(4)	7(4)
C19_3	19.9(16)	22.9(19)	25.8(15)	2.5(14)	3.5(12)	10.4(15)
C20_3	15(4)	20(3)	25(4)	6(4)	-3(3)	9(3)
C14_4	17.3(14)	17.0(17)	13.8(13)	0.8(16)	-2(1)	7.5(14)
C15_4	20(3)	23(2)	22.5(19)	0(3)	4.3(19)	10(2)
C16_4	16(4)	16(3)	27(4)	0(3)	2(3)	6(3)
C17_4	17(3)	20(3)	21(4)	2(2)	-2(2)	10(2)
C18_4	24(5)	23(3)	38(5)	2(3)	6(3)	13(3)
C19_4	19.9(16)	22.9(19)	25.8(15)	2.5(14)	3.5(12)	10.4(15)
C20_4	16(3)	25(3)	23(4)	3(3)	3(2)	9(2)
C14_5	14.6(13)	11.0(12)	15.4(13)	1.6(10)	2.8(10)	-1.3(10)
C15_5	23.0(15)	18.3(14)	18.1(14)	-2.4(11)	-3.9(11)	2.1(12)
C16_5	20.0(15)	20.1(15)	31.7(17)	-0.6(12)	-4.7(12)	6.8(12)
C17_5	19.3(14)	11.6(13)	28.1(15)	1.1(11)	6.3(12)	2.0(11)
C18_5	29.4(17)	19.5(15)	38.8(19)	-3.1(13)	7.1(14)	8.3(13)
C19_5	19.3(14)	15.1(13)	14.9(13)	-0.7(10)	1.6(11)	0.5(11)
C20_5	13.1(12)	16.1(13)	15.1(13)	3.1(10)	1.2(10)	2.4(10)
C14_6	25.4(16)	18.9(15)	32.4(17)	5.1(12)	-10.5(13)	8.4(12)
C15_6	33.1(19)	21.6(16)	47(2)	9.0(14)	-5.1(16)	10.6(14)
C16_6	33.8(19)	18.3(16)	63(2)	9.2(15)	-7.3(17)	8.2(14)
C17_6	34.0(18)	18.6(15)	55(2)	1.0(14)	-18.7(16)	12.5(13)
C18_6	52(3)	18.5(17)	75(3)	-3.0(18)	-19(2)	14.6(17)
C19_6	36.0(19)	28.7(17)	43(2)	-3.2(14)	-16.1(15)	19.3(15)
C20_6	29.8(17)	24.7(16)	36.4(19)	4.5(13)	-11.0(14)	10.5(13)

Table 3: Bond Lengths in Å for **CMW04_BuTsNH2OH**.

Atom	Atom	Length/Å
Zn1	N2	2.078(2)
Zn1	N1	2.247(2)
Zn1	N3	2.044(2)
Zn1	N5	2.111(2)
Zn1	N4	2.106(2)
S1	O1	1.449(2)
S1	O2	1.452(2)
S1	N4	1.570(2)
S1	C7	1.778(3)
S2	O3	1.443(2)
S2	O4	1.455(2)
S2	N3	1.576(2)
S2	C14_5	1.777(2)
S3	O5	1.448(3)
S3	O6	1.449(2)
S3	N2	1.571(2)
S3	C14_6	1.786(2)
O7	N5	1.440(3)
N2	C6	1.476(4)
N1	C1	1.473(3)
N1	C3	1.474(3)
N1	C5	1.474(3)
N3	C4	1.473(3)
N4	C2	1.478(3)
C7	C8	1.393(4)
C7	C12	1.394(4)
C8	C9	1.379(4)
C12	C11	1.390(4)
C1	C2	1.523(4)
C3	C4	1.515(4)
C10	C11	1.390(4)
C10	C13	1.509(4)
C10	C9	1.393(4)
C6	C5	1.513(4)
Zn1B	N1B	2.288(2)
Zn1B	N2BA	2.011(11)
Zn1B	N2BB	2.119(11)
Zn1B	N3B	2.095(2)
Zn1B	N4B	2.036(2)
Zn1B	N5B	2.130(2)
S1B	O1B	1.447(2)
S1B	O2B	1.446(2)
S1B	N3B	1.566(3)

Atom	Atom	Length/Å
S1B	C7B	1.778(3)
S2B	O3B	1.440(2)
S2B	O4B	1.448(2)
S2B	N4B	1.567(2)
S2B	C14_1	1.861(4)
S2B	C14_2	1.696(4)
S3BA	O5BA	1.38(2)
S3BA	O6BA	1.431(17)
S3BA	N2BA	1.576(3)
S3BA	C14_3	1.784(3)
S3BB	O5BB	1.53(2)
S3BB	O6BB	1.459(17)
S3BB	N2BB	1.577(3)
S3BB	C14_4	1.785(3)
O7B	N5B	1.440(3)
N1B	C3B	1.478(4)
N1B	C5B	1.467(4)
N1B	C1B	1.474(4)
N2BA	C2B	1.499(13)
N2BB	C2B	1.475(13)
N3B	C4B	1.484(4)
N4B	C6B	1.479(3)
C2B	C1B	1.512(5)
C3B	C4B	1.525(4)
C5B	C6B	1.519(4)
C7B	C8B	1.398(4)
C7B	C12B	1.386(4)
C8B	C9B	1.381(4)
C9B	C10B	1.396(4)
C10B	C11B	1.391(4)
C10B	C13B	1.514(4)
C11B	C12B	1.388(4)
N7	C28	1.527(4)
N7	C32	1.519(3)
N7	C36	1.523(4)
N7	C40	1.526(3)
C28	C29	1.534(4)
C29	C30	1.522(4)
C30	C31	1.483(5)
C32	C33	1.514(4)
C33	C34	1.519(4)
C34	C35	1.510(5)
C36	C37	1.518(4)
C37	C38	1.532(4)
C38	C39	1.517(5)
C40	C41	1.523(4)
C41	C42	1.524(4)
C42	C43	1.527(4)
N7A	C21A	1.509(6)
N7A	C25A	1.518(5)
N7A	C29A	1.522(6)
N7A	C33A	1.541(4)
C21A	C22A	1.493(6)
C22A	C23A	1.508(6)
C23A	C24A	1.488(6)
C25A	C26A	1.526(5)
C26A	C27A	1.522(6)

Atom	Atom	Length/Å
C27A	C28A	1.518(8)
C29A	C30A	1.515(3)
C30A	C31A	1.531(8)
C31A	C32A	1.506(7)
C33A	C34A	1.516(5)
C34A	C35A	1.535(4)
C35A	C36A	1.510(7)
N7B	C21B	1.504(6)
N7B	C25B	1.520(5)
N7B	C29B	1.522(6)
N7B	C33B	1.543(4)
C21B	C22B	1.491(6)
C22B	C23B	1.510(6)
C23B	C24B	1.488(6)
C25B	C26B	1.527(5)
C26B	C27B	1.520(6)
C27B	C28B	1.518(8)
C29B	C30B	1.514(3)
C30B	C31B	1.531(8)
C31B	C32B	1.506(7)
C33B	C34B	1.516(5)
C34B	C35B	1.534(4)
C35B	C36B	1.510(7)
C14_1	C15_1	1.386(3)
C14_1	C20_1	1.390(3)
C15_1	C16_1	1.387(3)
C16_1	C17_1	1.392(3)
C17_1	C18_1	1.510(3)
C17_1	C19_1	1.390(3)
C19_1	C20_1	1.389(3)
C14_2	C15_2	1.386(3)
C14_2	C20_2	1.390(3)
C15_2	C16_2	1.387(3)
C16_2	C17_2	1.391(3)
C17_2	C18_2	1.509(3)
C17_2	C19_2	1.390(3)
C19_2	C20_2	1.388(3)
C14_3	C15_3	1.386(3)
C14_3	C20_3	1.390(3)
C15_3	C16_3	1.387(3)
C16_3	C17_3	1.392(3)
C17_3	C18_3	1.510(3)
C17_3	C19_3	1.390(3)
C19_3	C20_3	1.388(3)
C14_4	C15_4	1.386(3)
C14_4	C20_4	1.390(3)
C15_4	C16_4	1.387(3)
C16_4	C17_4	1.392(3)
C17_4	C18_4	1.509(3)
C17_4	C19_4	1.390(3)
C19_4	C20_4	1.389(3)
C14_5	C15_5	1.386(2)
C14_5	C20_5	1.389(2)
C15_5	C16_5	1.387(3)
C16_5	C17_5	1.391(3)
C17_5	C18_5	1.510(3)
C17_5	C19_5	1.390(3)

Atom	Atom	Length/Å
C19_5	C20_5	1.388(3)
C14_6	C15_6	1.385(3)
C14_6	C20_6	1.390(2)
C15_6	C16_6	1.388(3)
C16_6	C17_6	1.391(3)
C17_6	C18_6	1.510(3)
C17_6	C19_6	1.390(3)
C19_6	C20_6	1.389(3)

Table 4: Bond Angles in ° for **CMW04_BuTsNH2OH**.

Atom	Atom	Atom	Angle/°
N2	Zn1	N1	80.13(9)
N2	Zn1	N5	97.43(10)
N2	Zn1	N4	117.83(9)
N3	Zn1	N2	116.20(10)
N3	Zn1	N1	81.19(8)
N3	Zn1	N5	112.22(9)
N3	Zn1	N4	117.90(9)
N5	Zn1	N1	165.67(9)
N4	Zn1	N1	80.07(8)
N4	Zn1	N5	88.79(9)
O1	S1	O2	115.95(13)
O1	S1	N4	108.70(13)
O1	S1	C7	106.96(13)
O2	S1	N4	112.45(12)
O2	S1	C7	104.84(13)
N4	S1	C7	107.42(13)
O3	S2	O4	115.56(14)
O3	S2	N3	113.85(13)
O3	S2	C14_5	105.15(11)
O4	S2	N3	108.69(12)
O4	S2	C14_5	105.56(12)
N3	S2	C14_5	107.32(13)
O5	S3	O6	116.17(15)
O5	S3	N2	108.92(13)
O5	S3	C14_6	105.66(13)
O6	S3	N2	112.20(14)
O6	S3	C14_6	104.75(13)
N2	S3	C14_6	108.62(14)
S3	N2	Zn1	128.44(14)
C6	N2	Zn1	112.08(17)
C6	N2	S3	114.71(19)
C1	N1	Zn1	107.89(16)
C1	N1	C3	112.6(2)
C1	N1	C5	111.8(2)
C3	N1	Zn1	105.85(15)
C5	N1	Zn1	106.62(16)
C5	N1	C3	111.7(2)
S2	N3	Zn1	131.06(13)
C4	N3	Zn1	112.49(16)
C4	N3	S2	113.42(17)
O7	N5	Zn1	127.36(18)
S1	N4	Zn1	129.04(13)
C2	N4	Zn1	110.69(16)
C2	N4	S1	114.48(18)
C8	C7	S1	119.9(2)
C8	C7	C12	119.6(3)
C12	C7	S1	120.2(2)
C9	C8	C7	120.0(3)
C11	C12	C7	119.4(3)
N1	C1	C2	109.5(2)
N4	C2	C1	109.5(2)
N1	C3	C4	111.3(2)
C11	C10	C13	120.4(3)
C11	C10	C9	118.0(3)
C9	C10	C13	121.6(3)
N3	C4	C3	109.1(2)
C12	C11	C10	121.6(3)
N2	C6	C5	108.2(2)
N1	C5	C6	110.6(2)
C8	C9	C10	121.5(3)
N2BA	Zn1B	N1B	78.4(3)
N2BA	Zn1B	N3B	113.1(3)
N2BA	Zn1B	N4B	120.3(3)
N2BA	Zn1B	N5B	98.4(3)
N2BB	Zn1B	N1B	81.3(3)
N2BB	Zn1B	N5B	97.2(3)
N3B	Zn1B	N1B	79.57(9)
N3B	Zn1B	N2BB	120.6(3)
N3B	Zn1B	N5B	90.22(10)
N4B	Zn1B	N1B	80.14(9)
N4B	Zn1B	N2BB	114.5(3)
N4B	Zn1B	N3B	116.65(9)
N4B	Zn1B	N5B	112.05(10)
N5B	Zn1B	N1B	166.89(9)
O1B	S1B	N3B	108.33(13)
O1B	S1B	C7B	106.16(13)
O2B	S1B	O1B	116.00(13)
O2B	S1B	N3B	112.72(13)
O2B	S1B	C7B	105.20(14)
N3B	S1B	C7B	107.90(14)
O3B	S2B	O4B	115.71(15)
O3B	S2B	N4B	113.71(13)
O3B	S2B	C14_1	107.4(2)
O3B	S2B	C14_2	102.9(3)
O4B	S2B	N4B	109.11(12)
O4B	S2B	C14_1	103.0(4)
O4B	S2B	C14_2	107.0(4)
N4B	S2B	C14_1	106.9(4)
N4B	S2B	C14_2	107.7(5)
O5BA	S3BA	O6BA	113.8(11)
O5BA	S3BA	N2BA	109.8(11)
O5BA	S3BA	C14_3	106.2(9)
O6BA	S3BA	N2BA	112.7(9)

Atom	Atom	Atom	Angle/°
O6BA	S3BA	C14_3	105.8(7)
N2BA	S3BA	C14_3	108.1(6)
O5BB	S3BB	N2BB	107.8(10)
O5BB	S3BB	C14_4	105.4(8)
O6BB	S3BB	O5BB	118.4(10)
O6BB	S3BB	N2BB	111.2(9)
O6BB	S3BB	C14_4	104.6(6)
N2BB	S3BB	C14_4	109.0(6)
C3B	N1B	Zn1B	107.45(17)
C5B	N1B	Zn1B	105.96(16)
C5B	N1B	C3B	112.5(2)
C5B	N1B	C1B	112.0(2)
C1B	N1B	Zn1B	106.10(17)
C1B	N1B	C3B	112.3(2)
S3BA	N2BA	Zn1B	128.4(8)
C2B	N2BA	Zn1B	113.9(5)
C2B	N2BA	S3BA	109.3(8)
S3BB	N2BB	Zn1B	128.4(8)
C2B	N2BB	Zn1B	109.3(4)
C2B	N2BB	S3BB	120.5(9)
S1B	N3B	Zn1B	129.11(13)
C4B	N3B	Zn1B	111.52(19)
C4B	N3B	S1B	114.4(2)
S2B	N4B	Zn1B	130.65(14)
C6B	N4B	Zn1B	113.52(17)
C6B	N4B	S2B	113.51(18)
O7B	N5B	Zn1B	128.28(17)
N2BA	C2B	C1B	103.5(4)
N2BB	C2B	C1B	113.7(4)
N1B	C3B	C4B	109.5(2)
N3B	C4B	C3B	109.5(2)
N1B	C5B	C6B	111.0(2)
N1B	C1B	C2B	110.4(2)
N4B	C6B	C5B	108.8(2)
C8B	C7B	S1B	119.3(2)
C12B	C7B	S1B	120.7(2)
C12B	C7B	C8B	119.9(3)
C9B	C8B	C7B	119.7(3)
C8B	C9B	C10B	121.4(3)
C9B	C10B	C13B	121.4(3)
C11B	C10B	C9B	117.9(3)
C11B	C10B	C13B	120.7(3)
C12B	C11B	C10B	121.5(3)
C7B	C12B	C11B	119.6(3)
C32	N7	C28	108.3(2)
C32	N7	C36	108.9(2)
C32	N7	C40	112.0(2)
C36	N7	C28	111.3(2)
C36	N7	C40	107.6(2)
C40	N7	C28	108.7(2)
N7	C28	C29	115.3(2)
C30	C29	C28	110.7(3)
C31	C30	C29	113.0(3)
C33	C32	N7	115.0(2)
C32	C33	C34	111.1(2)
C35	C34	C33	111.8(3)
C37	C36	N7	115.1(2)

Atom	Atom	Atom	Angle/°
C36	C37	C38	110.9(2)
C39	C38	C37	114.4(3)
C41	C40	N7	116.6(2)
C40	C41	C42	108.1(2)
C41	C42	C43	113.0(3)
C21A	N7A	C25A	109.8(3)
C21A	N7A	C29A	110.3(3)
C21A	N7A	C33A	108.3(3)
C25A	N7A	C29A	110.5(3)
C25A	N7A	C33A	109.8(3)
C29A	N7A	C33A	108.1(3)
C22A	C21A	N7A	117.3(3)
C21A	C22A	C23A	109.6(4)
C24A	C23A	C22A	114.7(4)
N7A	C25A	C26A	115.2(3)
C27A	C26A	C25A	110.7(4)
C28A	C27A	C26A	114.3(5)
C30A	C29A	N7A	117.5(3)
C29A	C30A	C31A	109.9(4)
C32A	C31A	C30A	112.0(6)
C34A	C33A	N7A	114.6(3)
C33A	C34A	C35A	111.6(3)
C36A	C35A	C34A	110.1(3)
C21B	N7B	C25B	110.0(3)
C21B	N7B	C29B	110.7(3)
C21B	N7B	C33B	108.2(3)
C25B	N7B	C29B	110.1(3)
C25B	N7B	C33B	109.6(3)
C29B	N7B	C33B	108.1(3)
C22B	C21B	N7B	118.1(3)
C21B	C22B	C23B	109.5(4)
C24B	C23B	C22B	114.7(4)
N7B	C25B	C26B	114.9(3)
C27B	C26B	C25B	110.9(4)
C28B	C27B	C26B	114.4(5)
C30B	C29B	N7B	117.7(3)
C29B	C30B	C31B	110.0(4)
C32B	C31B	C30B	112.0(6)
C34B	C33B	N7B	114.4(3)
C33B	C34B	C35B	111.6(3)
C36B	C35B	C34B	110.2(3)
C15_1	C14_1	S2B	117.4(4)
C15_1	C14_1	C20_1	119.77(19)
C20_1	C14_1	S2B	122.7(4)
C14_1	C15_1	C16_1	119.73(19)
C15_1	C16_1	C17_1	121.1(2)
C16_1	C17_1	C18_1	120.6(2)
C19_1	C17_1	C16_1	118.57(19)
C19_1	C17_1	C18_1	120.8(2)
C20_1	C19_1	C17_1	120.7(2)
C19_1	C20_1	C14_1	120.0(2)
C15_2	C14_2	S2B	121.0(4)
C15_2	C14_2	C20_2	119.77(19)
C20_2	C14_2	S2B	119.2(4)
C14_2	C15_2	C16_2	119.70(19)
C15_2	C16_2	C17_2	121.2(2)
C16_2	C17_2	C18_2	120.7(2)

Atom	Atom	Atom	Angle/°
C19_2	C17_2	C16_2	118.56(19)
C19_2	C17_2	C18_2	120.7(2)
C20_2	C19_2	C17_2	120.6(2)
C19_2	C20_2	C14_2	120.1(2)
C15_3	C14_3	S3BA	121.4(5)
C15_3	C14_3	C20_3	119.77(19)
C20_3	C14_3	S3BA	118.8(5)
C14_3	C15_3	C16_3	119.74(19)
C15_3	C16_3	C17_3	121.2(2)
C16_3	C17_3	C18_3	120.7(2)
C19_3	C17_3	C16_3	118.53(19)
C19_3	C17_3	C18_3	120.7(2)
C20_3	C19_3	C17_3	120.7(2)
C19_3	C20_3	C14_3	120.1(2)
C15_4	C14_4	S3BB	121.3(5)
C15_4	C14_4	C20_4	119.74(19)
C20_4	C14_4	S3BB	118.9(5)
C14_4	C15_4	C16_4	119.7(2)
C15_4	C16_4	C17_4	121.1(2)
C16_4	C17_4	C18_4	120.7(2)
C19_4	C17_4	C16_4	118.5(2)
C19_4	C17_4	C18_4	120.7(2)
C20_4	C19_4	C17_4	120.6(2)
C19_4	C20_4	C14_4	120.0(2)
C15_5	C14_5	S2	120.09(15)
C15_5	C14_5	C20_5	119.82(17)
C20_5	C14_5	S2	120.09(16)
C14_5	C15_5	C16_5	119.66(18)
C15_5	C16_5	C17_5	121.2(2)
C16_5	C17_5	C18_5	120.8(2)
C19_5	C17_5	C16_5	118.58(18)
C19_5	C17_5	C18_5	120.63(19)
C20_5	C19_5	C17_5	120.64(18)
C19_5	C20_5	C14_5	120.10(19)
C15_6	C14_6	S3	120.39(17)
C15_6	C14_6	C20_6	119.77(18)
C20_6	C14_6	S3	119.83(18)
C14_6	C15_6	C16_6	119.74(19)
C15_6	C16_6	C17_6	121.1(2)
C16_6	C17_6	C18_6	120.6(2)
C19_6	C17_6	C16_6	118.57(18)
C19_6	C17_6	C18_6	120.8(2)
C20_6	C19_6	C17_6	120.70(19)
C19_6	C20_6	C14_6	120.0(2)

Table 5: Hydrogen Fractional Atomic Coordinates ($\times 10^4$) and Equivalent Isotropic Displacement Parameters ($Å^2 \times 10^3$) for **CMW04_BuTsNH2OH**. U_{eq} is defined as 1/3 of the trace of the orthogonalised U_{ij}.

Atom	x	y	z	U_{eq}
H7	4468	4245	3050	53
H5A	6025	5454	3557	27
H5B	5073	5606	3249	27
H8	3378	5289	1412	24
H12	4132	7594	1289	28
H1A	5792	6541	951	18
H1B	7029	7101	1050	18
H2A	7111	7364	2212	17
H2B	6090	7519	1796	17
H3A	6927	5155	948	18
H3B	6520	5704	451	18
H4A	4816	5215	714	19
H4B	5111	4486	527	19
H11	3297	7362	142	31
H6A	8091	5254	1892	26
H6B	9028	5947	2376	26
H13D	2028	6463	-786	43
H13E	1728	5554	-743	43
H13F	2851	6072	-933	43
H5C	8252	6832	1968	21
H5D	8368	6379	1319	21
H9	2520	5071	278	27
H7B	-675	9005	3002	38
H5BA	777	10213	3573	24
H5BB	-160	10373	3246	24
H2BA	2956	10108	1987	33
H2BB	3922	10771	2488	33

Atom	x	y	z	U_{eq}
H2BC	3036	10138	1963	33
H2BD	3920	10800	2496	33
H3BA	826	11498	1021	27
H3BB	2070	12052	1175	27
H4BA	2046	12230	2334	26
H4BB	1060	12416	1906	26
H5BC	1926	10097	987	27
H5BD	1577	10686	511	27
H1BA	3221	11712	2089	31
H1BB	3379	11279	1443	31
H6BA	-166	10197	723	25
H6BB	114	9470	508	25
H8B	-1693	10197	1393	28
H9B	-2538	10036	255	29
H11B	-1719	12343	213	25
H12B	-895	12514	1359	25
H13A	-2198	11154	-914	43
H13B	-3095	11448	-727	43
H13C	-3283	10548	-742	43
H28A	4785	918	6094	24
H28B	4840	1762	6308	24
H29A	4123	1100	4925	31
H29B	4326	1974	5166	31
H30A	5858	2105	4802	41
H30B	6209	2096	5608	41
H31A	5643	817	4652	57
H31B	5943	783	5458	57
H31C	6833	1302	5059	57
H32A	2762	237	5212	20
H32B	3171	-149	5860	20
H33A	1144	40	5576	22
H33B	1558	-294	6260	22
H34A	1195	-1017	4921	31
H34B	1596	-1352	5607	31
H35A	-271	-1995	5211	50
H35B	-445	-1193	5281	50
H35C	-45	-1559	5947	50
H36A	2595	1474	5330	22
H36B	1925	1240	5925	22
H37A	3870	2553	6020	27
H37B	3248	2310	6639	27
H38A	2863	3312	5965	30
H38B	2212	2645	5369	30
H39A	1027	2882	5987	46
H39B	1645	2675	6672	46
H39C	988	2018	6067	46
H40A	3746	1433	7085	19
H40B	2557	801	6925	19
H41A	4361	333	7030	22
H41B	3158	-197	7091	22
H42A	3365	592	8112	29
H42B	4594	1044	8063	29
H43A	4934	-119	8225	43
H43B	3711	-555	8296	43
H43C	4508	114	8858	43
H21A	1954	5062	3321	24
H21B	2652	4548	3238	24

Atom	x	y	z	U_{eq}
H22A	440	4138	2653	44
H22B	1099	3584	2596	44
H23A	1721	5092	2123	46
H23B	2243	4469	2003	46
H24A	1174	4457	1002	66
H24B	200	4434	1359	66
H24C	523	3690	1324	66
H25A	3274	4660	4430	26
H25B	2468	4344	4942	26
H26A	2415	5664	4263	31
H26B	2115	5433	4990	31
H27A	3731	6446	5231	31
H27B	4003	5698	5427	31
H28C	4354	6439	4204	55
H28D	4621	5688	4396	55
H28E	5281	6491	4841	55
H29C	608	4685	4039	33
H29D	51	3841	3657	33
H30C	764	4151	5097	33
H30D	233	3299	4720	33
H31D	-841	4379	4730	42
H31E	-1370	3570	4279	42
H32C	-2053	3429	5273	73
H32D	-866	3745	5729	73
H32E	-1309	2926	5299	73
H33C	1532	3109	4321	20
H33D	1021	3031	3528	20
H34C	3292	3635	4001	25
H34D	2675	3358	3229	25
H35D	2593	2318	4293	24
H35E	2033	2053	3509	24
H36C	3730	2483	3199	40
H36D	3695	1873	3761	40
H36E	4302	2776	3975	40
H21C	1814	3834	2791	34
H21D	625	3608	2930	34
H22C	1976	5126	2745	29
H22D	783	4903	2891	29
H23C	1292	4311	1729	34
H23D	102	4059	1878	34
H24D	318	4940	1062	43
H24E	1328	5554	1564	43
H24F	149	5318	1733	43
H25C	2724	5260	3817	24
H25D	3339	4706	3667	24
H26C	2987	5080	4972	31
H26D	3418	4401	4854	31
H27C	4902	5507	5274	34
H27D	4941	5308	4503	34
H28F	4404	6306	4134	69
H28G	5359	6657	4782	69
H28H	4137	6449	4860	69
H29E	1376	4454	4629	33
H29F	713	4609	3941	33
H30E	258	3128	4463	33
H30F	-420	3299	3783	33
H31F	-210	4046	5092	28

Atom	x	y	z	U_{eq}
H31G	-995	4093	4409	28
H32F	-2057	2793	4414	46
H32G	-1945	3227	5135	46
H32H	-1245	2706	5066	46
H33E	2057	3354	4483	20
H33F	1283	2911	3788	20
H34E	3569	3624	4008	25
H34F	2854	3335	3259	25
H35F	2850	2312	4330	24
H35G	2243	2045	3554	24
H36F	3964	2527	3223	31
H36G	3837	1820	3692	31
H36H	4517	2685	4013	31
H15_1	744	8152	1921	23
H16_1	1204	7145	1549	24
H18A_1	967	6117	773	47
H18B_1	584	6232	-9	47
H18C_1	-262	5687	406	47
H19_1	-1019	6773	-183	21
H20_1	-1484	7780	185	22
H15_2	697	8112	1811	23
H16_2	1034	7133	1272	22
H18A_2	797	6315	273	37
H18B_2	-17	6336	-405	37
H18C_2	-454	5798	177	37
H19_2	-1299	7004	-344	17
H20_2	-1645	7981	194	15
H15_3	1156	8813	3631	26
H16_3	765	7499	3410	29
H18A_3	2212	6593	3244	46
H18B_3	2037	6649	2437	46
H18C_3	1040	6461	2814	46
H19_3	3389	7980	2558	27
H20_3	3777	9297	2768	24
H15_4	1011	8707	3638	26
H16_4	547	7377	3462	24
H18A_4	1154	6303	3316	41
H18B_4	2206	6440	3004	41
H18C_4	1096	6357	2514	41
H19_4	3136	7724	2603	27
H20_4	3645	9055	2816	25
H15_5	5725	3174	1888	27
H16_5	6041	2158	1394	30
H18A_5	5799	1305	409	44
H18B_5	4930	1268	-259	44
H18C_5	4560	779	366	44
H19_5	3650	1935	-212	22
H20_5	3320	2946	282	19
H15_6	6295	3940	3603	43
H16_6	5861	2611	3454	49
H18A_6	6756	1585	3345	78
H18B_6	7386	1688	2728	78
H18C_6	6128	1540	2579	78
H19_6	8323	2959	2469	44
H20_6	8785	4291	2638	39

2-1(H_2O_2)/2-1(OH_2)

EMORY UNIVERSITY | X-ray Crystallography Center

Submitted by: **Christian Wallen**
Emory University
Solved by: **John Bacsa**
Sample ID: **1-H2O2**

Crystal Data and Experimental

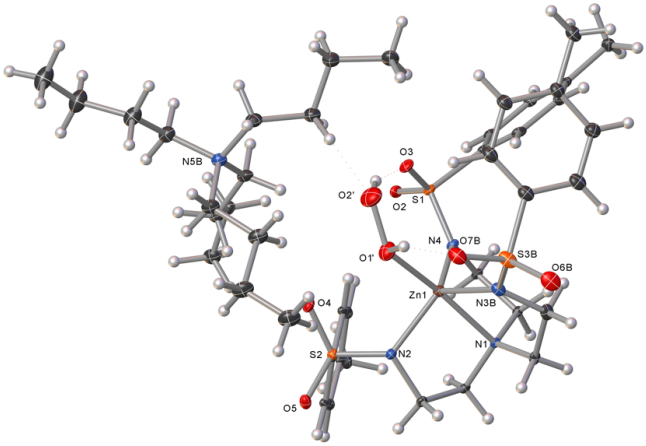

Experimental. Single colourless prism-shaped crystals of (**CMW04-BuZnTsO2H2xtal2**) were recrystallised from a mixture of diethyl ether and THF by vapor diffusion. A suitable crystal (0.78×0.44×0.40 mm) was selected and mounted on a loop with paratone oil on a Bruker APEX-II CCD diffractometer. The crystal was cooled to T = 100(2) K during data collection. The structure was solved with the **ShelXT**[2e] structure solution program using combined Patterson and dual-space recycling methods and by using **Olex2**[2c] as the graphical interface. The crystal structure was refined with version of **ShelXL**[2b] using Least Squares minimisation.

Crystal Data. $C_{86}H_{142}N_{10}O_{15}S_6Zn_2$, M_r = 1879.19, triclinic, P-1 (No. 2), a = 9.3583(12) Å, b = 13.4896(18) Å, c = 19.634(3) Å, α = 92.9514(19)°, β = 97.9613(18)°, γ = 109.1389(19)°, V = 2306.5(5) Å^3, T = 100(2) K, Z = 1, Z' = 0.5, μ(MoK$_\alpha$) = 0.723, 30794 reflections measured, 14175 unique (R_{int} = 0.0408) which were used in all calculations. The final wR_2 was 0.2157 (all data) and R_1 was 0.0864 (I > 2(I)).

Compound	**CMW04-BuZnTsO2H2xtal2**
Formula	$C_{86}H_{142}N_{10}O_{15}S_6Zn_2$
$D_{calc.}$/ g cm^{-3}	1.353
μ/mm^{-1}	0.723
Formula Weight	1879.19
Colour	colourless
Shape	prism
Max Size/mm	0.78
Mid Size/mm	0.44
Min Size/mm	0.40
T/K	100(2)
Crystal System	triclinic
Space Group	P-1
a/Å	9.3583(12)
b/Å	13.4896(18)
c/Å	19.634(3)
α/°	92.9514(19)
β/°	97.9613(18)
γ/°	109.1389(19)
V/Å^3	2306.5(5)
Z	1
Z'	0.5
Θ_{min}/°	1.827
Θ_{max}/°	31.162
Measured Refl.	30794
Independent Refl.	14175
$I > 2\sigma(I)$	10044
R_{int}	0.0408
Parameters	662
Restraints	495
Largest Peak	2.569
Deepest Hole	-1.172
GooF	1.066
wR_2 (all data)	0.2157
wR_2	0.1938
R_1 (all data)	0.1204
R_1	0.0864
CCDC number	1429663

Structure Quality Indicators

Reflections:	d min	0.69	I/σ	9.3	Rint	4.08%	complete	95%
Refinement:	Shift	0.001	Max Peak	2.6	Min Peak	-1.2	GooF	1.066

A colourless prism-shaped crystal with dimensions 0.78×0.44×0.40 mm was mounted on a loop with paratone oil. X-ray diffraction data were collected using a Bruker APEX-II CCD diffractometer equipped with an Oxford Cryosystems low-temperature apparatus operating at T = 100(2) K.

Data were measured using ϕ and ω scans with MoK$_\alpha$ radiation (fine-focus sealed tube, 45 kV, 35 mA). The total number of runs and images was based on the strategy calculation from the program **APEX2** (Bruker)[2a]. The maximum resolution achieved was Θ = 31.162°.

Unit cell indexing was performed by using the **APEX2** (Bruker)[2a] software and refined using **SAINT** (Bruker)[2d] on 9973 reflections, 32 percent of the observed reflections. Data reduction, scaling and absorption corrections were performed using **SAINT** (Bruker)[2d] and SADABS-2014/5 (Bruker)[2a,d] was used for absorption correction. wR_2(int) was 0.1252 before and 0.0520 after correction. The Ratio of minimum to maximum transmission is 0.8144.The $\lambda/2$ correction factor is 0.00150. The software also corrects for Lorentz polarisation. The final completeness is 99.70 out to 31.162 in Θ. The absorption coefficient (μ) of this material is 0.723 mm and the minimum and maximum transmissions are 0.6077 and 0.7462.

The structure was solved in the space group P1 with the **ShelXT**[2e] structure solution program using combined Patterson and dual-space recycling methods. The space group P-1 (# 2) was determined by **ShelXT**[2e] structure solution program. The crystal structure was refined by Least Squares using version 2014/7 of **ShelXL**.[2b] All non-hydrogen atoms were refined anisotropically. Hydrogen atom positions were calculated geometrically and refined using the riding model.

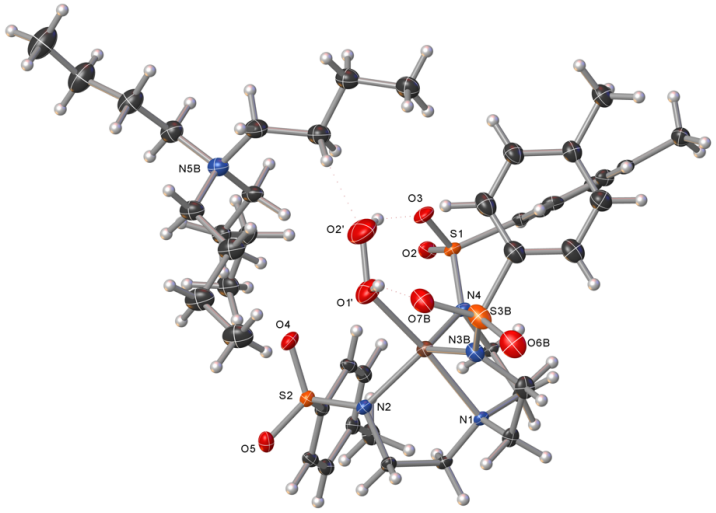

Figure 1: Plot of **1-H$_2$O$_2$**, one of the two disorder components of **1-H$_2$O$_2$/1-OH$_2$**.

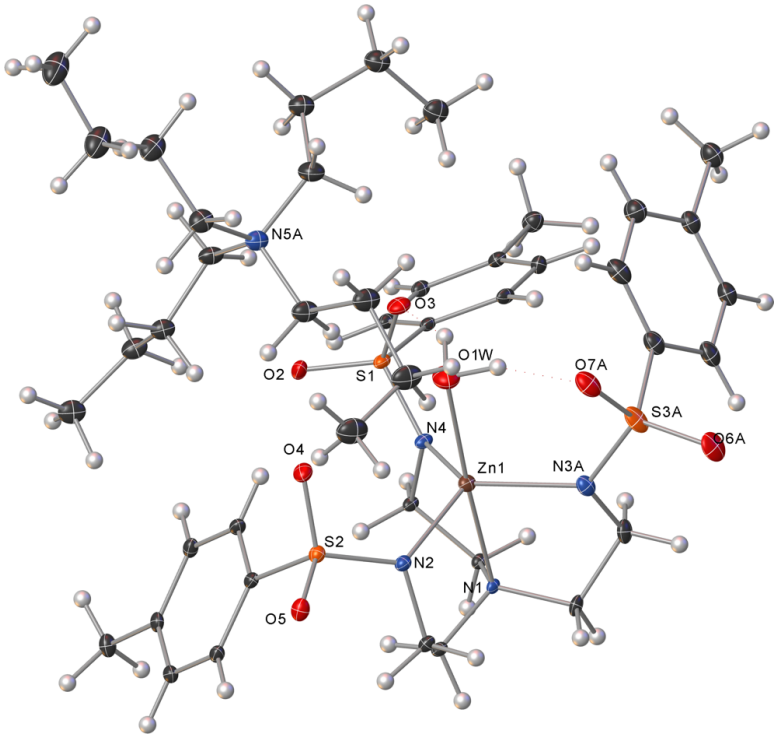

Figure 2: Plot of **1-OH$_2$**, one of the two disorder components of **1-H$_2$O$_2$/1-OH$_2$**.

Data Plots: Diffraction Data

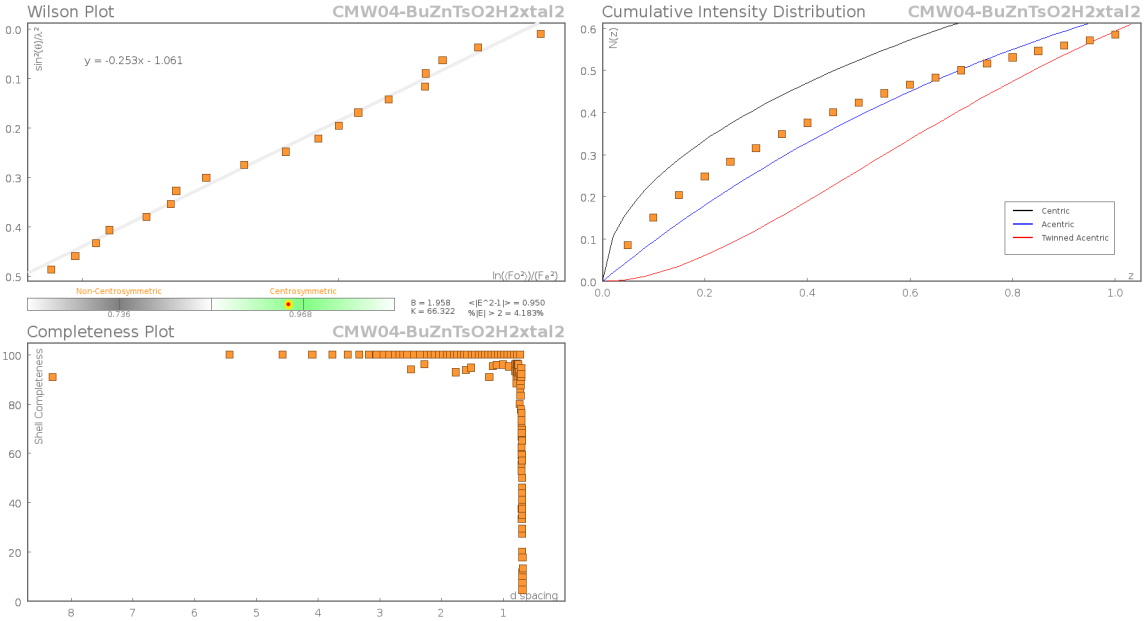

Data Plots: Refinement and Data

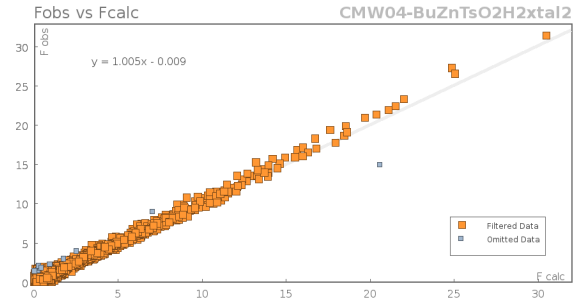

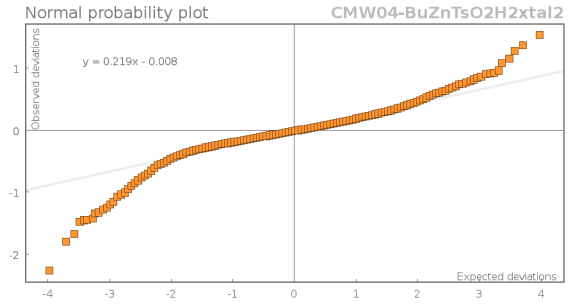

Reflection Statistics

Total reflections (after filtering)	30830	Unique reflections	14175
Completeness	0.95	Mean I/σ	9.34
hklsub>max</sub> collected	(13, 19, 27)	hklsub>min</sub> collected	(-13, -19, -28)
hkl_{max} used	(13, 19, 28)	hkl_{min} used	(-13, -19, 0)
Lim d_{max} collected	100.0	Lim d_{min} collected	0.36
d_{max} used	12.68	d_{min} used	0.69
Friedel pairs	9608	Friedel pairs merged	1
Inconsistent equivalents	0	R_{int}	0.0408
R_{sigma}	0.0668	Intensity transformed	0
Omitted reflections	0	Omitted by user (OMIT hkl)	36
Multiplicity	(17230, 6098, 468)	Maximum multiplicity	6
Removed systematic absences	0	Filtered off (Shel/OMIT)	0

Images of the Crystal on the Diffractometer

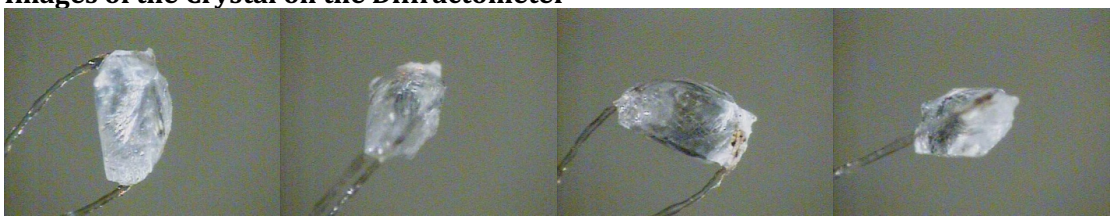

Table 1: Fractional Atomic Coordinates (×10⁴) and Equivalent Isotropic Displacement Parameters (Å²×10³) for **CMW04-BuZnTsO2H2xtal2**. U_{eq} is defined as 1/3 of the trace of the orthogonalised U_{ij}.

Atom	x	y	z	U_{eq}
Zn1	6405.9(5)	5378.5(4)	7333.4(2)	24.81(12)
S1	2987.3(10)	5218.5(8)	6548.5(5)	24.13(19)
S2	6038.7(11)	2908.5(7)	7380.4(5)	25.23(19)
N5A	1212(6)	2745(5)	8843(3)	38.3(9)
C28A	486(10)	2456(7)	8092(3)	39.8(12)
C29A	940(30)	1645(15)	7704(4)	38.6(12)
C30A	440(20)	1603(10)	6920(4)	43(2)
C31A	580(40)	640(20)	6539(6)	47(2)
C32A	584(7)	1828(7)	9255(4)	47.2(13)
C33A	-1083(8)	1458(9)	9326(6)	57.0(18)
C34A	-1475(15)	484(10)	9732(7)	70(2)
C35A	-3017(14)	154(12)	9899(7)	80(3)
C36A	2940(8)	3029(8)	8928(3)	46.6(13)
C37A	3849(9)	3552(9)	9621(4)	52.2(15)
C38A	5565(10)	3728(9)	9649(6)	61.5(19)

Atom	x	y	z	U_{eq}
C39A	5853(14)	2724(11)	9612(7)	68(2)
C40A	837(9)	3679(6)	9131(4)	50.8(11)
C41A	-522(8)	3999(6)	8879(5)	48.9(14)
C42A	-292(10)	5133(6)	9134(5)	50.3(16)
C43A	921(12)	5901(8)	8797(6)	50.7(17)
N5B	789(7)	2549(4)	8848(3)	38.3(9)
C28B	865(9)	2513(6)	8085(3)	39.8(12)
C29B	970(30)	1511(12)	7757(4)	38.6(12)
C30B	207(17)	1295(9)	6992(4)	43(2)
C31B	700(30)	490(20)	6607(6)	47(2)
C32B	-642(9)	1702(7)	8978(3)	47.2(13)
C33B	-957(12)	1555(9)	9702(4)	57.0(18)
C34B	-2307(16)	533(10)	9715(5)	70(2)
C35B	-2788(16)	383(12)	10386(6)	80(3)
C36B	2175(7)	2389(7)	9259(4)	46.6(13)
C37B	3724(7)	3170(7)	9217(5)	52.2(15)
C38B	5021(9)	2767(9)	9505(6)	61.5(19)
C39B	6529(11)	3542(11)	9480(7)	68(2)
C40B	717(10)	3617(5)	9096(4)	50.8(11)
C41B	1321(10)	4630(5)	8776(5)	48.9(14)
C42B	468(11)	5387(6)	8908(6)	50.3(16)
C43B	1323(12)	6481(6)	8722(6)	50.7(17)
S3A	7865(5)	7424(3)	8452(3)	47.6(5)
O6A	9322(9)	8191(6)	8765(4)	55.2(17)
O7A	7073(10)	6666(6)	8895(4)	50.8(15)
N3A	7979(10)	6781(5)	7775(4)	32.1(10)
C21A	6635(10)	8171(8)	8224(7)	43.5(11)
C22A	7190(13)	9081(11)	7906(10)	48.3(13)
C23A	6277(14)	9699(7)	7754(6)	43(2)
C24A	4834(11)	9436(7)	7923(6)	39.2(13)
C25A	4286(12)	8529(9)	8249(9)	47(2)
C26A	5218(16)	7919(15)	8411(16)	49.2(11)
C27A	3855(13)	10133(8)	7789(7)	48.4(19)
S3B	7995(5)	7618(3)	8406(3)	47.6(5)
O6B	9445(8)	8470(5)	8554(4)	55.2(17)
O7B	7564(9)	6964(6)	8964(4)	50.8(15)
N3B	7861(10)	6854(5)	7741(4)	32.1(10)
C21B	6569(9)	8235(8)	8251(6)	43.5(11)
C22B	6874(12)	9125(10)	7900(9)	48.3(13)
C23B	5794(13)	9630(8)	7791(6)	48(3)
C24B	4429(10)	9271(7)	8034(6)	39.2(13)
C25B	4084(11)	8339(9)	8346(7)	46(3)
C26B	5164(15)	7823(14)	8444(15)	49.2(11)
C27B	3275(12)	9848(8)	7949(6)	48.4(19)
O1'	5482(12)	5138(10)	8291(5)	61.9(18)
O2	1985(3)	4262(2)	6122.4(17)	33.2(6)
O2'	4054(11)	5199(9)	8457(4)	86(3)
O3	2717(4)	5323(3)	7255.3(16)	37.7(7)
O4	4779(3)	2904(2)	7731.7(16)	34.7(7)
O5	6945(3)	2268(2)	7629.1(16)	34.1(6)
N1	7821(3)	5723(2)	6500.0(15)	18.8(5)
N2	7067(3)	4086(2)	7351.2(16)	23.7(6)
N4	4747(3)	5412(3)	6561.4(15)	23.7(6)
C1	8189(4)	4760(3)	6334.0(19)	22.6(7)
C2	8404(4)	4234(3)	6994(2)	24.8(7)
C3	8784(5)	7405(3)	7246(2)	37.6(10)
C4	9197(4)	6629(3)	6788(2)	28.8(8)

Atom	x	y	z	U_{eq}
C5	6878(4)	5977(3)	5915.5(17)	20.2(6)
C6	5188(4)	5320(3)	5870.8(17)	20.3(6)
C7	2586(4)	6270(3)	6144.0(19)	22.3(7)
C8	1673(4)	6075(3)	5493.1(19)	24.7(7)
C9	1295(4)	6881(3)	5191(2)	27.2(8)
C10	1834(4)	7905(3)	5526(2)	28.3(8)
C11	2782(5)	8098(3)	6170(2)	31.2(8)
C12	3158(4)	7300(3)	6482(2)	28.8(8)
C13	1376(5)	8768(4)	5206(3)	39.4(10)
C14	5208(4)	2355(3)	6512(2)	23.0(7)
C15	3965(4)	2606(3)	6182(2)	27.1(8)
C16	3367(4)	2238(3)	5496(2)	28.7(8)
C17	3991(5)	1622(3)	5121(2)	27.3(8)
C18	5214(4)	1369(3)	5459(2)	28.2(8)
C19	5822(4)	1726(3)	6147(2)	26.2(7)
C20	3358(5)	1246(3)	4365(2)	36.0(9)
O1W	4978(11)	5137(11)	8143(5)	58.4(19)

Table 2: Anisotropic Displacement Parameters (×10^4) **CMW04-BuZnTsO2H2xtal2**. The anisotropic displacement factor exponent takes the form: $-2\pi^2[h^2a^{*2} \times U_{11} + \ldots + 2hka^* \times b^* \times U_{12}]$

Atom	U_{11}	U_{22}	U_{33}	U_{23}	U_{13}	U_{12}
Zn1	25.7(2)	30.4(2)	16.8(2)	0.45(16)	1.29(15)	8.65(17)
S1	18.2(4)	30.2(5)	22.6(4)	1.0(3)	6.1(3)	5.5(3)
S2	24.6(4)	25.3(4)	24.0(4)	4.1(3)	5.3(3)	5.3(3)
N5A	35.5(18)	50.3(18)	30.6(14)	3.1(12)	2.4(12)	17.8(14)
C28A	33(3)	58(2)	34.9(15)	6.7(13)	7.5(14)	22.1(18)
C29A	37(2)	51(3)	31.3(19)	12.0(19)	5.4(19)	20(3)
C30A	40(5)	60(6)	31(2)	15(2)	9(2)	18(5)
C31A	47(5)	69(6)	30(3)	11(4)	-2(3)	28(3)
C32A	48(2)	60(3)	33(3)	5(2)	4.4(19)	17(2)
C33A	53(3)	75(4)	32(3)	0(3)	5(3)	9(3)
C34A	68(4)	81(4)	40(3)	2(3)	6(3)	0(3)
C35A	77(5)	90(6)	45(4)	-3(4)	12(4)	-7(4)
C36A	40(2)	68(3)	34(3)	1(2)	0.5(16)	23.5(19)
C37A	43(2)	77(4)	34(3)	-3(3)	-3(2)	22(2)
C38A	44(3)	98(5)	41(4)	1(3)	-6(2)	28(3)
C39A	51(3)	100(5)	54(5)	-1(4)	-4(3)	32(3)
C40A	51(3)	60(2)	51(3)	5.9(17)	19(2)	25.5(19)
C41A	46(3)	59(3)	46(4)	5(2)	10(2)	23(2)
C42A	50(4)	59(3)	46(4)	2(3)	8(3)	24(3)
C43A	45(4)	61(4)	47(4)	4(3)	-2(3)	22(3)
N5B	35.5(18)	50.3(18)	30.6(14)	3.1(12)	2.4(12)	17.8(14)
C28B	33(3)	58(2)	34.9(15)	6.7(13)	7.5(14)	22.1(18)
C29B	37(2)	51(3)	31.3(19)	12.0(19)	5.4(19)	20(3)
C30B	40(5)	60(6)	31(2)	15(2)	9(2)	18(5)
C31B	47(5)	69(6)	30(3)	11(4)	-2(3)	28(3)
C32B	48(2)	60(3)	33(3)	5(2)	4.4(19)	17(2)
C33B	53(3)	75(4)	32(3)	0(3)	5(3)	9(3)
C34B	68(4)	81(4)	40(3)	2(3)	6(3)	0(3)
C35B	77(5)	90(6)	45(4)	-3(4)	12(4)	-7(4)
C36B	40(2)	68(3)	34(3)	1(2)	0.5(16)	23.5(19)
C37B	43(2)	77(4)	34(3)	-3(3)	-3(2)	22(2)
C38B	44(3)	98(5)	41(4)	1(3)	-6(2)	28(3)
C39B	51(3)	100(5)	54(5)	-1(4)	-4(3)	32(3)
C40B	51(3)	60(2)	51(3)	5.9(17)	19(2)	25.5(19)

Atom	U_{11}	U_{22}	U_{33}	U_{23}	U_{13}	U_{12}
C41B	46(3)	59(3)	46(4)	5(2)	10(2)	23(2)
C42B	50(4)	59(3)	46(4)	2(3)	8(3)	24(3)
C43B	45(4)	61(4)	47(4)	4(3)	-2(3)	22(3)
S3A	69.3(9)	50.4(12)	22.4(7)	-11.9(8)	-11.4(6)	29.1(9)
O6A	70(2)	60(3)	25(3)	-16(2)	-18(2)	21(2)
O7A	73(4)	54(3)	29(2)	-5(2)	-1(2)	31(3)
N3A	38.1(17)	33.3(15)	23.5(14)	-2.7(12)	-2.7(12)	14.1(13)
C21A	53.9(16)	39.7(16)	35.2(17)	-6.1(13)	-1.4(13)	18.6(13)
C22A	59(4)	38(2)	44(3)	-10.7(18)	-3(3)	18(2)
C23A	51(3)	32(3)	42(4)	-5(3)	3(3)	12(2)
C24A	47(2)	34(2)	34(2)	-2.3(16)	0.8(18)	12.8(18)
C25A	51(3)	44(3)	48(3)	6.0(18)	6.8(17)	17.0(18)
C26A	71(3)	43(3)	38(3)	0(2)	4(2)	28(2)
C27A	58(4)	41(3)	48(4)	2(3)	3(3)	21(3)
S3B	69.3(9)	50.4(12)	22.4(7)	-11.9(8)	-11.4(6)	29.1(9)
O6B	70(2)	60(3)	25(3)	-16(2)	-18(2)	21(2)
O7B	73(4)	54(3)	29(2)	-5(2)	-1(2)	31(3)
N3B	38.1(17)	33.3(15)	23.5(14)	-2.7(12)	-2.7(12)	14.1(13)
C21B	53.9(16)	39.7(16)	35.2(17)	-6.1(13)	-1.4(13)	18.6(13)
C22B	59(4)	38(2)	44(3)	-10.7(18)	-3(3)	18(2)
C23B	49(3)	47(3)	50(3)	1.8(19)	6.1(19)	19(2)
C24B	47(2)	34(2)	34(2)	-2.3(16)	0.8(18)	12.8(18)
C25B	59(5)	40(4)	43(5)	1(3)	9(3)	23(3)
C26B	71(3)	43(3)	38(3)	0(2)	4(2)	28(2)
C27B	58(4)	41(3)	48(4)	2(3)	3(3)	21(3)
O1'	72(3)	67(3)	46(2)	7(2)	26(2)	16(3)
O2	22.8(13)	26.1(14)	45.8(18)	-0.3(12)	2.7(12)	3.5(11)
O2'	88(4)	118(8)	68(6)	26(6)	42(4)	42(5)
O3	34.1(16)	51.4(19)	30.6(16)	8.4(14)	18.1(13)	12.8(14)
O4	35.1(16)	33.8(15)	33.0(16)	5.1(12)	15.9(13)	4.1(13)
O5	34.2(15)	30.1(15)	34.0(16)	9.3(12)	-0.9(12)	7.2(12)
N1	14.2(12)	21.6(13)	15.7(13)	-1.6(10)	0(1)	1.1(10)
N2	21.0(14)	26.4(15)	22.5(15)	2.8(12)	5.1(11)	5.8(12)
N4	19.2(14)	35.0(17)	15.4(14)	1.1(12)	4.5(11)	6.8(12)
C1	16.4(15)	28.5(17)	20.8(16)	-0.1(13)	3.9(12)	4.9(13)
C2	17.5(15)	27.0(18)	28.1(19)	4.5(14)	2.7(13)	5.2(13)
C3	37(2)	28(2)	34(2)	-6.7(17)	-7.1(18)	0.3(17)
C4	20.1(17)	26.5(18)	28.2(19)	0.2(15)	-4.8(14)	-3.7(14)
C5	18.4(15)	25.1(16)	14.1(15)	0.9(12)	1.3(11)	3.9(13)
C6	17.1(15)	29.1(17)	11.9(14)	-0.5(12)	1.4(11)	4.6(13)
C7	14.4(14)	27.9(17)	22.3(17)	-1.8(13)	2.6(12)	5.0(13)
C8	18.3(15)	30.9(18)	20.5(17)	-5.7(14)	2.7(13)	3.8(14)
C9	21.3(17)	38(2)	19.4(17)	-1.9(15)	1.4(13)	7.2(15)
C10	19.3(16)	31.4(19)	33(2)	3.2(16)	8.0(15)	6.2(14)
C11	24.8(18)	26.5(19)	38(2)	-3.8(16)	3.0(16)	4.5(15)
C12	16.3(16)	41(2)	23.4(18)	-9.9(16)	-1.9(13)	6.5(15)
C13	34(2)	40(2)	44(3)	9(2)	5.8(19)	13.4(19)
C14	18.9(15)	21.1(16)	26.8(18)	2.5(13)	5.1(13)	3.4(13)
C15	19.7(16)	24.3(17)	37(2)	0.7(15)	3.0(15)	7.9(14)
C16	23.2(17)	23.0(17)	36(2)	2.4(15)	-1.4(15)	4.8(14)
C17	28.4(18)	17.2(16)	30(2)	1.3(14)	2.8(15)	0.7(14)
C18	26.9(18)	20.2(16)	36(2)	-0.5(15)	6.1(15)	5.5(14)
C19	19.9(16)	22.0(17)	34(2)	0.3(14)	1.2(14)	5.7(13)
C20	40(2)	28(2)	33(2)	-1.2(16)	-2.2(18)	6.2(17)
O1W	67(3)	66(3)	46(3)	7(2)	29(3)	19(3)

Table 3: Bond Lengths in Å for **CMW04-BuZnTsO2H2xtal2**.

Atom	Atom	Length/Å
Zn1	N3A	2.037(5)
Zn1	N3B	2.053(4)
Zn1	O1'	2.171(10)
Zn1	N1	2.219(3)
Zn1	N2	2.032(3)
Zn1	N4	2.028(3)
Zn1	O1W	2.185(10)
S1	O2	1.457(3)
S1	O3	1.453(3)
S1	N4	1.576(3)
S1	C7	1.779(4)
S2	O4	1.444(3)
S2	O5	1.454(3)
S2	N2	1.573(3)
S2	C14	1.786(4)
N5A	C28A	1.509(6)
N5A	C32A	1.513(9)
N5A	C36A	1.517(8)
N5A	C40A	1.517(7)
C28A	C29A	1.504(4)
C29A	C30A	1.539(7)
C30A	C31A	1.521(9)
C32A	C33A	1.503(4)
C33A	C34A	1.539(12)
C34A	C35A	1.454(13)
C36A	C37A	1.504(4)
C37A	C38A	1.537(11)
C38A	C39A	1.465(11)
C40A	C41A	1.502(4)
C41A	C42A	1.521(4)
C42A	C43A	1.520(4)
N5B	C28B	1.510(6)
N5B	C32B	1.511(9)
N5B	C36B	1.514(8)
N5B	C40B	1.521(7)
C28B	C29B	1.503(4)
C29B	C30B	1.539(7)
C30B	C31B	1.521(9)
C32B	C33B	1.502(4)
C33B	C34B	1.539(12)
C34B	C35B	1.454(13)
C36B	C37B	1.503(4)
C37B	C38B	1.537(11)
C38B	C39B	1.465(11)
C40B	C41B	1.505(4)
C41B	C42B	1.520(4)
C42B	C43B	1.520(4)

Atom	Atom	Length/Å
S3A	O6A	1.444(5)
S3A	O7A	1.457(5)
S3A	N3A	1.585(4)
S3A	C21A	1.792(5)
N3A	C3	1.498(10)
C21A	C22A	1.383(8)
C21A	C26A	1.364(8)
C22A	C23A	1.391(10)
C23A	C24A	1.372(11)
C24A	C25A	1.389(10)
C24A	C27A	1.522(8)
C25A	C26A	1.400(8)
S3B	O6B	1.443(5)
S3B	O7B	1.459(5)
S3B	N3B	1.585(4)
S3B	C21B	1.791(5)
N3B	C3	1.459(9)
C21B	C22B	1.383(8)
C21B	C26B	1.365(8)
C22B	C23B	1.391(10)
C23B	C24B	1.372(11)
C24B	C25B	1.389(10)
C24B	C27B	1.522(8)
C25B	C26B	1.401(8)
O1'	O2'	1.445(14)
N1	C1	1.480(5)
N1	C4	1.472(4)
N1	C5	1.474(4)
N2	C2	1.481(5)
N4	C6	1.482(4)
C1	C2	1.529(5)
C3	C4	1.522(6)
C5	C6	1.526(5)
C7	C8	1.396(5)
C7	C12	1.405(5)
C8	C9	1.387(6)
C9	C10	1.398(6)
C10	C11	1.400(6)
C10	C13	1.504(6)
C11	C12	1.383(6)
C14	C15	1.400(5)
C14	C19	1.391(5)
C15	C16	1.385(6)
C16	C17	1.396(6)
C17	C18	1.391(6)
C17	C20	1.513(6)
C18	C19	1.386(6)

Table 4: Bond Angles in ° for **CMW04-BuZnTsO2H2xtal2**.

Atom	Atom	Atom	Angle/°
N3A	Zn1	N1	81.4(2)
N3A	Zn1	O1W	96.8(4)

Atom	Atom	Atom	Angle/°
N3B	Zn1	O1'	90.6(4)
N3B	Zn1	N1	81.7(2)
O1'	Zn1	N1	168.0(3)

Atom	Atom	Atom	Angle/°
N2	Zn1	N3A	117.4(4)
N2	Zn1	N3B	122.3(3)
N2	Zn1	O1'	94.1(4)
N2	Zn1	N1	82.34(12)
N2	Zn1	O1W	101.5(4)
N4	Zn1	N3A	117.9(4)
N4	Zn1	N3B	113.1(3)
N4	Zn1	O1'	109.7(3)
N4	Zn1	N1	81.98(11)
N4	Zn1	N2	118.85(13)
N4	Zn1	O1W	96.0(2)
O1W	Zn1	N1	176.1(4)
O2	S1	N4	113.57(17)
O2	S1	C7	105.10(18)
O3	S1	O2	115.77(19)
O3	S1	N4	108.65(18)
O3	S1	C7	106.28(18)
N4	S1	C7	106.78(17)
O4	S2	O5	117.22(19)
O4	S2	N2	108.60(18)
O4	S2	C14	106.29(18)
O5	S2	N2	111.96(18)
O5	S2	C14	104.80(18)
N2	S2	C14	107.33(17)
C28A	N5A	C32A	110.1(4)
C28A	N5A	C36A	111.1(4)
C28A	N5A	C40A	109.5(4)
C32A	N5A	C36A	108.6(4)
C32A	N5A	C40A	108.4(5)
C40A	N5A	C36A	109.1(5)
C29A	C28A	N5A	115.8(5)
C28A	C29A	C30A	111.0(4)
C31A	C30A	C29A	111.1(5)
C33A	C32A	N5A	119.9(5)
C32A	C33A	C34A	110.7(7)
C35A	C34A	C33A	114.2(9)
C37A	C36A	N5A	117.0(5)
C36A	C37A	C38A	111.4(6)
C39A	C38A	C37A	111.3(7)
C41A	C40A	N5A	127.2(5)
C40A	C41A	C42A	112.5(5)
C43A	C42A	C41A	110.8(5)
C28B	N5B	C32B	110.1(4)
C28B	N5B	C36B	111.3(4)
C28B	N5B	C40B	108.9(4)
C32B	N5B	C36B	108.9(4)
C32B	N5B	C40B	108.3(5)
C36B	N5B	C40B	109.2(5)
C29B	C28B	N5B	115.9(5)
C28B	C29B	C30B	111.0(4)
C31B	C30B	C29B	111.1(5)
C33B	C32B	N5B	120.3(6)
C32B	C33B	C34B	110.7(7)
C35B	C34B	C33B	114.2(9)
C37B	C36B	N5B	117.4(5)
C36B	C37B	C38B	111.5(6)
C39B	C38B	C37B	111.3(7)

Atom	Atom	Atom	Angle/°
C41B	C40B	N5B	126.4(5)
C40B	C41B	C42B	112.5(5)
C41B	C42B	C43B	110.8(5)
O6A	S3A	O7A	116.6(4)
O6A	S3A	N3A	112.5(3)
O6A	S3A	C21A	105.4(3)
O7A	S3A	N3A	107.8(3)
O7A	S3A	C21A	105.2(3)
N3A	S3A	C21A	108.9(2)
S3A	N3A	Zn1	125.1(4)
C3	N3A	Zn1	111.4(4)
C3	N3A	S3A	117.1(4)
C22A	C21A	S3A	119.1(5)
C26A	C21A	S3A	121.5(4)
C26A	C21A	C22A	119.1(5)
C21A	C22A	C23A	120.0(7)
C24A	C23A	C22A	121.3(6)
C23A	C24A	C25A	118.6(6)
C23A	C24A	C27A	121.8(7)
C25A	C24A	C27A	119.6(7)
C24A	C25A	C26A	119.8(7)
C21A	C26A	C25A	121.0(6)
O6B	S3B	O7B	116.5(3)
O6B	S3B	N3B	112.8(3)
O6B	S3B	C21B	105.6(3)
O7B	S3B	N3B	107.6(3)
O7B	S3B	C21B	105.1(3)
N3B	S3B	C21B	108.9(2)
S3B	N3B	Zn1	134.7(4)
C3	N3B	Zn1	112.4(4)
C3	N3B	S3B	111.7(4)
C22B	C21B	S3B	119.2(5)
C26B	C21B	S3B	121.7(4)
C26B	C21B	C22B	119.1(5)
C21B	C22B	C23B	119.9(7)
C24B	C23B	C22B	121.3(6)
C23B	C24B	C25B	118.6(6)
C23B	C24B	C27B	121.7(7)
C25B	C24B	C27B	119.7(7)
C24B	C25B	C26B	119.8(7)
C21B	C26B	C25B	121.0(6)
O2'	O1'	Zn1	129.7(8)
C1	N1	Zn1	106.5(2)
C4	N1	Zn1	106.0(2)
C4	N1	C1	112.4(3)
C4	N1	C5	112.3(3)
C5	N1	Zn1	106.3(2)
C5	N1	C1	112.8(3)
S2	N2	Zn1	127.72(18)
C2	N2	Zn1	110.8(2)
C2	N2	S2	115.6(3)
S1	N4	Zn1	131.15(18)
C6	N4	Zn1	112.0(2)
C6	N4	S1	114.6(2)
N1	C1	C2	109.5(3)
N2	C2	C1	109.7(3)
N3A	C3	C4	106.0(4)

Atom	Atom	Atom	Angle/°
N3B	C3	C4	110.4(4)
N1	C4	C3	110.5(3)
N1	C5	C6	110.9(3)
N4	C6	C5	108.7(3)
C8	C7	S1	120.2(3)
C8	C7	C12	119.4(4)
C12	C7	S1	120.5(3)
C9	C8	C7	120.4(3)
C8	C9	C10	120.8(4)
C9	C10	C11	118.3(4)
C9	C10	C13	120.5(4)
C11	C10	C13	121.2(4)

Atom	Atom	Atom	Angle/°
C12	C11	C10	121.6(4)
C11	C12	C7	119.6(4)
C15	C14	S2	119.1(3)
C19	C14	S2	121.3(3)
C19	C14	C15	119.5(4)
C16	C15	C14	119.9(4)
C15	C16	C17	121.0(4)
C16	C17	C20	120.7(4)
C18	C17	C16	118.3(4)
C18	C17	C20	121.0(4)
C19	C18	C17	121.5(4)
C18	C19	C14	119.8(3)

Table 5: Hydrogen Fractional Atomic Coordinates ($\times 10^4$) and Equivalent Isotropic Displacement Parameters ($Å^2 \times 10^3$) for **CMW04-BuZnTsO2H2xtal2**. U_{eq} is defined as 1/3 of the trace of the orthogonalised U_{ij}.

Atom	x	y	z	U_{eq}
H28A	-642	2190	8065	48
H28B	751	3106	7853	48
H29A	454	943	7859	46
H29B	2065	1821	7809	46
H30A	-636	1584	6825	51
H30B	1091	2247	6748	51
H31A	197	605	6045	71
H31B	-33	-2	6723	71
H31C	1654	679	6605	71
H32A	799	1218	9048	57
H32B	1187	2015	9728	57
H33A	-1721	1278	8861	68
H33B	-1318	2032	9570	68
H34A	-1353	-110	9456	84
H34B	-730	640	10167	84
H35A	-3758	-196	9483	120
H35B	-3237	774	10073	120
H35C	-3095	-336	10255	120
H36A	3168	2375	8827	56
H36B	3312	3503	8574	56
H37A	3462	3105	9986	63
H37B	3708	4239	9715	63
H38A	5930	4119	9258	74
H38B	6148	4162	10084	74
H39A	5629	2419	9129	103
H39B	5193	2236	9884	103
H39C	6930	2846	9799	103
H40A	807	3592	9627	61
H40B	1748	4305	9115	61
H41A	-1439	3523	9038	59
H41B	-714	3916	8367	59
H42A	-1273	5267	9026	60
H42B	28	5244	9643	60
H43A	591	5805	8295	76
H43B	1892	5769	8904	76
H43C	1062	6626	8974	76
H28C	-57	2628	7840	48
H28D	1770	3108	8012	48

Atom	x	y	z	U_{eq}
H29C	452	914	8009	46
H29D	2057	1569	7791	46
H30C	-922	1032	6961	51
H30D	497	1961	6772	51
H31D	271	408	6114	71
H31E	319	-194	6794	71
H31F	1819	723	6664	71
H32C	-1530	1835	8714	57
H32D	-628	1021	8772	57
H33C	-1201	2165	9890	68
H33D	-30	1525	9999	68
H34C	-3190	536	9374	84
H34D	-2011	-75	9566	84
H35D	-3613	-298	10358	120
H35E	-3158	952	10522	120
H35F	-1916	393	10730	120
H36C	2047	2391	9751	56
H36D	2174	1678	9105	56
H37C	3854	3847	9482	63
H37D	3787	3301	8728	63
H38C	4943	2619	9990	74
H38D	4907	2100	9233	74
H39D	6632	3658	8997	103
H39E	7332	3278	9685	103
H39F	6633	4210	9739	103
H40C	-381	3503	9102	61
H40D	1225	3767	9585	61
H41C	1229	4468	8271	59
H41D	2422	4977	8966	59
H42C	358	5430	9402	60
H42D	-572	5118	8628	60
H43D	1528	6428	8248	76
H43E	2296	6786	9041	76
H43F	697	6932	8757	76
H22A	8193	9284	7793	58
H23A	6660	10315	7528	52
H25A	3281	8323	8362	57
H26A	4858	7320	8655	59
H27A	4201	10731	8149	73
H27B	2779	9721	7798	73
H27C	3953	10394	7336	73
H22B	7819	9391	7733	58
H23B	6007	10234	7543	58
H25B	3119	8052	8493	55
H26B	4914	7177	8648	59
H27D	3815	10600	7925	73
H27E	2727	9764	8344	73
H27F	2540	9554	7522	73
H1A	9140	4948	6129	27
H1B	7346	4265	5992	27
H2A	8509	3541	6876	30
H2B	9351	4680	7303	30
H3A	9720	7982	7473	45
H3B	8103	7716	6970	45
H4A	9669	6989	6407	35
H4B	9956	6378	7063	35
H5A	7230	5836	5479	24

Atom	x	y	z	U_{eq}
H5B	7005	6736	5975	24
H6A	4552	5579	5527	24
H6B	5020	4573	5722	24
H8	1309	5385	5256	30
H9	662	6736	4750	33
H11	3177	8794	6400	37
H12	3798	7447	6920	35
H13A	1288	8663	4703	59
H13B	2155	9453	5382	59
H13C	386	8751	5326	59
H15	3531	3029	6429	32
H16	2518	2407	5276	34
H18	5642	942	5213	34
H19	6655	1542	6368	31
H20A	2267	1165	4275	54
H20B	3483	566	4253	54
H20C	3915	1765	4079	54
H1WA	4161	5424	7947	88
H1WB	5592	5698	8512	88
H2'	3304	5101	8022	70
H1'	6040(140)	5730(50)	8660(40)	88

Table 6: Hydrogen Bond information for **CMW04-BuZnTsO2H2xtal2**.

D	H	A	d(D-H)/Å	d(H-A)/Å	d(D-A)/Å	D-H-A/deg
C41B	H41D	O2'	0.99	1.89	2.595(12)	125.5
O1W	H1WA	O3	1.01	1.74	2.636(9)	145.7
O1W	H1WB	O7A	0.99	1.62	2.552(15)	156.6
O2'	H2'	O3	1.00	1.61	2.552(9)	155.9
O1'	H1'	O7B	0.995(2)	1.81(6)	2.723(15)	151(10)

3-1

EMORY UNIVERSITY | X-ray Crystallography Center

Submitted by: **Christian Wallen**
Emory University
Solved by: **Thomas C. Pickel**
Sample ID: **CMW04BuCoTs**

Crystal Data and Experimental[1-6]

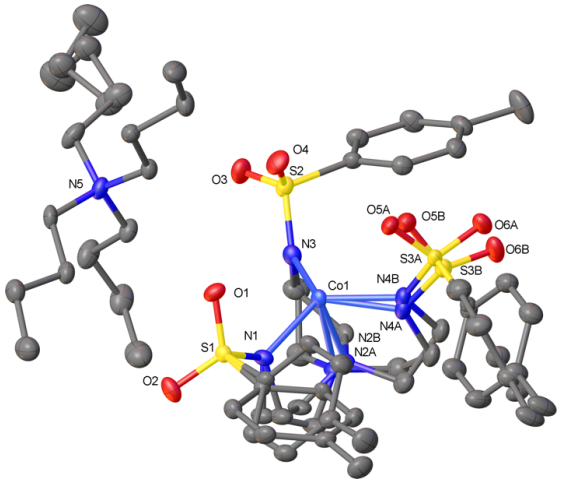

Experimental. Single violet prism-shaped crystals of (**CMW04BuCoTs**) were recrystallised from a mixture of CH_2Cl_2 and diethyl ether by vapor diffusion. A suitable crystal (0.43×0.43×0.38) was selected and mounted on a loop with paratone oil on a Bruker APEX-II CCD diffractometer. The crystal was kept at T = 100(2) K during data collection. The structure was solved with the **XT** (Sheldrick, 2008) structure solution program, using direct and dual-space solution methods and by using **Olex2** (Dolomanov et al., 2009), as the graphical interface. The model was refined with version 2014/7 of **ShelXL-97** (Sheldrick, 2008) using Least Squares minimisation.

Crystal Data. $C_{43}H_{69}CoN_5O_6S_3$, M_r = 907.17, monoclinic, $P2_1/n$ (No. 14), a = 14.2734(9) Å, b = 14.8425(9) Å, c = 21.9158(14) Å, β = 102.4610(10)°, $\alpha = \gamma$ = 90°, V = 4533.6(5) Å^3, T = 100(2) K, Z = 4, Z' = 1, μ(MoK$_\alpha$) = 0.568, 104077 reflections measured, 13895 unique (R_{int} = 0.0651) which were used in all calculations. The final wR_2 was 0.1875 (all data) and R_1 was 0.0711 (I > 2(I)).

Compound	**CMW04BuCoTs**
Formula	$C_{43}H_{69}CoN_5O_6S_3$
$D_{calc.}$/ g cm^{-3}	1.329
μ/mm^{-1}	0.568
Formula Weight	907.17
Colour	violet
Shape	prism
Max Size/mm	0.43
Mid Size/mm	0.43
Min Size/mm	0.38
T/K	100(2)
Crystal System	monoclinic
Space Group	$P2_1/n$
a/Å	14.2734(9)
b/Å	14.8425(9)
c/Å	21.9158(14)
α/°	90
β/°	102.4610(10)
γ/°	90
V/Å^3	4533.6(5)
Z	4
Z'	1
Θ_{min}/°	1.562
Θ_{max}/°	30.581
Measured Refl.	104077
Independent Refl.	13895
Reflections Used	10880
R_{int}	0.0651
Parameters	762
Restraints	561
Largest Peak	1.980
Deepest Hole	-1.667
GooF	1.041
wR_2 (all data)	0.1875
wR_2	0.1701
R_1 (all data)	0.0919
R_1	0.0711
CCDC #	1434440

Structure Quality Indicators

Reflections:	d min	0.70	I/σ	17.2	Rint	6.51%	complete 100%
Refinement:	Max Peak	2.0	Min Peak	-1.7	GooF	1.041	

A violet prism-shaped crystal with dimensions 0.43×0.43×0.38 was mounted on a loop with paratone oil. Data were collected using a Bruker APEX-II CCD diffractometer equipped with an Oxford Cryosystems low-temperature apparatus operating at T = 100(2) K.

Data were measured using ϕ and ω scans using MoK$_\alpha$ radiation (fine-focus sealed tube, 45 kV, 35 mA). The total number of runs and images was based on the strategy calculation from the program **APEX2** (Bruker). The actually achieved resolution was Θ = 30.581.

Cell parameters were retrieved using the **SAINT** (Bruker, V8.34A, 2013) software and refined using **SAINT** (Bruker, V8.34A, 2013) on 9735 reflections, 9 of the observed reflections. Data reduction was performed using the **SAINT** (Bruker, V8.34A, 2013) software which corrects for Lorentz polarisation. The final completeness is 99.9% out to 30.581 in Θ. The absorption coefficient (μ) of this material is 0.568 mm^{-1} and the minimum and maximum transmissions are 0.6511 and 0.7461.

The structure was solved with **ShelXT** (Sheldrick, 2015) in the space group P1 using combined Patterson and dual-space recycling methods. **ShelXT** (Sheldrick, 2015) determined that structure belongs to the space group P2$_1$ (# 4). The structure was refined by Least Squares using version of **ShelXL-97** (Sheldrick, 2008). All non-hydrogen atoms were refined anisotropically. Hydrogen atom positions were calculated geometrically and refined using the riding model.

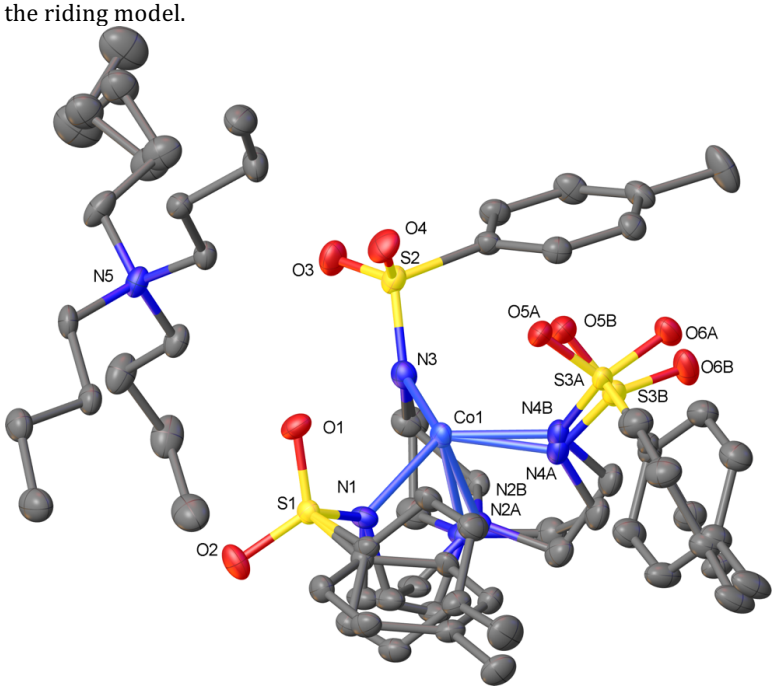

Figure S6:

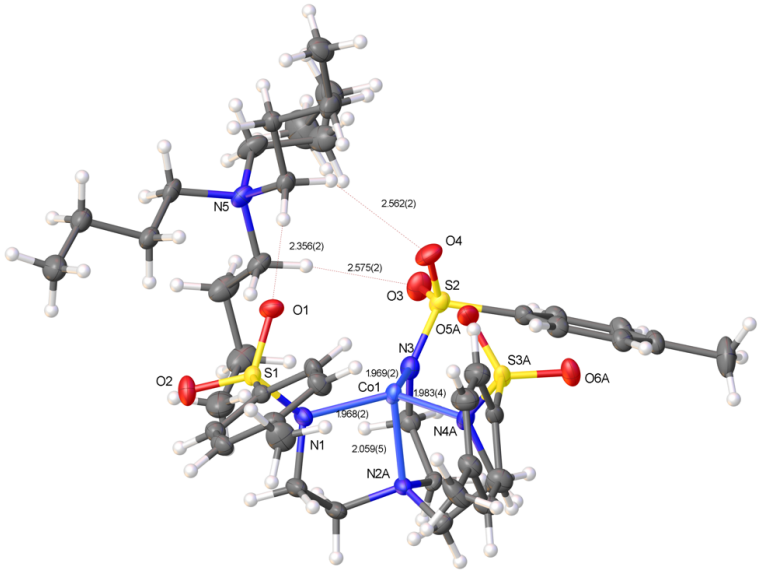

Figure S7: Component 1 and undisordered component.

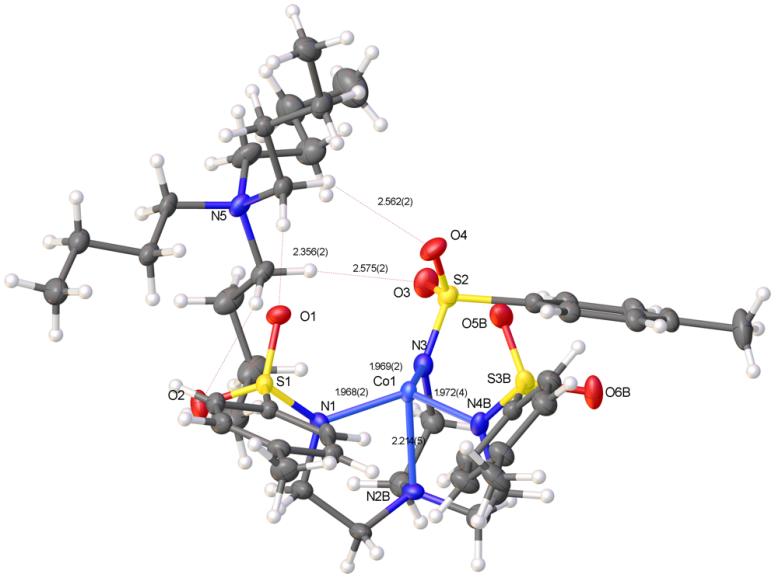

Figure S8: Component 2 and undisordered component.

Data Plots: Diffraction Data

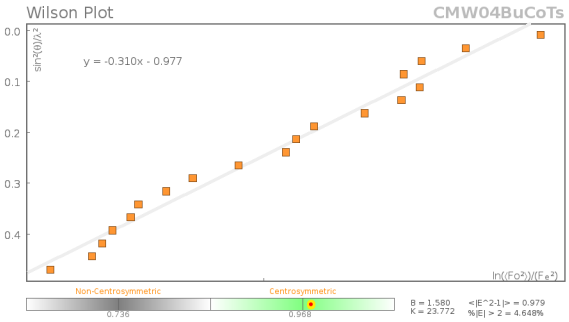

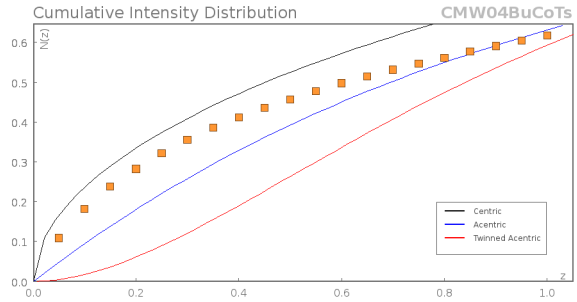

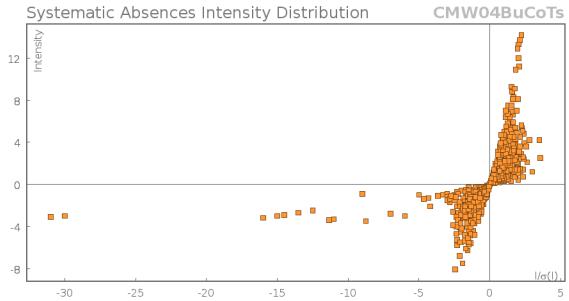

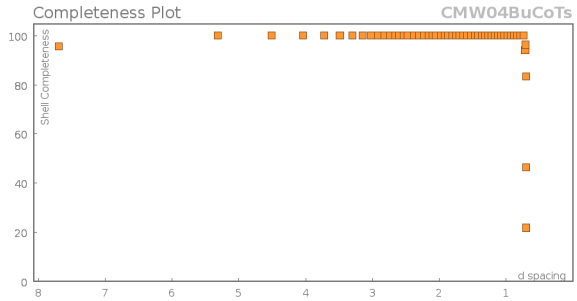

Data Plots: Refinement and Data

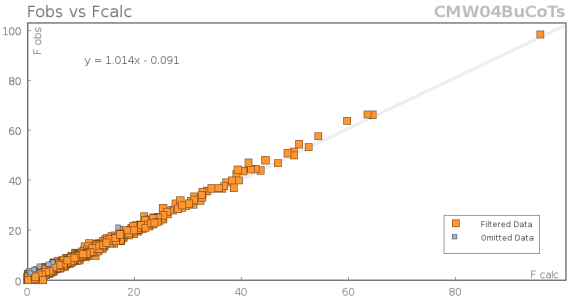

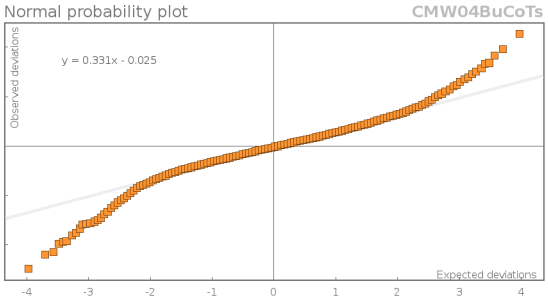

Reflection Statistics

Total reflections (after filtering)	106471	Unique reflections	13895
Completeness	0.997	Mean I/σ	17.17
hklsub>max</sub> collected	(20, 21, 31)	hklsub>min</sub> collected	(-20, -21, -31)
hkl_{max} used	(19, 21, 31)	hkl_{min} used	(-20, 0, 0)
Lim d_{max} collected	100.0	Lim d_{min} collected	0.36
d_{max} used	14.84	d_{min} used	0.7
Friedel pairs	23750	Friedel pairs merged	1
Inconsistent equivalents	0	R_{int}	0.0651
R_{sigma}	0.0365	Intensity transformed	0
Omitted reflections	0	Omitted by user (OMIT hkl)	54
Multiplicity	(22470, 12299, 9794, 4957, 1381, 548)	Maximum mulitplicity	18
Removed systematic absences	2340	Filtered off (Shel/OMIT)	0

Images of the Crystal on the Diffractometer

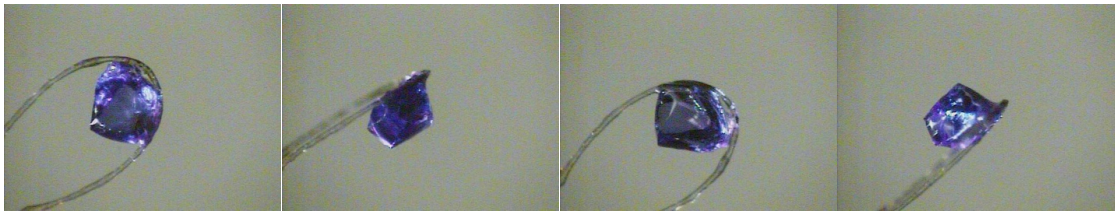

Table S1: Fractional Atomic Coordinates (×10⁴) and Equivalent Isotropic Displacement Parameters (Å²×10³) for **CMW04BuCoTs**. U_{eq} is defined as 1/3 of the trace of the orthogonalised U_{ij}.

Atom	x	y	z	U_{eq}
Co1	6312.8(2)	5578.1(3)	7640.4(2)	17.85(10)
S1	4194.1(4)	5795.1(4)	6820.2(3)	17.69(13)
S2	6685.0(5)	4179.0(5)	8767.8(3)	21.99(14)
O1	4241.4(15)	4822.5(14)	6863.8(10)	25.1(4)
O2	3303.0(14)	6216.0(17)	6883.7(10)	29.2(5)
O3	6342.3(16)	4027.4(17)	9336.4(11)	32.0(5)
O4	6353.8(16)	3567.0(16)	8252.5(11)	31.0(5)
N1	5086.2(16)	6185.6(15)	7300.6(11)	19.0(4)
N3	6480.6(16)	5170.2(17)	8512.9(11)	21.7(4)
C12	7952.5(19)	4076.0(18)	8984.0(12)	19.4(5)
C13	8473(2)	4124.3(19)	8512.8(13)	21.8(5)
C14	9465(2)	4095(2)	8668.3(13)	23.2(5)
C15	9955(2)	4012(2)	9289.3(14)	25.4(6)
C16	9428(2)	3973(2)	9751.0(14)	28.4(6)
C17	8432(2)	4002(2)	9603.0(13)	23.4(5)
C18	11039(2)	3980(3)	9447.1(18)	46.1(10)
N4A	7435(3)	5691(3)	7252.3(16)	22.7(7)
S3A	7828.2(14)	4997.6(13)	6826.0(8)	23.3(4)
O5A	7131(3)	4272(2)	6679(2)	31.9(9)
O6A	8807(3)	4727(4)	7073.2(19)	36.1(10)
C21A	7829(3)	5541(2)	6101.5(15)	21.4(9)
C22A	8129(3)	6423(3)	6037(2)	32.6(10)
C23A	8024(3)	6795(3)	5444(2)	30.6(10)
C24A	7633(3)	6307(3)	4918.7(18)	27.6(10)
C25A	7335(3)	5423(3)	4992(2)	37.1(11)
C26A	7435(3)	5051(3)	5577(2)	37.4(11)
C27A	7509(4)	6701(4)	4269(2)	33.8(11)
N2A	6774(3)	6816(3)	8033.0(17)	19.4(8)
C9A	5892(3)	7370(3)	7970(2)	25.0(8)
C8A	5220(3)	7177(3)	7342(2)	22.9(9)
C10A	7217(3)	6637(3)	8698(2)	21.3(7)
C11A	6669(10)	5890(5)	8952(3)	23.6(13)
C19A	7462(3)	7199(3)	7689(2)	26.0(8)
C20A	8089(3)	6441(3)	7520(2)	26.1(8)
C1A	4368(3)	6025(3)	6054.0(16)	19.8(11)
C2A	3831(3)	6681(3)	5689(2)	27.1(9)
C3A	3967(3)	6845(3)	5089(2)	29.8(10)
C4A	4626(3)	6370(3)	4845.8(18)	26.7(13)
C5A	5172(3)	5697(3)	5219(2)	32.2(10)
C6A	5046(3)	5525(3)	5821(2)	28.5(10)
C7A	4768(4)	6552(5)	4192(2)	42.1(16)
N4B	7414(4)	5888(3)	7265.1(19)	22.1(9)
S3B	7985.3(18)	5227.5(18)	6914.2(10)	24.4(6)
O5B	7501(4)	4361(3)	6868(3)	29.0(11)
O6B	9001(3)	5218(4)	7173(2)	27.6(11)

Atom	x	y	z	U_{eq}
C21B	7839(3)	5629(3)	6132.3(16)	19.9(11)
C22B	7334(3)	6413(3)	5917(2)	25.0(11)
C23B	7314(4)	6720(3)	5318(2)	25.4(11)
C24B	7786(4)	6266(3)	4927.5(18)	25.2(12)
C25B	8288(4)	5482(4)	5148(2)	25.3(11)
C26B	8308(4)	5170(3)	5745(2)	25.0(11)
C27B	7765(6)	6596(5)	4271(2)	33.8(11)
N2B	6605(3)	6923(3)	8084(2)	21.8(11)
C9B	5937(3)	7582(3)	7709(3)	25.0(8)
C8B	4966(4)	7140(3)	7460(3)	22.9(9)
C10B	6439(4)	6849(5)	8728(3)	29.0(9)
C11B	6760(15)	5923(6)	9000(4)	25.9(16)
C19B	7618(4)	7116(5)	8080(2)	28.2(9)
C20B	7840(4)	6784(5)	7466(3)	26.1(8)
C1B	4302(4)	6140(3)	6065.0(17)	15.6(13)
C2B	3515(3)	6177(3)	5571(2)	15(1)
C3B	3633(3)	6446(3)	4984(2)	17.6(10)
C4B	4517(4)	6679(3)	4881(2)	17.9(14)
C5B	5320(3)	6638(3)	5387(2)	16.7(10)
C6B	5214(3)	6370(3)	5978(2)	14.9(10)
C7B	4639(5)	6970(4)	4240(2)	24.6(14)
N5	3444.6(17)	3385.0(17)	8230.0(11)	22.1(5)
C28	2402.8(18)	3541(2)	7909.0(13)	22.9(5)
C29	2229.5(19)	4258(2)	7405.6(14)	23.7(5)
C30	1176(2)	4240(2)	7057.1(15)	28.0(6)
C31	951(2)	4981(2)	6576.4(17)	35.5(7)
C32	3932(2)	4251(2)	8503.4(14)	24.6(6)
C33	3516(3)	4698(3)	9010.2(16)	34.4(7)
C34	4027(3)	5594(3)	9199.9(16)	36.9(8)
C35	3861(3)	6291(3)	8679.5(19)	41.3(8)
C36	4023.2(19)	3056(2)	7769.2(13)	21.8(5)
C37	3600.5(19)	2268.4(19)	7359.2(13)	22.2(5)
C38	4389(2)	1861(2)	7071.5(16)	31.0(6)
C39	4039(3)	1135(2)	6588.5(17)	33.7(7)
C40	3433(2)	2681(2)	8734.1(15)	31.9(7)
C41	4432(4)	2323(5)	9048(3)	36.4(14)
C42	4390(5)	1720(4)	9624(3)	36.9(11)
C43	4120(6)	2267(6)	10141(3)	53.9(15)
C41B	4371(4)	2455(8)	9188(4)	37.1(14)
C42B	3991(5)	1939(7)	9707(4)	38.2(11)
C43B	4806(8)	1508(8)	10169(4)	56.5(17)

Table S2: Anisotropic Displacement Parameters (×10^4) **CMW04BuCoTs**. The anisotropic displacement factor exponent takes the form: $-2\pi^2[h^2a^{*2} \times U_{11} + ... + 2hka^* \times b^* \times U_{12}]$

Atom	U_{11}	U_{22}	U_{33}	U_{23}	U_{13}	U_{12}
Co1	12.63(16)	21.38(18)	18.37(17)	3.34(13)	0.76(12)	0.14(12)
S1	14.0(3)	19.3(3)	19.1(3)	2.0(2)	2.0(2)	0.1(2)
S2	18.6(3)	24.3(3)	22.5(3)	4.2(2)	3.5(2)	-3.5(2)
O1	27(1)	18.8(10)	28.3(10)	4.8(8)	3.3(8)	-4.7(8)
O2	17.4(9)	40.7(13)	28.5(11)	-0.8(9)	2.7(8)	7.4(8)
O3	27.5(11)	41.1(13)	29.7(11)	11.3(10)	11.2(9)	-0.8(9)
O4	28.2(11)	28.3(11)	34.3(12)	-2.1(9)	1.8(9)	-11.4(9)
N1	18.3(10)	16.3(9)	20.2(10)	0.5(8)	-0.5(8)	2.7(7)
N3	17.6(10)	26.4(12)	20.1(10)	1.6(9)	2.1(8)	1.1(8)
C12	19.1(11)	18.0(12)	19.8(12)	2.9(9)	1.6(9)	1.6(9)

Atom	U_{11}	U_{22}	U_{33}	U_{23}	U_{13}	U_{12}
C13	24.3(12)	22.0(13)	18.4(12)	-0.2(10)	2.8(10)	1(1)
C14	23.4(13)	23.8(13)	23.4(13)	-2.2(10)	7.5(10)	2.9(10)
C15	20.8(12)	25.1(14)	28.0(14)	-1.6(11)	0.5(10)	6.3(10)
C16	28.9(14)	33.5(16)	20.1(13)	3.1(11)	-1.0(11)	6.1(12)
C17	26.8(13)	24.0(13)	18.5(12)	3.4(10)	2.8(10)	3.6(10)
C18	22.0(15)	75(3)	38.1(19)	-4.2(19)	-0.4(13)	16.3(17)
N4A	14.8(12)	27.0(16)	26.3(13)	7.5(11)	4.7(10)	-1.6(11)
S3A	17.5(7)	24.9(8)	30.2(7)	13.8(6)	10.8(5)	5.6(6)
O5A	29(2)	22.8(16)	48(2)	9.1(15)	17.1(17)	0.5(14)
O6A	26.0(16)	47(2)	37(2)	19(2)	11.5(14)	14.1(16)
C21A	17.4(18)	20.6(17)	27.3(16)	5.6(13)	7.0(13)	2.7(14)
C22A	40(2)	31.0(19)	26.7(18)	2.3(15)	7.2(17)	0.0(17)
C23A	42(2)	22.6(19)	28.2(17)	2.1(14)	9.5(16)	-2.1(17)
C24A	29(2)	26.0(18)	28.2(17)	2.0(14)	5.7(15)	4.9(16)
C25A	41(3)	30(2)	37(2)	-1.3(15)	0.6(18)	-3.4(18)
C26A	38(2)	30(2)	41.6(19)	2.4(16)	2.9(17)	-1.7(18)
C27A	41(3)	33.8(17)	29.6(13)	5.7(12)	13.8(13)	20.8(17)
N2A	17.4(15)	16.5(17)	21.9(15)	-1.6(13)	-0.7(12)	-0.3(12)
C9A	23.7(12)	14.7(15)	33.5(18)	-0.2(13)	-0.2(13)	1.5(11)
C8A	20.9(17)	16.3(12)	30.0(19)	1.1(11)	2.3(14)	1.0(11)
C10A	17.1(16)	22.5(18)	22.0(15)	-4.6(13)	-0.8(12)	-1.7(13)
C11A	26(3)	24(2)	20(2)	-4.6(18)	3(2)	1.4(19)
C19A	22.2(15)	24.3(17)	29.2(17)	2.2(15)	0.5(14)	-4.9(13)
C20A	15.4(16)	29(2)	32.6(17)	8.4(16)	1.7(14)	-3.2(13)
C1A	18(2)	20(2)	20(2)	3.3(17)	-0.5(17)	-0.6(17)
C2A	27(2)	27(2)	26(2)	-0.9(18)	3.8(17)	3.9(18)
C3A	32(3)	25(3)	29(2)	4(2)	0(2)	4.9(19)
C4A	28(2)	26(4)	26(2)	2(2)	5.0(17)	-1(2)
C5A	35(2)	30(2)	33(2)	1(2)	11(2)	5(2)
C6A	25(2)	29(2)	30(2)	5.3(19)	2.8(17)	6.4(18)
C7A	46(3)	53(4)	29(3)	11(3)	13(2)	3(3)
N4B	15.2(14)	25.3(18)	26.0(15)	9.0(14)	4.7(12)	-0.6(14)
S3B	17.9(9)	23.7(11)	32.4(10)	12.9(8)	7.2(7)	1.7(8)
O5B	22(2)	24.4(18)	42(3)	11.2(17)	10(2)	1.5(16)
O6B	14.8(17)	36(3)	32(2)	14(2)	5.5(15)	4.5(17)
C21B	16(2)	18(2)	25.9(18)	3.2(15)	4.0(16)	-0.9(17)
C22B	30(2)	24(2)	23(2)	2.2(17)	11.2(18)	6.1(19)
C23B	35(3)	17(2)	26(2)	4.7(16)	11.9(18)	8(2)
C24B	30(3)	24(2)	23.7(19)	2.9(16)	9.6(18)	8(2)
C25B	25(2)	22(2)	29(2)	-2.4(17)	6.3(18)	2.7(18)
C26B	22(2)	19(2)	33(2)	5.5(17)	4.9(17)	1.8(18)
C27B	41(3)	33.8(17)	29.6(13)	5.7(12)	13.8(13)	20.8(17)
N2B	22.4(19)	14(2)	27(2)	-1.9(17)	1.0(15)	-0.6(16)
C9B	23.7(12)	14.7(15)	33.5(18)	-0.2(13)	-0.2(13)	1.5(11)
C8B	20.9(17)	16.3(12)	30.0(19)	1.1(11)	2.3(14)	1.0(11)
C10B	26.5(19)	29.0(19)	29.1(18)	-2.4(15)	0.7(15)	2.0(16)
C11B	27(3)	27(2)	22(2)	-3.7(19)	1(2)	3(2)
C19B	24.1(16)	26.4(18)	31.6(18)	1.1(17)	0.6(15)	-3.5(14)
C20B	15.4(16)	29(2)	32.6(17)	8.4(16)	1.7(14)	-3.2(13)
C1B	15(2)	14(2)	18(2)	0(2)	4(2)	1(2)
C2B	11(2)	16(2)	17(2)	0.0(19)	0.2(18)	-1.7(18)
C3B	17(2)	15(3)	18(2)	4(2)	-3.2(19)	-0.7(19)
C4B	22(2)	12(4)	19(2)	2(2)	4(2)	4(2)
C5B	15(2)	16(2)	20(2)	3.7(19)	7.1(19)	-1.6(18)
C6B	9(2)	19(2)	16(2)	7.7(18)	1.0(17)	5.5(17)
C7B	32(3)	21(3)	21(3)	6(3)	5(2)	0(3)
N5	19.7(10)	26.8(12)	20.4(10)	0.9(9)	5.8(8)	-6.7(9)

Atom	U_{11}	U_{22}	U_{33}	U_{23}	U_{13}	U_{12}
C28	14.1(11)	31.6(15)	24.2(13)	-3.4(11)	7.1(9)	-4.7(10)
C29	17.8(12)	26.1(14)	28.3(14)	-2.8(11)	7.3(10)	-3.8(10)
C30	20.5(13)	31.5(16)	31.3(15)	-3.7(12)	4.5(11)	-3.1(11)
C31	28.1(15)	33.8(17)	41.6(18)	-0.4(14)	1.0(13)	-0.2(13)
C32	22.9(13)	27.9(14)	23.2(13)	-3.4(11)	5.4(10)	-9(1)
C33	38.4(17)	41.4(19)	26.7(15)	-9.4(13)	14.0(13)	-14.2(14)
C34	38.6(17)	45(2)	29.5(16)	-15.8(14)	12.1(13)	-12.1(15)
C35	38.8(18)	35.1(19)	49(2)	-12.5(16)	6.3(16)	-3.3(15)
C36	16.6(11)	24.4(13)	24.8(13)	0.8(10)	5.8(9)	-1.7(9)
C37	20.0(12)	20.9(13)	25.7(13)	2.4(10)	5.1(10)	-0.6(9)
C38	21.9(13)	34.5(17)	39.0(17)	-4.7(13)	11.4(12)	-2.2(12)
C39	37.3(17)	27.6(16)	39.7(18)	-1.9(13)	16.0(14)	3.2(13)
C40	36.4(16)	34.9(17)	23.8(14)	5.7(12)	5.4(12)	-15.6(13)
C41	42.4(18)	36(2)	26(2)	2.4(19)	-2.7(15)	-5.4(15)
C42	37(3)	42(3)	31.4(19)	7.6(18)	5.4(18)	7(2)
C43	61(3)	65(4)	33(2)	5(2)	4(2)	15(3)
C41B	43.2(18)	37(2)	26(2)	3(2)	-3.1(15)	-5.7(16)
C42B	38(3)	43(3)	32(2)	8.0(19)	5.1(19)	6(2)
C43B	62(3)	68(4)	36(2)	8(2)	3(2)	17(3)

Table S3: Bond Lengths in Å for **CMW04BuCoTs**.

Atom	Atom	Length/Å
Co1	N1	1.967(2)
Co1	N3	1.970(2)
Co1	N4A	1.976(3)
Co1	N2A	2.075(4)
Co1	N4B	1.979(4)
Co1	N2B	2.220(5)
S1	O1	1.447(2)
S1	O2	1.451(2)
S1	N1	1.577(2)
S1	C1A	1.783(3)
S1	C1B	1.770(3)
S2	O3	1.451(2)
S2	O4	1.447(2)
S2	N3	1.578(3)
S2	C12	1.775(3)
N1	C8A	1.484(4)
N1	C8B	1.478(5)
N3	C11A	1.423(8)
N3	C11B	1.536(13)
C12	C13	1.398(4)
C12	C17	1.386(4)
C13	C14	1.384(4)
C14	C15	1.395(4)
C15	C16	1.387(4)
C15	C18	1.511(4)
C16	C17	1.388(4)
N4A	S3A	1.572(4)
N4A	C20A	1.489(5)
S3A	O5A	1.455(4)
S3A	O6A	1.442(3)
S3A	C21A	1.781(3)
C21A	C22A	1.394(6)
C21A	C26A	1.373(6)
C22A	C23A	1.390(6)
C23A	C24A	1.372(6)
C24A	C25A	1.399(6)
C24A	C27A	1.514(5)
C25A	C26A	1.376(7)
N2A	C9A	1.484(5)
N2A	C10A	1.482(5)
N2A	C19A	1.475(5)
C9A	C8A	1.526(4)
C10A	C11A	1.528(6)
C19A	C20A	1.532(5)
C1A	C2A	1.382(5)
C1A	C6A	1.400(5)
C2A	C3A	1.391(6)
C3A	C4A	1.373(6)
C4A	C5A	1.414(6)
C4A	C7A	1.514(5)
C5A	C6A	1.394(6)
N4B	S3B	1.577(4)
N4B	C20B	1.489(6)
S3B	O5B	1.454(4)
S3B	O6B	1.438(3)
S3B	C21B	1.783(3)
C21B	C22B	1.397(6)
C21B	C26B	1.370(6)
C22B	C23B	1.384(6)
C23B	C24B	1.375(6)
C24B	C25B	1.396(6)
C24B	C27B	1.514(5)
C25B	C26B	1.385(7)
N2B	C9B	1.484(5)
N2B	C10B	1.485(5)
N2B	C19B	1.476(5)
C9B	C8B	1.523(4)

Atom	Atom	Length/Å
C10B	C11B	1.528(5)
C19B	C20B	1.530(5)
C1B	C2B	1.382(5)
C1B	C6B	1.399(6)
C2B	C3B	1.392(6)
C3B	C4B	1.374(6)
C4B	C5B	1.414(6)
C4B	C7B	1.514(5)
C5B	C6B	1.394(6)
N5	C28	1.519(4)
N5	C32	1.522(4)
N5	C36	1.517(4)
N5	C40	1.523(4)
C28	C29	1.515(4)

Atom	Atom	Length/Å
C29	C30	1.533(4)
C30	C31	1.509(5)
C32	C33	1.520(4)
C33	C34	1.531(5)
C34	C35	1.519(6)
C36	C37	1.518(4)
C37	C38	1.529(4)
C38	C39	1.518(5)
C40	C41	1.537(6)
C40	C41B	1.523(6)
C41	C42	1.560(6)
C42	C43	1.510(7)
C41B	C42B	1.561(6)
C42B	C43B	1.510(7)

Table S4: Bond Angles in ° for **CMW04BuCoTs**.

Atom	Atom	Atom	Angle/°
N1	Co1	N3	114.84(10)
N1	Co1	N4A	122.42(13)
N1	Co1	N2A	85.84(12)
N1	Co1	N4B	117.25(16)
N1	Co1	N2B	79.70(14)
N3	Co1	N4A	120.24(13)
N3	Co1	N2A	84.75(12)
N3	Co1	N4B	122.25(16)
N3	Co1	N2B	83.10(13)
N4A	Co1	N2A	83.67(17)
N4B	Co1	N2B	83.20(18)
O1	S1	O2	116.91(14)
O1	S1	N1	107.64(12)
O1	S1	C1A	103.85(19)
O1	S1	C1B	109.76(18)
O2	S1	N1	112.08(13)
O2	S1	C1A	108.12(17)
O2	S1	C1B	102.70(18)
N1	S1	C1A	107.59(15)
N1	S1	C1B	107.3(2)
O3	S2	N3	112.20(14)
O3	S2	C12	105.69(13)
O4	S2	O3	117.33(14)
O4	S2	N3	107.73(13)
O4	S2	C12	107.26(14)
N3	S2	C12	105.94(13)
S1	N1	Co1	127.48(14)
C8A	N1	Co1	109.8(2)
C8A	N1	S1	118.7(2)
C8B	N1	Co1	119.3(2)
C8B	N1	S1	113.1(2)
S2	N3	Co1	127.19(15)
C11A	N3	Co1	113.0(2)
C11A	N3	S2	117.8(3)
C11B	N3	Co1	114.2(2)
C11B	N3	S2	115.6(3)

Atom	Atom	Atom	Angle/°
C13	C12	S2	118.2(2)
C17	C12	S2	121.9(2)
C17	C12	C13	119.9(3)
C14	C13	C12	119.7(3)
C13	C14	C15	120.9(3)
C14	C15	C18	119.9(3)
C16	C15	C14	118.6(3)
C16	C15	C18	121.5(3)
C17	C16	C15	121.2(3)
C12	C17	C16	119.7(3)
S3A	N4A	Co1	128.8(3)
C20A	N4A	Co1	113.0(3)
C20A	N4A	S3A	116.7(3)
N4A	S3A	C21A	107.60(17)
O5A	S3A	N4A	107.54(18)
O5A	S3A	C21A	105.7(2)
O6A	S3A	N4A	113.6(2)
O6A	S3A	O5A	115.9(3)
O6A	S3A	C21A	105.92(16)
C22A	C21A	S3A	125.1(3)
C26A	C21A	S3A	115.3(3)
C26A	C21A	C22A	119.4(3)
C23A	C22A	C21A	119.6(4)
C24A	C23A	C22A	121.1(4)
C23A	C24A	C25A	118.5(4)
C23A	C24A	C27A	121.9(4)
C25A	C24A	C27A	119.6(4)
C26A	C25A	C24A	120.7(4)
C21A	C26A	C25A	120.6(4)
C9A	N2A	Co1	105.4(2)
C10A	N2A	Co1	106.1(3)
C10A	N2A	C9A	111.4(3)
C19A	N2A	Co1	108.4(3)
C19A	N2A	C9A	112.6(3)
C19A	N2A	C10A	112.4(3)
N2A	C9A	C8A	109.6(3)
N1	C8A	C9A	106.8(3)

Atom	Atom	Atom	Angle/°
N2A	C10A	C11A	110.2(4)
N3	C11A	C10A	109.6(5)
N2A	C19A	C20A	109.2(3)
N4A	C20A	C19A	107.1(3)
C2A	C1A	S1	120.5(3)
C2A	C1A	C6A	120.2(3)
C6A	C1A	S1	119.3(3)
C1A	C2A	C3A	119.8(4)
C4A	C3A	C2A	121.6(4)
C3A	C4A	C5A	118.5(4)
C3A	C4A	C7A	121.3(4)
C5A	C4A	C7A	120.3(4)
C6A	C5A	C4A	120.6(4)
C5A	C6A	C1A	119.3(3)
S3B	N4B	Co1	126.8(3)
C20B	N4B	Co1	113.3(3)
C20B	N4B	S3B	118.5(4)
N4B	S3B	C21B	107.17(18)
O5B	S3B	N4B	107.24(19)
O5B	S3B	C21B	105.8(2)
O6B	S3B	N4B	113.3(3)
O6B	S3B	O5B	116.3(3)
O6B	S3B	C21B	106.38(18)
C22B	C21B	S3B	123.2(3)
C26B	C21B	S3B	117.2(3)
C26B	C21B	C22B	119.4(3)
C23B	C22B	C21B	119.9(4)
C24B	C23B	C22B	121.1(4)
C23B	C24B	C25B	118.5(4)
C23B	C24B	C27B	121.4(4)
C25B	C24B	C27B	120.1(4)
C26B	C25B	C24B	120.7(4)
C21B	C26B	C25B	120.4(4)
C9B	N2B	Co1	108.2(3)
C9B	N2B	C10B	111.1(4)
C10B	N2B	Co1	107.2(3)
C19B	N2B	Co1	105.3(3)
C19B	N2B	C9B	112.5(3)
C19B	N2B	C10B	112.1(3)
N2B	C9B	C8B	110.0(3)
N1	C8B	C9B	110.8(4)
N2B	C10B	C11B	110.0(4)
C10B	C11B	N3	111.8(7)
N2B	C19B	C20B	109.4(3)
N4B	C20B	C19B	113.5(4)
C2B	C1B	S1	121.6(4)
C2B	C1B	C6B	120.4(3)
C6B	C1B	S1	118.0(3)
C1B	C2B	C3B	119.7(4)
C4B	C3B	C2B	121.6(4)
C3B	C4B	C5B	118.6(4)
C3B	C4B	C7B	121.2(4)
C5B	C4B	C7B	120.2(4)
C6B	C5B	C4B	120.6(4)
C5B	C6B	C1B	119.2(3)
C28	N5	C32	111.9(2)
C28	N5	C40	106.1(2)
C32	N5	C40	111.7(2)
C36	N5	C28	111.1(2)
C36	N5	C32	105.4(2)
C36	N5	C40	110.8(2)
C29	C28	N5	115.7(2)
C28	C29	C30	109.8(2)
C31	C30	C29	111.9(3)
C33	C32	N5	116.0(2)
C32	C33	C34	109.8(3)
C35	C34	C33	113.5(3)
N5	C36	C37	116.0(2)
C36	C37	C38	108.4(2)
C39	C38	C37	114.1(3)
N5	C40	C41	114.0(3)
C41B	C40	N5	118.7(4)
C40	C41	C42	111.5(4)
C43	C42	C41	111.1(5)
C40	C41B	C42B	100.9(5)
C43B	C42B	C41B	110.9(5)

Table S5: Hydrogen Fractional Atomic Coordinates (×10⁴) and Equivalent Isotropic Displacement Parameters (Å²×10³) for **CMW04BuCoTs**. U_{eq} is defined as 1/3 of the trace of the orthogonalised U_{ij}.

Atom	x	y	z	U_{eq}
H13	8148	4177	8088	26
H14	9818	4131	8348	28
H16	9753	3925	10176	34
H17	8081	3971	9925	28
H18A	11259	3450	9250	69
H18B	11267	3942	9901	69
H18C	11294	4527	9292	69
H22A	8402	6768	6396	39
H23A	8228	7396	5401	37
H25A	7060	5076	4634	45
H26A	7230	4450	5620	45
H27A	7222	7302	4261	51
H27B	7089	6310	3969	51
H27C	8137	6747	4158	51
H9AA	6063	8017	7999	30
H9AB	5565	7225	8313	30
H8AA	4596	7482	7316	27
H8AB	5505	7396	6995	27
H10A	7207	7193	8946	26
H10B	7894	6453	8737	26
H11A	7054	5666	9354	28
H11B	6057	6131	9027	28
H19A	7869	7654	7951	31
H19B	7111	7499	7303	31
H20A	8452	6656	7211	31
H20B	8553	6234	7898	31
H2A	3371	7020	5848	33
H3A	3593	7297	4842	36
H5A	5630	5359	5058	39
H6A	5415	5073	6071	34
H7AA	4208	6336	3886	63
H7AB	5344	6237	4130	63
H7AC	4844	7201	4137	63
H22B	7005	6736	6181	30
H23B	6968	7254	5174	30
H25B	8619	5161	4884	30
H26B	8649	4633	5888	30
H27D	7263	6276	3975	51
H27E	8389	6482	4167	51
H27F	7631	7244	4247	51
H9BA	6206	7799	7355	30
H9BB	5857	8106	7972	30
H8BA	4573	7178	7780	27
H8BB	4625	7467	7083	27
H10C	5749	6935	8720	35
H10D	6804	7325	8994	35
H11C	6462	5802	9360	31
H11D	7465	5923	9154	31

Atom	x	y	z	U_{eq}
H19C	8042	6809	8437	34
H19D	7738	7773	8124	34
H20C	7595	7231	7134	31
H20D	8545	6748	7513	31
H2B	2896	6020	5633	18
H3B	3089	6469	4647	21
H5B	5938	6794	5323	20
H6B	5755	6343	6317	18
H7BA	4132	6699	3920	37
H7BB	5267	6770	4179	37
H7BC	4598	7628	4208	37
H28A	2134	2965	7720	27
H28B	2043	3708	8231	27
H29A	2649	4148	7108	28
H29B	2388	4858	7597	28
H30A	1032	3650	6848	34
H30B	760	4307	7362	34
H31A	1370	4923	6278	53
H31B	1057	5567	6785	53
H31C	279	4933	6354	53
H3	4617	4119	8678	29
H2	3904	4689	8159	29
H33A	3597	4296	9378	41
H33B	2821	4805	8853	41
H34A	3801	5843	9562	44
H34B	4724	5481	9335	44
H35A	4200	6107	8356	62
H35B	4103	6877	8850	62
H35C	3172	6337	8497	62
H4	4668	2880	8006	26
H1	4108	3565	7495	26
H37A	3062	2477	7025	27
H37B	3353	1810	7612	27
H38A	4691	2348	6873	37
H38B	4889	1601	7410	37
H39A	3567	1393	6240	51
H39B	3740	647	6780	51
H39C	4583	896	6433	51
H40A	3029	2168	8546	38
H40B	3132	2948	9059	38
H40C	2971	2884	8983	38
H40D	3177	2115	8523	38
H41A	4869	2838	9183	44
H41B	4695	1968	8741	44
H42A	3913	1235	9496	44
H42B	5024	1436	9780	44
H43A	3500	2561	9985	81
H43B	4612	2726	10285	81
H43C	4073	1869	10490	81
H41C	4727	3006	9355	44
H41D	4788	2068	8992	44
H42C	3646	2364	9929	46
H42D	3532	1468	9511	46

Atom	x	y	z	U_{eq}
H43D	5074	1012	9966	85
H43E	4567	1276	10525	85
H43F	5307	1958	10316	85

3-1(NH_2OH)

EMORY UNIVERSITY | X-ray Crystallography Center

Submitted by: **Christian Wallen**

Solved by: **John Bacsa**

Sample ID: **CMW04-73NN (1–NH_2OH)**

Crystal Data and Experimental

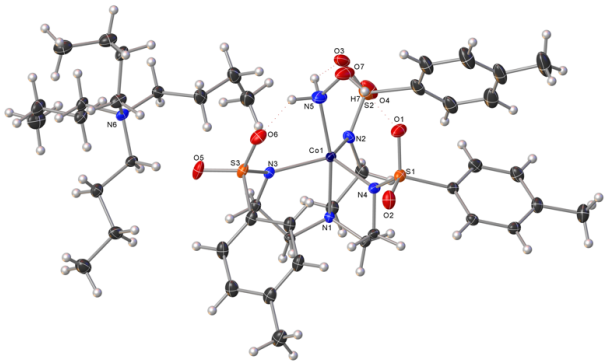

Experimental. Single violet prism-shaped crystals of (**CMW04-73NN**) were obtained by vapor diffusion from DCM and diethyl ether. A suitable crystal (0.43×0.30×0.26 mm) was selected and mounted on a loop with paratone oil on a Bruker APEX-II CCD diffractometer. The crystal was cooled to T = 100(2) K during data collection. The structure was solved with the **ShelXT-2014/4** (Sheldrick, 2015) structure solution program using direct and dual-space solution methods and by using **Olex2** (Dolomanov et al., 2009) as the graphical interface. The structure was refined with version 2014/7 of **ShelXL** (Sheldrick, 2008) using Least Squares minimisation.

Crystal Data. $C_{43}H_{72}CoN_6O_7S_3$, M_r = 940.17, triclinic, P-1 (No. 2), a = 13.5871(16) Å, b = 18.615(2) Å, c = 20.023(2) Å, α = 90.4613(16)°, β = 100.2779(15)°, γ = 111.1181(14)°, V = 4633.8(9) Å^3, T = 100(2) K, Z = 4, Z' = 2, μ(MoK$_\alpha$) = 0.560, 99178 reflections measured, 29052 unique (R_{int}# = 0.0480) which were used in all calculations. The final wR_2 was 0.1987 (all data) and R_1 was 0.0703 (I > 2σ(I)).

Compound	**CMW04-73NN** (CCDC 1447762)
Formula	$C_{43}H_{72}CoN_6O_7S_3$
$D_{calc.}$/ g cm^{-3}	1.348
μ/mm^{-1}	0.560
Formula Weight	940.17
Colour	violet
Shape	prism
Max Size/mm	0.43
Mid Size/mm	0.30
Min Size/mm	0.26
T/K	100(2)
Crystal System	triclinic
Space Group	P-1
a/Å	13.5871(16)
b/Å	18.615(2)
c/Å	20.023(2)
α/°	90.4613(16)
β/°	100.2779(15)
γ/°	111.1181(14)
V/Å^3	4633.8(9)
Z	4
Z'	2
Θ_{min}/°	1.506
Θ_{max}/°	31.043
Measured Refl.	99178
Independent Refl.	29052
Reflections I >2sigma(I)	20164
R_{int}	0.0480
Parameters	1158
Restraints	340
Largest Peak	2.922
Deepest Hole	-3.075
GooF	1.025
wR_2 (all data)	0.1987
wR_2	0.1687
R_1 (all data)	0.1062
R_1	0.0703

Structure Quality Indicators

Reflections:		Rint 4.80%	complete 98%	
Refinement:	Shift -0.004	Max Peak 2.9	Min Peak -3.1	GooF 1.025

Experimental Extended. A violet prism-shaped crystal with dimensions 0.43×0.30×0.26 mm was mounted on a loop with paratone oil. Data were collected using a Bruker APEX-II CCD diffractometer equipped with an Oxford Cryosystems low-temperature apparatus operating at $T = 100(2)$ K.

Data were measured using MoK↙ radiation (fine-focus sealed tube, 45 kV, 35 mA). The total number of runs and images was based on the strategy calculation from the program **APEX2** (Bruker, 2014). The maximum resolution achieved was $\theta = 31.043°$.

Unit cell indexing was performed by using the **APEX2** (Bruker, 2014) software and refined using **SAINT** (Bruker, V8.34A, 2013) on 9862 reflections. Data reduction, scaling and absorption corrections were performed using **SAINT** (Bruker, V8.34A, 2013) and **SADABS-2014/5** (Bruker, 2014/5). wR_2(int) was 0.0851 before and 0.0544 after correction. The ratio of minimum to maximum transmission is 0.8921. The λ/2 correction factor is 0.00150. The final completeness is 99.9% out to 31.043 in θ. The absorption coefficient (μ) of this material is 0.560 mm^{-1} and the minimum and maximum transmissions are 0.6657 and 0.7462.

The structure was solved with **ShelXT-2014/4** (Sheldrick, 2015) in the space group P-1 (# 2) by Direct Methods using the Direct Methods solution method and by using **Olex2** (Dolomanov et al., 2009) as the graphical interface. The structure was refined by Least Squares using **ShelXL-2014/7** (Sheldrick, 2008). All non-hydrogen atoms were refined anisotropically. Hydrogen atom positions were calculated geometrically and refined using the riding model.

The value of Z' is 2. There are four independent molecules (two cation-anion assemblies) in the asymmetric unit. Parts of the structure are disordered and the disorder was modelled by splitting the atoms in two parts and refining with similarity restraints.

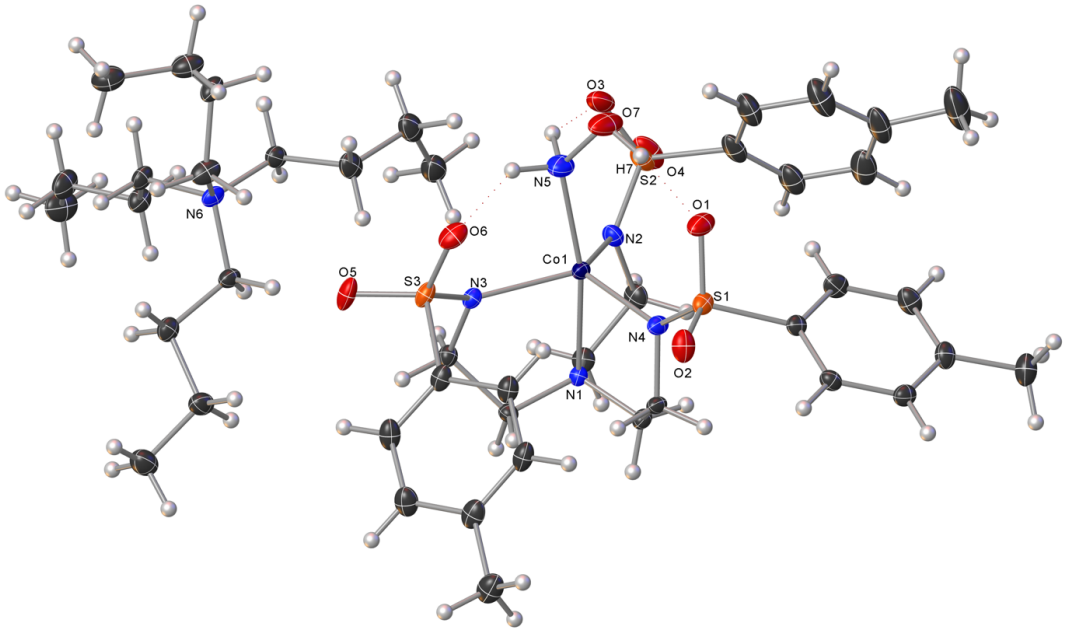

Figure S11:

One of the two formula units in the asymmetric. Only one disorder component is plotted for clarity.

Data Plots: Diffraction Data

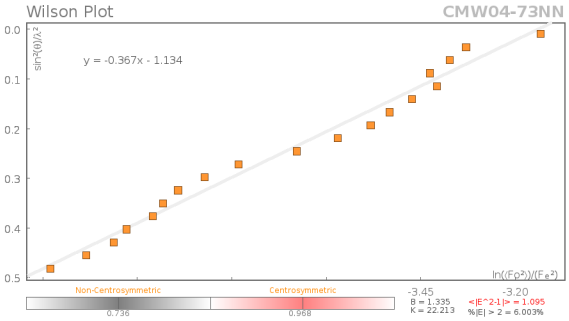

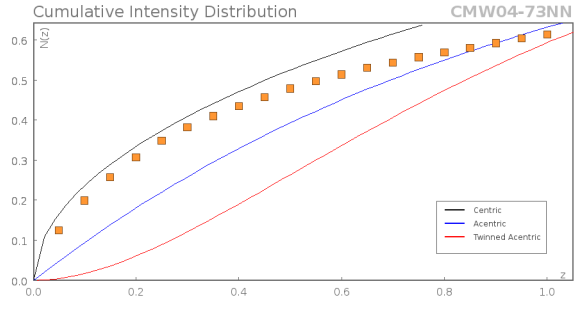

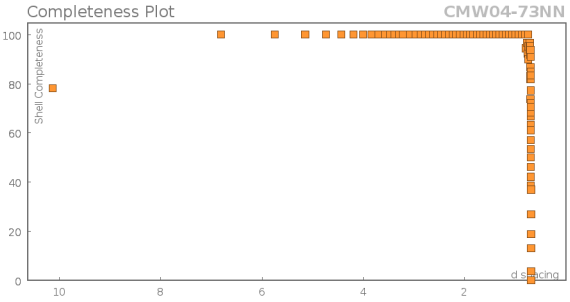

Data Plots: Refinement and Data

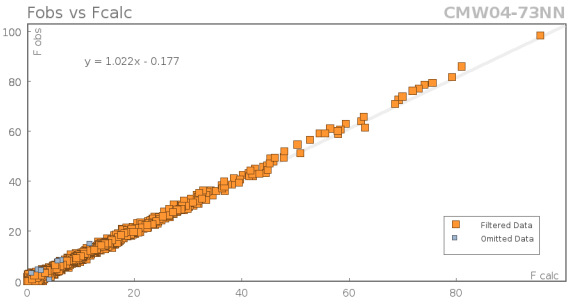

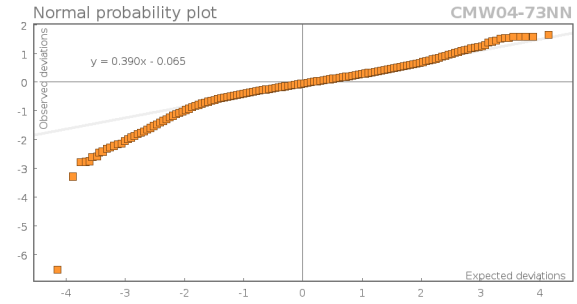

Reflection Statistics

Total reflections (after filtering)	99221	Unique reflections	29052
Completeness	0.98	Mean I/σ	10.75
hklsub>max</sub> collected	(19, 26, 28)	hklsub>min</sub> collected	(-19, -26, -28)
hkl_{max} used	(19, 26, 28)	hkl_{min} used	(-19, -26, 0)
Lim d_{max} collected	100.0	Lim d_{min} collected	0.36
d_{max} used	13.53	d_{min} used	0.69
Friedel pairs	26842	Friedel pairs merged	1
Inconsistent equivalents	0	R_{int}	0.048
R_{sigma}	0.0534	Intensity transformed	0
Omitted reflections	0	Omitted by user (OMIT hkl)	43
Multiplicity	(21770, 26678, 6281, 618, 556)	Maximum multiplicity	9
Removed systematic absences	0	Filtered off (Shel/OMIT)	0

Images of the Crystal on the Diffractometer

Table S9: Fractional Atomic Coordinates (×10^4) and Equivalent Isotropic Displacement Parameters (Å^2×10^3) for **CMW04-73NN**. U_{eq} is defined as 1/3 of of the trace of the orthogonalised U_{ij}.

Atom	x	y	z	U_{eq}
N6B	1730.8(17)	4129.8(12)	8854.6(12)	30.8(6)
C32A	2805(3)	4765(2)	9003(2)	29.7(9)
C33A	3413(5)	4889(3)	9712(3)	33.4(10)
C34A	4535(5)	5491(3)	9786(3)	37.1(10)
C35A	4593(9)	6289(4)	9607(7)	43.8(14)
C36A	1319(4)	4089(3)	8071.6(18)	33.7(10)
C37A	1253(6)	4742(3)	7678(3)	39.9(16)
C38A	801(7)	4491(4)	6929(3)	46.6(18)
C39A	602(6)	5116(4)	6512(3)	41.9(16)
C40A	922(4)	4255(3)	9194(3)	33.0(11)
C41A	8(5)	3570(3)	9314(3)	33.6(10)
C42A	-707(9)	3796(6)	9699(7)	40(1)
C43A	-1205(6)	3382(5)	10264(4)	48.3(14)
C32B	2555(5)	4628(3)	9470(3)	29.7(9)
C33B	2660(5)	5433(3)	9677(4)	33.4(10)
C34B	3789(5)	5936(3)	10022(3)	37.1(10)
C35B	4645(7)	6117(5)	9595(7)	43.8(14)
C36B	1989(5)	4569(3)	8250(2)	33.7(10)
C37B	1186(5)	4130(3)	7639(2)	27.3(12)
C38B	1566(5)	4524(4)	7022(2)	35.9(16)
C39B	790(6)	4245(4)	6357(3)	36.1(16)
C40B	667(4)	4107(4)	9028(3)	33.0(11)
C41B	315(4)	3839(4)	9689(3)	33.6(10)
C42B	-824(7)	3789(6)	9664(7)	40(1)
C43B	-1587(5)	3043(5)	9852(4)	48.3(14)
C37'	5427(6)	8520(6)	9759(3)	21.8(12)
C38'	4210(6)	8214(5)	9739(4)	27.3(10)
C39'	3819(5)	8341(4)	10376(3)	29.5(9)
C37	5440(7)	8384(6)	9726(3)	21.8(12)
C38	4309(6)	8217(4)	9873(4)	27.3(10)
C39	3936(5)	8889(4)	9914(3)	29.5(9)
S1B	-869.6(5)	-1205.6(4)	6457.5(4)	18.28(13)
C7'	-474(10)	-1921(6)	6109(4)	18.2(6)
C8'	339(7)	-2123(5)	6502(4)	20.7(7)
C9'	624(5)	-2715(4)	6278(3)	22.9(8)
C10'	99(5)	-3149(3)	5658(3)	18.1(8)
C11'	-686(5)	-2950(3)	5255(3)	17.8(8)
C12'	-964(5)	-2346(3)	5466(3)	16.2(7)
C13'	364(6)	-3830(4)	5449(4)	28.6(10)
C7B	-506(10)	-1896(7)	6055(4)	18.2(6)
C8B	303(7)	-2113(5)	6397(4)	20.7(7)
C9B	495(5)	-2703(4)	6075(3)	22.9(8)
C10B	-119(5)	-3052(3)	5437(3)	18.1(8)
C11B	-889(5)	-2788(3)	5111(3)	17.8(8)

Atom	x	y	z	U_{eq}
C12B	-1109(5)	-2199(3)	5418(3)	16.2(7)
C13B	90(6)	-3715(4)	5122(4)	28.6(10)
C36	5561(2)	8690.9(18)	9023.0(15)	22.7(6)
C2B	3153(2)	602(2)	7256.7(16)	26.5(6)
C1E	7925(3)	3153(2)	7725(2)	35.7(8)
O7B	-476(2)	-702.5(13)	8350.8(12)	27.5(5)
C1C	8193(3)	3946.5(19)	7821.2(18)	29.6(7)
C1D	6709(3)	3725.3(19)	8382.0(19)	31.7(7)
C1	7981(2)	6314.7(16)	6712.1(15)	17.5(5)
C1B	2950(2)	1206.4(19)	6810.1(16)	24.4(6)
C3B	1333(2)	1995.5(16)	6996.9(15)	21.4(6)
C4	6478(2)	6708.8(14)	6270.5(13)	14.3(5)
C2	8239(2)	5736.0(17)	7168.5(16)	21.0(5)
C4B	1486(2)	1641.4(16)	6355.6(14)	20.4(5)
O3B	2263.3(19)	196.0(14)	8946.0(11)	27.7(5)
C5	6456(2)	5449.4(15)	5892.8(14)	15.6(5)
C5B	1471(2)	397.9(17)	5931.9(14)	21.1(6)
N1B	1790.7(18)	965.1(14)	6522.4(11)	17.8(4)
C3	6380(2)	7107.4(15)	6908.8(14)	15.3(5)
C8	5286(2)	2922.1(16)	6475.0(15)	21.0(6)
C9	5480(2)	2319.7(17)	6184.3(16)	22.9(6)
C10	4877(2)	1939.0(15)	5558.2(16)	20.2(5)
C11	4075(2)	2182.9(15)	5220.1(14)	18.2(5)
C12	3875(2)	2785.5(15)	5509.3(14)	16.1(5)
N3B	585.9(19)	1380.9(14)	7328.1(12)	17.9(4)
C13	5059(3)	1264.8(18)	5254.2(19)	28.7(7)
O1B	-1015.6(19)	-1449.9(12)	7128.2(12)	26.3(5)
N5B	205(2)	50.6(15)	8201.7(13)	21.8(5)
O5B	-353.3(19)	2264.6(13)	7595.3(11)	26.6(5)
C15B	1525(3)	-1429(2)	8425.5(17)	28.5(6)
C16B	1274(3)	-2220(2)	8308.5(19)	32.9(7)
C17	7595(3)	4232.1(17)	8167.6(17)	25.6(6)
C6	5289(2)	4924.6(14)	5857.7(13)	15.2(5)
C17B	1930(3)	-2499(2)	8009.0(19)	38.3(8)
C6B	289(2)	-114.8(16)	5857.8(13)	19.6(5)
C7	4469(2)	3149.1(14)	6137.7(14)	14.8(5)
C19	7072(3)	2641.4(19)	7969(2)	35.2(8)
C20	6816(4)	1781(2)	7904(3)	49.9(12)
C20B	1672(4)	-3357(3)	7909(2)	52.4(11)
C21	3836(2)	6461.8(16)	6466.7(15)	17.7(5)
C21B	-1214(2)	1375.5(16)	6489.8(15)	18.3(5)
C22	3810(2)	7082.9(16)	6090.9(16)	22.2(6)
C22B	-1229(2)	2012.8(16)	6139.6(15)	20.9(5)
C23	3315(2)	6946.8(17)	5409.4(17)	24.2(6)
C23B	-1724(2)	1910.7(17)	5456.1(15)	21.7(6)
C24	2833(2)	6199.9(18)	5088.5(16)	22.3(6)
C24B	-2216(2)	1178.5(18)	5114.9(15)	21.6(6)
C25	2855(2)	5585.9(17)	5474.9(16)	21.8(6)
N2B	2437.9(19)	449.4(16)	7754.5(12)	22.4(5)
C25B	-2201(2)	540.8(17)	5478.4(15)	22.4(6)
N4B	106.5(18)	-409.0(13)	6526.7(11)	16.7(4)
C26	3354(2)	5710.7(16)	6156.1(15)	19.6(5)
C14B	2443(3)	-913(2)	8248.1(15)	26.5(6)
C26B	-1700(2)	636.8(16)	6157.6(15)	21.4(6)
O2B	-1826.3(18)	-1210.1(14)	6000.2(14)	33.9(6)
C27	2317(3)	6072(2)	4339.8(17)	28.0(7)
O4B	3994(2)	396.3(17)	8613.9(13)	38.3(6)

Atom	x	y	z	U_{eq}
C27B	-2744(3)	1077(2)	4372.8(16)	28.2(7)
O6B	-1159.6(17)	863.9(13)	7690.5(11)	22.8(4)
C28	7339(2)	8521.0(15)	9172.7(14)	18.4(5)
C28A	1796(3)	3346.8(15)	8946.1(17)	33.3(8)
C29	6843(3)	7684.1(16)	8865.1(16)	24.5(6)
C29A	2744(3)	3242.2(18)	8715.5(18)	32.7(7)
C30	7562(3)	7237.7(17)	9128.6(17)	28.1(7)
C30A	2742(3)	2429.2(18)	8822.7(17)	30.8(7)
S2B	2832.2(6)	103.2(5)	8423.7(4)	25.24(16)
C31	8562(3)	7424.6(19)	8816.6(17)	30.5(7)
C18	6455(3)	2934(2)	8289(2)	38.8(9)
C31A	3769(3)	2371(2)	8668.2(18)	33.9(7)
C18B	2826(3)	-1969(3)	7813(2)	41.3(8)
C33	6702(2)	9077.4(15)	8152.2(13)	17.1(5)
C34	6008(3)	9455.2(17)	7042.3(15)	24.4(6)
C35	5683(3)	10049.1(19)	6631.2(17)	29.2(7)
C19B	3083(3)	-1189(3)	7929.8(19)	36.2(8)
C40	7261(2)	9820.4(15)	9302.2(14)	18.3(5)
C41	8415(2)	10248.2(15)	9232.0(15)	19.2(5)
C42	8862(3)	11050.9(17)	9599.0(18)	28.3(7)
C43	10013(3)	11487.3(19)	9533.3(19)	33.8(8)
Co1	6020.0(3)	5520.5(2)	7300.2(2)	12.48(8)
Co1B	917.8(3)	381.7(2)	7326.9(2)	14.63(8)
S3B	-507.8(6)	1490.2(4)	7345.8(4)	18.24(13)
N1	6805.7(17)	6049.8(12)	6459.8(11)	12.2(4)
N2	7563.5(19)	5593.3(13)	7690.4(12)	17.4(4)
N3	5669.1(17)	6517.6(12)	7283.4(11)	13.5(4)
N4	5158.5(18)	4672.0(12)	6544.8(11)	15.4(4)
N5	5412(2)	5266.0(15)	8207.3(13)	25.6(5)
N6	6715.9(18)	9030.4(13)	8911.5(11)	15.8(4)
O1	4089.3(19)	3685.5(12)	7216.5(11)	27.1(5)
O2	3185.5(17)	3887.3(12)	6096.0(12)	24.9(5)
O3	7477(2)	5345.5(13)	8889.4(11)	29.2(5)
O4	9166.2(19)	5534.5(14)	8503.6(13)	34.3(6)
O5	4737.3(16)	7411.3(12)	7527.2(12)	23.9(5)
O6	3969.0(16)	6026.8(13)	7701.3(11)	24.0(4)
O7	4747(2)	4534.1(14)	8396.5(12)	38.6(6)
S1	4168.3(5)	3889.5(4)	6522.9(3)	16.47(13)
S2	8000.5(6)	5250.7(4)	8343.9(4)	23.00(15)
S3	4579.9(5)	6624.2(4)	7314.9(4)	16.73(13)
C32	6285(2)	9664.2(15)	7806.5(14)	18.8(5)

Table S10: Anisotropic Displacement Parameters (×10^4) **CMW04-73NN**. The anisotropic displacement factor exponent takes the form: -2PI^2[a*^2 × U_{11} + ... 2hka* × b* × U_{12}]

Atom	U_{11}	U_{22}	U_{33}	U_{23}	U_{13}	U_{12}
N6B	19.8(12)	18.6(12)	42.9(17)	11.3(11)	-5.5(11)	-0.8(10)
C32A	29.3(19)	18.2(15)	34.7(19)	-1.6(14)	4.4(15)	1.6(14)
C33A	41(2)	21.4(17)	31(2)	1.1(14)	2.7(16)	5.0(15)
C34A	43(2)	27.2(19)	29(2)	-3.6(16)	5.3(17)	-0.3(16)
C35A	58(2)	26(3)	33(2)	-2(2)	11.1(18)	-3(2)
C36A	31(2)	33(2)	28(2)	9.4(16)	1.7(17)	3.2(16)
C37A	38(4)	35(3)	43(3)	7(2)	8(3)	9(3)
C38A	48(3)	48(3)	42(3)	5(2)	11(2)	15(2)
C39A	38(4)	43(4)	40(3)	-2(3)	11(3)	7(3)
C40A	39.9(17)	24.9(16)	31.4(18)	2.3(13)	10.5(14)	6.8(13)

Atom	U_{11}	U_{22}	U_{33}	U_{23}	U_{13}	U_{12}
C41A	32(2)	34(2)	26(2)	8.8(16)	-0.9(15)	5.2(16)
C42A	37(2)	47(2)	27(2)	11.7(15)	4.6(18)	6.0(16)
C43A	36(3)	54(3)	35(3)	13(2)	1(2)	-5(2)
C32B	29.3(19)	18.2(15)	34.7(19)	-1.6(14)	4.4(15)	1.6(14)
C33B	41(2)	21.4(17)	31(2)	1.1(14)	2.7(16)	5.0(15)
C34B	43(2)	27.2(19)	29(2)	-3.6(16)	5.3(17)	-0.3(16)
C35B	58(2)	26(3)	33(2)	-2(2)	11.1(18)	-3(2)
C36B	31(2)	33(2)	28(2)	9.4(16)	1.7(17)	3.2(16)
C37B	26(2)	30(2)	19.4(19)	11.0(17)	3.4(17)	2.8(19)
C38B	37(3)	39(3)	24(2)	14(2)	9(2)	3(3)
C39B	35(3)	38(4)	21(3)	9(2)	5(2)	-3(3)
C40B	39.9(17)	24.9(16)	31.4(18)	2.3(13)	10.5(14)	6.8(13)
C41B	32(2)	34(2)	26(2)	8.8(16)	-0.9(15)	5.2(16)
C42B	37(2)	47(2)	27(2)	11.7(15)	4.6(18)	6.0(16)
C43B	36(3)	54(3)	35(3)	13(2)	1(2)	-5(2)
C37'	23.5(13)	18(3)	22.4(15)	-3.0(14)	10.8(11)	2.4(13)
C38'	22.6(14)	34.3(13)	19.8(19)	0.8(12)	6.3(14)	3.5(11)
C39'	24(2)	38.3(19)	23(2)	2.9(15)	6.2(16)	8.1(16)
C37	23.5(13)	18(3)	22.4(15)	-3.0(14)	10.8(11)	2.4(13)
C38	22.6(14)	34.3(13)	19.8(19)	0.8(12)	6.3(14)	3.5(11)
C39	24(2)	38.3(19)	23(2)	2.9(15)	6.2(16)	8.1(16)
S1B	13.0(3)	17.9(3)	19.0(3)	2.4(2)	1.8(2)	0.4(2)
C36	13.9(12)	25.9(14)	21.1(14)	-2.5(11)	5.7(10)	-2.1(10)
C2B	14.2(13)	43.1(18)	19.4(14)	0.0(12)	3.5(11)	7.2(12)
C1E	35.6(19)	32.0(17)	39(2)	-4.0(14)	-10.7(15)	21.0(15)
O7B	36.8(13)	25.0(11)	24.4(11)	9.7(9)	17.7(10)	10.2(9)
C1C	27.7(16)	25.2(15)	34.8(18)	4.7(13)	-4.9(13)	13.5(13)
C1D	32.0(17)	22.3(15)	42(2)	5.9(13)	0.6(15)	13.8(13)
C1	11.1(11)	18.4(12)	22.2(13)	0.5(10)	4.2(10)	4.0(9)
C1B	13.7(12)	32.1(15)	20.2(14)	-2.5(11)	5.9(10)	-1.2(11)
C3B	19.1(13)	19.5(13)	19.6(13)	2.1(10)	5(1)	-0.4(10)
C4	15.6(11)	13.6(11)	14.7(12)	3.6(9)	4.8(9)	5.7(9)
C2	16.7(12)	24.7(13)	25.2(14)	2.1(11)	3.1(11)	12.3(11)
C4B	19.5(13)	20.1(13)	15.0(12)	3.9(10)	5.1(10)	-1.5(10)
O3B	35.3(13)	36.3(12)	10.6(9)	-2.1(8)	-1.8(8)	15(1)
C5	17.9(12)	14.5(11)	14.7(12)	-0.5(9)	5.6(9)	5.0(9)
C5B	22.5(14)	23.3(13)	12.0(12)	-0.2(10)	6.3(10)	0.8(11)
N1B	15(1)	21.4(11)	10.6(10)	-0.2(8)	3.4(8)	-1.1(8)
C3	14.4(11)	13.7(11)	17.4(12)	0.2(9)	4.2(9)	4.4(9)
C8	18.7(13)	18.6(12)	18.8(13)	-2(1)	-4.3(10)	2.4(10)
C9	18.0(13)	19.8(13)	28.3(15)	2.5(11)	-2.1(11)	7.1(10)
C10	18.1(13)	13.8(11)	27.5(15)	-0.5(10)	5.4(11)	3.9(10)
C11	18.3(12)	15.8(11)	16.5(12)	-0.6(9)	2(1)	2.2(10)
C12	14.6(11)	15.3(11)	16.7(12)	3.0(9)	1.3(9)	4.3(9)
N3B	16.1(11)	19.7(11)	15.6(11)	3.4(8)	4.6(8)	3.2(9)
C13	29.6(16)	20.2(14)	37.3(18)	-3.3(12)	7.1(14)	10.1(12)
O1B	30.9(12)	20(1)	25.3(11)	3.9(8)	15.7(9)	1.3(9)
N5B	21.3(12)	26.0(12)	19.4(12)	8.4(9)	8.9(10)	7.6(10)
O5B	29.4(12)	25.7(11)	23.7(11)	-4.1(8)	0.2(9)	11.5(9)
C15B	28.0(14)	39.6(15)	22.9(15)	-5.3(11)	-1.9(11)	21.8(12)
C16B	31.7(16)	38.0(16)	32.8(17)	-8.2(13)	-3.3(13)	21.9(13)
C17	24.3(15)	19.4(13)	29.2(16)	4.3(11)	-8.4(12)	9.7(11)
C6	19.3(12)	13.1(11)	10.9(11)	0.1(8)	3.1(9)	3.0(9)
C17B	36.9(16)	55.7(18)	30.6(17)	-14.0(14)	-9.7(13)	34.8(14)
C6B	20.1(13)	22.1(13)	8.8(11)	1.0(9)	-1.0(9)	0.4(10)
C7	14.1(11)	11.3(10)	15.9(12)	0.5(9)	2.3(9)	1.2(9)
C19	34.7(18)	22.5(15)	45(2)	-0.9(14)	-12.9(15)	15.9(14)

Atom	U_{11}	U_{22}	U_{33}	U_{23}	U_{13}	U_{12}
C20	53(3)	22.9(17)	67(3)	-3.0(17)	-12(2)	17.0(17)
C20B	62(3)	56(2)	51(3)	-15.2(18)	-5(2)	44(2)
C21	11.1(11)	19.8(12)	22.3(13)	-4.3(10)	1.5(10)	6.6(9)
C21B	13.2(11)	19.6(12)	19.7(13)	3.7(10)	3.4(10)	2.8(10)
C22	14.9(12)	17.4(12)	32.0(16)	-4.5(11)	-1.2(11)	6.1(10)
C22B	17.2(13)	19.1(12)	23.4(14)	2.7(10)	1.4(11)	4.4(10)
C23	19.7(14)	21.8(13)	29.9(16)	-1.2(11)	-1.4(12)	9.3(11)
C23B	17.9(13)	24.5(14)	23.4(14)	7.6(11)	3.6(11)	8.7(11)
C24	15.0(12)	27.1(14)	26.6(15)	-4.6(11)	0.4(11)	11.8(11)
C24B	13.8(12)	31.9(15)	19.9(14)	2.8(11)	3.6(10)	9.4(11)
C25	16.7(13)	20.8(13)	26.9(15)	-7.3(11)	0.6(11)	7.9(10)
N2B	15.0(11)	36.8(14)	14.1(11)	-0.6(10)	0.3(9)	9.1(10)
C25B	17.5(13)	23.4(13)	21.1(14)	-0.7(11)	0.6(11)	2.9(11)
N4B	15.8(10)	17.3(10)	11.2(10)	2.3(8)	1.8(8)	-0.3(8)
C26	15.3(12)	18.0(12)	24.4(14)	-3.3(10)	1.5(10)	6.1(10)
C14B	22.6(13)	43.3(16)	16.6(13)	-5.2(11)	-6.3(10)	20.4(12)
C26B	19.5(13)	18.9(12)	22.2(14)	4.2(10)	2.7(11)	3.3(10)
O2B	16.2(10)	25.7(11)	49.0(15)	3.8(10)	-7.7(10)	1.5(9)
C27	24.1(15)	33.8(16)	26.6(16)	-5.1(13)	-1.9(12)	14.6(13)
O4B	21.6(12)	57.0(17)	26.4(13)	-1.8(11)	-10.4(10)	10.2(11)
C27B	26.9(16)	39.9(18)	19.3(14)	-0.5(12)	1.4(12)	15.7(14)
O6B	22.1(10)	29.5(11)	19.4(10)	7.7(8)	9.5(8)	9.7(9)
C28	21.2(13)	14.5(11)	16.2(12)	-0.7(9)	1.3(10)	3.9(10)
C28A	53(2)	16.0(13)	29.1(17)	8.4(12)	14.6(15)	7.7(13)
C29	28.1(15)	14.5(12)	23.8(15)	-2.4(10)	-1.6(12)	2.7(11)
C29A	46(2)	18.7(13)	26.2(16)	1.9(11)	9.5(14)	2.8(13)
C30	33.0(17)	17.5(13)	28.6(16)	-0.1(11)	-1.4(13)	6.7(12)
C30A	42.4(19)	21.4(14)	23.3(15)	1.1(11)	7.3(13)	5.2(13)
S2B	20.1(3)	38.8(4)	13.4(3)	-3.4(3)	-5.3(3)	11.0(3)
C31	40.4(19)	24.8(15)	25.6(16)	-0.7(12)	0.0(14)	14.1(14)
C18	34.2(19)	20.5(15)	56(2)	6.2(15)	-1.6(17)	8.6(13)
C31A	41.5(19)	28.1(16)	24.2(16)	-0.7(12)	5.1(14)	4.3(14)
C18B	35.0(16)	64.5(19)	35.9(19)	-11.7(15)	-4.6(14)	37.7(15)
C33	20.3(13)	14.9(11)	12.8(12)	-0.8(9)	3.8(10)	2.3(10)
C34	30.9(16)	20.6(13)	17.6(14)	0.4(10)	1.4(12)	6.4(12)
C35	33.6(17)	25.8(15)	25.5(16)	3.8(12)	0.0(13)	10.4(13)
C19B	25.3(15)	62(2)	29.8(17)	-5.7(14)	-1.4(12)	29.5(15)
C40	18.0(12)	15.3(11)	17.6(13)	-5.2(9)	3(1)	1.8(10)
C41	16.6(12)	16.2(12)	21.1(13)	-1.6(10)	5.1(10)	1.2(10)
C42	30.3(16)	18.3(13)	28.6(16)	-6.2(11)	6.7(13)	-0.4(12)
C43	30.1(17)	23.0(15)	32.4(18)	-3.6(13)	2.5(14)	-7.1(13)
Co1	13.36(16)	11.97(15)	11.08(16)	0.07(12)	2.54(12)	3.36(12)
Co1B	12.19(16)	19.86(17)	8.91(16)	1.44(12)	1.65(12)	2.60(13)
S3B	17.8(3)	19.8(3)	16.1(3)	2.0(2)	3.4(2)	5.6(2)
N1	10.0(9)	11.9(9)	14.1(10)	-0.3(7)	2.7(8)	3.2(7)
N2	18.4(11)	17.2(10)	18.3(11)	3.6(8)	2.0(9)	9.0(9)
N3	11.4(9)	14.7(9)	14.6(10)	-1.0(8)	4.0(8)	4.4(8)
N4	17(1)	12.7(9)	13.7(10)	0.8(8)	4.4(8)	1.4(8)
N5	32.0(14)	23.3(12)	20.5(12)	5.5(9)	10.7(11)	6.2(10)
N6	14(1)	16.6(10)	12.9(10)	-3.3(8)	1.4(8)	1.7(8)
O1	36.1(13)	19.4(10)	20.8(11)	1.6(8)	14.9(9)	-0.3(9)
O2	15.5(9)	18.7(9)	37.8(13)	-3.2(9)	3.7(9)	4.0(8)
O3	42.3(14)	24.0(11)	16.8(10)	4.0(8)	-1.8(9)	10.4(10)
O4	27.1(12)	25.7(11)	39.3(14)	5.1(10)	-13.6(10)	6.3(9)
O5	16.9(10)	24.1(10)	30.5(12)	-13.0(9)	-0.1(8)	9.9(8)
O6	16.2(9)	31.1(11)	23.0(11)	-3.0(8)	8.8(8)	4.6(8)
O7	56.0(17)	24.5(11)	21.8(12)	4.4(9)	15.0(11)	-4.6(11)

Atom	U_{11}	U_{22}	U_{33}	U_{23}	U_{13}	U_{12}
S1	15.7(3)	12.9(3)	18.1(3)	-0.3(2)	6.0(2)	0.8(2)
S2	24.3(4)	17.8(3)	22.4(4)	3.1(3)	-6.5(3)	7.6(3)
S3	12.0(3)	18.8(3)	18.9(3)	-6.1(2)	2.8(2)	5.4(2)
C32	17.1(12)	15.9(12)	20.3(13)	-2.2(10)	2.8(10)	3.1(10)

Table S12: Bond Lengths in Å for **CMW04-73NN**.

Atom	Atom	Length/Å
N6B	C32A	1.488(3)
N6B	C36A	1.559(3)
N6B	C40A	1.474(3)
N6B	C32B	1.541(3)
N6B	C36B	1.489(3)
N6B	C40B	1.532(3)
N6B	C28A	1.502(3)
C32A	C33A	1.480(5)
C33A	C34A	1.513(5)
C34A	C35A	1.508(5)
C36A	C37A	1.474(5)
C37A	C38A	1.515(5)
C38A	C39A	1.513(3)
C40A	C41A	1.483(4)
C41A	C42A	1.507(5)
C42A	C43A	1.498(5)
C32B	C33B	1.500(5)
C33B	C34B	1.511(5)
C34B	C35B	1.507(5)
C36B	C37B	1.490(5)
C37B	C38B	1.517(5)
C38B	C39B	1.499(5)
C40B	C41B	1.515(5)
C41B	C42B	1.508(5)
C42B	C43B	1.501(5)
C37'	C38'	1.536(5)
C37'	C36	1.538(5)
C38'	C39'	1.513(3)
C37	C38	1.538(5)
C37	C36	1.537(5)
C38	C39	1.515(3)
S1B	C7'	1.785(4)
S1B	C7B	1.768(4)
S1B	O1B	1.446(2)
S1B	N4B	1.578(2)
S1B	O2B	1.448(2)
C7'	C8'	1.405(8)
C7'	C12'	1.423(8)
C8'	C9'	1.388(8)
C9'	C10'	1.398(8)
C10'	C11'	1.382(8)
C10'	C13'	1.512(8)
C11'	C12'	1.392(7)
C7B	C8B	1.377(8)
C7B	C12B	1.378(8)
C8B	C9B	1.395(8)
C9B	C10B	1.403(8)
C10B	C11B	1.375(8)
C10B	C13B	1.519(8)
C11B	C12B	1.401(7)
C36	N6	1.525(4)
C2B	C1B	1.515(5)
C2B	N2B	1.473(4)
C1E	C1C	1.391(5)
C1E	C19	1.380(6)
O7B	N5B	1.443(3)
C1C	C17	1.390(5)
C1D	C17	1.377(5)
C1D	C18	1.389(5)
C1	C2	1.514(4)
C1	N1	1.479(3)
C1B	N1B	1.475(4)
C3B	C4B	1.519(4)
C3B	N3B	1.481(4)
C4	C3	1.523(4)
C4	N1	1.479(3)
C2	N2	1.475(4)
C4B	N1B	1.483(4)
O3B	S2B	1.450(2)
C5	C6	1.523(4)
C5	N1	1.473(3)
C5B	N1B	1.472(3)
C5B	C6B	1.523(4)
N1B	Co1B	2.228(2)
C3	N3	1.486(3)
C8	C9	1.387(4)
C8	C7	1.394(4)
C9	C10	1.395(4)
C10	C11	1.396(4)
C10	C13	1.508(4)
C11	C12	1.390(4)
C12	C7	1.386(4)
N3B	Co1B	2.066(2)
N3B	S3B	1.577(3)
N5B	Co1B	2.140(2)
O5B	S3B	1.451(2)
C15B	C16B	1.394(5)
C15B	C14B	1.380(5)
C16B	C17B	1.394(5)
C17	S2	1.786(3)
C6	N4	1.477(3)
C17B	C20B	1.509(6)

Atom	Atom	Length/Å
C17B	C18B	1.386(6)
C6B	N4B	1.479(3)
C7	S1	1.778(3)
C19	C20	1.511(5)
C19	C18	1.389(6)
C21	C22	1.392(4)
C21	C26	1.397(4)
C21	S3	1.777(3)
C21B	C22B	1.388(4)
C21B	C26B	1.394(4)
C21B	S3B	1.779(3)
C22	C23	1.386(4)
C22B	C23B	1.391(4)
C23	C24	1.398(4)
C23B	C24B	1.392(4)
C24	C25	1.392(4)
C24	C27	1.515(4)
C24B	C25B	1.401(4)
C24B	C27B	1.509(4)
C25	C26	1.387(4)
N2B	S2B	1.582(3)
N2B	Co1B	2.048(2)
C25B	C26B	1.387(4)
N4B	Co1B	2.028(2)
C14B	S2B	1.784(4)
C14B	C19B	1.393(4)
O4B	S2B	1.448(2)
O6B	S3B	1.452(2)
C28	C29	1.530(4)
C28	N6	1.523(4)
C28A	C29A	1.518(5)
C29	C30	1.527(4)
C29A	C30A	1.529(5)
C30	C31	1.524(5)
C30A	C31A	1.522(5)
C18B	C19B	1.374(6)
C33	N6	1.521(3)
C33	C32	1.520(4)
C34	C35	1.527(4)
C34	C32	1.521(4)
C40	C41	1.514(4)
C40	N6	1.521(3)
C41	C42	1.520(4)
C42	C43	1.510(5)
Co1	N1	2.202(2)
Co1	N2	2.058(2)
Co1	N3	2.075(2)
Co1	N4	2.037(2)
Co1	N5	2.115(3)
N2	S2	1.575(2)
N3	S3	1.574(2)
N4	S1	1.581(2)
N5	O7	1.435(3)
O1	S1	1.455(2)
O2	S1	1.450(2)
O3	S2	1.447(3)
O4	S2	1.450(3)
O5	S3	1.451(2)
O6	S3	1.450(2)

Table S13: Bond Angles in ° for **CMW04-73NN**.

Atom	Atom	Atom	Angle/°
C32A	N6B	C36A	106.0(2)
C32A	N6B	C28A	112.7(2)
C40A	N6B	C32A	114.5(2)
C40A	N6B	C36A	107.4(2)
C40A	N6B	C28A	113.0(2)
C36B	N6B	C32B	105.7(3)
C36B	N6B	C40B	112.4(4)
C36B	N6B	C28A	123.4(4)
C40B	N6B	C32B	101.8(4)
C28A	N6B	C36A	102.2(2)
C28A	N6B	C32B	102.8(3)
C28A	N6B	C40B	108.1(3)
C33A	C32A	N6B	117.0(4)
C32A	C33A	C34A	112.3(4)
C35A	C34A	C33A	115.5(5)
C37A	C36A	N6B	125.9(4)
C36A	C37A	C38A	111.6(4)
C39A	C38A	C37A	114.1(4)
N6B	C40A	C41A	118.3(4)
C40A	C41A	C42A	111.4(5)
C43A	C42A	C41A	125.9(6)
C33B	C32B	N6B	123.5(4)
C32B	C33B	C34B	113.1(4)
C35B	C34B	C33B	116.8(5)
N6B	C36B	C37B	108.3(4)
C36B	C37B	C38B	107.0(4)
C39B	C38B	C37B	115.8(4)
C41B	C40B	N6B	123.5(4)
C42B	C41B	C40B	110.2(5)
C43B	C42B	C41B	116.2(5)
C38'	C37'	C36	105.7(5)
C39'	C38'	C37'	118.4(4)
C36	C37	C38	112.6(5)
C39	C38	C37	118.0(4)
O1B	S1B	C7'	103.1(4)
O1B	S1B	C7B	106.9(4)
O1B	S1B	N4B	109.36(13)
O1B	S1B	O2B	115.65(15)
N4B	S1B	C7'	107.5(5)
N4B	S1B	C7B	107.1(5)
O2B	S1B	C7'	107.0(3)
O2B	S1B	C7B	103.8(3)
O2B	S1B	N4B	113.33(13)

Atom	Atom	Atom	Angle/°
C8'	C7'	S1B	119.0(5)
C8'	C7'	C12'	116.1(4)
C12'	C7'	S1B	124.8(5)
C9'	C8'	C7'	121.5(6)
C8'	C9'	C10'	121.5(6)
C9'	C10'	C13'	120.7(6)
C11'	C10'	C9'	118.0(5)
C11'	C10'	C13'	121.3(5)
C10'	C11'	C12'	121.1(5)
C11'	C12'	C7'	121.7(5)
C8B	C7B	S1B	119.3(5)
C8B	C7B	C12B	125.1(5)
C12B	C7B	S1B	115.5(5)
C7B	C8B	C9B	116.6(6)
C8B	C9B	C10B	120.7(6)
C9B	C10B	C13B	118.6(6)
C11B	C10B	C9B	119.7(5)
C11B	C10B	C13B	121.7(5)
C10B	C11B	C12B	121.2(5)
C7B	C12B	C11B	116.5(5)
N6	C36	C37'	115.8(4)
N6	C36	C37	114.8(4)
N2B	C2B	C1B	108.1(3)
C19	C1E	C1C	121.0(4)
C17	C1C	C1E	119.8(3)
C17	C1D	C18	120.1(4)
N1	C1	C2	109.8(2)
N1B	C1B	C2B	109.9(2)
N3B	C3B	C4B	108.9(2)
N1	C4	C3	109.3(2)
N2	C2	C1	108.0(2)
N1B	C4B	C3B	109.5(2)
N1	C5	C6	110.4(2)
N1B	C5B	C6B	109.8(2)
C1B	N1B	C4B	111.3(2)
C1B	N1B	Co1B	106.82(17)
C4B	N1B	Co1B	107.79(17)
C5B	N1B	C1B	111.2(2)
C5B	N1B	C4B	112.0(2)
C5B	N1B	Co1B	107.48(16)
N3	C3	C4	108.6(2)
C9	C8	C7	119.4(3)
C8	C9	C10	121.3(3)
C9	C10	C11	118.7(3)
C9	C10	C13	121.3(3)
C11	C10	C13	120.1(3)
C12	C11	C10	120.4(3)
C7	C12	C11	120.3(3)
C3B	N3B	Co1B	111.69(18)
C3B	N3B	S3B	113.8(2)
S3B	N3B	Co1B	129.68(14)
O7B	N5B	Co1B	129.19(19)
C14B	C15B	C16B	119.6(3)
C15B	C16B	C17B	121.1(4)
C1C	C17	S2	119.6(3)
C1D	C17	C1C	119.6(3)
C1D	C17	S2	120.8(3)

Atom	Atom	Atom	Angle/°
N4	C6	C5	108.4(2)
C16B	C17B	C20B	120.6(4)
C18B	C17B	C16B	118.2(4)
C18B	C17B	C20B	121.2(4)
N4B	C6B	C5B	108.3(2)
C8	C7	S1	119.9(2)
C12	C7	C8	120.0(2)
C12	C7	S1	120.1(2)
C1E	C19	C20	121.4(4)
C1E	C19	C18	118.5(3)
C18	C19	C20	120.1(4)
C22	C21	C26	119.7(3)
C22	C21	S3	120.3(2)
C26	C21	S3	119.7(2)
C22B	C21B	C26B	119.9(3)
C22B	C21B	S3B	120.9(2)
C26B	C21B	S3B	119.1(2)
C23	C22	C21	119.4(3)
C21B	C22B	C23B	119.7(3)
C22	C23	C24	121.7(3)
C22B	C23B	C24B	121.3(3)
C23	C24	C27	120.4(3)
C25	C24	C23	118.0(3)
C25	C24	C27	121.5(3)
C23B	C24B	C25B	118.2(3)
C23B	C24B	C27B	120.7(3)
C25B	C24B	C27B	121.1(3)
C26	C25	C24	121.1(3)
C2B	N2B	S2B	114.6(2)
C2B	N2B	Co1B	112.47(18)
S2B	N2B	Co1B	129.36(15)
C26B	C25B	C24B	121.0(3)
S1B	N4B	Co1B	132.14(14)
C6B	N4B	S1B	112.33(17)
C6B	N4B	Co1B	113.89(16)
C25	C26	C21	120.0(3)
C15B	C14B	S2B	121.2(2)
C15B	C14B	C19B	119.5(3)
C19B	C14B	S2B	119.2(3)
C25B	C26B	C21B	119.9(3)
N6	C28	C29	115.1(2)
N6B	C28A	C29A	114.8(2)
C30	C29	C28	110.8(2)
C28A	C29A	C30A	111.2(3)
C31	C30	C29	114.6(3)
C31A	C30A	C29A	110.0(3)
O3B	S2B	N2B	109.11(14)
O3B	S2B	C14B	106.00(15)
N2B	S2B	C14B	108.28(14)
O4B	S2B	O3B	116.03(15)
O4B	S2B	N2B	111.72(15)
O4B	S2B	C14B	105.22(16)
C1D	C18	C19	120.9(4)
C19B	C18B	C17B	121.0(3)
C32	C33	N6	116.8(2)
C32	C34	C35	113.3(3)
C18B	C19B	C14B	120.5(4)

Atom	Atom	Atom	Angle/°
C41	C40	N6	115.1(2)
C40	C41	C42	111.0(2)
C43	C42	C41	111.8(3)
N2	Co1	N1	80.63(9)
N2	Co1	N3	119.24(9)
N2	Co1	N5	97.15(11)
N3	Co1	N1	80.94(8)
N3	Co1	N5	89.40(10)
N4	Co1	N1	81.16(8)
N4	Co1	N2	116.32(9)
N4	Co1	N3	117.09(9)
N4	Co1	N5	110.77(10)
N5	Co1	N1	167.29(9)
N3B	Co1B	N1B	80.53(9)
N3B	Co1B	N5B	90.54(10)
N5B	Co1B	N1B	168.41(10)
N2B	Co1B	N1B	80.51(10)
N2B	Co1B	N3B	118.26(10)
N2B	Co1B	N5B	97.48(10)
N4B	Co1B	N1B	80.41(9)
N4B	Co1B	N3B	116.20(10)
N4B	Co1B	N5B	110.37(10)
N4B	Co1B	N2B	117.51(10)
N3B	S3B	C21B	107.25(13)
O5B	S3B	N3B	112.77(13)
O5B	S3B	C21B	105.30(13)
O5B	S3B	O6B	116.01(14)
O6B	S3B	N3B	108.64(13)
O6B	S3B	C21B	106.27(13)
C1	N1	Co1	107.32(16)
C4	N1	C1	110.9(2)
C4	N1	Co1	108.17(15)
C5	N1	C1	111.0(2)
C5	N1	C4	111.9(2)
C5	N1	Co1	107.37(15)
C2	N2	Co1	112.50(17)
C2	N2	S2	114.12(19)
S2	N2	Co1	129.55(14)
C3	N3	Co1	110.88(15)
C3	N3	S3	113.97(17)
S3	N3	Co1	129.80(13)
C6	N4	Co1	113.05(16)
C6	N4	S1	112.32(17)
S1	N4	Co1	132.39(14)
O7	N5	Co1	128.53(19)
C28	N6	C36	111.2(2)
C33	N6	C36	108.9(2)
C33	N6	C28	107.8(2)
C33	N6	C40	112.0(2)
C40	N6	C36	108.3(2)
C40	N6	C28	108.7(2)
N4	S1	C7	107.54(12)
O1	S1	C7	105.52(13)
O1	S1	N4	108.90(13)
O2	S1	C7	105.14(13)
O2	S1	N4	113.42(13)
O2	S1	O1	115.65(14)
N2	S2	C17	108.30(14)
O3	S2	C17	105.70(16)
O3	S2	N2	109.15(13)
O3	S2	O4	116.07(16)
O4	S2	C17	104.81(15)
O4	S2	N2	112.26(14)
N3	S3	C21	106.75(12)
O5	S3	C21	104.87(13)
O5	S3	N3	112.54(12)
O6	S3	C21	107.14(13)
O6	S3	N3	108.81(13)
O6	S3	O5	116.12(13)
C33	C32	C34	108.3(2)

Table S14: Hydrogen Fractional Atomic Coordinates (×10^4) and Equivalent Isotropic Displacement Parameters (Å^2×10^3) for **CMW04-73NN**. U_{eq} is defined as 1/3 of of the trace of the orthogonalised U_{ij}.

Atom	x	y	z	U_{eq}
H32A	3252	4663	8702	36
H32B	2708	5252	8878	36
H33A	3463	4395	9860	40
H33B	3018	5054	10014	40
H34A	4912	5528	10264	45
H34B	4930	5312	9494	45
H35A	4445	6300	9110	66
H35B	5314	6665	9794	66
H35C	4058	6420	9798	66
H36A	1767	3875	7857	40
H36B	584	3691	7979	40
H37A	1980	5147	7730	48
H37B	789	4967	7862	48
H38A	1309	4317	6739	56
H38B	115	4044	6886	56

Atom	x	y	z	U_{eq}
H39A	320	4915	6035	63
H39B	1279	5559	6546	63
H39C	78	5280	6685	63
H40A	621	4594	8918	40
H40B	1300	4544	9640	40
H41A	289	3213	9578	40
H41B	-419	3294	8872	40
H42A	-289	4336	9888	48
H42B	-1311	3816	9350	48
H43A	-1947	3359	10208	72
H43B	-791	3659	10702	72
H43C	-1202	2856	10250	72
H32C	2421	4327	9871	36
H32D	3272	4663	9396	36
H33C	2164	5406	9990	40
H33D	2440	5675	9267	40
H34C	3772	6431	10194	45
H34D	4007	5680	10422	45
H35D	4572	6506	9283	66
H35E	4562	5646	9332	66
H35F	5357	6318	9892	66
H36C	2723	4633	8191	40
H36D	1958	5088	8312	40
H37C	467	4133	7663	33
H37D	1139	3587	7611	33
H38C	1735	5085	7104	43
H38D	2242	4455	6980	43
H39D	1127	4509	5988	54
H39E	142	4356	6373	54
H39F	594	3687	6274	54
H40C	667	4637	8995	40
H40D	90	3779	8657	40
H41C	360	3326	9765	40
H41D	800	4207	10074	40
H42C	-805	4213	9974	48
H42D	-1119	3878	9197	48
H43D	-2260	2871	9515	72
H43E	-1737	3122	10303	72
H43F	-1262	2650	9863	72
H37E	5733	8128	9917	26
H37F	5795	8995	10069	26
H38E	3880	8451	9367	33
H38F	3925	7651	9614	33
H39G	3958	8892	10458	44
H39H	4200	8168	10765	44
H39I	3045	8046	10316	44
H37G	5976	8769	10081	26
H37H	5595	7903	9751	26
H38G	3786	7830	9515	33
H38H	4272	7974	10311	33
H39J	4056	9182	9513	44
H39K	4344	9226	10326	44
H39L	3168	8692	9929	44
H8'	702	-1848	6931	25
H9'	1189	-2828	6553	28
H11'	-1042	-3230	4827	21
H12'	-1494	-2215	5173	19

Atom	x	y	z	U_{eq}
H13A	586	-3756	5007	43
H13B	-273	-4305	5413	43
H13C	950	-3872	5791	43
H8B	709	-1873	6831	25
H9B	1048	-2871	6291	28
H11B	-1280	-3010	4669	21
H12B	-1645	-2018	5199	19
H13D	790	-3717	5352	43
H13E	92	-3652	4637	43
H13F	-476	-4205	5175	43
H36G	5181	8204	8728	27
H36H	5201	9055	8871	27
H36E	5142	8263	8669	27
H36F	5243	9094	8960	27
H2BA	3004	121	6975	32
H2BB	3914	791	7496	32
H1E	8336	2960	7487	43
H7B	-738	-1042	7945	41
H1C	8783	4292	7651	36
H1D	6271	3917	8594	38
H1A	8238	6825	6970	21
H1B	8353	6370	6322	21
H1BA	3201	1707	7083	29
H1BB	3357	1275	6437	29
H3BA	2034	2236	7312	26
H3BB	1034	2401	6880	26
H4A	5779	6523	5947	17
H4B	7020	7079	6045	17
H2A	8088	5248	6897	25
H2B	9010	5943	7388	25
H4BA	811	1477	6011	25
H4BB	2057	2029	6163	25
H5A	6919	5139	5958	19
H5B	6533	5696	5459	19
H5BA	1918	76	5994	25
H5BB	1588	670	5514	25
H3A	7099	7363	7201	18
H3B	6071	7506	6782	18
H8	5707	3178	6900	25
H9	6034	2163	6416	27
H11	3664	1936	4790	22
H12	3330	2949	5275	19
H13G	4562	781	5383	43
H13H	5802	1306	5425	43
H13I	4933	1268	4757	43
H5BC	810(20)	190(20)	8591(13)	29(10)
H5BD	-240(30)	364(18)	8193(19)	28(10)
H15B	1068	-1246	8626	34
H16B	646	-2574	8435	40
H6A	4808	5207	5700	18
H6B	5097	4470	5532	18
H6BA	-170	186	5707	23
H6BB	102	-551	5514	23
H20D	7430	1682	7789	75
H20E	6181	1536	7545	75
H20F	6672	1566	8337	75
H20A	1251	-3622	8245	79

Atom	x	y	z	U_{eq}
H20B	2342	-3456	7969	79
H20C	1255	-3549	7449	79
H22	4128	7595	6299	27
H22B	-903	2517	6365	25
H23	3303	7372	5154	29
H23B	-1726	2349	5218	26
H25	2524	5073	5269	26
H25B	-2540	36	5256	27
H26	3368	5285	6411	24
H26B	-1688	200	6396	26
H27D	2854	6081	4068	42
H27E	2043	6482	4214	42
H27F	1722	5570	4253	42
H27A	-3085	1458	4278	42
H27B	-3290	555	4267	42
H27C	-2200	1153	4091	42
H28C	7403	8520	9673	22
H28D	8075	8754	9079	22
H28A	1124	2952	8689	40
H28B	1836	3251	9434	40
H29C	6127	7431	8985	29
H29D	6744	7676	8363	29
H29A	3422	3627	8975	39
H29B	2711	3334	8227	39
H30C	7790	7348	9628	34
H30D	7134	6678	9037	34
H30A	2689	2313	9300	37
H30B	2110	2046	8520	37
H31D	8347	7297	8323	46
H31E	8982	7120	9016	46
H31F	9001	7976	8910	46
H18	5851	2589	8447	47
H31A	3824	2495	8198	51
H31B	3751	1845	8726	51
H31C	4391	2737	8981	51
H18B	3270	-2149	7595	50
H33E	7444	9196	8079	21
H33F	6256	8561	7921	21
H34E	5410	8947	6943	29
H34F	6638	9404	6894	29
H35G	5497	9877	6146	44
H35H	6283	10549	6709	44
H35I	5059	10103	6775	44
H19B	3702	-835	7793	43
H40E	6838	10144	9144	22
H40F	7244	9755	9791	22
H41E	8451	10292	8744	23
H41F	8861	9952	9424	23
H42E	8413	11345	9407	34
H42F	8826	11005	10087	34
H43G	10045	11563	9053	51
H43H	10456	11191	9711	51
H43I	10284	11991	9793	51
H5C	6056	5455	8581	31
H5D	5012	5615	8243	31
H7	4424	4181	8001	58
H32E	6842	10190	7912	23

Atom	x	y	z	U_{eq}
H32F	5638	9656	7973	23

3-1(N_2H_4)

EMORY UNIVERSITY | X-ray Crystallography Center

Submitted by: **Christian Wallen**
Emory University
Solved by: **John Bacsa**
Sample ID: **CMW04073_BuCoTsH4N2 (1–N_2H_4)**

Crystal Data and Experimental

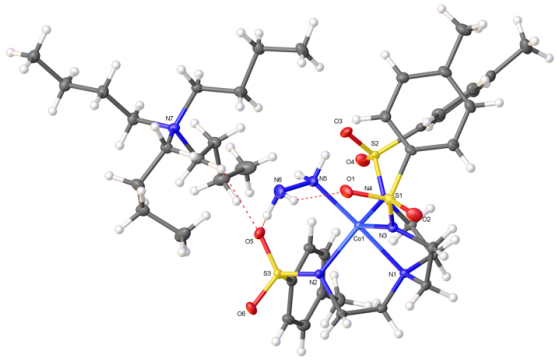

Experimental. Single violet block-shaped crystals of (**CMW04-073-BuCoTsH4N2**) were recrystallised from a mixture of THF and diethyl ether by vapor diffusion. A suitable crystal (0.60×0.40×0.30 mm) was selected and mounted on a loop with paratone oil on a Bruker APEX-II CCD diffractometer. The crystal was cooled to T = 100(2) K during the data collection. The structure was solved with **XT** (Sheldrick, 2015) structure solution program, using direct and dual-space solution methods and by using **Olex2** (Dolomanov et al., 2009) as the graphical interface. The model was refined with version 2013-4 of **ShelXL-97** (Sheldrick, 2008) using Least Squares minimisation.

Crystal Data. $C_{43}H_{73}CoN_7O_6S_3$, M_r = 939.19, triclinic, P-1 (No. 2), a = 9.1127(15) Å, b = 13.390(2) Å, c = 20.684(3) Å, α = 97.417(2)°, β = 97.035(2)°, γ = 109.643(2)°, V = 2319.5(7) Å^3, T = 100(2) K, Z = 2, Z' = 1, μ(MoK$_\alpha$) = 0.559, 41686 reflections measured, 13755 unique (R_{int} = 0.0442) which were used in all calculations. The final wR_2 was 0.1227 (all data) and R_1 was 0.0448 (I > 2(I)).

Compound	**CMW04-073-BuCoTsH4N2** (CCDC 1447761)
Formula	$C_{43}H_{73}CoN_7O_6S_3$
$D_{calc.}$/ g cm^{-3}	1.345
μ/mm^{-1}	0.559
Formula Weight	939.19
Colour	violet
Shape	block
Max Size/mm	0.60
Mid Size/mm	0.40
Min Size/mm	0.30
T/K	100(2)
Crystal System	triclinic
Space Group	P-1
a/Å	9.1127(15)
b/Å	13.390(2)
c/Å	20.684(3)
α/°	97.417(2)
β/°	97.035(2)
γ/°	109.643(2)
V/Å^3	2319.5(7)
Z	2
Z'	1
Θ_{min}/°	1.642
Θ_{max}/°	30.302
Measured Refl.	41686
Independent Refl.	13755
Reflections Used	10819
R_{int}	0.0442
Parameters	564
Restraints	10
Largest Peak	0.777
Deepest Hole	-0.363
GooF	1.066
wR_2 (all data)	0.1227
wR_2	0.1085
R_1 (all data)	0.0603
R_1	0.0448

Structure Quality Indicators

Refinement: Shift -0.003 | Max Peak 0.8 | Min Peak -0.4 | GooF 1.066

A violet block-shaped crystal with dimensions 0.60×0.40×0.30 mm was mounted on a loop with paratone oil. Data were collected using a Bruker APEX-II CCD diffractometer equipped with an Oxford Cryosystems low-temperature apparatus operating at T = 100(2) K.

Data were measured using ω scans scans of 1° per frame for 10 s using MoK_α radiation (fine-focus sealed tube, 45 kV, 35 mA). The total number of runs and images was based on the strategy calculation from the program **APEX2** (Bruker). The maximum resolution achieved was Θ = 30.302.

Unit cell indexing was performed by using the **APEX2** (Bruker, 2014) software and refined using **SAINT** (Bruker, V8.34A, 2013) on 9988 reflections, 24% of the observed reflections. Data reduction, scaling and absorption corrections were performed using **SAINT** (Bruker, V8.34A, 2013) and **SADABS-2014/5** (Bruker, 2014/5) was used for absorption correction. wR_2(int) was 0.1207 before and 0.0562 after correction. The Ratio of minimum to maximum transmission is 0.8418. The $\lambda/2$ correction factor is 0.00150. The final completeness is 100.00% out to 30.302° in Θ. The absorption coefficient (μ) of this material is 0.559 mm^{-1} and the minimum and maximum transmissions are 0.628 and 0.746.

The structure was solved with **XT** (Sheldrick, 2015) structure solution program, using direct and dual-space solution methods which confirmed that the crystal belongs the space group P-1 (# 2) and by using **Olex2** (Dolomanov et al., 2009) as the graphical interface. The structure was refined by Least Squares using version 2013-4 of **ShelXL-97** (Sheldrick, 2008). All non-hydrogen atoms were refined anisotropically. Hydrogen atom positions were calculated geometrically and refined using the riding model.

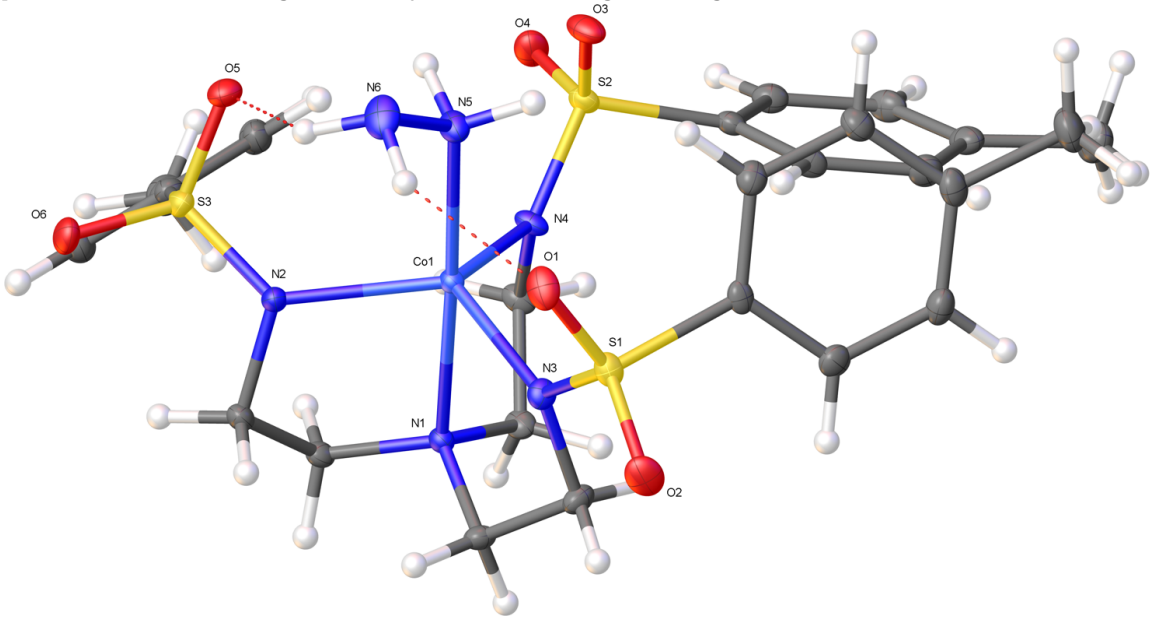

Figure S9:

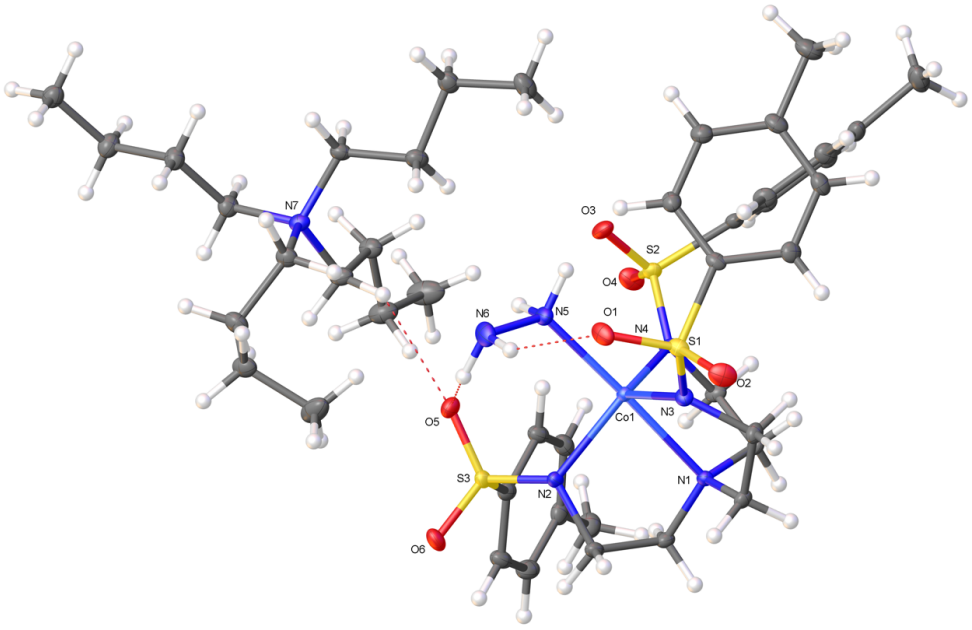

Figure S10: Plot of the asymmetric unit with H-bonds shown.

Data Plots: Diffraction Data

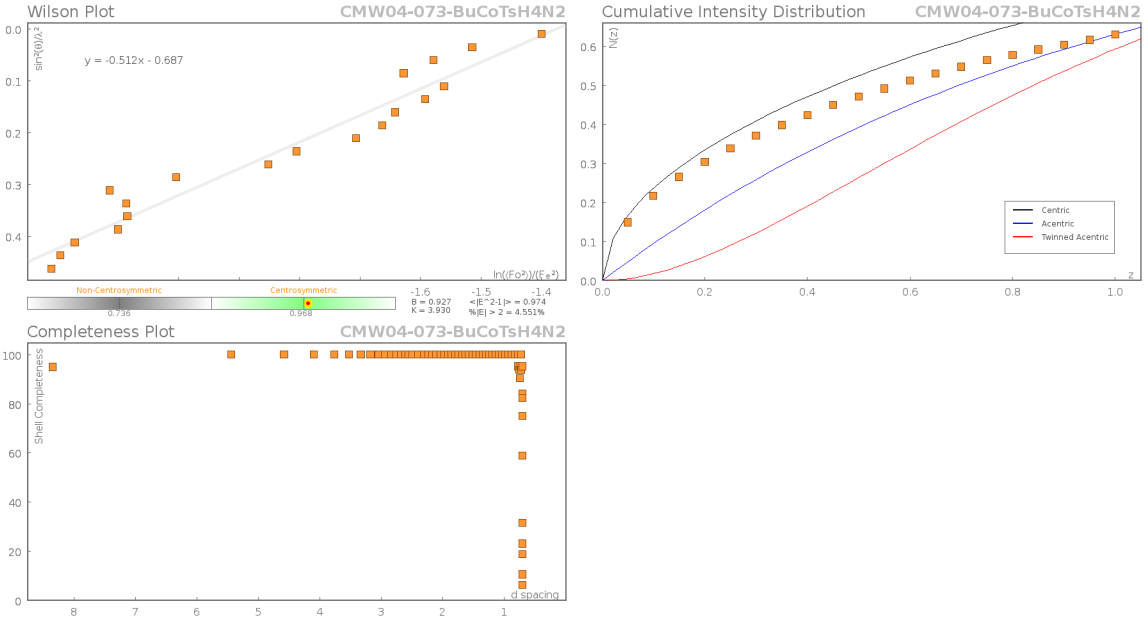

Data Plots: Refinement and Data

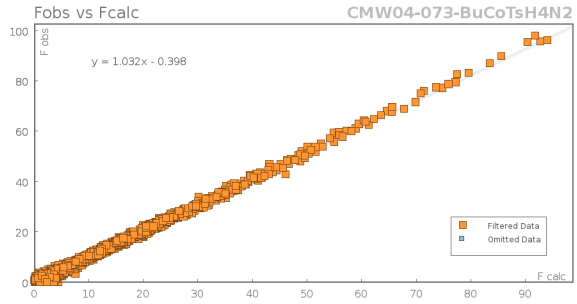

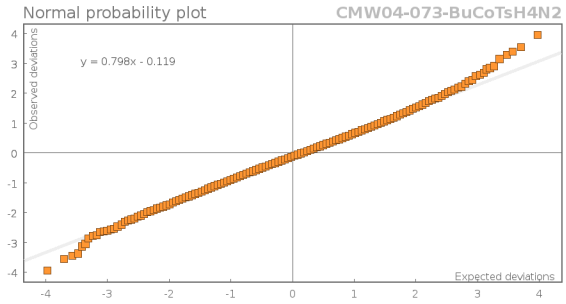

Reflection Statistics

Total reflections (after filtering)	41686	Unique reflections	13755
Completeness	0.991	Mean I/σ	13.36
hklsub>max</sub> collected	(12, 18, 29)	hklsub>min</sub> collected	(-12, -18, -29)
hkl_{max} used	(12, 18, 29)	hkl_{min} used	(-12, -18, 0)
Lim d_{max} collected	100.0	Lim d_{min} collected	0.36
d_{max} used	12.4	d_{min} used	0.7
Friedel pairs	12406	Friedel pairs merged	1
Inconsistent equivalents	0	R_{int}	0.0442
R_{sigma}	0.049	Intensity transformed	0
Omitted reflections	0	Omitted by user (OMIT hkl)	0
Multiplicity	(13450, 10270, 2068, 373)	Maximum mulitplicity	8
Removed systematic absences	0	Filtered off (Shel/OMIT)	0

Table S3: Fractional Atomic Coordinates (×10⁴) and Equivalent Isotropic Displacement Parameters (Å²×10³) for **CMW04-073-BuCoTsH4N2**. U_{eq} is defined as 1/3 of the trace of the orthogonalised U_{ij}.

Atom	x	y	z	U_{eq}
Co1	6409.5(3)	5718.4(2)	7282.2(2)	9.21(6)
S2	2935.1(5)	5400.1(3)	6422.9(2)	12.69(9)
S3	6019.9(5)	3213.7(3)	7353.1(2)	12.65(9)
S1	8136.2(5)	8036.9(3)	8312.9(2)	13.01(9)
O6	6933.5(16)	2602.3(10)	7611.4(7)	18.5(3)
O3	2535.6(16)	5486.7(11)	7080.0(7)	18.8(3)
O5	4714.3(16)	3247.2(10)	7684.0(7)	16.9(3)
O1	7632.7(17)	7446.5(11)	8835.2(6)	18.5(3)
O4	1948.2(16)	4438.8(11)	5949.3(7)	20.0(3)
O2	9638.8(16)	8932.4(11)	8484.7(7)	20.5(3)
N1	7908.6(17)	5906.6(11)	6502.3(7)	10.2(3)
N2	7084.3(17)	4400.6(11)	7323.3(7)	11.4(3)
N3	8070.6(18)	7221.3(11)	7679.1(7)	12.2(3)
N4	4765.6(17)	5597.0(12)	6488.2(7)	12.0(3)
N7	991.0(18)	2686.4(12)	8923.8(7)	13.3(3)
N5	4941.5(19)	5458.0(13)	8010.0(8)	15.0(3)
N6	5520(2)	5226.0(14)	8648.6(8)	20.8(3)
C7	6706(2)	8642.4(13)	8128.2(9)	12.2(3)
C14	2633(2)	6488.7(14)	6087.7(9)	12.1(3)
C21	5169(2)	2548.0(14)	6520.3(9)	14.2(3)
C3	9370(2)	6840.8(14)	6773.7(9)	13.0(3)
C15	3304(2)	7527.0(15)	6462.4(9)	15.5(3)
C28	224(2)	3532.9(14)	8910.4(9)	14.7(3)
C6	5260(2)	5453.1(14)	5838.2(8)	13.3(3)

Atom	x	y	z	U_{eq}
C4	8990(2)	7712.0(14)	7189.4(9)	14.6(3)
C1	8242(2)	4904.5(13)	6354.5(9)	12.5(3)
C19	1684(2)	6307.1(15)	5473.5(9)	14.9(3)
C8	5266(2)	8308.2(14)	8350.1(9)	15.4(3)
C5	7017(2)	6105.3(14)	5916.1(9)	13.4(3)
C24	4034(2)	1695.5(14)	5170(1)	17.0(4)
C18	1336(2)	7149.4(16)	5246.9(9)	16.6(4)
C16	2962(2)	8363.3(15)	6228(1)	17.4(4)
C26	5812(2)	1870.1(14)	6186.3(10)	17.5(4)
C9	4201(2)	8833.1(15)	8230.6(9)	17.2(4)
C17	1951(2)	8186.1(15)	5629.2(10)	16.8(4)
C11	5990(2)	10008.7(14)	7663.8(10)	17.1(4)
C2	8461(2)	4477.1(14)	6988.4(9)	13.5(3)
C10	4559(2)	9701.9(14)	7901.1(10)	16.9(4)
C34	4855(2)	2778.4(16)	10007.6(10)	19.0(4)
C30	329(2)	5384.5(15)	8802.2(10)	18.0(4)
C12	7053(2)	9482.7(14)	7772.2(9)	15.5(3)
C25	5241(2)	1453.5(15)	5513.6(10)	19.8(4)
C41	-836(2)	1673.3(15)	9679.7(9)	17.2(4)
C23	3384(2)	2361.5(15)	5516.8(10)	17.8(4)
C42	-2102(2)	584.6(15)	9674.8(10)	19.9(4)
C32	2434(2)	3081.8(15)	9476.3(9)	15.5(3)
C29	1224(2)	4592.5(15)	8742.1(10)	17.3(4)
C37	335(2)	2226.2(16)	7643.3(9)	17.6(4)
C40	-240(2)	1644.8(14)	9024.3(9)	16.4(4)
C31	1279(3)	6466.0(15)	8637.3(11)	21.5(4)
C33	3172(2)	2242.1(15)	9608(1)	19.3(4)
C43	-2802(2)	548.0(16)	10305.4(10)	18.6(4)
C22	3949(2)	2792.0(14)	6183.9(10)	16.2(4)
C36	1540(2)	2454.8(16)	8274.0(9)	17.0(4)
C27	3446(3)	1253.3(16)	4440.9(10)	22.6(4)
C38	808(3)	1589.3(18)	7087.8(10)	24.4(4)
C20	1504(3)	9094.2(17)	5412.5(12)	26.6(5)
C13	3444(3)	10305.3(17)	7805.0(12)	24.8(4)
C35	6081(3)	3374(2)	9615.8(12)	30.2(5)
C39	-120(3)	1503(2)	6409.2(11)	31.9(5)

Table S4: Anisotropic Displacement Parameters (×10^4) **CMW04-073-BuCoTsH4N2**. The anisotropic displacement factor exponent takes the form: $-2\pi^2[h^2a^{*2} \times U_{11} + \ldots + 2hka^* \times b^* \times U_{12}]$

Atom	U_{11}	U_{22}	U_{33}	U_{23}	U_{13}	U_{12}
Co1	8.96(11)	10.13(11)	9.14(11)	2.10(8)	1.82(8)	3.97(9)
S2	8.66(19)	15.19(19)	14.6(2)	3.24(15)	1.83(16)	4.63(16)
S3	11.4(2)	10.63(18)	16.7(2)	4.85(15)	3.13(16)	3.91(15)
S1	14.1(2)	13.63(19)	10.37(19)	-1.09(15)	-1.64(16)	6.32(16)
O6	18.5(7)	14.5(6)	24.8(7)	8.6(5)	1.8(6)	7.5(5)
O3	14.8(6)	28.8(7)	18.4(7)	10.1(6)	8.3(5)	11.2(6)
O5	15.2(6)	15.9(6)	19.9(7)	5.7(5)	7.2(5)	3.9(5)
O1	26.4(7)	22.4(7)	9.8(6)	3.0(5)	0.6(5)	13.8(6)
O4	13.9(6)	15.0(6)	27.3(8)	0.7(5)	-2.0(6)	3.3(5)
O2	15.3(7)	19.0(6)	20.7(7)	-4.9(5)	-5.6(5)	4.0(5)
N1	9.5(7)	10.8(6)	10.9(7)	2.2(5)	2.0(5)	4.3(5)
N2	9.7(7)	10.2(6)	15.1(7)	3.6(5)	3.2(6)	3.6(5)
N3	15.2(7)	11.8(6)	9.7(7)	0.7(5)	2.8(6)	5.3(6)
N4	8.6(7)	19.1(7)	9.4(7)	1.9(5)	2.3(5)	6.4(6)
N7	12.3(7)	15.5(7)	11.7(7)	0.2(5)	1.9(6)	5.5(6)

Atom	U_{11}	U_{22}	U_{33}	U_{23}	U_{13}	U_{12}
N5	17.7(8)	18.4(7)	13.1(7)	6.1(6)	5.8(6)	9.4(6)
N6	32(1)	24.2(8)	11.5(7)	7.0(6)	6.6(7)	14.4(8)
C7	14.5(8)	10.5(7)	10.6(8)	-1.8(6)	-0.9(6)	5.8(6)
C14	8.8(8)	15.0(8)	13.6(8)	3.2(6)	3.4(6)	4.9(6)
C21	11.7(8)	10.6(7)	19.5(9)	2.7(6)	4.5(7)	2.6(6)
C3	10.4(8)	12.5(7)	14.7(8)	2.6(6)	4.0(6)	1.7(6)
C15	11.1(8)	19.1(8)	13.8(8)	-0.4(7)	-1.2(7)	4.5(7)
C28	13.1(8)	15.1(8)	17.5(9)	2.4(7)	2.9(7)	7.2(7)
C6	12.4(8)	19.1(8)	9.0(8)	0.8(6)	1.5(6)	7.0(7)
C4	16.2(9)	10.3(7)	16.0(8)	2.5(6)	5.6(7)	2.1(6)
C1	11.2(8)	12.4(7)	14.7(8)	1.6(6)	4.7(6)	4.8(6)
C19	12.3(8)	17.7(8)	12.7(8)	1.1(6)	1.7(7)	3.7(7)
C8	19.7(9)	14.7(8)	13.2(8)	2.5(6)	4.5(7)	7.4(7)
C5	14.7(8)	17.3(8)	10.5(8)	5.5(6)	4.4(6)	6.8(7)
C24	18.3(9)	11.9(8)	18.9(9)	4.2(7)	4.8(7)	2.1(7)
C18	13.4(8)	24.3(9)	12.4(8)	6.5(7)	0.1(7)	6.7(7)
C16	13.9(9)	14.7(8)	21.1(9)	1.6(7)	1.6(7)	3.0(7)
C26	14.3(9)	14.6(8)	25.3(10)	4.1(7)	3.4(7)	7.1(7)
C9	17.4(9)	18.3(8)	17.2(9)	1.8(7)	4.4(7)	8.3(7)
C17	13.1(8)	20.1(8)	19.0(9)	8.9(7)	4.7(7)	5.6(7)
C11	19.4(9)	12.2(8)	19.0(9)	3.7(7)	0.5(7)	5.6(7)
C2	10.5(8)	12.7(7)	18.7(9)	3.5(6)	3.8(7)	5.3(6)
C10	19.5(9)	13.5(8)	18.1(9)	-0.5(7)	0.5(7)	8.6(7)
C34	17.9(9)	25.5(9)	15.8(9)	4.0(7)	0.8(7)	11.3(8)
C30	15.9(9)	17.6(8)	20.4(9)	4.6(7)	0.5(7)	6.3(7)
C12	15.2(9)	11.0(7)	17.9(9)	0.8(6)	2.0(7)	2.5(7)
C25	19.0(9)	15.9(8)	25.8(10)	1.7(7)	7.8(8)	7.4(7)
C41	20.1(9)	15.7(8)	15.1(9)	2.8(7)	3.4(7)	5.2(7)
C23	16.8(9)	15.3(8)	21.4(9)	4.9(7)	1.8(7)	6.0(7)
C42	21.5(10)	18.0(8)	18.2(9)	2.2(7)	5.6(8)	4.2(8)
C32	14.7(9)	17.8(8)	14.0(8)	2.2(7)	0.1(7)	6.9(7)
C29	13.5(9)	16.9(8)	21.5(9)	2.0(7)	1.8(7)	6.4(7)
C37	18.0(9)	22.9(9)	13.5(9)	2.5(7)	2.3(7)	10.0(8)
C40	17.4(9)	13.3(8)	16.8(9)	1.3(7)	2.7(7)	4.0(7)
C31	21.9(10)	15.1(8)	25.9(10)	4.7(7)	-2.1(8)	6.5(8)
C33	20.4(10)	19.2(9)	19.8(9)	3.6(7)	-0.1(8)	10.3(8)
C43	15.7(9)	21.2(9)	17.8(9)	4.8(7)	2.5(7)	5.1(7)
C22	13.8(8)	13.2(8)	22.5(9)	3.1(7)	3.9(7)	5.9(7)
C36	16.0(9)	23.5(9)	14.1(9)	2.9(7)	3.8(7)	10.3(7)
C27	27.3(11)	20.6(9)	20.3(10)	3.3(8)	6.4(8)	8.5(8)
C38	20(1)	32.9(11)	21.1(10)	1.3(8)	4.0(8)	11.6(9)
C20	23.8(11)	24.8(10)	34.3(12)	15.3(9)	3.1(9)	9.6(9)
C13	26.8(11)	22.0(9)	31.0(11)	4.2(8)	4.5(9)	16.2(9)
C35	19.5(10)	52.0(14)	25.4(11)	17.1(10)	5.9(9)	16.3(10)
C39	26.9(12)	50.8(14)	17.7(10)	-5.7(10)	-1.9(9)	20.0(11)

Table S5: Bond Lengths in Å for **CMW04-073-BuCoTsH4N2**.

Atom	Atom	Length/Å
Co1	N1	2.2237(15)
Co1	N2	2.0625(14)
Co1	N3	2.0581(15)
Co1	N4	2.0329(15)
Co1	N5	2.1195(16)
S2	O3	1.4499(14)
S2	O4	1.4511(14)
S2	N4	1.5843(15)
S2	C14	1.7791(18)
S3	O6	1.4528(13)
S3	O5	1.4538(14)
S3	N2	1.5729(15)
S3	C21	1.782(2)
S1	O1	1.4492(14)
S1	O2	1.4512(15)

Atom	Atom	Length/Å
S1	N3	1.5755(15)
S1	C7	1.7804(18)
N1	C3	1.473(2)
N1	C1	1.476(2)
N1	C5	1.479(2)
N2	C2	1.486(2)
N3	C4	1.473(2)
N4	C6	1.479(2)
N7	C28	1.520(2)
N7	C32	1.524(2)
N7	C40	1.525(2)
N7	C36	1.521(2)
N5	N6	1.471(2)
C7	C8	1.393(3)
C7	C12	1.393(2)
C14	C15	1.393(2)
C14	C19	1.389(3)
C21	C26	1.393(2)
C21	C22	1.392(3)
C3	C4	1.518(2)
C15	C16	1.387(3)
C28	C29	1.517(3)
C6	C5	1.520(3)
C1	C2	1.514(2)
C19	C18	1.391(3)
C8	C9	1.393(3)
C24	C25	1.388(3)
C24	C23	1.398(3)
C24	C27	1.507(3)
C18	C17	1.397(3)
C16	C17	1.392(3)
C26	C25	1.394(3)
C9	C10	1.389(3)
C17	C20	1.508(3)
C11	C10	1.399(3)
C11	C12	1.390(3)
C10	C13	1.506(3)
C34	C33	1.532(3)
C34	C35	1.527(3)
C30	C29	1.542(3)
C30	C31	1.523(3)
C41	C42	1.523(3)
C41	C40	1.521(3)
C23	C22	1.387(3)
C42	C43	1.520(3)
C32	C33	1.528(2)
C37	C36	1.524(3)
C37	C38	1.532(3)
C38	C39	1.517(3)

Table S6: Bond Angles in ° for **CMW04-073-BuCoTsH4N2**.

Atom	Atom	Atom	Angle/°
N2	Co1	N1	80.54(5)
N2	Co1	N5	97.28(6)
N3	Co1	N1	80.54(6)
N3	Co1	N2	117.82(6)
N3	Co1	N5	102.00(6)
N4	Co1	N1	80.30(6)
N4	Co1	N2	116.36(6)
N4	Co1	N3	117.75(6)
N4	Co1	N5	99.29(6)
N5	Co1	N1	177.26(6)
O3	S2	O4	116.21(9)
O3	S2	N4	108.94(8)
O3	S2	C14	106.08(8)
O4	S2	N4	113.03(8)
O4	S2	C14	105.00(8)
N4	S2	C14	106.86(8)
O6	S3	O5	115.95(8)
O6	S3	N2	112.59(8)
O6	S3	C21	105.57(8)
O5	S3	N2	108.73(8)
O5	S3	C21	106.56(9)
N2	S3	C21	106.85(8)
O1	S1	O2	116.42(9)
O1	S1	N3	109.36(8)
O1	S1	C7	105.24(8)
O2	S1	N3	111.95(9)
O2	S1	C7	104.64(8)
N3	S1	C7	108.66(8)
C3	N1	Co1	106.93(10)
C3	N1	C1	111.50(13)
C3	N1	C5	110.91(13)
C1	N1	Co1	107.78(10)
C1	N1	C5	111.84(14)
C5	N1	Co1	107.63(10)
S3	N2	Co1	128.13(9)
C2	N2	Co1	111.73(10)
C2	N2	S3	114.07(11)
S1	N3	Co1	129.50(9)
C4	N3	Co1	112.40(11)
C4	N3	S1	114.89(12)
S2	N4	Co1	131.18(9)
C6	N4	Co1	114.92(11)
C6	N4	S2	112.68(12)
C28	N7	C32	109.94(14)
C28	N7	C40	108.20(14)
C28	N7	C36	111.44(14)
C32	N7	C40	111.31(14)
C36	N7	C32	107.85(14)
C36	N7	C40	108.12(14)
N6	N5	Co1	119.87(12)
C8	C7	S1	120.97(13)
C12	C7	S1	119.42(14)
C12	C7	C8	119.59(16)

Atom	Atom	Atom	Angle/°
C15	C14	S2	119.12(14)
C19	C14	S2	120.82(14)
C19	C14	C15	120.00(16)
C26	C21	S3	120.52(15)
C22	C21	S3	119.28(13)
C22	C21	C26	119.90(18)
N1	C3	C4	109.98(14)
C16	C15	C14	119.34(17)
C29	C28	N7	115.60(15)
N4	C6	C5	108.61(14)
N3	C4	C3	108.20(14)
N1	C1	C2	109.33(14)
C14	C19	C18	120.10(17)
C7	C8	C9	119.95(17)
N1	C5	C6	110.40(14)
C25	C24	C23	118.34(18)
C25	C24	C27	120.68(17)
C23	C24	C27	120.98(18)
C19	C18	C17	120.44(17)
C15	C16	C17	121.41(17)
C21	C26	C25	119.52(18)
C10	C9	C8	121.11(18)
C18	C17	C20	121.22(18)
C16	C17	C18	118.59(17)
C16	C17	C20	120.16(18)
C12	C11	C10	121.11(17)
N2	C2	C1	109.07(14)
C9	C10	C11	118.30(17)
C9	C10	C13	120.98(18)
C11	C10	C13	120.72(17)
C35	C34	C33	114.36(17)
C31	C30	C29	111.27(16)
C11	C12	C7	119.85(18)
C24	C25	C26	121.28(17)
C40	C41	C42	108.93(15)
C22	C23	C24	121.14(18)
C43	C42	C41	112.65(16)
N7	C32	C33	115.08(15)
C28	C29	C30	108.93(15)
C36	C37	C38	108.53(16)
C41	C40	N7	116.64(15)
C32	C33	C34	111.09(16)
C23	C22	C21	119.81(17)
N7	C36	C37	116.38(15)
C39	C38	C37	112.93(17)

Table S7: Hydrogen Fractional Atomic Coordinates ($\times 10^4$) and Equivalent Isotropic Displacement Parameters ($Å^2 \times 10^3$) for **CMW04-073-BuCoTsH4N2**. U_{eq} is defined as 1/3 of the trace of the orthogonalised U_{ij}.

Atom	x	y	z	U_{eq}
H3A	9875	7130	6407	16
H3B	10123	6613	7050	16
H15	3989	7661	6874	19
H28A	-773	3226	8583	18
H28B	-58	3684	9350	18
H6C	4647	5703	5509	16
H6D	5058	4681	5680	16
H4A	9982	8300	7418	18
H4B	8369	8020	6903	18
H1A	9213	5051	6158	15
H1B	7352	4360	6031	15
H19	1273	5606	5208	18
H8	5009	7723	8583	19
H5C	7415	5901	5514	16
H5D	7181	6883	5967	16
H18	674	7019	4829	20
H16	3429	9072	6482	21
H26	6633	1693	6415	21
H9	3214	8593	8377	21
H11	6239	10586	7425	20
H2A	8542	3757	6886	16
H2B	9450	4967	7284	16
H34A	4840	3296	10393	23
H34B	5188	2218	10181	23
H30A	-703	5070	8497	22

Atom	x	y	z	U_{eq}
H30B	120	5496	9259	22
H12	8015	9696	7604	19
H25	5686	995	5286	24
H41A	-1285	2250	9742	21
H41B	52	1829	10051	21
H23	2541	2522	5292	21
H42A	-2960	425	9291	24
H42B	-1633	17	9619	24
H32A	2124	3340	9890	19
H32B	3250	3706	9364	19
H29A	1431	4472	8285	21
H29B	2253	4897	9049	21
H37A	315	2912	7520	21
H37B	-735	1803	7715	21
H40A	-1162	1435	8662	20
H40B	218	1071	8979	20
H31A	1536	6352	8194	32
H31B	2261	6807	8963	32
H31C	653	6935	8649	32
H33A	3201	1826	9181	23
H33B	2510	1733	9856	23
H43A	-3615	-164	10276	28
H43B	-3278	1103	10361	28
H43C	-1963	681	10686	28
H22	3506	3252	6411	19
H36A	1878	1826	8282	20
H36B	2483	3081	8251	20
H27A	3984	1789	4185	34
H27B	2302	1090	4340	34
H27C	3671	593	4324	34
H38A	1951	1945	7086	29
H38B	637	855	7180	29
H20A	1750	9176	4970	40
H20B	2104	9766	5726	40
H20C	368	8931	5401	40
H13A	2971	10162	7335	37
H13B	4030	11081	7950	37
H13C	2606	10066	8067	37
H35A	6041	2887	9212	45
H35B	7139	3621	9888	45
H35C	5849	3997	9496	45
H39A	239	1099	6073	48
H39B	50	2227	6313	48
H39C	-1250	1126	6402	48
H5A	4017(19)	4823(13)	7822(12)	29(7)
H5B	4510(30)	6020(15)	8080(13)	40(8)
H6A	6505(16)	5823(11)	8821(11)	23(6)
H6B	5770(20)	4590(11)	8521(12)	30(7)

Table S8: Hydrogen Bond information for **CMW04-073-BuCoTsH4N2**.

D	H	A	d(D-H)/Å	d(H-A)/Å	d(D-A)/Å	D-H-A/deg
C36	H36B	O5	0.99	2.43	3.181(2)	132.2

D	H	A	d(D-H)/Å	d(H-A)/Å	d(D-A)/Å	D-H-A/deg
N6	H6A	O1	0.969(9)	2.064(14)	2.893(2)	142.5(18)
N6	H6B	O5	0.968(8)	2.187(17)	2.917(2)	131.2(18)

3-1(NH_3)

EMORY UNIVERSITY | X-ray Crystallography Center

Submitted by: Christian Wallen

Solved by: John Bacsa

Sample ID: CMW05-034_BuCoTsNH3 (1–NH_3)

Crystal Data and Experimental

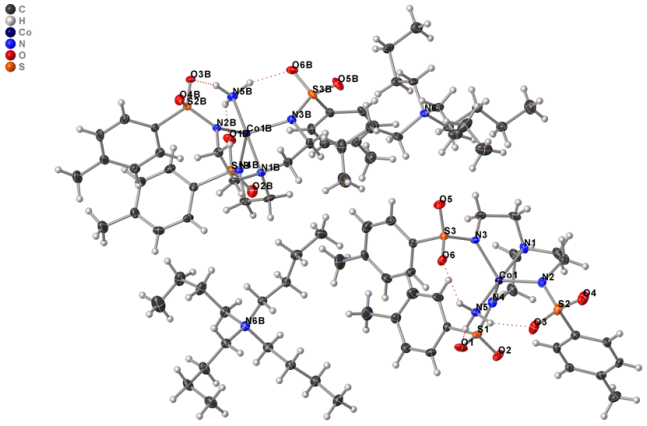

Experimental. Block-shaped crystals of (**CMW05-034_BuCoTsNH3**) were obtained by vapor diffusion of ether into DCM. A suitable crystal (0.41×0.26×0.24 mm) was selected and mounted on a loop with paratone oil on a Bruker APEX2 diffractometer. The crystal was cooled to T = 100(2) K during data collection. The structure was solved with the **XT** (Sheldrick, 2015) structure solution program using combined Patterson and dual-space recycling methods and by using **Olex2** (Dolomanov et al., 2009) as the graphical interface. The crystal structure was refined with version 2014/7 of **XL** (Sheldrick, 2008) using Least Squares minimisation.

Crystal Data. $C_{86}H_{144}Co_2N_{12}O_{12}S_6$, M_r = 1848.34, monoclinic, $P2_1$ (No. 4), a = 14.4778(3) Å, b = 14.7981(4) Å, c = 22.2441(7) Å, β = 104.747(3)°, $\alpha = \gamma$ = 90°, V = 4608.7(2) Å^3, T = 100(2) K, Z = 2, Z' = 1, μ(MoK$_\alpha$) = 0.561 mm^{-1}, 59676 reflections measured, 28087 unique (R_{int}= 0.0580) which were used in all calculations. The final wR_2 was 0.1383 (all data) and R_1 was 0.0584 (I > 2σ(I)).

Compound	**CMW05-034_BuCoTsNH3** (CCDC 1489712)
Formula	$C_{86}H_{144}Co_2N_{12}O_{12}S_6$
$D_{calc.}$/ g cm^{-3}	1.332
μ/mm^{-1}	0.561
Formula Weight	1848.34
Colour	pink
Shape	block
Max Size/mm	0.41
Mid Size/mm	0.26
Min Size/mm	0.24
T/K	100(2)
Crystal System	monoclinic
Flack Parameter	0.496(14)
Hooft Parameter	0.507(8)
Space Group	$P2_1$
a/Å	14.4778(3)
b/Å	14.7981(4)
c/Å	22.2441(7)
α/°	90
β/°	104.747(3)
γ/°	90
V/Å^3	4608.7(2)
Z	2
Z'	1
Θ_{min}/°	1.670
Θ_{max}/°	31.036
Measured Refl.	59676
Independent Refl.	28087
Reflections I >2sigma(I)	20390
R_{int}	0.0580
Parameters	1088
Restraints	8
Largest Peak	1.343
Deepest Hole	-0.481
GooF	1.022
wR_2 (all data)	0.1383
wR_2	0.1208
R_1 (all data)	0.0883
R_1	0.0584

Structure Quality Indicators

Reflections:	d min (Mo)	0.69	I/σ	8.0	Rint	5.80%	
Refinement:	Shift	-0.001	Max Peak	1.3	Min Peak	-0.5	GooF 1.022

Experimental Extended. A pink block-shaped crystal with dimensions 0.41×0.26×0.24 mm was mounted on a loop with paratone oil. X-ray diffraction data were collected using a Bruker APEX-II CCD diffractometer equipped with an Oxford Cryosystems low-temperature apparatus operating at T = 100(2) K.
Data were measured using ω scans with a narrow frame width scans of 1.00° per frame for 20.00 s using MoK_α radiation (fine-focus sealed tube, 45 kV, 35 mA). The total number of runs and images was based on the strategy calculation from the program **APEX2** (Bruker). The maximum resolution achieved was Θ = 31.036°. Unit cell indexing was performed by using the **APEX2** (Bruker) software and refined using **SAINT** (Bruker, V8.34A, 2013) on 9925 reflections. Data reduction, scaling and absorption corrections were performed using **SAINT** (Bruker, V8.34A, 2013) and **SADABS-2014/5** (Bruker, 2014). wR_2(int) was 0.1124 before and 0.0619 after correction. The ratio of minimum to maximum transmission is 0.8335. The final completeness is 99.9% out to 31.04° in Θ. The absorption coefficient μ of this material is 0.561 at this wavelength (λ = 0.71073 Å) and the minimum and maximum transmissions are 0.7874 and 0.9447.
The structure was solved in the space group P1 with **ShelXT-2014/4** (Sheldrick, 2015) structure solution program using combined Patterson and dual-space recycling methods. The space group $P2_1$ (# 4) was determined by **ShelXT-2014/4** (Sheldrick, 2015). The crystal structure was refined by Least Squares using version 2014/7 of **XL** (Sheldrick, 2008). All non-hydrogen atoms were refined anisotropically. Hydrogen atom positions were located from the residual electron density and refined with restraints or calculated geometrically and refined using the riding model.

Refined as a 2-component inversion twin.
There are two independent molecules in the asymmetric unit.
The Flack parameter was refined to 0.496(14) meaning that the crystal consists of a racemic mixture of the two enantiomers.

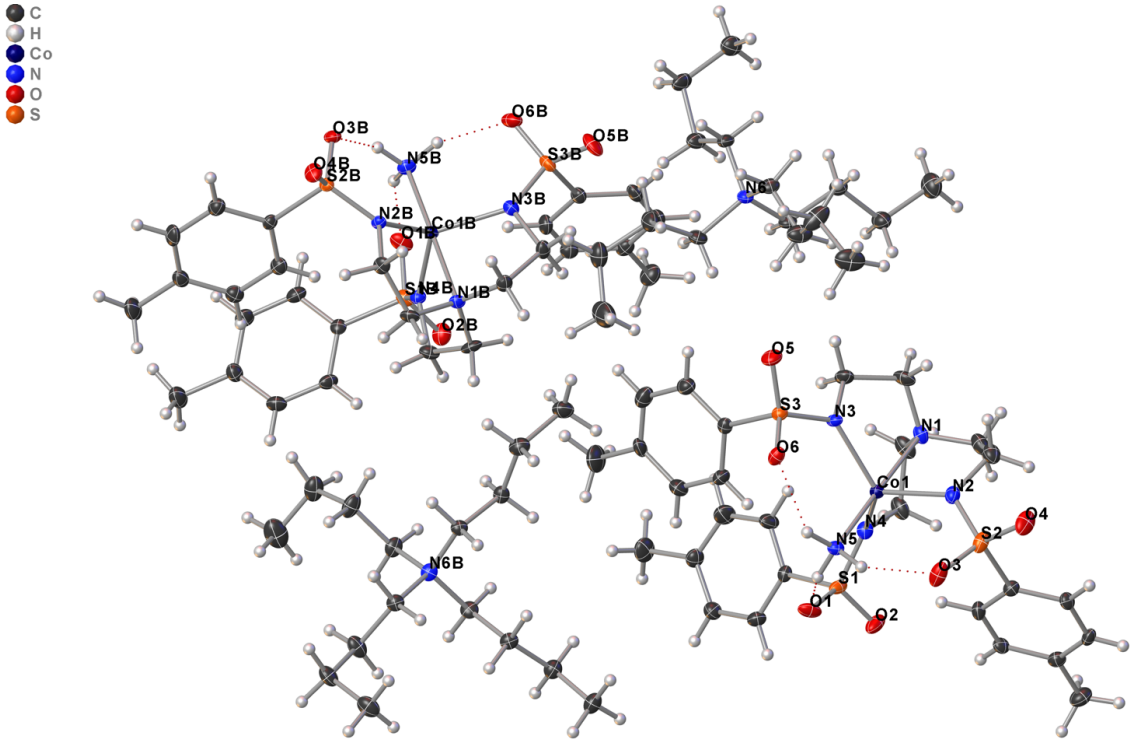

Figure S15:

Plot of the asymmetric unit. There are two independent molecules in the asymmetric unit.

Data Plots: Diffraction Data

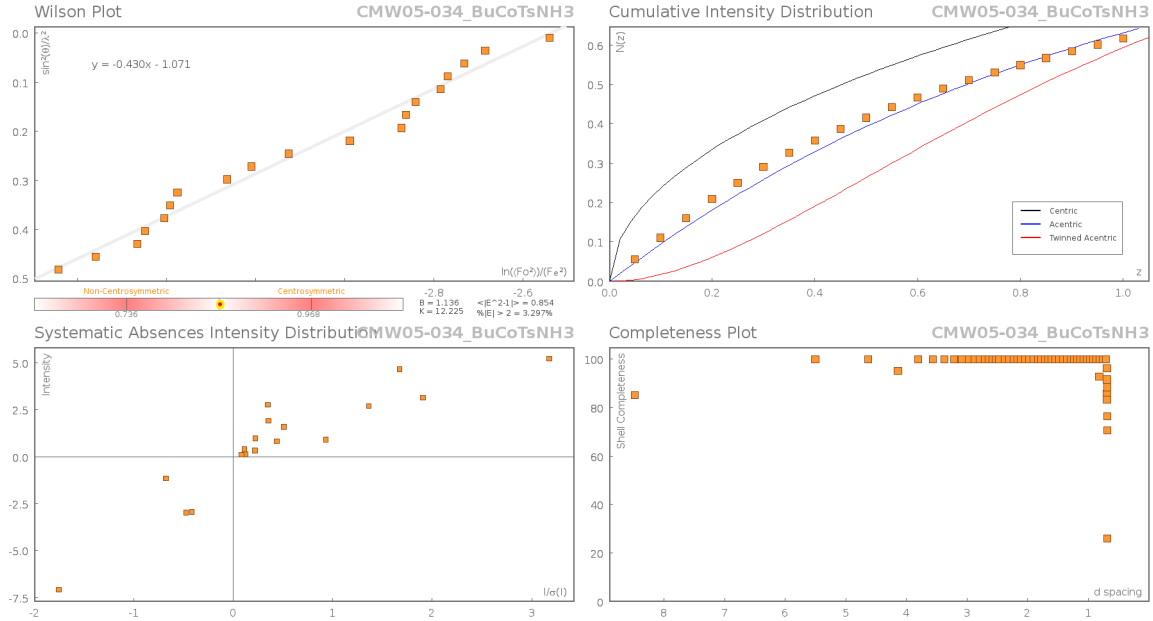

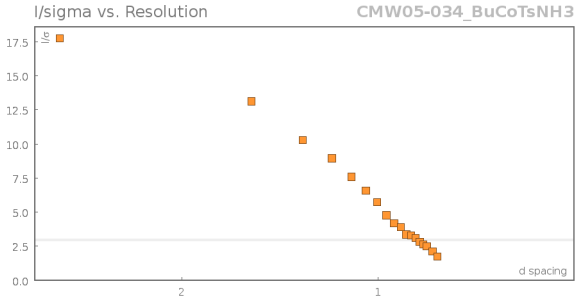

Data Plots: Refinement and Data

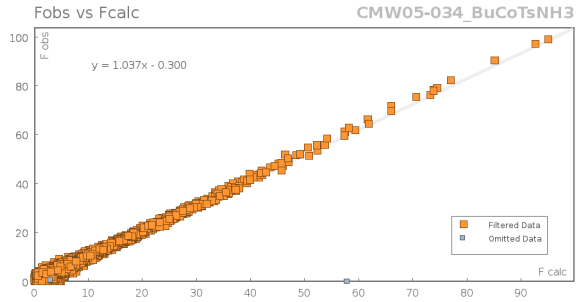

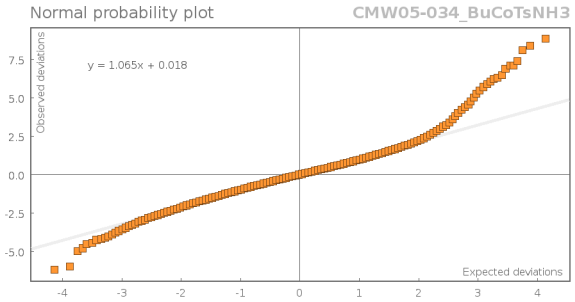

Reflection Statistics

Total reflections (after filtering)	59699	Unique reflections	28087
Completeness	0.953	Mean I/σ	8.03
hkl_{max} collected	(20, 20, 27)	hkl_{min} collected	(-20, -21, -32)
hkl_{max} used	(20, 20, 32)	hkl_{min} used	(-20, -21, 0)
Lim d_{max} collected	100.0	Lim d_{min} collected	0.36
d_{max} used	14.0	d_{min} used	0.69
Friedel pairs	14401	Friedel pairs merged	0
Inconsistent equivalents	0	R_{int}	0.058
R_{sigma}	0.095	Intensity transformed	0
Omitted reflections	0	Omitted by user (OMIT hkl)	5
Multiplicity	(28473, 11833, 2520)	Maximum multiplicity	5
Removed systematic absences	18	Filtered off (Shel/OMIT)	0

Images of the Crystal on the Diffractometer

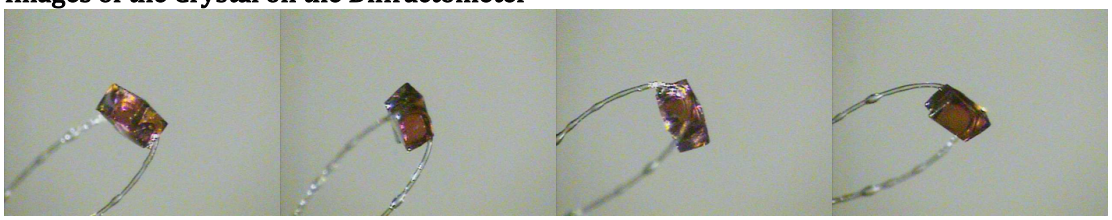

Table S19: Fractional Atomic Coordinates (×10⁴) and Equivalent Isotropic Displacement Parameters (Å²×10³) for **CMW05-034_BuCoTsNH3**. *Ueq* is defined as 1/3 of of the trace of the orthogonalised *Uij*.

Atom	x	y	z	*Ueq*
Co1	1212.6(4)	2440.7(4)	-111.1(3)	12.42(13)
S3	3405.3(8)	2827.8(8)	716.0(6)	14.7(2)
S1	-422.4(8)	2004.5(9)	682.7(5)	16.9(2)
S2	654.2(8)	1237.8(10)	-1407.0(5)	19.9(3)

Atom	x	y	z	*Ueq*
O1	157(2)	1194(2)	870.7(16)	22.6(7)
O6	3511(2)	1858(2)	666.5(16)	18.5(8)
O3	1044(3)	485(3)	-998.6(18)	26.0(9)
N5	1618(3)	1149(3)	241.7(18)	16.2(8)
O2	-1420(2)	1840(3)	397.7(16)	26.6(9)
O4	857(2)	1228(3)	-2010.5(16)	29.2(9)
O5	4236(2)	3362(3)	689.9(17)	23.9(8)
N2	957(3)	2151(3)	-1040.9(19)	18.5(9)
N3	2470(3)	3144(3)	230.0(18)	14.4(8)
N4	75(3)	2638(3)	285.5(18)	16.7(8)
N1	752(3)	3784(3)	-478.6(18)	17.4(9)
C16	-1990(3)	1137(3)	-1142(2)	17(1)
C18	-2169(3)	966(3)	-2233(2)	17.4(10)
C17	-2589(3)	1027(3)	-1739(2)	17.8(10)
C24	2887(4)	3337(4)	2634(2)	22.7(11)
C21	3224(3)	3031(3)	1464(2)	15(1)
C12	-827(3)	2131(3)	1809(2)	19.4(10)
C19	-1187(3)	1037(3)	-2149(2)	16.6(10)
C8	72(4)	3377(4)	1561(2)	24.0(11)
C6	-534(3)	3409(4)	17(2)	23.5(11)
C10	-270(4)	3311(4)	2570(2)	21.0(11)
C5	98(4)	4143(4)	-124(2)	25.5(11)
C26	2468(3)	2596(3)	1632(2)	20.7(10)
C20	-3656(3)	982(4)	-1832(3)	28.0(13)
C4	1602(3)	4357(3)	-398(2)	23.8(11)
C13	-161(4)	3681(4)	3218(2)	32.7(14)
C25	2316(4)	2741(4)	2215(2)	25.4(11)
C9	114(4)	3739(4)	2145(2)	30.7(12)
C14	-610(3)	1142(3)	-1548(2)	15.0(9)
C7	-395(3)	2567(3)	1395(2)	13.9(9)
C15	-1014(3)	1192(4)	-1047(2)	18.6(10)
C22	3807(3)	3605(4)	1884(2)	22.2(10)
C11	-770(3)	2510(4)	2385(2)	22(1)
C23	3634(4)	3755(4)	2464(2)	27.0(12)
C2	758(4)	2963(4)	-1438(2)	24.1(12)
C1	249(3)	3656(4)	-1140(2)	24.8(11)
C3	2324(3)	4127(3)	204(2)	21.7(11)
C27	2681(5)	3522(5)	3250(3)	43.3(17)
Co1B	6203.3(4)	6315.7(4)	4836.0(3)	11.35(13)
S2B	8404.3(7)	6098.0(8)	5715.5(5)	13.0(2)
S1B	4427.8(8)	6559.5(9)	5550.7(6)	17.1(2)
S3B	5725.1(8)	7508.3(9)	3541.0(5)	17.4(2)
O3B	8404(2)	7076(2)	5710.9(15)	17.9(7)
O2B	3416(2)	6426(3)	5276.0(15)	24.5(8)
O4B	9296(2)	5684(3)	5675.6(16)	21.1(8)
O5B	5905(2)	7496(3)	2930.5(16)	27.2(9)
O6B	6201(2)	8228(2)	3952.2(18)	23.2(8)
O1B	4760(2)	7484(2)	5593.7(16)	22.7(7)
N5B	6470(3)	7621(3)	5194.6(19)	17.1(9)
N1B	5913(3)	4950(3)	4471.9(18)	14.4(8)
N2B	7519(3)	5738(3)	5203.9(18)	12.7(8)
N4B	5063(3)	5977(3)	5213.8(18)	14.1(8)
N3B	5963(3)	6579(3)	3892.4(18)	15.7(8)
C12B	5051(3)	6733(4)	6821(2)	21.7(10)
C3B	5639(4)	5787(3)	3493(2)	18.3(10)
C17B	7946(4)	5329(4)	7611(2)	20.3(11)
C4B	6065(3)	4941(3)	3841(2)	17.5(9)

Atom	x	y	z	*Ueq*
C14B	8227(3)	5778(3)	6449(2)	13.8(9)
C9B	4486(3)	5009(3)	7062(2)	21(1)
C26B	4058(3)	7615(4)	3910(2)	20.8(11)
C22B	3906(4)	7897(3)	2826(2)	19(1)
C11B	5186(3)	6427(3)	7430(2)	23.5(11)
C18B	8842(4)	5544(4)	7548(2)	24.4(11)
C23B	2941(4)	8033(4)	2746(2)	21.9(11)
C21B	4478(3)	7693(3)	3412(2)	17.1(10)
C5B	4923(3)	4736(3)	4473(2)	19.1(10)
C27B	1452(3)	8117(4)	3137(3)	27.3(12)
C19B	8990(3)	5768(3)	6975(2)	20.7(10)
C20B	7772(4)	5097(4)	8236(2)	30.6(13)
C13B	5061(4)	5230(4)	8216(2)	31.6(13)
C6B	4719(3)	5034(3)	5072(2)	19.3(10)
C16B	7187(3)	5324(3)	7078(2)	20.1(10)
C15B	7324(3)	5551(3)	6503(2)	19.1(10)
C7B	4620(3)	6171(4)	6331(2)	15.1(9)
C10B	4900(4)	5564(4)	7554(2)	20.8(11)
C24B	2509(3)	7960(3)	3233(2)	18.3(10)
C8B	4336(3)	5301(3)	6453(2)	18.9(10)
C2B	7589(3)	4751(3)	5081(2)	17.2(10)
C25B	3082(3)	7748(3)	3815(2)	19.1(10)
C1B	6599(3)	4344(3)	4893(2)	18(1)
N6B	954(3)	3512(3)	5719.8(18)	15.9(8)
C33B	-312(3)	2651(3)	4894(2)	17.4(10)
C34B	-1365(3)	2679(4)	4550(2)	21.5(11)
C32B	-98(3)	3360(4)	5408(2)	17.1(10)
C35B	-1642(4)	1965(4)	4049(2)	24.1(11)
C41B	1073(3)	4642(3)	4858(2)	16.6(10)
C37B	1974(4)	4515(4)	6581(2)	26.8(12)
C38B	1907(4)	5145(4)	7115(2)	29.2(12)
C43B	1463(4)	5760(4)	4075(3)	27.8(12)
C40B	1484(3)	3837(3)	5254(2)	15.5(10)
C36B	982(3)	4221(3)	6217(2)	18.9(10)
C29B	1110(4)	2219(4)	6514(2)	23.7(12)
C28B	1451(3)	2646(3)	5989(2)	16.7(10)
C30B	1641(4)	1322(4)	6705(2)	24.3(11)
C42B	1783(3)	4962(4)	4508(2)	22.3(11)
C31B	1426(4)	626(4)	6192(3)	27.0(12)
C39B	1583(5)	4686(4)	7628(3)	42.5(16)
N6	6066(3)	5393(3)	805.1(18)	16.1(8)
C34	6876(4)	3860(5)	-373(3)	34.7(15)
C30	3719(3)	6067(4)	-409(2)	24.6(12)
C32	6607(3)	5030(4)	357(2)	18.5(10)
C36	6523(3)	6306(4)	1029(2)	17.6(10)
C29	4774(3)	6135(4)	-68(2)	19.9(10)
C33	6200(4)	4187(4)	0(3)	29.0(13)
C42	7108(4)	4131(4)	2369(2)	31.6(13)
C41	7135(4)	4527(4)	1739(2)	28.7(13)
C31	3472(4)	6720(5)	-949(3)	34.6(15)
C39	6423(4)	8368(4)	1126(3)	27.7(12)
C40	6135(3)	4749(4)	1351(2)	21.0(11)
C35	6537(5)	3068(4)	-787(3)	37.2(15)
C28	5008(3)	5500(3)	486(2)	17(1)
C37	6142(4)	6793(4)	1514(2)	22.6(11)
C38	6640(4)	7704(4)	1664(2)	25.6(12)
C43	6652(4)	3226(5)	2330(3)	48.2(18)

Table S20: Anisotropic Displacement Parameters ($\times 10^4$) for **CMW05-034_BuCoTsNH3**. The anisotropic displacement factor exponent takes the form: $-2\pi^2[a^{*2} \times U_{11} + ... \; 2hka^* \times b^* \times U_{12}]$

Atom	U_{11}	U_{22}	U_{33}	U_{23}	U_{13}	U_{12}
Co1	10.0(3)	13.0(3)	14.6(3)	0.4(3)	3.7(2)	0.9(2)
S3	11.0(5)	15.0(6)	18.0(6)	-0.2(5)	3.8(4)	-0.2(4)
S1	15.9(5)	19.3(6)	17.9(6)	-5.9(5)	8.8(4)	-6.5(5)
S2	13.4(5)	29.0(7)	17.1(6)	-7.1(6)	3.5(4)	3.0(5)
O1	30.9(18)	10.4(17)	31.7(19)	-2.1(15)	17.7(15)	-2.5(15)
O6	15.0(16)	17.2(19)	20.7(17)	-3.8(14)	0.0(13)	3.0(13)
O3	22.6(18)	25(2)	25(2)	-9.7(16)	-2.5(15)	10.0(15)
N5	16.7(18)	15(2)	17.8(19)	0.4(17)	5.8(15)	-2.0(16)
O2	17.7(16)	41(2)	22.0(18)	-8.6(17)	6.7(14)	-12.1(16)
O4	21.7(17)	48(3)	20.8(18)	-10.8(19)	11.1(14)	-1.7(19)
O5	14.2(15)	28(2)	30(2)	-0.6(16)	6.2(14)	-6.7(14)
N2	14.9(19)	25(3)	15(2)	0.4(17)	2.6(16)	-0.9(17)
N3	11.2(17)	11(2)	20(2)	2.3(16)	1.7(15)	-1.5(14)
N4	13.9(17)	20(2)	16.9(19)	-0.6(16)	5.2(15)	3.4(15)
N1	18.1(19)	19(2)	16(2)	4.1(17)	4.5(16)	6.7(16)
C16	19(2)	19(3)	15(2)	0(2)	8.6(18)	-1.1(19)
C18	18(2)	17(3)	15(2)	-3.3(19)	-1.1(17)	-1.1(18)
C17	17(2)	15(3)	22(2)	-1.2(19)	5.1(18)	-0.6(18)
C24	33(3)	22(3)	12(2)	3(2)	4(2)	-2(2)
C21	16(2)	13(2)	16(2)	0.7(19)	2.5(18)	3.2(18)
C12	19(2)	16(2)	23(2)	-2.0(19)	6.1(19)	-3.4(18)
C19	19(2)	19(3)	13(2)	-0.5(19)	6.1(17)	1.8(18)
C8	32(3)	23(3)	20(3)	-1(2)	13(2)	-10(2)
C6	21(2)	28(3)	23(3)	8(2)	8(2)	12(2)
C10	24(2)	18(3)	20(3)	-4(2)	5(2)	1(2)
C5	28(3)	24(3)	28(3)	9(2)	13(2)	14(2)
C26	21(2)	21(3)	19(2)	-3(2)	3.0(18)	-6.5(19)
C20	19(2)	32(3)	32(3)	-6(2)	6(2)	-6(2)
C4	22(2)	15(3)	35(3)	10(2)	9(2)	1.0(19)
C13	45(3)	32(3)	21(3)	-10(2)	9(2)	0(3)
C25	30(3)	26(3)	22(3)	4(2)	9(2)	-7(2)
C9	43(3)	21(3)	28(3)	-5(2)	8(2)	-6(2)
C14	13.0(19)	16(2)	17(2)	-2.1(19)	5.0(17)	1.4(18)
C7	11.2(19)	17(3)	13(2)	-2.2(19)	3.3(16)	2.4(18)
C15	19(2)	23(3)	12(2)	1(2)	2.4(17)	1(2)
C22	19(2)	22(3)	24(3)	2(2)	2.7(19)	-2(2)
C11	23(2)	24(3)	20(2)	1(2)	7.0(19)	-2(2)
C23	28(3)	25(3)	24(3)	-6(2)	0(2)	-2(2)
C2	22(2)	32(3)	20(3)	4(2)	8(2)	0(2)
C1	21(2)	32(3)	22(3)	10(2)	7(2)	5(2)
C3	23(2)	13(3)	27(3)	2(2)	2(2)	-3.5(19)
C27	58(4)	55(5)	17(3)	-5(3)	9(3)	-8(3)
Co1B	9.4(3)	10.9(3)	13.6(3)	1.5(2)	2.6(2)	0.8(2)
S2B	8.3(4)	14.6(6)	15.7(5)	2.4(4)	2.2(4)	0.0(4)
S1B	14.3(5)	17.6(6)	21.0(6)	3.6(5)	7.6(4)	4.3(4)
S3B	15.2(5)	19.2(7)	18.5(6)	8.3(5)	5.6(4)	2.5(5)
O3B	16.0(16)	14.9(18)	21.4(18)	1.8(14)	2.4(13)	-4.9(13)
O2B	17.1(15)	31(2)	24.8(18)	0.2(16)	4.4(14)	6.9(15)
O4B	9.4(14)	30(2)	23.3(18)	3.0(15)	2.3(13)	2.1(14)
O5B	23.6(18)	37(2)	25.1(19)	16.2(18)	14.1(15)	8.3(18)
O6B	18.6(17)	16.7(19)	33(2)	6.5(16)	4.1(15)	-2.7(14)
O1B	28.3(17)	13.1(18)	31.0(19)	2.9(16)	15.6(15)	7.3(15)
N5B	16.8(18)	11(2)	23(2)	-2.4(17)	5.5(16)	0.4(15)

Atom	U_{11}	U_{22}	U_{33}	U_{23}	U_{13}	U_{12}
N1B	14.8(17)	11(2)	18(2)	-0.3(16)	4.3(15)	-0.7(15)
N2B	12.5(17)	9.0(19)	16.0(19)	0.7(16)	2.2(15)	1.1(14)
N4B	11.2(16)	14(2)	17.0(19)	0.4(15)	4.1(14)	-0.4(14)
N3B	16.7(18)	15(2)	16.3(19)	2.2(17)	5.2(15)	0.9(16)
C12B	18(2)	21(3)	26(3)	-4(2)	4.8(19)	-5.4(19)
C3B	24(2)	16(3)	13(2)	-1.5(19)	1.9(19)	2(2)
C17B	28(3)	15(3)	17(2)	0(2)	5(2)	-1(2)
C4B	21(2)	14(2)	17(2)	-2.0(18)	3.2(18)	0.5(18)
C14B	14(2)	13(2)	15(2)	-2.5(19)	2.3(18)	0.5(18)
C9B	22(2)	15(3)	27(3)	0(2)	8(2)	-2.0(19)
C26B	20(2)	24(3)	16(2)	3(2)	0.0(19)	3(2)
C22B	26(2)	15(3)	16(2)	4.7(19)	5.7(19)	3(2)
C11B	29(2)	17(3)	23(2)	-5(2)	5(2)	-4(2)
C18B	25(2)	24(3)	19(2)	5(2)	-4(2)	5(2)
C23B	23(2)	21(3)	19(2)	4(2)	1(2)	1(2)
C21B	18(2)	15(3)	17(2)	3.4(19)	2.2(18)	1.8(18)
C5B	12.3(19)	12(2)	32(3)	-4(2)	3.2(19)	-3.7(17)
C27B	17(2)	30(3)	31(3)	-1(2)	1(2)	3(2)
C19B	19(2)	20(3)	22(2)	0(2)	1.3(19)	-0.1(19)
C20B	44(3)	32(3)	15(3)	-1(2)	8(2)	-4(3)
C13B	46(3)	29(3)	20(3)	1(2)	7(2)	-4(3)
C6B	20(2)	16(3)	25(3)	1(2)	12.3(19)	-2.2(19)
C16B	22(2)	18(3)	22(2)	-1(2)	7.4(19)	0.4(19)
C15B	18(2)	17(3)	21(2)	2.4(19)	1.4(18)	2.8(18)
C7B	9.3(18)	20(3)	17(2)	0(2)	5.4(16)	0.3(18)
C10B	25(2)	21(3)	17(2)	1(2)	6(2)	1(2)
C24B	17(2)	12(2)	24(3)	-3(2)	2.1(19)	1.9(18)
C8B	21(2)	18(3)	20(2)	-6.4(19)	9.1(19)	-6.1(18)
C2B	16(2)	12(2)	22(2)	1.6(19)	1.1(18)	5.7(17)
C25B	19(2)	18(3)	21(2)	-1(2)	7.0(19)	-0.4(19)
C1B	19(2)	10(2)	26(3)	2.6(19)	7.3(19)	-1.4(17)
N6B	12.8(17)	17(2)	18(2)	-2.2(16)	4.7(15)	4.3(15)
C33B	16(2)	15(3)	22(2)	-2(2)	6.4(18)	2.2(18)
C34B	20(2)	23(3)	21(3)	-2(2)	6(2)	1(2)
C32B	10.2(19)	21(3)	22(2)	0(2)	7.5(18)	3.1(18)
C35B	22(2)	26(3)	22(3)	-5(2)	2(2)	0(2)
C41B	17(2)	15(2)	18(2)	-1.3(19)	3.7(18)	4.3(18)
C37B	24(2)	27(3)	26(3)	-11(2)	-1(2)	5(2)
C38B	35(3)	26(3)	24(3)	-6(2)	3(2)	9(2)
C43B	34(3)	21(3)	29(3)	0(2)	9(2)	-7(2)
C40B	14(2)	17(3)	18(2)	-1.1(19)	7.0(17)	0.3(18)
C36B	18(2)	21(3)	19(2)	-6(2)	5.8(18)	4.6(19)
C29B	32(3)	23(3)	20(2)	2(2)	14(2)	8(2)
C28B	15(2)	15(3)	20(2)	-1.5(19)	6.1(18)	2.8(18)
C30B	30(3)	26(3)	21(2)	6(2)	12(2)	5(2)
C42B	17(2)	21(3)	30(3)	-2(2)	7(2)	1(2)
C31B	29(3)	22(3)	32(3)	8(2)	13(2)	8(2)
C39B	61(4)	33(4)	35(3)	1(3)	15(3)	14(3)
N6	14.3(18)	16(2)	18(2)	1.9(16)	4.8(15)	-3.5(15)
C34	18(2)	43(4)	44(4)	-21(3)	9(2)	0(2)
C30	19(2)	26(3)	28(3)	5(2)	4(2)	-2(2)
C32	13(2)	21(3)	24(3)	-1(2)	8.0(19)	-2.3(19)
C36	18(2)	17(2)	18(2)	-1(2)	5.0(17)	-6.5(19)
C29	17(2)	22(3)	22(2)	0(2)	6.0(18)	-2(2)
C33	31(3)	26(3)	37(3)	-7(2)	20(2)	-6(2)
C42	33(3)	36(3)	22(3)	1(2)	0(2)	9(2)
C41	22(2)	36(3)	25(3)	8(2)	0(2)	-1(2)

Atom	U_{11}	U_{22}	U_{33}	U_{23}	U_{13}	U_{12}
C31	26(3)	43(4)	33(3)	7(3)	3(2)	7(3)
C39	32(3)	25(3)	27(3)	-4(2)	10(2)	-3(2)
C40	21(2)	22(3)	22(3)	4(2)	10(2)	-5(2)
C35	44(4)	24(3)	52(4)	-8(3)	28(3)	2(3)
C28	13(2)	18(3)	22(2)	0(2)	7.0(18)	-4.6(18)
C37	26(2)	24(3)	21(3)	-3(2)	12(2)	-8(2)
C38	30(3)	27(3)	21(3)	-10(2)	9(2)	-11(2)
C43	34(3)	57(5)	48(4)	24(4)	-1(3)	2(3)

Table S21: Bond Lengths in Å for **CMW05-034_BuCoTsNH3**.

Atom	Atom	Length/Å
Co1	N5	2.093(4)
Co1	N2	2.051(4)
Co1	N3	2.066(4)
Co1	N4	2.077(4)
Co1	N1	2.187(4)
S3	O6	1.450(4)
S3	O5	1.453(4)
S3	N3	1.574(4)
S3	C21	1.776(5)
S1	O1	1.463(4)
S1	O2	1.443(3)
S1	N4	1.581(4)
S1	C7	1.781(5)
S2	O3	1.457(4)
S2	O4	1.445(4)
S2	N2	1.582(4)
S2	C14	1.782(4)
N2	C2	1.475(7)
N3	C3	1.469(6)
N4	C6	1.473(6)
N1	C5	1.477(6)
N1	C4	1.468(6)
N1	C1	1.479(6)
C16	C17	1.398(6)
C16	C15	1.377(6)
C18	C17	1.389(7)
C18	C19	1.389(6)
C17	C20	1.507(7)
C24	C25	1.392(7)
C24	C23	1.379(7)
C24	C27	1.501(7)
C21	C26	1.400(6)
C21	C22	1.380(7)
C12	C7	1.397(6)
C12	C11	1.381(7)
C19	C14	1.393(6)
C8	C9	1.391(7)
C8	C7	1.379(7)
C6	C5	1.504(7)
C10	C13	1.511(7)
C10	C9	1.369(8)
C10	C11	1.395(7)
C26	C25	1.386(7)
C4	C3	1.514(7)
C14	C15	1.386(6)
C22	C23	1.393(7)
C2	C1	1.511(7)
Co1B	N5B	2.088(4)
Co1B	N1B	2.177(4)
Co1B	N2B	2.058(4)
Co1B	N4B	2.095(4)
Co1B	N3B	2.075(4)
S2B	O3B	1.447(4)
S2B	O4B	1.452(3)
S2B	N2B	1.574(4)
S2B	C14B	1.780(5)
S1B	O2B	1.450(3)
S1B	O1B	1.446(4)
S1B	N4B	1.582(4)
S1B	C7B	1.781(5)
S3B	O5B	1.446(4)
S3B	O6B	1.458(4)
S3B	N3B	1.576(4)
S3B	C21B	1.776(5)
N1B	C4B	1.474(6)
N1B	C5B	1.468(6)
N1B	C1B	1.481(6)
N2B	C2B	1.493(6)
N4B	C6B	1.488(6)
N3B	C3B	1.474(6)
C12B	C11B	1.394(7)
C12B	C7B	1.387(6)
C3B	C4B	1.518(7)
C17B	C18B	1.377(7)
C17B	C20B	1.513(7)
C17B	C16B	1.397(7)
C14B	C19B	1.389(6)
C14B	C15B	1.384(6)
C9B	C10B	1.377(7)
C9B	C8B	1.385(7)
C26B	C21B	1.398(7)
C26B	C25B	1.389(7)
C22B	C23B	1.378(7)
C22B	C21B	1.387(6)
C11B	C10B	1.391(7)
C18B	C19B	1.386(7)
C23B	C24B	1.385(7)
C5B	C6B	1.503(7)
C27B	C24B	1.509(7)

Atom	Atom	Length/Å
C13B	C10B	1.514(7)
C16B	C15B	1.385(7)
C7B	C8B	1.399(7)
C24B	C25B	1.385(7)
C2B	C1B	1.513(6)
N6B	C32B	1.520(6)
N6B	C40B	1.516(6)
N6B	C36B	1.518(6)
N6B	C28B	1.516(6)
C33B	C34B	1.523(6)
C33B	C32B	1.524(7)
C34B	C35B	1.516(7)
C41B	C40B	1.510(7)
C41B	C42B	1.515(7)
C37B	C38B	1.532(7)
C37B	C36B	1.521(7)
C38B	C39B	1.503(8)
C43B	C42B	1.520(8)
C29B	C28B	1.518(7)
C29B	C30B	1.538(7)
C30B	C31B	1.510(8)
N6	C32	1.514(6)
N6	C36	1.530(6)
N6	C40	1.526(6)
N6	C28	1.524(6)
C34	C33	1.514(7)
C34	C35	1.494(8)
C30	C29	1.525(6)
C30	C31	1.512(8)
C32	C33	1.514(7)
C36	C37	1.514(7)
C29	C28	1.518(7)
C42	C41	1.528(7)
C42	C43	1.487(9)
C41	C40	1.521(7)
C39	C38	1.519(8)
C37	C38	1.525(7)

Table S22: Bond Angles in ° for **CMW05-034_BuCoTsNH3**.

Atom	Atom	Atom	Angle/°
N5	Co1	N1	178.57(15)
N2	Co1	N5	98.55(16)
N2	Co1	N3	113.04(16)
N2	Co1	N4	119.91(16)
N2	Co1	N1	81.57(16)
N3	Co1	N5	100.68(15)
N3	Co1	N4	119.53(16)
N3	Co1	N1	80.56(15)
N4	Co1	N5	98.40(16)
N4	Co1	N1	80.33(16)
O6	S3	O5	115.5(2)
O6	S3	N3	109.3(2)
O6	S3	C21	106.4(2)
O5	S3	N3	112.8(2)
O5	S3	C21	105.5(2)
N3	S3	C21	106.7(2)
O1	S1	N4	109.7(2)
O1	S1	C7	104.3(2)
O2	S1	O1	115.1(2)
O2	S1	N4	113.7(2)
O2	S1	C7	105.2(2)
N4	S1	C7	108.1(2)
O3	S2	N2	108.6(2)
O3	S2	C14	105.4(2)
O4	S2	O3	115.7(2)
O4	S2	N2	113.1(2)
O4	S2	C14	106.1(2)
N2	S2	C14	107.3(2)
S2	N2	Co1	130.7(3)
C2	N2	Co1	113.1(3)
C2	N2	S2	113.6(3)
S3	N3	Co1	128.8(2)
C3	N3	Co1	112.4(3)
C3	N3	S3	114.3(3)
S1	N4	Co1	132.6(2)
C6	N4	Co1	113.2(3)
C6	N4	S1	112.0(3)
C5	N1	Co1	107.7(3)
C5	N1	C1	110.9(4)
C4	N1	Co1	108.3(3)
C4	N1	C5	111.0(4)
C4	N1	C1	112.3(4)
C1	N1	Co1	106.4(3)
C15	C16	C17	121.0(4)
C17	C18	C19	121.8(4)
C16	C17	C20	120.1(4)
C18	C17	C16	118.0(4)
C18	C17	C20	121.9(5)
C25	C24	C27	120.2(5)
C23	C24	C25	118.4(5)
C23	C24	C27	121.4(5)
C26	C21	S3	119.0(4)
C22	C21	S3	121.8(4)
C22	C21	C26	119.2(4)
C11	C12	C7	119.6(4)
C18	C19	C14	118.8(4)
C7	C8	C9	119.1(5)
N4	C6	C5	108.1(4)
C9	C10	C13	121.9(5)
C9	C10	C11	117.4(5)
C11	C10	C13	120.6(5)
N1	C5	C6	111.0(4)
C25	C26	C21	120.0(4)
N1	C4	C3	110.2(4)
C26	C25	C24	121.0(5)
C10	C9	C8	122.5(5)
C19	C14	S2	121.1(3)
C15	C14	S2	118.6(3)

Atom	Atom	Atom	Angle/°
C15	C14	C19	120.2(4)
C12	C7	S1	117.3(4)
C8	C7	S1	122.9(4)
C8	C7	C12	119.7(4)
C16	C15	C14	120.1(4)
C21	C22	C23	120.1(5)
C12	C11	C10	121.5(5)
C24	C23	C22	121.3(5)
N2	C2	C1	109.4(4)
N1	C1	C2	110.6(4)
N3	C3	C4	108.5(4)
N5B	Co1B	N1B	179.16(16)
N5B	Co1B	N4B	98.99(16)
N2B	Co1B	N5B	99.80(15)
N2B	Co1B	N1B	80.42(15)
N2B	Co1B	N4B	119.01(15)
N2B	Co1B	N3B	112.32(16)
N4B	Co1B	N1B	80.21(15)
N3B	Co1B	N5B	100.35(16)
N3B	Co1B	N1B	80.29(16)
N3B	Co1B	N4B	120.30(15)
O3B	S2B	O4B	114.8(2)
O3B	S2B	N2B	109.6(2)
O3B	S2B	C14B	105.8(2)
O4B	S2B	N2B	112.7(2)
O4B	S2B	C14B	106.4(2)
N2B	S2B	C14B	107.0(2)
O2B	S1B	N4B	111.9(2)
O2B	S1B	C7B	104.9(2)
O1B	S1B	O2B	116.1(2)
O1B	S1B	N4B	108.9(2)
O1B	S1B	C7B	105.9(2)
N4B	S1B	C7B	108.7(2)
O5B	S3B	O6B	115.4(2)
O5B	S3B	N3B	112.7(2)
O5B	S3B	C21B	105.6(2)
O6B	S3B	N3B	108.5(2)
O6B	S3B	C21B	106.7(2)
N3B	S3B	C21B	107.4(2)
C4B	N1B	Co1B	107.6(3)
C4B	N1B	C1B	111.0(4)
C5B	N1B	Co1B	107.2(3)
C5B	N1B	C4B	112.4(4)
C5B	N1B	C1B	111.4(4)
C1B	N1B	Co1B	107.0(3)
S2B	N2B	Co1B	130.3(2)
C2B	N2B	Co1B	115.6(3)
C2B	N2B	S2B	112.5(3)
S1B	N4B	Co1B	132.2(2)
C6B	N4B	Co1B	113.2(3)
C6B	N4B	S1B	114.1(3)
S3B	N3B	Co1B	128.7(2)
C3B	N3B	Co1B	114.0(3)
C3B	N3B	S3B	113.5(3)
C7B	C12B	C11B	119.6(5)
N3B	C3B	C4B	108.8(4)
C18B	C17B	C20B	121.9(5)
C18B	C17B	C16B	118.1(5)
C16B	C17B	C20B	120.0(5)
N1B	C4B	C3B	109.8(4)
C19B	C14B	S2B	120.3(4)
C15B	C14B	S2B	120.2(3)
C15B	C14B	C19B	119.5(4)
C10B	C9B	C8B	121.2(5)
C25B	C26B	C21B	120.0(4)
C23B	C22B	C21B	119.8(5)
C10B	C11B	C12B	121.0(5)
C17B	C18B	C19B	121.4(5)
C22B	C23B	C24B	122.1(5)
C26B	C21B	S3B	119.2(4)
C22B	C21B	S3B	121.6(4)
C22B	C21B	C26B	119.1(4)
N1B	C5B	C6B	110.5(4)
C18B	C19B	C14B	120.0(4)
N4B	C6B	C5B	109.4(4)
C15B	C16B	C17B	121.1(4)
C14B	C15B	C16B	119.9(4)
C12B	C7B	S1B	120.0(4)
C12B	C7B	C8B	119.6(4)
C8B	C7B	S1B	120.3(4)
C9B	C10B	C11B	118.8(5)
C9B	C10B	C13B	120.4(5)
C11B	C10B	C13B	120.8(5)
C23B	C24B	C27B	121.4(5)
C23B	C24B	C25B	117.9(5)
C25B	C24B	C27B	120.7(5)
C9B	C8B	C7B	119.8(4)
N2B	C2B	C1B	109.7(4)
C24B	C25B	C26B	121.2(5)
N1B	C1B	C2B	111.6(4)
C40B	N6B	C32B	111.0(4)
C40B	N6B	C36B	110.8(4)
C36B	N6B	C32B	105.8(3)
C28B	N6B	C32B	111.9(4)
C28B	N6B	C40B	105.4(3)
C28B	N6B	C36B	112.0(4)
C34B	C33B	C32B	110.1(4)
C35B	C34B	C33B	113.2(4)
N6B	C32B	C33B	115.7(4)
C40B	C41B	C42B	109.2(4)
C36B	C37B	C38B	110.4(4)
C39B	C38B	C37B	114.1(5)
C41B	C40B	N6B	117.1(4)
N6B	C36B	C37B	115.6(4)
C28B	C29B	C30B	109.6(4)
N6B	C28B	C29B	116.2(4)
C31B	C30B	C29B	112.8(4)
C41B	C42B	C43B	115.5(4)
C32	N6	C36	105.9(3)
C32	N6	C40	111.2(4)
C32	N6	C28	110.9(4)
C40	N6	C36	110.9(4)
C28	N6	C36	111.1(4)
C28	N6	C40	106.8(3)

Atom	Atom	Atom	Angle/°
C35	C34	C33	115.6(5)
C31	C30	C29	110.9(5)
N6	C32	C33	116.1(4)
C37	C36	N6	116.6(4)
C28	C29	C30	110.6(4)
C34	C33	C32	109.4(4)

Atom	Atom	Atom	Angle/°
C43	C42	C41	114.0(5)
C40	C41	C42	111.2(4)
C41	C40	N6	116.5(4)
C29	C28	N6	115.7(4)
C36	C37	C38	109.9(4)
C39	C38	C37	114.0(4)

Table S23: Hydrogen Fractional Atomic Coordinates (×10⁴) and Equivalent Isotropic Displacement Parameters (Å²×10³) for **CMW05-034_BuCoTsNH3**. U_{eq} is defined as 1/3 of the trace of the orthogonalised U_{ij}.

Atom	x	y	z	U_{eq}
H5A	1510(30)	700(30)	-92(16)	33(9)
H5B	1260(20)	940(30)	531(13)	33(9)
H16	-2234	1167	-828	20
H18	-2527	883	-2602	21
H12	-1151	1589	1698	23
H19	-921	1014	-2487	20
H8	355	3677	1286	29
H6A	-878	3627	309	28
H6B	-996	3225	-361	28
H5D	-294	4615	-363	31
H5E	468	4405	262	31
H26	2067	2211	1353	25
H20A	-3958	889	-2265	42
H20B	-3879	1538	-1697	42
H20C	-3811	490	-1594	42
H4A	1420	4987	-394	29
H4B	1886	4267	-745	29
H13A	-730	3557	3350	49
H13B	-60	4322	3216	49
H13C	376	3399	3498	49
H25	1825	2434	2329	30
H9	415	4293	2250	37
H15	-626	1263	-647	22
H22	4315	3893	1779	27
H11	-1072	2224	2656	26
H23	4031	4145	2742	32
H2A	363	2802	-1846	29
H2B	1352	3214	-1490	29
H1A	221	4226	-1359	30
H1B	-400	3457	-1172	30
H3A	2923	4433	223	26
H3B	2091	4324	555	26
H27A	3259	3702	3545	65
H27B	2435	2985	3395	65
H27C	2217	3998	3204	65
H5BA	6367	8048	4859	26
H5BB	7120	7660	5438	26
H5BC	6047	7755	5453	26
H12B	5248	7310	6744	26
H3BA	5843	5841	3111	22
H3BB	4948	5752	3386	22
H4BA	5765	4410	3619	21
H4BB	6743	4914	3867	21

Atom	x	y	z	U_{eq}
H9B	4303	4427	7140	25
H26B	4432	7473	4304	25
H22B	4174	7941	2489	23
H11B	5472	6805	7759	28
H18B	9358	5538	7896	29
H23B	2567	8179	2352	26
H5BD	4820	4090	4421	23
H5BE	4490	5039	4127	23
H27D	1191	7657	3350	41
H27E	1142	8095	2701	41
H27F	1349	8699	3299	41
H19B	9601	5913	6942	25
H20D	8372	5064	8543	46
H20E	7453	4524	8209	46
H20F	7381	5555	8351	46
H13D	4456	5137	8308	47
H13E	5422	5671	8496	47
H13F	5408	4671	8262	47
H6BA	4037	5004	5035	23
H6BB	5039	4635	5406	23
H16B	6579	5166	7109	24
H15B	6810	5551	6153	23
H8B	4047	4920	6126	23
H2BA	7962	4454	5453	21
H2BB	7909	4663	4752	21
H25B	2808	7695	4149	23
H1BA	6625	3771	4686	22
H1BB	6377	4228	5262	22
H33A	75	2766	4605	21
H33B	-151	2056	5072	21
H34A	-1746	2597	4848	26
H34B	-1514	3271	4363	26
H32A	-373	3929	5235	21
H32B	-416	3183	5725	21
H35A	-1264	2038	3755	36
H35B	-2306	2028	3839	36
H35C	-1532	1376	4234	36
H41A	942	5125	5119	20
H41B	478	4474	4566	20
H37A	2291	4826	6305	32
H37B	2350	3988	6747	32
H38A	2529	5414	7288	35
H38B	1466	5631	6949	35
H43A	903	5596	3759	42
H43B	1964	5925	3885	42
H43C	1319	6263	4309	42
H40A	2132	3985	5480	19
H40B	1522	3338	4979	19
H36A	644	3987	6509	23
H36B	637	4750	6022	23
H29A	428	2108	6380	28
H29B	1231	2626	6867	28
H28A	2129	2770	6138	20
H28B	1373	2208	5655	20
H30A	2323	1437	6824	29
H30B	1463	1080	7065	29
H42A	1926	4461	4265	27

Atom	x	y	z	U_{eq}
H42B	2372	5125	4808	27
H31A	1755	783	5882	40
H31B	751	611	6006	40
H31C	1636	42	6361	40
H39A	908	4578	7496	64
H39B	1722	5066	7990	64
H39C	1913	4122	7727	64
H34C	6999	4356	-626	42
H34D	7479	3701	-85	42
H30C	3575	5456	-560	30
H30D	3332	6201	-122	30
H32C	7257	4901	590	22
H32D	6637	5501	60	22
H36C	7203	6213	1196	21
H36D	6443	6699	670	21
H29C	5162	5982	-351	24
H29D	4923	6751	73	24
H33C	6116	3720	287	35
H33D	5581	4321	-277	35
H42C	7757	4087	2627	38
H42D	6763	4544	2572	38
H41C	7520	5072	1803	34
H41D	7430	4096	1517	34
H31D	3823	6561	-1247	52
H31E	3638	7323	-801	52
H31F	2800	6689	-1142	52
H39D	6716	8163	809	41
H39E	6672	8952	1271	41
H39F	5745	8409	958	41
H40C	5778	5010	1623	25
H40D	5822	4188	1190	25
H35D	6412	2570	-543	56
H35E	7020	2899	-992	56
H35F	5962	3227	-1092	56
H28C	4749	4908	349	20
H28D	4685	5716	790	20
H37C	6253	6429	1888	27
H37D	5460	6885	1360	27
H38C	6449	7972	2012	31
H38D	7325	7605	1793	31
H43D	6008	3263	2078	72
H43E	6649	3025	2740	72
H43F	7006	2804	2148	72
H5C	2293(10)	1080(40)	465(15)	33(9)

Table S24: Hydrogen Bond information for **CMW05-034_BuCoTsNH3**.

D	H	A	d(D-H)/Å	d(H-A)/Å	d(D-A)/Å	D-H-A/deg
N5	H5A	O3	0.979(8)	1.98(3)	2.846(5)	146(4)
N5	H5B	O1	0.979(8)	1.96(3)	2.819(5)	144(4)
N5B	H5BA	O6B	0.96	1.99	2.837(6)	146.3
N5B	H5BB	O3B	0.96	2.00	2.859(5)	147.9
N5B	H5BC	O1B	0.96	2.01	2.841(5)	144.1
N5	H5C	O6	0.982(7)	2.06(4)	2.861(5)	138(4)

3-2

EMORY UNIVERSITY | X-ray Crystallography Center

Submitted by: **Christian Wallen**

Solved by: **John Bacsa**

Sample ID: **CMW-04-051 vial1 (2**

Crystal Data and Experimental

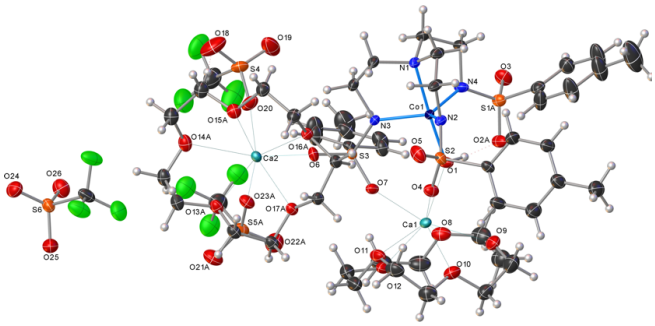

Experimental. Single green prism-shaped crystals of (**A244-0m**) were obtained by vapor diffusion from DCM and diethyl ether. A suitable crystal (0.48×0.20×0.10 mm) was selected and mounted on a loop with paratone oil on a Bruker APEX-II CCD diffractometer. The crystal was cooled to T = 110(2) K during data collection. The structure was solved with the **XT** (Sheldrick, 2015) structure solution program using direct and dual-space solution methods and by using **Olex2** (Dolomanov et al., 2009) as the graphical interface. The structure was refined with version 2014/7 of **XL** (Sheldrick, 2008) using Least Squares minimisation.

Crystal Data. $C_{54}H_{82}Ca_2CoF_9N_4O_{27}S_6$, M_r = 1721.75, triclinic, P-1 (No. 2), a = 12.8230(17) Å, b = 14.7189(19) Å, c = 19.625(3) Å, α = 86.108(3)°, β = 78.897(3)°, γ = 89.474(3)°, V = 3626.3(9) Å^3, T = 110(2) K, Z = 2, Z' = 1, μ(MoK$_\alpha$) = 0.655, 24718 reflections measured, 15868 unique (R_{int}# = 0.0468) which were used in all calculations. The final wR_2 was 0.2035 (all data) and R_1 was 0.0742 (I > 2σ(I)).

Compound	**A244-0m**
	(CCDC 1447763)
Formula	$C_{54}H_{82}Ca_2CoF_9N_4O_{27}S_6$
$D_{calc.}$/ g cm^{-3}	1.577
μ/mm^{-1}	0.655
Formula Weight	1721.75
Colour	green
Shape	prism
Max Size/mm	0.48
Mid Size/mm	0.20
Min Size/mm	0.10
T/K	110(2)
Crystal System	triclinic
Space Group	P-1
a/Å	12.8230(17)
b/Å	14.7189(19)
c/Å	19.625(3)
α/°	86.108(3)
β/°	78.897(3)
γ/°	89.474(3)
V/Å^3	3626.3(9)
Z	2
Z'	1
Θ_{min}/°	1.618
Θ_{max}/°	27.502
Measured Refl.	24718
Independent Refl.	15868
Reflections I > 2σ(I)	10297
R_{int}	0.0468
Parameters	1167
Restraints	1273
Largest Peak	0.991
Deepest Hole	-1.450
GooF	1.041
wR_2 (all data)	0.2035
wR_2	0.1690
R_1 (all data)	0.1217
R_1	0.0742

Structure Quality Indicators

Reflections:	d min	0.77	I/σ	7.6	Rint	4.68%	complete	95%
Refinement:	Shift	-0.001	Max Peak	1.0	Min Peak	-1.4	GooF	1.041

Experimental Extended. A green prism-shaped crystal with dimensions 0.48×0.20×0.10 mm was mounted on a loop with paratone oil. Data were collected using a Bruker APEX-II CCD diffractometer equipped with an Oxford Cryosystems low-temperature apparatus operating at $T = 110(2)$ K.

Data were measured using and scans of 1.00° per frame for 30.00 s using MoK$_\alpha$ radiation (fine-focus sealed tube, 45 kV, 35 mA). The total number of runs and images was based on the strategy calculation from the program **APEX2** (Bruker). The maximum resolution achieved was $\Theta = 27.502°$.

Unit cell indexing was performed by using the **APEX2** (Bruker, 2014) software and refined using **SAINT** (Bruker, V8.34A, 2013) on 9951 reflections, 40% of the observed reflections. Data reduction, scaling and absorption corrections were performed using **SAINT** (Bruker, V8.34A, 2013) and **SADABS-2014/5** (Bruker,2014/5) was used for absorption correction.wR_2(int) was 0.1138 before and 0.0409 after correction. The Ratio of minimum to maximum transmission is 0.7886.The /2 correction factor is 0.00150. software. The final completeness is 96.80 out to 27.502 in Θ. The absorption coefficient (μ) of this material is 0.655 and the minimum and maximum transmissions are 0.5880 and 0.7456.

The structure was solved with XT (Sheldrick, 2015) in the space group P-1 (# 2) using direct and dual-space solution methods and by using **Olex2** (Dolomanov et al., 2009) as the graphical interface. The structure was refined by Least Squares using **XL** (Sheldrick, 2008). All non-hydrogen atoms were refined anisotropically. Hydrogen atom positions were calculated geometrically and refined using the riding model.

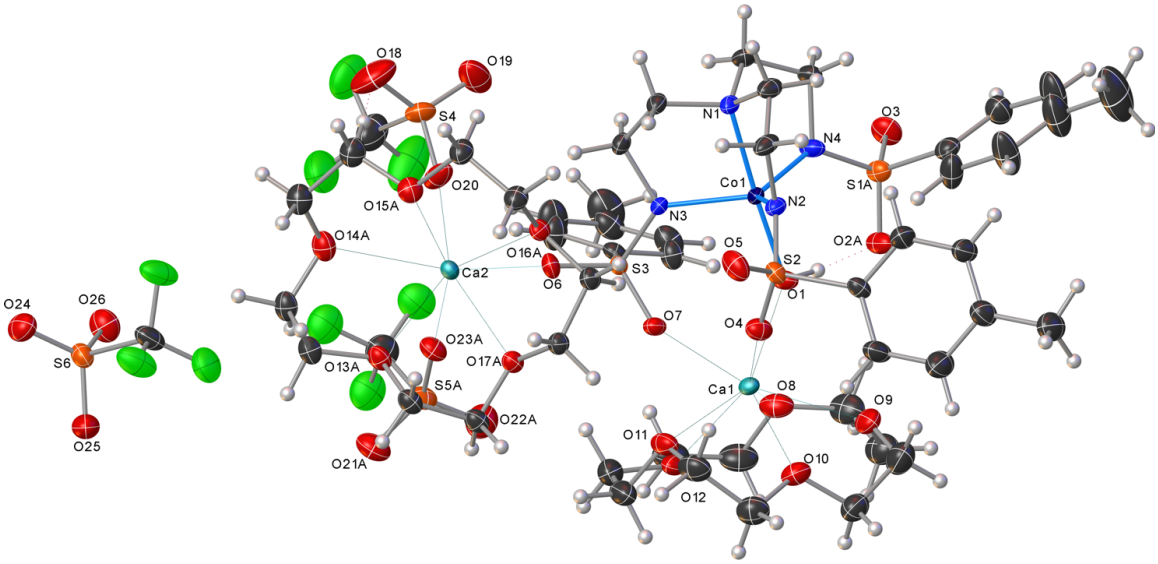

Figure S13:

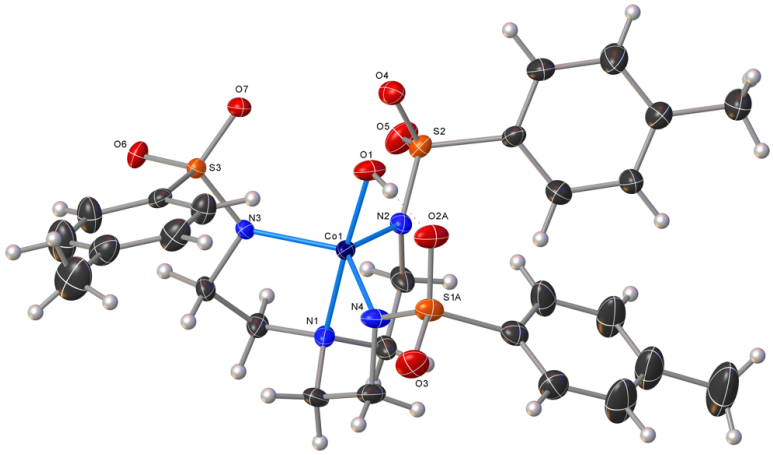

Figure S14:

Data Plots: Diffraction Data

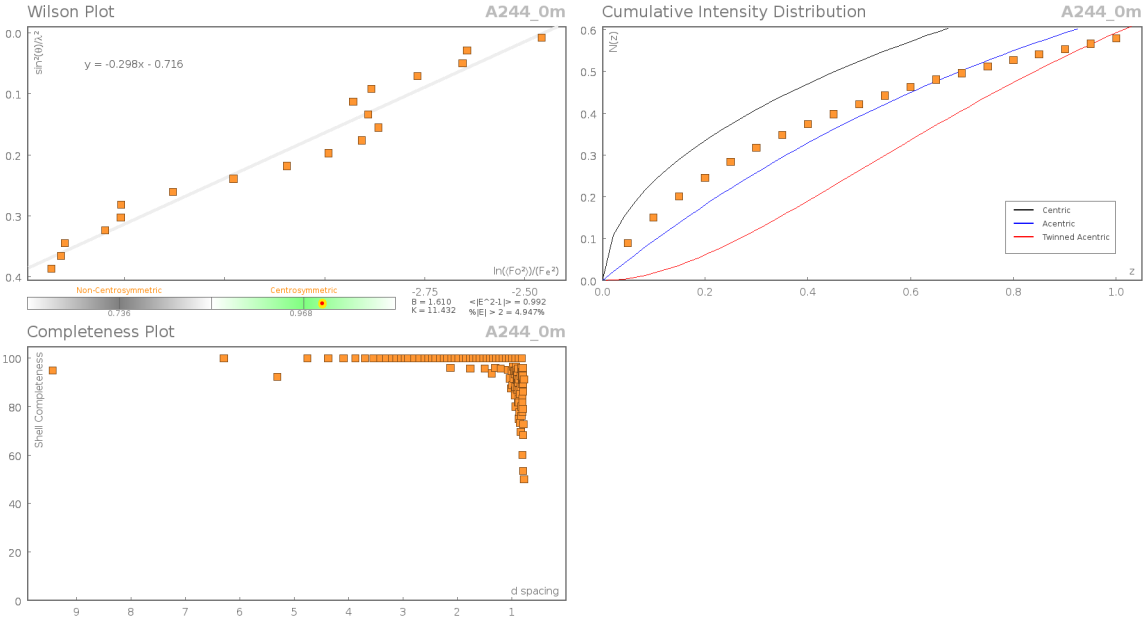

Data Plots: Refinement and Data

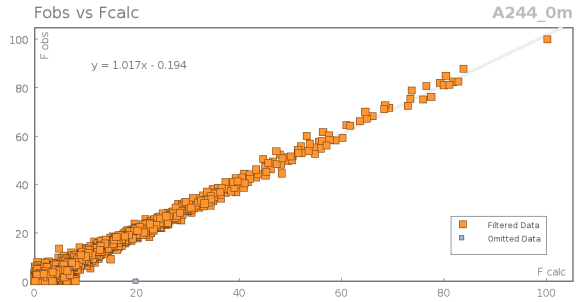

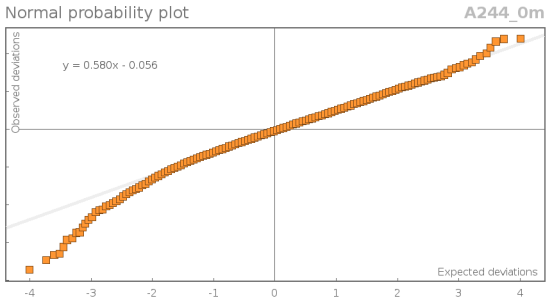

Reflection Statistics

Total reflections (after filtering)	24719	Unique reflections	15868
Completeness	0.951	Mean I/σ	7.55
hklsub>max</sub> collected	(16, 15, 25)	hklsub>min</sub> collected	(-16, -19, -24)
hkl_{max} used	(16, 19, 25)	hkl_{min} used	(-16, -19, 0)
Lim d_{max} collected	100.0	Lim d_{min} collected	0.36
d_{max} used	19.21	d_{min} used	0.77
Friedel pairs	4768	Friedel pairs merged	1
Inconsistent equivalents	4	R_{int}	0.0468
R_{sigma}	0.0901	Intensity transformed	0
Omitted reflections	0	Omitted by user (OMIT hkl)	1
Multiplicity	(16588, 4016, 33)	Maximum multiplicity	5
Removed systematic absences	0	Filtered off (Shel/OMIT)	0

Images of the Crystal on the Diffractometer

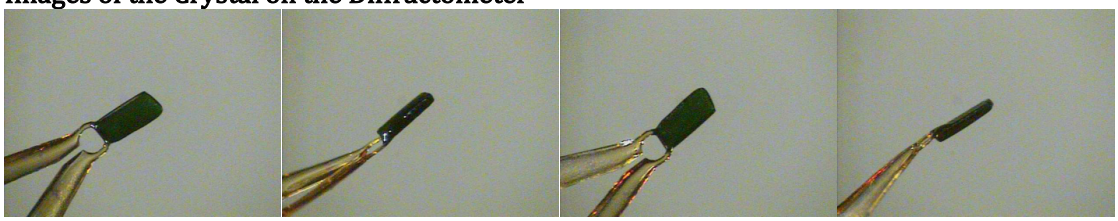

Table S74: Fractional Atomic Coordinates (×10^4) and Equivalent Isotropic Displacement Parameters (Å^2×10^3) for **A244_0m**. U_{eq} is defined as 1/3 of of the trace of the orthogonalised U_{ij}.

Atom	x	y	z	U_{eq}
C50B	-986(17)	7041(9)	4182(9)	56.9(16)
C51B	-912(17)	8046(10)	4313(7)	61(3)
C52B	-1040(20)	8512(10)	3621(8)	69(5)
C53B	-1679(15)	7856(10)	3312(7)	56(2)
O27B	-1765(14)	7011(10)	3737(8)	53.4(12)
C50A	-1040(18)	6936(10)	4216(9)	56.9(16)
C51A	-564(17)	7873(13)	4250(7)	61(3)
C52A	-472(17)	8274(12)	3507(8)	61(2)
C53A	-1325(17)	7808(12)	3232(8)	56(2)
O27A	-1762(16)	7082(11)	3733(10)	53.4(12)
C4	6298(4)	5238(3)	2610(3)	23.5(11)
S1B	2943(8)	5837(5)	4740(7)	23.9(7)
O2B	2141(12)	5182(7)	4655(11)	27(2)
C7B	2474(11)	6943(6)	4551(5)	26.9(9)
C8B	2177(15)	7156(9)	3920(6)	42(2)

Atom	x	y	z	U_{eq}
C9B	1969(15)	8061(9)	3727(7)	45(4)
C10B	2000(20)	8734(9)	4182(9)	63(3)
C11B	2280(20)	8512(8)	4821(9)	53(5)
C12B	2510(20)	7624(8)	5011(7)	38.1(16)
C13B	1700(30)	9712(10)	3984(11)	94(5)
C5	5827(4)	5842(4)	3759(3)	26.4(11)
F8A	8629(7)	-1442(4)	985(4)	53.4(15)
F7A	7881(8)	-1795(5)	150(4)	51.1(18)
F9A	6964(7)	-1705(5)	1124(4)	55.2(15)
C49A	7893(9)	-1971(4)	821(8)	38.2(13)
C6	4899(4)	6169(4)	4265(3)	29.8(12)
C1	5538(4)	6775(3)	2726(3)	27.4(10)
O15B	7975(4)	2653(4)	591(4)	29.3(14)
O13B	5709(5)	1577(4)	227(3)	25.4(9)
O17B	4698(4)	3001(3)	870(2)	20.7(8)
O14B	7411(4)	893(4)	721(3)	32(1)
O16B	6496(4)	3876(3)	1048(3)	19.9(8)
C38B	6000(6)	656(4)	123(5)	39.3(17)
C39B	7164(6)	601(6)	90(4)	40.5(17)
C40B	8503(5)	1113(5)	653(4)	34.6(14)
C41B	8751(7)	2025(5)	285(5)	38.5(19)
C42B	8142(6)	3564(4)	295(4)	28.0(11)
C43B	7575(5)	4164(5)	816(4)	25.8(10)
C44B	5761(5)	4356(4)	690(4)	22.3(10)
C45B	4671(5)	3966(4)	940(4)	21.4(9)
C46B	4460(6)	2771(4)	219(3)	26(1)
C47B	4633(5)	1777(4)	155(4)	26.3(10)
C2	5007(4)	6761(3)	2112(3)	27.1(10)
C3	5983(4)	4262(3)	2829(3)	21.8(10)
F8B	9122(14)	-1590(9)	938(9)	53.4(15)
F7B	8358(11)	-1731(10)	116(8)	40(3)
F9B	7406(14)	-1548(10)	1202(9)	55.2(15)
C49B	8221(18)	-1948(5)	791(15)	38.2(13)
C22	5057(5)	1950(4)	3688(3)	36.1(12)
C23	5046(6)	1505(4)	4331(3)	47.3(15)
C24	4329(5)	1744(4)	4916(3)	36.6(11)
O15A	7846(6)	2978(6)	483(7)	27(2)
O13A	5922(9)	1381(8)	251(5)	25.4(9)
O17A	4618(8)	2714(5)	753(4)	20.7(8)
O14A	7724(8)	1163(6)	737(4)	32(1)
O16A	6071(6)	3927(6)	1033(4)	19.9(8)
C38A	6714(8)	811(8)	-108(5)	26(2)
C39A	7335(8)	434(6)	409(6)	28.0(18)
C40A	8678(8)	1548(6)	337(7)	34(2)
C41A	8816(8)	2505(6)	505(8)	35(3)
C42A	7924(7)	3937(6)	530(8)	28.0(11)
C43A	6870(6)	4322(6)	484(6)	25.8(10)
C44A	5017(6)	4229(6)	998(5)	22.3(10)
C45A	4560(9)	3658(5)	525(6)	21.4(9)
C46A	4271(7)	2127(6)	288(6)	26(1)
C47A	5224(9)	1779(7)	-178(5)	26.3(10)
C14B	2465(8)	7081(5)	1784(6)	21.6(10)
C15B	2896(7)	7934(7)	1642(7)	26(3)
C16B	2244(9)	8693(6)	1652(7)	30(3)
C17B	1172(8)	8610(6)	1801(5)	34.7(13)
C18B	730(8)	7755(8)	1944(7)	45(3)
C19B	1384(9)	6982(6)	1936(8)	48(6)

Atom	x	y	z	U_{eq}
C20B	475(12)	9448(8)	1808(9)	45(2)
C26	3640(5)	2906(4)	4207(3)	28.8(10)
C21	4341(4)	2638(3)	3628(3)	19.7(8)
C27	4325(7)	1246(5)	5620(4)	57.8(18)
C28	133(5)	3962(5)	4219(3)	45.1(13)
C29	-562(5)	4436(5)	3804(4)	48.7(14)
C31	-609(5)	4891(4)	2204(3)	38.0(12)
C32	504(5)	4319(4)	1209(3)	39.8(13)
C33	1636(5)	4106(4)	944(3)	40.2(12)
C34	1747(5)	2580(4)	1399(3)	40.7(13)
C25	3639(5)	2454(4)	4848(3)	35.2(11)
C35	1923(5)	2059(4)	2042(4)	41.7(13)
O22A	3512(6)	383(5)	2515(4)	46.7(13)
O21A	4368(7)	-481(5)	1544(4)	43.0(14)
O23A	5119(6)	940(4)	1763(4)	28.2(13)
S5A	4460(3)	167(3)	2044.1(19)	29.7(6)
C48A	5237(9)	-444(7)	2605(5)	46.4(10)
F4A	4736(7)	-1199(5)	2900(4)	57.4(10)
F5A	5471(7)	34(5)	3090(4)	54.6(13)
F6A	6186(6)	-689(5)	2247(4)	57.4(10)
C36	1261(6)	2000(4)	3270(4)	45.0(13)
C37	508(5)	2463(4)	3793(4)	45.5(14)
C54	8167(6)	1002(5)	2875(5)	57.6(14)
Ca1	1749.1(7)	4129.3(6)	2635.6(5)	17.6(2)
O22B	3673(7)	476(6)	1992(6)	46.7(13)
O21B	4961(9)	-551(6)	1381(5)	43.0(14)
O23B	5538(7)	838(6)	1788(6)	28.2(13)
S5B	4721(4)	150(4)	1856(2)	29.7(6)
C48B	4876(11)	-458(8)	2672(6)	46.4(10)
F4B	4149(9)	-1138(6)	2839(5)	61(3)
F5B	4778(9)	54(6)	3195(4)	54.6(13)
F6B	5812(8)	-854(6)	2638(6)	57.4(10)
Co1	4072.5(5)	5349.3(4)	3167.1(3)	15.87(15)
F1	9007(4)	885(3)	3185(3)	74.5(13)
F2	8203(4)	376(3)	2418(3)	90.6(15)
F3	7299(4)	843(3)	3350(3)	96.9(17)
C30	-511(6)	5422(5)	2793(4)	50.1(15)
S1A	2902(5)	5950(3)	4693(4)	23.6(6)
O2A	1973(7)	5474(5)	4568(6)	31(2)
C7A	2679(7)	7135(5)	4588(4)	26.9(9)
C8A	2547(9)	7523(7)	3950(5)	42(2)
C9A	2362(12)	8458(7)	3872(5)	56(3)
C10A	2280(12)	8988(7)	4436(7)	63(3)
C11A	2376(14)	8588(7)	5079(6)	61(4)
C12A	2588(15)	7670(6)	5160(5)	38.1(16)
C13A	2108(18)	10016(8)	4340(9)	94(5)
Ca2	6195.9(7)	2199.7(6)	1282.9(5)	16.4(2)
N1	5542(3)	5838(3)	3056(2)	20.8(8)
N2	4027(3)	6194(3)	2344(2)	19.1(8)
N3	4826(3)	4229(2)	2862(2)	16.3(8)
N4	3937(3)	5709(3)	4130(2)	24.6(9)
O1	2667(3)	4942(2)	3290.7(19)	27.5(8)
O3	3152(3)	5810(3)	5398.7(19)	34.3(9)
O4	2659(3)	5315(2)	1911.6(19)	25.9(8)
O5	3966(3)	6204(3)	1081.1(19)	34.8(9)
O6	5091(3)	2743(2)	2311.0(18)	23.2(8)
O7	3300(3)	3306(2)	2704.4(18)	21.1(7)

Atom	x	y	z	U_{eq}
O8	884(3)	3379(3)	3814(2)	34.3(9)
O9	109(3)	4933(3)	3239(2)	34.7(9)
O10	428(3)	4645(3)	1885(2)	32.7(8)
O11	2048(3)	3506(3)	1433.7(19)	32.4(8)
O12	1315(3)	2492(2)	2619(2)	29.0(8)
O18	9182(4)	2179(4)	2010(3)	68.7(15)
O19	8017(4)	2699(3)	3037(3)	56.1(13)
O20	7280(3)	2136(3)	2119(2)	40.4(10)
O24	9154(3)	-3408(3)	602(2)	38.1(9)
O25	7239(3)	-3549(3)	814(2)	41.4(10)
O26	8132(4)	-3231(3)	1754(2)	41.2(10)
S2	3322(1)	6121.8(7)	1767.7(6)	19.6(3)
S3	4377.1(9)	3238.8(7)	2817.4(6)	15.3(2)
S4	8166.8(11)	2138(1)	2470.7(7)	30.6(3)
S6	8152.9(11)	-3178.6(8)	1018.2(7)	26.4(3)
C14A	2417(5)	7053(4)	1832(4)	21.6(10)
C15A	2665(6)	7874(5)	2046(4)	37(3)
C16A	1990(6)	8612(5)	2017(4)	31(2)
C17A	1073(6)	8540(4)	1778(4)	34.7(13)
C18A	816(6)	7717(5)	1562(5)	45(3)
C19A	1496(6)	6966(5)	1588(4)	35(2)
C20A	347(7)	9354(5)	1749(6)	45(2)

Table S15: Anisotropic Displacement Parameters (×10^4) **A244_0m**. The anisotropic displacement factor exponent takes the form: -2PI^2[a*^2 × U_{11} + ... 2hka* × b* × U_{12}]

Atom	U_{11}	U_{22}	U_{33}	U_{23}	U_{13}	U_{12}
C50B	67(3)	54(3)	50(3)	-7(2)	-9(3)	-5(2)
C51B	77(6)	54(3)	55(3)	-5(2)	-15(3)	-8(4)
C52B	89(11)	59(4)	63(5)	1(4)	-24(7)	-14(5)
C53B	62(5)	56(3)	50(3)	-6(3)	-6(3)	-3(3)
O27B	62(3)	51(2)	46(2)	-11.4(18)	-3.5(19)	-1(2)
C50A	67(3)	54(3)	50(3)	-7(2)	-9(3)	-5(2)
C51A	77(6)	54(3)	55(3)	-5(2)	-15(3)	-8(4)
C52A	67(4)	58(3)	57(3)	-3(2)	-13(3)	-6(3)
C53A	62(5)	56(3)	50(3)	-6(3)	-6(3)	-3(3)
O27A	62(3)	51(2)	46(2)	-11.4(18)	-3.5(19)	-1(2)
C4	15(2)	20(2)	34(3)	-5(2)	-1(2)	-0.3(18)
S1B	22.6(13)	32.3(14)	16.7(13)	-3.9(12)	-2.5(10)	-2.2(12)
O2B	23(4)	35(4)	21(4)	-8(4)	0(3)	-3(3)
C7B	17.5(18)	33.9(13)	28.7(15)	-3.1(12)	-2.4(15)	-1.5(13)
C8B	50(6)	45(3)	33(2)	-13(2)	-14(3)	23(3)
C9B	50(10)	44(4)	43(5)	-10(3)	-14(5)	22(4)
C10B	96(8)	47(4)	54(5)	-19(3)	-30(5)	31(4)
C11B	71(13)	40(4)	53(6)	-13(3)	-21(7)	14(4)
C12B	40(4)	40(2)	37(3)	-11(2)	-11(3)	5(2)
C13B	156(15)	49(4)	87(8)	-17(4)	-49(8)	44(6)
C5	20(2)	32(3)	32(3)	-9(2)	-13.4(19)	1.9(18)
F8A	61(4)	28(2)	82(3)	-4(2)	-41(3)	-5(2)
F7A	69(5)	39(3)	53(2)	1(2)	-32(3)	-5(3)
F9A	57(3)	35(3)	78(3)	-19(2)	-19(3)	7(2)
C49A	48(3)	26.7(17)	46(2)	-8.1(14)	-22(2)	-1.3(15)
C6	22(2)	35(3)	36(3)	-15(2)	-10(2)	-1.6(19)
C1	20(2)	17.5(17)	46(2)	1.5(15)	-10.4(18)	-2.7(14)
O15B	26(3)	22.4(19)	35(3)	-1.7(17)	5(2)	2.4(15)
O13B	32.9(19)	25(2)	20.0(17)	-5.3(14)	-7.6(14)	1.3(13)

Atom	U_{11}	U_{22}	U_{33}	U_{23}	U_{13}	U_{12}
O17B	23.7(19)	18.6(16)	20.8(16)	-0.5(12)	-6.8(13)	1.0(13)
O14B	39(2)	31(2)	25.6(19)	-6.0(15)	-3.8(16)	6.1(16)
O16B	21.1(17)	15.0(15)	23.2(16)	0.2(12)	-4.0(14)	-0.5(12)
C38B	51(3)	30(2)	41(4)	-12(2)	-15(2)	9.8(18)
C39B	49(3)	40(4)	35(3)	-15(3)	-12(2)	13(2)
C40B	40(2)	28(2)	35(3)	-6(2)	-5(2)	7.3(17)
C41B	36(3)	29(2)	44(4)	-3(2)	9(3)	10.5(18)
C42B	24.2(19)	25(2)	33(3)	-0.4(16)	-0.6(16)	-0.7(14)
C43B	23.0(17)	22.5(19)	30(2)	1.5(15)	-1.6(14)	-2.2(13)
C44B	23.2(17)	18.6(18)	25(2)	-1.7(14)	-5.5(14)	1.4(13)
C45B	21.7(19)	18.9(16)	24(2)	-0.9(13)	-5.3(16)	1.3(13)
C46B	32(2)	23.6(17)	24.2(19)	-3.3(15)	-9.5(16)	-0.2(15)
C47B	34(2)	22.7(18)	24(2)	-3.3(16)	-8.5(15)	-0.1(15)
C2	15.6(18)	21.9(19)	43(2)	4.7(16)	-5.8(15)	-3.0(15)
C3	16(2)	19(2)	30(3)	-2(2)	-3(2)	3.5(18)
F8B	61(4)	28(2)	82(3)	-4(2)	-41(3)	-5(2)
F7B	33(6)	38(5)	52(3)	0(2)	-18(3)	-2(4)
F9B	57(3)	35(3)	78(3)	-19(2)	-19(3)	7(2)
C49B	48(3)	26.7(17)	46(2)	-8.1(14)	-22(2)	-1.3(15)
C22	43(2)	33(2)	31.1(19)	2.2(15)	-5.4(16)	13(2)
C23	65(3)	40(2)	34.8(18)	7.2(15)	-9.9(17)	16(2)
C24	52(3)	26.6(19)	32.8(18)	1.2(14)	-12.4(16)	-2.7(18)
O15A	29(3)	25(2)	26(6)	1(2)	-3(3)	-1.8(18)
O13A	32.9(19)	25(2)	20.0(17)	-5.3(14)	-7.6(14)	1.3(13)
O17A	23.7(19)	18.6(16)	20.8(16)	-0.5(12)	-6.8(13)	1.0(13)
O14A	39(2)	31(2)	25.6(19)	-6.0(15)	-3.8(16)	6.1(16)
O16A	21.1(17)	15.0(15)	23.2(16)	0.2(12)	-4.0(14)	-0.5(12)
C38A	36(3)	23(4)	20(3)	-1(3)	-3(2)	3(3)
C39A	36(3)	28(3)	19(4)	-2(2)	-3(3)	7(2)
C40A	38(3)	32(3)	31(5)	-1(2)	-4(3)	5(2)
C41A	34(3)	34(3)	37(7)	-3(2)	-7(3)	5(2)
C42A	24.2(19)	25(2)	33(3)	-0.4(16)	-0.6(16)	-0.7(14)
C43A	23.0(17)	22.5(19)	30(2)	1.5(15)	-1.6(14)	-2.2(13)
C44A	23.2(17)	18.6(18)	25(2)	-1.7(14)	-5.5(14)	1.4(13)
C45A	21.7(19)	18.9(16)	24(2)	-0.9(13)	-5.3(16)	1.3(13)
C46A	32(2)	23.6(17)	24.2(19)	-3.3(15)	-9.5(16)	-0.2(15)
C47A	34(2)	22.7(18)	24(2)	-3.3(16)	-8.5(15)	-0.1(15)
C14B	28(2)	19(2)	20(3)	-2.9(17)	-9.0(19)	-1.8(15)
C15B	32(3)	19(2)	31(9)	1(2)	-14(3)	-2.7(19)
C16B	37(3)	21(3)	35(10)	-1(3)	-16(3)	0.8(18)
C17B	37(3)	27(2)	44(3)	-6(2)	-15(2)	1.0(16)
C18B	34(3)	29(2)	73(8)	-8(3)	-15(3)	0(2)
C19B	29(3)	21(4)	93(18)	-4(4)	-8(3)	-3(2)
C20B	42(4)	30(3)	67(5)	-9(3)	-20(3)	6(2)
C26	36(2)	26.0(19)	22.3(16)	-1.3(13)	-1.9(15)	4.0(17)
C21	23.5(19)	16.3(16)	20.4(17)	-1.9(13)	-6.6(14)	-4.9(14)
C27	89(5)	47(3)	37(2)	8.9(19)	-15(2)	6(3)
C28	40(3)	59(3)	32(3)	-4(2)	7(2)	-13(2)
C29	40(3)	61(3)	43(3)	-10(2)	1(2)	-7(2)
C31	30(2)	38(3)	47(3)	-3(2)	-9(2)	3(2)
C32	41(3)	47(3)	33(2)	-1(2)	-11(2)	-4(2)
C33	42(3)	52(3)	29(3)	-10(2)	-9(2)	-8(2)
C34	31(3)	43(2)	49(3)	-20.7(19)	-4(2)	-4(2)
C25	52(3)	29.1(19)	23.2(17)	1.0(14)	-6.1(16)	-1.1(18)
C35	34(3)	35(3)	60(3)	-16.3(19)	-12(2)	4(2)
O22A	44.1(18)	39(2)	54(2)	6(2)	-4.7(18)	0.1(16)
O21A	54(4)	32.7(18)	45(2)	-4.2(16)	-13(2)	-12(2)

Atom	U_{11}	U_{22}	U_{33}	U_{23}	U_{13}	U_{12}
O23A	36(3)	21.1(16)	28.7(19)	-2.2(14)	-8(2)	-5.1(19)
S5A	33.9(13)	21.0(6)	36.3(13)	2.6(9)	-13(1)	-6.1(8)
C48A	52.1(17)	43.2(15)	45.2(15)	3.8(11)	-15.5(13)	4.1(12)
F4A	61.0(18)	50.2(15)	60(2)	9.5(13)	-13.6(15)	7.6(13)
F5A	66(3)	52(2)	48.5(19)	3.8(16)	-22(2)	2(2)
F6A	61.0(18)	50.2(15)	60(2)	9.5(13)	-13.6(15)	7.6(13)
C36	47(3)	38(3)	54(3)	6(2)	-22(2)	-9(2)
C37	45(3)	46(3)	45(3)	10(2)	-10(2)	-19(2)
C54	46(3)	40(2)	85(3)	4(2)	-9(2)	8(2)
Ca1	13.1(5)	22.6(5)	16.9(5)	-3.1(4)	-1.3(4)	-2.3(3)
O22B	44.1(18)	39(2)	54(2)	6(2)	-4.7(18)	0.1(16)
O21B	54(4)	32.7(18)	45(2)	-4.2(16)	-13(2)	-12(2)
O23B	36(3)	21.1(16)	28.7(19)	-2.2(14)	-8(2)	-5.1(19)
S5B	33.9(13)	21.0(6)	36.3(13)	2.6(9)	-13(1)	-6.1(8)
C48B	52.1(17)	43.2(15)	45.2(15)	3.8(11)	-15.5(13)	4.1(12)
F4B	82(5)	36(4)	57(5)	2(4)	6(4)	-15(4)
F5B	66(3)	52(2)	48.5(19)	3.8(16)	-22(2)	2(2)
F6B	61.0(18)	50.2(15)	60(2)	9.5(13)	-13.6(15)	7.6(13)
Co1	11.3(3)	16.7(3)	19.5(3)	-5.0(2)	-1.6(3)	0.6(2)
F1	64(3)	63(3)	96(3)	12(2)	-23(2)	23(2)
F2	78(3)	52(2)	146(4)	-30(2)	-24(3)	13(2)
F3	70(3)	65(3)	134(4)	40(3)	16(3)	14(2)
C30	37(3)	59(3)	56(3)	-15(2)	-11(2)	12(3)
S1A	22.2(10)	32.9(12)	15.5(12)	-4.8(10)	-2.1(8)	-2.8(10)
O2A	22(3)	48(4)	22(4)	-15(4)	2(2)	-8(3)
C7A	17.5(18)	33.9(13)	28.7(15)	-3.1(12)	-2.4(15)	-1.5(13)
C8A	50(6)	45(3)	33(2)	-13(2)	-14(3)	23(3)
C9A	98(10)	47(4)	32(6)	-16(3)	-30(6)	32(4)
C10A	96(8)	47(4)	54(5)	-19(3)	-30(5)	31(4)
C11A	97(11)	55(7)	34(7)	-22(6)	-17(7)	31(7)
C12A	40(4)	40(2)	37(3)	-11(2)	-11(3)	5(2)
C13A	156(15)	49(4)	87(8)	-17(4)	-49(8)	44(6)
Ca2	18.6(5)	15.4(4)	15.8(5)	-3.2(3)	-3.8(4)	0.3(3)
N1	14.1(19)	16.3(15)	32(2)	-4.2(14)	-3.9(16)	-0.6(13)
N2	14.2(16)	19.0(17)	24(2)	-0.9(15)	-3.7(14)	-1.1(13)
N3	11.9(19)	17.8(18)	20(2)	-3.6(15)	-3.9(16)	2.1(14)
N4	18.6(19)	34(2)	23(2)	-7.8(16)	-5.4(15)	-5.4(16)
O1	22.2(19)	36(2)	24.8(19)	-9.6(16)	-3.5(16)	-8.7(15)
O3	45(2)	40(2)	19.7(13)	-2.9(12)	-9.9(13)	-2.3(17)
O4	29(2)	21.7(17)	29(2)	2.6(14)	-10.3(16)	-4.0(14)
O5	46(3)	33(2)	22(2)	-7.6(16)	4.4(18)	-5.8(17)
O6	27.9(19)	17.4(16)	23.6(18)	-6.2(13)	-1.8(15)	3.7(14)
O7	19.4(17)	20.7(16)	25.2(18)	-2.6(14)	-9.1(15)	-1.8(13)
O8	32(2)	44.7(19)	24.9(19)	3.9(15)	-3.9(16)	-14.7(15)
O9	20.1(18)	43(2)	39(2)	-11.1(16)	0.7(15)	-0.4(15)
O10	23.2(18)	41(2)	34.5(19)	-0.5(16)	-8.9(15)	-2.4(15)
O11	27.2(19)	44.4(19)	26.3(18)	-15.0(14)	-2.2(15)	-6.4(14)
O12	24.5(18)	20.9(16)	44.6(19)	-5.1(13)	-13.0(15)	-2.2(14)
O18	29(2)	105(4)	69(3)	11(3)	-8.0(19)	-7(2)
O19	72(3)	51(2)	60(3)	-21(2)	-42(2)	16(2)
O20	23.2(19)	70(3)	32(2)	-17.8(19)	-11.0(16)	9.2(17)
O24	28.9(18)	47(2)	37(2)	-7.4(17)	-1.1(15)	-0.2(15)
O25	29.7(19)	40(2)	57(3)	-16.1(19)	-11.4(18)	0.1(15)
O26	51(3)	41(2)	30.7(17)	-3.2(15)	-4.7(16)	0.3(18)
S2	24.4(6)	16.4(5)	17.7(6)	-2.1(4)	-2.8(5)	-1.5(4)
S3	16.0(5)	15.0(5)	14.9(5)	-2.1(4)	-2.5(4)	0.6(4)
S4	23.9(7)	39.5(7)	31.1(7)	0.0(6)	-12.8(6)	-5.7(5)

Atom	U_{11}	U_{22}	U_{33}	U_{23}	U_{13}	U_{12}
S6	28.0(7)	23.2(6)	27.1(7)	-6.3(5)	-1.6(5)	-1.6(5)
C14A	28(2)	19(2)	20(3)	-2.9(17)	-9.0(19)	-1.8(15)
C15A	28(5)	36(5)	54(7)	-16(5)	-20(5)	7(4)
C16A	31(5)	23(4)	43(6)	-4(4)	-17(4)	3(3)
C17A	37(3)	27(2)	44(3)	-6(2)	-15(2)	1.0(16)
C18A	34(3)	29(2)	73(8)	-8(3)	-15(3)	0(2)
C19A	35(3)	28(4)	48(6)	-9(4)	-21(4)	-1(3)
C20A	42(4)	30(3)	67(5)	-9(3)	-20(3)	6(2)

Table S16: Bond Lengths in Å for **A244_0m**.

Atom	Atom	Length/Å
C50B	C51B	1.525(11)
C50B	O27B	1.452(9)
C51B	C52B	1.520(12)
C52B	C53B	1.500(13)
C53B	O27B	1.441(10)
C50A	C51A	1.525(11)
C50A	O27A	1.452(9)
C51A	C52A	1.520(12)
C52A	C53A	1.500(13)
C53A	O27A	1.441(10)
C4	C3	1.508(6)
C4	N1	1.499(6)
S1B	O2B	1.457(4)
S1B	C7B	1.770(6)
S1B	N4	1.591(14)
S1B	O3	1.368(12)
C7B	C8B	1.379(9)
C7B	C12B	1.401(9)
C8B	C9B	1.398(12)
C9B	C10B	1.385(14)
C10B	C11B	1.383(15)
C10B	C13B	1.531(13)
C11B	C12B	1.381(10)
C5	C6	1.495(7)
C5	N1	1.493(7)
F8A	C49A	1.329(11)
F7A	C49A	1.327(14)
F9A	C49A	1.295(13)
C49A	S6	1.834(6)
C6	N4	1.489(6)
C1	C2	1.496(8)
C1	N1	1.484(6)
O15B	C41B	1.426(6)
O15B	C42B	1.426(6)
O13B	C38B	1.420(6)
O13B	C47B	1.439(6)
O17B	C45B	1.436(6)
O17B	C46B	1.431(6)
O14B	C39B	1.429(6)
O14B	C40B	1.419(6)
O16B	C43B	1.430(6)
O16B	C44B	1.433(6)
C38B	C39B	1.484(7)
C40B	C41B	1.488(7)
C42B	C43B	1.476(7)
C44B	C45B	1.496(6)
C46B	C47B	1.488(6)
C2	N2	1.494(6)
C3	N3	1.474(6)
F8B	C49B	1.36(2)
F7B	C49B	1.32(3)
F9B	C49B	1.35(3)
C49B	S6	1.834(7)
C22	C23	1.381(8)
C22	C21	1.374(7)
C23	C24	1.388(9)
C24	C27	1.519(9)
C24	C25	1.380(8)
O15A	C41A	1.427(6)
O15A	C42A	1.427(6)
O13A	C38A	1.420(6)
O13A	C47A	1.438(6)
O17A	C45A	1.436(5)
O17A	C46A	1.431(6)
O14A	C39A	1.429(6)
O14A	C40A	1.420(6)
O16A	C43A	1.431(6)
O16A	C44A	1.432(6)
C38A	C39A	1.484(7)
C40A	C41A	1.487(7)
C42A	C43A	1.477(7)
C44A	C45A	1.496(6)
C46A	C47A	1.488(6)
C14B	C15B	1.366(8)
C14B	C19B	1.367(9)
C14B	S2	1.780(5)
C15B	C16B	1.388(9)
C16B	C17B	1.354(9)
C17B	C18B	1.374(9)
C17B	C20B	1.516(8)
C18B	C19B	1.406(10)
C26	C21	1.385(7)
C26	C25	1.381(8)
C21	S3	1.760(5)
C28	C29	1.462(10)
C28	O8	1.442(7)
C29	O9	1.427(8)
C31	C30	1.466(9)
C31	O10	1.412(7)

Atom	Atom	Length/Å
C32	C33	1.483(9)
C32	O10	1.426(7)
C33	O11	1.433(7)
C34	C35	1.485(9)
C34	O11	1.429(7)
C35	O12	1.430(7)
O22A	S5A	1.426(8)
O21A	S5A	1.436(7)
O23A	S5A	1.437(6)
S5A	C48A	1.812(10)
C48A	F4A	1.328(12)
C48A	F5A	1.301(11)
C48A	F6A	1.343(12)
C36	C37	1.467(10)
C36	O12	1.414(7)
C37	O8	1.442(7)
C54	F1	1.340(9)
C54	F2	1.324(9)
C54	F3	1.319(9)
C54	S4	1.801(7)
O22B	S5B	1.405(10)
O21B	S5B	1.429(9)
O23B	S5B	1.445(8)
S5B	C48B	1.826(11)
C48B	F4B	1.355(13)
C48B	F5B	1.299(12)
C48B	F6B	1.322(14)
Co1	N1	1.991(4)
Co1	N2	1.980(4)
Co1	N3	1.973(4)
Co1	N4	1.972(4)
Co1	O1	1.870(3)

Atom	Atom	Length/Å
C30	O9	1.444(8)
S1A	O2A	1.457(4)
S1A	C7A	1.769(6)
S1A	N4	1.609(9)
S1A	O3	1.480(8)
C7A	C8A	1.379(9)
C7A	C12A	1.401(9)
C8A	C9A	1.398(12)
C9A	C10A	1.384(14)
C10A	C11A	1.383(15)
C10A	C13A	1.531(13)
C11A	C12A	1.381(10)
N2	S2	1.588(4)
N3	S3	1.585(4)
O4	S2	1.447(3)
O5	S2	1.436(4)
O6	S3	1.447(3)
O7	S3	1.442(3)
O18	S4	1.434(5)
O19	S4	1.411(5)
O20	S4	1.439(4)
O24	S6	1.433(4)
O25	S6	1.434(4)
O26	S6	1.435(4)
S2	C14A	1.782(5)
C14A	C15A	1.366(8)
C14A	C19A	1.368(9)
C15A	C16A	1.388(9)
C16A	C17A	1.354(9)
C17A	C18A	1.374(9)
C17A	C20A	1.516(8)
C18A	C19A	1.406(10)

Table S17: Bond Angles in ° for **A244_0m**.

Atom	Atom	Atom	Angle/°
O27B	C50B	C51B	104.5(7)
C52B	C51B	C50B	102.2(7)
C53B	C52B	C51B	104.9(8)
O27B	C53B	C52B	108.2(7)
C53B	O27B	C50B	107.3(6)
O27A	C50A	C51A	104.5(7)
C52A	C51A	C50A	102.2(7)
C53A	C52A	C51A	104.9(8)
O27A	C53A	C52A	108.2(7)
C53A	O27A	C50A	107.3(6)
N1	C4	C3	108.0(4)
O2B	S1B	C7B	108.1(4)
O2B	S1B	N4	106.6(10)
N4	S1B	C7B	104.2(6)
O3	S1B	O2B	113.8(11)
O3	S1B	C7B	107.5(5)
O3	S1B	N4	116.1(6)
C8B	C7B	S1B	119.9(6)

Atom	Atom	Atom	Angle/°
C8B	C7B	C12B	120.1(7)
C12B	C7B	S1B	119.7(5)
C7B	C8B	C9B	119.7(8)
C10B	C9B	C8B	120.2(9)
C9B	C10B	C13B	119.7(11)
C11B	C10B	C9B	119.7(8)
C11B	C10B	C13B	120.5(11)
C12B	C11B	C10B	120.7(10)
C11B	C12B	C7B	119.6(8)
N1	C5	C6	109.3(4)
F8A	C49A	S6	111.3(6)
F7A	C49A	F8A	107.8(8)
F7A	C49A	S6	111.6(8)
F9A	C49A	F8A	108.9(9)
F9A	C49A	F7A	103.1(8)
F9A	C49A	S6	113.7(7)
N4	C6	C5	107.0(4)
N1	C1	C2	109.0(4)
C41B	O15B	C42B	113.8(5)

Atom	Atom	Atom	Angle/°
C38B	O13B	C47B	113.5(6)
C46B	O17B	C45B	112.1(4)
C40B	O14B	C39B	112.4(4)
C43B	O16B	C44B	113.8(4)
O13B	C38B	C39B	106.8(6)
O14B	C39B	C38B	109.4(5)
O14B	C40B	C41B	111.2(6)
O15B	C41B	C40B	108.2(6)
O15B	C42B	C43B	106.9(5)
O16B	C43B	C42B	110.7(5)
O16B	C44B	C45B	109.5(5)
O17B	C45B	C44B	109.5(5)
O17B	C46B	C47B	108.4(5)
O13B	C47B	C46B	108.0(5)
N2	C2	C1	106.3(4)
N3	C3	C4	105.2(4)
F8B	C49B	S6	110.4(12)
F7B	C49B	F8B	100.6(16)
F7B	C49B	F9B	116.9(15)
F7B	C49B	S6	113.8(16)
F9B	C49B	F8B	105.9(18)
F9B	C49B	S6	108.5(14)
C21	C22	C23	119.1(6)
C22	C23	C24	121.1(6)
C23	C24	C27	120.5(6)
C25	C24	C23	118.8(6)
C25	C24	C27	120.7(6)
C41A	O15A	C42A	113.7(6)
C38A	O13A	C47A	113.6(6)
C46A	O17A	C45A	112.1(4)
C40A	O14A	C39A	112.4(5)
C43A	O16A	C44A	113.7(4)
O13A	C38A	C39A	106.7(6)
O14A	C39A	C38A	109.4(6)
O14A	C40A	C41A	111.1(6)
O15A	C41A	C40A	108.2(6)
O15A	C42A	C43A	106.8(5)
O16A	C43A	C42A	110.6(5)
O16A	C44A	C45A	109.5(5)
O17A	C45A	C44A	109.5(5)
O17A	C46A	C47A	108.4(5)
O13A	C47A	C46A	108.1(5)
C15B	C14B	C19B	119.3(5)
C15B	C14B	S2	119.3(7)
C19B	C14B	S2	121.4(7)
C14B	C15B	C16B	120.4(6)
C17B	C16B	C15B	121.2(6)
C16B	C17B	C18B	118.9(6)
C16B	C17B	C20B	120.4(6)
C18B	C17B	C20B	120.7(6)
C17B	C18B	C19B	120.3(7)
C14B	C19B	C18B	119.9(6)
C25	C26	C21	119.3(5)
C22	C21	C26	120.8(5)
C22	C21	S3	119.6(4)
C26	C21	S3	119.4(4)
O8	C28	C29	112.3(5)
O9	C29	C28	107.0(5)
O10	C31	C30	107.2(5)
O10	C32	C33	107.6(5)
O11	C33	C32	110.8(5)
O11	C34	C35	108.2(5)
C24	C25	C26	120.8(6)
O12	C35	C34	107.2(5)
O22A	S5A	O21A	117.0(5)
O22A	S5A	O23A	114.4(5)
O22A	S5A	C48A	103.0(5)
O21A	S5A	O23A	114.0(5)
O21A	S5A	C48A	102.8(5)
O23A	S5A	C48A	103.1(5)
F4A	C48A	S5A	110.6(8)
F4A	C48A	F6A	107.5(8)
F5A	C48A	S5A	114.0(7)
F5A	C48A	F4A	108.9(9)
F5A	C48A	F6A	104.1(9)
F6A	C48A	S5A	111.4(7)
O12	C36	C37	108.2(5)
O8	C37	C36	108.5(5)
F1	C54	S4	110.4(5)
F2	C54	F1	108.3(6)
F2	C54	S4	111.9(6)
F3	C54	F1	108.1(7)
F3	C54	F2	106.9(7)
F3	C54	S4	111.2(5)
O22B	S5B	O21B	117.8(7)
O22B	S5B	O23B	115.1(6)
O22B	S5B	C48B	104.1(7)
O21B	S5B	O23B	114.5(6)
O21B	S5B	C48B	101.3(6)
O23B	S5B	C48B	100.5(6)
F4B	C48B	S5B	109.7(9)
F5B	C48B	S5B	114.0(8)
F5B	C48B	F4B	108.3(10)
F5B	C48B	F6B	105.4(11)
F6B	C48B	S5B	113.2(9)
F6B	C48B	F4B	105.7(10)
N2	Co1	N1	83.06(17)
N3	Co1	N1	83.01(15)
N3	Co1	N2	109.30(16)
N4	Co1	N1	83.74(17)
N4	Co1	N2	125.24(17)
N4	Co1	N3	121.37(18)
O1	Co1	N1	177.24(16)
O1	Co1	N2	96.35(16)
O1	Co1	N3	99.73(16)
O1	Co1	N4	94.44(16)
O9	C30	C31	110.5(5)
O2A	S1A	C7A	108.2(4)
O2A	S1A	N4	110.3(6)
O2A	S1A	O3	116.8(7)
N4	S1A	C7A	107.7(4)
O3	S1A	C7A	104.5(4)
O3	S1A	N4	108.8(4)
C8A	C7A	S1A	120.0(6)

Atom	Atom	Atom	Angle/°
C8A	C7A	C12A	120.1(7)
C12A	C7A	S1A	119.8(5)
C7A	C8A	C9A	119.7(8)
C10A	C9A	C8A	120.2(9)
C9A	C10A	C13A	119.7(11)
C11A	C10A	C9A	119.7(8)
C11A	C10A	C13A	120.5(11)
C12A	C11A	C10A	120.7(10)
C11A	C12A	C7A	119.5(8)
C4	N1	Co1	109.3(3)
C5	N1	C4	109.5(4)
C5	N1	Co1	108.6(3)
C1	N1	C4	111.2(4)
C1	N1	C5	111.3(4)
C1	N1	Co1	106.9(3)
C2	N2	Co1	114.0(3)
C2	N2	S2	114.2(3)
S2	N2	Co1	128.3(2)
C3	N3	Co1	114.2(3)
C3	N3	S3	114.0(3)
S3	N3	Co1	130.1(2)
S1B	N4	Co1	133.0(4)
C6	N4	S1B	111.2(5)
C6	N4	Co1	113.8(3)
C6	N4	S1A	110.9(4)
S1A	N4	Co1	130.6(3)
C37	O8	C28	114.4(5)
C29	O9	C30	111.1(5)
C31	O10	C32	114.3(4)
C34	O11	C33	112.1(4)
C36	O12	C35	114.4(5)
N2	S2	C14B	109.1(4)
N2	S2	C14A	108.0(3)
O4	S2	C14B	107.5(4)
O4	S2	N2	110.7(2)
O4	S2	C14A	105.1(3)
O5	S2	C14B	103.8(4)
O5	S2	N2	111.0(2)
O5	S2	O4	114.4(2)
O5	S2	C14A	107.2(3)
N3	S3	C21	107.8(2)
O6	S3	C21	106.3(2)
O6	S3	N3	110.8(2)
O7	S3	C21	107.5(2)
O7	S3	N3	109.32(19)
O7	S3	O6	114.8(2)
O18	S4	C54	101.9(4)
O18	S4	O20	113.8(3)
O19	S4	C54	103.8(4)
O19	S4	O18	117.3(3)
O19	S4	O20	113.7(3)
O20	S4	C54	103.9(3)
O24	S6	C49A	108.2(5)
O24	S6	C49B	97.2(8)
O24	S6	O25	115.1(2)
O24	S6	O26	114.6(3)
O25	S6	C49A	97.9(4)
O25	S6	C49B	109.3(8)
O25	S6	O26	115.3(3)
O26	S6	C49A	103.2(5)
O26	S6	C49B	102.7(9)
C15A	C14A	S2	122.2(5)
C15A	C14A	C19A	119.2(5)
C19A	C14A	S2	118.3(5)
C14A	C15A	C16A	120.5(6)
C17A	C16A	C15A	121.3(6)
C16A	C17A	C18A	118.8(6)
C16A	C17A	C20A	120.5(6)
C18A	C17A	C20A	120.7(6)
C17A	C18A	C19A	120.4(7)
C14A	C19A	C18A	119.9(6)

Table S18: Hydrogen Fractional Atomic Coordinates (×10^4) and Equivalent Isotropic Displacement Parameters (Å^2×10^3) for **A244_0m**. U_{eq} is defined as 1/3 of of the trace of the orthogonalised U_{ij}.

Atom	x	y	z	U_{eq}
H50A	-290	6811	3948	68
H50B	-1224	6671	4625	68
H51A	-1484	8220	4696	74
H51B	-214	8193	4425	74
H52A	-1426	9097	3691	83
H52B	-344	8633	3314	83
H53A	-2396	8105	3301	68
H53B	-1323	7752	2830	68
H50C	-479	6495	4043	68
H50D	-1428	6703	4680	68
H51C	-1039	8242	4583	74
H51D	140	7824	4385	74
H52C	-587	8941	3497	73
H52D	238	8151	3227	73
H53C	-1889	8247	3160	68
H53D	-1023	7558	2781	68
H4A	7035	5347	2671	28
H4B	6265	5373	2114	28
H8B	2114	6689	3619	50
H9B	1805	8215	3281	54
H11B	2303	8975	5131	64
H12B	2695	7476	5452	46
H13A	1887	10120	4317	141
H13B	935	9745	3992	141
H13C	2089	9898	3515	141
H5A	6446	6247	3738	32
H5B	6022	5219	3912	32
H6A	4992	6013	4749	36
H6B	4830	6838	4199	36
H1A	6277	7002	2574	33
H1B	5152	7188	3065	33
H38A	5819	472	-316	47
H38B	5620	250	512	47
H39A	7405	-34	26	49
H39B	7539	992	-311	49
H40A	8941	647	392	42
H40B	8685	1109	1121	42
H41A	9470	2223	328	46
H41B	8735	1998	-216	46
H42A	7859	3642	-140	34
H42B	8910	3711	187	34
H43A	7937	4154	1219	31
H43B	7592	4798	609	31
H44A	5979	4301	183	27
H44B	5761	5010	780	27
H45A	4416	4091	1433	26
H45B	4173	4254	663	26
H46A	4927	3120	-169	31
H46B	3712	2926	200	31

Atom	x	y	z	U_{eq}
H47A	4129	1427	523	32
H47B	4516	1606	-303	32
H2A	4820	7387	1960	33
H2B	5483	6493	1718	33
H3A	6355	3849	2485	26
H3B	6157	4082	3289	26
H22	5552	1783	3291	43
H23	5537	1027	4375	57
H38C	7181	1167	-492	32
H38D	6380	313	-307	32
H39C	6879	25	764	34
H39D	7938	73	175	34
H40C	8661	1533	-164	41
H40D	9291	1181	433	41
H41C	8991	2517	974	42
H41D	9404	2800	163	42
H42C	8473	4203	144	34
H42D	8120	4070	977	34
H43C	6887	4990	516	31
H43D	6694	4202	29	31
H44C	5034	4876	821	27
H44D	4566	4179	1469	27
H45C	3810	3830	531	26
H45D	4962	3763	42	26
H46C	3811	2467	8	31
H46D	3855	1612	556	31
H47C	5011	1316	-469	32
H47D	5590	2284	-489	32
H15B	3646	8008	1536	32
H16B	2556	9282	1552	36
H18B	-20	7686	2050	54
H19B	1075	6392	2036	58
H20A	325	9666	2278	68
H20B	-195	9292	1672	68
H20C	842	9926	1480	68
H26	3163	3395	4165	35
H27A	3877	701	5669	87
H27B	4043	1648	5990	87
H27C	5052	1069	5655	87
H28A	525	4416	4423	54
H28B	-307	3591	4607	54
H29A	-1003	3993	3626	58
H29B	-1040	4856	4090	58
H31A	-1046	4339	2368	46
H31B	-953	5258	1869	46
H32A	252	4789	894	48
H32B	61	3766	1235	48
H33A	1703	3817	497	48
H33B	2057	4677	858	48
H34A	2181	2321	985	49
H34B	990	2546	1362	49
H25	3159	2635	5246	42
H35A	1687	1420	2046	50

Atom	x	y	z	U_{eq}
H35B	2686	2061	2067	50
H36A	1972	1976	3397	54
H36B	1019	1368	3244	54
H37A	-205	2476	3669	55
H37B	454	2133	4255	55
H30A	-164	6013	2619	60
H30B	-1227	5547	3064	60
H8A	2581	7157	3566	50
H9A	2291	8731	3430	67
H11A	2294	8948	5470	73
H12A	2672	7402	5600	46
H13D	1350	10139	4366	141
H13E	2506	10247	3884	141
H13F	2360	10321	4707	141
H1	2380	5088	3751	41
H15A	3304	7941	2216	45
H16A	2174	9179	2167	37
H18A	176	7655	1393	54
H19A	1315	6399	1437	42
H20D	334	9544	1263	68
H20E	611	9857	1973	68
H20F	-373	9188	1994	68

4-1

EMORY UNIVERSITY | X-ray Crystallography Center

Submitted by: **Christian Wallen**
Emory University
Solved by: **Marika Wieliczko**
Sample ID: **MW03045**

Crystal Data and Experimental

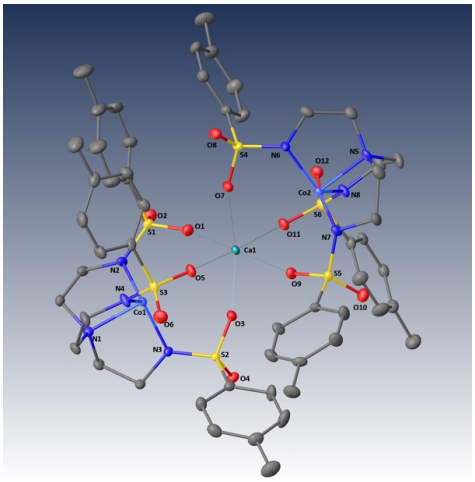

Experimental. Single clear bluish violet hexagonal-shaped crystals of (**MW03045**) were recrystallised from toluene by slow evaporation. A suitable crystal (0.33×0.28×0.07) was selected and mounted on a loop with paratone oil on a Bruker APEX-II CCD diffractometer. The crystal was cooled to T = 109.01 K during data collection. The structure was solved with the **Superflip** (L. Palatinus & G. Chapuis, 2007) structure solution program using charge flipping methods and by using **Olex2** (Dolomanov et al., 2009) as the graphical interface. The crystal structure was refined with version of **XL** (Sheldrick, 2008) using Least Squares minimisation.

Crystal Data. $C_{54}H_{66}CaCo_2N_8O_{12}S_6$, M_r = 1369.44, monoclinic, $P2_1$ (No. 4), a = 13.9236(11) Å, b = 13.3642(10) Å, c = 17.2950(13) Å, β = 112.3550(10)°, α = γ = 90°, V = 2976.3(4) Å^3, T = 109.01 K, Z = 2, Z' = 1, μ(MoK$_\alpha$) = 0.921, 22136 reflections measured, 14778 unique (R_{int} = 0.0328) which were used in all calculations. The final wR_2 was 0.1150 (all data) and R_1 was 0.0476 (I > 2(I)).

Compound	**MW03045**
Formula	$C_{54}H_{66}CaCo_2N_8O_{12}S_6$
$D_{calc.}$/ g cm^{-3}	1.528
μ/mm^{-1}	0.921
Formula Weight	1369.44
Colour	clear bluish violet
Shape	hexagonal
Max Size/mm	0.33
Mid Size/mm	0.28
Min Size/mm	0.07
T/K	109.01
Crystal System	monoclinic
Flack Parameter	0.202(8)
Hooft Parameter	0.200(8)
Space Group	$P2_1$
a/Å	13.9236(11)
b/Å	13.3642(10)
c/Å	17.2950(13)
α/°	90
β/°	112.3550(10)
γ/°	90
V/Å^3	2976.3(4)
Z	2
Z'	1
Θ_{min}/°	1.581
Θ_{max}/°	29.216
Measured Refl.	22136
Independent Refl.	14778
$I > 2\sigma(I)$	13032
R_{int}	0.0328
Parameters	754
Restraints	1
Largest Peak	1.052
Deepest Hole	-0.448
GooF	1.009
wR_2 (all data)	0.1150
wR_2	0.1096
R_1 (all data)	0.0561
R_1	0.0476
CCDC #	1434437

Structure Quality Indicators

Reflections:	d min 0.73	I/σ 10.9	Rint 3.28%	complete 91%
Refinement:	Shift -0.001	Max Peak 1.1	Min Peak -0.5	GooF 1.009

A clear bluish violet hexagonal-shaped crystal with dimensions 0.33×0.28×0.07 mm was mounted on a loop with paratone oil.X-ray diffraction data were collected using a Bruker APEX-II CCD diffractometer equipped with an Oxford low-temperature apparatus operating at T = 109.01 K.

Data were measured using ϕ using MoK_α radiation (fine-focus sealed tube, 45 kV, 35 mA). The total number of runs and images was based on the strategy calculation from the program **APEX2** (Bruker, 2014). The maximum resolution achieved was Θ = 29.216°.

Unit cell indexing was performed by using the **APEX2** (Bruker, 2014) software and refined using **SAINT** (Bruker, V8.27A, 2012) on 7388 reflections, 33% of the observed reflections. Data reduction, scaling and absorption corrections were performed using **SAINT** (Bruker, V8.27A, 2012) and **SADABS-2012/1** (Bruker, 2012) was used for absorption correction.wR_2(int) was 0.0641 before and 0.0505 after correction.The Ratio of minimum to maximum transmission is 0.7802.The $\lambda/2$ correction factor is 0.0015. software which corrects for Lorentz polarisation. The final completeness is 100.00% out to 29.216 in Θ. The absorption coefficient (μ) of this material is 0.921 mm^{-1} and the minimum and maximum transmissions are 0.5819 and 0.7458.

The structure was solved in the space group P1 with the **Superflip** (L. Palatinus & G. Chapuis, 2007) structure solution program using using charge flipping methods. The space group $P2_1$ (# 4) was determined by the**Superflip** (L. Palatinus & G. Chapuis, 2007) structure solution program.The crystal structure was refined by Least Squares using version of **XL** (Sheldrick, 2008). All non-hydrogen atoms were refined anisotropically. Hydrogen atom positions were calculated geometrically and refined using the riding model.?

There are two independent molecules in the asymmetric unit.

The Flack parameter was refined to 0.202(8). Determination of absolute structure using Bayesian statistics on Bijvoet differences using the Olex2 results in 0.200(8). Note: The Flack parameter is used to determine chirality of the crystal studied, the value should be near 0, a value of 1 means that the stereochemistry is wrong and the model should be inverted. A value of 0.5 means that the crystal consists of a racemic mixture of the two enantiomers.

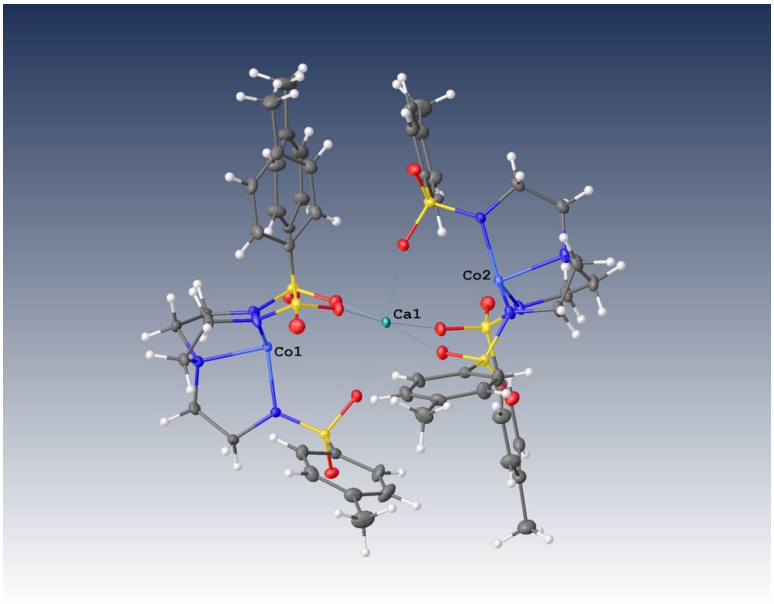

Figure S9:

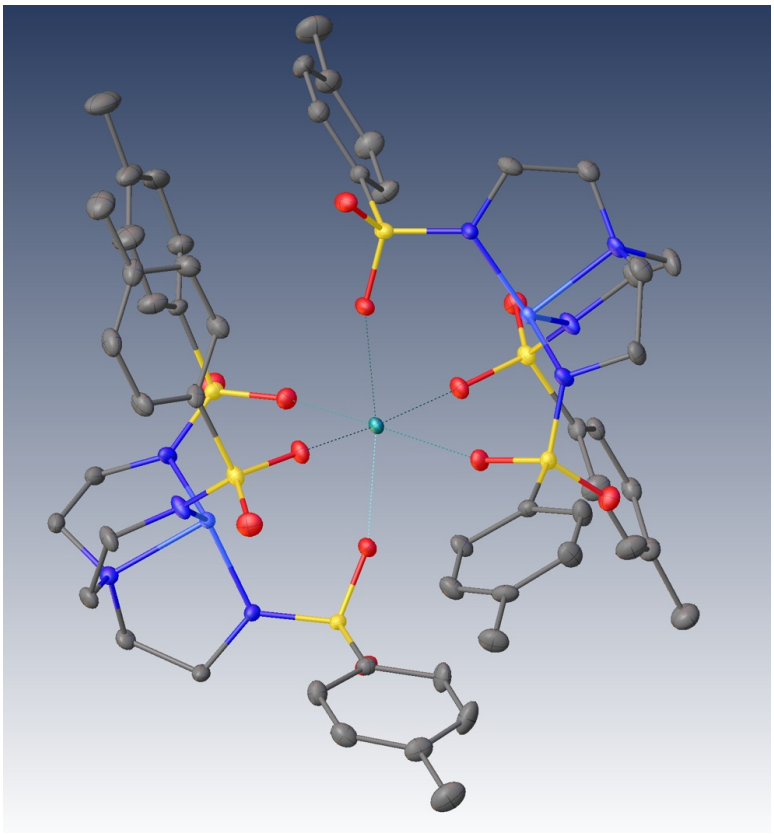

Figure S10:

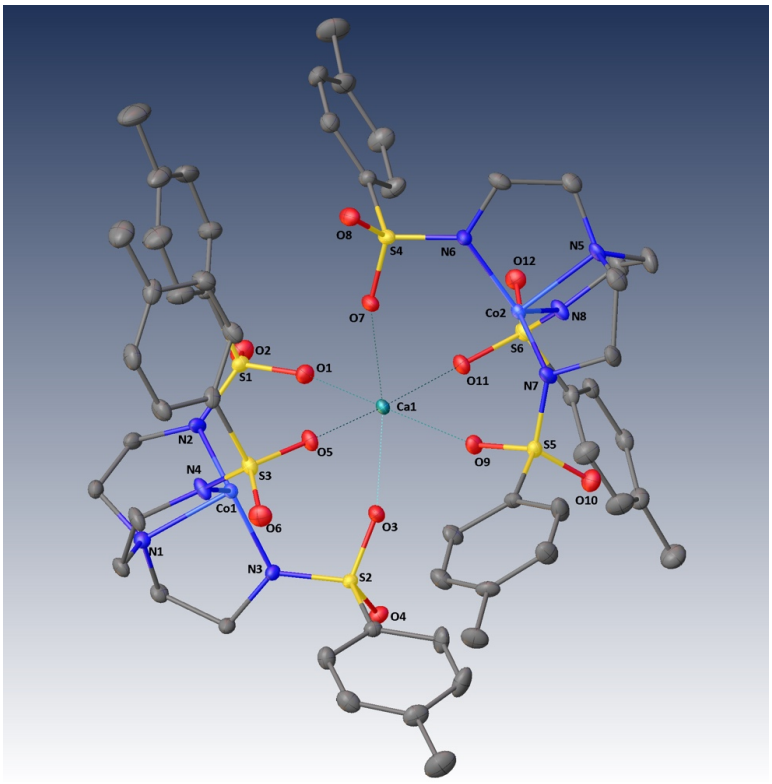

Figure S11:

Data Plots: Diffraction Data

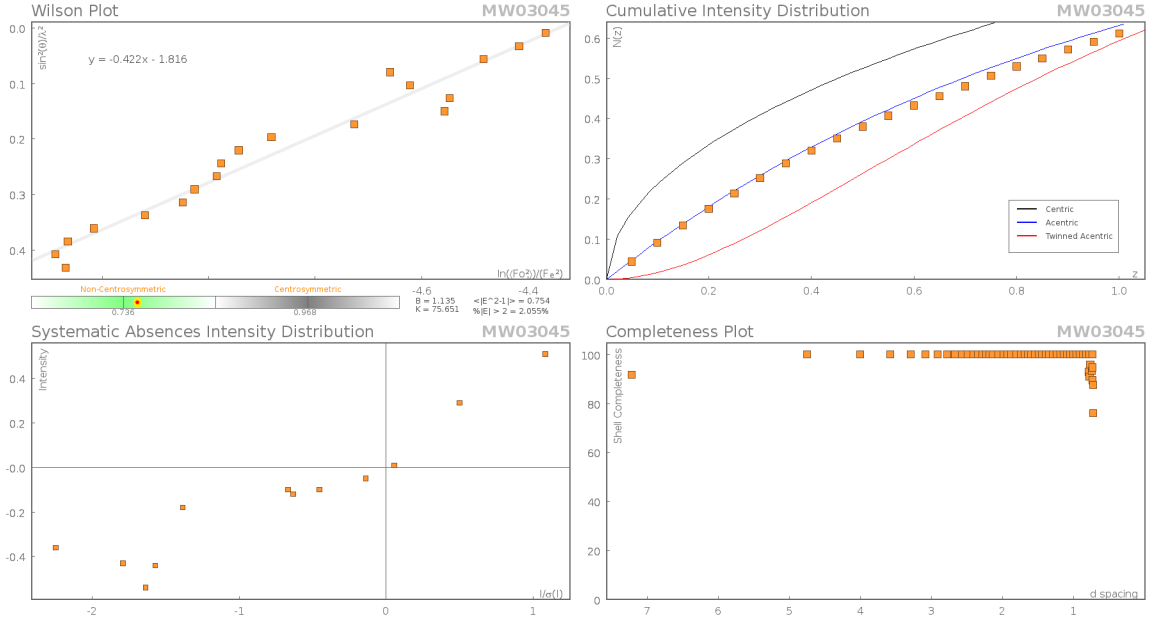

Data Plots: Refinement and Data

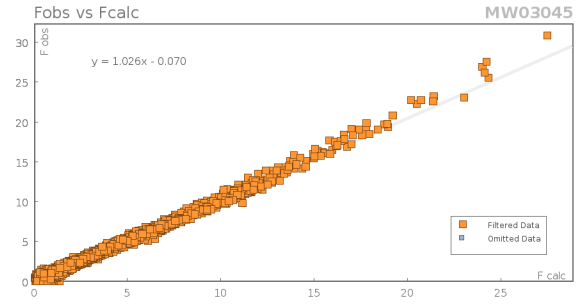

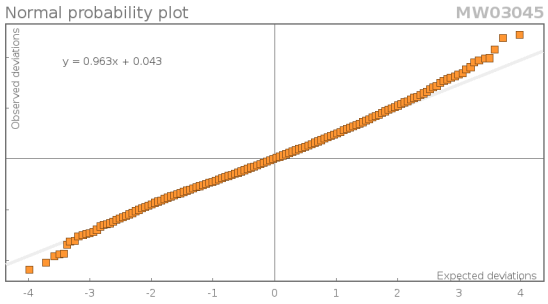

Reflection Statistics

Total reflections (after filtering)	22148	Unique reflections	14778
Completeness	0.914	Mean I/σ	10.93
hklsub>max</sub> collected	(19, 17, 23)	hklsub>min</sub> collected	(-19, -18, -23)
hkl_{max} used	(17, 17, 23)	hkl_{min} used	(-19, -18, 0)
Lim d_{max} collected	100.0	Lim d_{min} collected	0.36
d_{max} used	12.88	d_{min} used	0.73
Friedel pairs	6633	Friedel pairs merged	0
Inconsistent equivalents	2	R_{int}	0.0328
R_{sigma}	0.0676	Intensity transformed	0
Omitted reflections	0	Omitted by user (OMIT hkl)	0
Multiplicity	(20902, 620, 2)	Maximum multiplicity	4
Removed systematic absences	12	Filtered off (Shel/OMIT)	0

Images of the Crystal on the Diffractometer

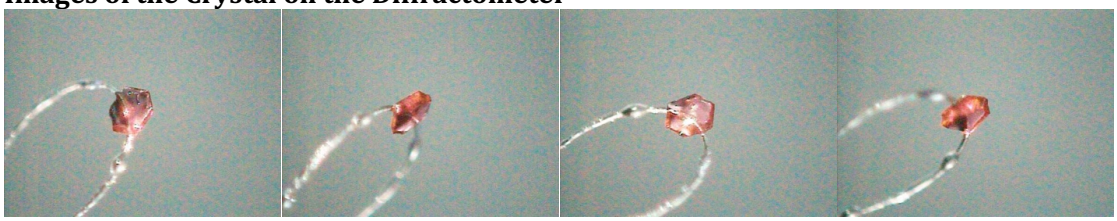

Table S7: Fractional Atomic Coordinates (×10⁴) and Equivalent Isotropic Displacement Parameters (Å²×10³) for **MW03045**. U_{eq} is defined as 1/3 of the trace of the orthogonalised U_{ij}.

Atom	x	y	z	U_{eq}
Co1	9157.2(4)	6608.7(5)	4462.4(4)	12.76(13)
Co2	5726.5(5)	4656.6(4)	649.4(4)	13.25(13)
Ca1	7590.4(7)	5412.6(7)	2585.5(5)	12.63(18)
S2	10457.8(8)	5666.3(8)	3586.5(7)	13.6(2)
S1	7741.0(9)	5054.3(9)	4769.4(7)	16.0(2)
S5	7471.4(9)	5570.9(9)	380.8(7)	14.9(2)
S6	6832.9(9)	2847.4(9)	1739.2(7)	16.1(2)
S4	4695.6(8)	5682.4(9)	1717.3(7)	16.0(2)
S3	7974.4(9)	8163.1(9)	3149.0(7)	16.1(2)
O4	11221(3)	4884(3)	3765(2)	19.6(7)
O11	7267(3)	3732(3)	2257(2)	19.2(7)
O7	5823(3)	5739(3)	2180(2)	19.3(7)
O3	9385(3)	5344(3)	3129(2)	19.2(7)
O10	8025(3)	4859(3)	85(2)	23.6(8)
O9	7701(3)	5552(3)	1281.8(19)	18.4(7)

Atom	x	y	z	U_{eq}
O12	6338(3)	2127(3)	2090(2)	22.0(7)
O8	4138(3)	6608(3)	1636(2)	22.0(7)
O2	7937(3)	4140(3)	5246(2)	26.3(8)
O6	8415(3)	8874(3)	2754(2)	25.2(8)
O1	7633(3)	4966(3)	3896(2)	20.7(7)
O5	7705(3)	7182(3)	2743(2)	20.2(7)
N3	10447(3)	6226(3)	4374(2)	15.1(8)
N4	8676(3)	7930(3)	4082(3)	19.5(9)
N8	6115(3)	3265(3)	859(3)	18.3(8)
N2	8573(3)	5896(3)	5140(2)	17.6(8)
N7	6251(3)	5477(3)	-45(2)	18.0(8)
N1	10081(3)	7282(3)	5569(2)	16.2(8)
N5	4605(3)	4152(3)	-454(3)	17.3(8)
N6	4564(3)	5164(3)	874(2)	17.7(8)
C48	7910(4)	2223(4)	1646(3)	18.4(10)
C12	10752(3)	6511(4)	2918(3)	16.6(9)
C30	4209(4)	4852(4)	2280(3)	18(1)
C49	8129(4)	1244(4)	1910(3)	18.5(9)
C3	6523(3)	5508(4)	4724(3)	18.8(10)
C21	6802(4)	8713(4)	3120(3)	18.1(10)
C1	9544(4)	7144(4)	6152(3)	19.3(10)
C2	9045(4)	6101(4)	6043(3)	21.1(10)
C11	11392(3)	6535(4)	5076(3)	17.0(9)
C54	8536(4)	2747(4)	1321(4)	28.3(12)
C50	9009(4)	796(4)	1873(3)	20.5(10)
C42	8654(4)	8545(4)	-174(3)	21.5(10)
C45	8448(4)	7396(4)	831(3)	21.3(10)
C24	4973(4)	9625(4)	3063(3)	25.6(11)
C10	11093(4)	6757(4)	5829(3)	19(1)
C33	3375(4)	3511(5)	3081(4)	30.6(13)
C39	7881(3)	6758(3)	185(3)	15.3(9)
C14	11351(4)	8085(4)	2615(3)	25.6(11)
C51	9665(4)	1295(4)	1579(3)	24.6(11)
C46	4930(4)	3142(4)	-595(3)	26.9(12)
C19	10155(4)	8347(4)	5348(3)	19.1(10)
C17	11094(5)	6719(4)	1670(4)	32.5(13)
C38	5740(4)	5224(4)	-934(3)	21.3(10)
C41	8059(4)	7918(4)	-814(3)	27.6(12)
C29	3539(4)	5026(4)	211(3)	22(1)
C47	5416(4)	2568(4)	231(3)	23.5(11)
C43	9082(4)	9509(4)	-371(4)	30.0(12)
C40	7685(4)	7026(4)	-646(3)	27.0(12)
C22	6799(4)	9723(4)	3313(3)	23.4(10)
C26	4994(4)	8608(4)	2861(4)	27.5(12)
C18	10772(5)	6128(4)	2172(3)	25.6(11)
C53	9406(5)	2287(5)	1291(4)	31.9(13)
C23	5888(4)	10160(4)	3287(3)	27.2(12)
C27	5898(4)	8154(4)	2900(3)	22.5(10)
C13	11011(4)	7500(4)	3130(3)	22.4(10)
C20	9128(4)	8733(4)	4698(3)	22.8(11)
C28	3605(4)	4157(4)	-336(3)	24.0(11)
C36	3362(4)	5126(4)	2466(3)	24.7(11)
C15	11423(4)	7695(4)	1895(4)	27.3(12)
C31	4653(4)	3905(4)	2500(4)	29.2(12)
C16	11826(5)	8311(5)	1347(4)	40.2(16)
C32	4227(5)	3249(5)	2895(4)	33.8(13)
C35	2963(4)	4457(4)	2866(3)	28.5(12)

Atom	x	y	z	U_{eq}
C44	8830(4)	8277(4)	642(3)	25.9(11)
C9	5812(4)	4856(5)	4833(4)	29.9(12)
C37	4623(4)	4899(4)	-1090(3)	25.8(11)
C25	3970(5)	10108(5)	3012(4)	38.9(15)
C6	4590(4)	6210(6)	4573(4)	36.5(15)
C4	6266(4)	6496(5)	4531(4)	30.0(12)
C8	4847(4)	5212(5)	4751(4)	35.6(14)
C5	5301(5)	6836(5)	4454(4)	38.8(15)
C7	3536(5)	6583(8)	4487(5)	58(2)
C52	10646(5)	826(5)	1572(4)	33.3(13)
C34	2892(6)	2771(6)	3487(5)	46.8(17)

Table S8: Anisotropic Displacement Parameters (×10^4) **MW03045**. The anisotropic displacement factor exponent takes the form: $-2\pi^2[h^2a^{*2} \times U_{11} + \ldots + 2hka^* \times b^* \times U_{12}]$

Atom	U_{11}	U_{22}	U_{33}	U_{23}	U_{13}	U_{12}
Co1	12.2(3)	12.9(3)	11.7(3)	-0.2(2)	2.9(2)	0.6(2)
Co2	14.5(3)	10.3(3)	13.0(3)	-0.5(2)	3.1(2)	-1.2(2)
Ca1	13.1(4)	11.9(4)	11.5(4)	-1.3(3)	3.1(3)	-1.3(3)
S2	12.3(5)	15.0(5)	13.9(5)	0.3(4)	5.3(4)	0.4(4)
S1	15.9(5)	18.6(6)	14.4(5)	2.6(4)	6.6(4)	0.8(4)
S5	18.0(5)	13.8(6)	13.3(5)	0.1(4)	6.4(4)	-1.0(4)
S6	18.2(5)	10.3(5)	17.7(6)	-0.5(4)	4.3(4)	0.2(4)
S4	12.7(5)	14.6(6)	20.2(5)	-1.6(4)	5.8(4)	0.1(4)
S3	18.6(5)	11.3(5)	15.0(5)	-0.2(4)	2.4(4)	0.3(4)
O4	18.7(16)	20.1(19)	22.2(17)	3.2(14)	10.4(14)	3.3(14)
O11	21.4(17)	14.0(17)	19.5(17)	-2.9(14)	4.9(14)	-2.2(14)
O7	16.2(15)	18.5(17)	21.4(17)	-4.7(14)	5.2(13)	-2.3(14)
O3	17.9(16)	20.3(18)	18.3(16)	-4.8(14)	5.7(13)	-3.3(14)
O10	27.3(18)	20(2)	23.5(18)	1.1(15)	10.1(15)	4.5(15)
O9	22.4(16)	18.7(18)	13.7(15)	1.3(14)	6.2(13)	-2.5(14)
O12	25.1(18)	16.2(18)	24.6(19)	1.4(14)	9.5(15)	-0.9(14)
O8	18.6(16)	17.3(17)	29.3(19)	-2.0(16)	8.3(14)	0.5(14)
O2	32(2)	24(2)	26(2)	8.5(16)	14.7(17)	4.0(16)
O6	28.7(19)	16.0(18)	31(2)	4.0(15)	11.5(17)	-0.8(15)
O1	22.1(17)	23.1(19)	17.8(17)	1.1(14)	8.6(14)	-1.8(14)
O5	23.1(17)	14.7(17)	19.5(18)	-3.3(13)	4.5(14)	-0.7(14)
N3	12.7(17)	20(2)	12.2(18)	0.2(15)	4.2(15)	1.8(15)
N4	21(2)	12(2)	16.3(19)	-1.6(16)	-3.6(16)	2.3(16)
N8	18.3(19)	9.7(19)	19(2)	-0.9(16)	-1.7(16)	1.2(15)
N2	15.0(18)	26(2)	11.3(18)	0.9(16)	4.3(15)	-4.8(16)
N7	17.7(19)	20(2)	13.4(18)	0.5(16)	2.6(15)	-5.5(16)
N1	14.6(18)	17(2)	15.3(19)	0.3(16)	3.4(15)	1.9(15)
N5	21(2)	11.3(19)	15.7(19)	-1.7(15)	2.5(16)	-5.2(16)
N6	12.5(18)	21(2)	18(2)	-5.6(17)	4.2(15)	-1.4(15)
C48	21(2)	14(2)	18(2)	-0.3(18)	4.2(19)	5.0(18)
C12	14(2)	19(2)	16(2)	3.5(19)	5.3(17)	1.1(18)
C30	17(2)	18(3)	19(2)	-0.6(18)	7.0(18)	-1.7(18)
C49	23(2)	15(2)	14(2)	-1.3(18)	3.1(18)	-1.7(19)
C3	13(2)	28(3)	17(2)	-2(2)	6.9(17)	2.2(19)
C21	22(2)	17(2)	11(2)	3.0(18)	2.2(18)	7.4(19)
C1	19(2)	23(3)	16(2)	-3.9(19)	6.0(19)	1.0(19)
C2	16(2)	32(3)	15(2)	1(2)	6.2(19)	-1(2)
C11	13(2)	21(2)	15(2)	-0.2(19)	4.2(17)	2.2(18)
C54	33(3)	21(3)	34(3)	11(2)	17(2)	6(2)
C50	24(2)	14(2)	18(2)	0.5(18)	2.1(19)	3.1(19)

Atom	U_{11}	U_{22}	U_{33}	U_{23}	U_{13}	U_{12}
C42	16(2)	17(2)	31(3)	7(2)	10(2)	-0.6(19)
C45	20(2)	23(3)	15(2)	4(2)	0.1(19)	-1(2)
C24	30(3)	26(3)	18(2)	2(2)	6(2)	10(2)
C10	18(2)	21(3)	14(2)	2.0(19)	1.1(17)	1.9(19)
C33	30(3)	35(3)	30(3)	2(2)	15(2)	-6(2)
C39	16(2)	13(2)	19(2)	2.1(17)	8.0(17)	-1.1(17)
C14	26(3)	18(3)	26(3)	5(2)	3(2)	-1(2)
C51	24(3)	23(3)	24(3)	0(2)	6(2)	6(2)
C46	31(3)	19(3)	22(3)	-7(2)	0(2)	4(2)
C19	20(2)	13(2)	20(2)	-3.7(19)	3.0(19)	-2.2(18)
C17	53(4)	26(3)	29(3)	5(2)	29(3)	10(3)
C38	27(2)	23(3)	12(2)	-1.0(19)	4.7(19)	-5(2)
C41	33(3)	29(3)	20(3)	6(2)	10(2)	-5(2)
C29	15(2)	20(2)	24(3)	2(2)	0.8(19)	-2.6(19)
C47	25(3)	16(3)	22(3)	-2(2)	1(2)	-2(2)
C43	29(3)	21(3)	38(3)	7(2)	11(2)	-5(2)
C40	36(3)	26(3)	20(3)	-3(2)	12(2)	-8(2)
C22	24(2)	15(2)	25(3)	-2(2)	3(2)	-1(2)
C26	23(3)	26(3)	31(3)	0(2)	7(2)	-2(2)
C18	41(3)	15(2)	24(3)	-3(2)	16(2)	2(2)
C53	32(3)	30(3)	39(3)	12(3)	20(3)	2(2)
C23	35(3)	19(3)	23(3)	-4(2)	5(2)	5(2)
C27	24(2)	16(2)	23(3)	1(2)	4(2)	0(2)
C13	28(3)	19(3)	18(2)	-0.1(19)	7(2)	1(2)
C20	25(3)	16(2)	19(2)	-5(2)	-1(2)	3(2)
C28	20(2)	25(3)	21(3)	0(2)	2(2)	1(2)
C36	22(2)	28(3)	22(3)	-2(2)	6(2)	1(2)
C15	27(3)	27(3)	29(3)	12(2)	13(2)	5(2)
C31	30(3)	23(3)	43(3)	4(2)	23(3)	4(2)
C16	47(4)	35(4)	49(4)	18(3)	30(3)	7(3)
C32	38(3)	26(3)	43(3)	8(3)	21(3)	5(3)
C35	27(3)	36(3)	27(3)	-6(2)	17(2)	-4(2)
C44	24(3)	23(3)	25(3)	-1(2)	2(2)	-5(2)
C9	24(3)	35(3)	33(3)	-2(2)	13(2)	-3(2)
C37	28(3)	23(3)	19(2)	4(2)	0(2)	0(2)
C25	34(3)	43(4)	39(3)	2(3)	13(3)	14(3)
C6	20(3)	62(4)	26(3)	0(3)	7(2)	9(3)
C4	24(3)	32(3)	38(3)	10(3)	15(2)	3(2)
C8	26(3)	49(4)	36(3)	-6(3)	18(3)	-14(3)
C5	29(3)	44(4)	44(4)	8(3)	15(3)	13(3)
C7	25(3)	99(7)	52(4)	3(5)	17(3)	10(4)
C52	31(3)	32(3)	38(3)	5(3)	14(3)	9(3)
C34	45(4)	52(4)	53(4)	14(4)	30(3)	-7(3)

Table S9: Bond Lengths in Å for **MW03045**.

Atom	Atom	Length/Å
Co1	Ca1	3.5305(11)
Co1	N3	1.928(4)
Co1	N4	1.915(4)
Co1	N2	1.914(4)
Co1	N1	2.063(4)
Co2	Ca1	3.5155(10)
Co2	N8	1.933(4)
Co2	N7	1.961(4)
Co2	N5	2.066(4)
Co2	N6	1.925(4)
Ca1	O11	2.318(3)
Ca1	O7	2.329(3)
Ca1	O3	2.313(3)
Ca1	O9	2.325(3)
Ca1	O1	2.323(3)
Ca1	O5	2.379(4)
S2	O4	1.438(3)
S2	O3	1.464(3)
S2	N3	1.560(4)

Atom	Atom	Length/Å
S2	C12	1.772(5)
S1	O2	1.441(4)
S1	O1	1.465(4)
S1	N2	1.566(4)
S1	C3	1.774(5)
S5	O10	1.436(4)
S5	O9	1.467(3)
S5	N7	1.579(4)
S5	C39	1.762(5)
S6	O11	1.467(4)
S6	O12	1.445(4)
S6	N8	1.571(4)
S6	C48	1.776(5)
S4	O7	1.468(3)
S4	O8	1.439(4)
S4	N6	1.562(4)
S4	C30	1.771(5)
S3	O6	1.438(4)
S3	O5	1.467(4)
S3	N4	1.567(4)
S3	C21	1.774(5)
N3	C11	1.470(6)
N4	C20	1.475(6)
N8	C47	1.480(6)
N2	C2	1.472(6)
N7	C38	1.467(6)
N1	C1	1.478(6)
N1	C10	1.483(6)
N1	C19	1.487(6)
N5	C46	1.473(7)
N5	C28	1.482(6)
N5	C37	1.493(6)
N6	C29	1.463(6)
C48	C49	1.382(7)
C48	C54	1.393(7)
C12	C18	1.398(7)
C12	C13	1.382(7)
C30	C36	1.384(7)
C30	C31	1.397(7)
C49	C50	1.387(7)
C3	C9	1.385(7)
C3	C4	1.375(8)
C21	C22	1.391(7)
C21	C27	1.386(7)
C1	C2	1.538(7)
C11	C10	1.540(6)
C54	C53	1.376(8)
C50	C51	1.375(7)
C42	C41	1.384(8)
C42	C43	1.512(7)
C42	C44	1.383(7)
C45	C39	1.388(7)
C45	C44	1.381(7)
C24	C26	1.406(8)
C24	C23	1.382(8)
C24	C25	1.510(8)
C33	C32	1.388(8)
C33	C35	1.380(8)
C33	C34	1.509(8)
C39	C40	1.402(7)
C14	C13	1.397(7)
C14	C15	1.389(8)
C51	C53	1.414(8)
C51	C52	1.507(7)
C46	C47	1.534(7)
C19	C20	1.534(7)
C17	C18	1.369(8)
C17	C15	1.389(9)
C38	C37	1.536(7)
C41	C40	1.376(8)
C29	C28	1.522(8)
C22	C23	1.382(7)
C26	C27	1.376(7)
C36	C35	1.372(8)
C15	C16	1.514(8)
C31	C32	1.377(8)
C9	C8	1.381(8)
C6	C8	1.384(10)
C6	C5	1.369(9)
C6	C7	1.504(8)
C4	C5	1.376(8)

Table S10: Bond Angles in ° for **MW03045**.

Atom	Atom	Atom	Angle/°
N3	Co1	Ca1	94.34(12)
N3	Co1	N1	85.30(16)
N4	Co1	Ca1	95.07(12)
N4	Co1	N3	115.59(18)
N4	Co1	N1	85.98(17)
N2	Co1	Ca1	94.57(12)
N2	Co1	N3	122.81(18)
N2	Co1	N4	119.65(19)
N2	Co1	N1	84.81(16)
N1	Co1	Ca1	178.95(12)
N8	Co2	Ca1	92.59(12)
N8	Co2	N7	120.67(18)
N8	Co2	N5	85.32(16)
N7	Co2	Ca1	96.35(11)
N7	Co2	N5	86.78(16)
N5	Co2	Ca1	176.83(11)
N6	Co2	Ca1	94.55(12)
N6	Co2	N8	119.87(18)
N6	Co2	N7	117.65(18)
N6	Co2	N5	84.45(17)
O11	Ca1	O7	91.35(12)

Atom	Atom	Atom	Angle/°
O11	Ca1	O9	85.27(12)
O11	Ca1	O1	85.48(13)
O11	Ca1	O5	171.65(13)
O7	Ca1	O5	82.27(12)
O3	Ca1	O11	98.04(13)
O3	Ca1	O7	169.82(13)
O3	Ca1	O9	86.41(12)
O3	Ca1	O1	88.30(12)
O3	Ca1	O5	88.73(12)
O9	Ca1	O7	98.34(12)
O9	Ca1	O5	90.30(12)
O1	Ca1	O7	88.53(12)
O1	Ca1	O9	168.60(13)
O1	Ca1	O5	99.67(13)
O4	S2	O3	114.9(2)
O4	S2	N3	114.4(2)
O4	S2	C12	105.6(2)
O3	S2	N3	105.5(2)
O3	S2	C12	106.0(2)
N3	S2	C12	110.2(2)
O2	S1	O1	116.4(2)
O2	S1	N2	115.2(2)
O2	S1	C3	106.6(2)
O1	S1	N2	104.4(2)
O1	S1	C3	105.1(2)
N2	S1	C3	108.5(2)
O10	S5	O9	115.9(2)
O10	S5	N7	114.2(2)
O10	S5	C39	105.7(2)
O9	S5	N7	104.8(2)
O9	S5	C39	105.3(2)
N7	S5	C39	110.6(2)
O11	S6	N8	105.5(2)
O11	S6	C48	105.5(2)
O12	S6	O11	115.7(2)
O12	S6	N8	114.4(2)
O12	S6	C48	106.2(2)
N8	S6	C48	109.0(2)
O7	S4	N6	104.6(2)
O7	S4	C30	106.6(2)
O8	S4	O7	115.7(2)
O8	S4	N6	115.0(2)
O8	S4	C30	106.7(2)
N6	S4	C30	107.6(2)
O6	S3	O5	116.2(2)
O6	S3	N4	114.2(2)
O6	S3	C21	105.5(2)
O5	S3	N4	105.1(2)
O5	S3	C21	107.0(2)
N4	S3	C21	108.5(2)
S6	O11	Ca1	157.9(2)
S4	O7	Ca1	160.5(2)
S2	O3	Ca1	158.5(2)
S5	O9	Ca1	164.4(2)
S1	O1	Ca1	160.1(2)
S3	O5	Ca1	159.6(2)
S2	N3	Co1	121.0(2)

Atom	Atom	Atom	Angle/°
C11	N3	Co1	115.4(3)
C11	N3	S2	123.6(3)
S3	N4	Co1	122.5(2)
C20	N4	Co1	115.2(3)
C20	N4	S3	121.8(3)
S6	N8	Co2	123.6(2)
C47	N8	Co2	114.1(3)
C47	N8	S6	119.1(3)
S1	N2	Co1	121.8(2)
C2	N2	Co1	115.8(3)
C2	N2	S1	122.0(3)
S5	N7	Co2	110.1(2)
C38	N7	Co2	111.5(3)
C38	N7	S5	121.0(3)
C1	N1	Co1	106.2(3)
C1	N1	C10	113.8(4)
C1	N1	C19	113.4(4)
C10	N1	Co1	105.1(3)
C10	N1	C19	112.3(4)
C19	N1	Co1	105.0(3)
C46	N5	Co2	106.3(3)
C46	N5	C28	113.0(4)
C46	N5	C37	113.5(4)
C28	N5	Co2	106.9(3)
C28	N5	C37	112.2(4)
C37	N5	Co2	104.1(3)
S4	N6	Co2	122.4(2)
C29	N6	Co2	116.2(3)
C29	N6	S4	121.4(3)
C49	C48	S6	120.2(4)
C49	C48	C54	121.1(5)
C54	C48	S6	118.7(4)
C18	C12	S2	117.4(4)
C13	C12	S2	122.5(4)
C13	C12	C18	120.0(5)
C36	C30	S4	120.0(4)
C36	C30	C31	120.2(5)
C31	C30	S4	119.7(4)
C48	C49	C50	118.8(5)
C9	C3	S1	120.0(4)
C4	C3	S1	119.7(4)
C4	C3	C9	120.2(5)
C22	C21	S3	118.8(4)
C27	C21	S3	120.9(4)
C27	C21	C22	120.3(5)
N1	C1	C2	110.6(4)
N2	C2	C1	107.3(4)
N3	C11	C10	107.9(4)
C53	C54	C48	119.1(5)
C51	C50	C49	122.0(5)
C41	C42	C43	120.1(5)
C44	C42	C41	118.6(5)
C44	C42	C43	121.3(5)
C44	C45	C39	119.0(5)
C26	C24	C25	120.4(5)
C23	C24	C26	117.7(5)
C23	C24	C25	121.9(5)

Atom	Atom	Atom	Angle/°
N1	C10	C11	111.5(4)
C32	C33	C34	120.9(6)
C35	C33	C32	118.2(5)
C35	C33	C34	120.8(5)
C45	C39	S5	121.7(4)
C45	C39	C40	119.8(4)
C40	C39	S5	118.4(4)
C15	C14	C13	121.3(5)
C50	C51	C53	118.0(5)
C50	C51	C52	122.2(5)
C53	C51	C52	119.8(5)
N5	C46	C47	111.0(4)
N1	C19	C20	112.0(4)
C18	C17	C15	121.1(5)
N7	C38	C37	107.8(4)
C40	C41	C42	121.0(5)
N6	C29	C28	108.2(4)
N8	C47	C46	107.6(4)
C41	C40	C39	119.7(5)
C23	C22	C21	119.2(5)
C27	C26	C24	121.3(5)
C17	C18	C12	120.0(5)

Atom	Atom	Atom	Angle/°
C54	C53	C51	121.0(5)
C24	C23	C22	121.9(5)
C26	C27	C21	119.6(5)
C12	C13	C14	118.9(5)
N4	C20	C19	107.9(4)
N5	C28	C29	111.8(4)
C35	C36	C30	119.3(5)
C14	C15	C17	118.3(5)
C14	C15	C16	121.8(6)
C17	C15	C16	119.8(5)
C32	C31	C30	118.9(5)
C31	C32	C33	121.4(6)
C36	C35	C33	121.8(5)
C45	C44	C42	121.8(5)
C8	C9	C3	119.1(6)
N5	C37	C38	111.1(4)
C8	C6	C7	120.1(7)
C5	C6	C8	118.8(5)
C5	C6	C7	121.1(7)
C3	C4	C5	119.7(5)
C9	C8	C6	120.9(5)
C6	C5	C4	121.2(6)

Table S11: Hydrogen Fractional Atomic Coordinates (×10⁴) and Equivalent Isotropic Displacement Parameters (Å²×10³) for **MW03045**. U_{eq} is defined as 1/3 of the trace of the orthogonalised U_{ij}.

Atom	x	y	z	U_{eq}
H49	7685	884	2114	22
H1A	9000	7663	6045	23
H1B	10047	7224	6734	23
H2A	9578	5590	6327	25
H2B	8509	6085	6289	25
H11A	11691	7140	4924	20
H11B	11918	5994	5217	20
H54	8366	3412	1123	34
H50	9164	123	2057	25
H45	8572	7229	1394	26
H10A	11053	6121	6109	23
H10B	11639	7176	6237	23
H14	11536	8764	2760	31
H46A	5441	3196	-864	32
H46B	4320	2769	-977	32
H19A	10709	8415	5124	23
H19B	10351	8762	5859	23
H17	11092	6456	1159	39
H38A	6117	4674	-1079	26
H38B	5734	5813	-1283	26
H41	7908	8106	-1378	33
H29A	3325	5643	-128	26
H29B	3019	4878	458	26
H47A	4867	2322	416	28
H47B	5813	1985	158	28
H43A	9810	9412	-295	45
H43B	9035	10039	5	45

Atom	x	y	z	U_{eq}
H43C	8679	9701	-952	45
H40	7295	6593	-1090	32
H22	7417	10108	3461	28
H26	4372	8227	2695	33
H18	10562	5457	2014	31
H53	9839	2642	1073	38
H23	5891	10847	3427	33
H27	5903	7462	2776	27
H13	10958	7777	3618	27
H20A	8646	8914	4973	27
H20B	9254	9336	4417	27
H28A	3527	3519	-75	29
H28B	3026	4207	-889	29
H36	3061	5771	2318	30
H31	5239	3717	2379	35
H16A	11321	8295	769	60
H16B	12488	8034	1371	60
H16C	11929	9005	1546	60
H32	4524	2602	3043	41
H35	2387	4650	2999	34
H44	9224	8711	1084	31
H9	5986	4172	4963	36
H37A	4209	5493	-1067	31
H37B	4303	4603	-1655	31
H25A	3602	10371	2447	58
H25B	4123	10657	3417	58
H25C	3535	9610	3139	58
H4	6752	6941	4452	36
H8	4353	4767	4818	43
H5	5124	7517	4316	47
H7A	3078	6012	4449	87
H7B	3241	6992	3981	87
H7C	3600	6988	4977	87
H52A	11248	1125	2015	50
H52B	10694	944	1029	50
H52C	10633	104	1668	50
H34A	2323	2418	3053	70
H34B	2622	3128	3856	70
H34C	3419	2286	3813	70

4-2

EMORY UNIVERSITY | X-ray Crystallography Center

Submitted by: **Christian Wallen**
Emory University
Solved by:
Sample ID: **CMW-030086SRTS**

Crystal Data and Experimental

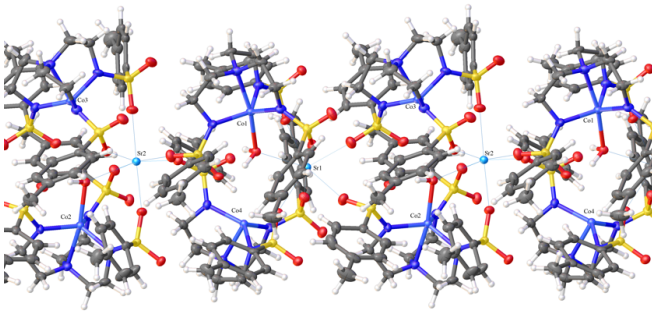

Experimental. Single violet plate-shaped crystals of (**CMW-03-086SRTS**) were recrystallised from a mixture of CH_2Cl_2 and methanol by vapor diffusion. A suitable crystal (0.92×0.28×0.10 mm) was selected and mounted on a loop with paratone oil on a Bruker APEX-II CCD diffractometer. The crystal was cooled to T = 100(2) K during data collection. The structure was solved with the **ShelXT** (Sheldrick, 2015) structure solution program using combined Patterson and dual-space recycling methods and by using **Olex2** (Dolomanov et al., 2009) as the graphical interface. The crystal structure was refined with version of **ShelXL** (Sheldrick, 2008) using Least Squares minimisation.

Crystal Data. $C_{108}H_{138}Co_4N_{16}O_{27}S_{12}Sr_2$, M_r = 2888.02, monoclinic, $P2_1/c$ (No. 14), a = 29.583(7) Å, b = 16.185(4) Å, c = 25.822(6) Å, β = 95.585(4)°, $\alpha = \gamma = 90°$, V = 12305(5) Å^3, T = 100(2) K, Z = 4, Z' = 1, μ(MoK$_\alpha$) = 1.669, 97100 reflections measured, 32412 unique (R_{int} = 0.0842) which were used in all calculations. The final wR_2 was 0.1594 (all data) and R_1 was 0.0630 (I > 2σ(I)).

Compound	**CMW-03-086SRTS**
Formula	$C_{108}H_{138}Co_4N_{16}O_{27}S_{12}Sr_2$
$D_{calc.}$/ g cm^{-3}	1.559
μ/mm^{-1}	1.669
Formula Weight	2888.02
Colour	violet
Shape	plate
Max Size/mm	0.92
Mid Size/mm	0.28
Min Size/mm	0.10
T/K	100(2)
Crystal System	monoclinic
Space Group	$P2_1/c$
a/Å	29.583(7)
b/Å	16.185(4)
c/Å	25.822(6)
α/°	90
β/°	95.585(4)
γ/°	90
V/Å^3	12305(5)
Z	4
Z'	1
Θ_{min}/°	0.692
Θ_{max}/°	29.603
Measured Refl.	97100
Independent Refl.	32412
$I > 2\sigma(I)$	20137
R_{int}	0.0842
Parameters	1537
Restraints	10
Largest Peak	1.516
Deepest Hole	-0.936
GooF	1.033
wR_2 (all data)	0.1594
wR_2	0.1350
R_1 (all data)	0.1207
R_1	0.0630
CCDC #	1434441

Structure Quality Indicators

Reflections:

Refinement:

A violet plate-shaped crystal with dimensions 0.92×0.28×0.10 mm was mounted on a loop with paratone oil. X-ray diffraction data were collected using a Bruker APEX-II CCD diffractometer equipped with an Oxford Cryosystems low-temperature apparatus operating at T = 100(2) K.

Data were measured using ω scans with MoK$_\alpha$ radiation (fine-focus sealed tube, 45 kV, 35 mA). The total number of runs and images was based on the strategy calculation from the program **APEX2** (Bruker, 2014). The maximum resolution achieved was Θ = 29.603°.

Unit cell indexing was performed by using the **APEX2** (Bruker) software and refined using **SAINT** (Bruker, V8.34A, 2013) on 9882 reflections, 10% of the observed reflections. Data reduction, scaling and absorption corrections were performed using **SAINT** (Bruker, V8.34A, 2013) and **SADABS-2014/2** (Bruker, 2014) was used for absorption correction. wR_2(int) was 0.1695 before and 0.0606 after correction. The ratio of minimum to maximum transmission is 0.4684. The $\lambda/2$ correction factor is Not present. software which corrects for Lorentz polarisation. The final completeness is 100.00 out to 29.603 in Θ. The absorption coefficient (μ) of this material is 1.669 mm^{-1} and the minimum and maximum transmissions are 0.3494 and 0.7459.

The structure was solved in the space group P1 with the **ShelXT** (Sheldrick, 2015) structure solution program using combined Patterson and dual-space recycling methods. The space group P2$_1$/c (# 14) was determined by **ShelXT** (Sheldrick, 2015) structure solution program.The crystal structure was refined by Least Squares using version 2014/7 of **ShelXL** (Sheldrick, 2008). All non-hydrogen atoms were refined anisotropically. Hydrogen atom positions were calculated geometrically and refined using the riding model.

There are two independent molecules in the asymmetric unit.

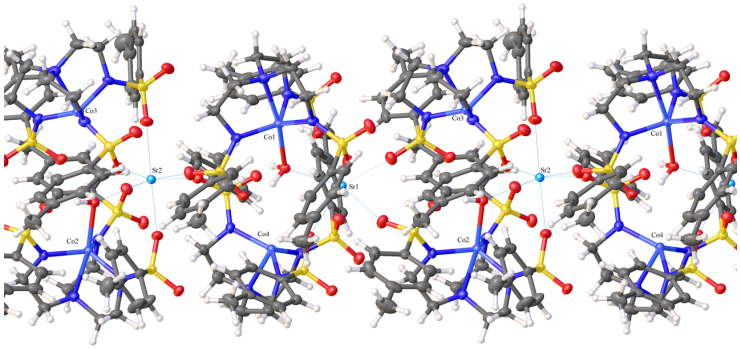

Figure S12:

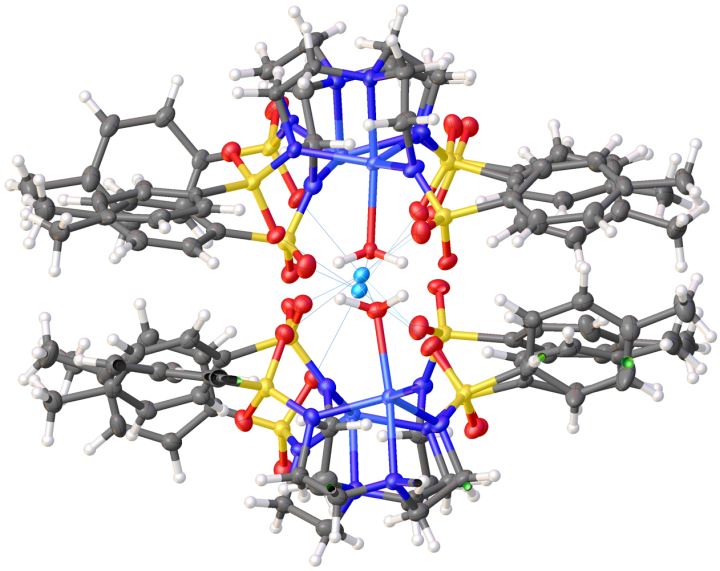

Figure S13:

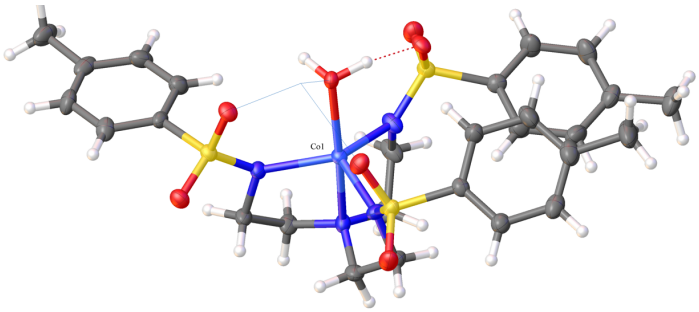

Figure S14:

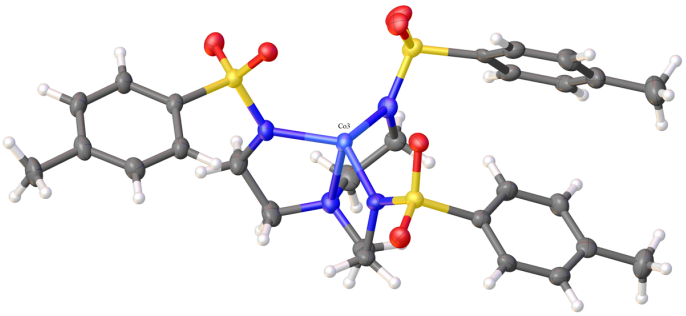

Figure S15:

Data Plots: Diffraction Data

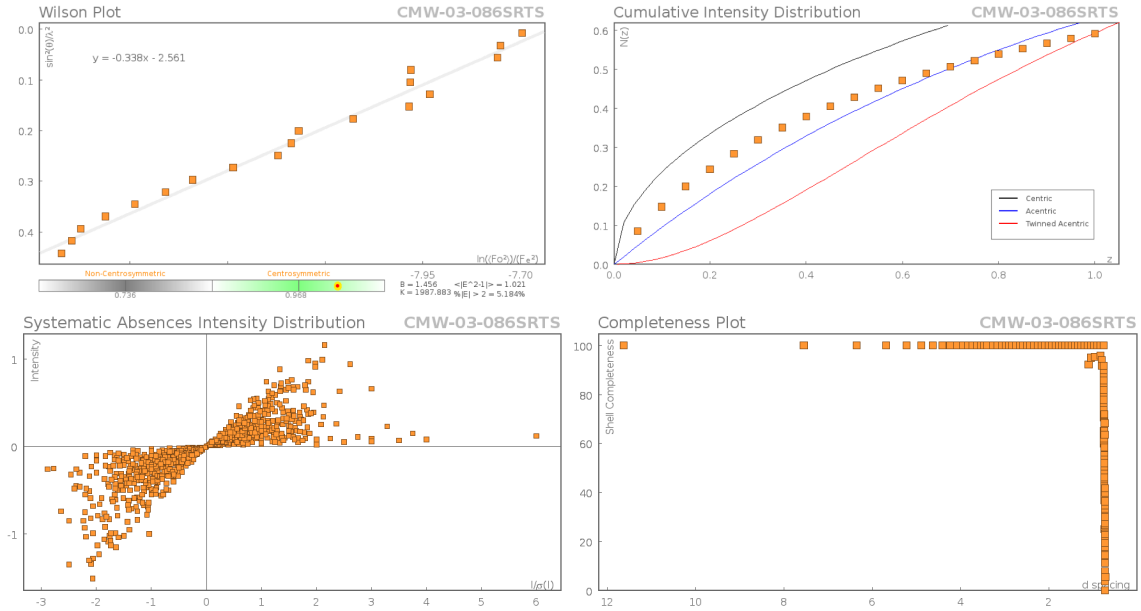

Data Plots: Refinement and Data

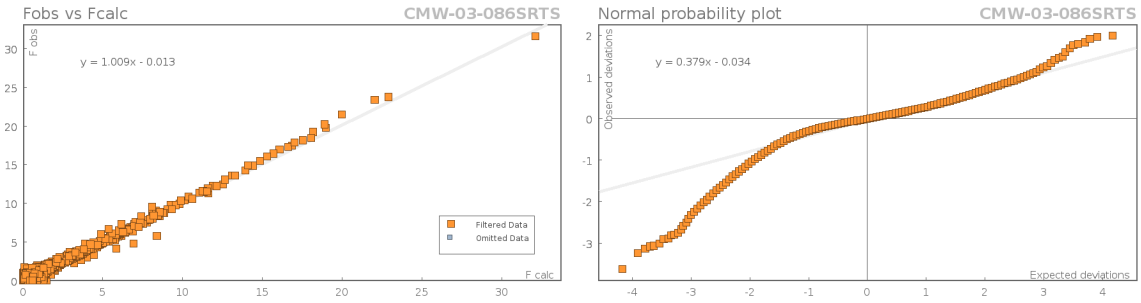

Reflection Statistics

Total reflections (after filtering)	98878	Unique reflections	32412
Completeness	0.936	Mean I/σ	6.7
hklsub>max</sub> collected	(38, 22, 35)	hklsub>min</sub> collected	(-41, -22, -31)
hkl_{max} used	(40, 22, 35)	hkl_{min} used	(-41, 0, 0)
Lim d_{max} collected	100.0	Lim d_{min} collected	0.36
d_{max} used	29.44	d_{min} used	0.72
Friedel pairs	24046	Friedel pairs merged	1
Inconsistent equivalents	0	R_{int}	0.0842
R_{sigma}	0.1104	Intensity transformed	0
Omitted reflections	0	Omitted by user (OMIT hkl)	0
Multiplicity	(68410, 15135, 66)	Maximum multiplicity	9
Removed systematic absences	1778	Filtered off (Shel/OMIT)	0

Images of the Crystal on the Diffractometer

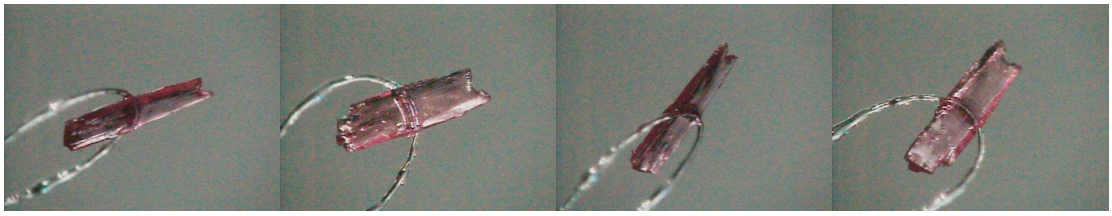

Table S12: Fractional Atomic Coordinates (×10⁴) and Equivalent Isotropic Displacement Parameters (Å²×10³) for **CMW-03-086SRTS**. U_{eq} is defined as 1/3 of the trace of the orthogonalised U_{ij}.

Atom	x	y	z	U_{eq}
Co1	3090.1(2)	1499.8(3)	1633.4(2)	18.14(13)
S3	2142.3(4)	747.6(6)	1070.5(4)	19.6(2)
S1	3624.6(4)	-148.1(6)	2053.4(4)	20.9(2)
S2	3347.5(4)	3010.6(6)	2451.5(4)	21.0(2)
O2	3817.9(10)	-860.2(17)	1816.0(12)	30.2(7)
O1	2677.0(8)	1364.1(15)	2276.9(10)	18.9(6)
O4	3178.1(10)	2430.5(17)	2813.2(10)	23.8(7)
O5	3119.3(11)	3801.1(17)	2430.4(12)	29.4(7)
O3	3193.8(10)	-272.1(17)	2266.2(12)	25.5(7)
O6	2076.3(10)	537.8(17)	1607.8(10)	22.8(7)
O7	2125.2(10)	60.0(16)	712.5(11)	24.5(7)
N1	3563.0(12)	616(2)	1678.2(13)	22.7(8)
N2	3439.3(12)	1885(2)	966.9(13)	22.6(8)
N3	3348.2(13)	2594(2)	1907.9(13)	24.8(8)
N4	2584.7(12)	1286(2)	1066.6(13)	21.0(8)
C22	1332.0(15)	1093(3)	499.0(17)	28.4(10)
C23	968.2(16)	1603(3)	329.7(18)	31.9(11)
C8	3931.6(15)	769(3)	1348.4(17)	28.2(10)
C2	3884.4(16)	670(3)	2958.0(17)	27.2(10)
C14	4416.7(17)	3992(3)	3311.2(18)	34.0(12)
C3	4194.9(17)	894(3)	3375.9(18)	35.4(12)
C20	2706.5(15)	1428(3)	529.8(16)	24.8(10)
C13	3995.2(17)	3899(3)	3036.8(18)	32.1(11)
C9	3719.9(16)	1172(3)	847.2(16)	27.5(10)
C1	4016.7(15)	117(2)	2591.1(16)	20.5(9)
C16	4677.1(17)	2779(3)	2923.4(18)	34.4(12)
C12	3908.6(15)	3221(2)	2713.9(16)	22.3(9)
C26	1679.3(16)	2228(3)	981.4(17)	27.6(10)
C10	3715.8(16)	2624(3)	1118.3(17)	29.7(11)
C15	4765.2(16)	3430(3)	3266.4(18)	29.8(11)
C21	1678.8(14)	1397(3)	833.3(16)	22.1(9)
C17	4256.4(16)	2667(3)	2654.5(18)	29.4(11)
C4	4630.1(18)	573(3)	3432.9(18)	36.2(12)
C18	5213.9(16)	3517(3)	3587(2)	41.5(13)
C11	3491.9(18)	3146(3)	1493.3(17)	30.5(11)
C24	953.9(16)	2416(3)	480.9(18)	32.0(11)
C6	4447.0(16)	-216(3)	2644.9(17)	27.6(10)
C5	4751.2(17)	11(3)	3065.7(18)	33.5(11)
C7	4957.1(18)	819(4)	3890.5(19)	52.0(16)
C19	3075.5(15)	2073(3)	548.9(16)	25.9(10)
C25	1317.9(17)	2725(3)	804.0(17)	32.0(11)
C27	552.6(17)	2964(3)	316(2)	42.4(14)
Co2	2166.3(2)	6453.6(3)	3502.6(2)	18.44(13)
S4	2825.4(4)	8051.4(6)	3336.7(4)	21.0(2)
S5	2713.8(4)	4808.7(6)	3913.4(4)	20.7(2)

Atom	x	y	z	U_{eq}
S6	1328.4(4)	5726.5(6)	2709.2(4)	21.5(2)
O11	2628.5(10)	4110.4(16)	4238.2(11)	25.1(7)
O8	2457.5(9)	6280.2(15)	2770.3(11)	22.6(7)
O9	2679.6(11)	8857.5(18)	3147.0(12)	30.4(7)
O13	1024.8(10)	5071.6(16)	2831.0(12)	25.1(7)
O14	1699.1(10)	5476.3(17)	2414.0(11)	25.8(7)
O12	2681.9(11)	4656.3(17)	3357.1(11)	25.9(7)
O10	3000(1)	7509.6(17)	2955.7(11)	27.8(7)
N6	1824.3(12)	6844(2)	4171.1(13)	22.6(8)
N5	2450.8(12)	7592.6(19)	3614.1(13)	21.4(8)
N8	1523.6(12)	6224(2)	3205.4(14)	22.5(8)
N7	2402.8(13)	5570(2)	4003.2(13)	23.5(8)
C47	1177.4(15)	6365(3)	3577.6(17)	27.3(10)
C43	3961.1(16)	5785(3)	3902.1(18)	30.8(11)
C41	3937(2)	5150(3)	4722(2)	49.4(15)
C51	401.5(16)	7478(3)	1703.8(17)	26.6(10)
C28	3298.2(15)	8258(2)	3790.8(16)	21.7(9)
C48	977.1(14)	6421(2)	2312.6(16)	19.6(9)
C42	4176.4(17)	5602(3)	4383(2)	34.7(12)
C36	2054.0(16)	7590(3)	4388.6(16)	26.2(10)
C29	3488.4(16)	7616(3)	4095.0(17)	29.4(11)
C35	2210.2(16)	8133(2)	3960.0(17)	25.7(10)
C50	355.7(16)	6630(3)	1657.1(18)	29.6(11)
C49	640.0(15)	6097(3)	1964.4(17)	25.9(10)
C38	2321.4(16)	5736(3)	4548.4(16)	27.5(10)
C31	4082.3(17)	8528(3)	4461.5(19)	36.1(12)
C53	1031.1(16)	7269(3)	2358.1(17)	25.6(10)
C54	74.1(17)	8051(3)	1400.0(19)	37.4(12)
C40	3495.4(18)	4893(3)	4574.5(19)	40.6(13)
C30	3878.5(17)	7765(3)	4424.7(18)	33.9(12)
C44	3524.5(15)	5544(3)	3748.8(17)	25(1)
C37	1860.3(16)	6148(3)	4547.4(17)	28.9(10)
C32	3888.9(17)	9157(3)	4147(2)	39.0(13)
C46	1354.3(15)	7015(3)	3960.9(17)	26.4(10)
C39	3290.1(16)	5088(2)	4085.3(16)	23.3(10)
C34	4494.5(19)	8695(4)	4840(2)	58.5(17)
C33	3502.4(16)	9037(3)	3811.7(18)	28.8(11)
C52	739.8(15)	7787(3)	2057.3(18)	27.2(10)
C45	4660.7(17)	5875(3)	4540(2)	47.5(15)
Co3	2883.5(2)	-3325.1(3)	1385.9(2)	20.70(13)
S7	3675.2(4)	-4157.3(6)	2100.0(4)	21.2(2)
S8	2431.9(4)	-4966.7(6)	905.3(4)	24.3(2)
S9	2124.7(4)	-2099.6(6)	1715.3(4)	22.1(2)
O15	3282.9(10)	-4362.6(17)	2369.5(11)	24.5(7)
O16	3922.7(11)	-4844.3(18)	1909.9(12)	29.0(7)
O17	2644.2(12)	-5629.0(18)	646.8(11)	35.2(8)
O18	2393.9(11)	-5068.1(18)	1458.1(11)	28.1(7)
O19	2010.9(10)	-2845.9(17)	1986.5(11)	26.6(7)
O20	2151.7(11)	-1348.8(17)	2023.0(12)	30.2(7)
N9	3509.4(12)	-3509(2)	1663.0(13)	22.8(8)
N11	2665.7(13)	-4106(2)	840.8(13)	24.4(8)
N12	2560.9(13)	-2284(2)	1442.1(14)	24.2(8)
N10	3188.3(13)	-2722(2)	786.3(14)	25.9(8)
C62	3861.0(16)	-3230(3)	1332.8(18)	32.5(11)
C78	939.1(16)	-1697(3)	468.0(17)	27.5(10)
C77	1192.2(16)	-2418(3)	492.3(17)	29.1(11)
C76	1550.1(16)	-2533(3)	865.5(18)	28.8(11)

Atom	x	y	z	U_{eq}
C63	3656.9(16)	-2544(3)	997.3(19)	35.3(12)
C64	3178.7(19)	-3332(3)	350.0(18)	38.4(13)
C65	2756.5(16)	-3851(3)	315.4(16)	28.3(10)
C74	2746.0(16)	-1598(3)	1137.1(17)	27.8(10)
C73	2914.7(17)	-1992(3)	655.7(19)	34.4(12)
C55	4070.9(15)	-3617(3)	2539.8(16)	21.6(9)
C56	4483.8(15)	-3957(3)	2712.4(17)	26.1(10)
C57	4788.2(16)	-3508(3)	3042.3(18)	31.1(11)
C58	4688.2(16)	-2720(3)	3204.6(17)	28.9(11)
C59	4267.7(16)	-2389(3)	3023.8(17)	28.7(10)
C60	3960.8(16)	-2820(3)	2684.7(17)	26.8(10)
C61	5017.9(17)	-2228(3)	3563(2)	41.2(13)
C75	1667.0(15)	-1929(2)	1231.0(16)	22.9(10)
C80	1424.4(15)	-1192(2)	1211.6(18)	25(1)
C79	1064.8(16)	-1088(3)	836.5(18)	28.9(11)
C81	547.9(17)	-1558(3)	63(2)	42.6(13)
C66	1873.0(15)	-4873(2)	602.0(17)	22.1(9)
C67	1507.9(16)	-4750(2)	892.7(18)	27.5(10)
C68	1082.4(17)	-4625(3)	642.2(19)	33.9(12)
C69	1009.4(18)	-4592(3)	99.1(19)	34.6(12)
C70	1377.3(17)	-4719(3)	-188.5(17)	29.0(11)
C71	1808.6(17)	-4859(2)	58.4(16)	25.5(10)
C72	546.1(18)	-4424(4)	-176(2)	52.7(16)
Co4	1824.5(2)	1748.2(3)	3422.6(2)	18.01(13)
S10	2694.7(4)	895.8(6)	3932.6(4)	18.9(2)
S11	1721.9(4)	2914.7(6)	2461.3(4)	19.8(2)
S12	1261.5(4)	155.9(6)	3116.3(4)	20.0(2)
O21	2713.0(9)	746.5(16)	3376(1)	20.2(6)
O22	2664.6(10)	171.2(16)	4254.6(11)	23.6(7)
O23	1959.4(10)	3634.8(16)	2290.0(11)	23.7(7)
O24	1856.5(10)	2135.3(17)	2242.4(11)	23.0(7)
O25	1701.8(10)	18.0(17)	2920.9(11)	24.2(7)
O26	1093.5(10)	-477.9(17)	3440.1(11)	27.1(7)
N13	2300.3(11)	1532(2)	3972.2(12)	19.5(8)
N15	1762.3(12)	2809.2(19)	3062.5(13)	20.9(8)
N16	1294.3(12)	1029(2)	3389.8(13)	21.5(8)
N14	1506.7(12)	2365.9(19)	4011.0(13)	20.2(8)
C89	2203.3(15)	1807(2)	4496.8(16)	22.8(9)
C90	1869.3(18)	2520(3)	4425.3(18)	39.0(13)
C91	1314(2)	3131(3)	3770(2)	43.2(14)
C92	1610.8(16)	3489(2)	3388.6(16)	23.7(10)
C101	937.6(15)	1296(3)	3704.6(17)	24.4(10)
C100	1154.8(19)	1800(3)	4163(2)	43.2(14)
C82	3197.3(14)	1417(3)	4175.8(15)	20.1(9)
C83	3276.0(15)	2205(3)	3991.3(16)	23.5(10)
C84	3666.3(17)	2622(3)	4180.8(17)	29.0(11)
C85	3980.4(16)	2265(3)	4552.5(17)	26.4(10)
C86	3890.3(16)	1490(3)	4741.2(17)	28.3(10)
C87	3497.8(15)	1064(3)	4554.7(16)	24.4(10)
C88	4412.8(17)	2721(3)	4742(2)	39.3(13)
C102	867.5(15)	225(2)	2554.3(16)	21.3(9)
C103	418.6(16)	7(3)	2572.6(18)	27.9(10)
C104	113.2(16)	75(3)	2135.2(19)	34.4(12)
C105	255.0(17)	372(3)	1665.8(18)	33.8(12)
C106	705.2(17)	597(3)	1654.6(18)	31.1(11)
C107	1016.9(15)	527(3)	2094.3(17)	24.7(10)
C108	-69.9(19)	441(4)	1186(2)	52.8(16)

Atom	x	y	z	U_{eq}
C93	1145.1(15)	3052(2)	2237.4(16)	20.7(9)
C94	828.4(15)	2492(2)	2386.9(17)	23.5(10)
C95	380.0(16)	2538(3)	2181.8(17)	26.1(10)
C96	235.8(15)	3146(2)	1821.6(17)	23.4(10)
C97	551.4(16)	3719(3)	1691.9(17)	25.4(10)
C98	1001.8(16)	3690(2)	1894.7(16)	23.7(10)
C99	-247.0(16)	3154(3)	1574.5(18)	31.4(11)
O27	3712.2(16)	4788(3)	772.7(17)	71.1(13)
Sr1	2422.7(2)	-87.1(2)	2515.4(2)	17.64(9)
Sr2	2506.3(2)	4814.1(2)	2413.1(2)	17.26(9)

Table S13: Anisotropic Displacement Parameters (×10⁴) **CMW-03-086SRTS**. The anisotropic displacement factor exponent takes the form: $-2\pi^2[h^2a^{*2} \times U_{11} + \ldots + 2hka^* \times b^* \times U_{12}]$

Atom	U_{11}	U_{22}	U_{33}	U_{23}	U_{13}	U_{12}
Co1	18.8(3)	20.8(3)	14.8(3)	-0.7(2)	1.2(2)	0.0(2)
S3	21.7(6)	21.7(5)	15.2(5)	0.7(4)	0.7(4)	0.5(4)
S1	17.6(6)	20.8(5)	23.9(6)	-3.2(4)	0.9(4)	1.5(4)
S2	24.1(6)	18.6(5)	20.5(5)	-2.4(4)	2.7(5)	-0.1(4)
O2	24.2(18)	26.4(16)	39.2(19)	-11.2(14)	-1.0(15)	3.3(14)
O1	15.6(15)	22.4(14)	18.1(14)	-0.6(12)	-1.6(12)	-0.1(12)
O4	28.9(18)	27.7(15)	14.8(15)	-1.8(12)	3.0(13)	-4.3(13)
O5	27.5(18)	24.4(15)	35.1(18)	-3.6(14)	-2.5(15)	5.8(14)
O3	21.2(17)	21.9(15)	33.6(18)	0.9(13)	3.1(14)	-2.0(13)
O6	28.1(18)	23.9(15)	16.2(15)	3.9(12)	1.0(13)	-1.5(13)
O7	28.6(18)	22.3(15)	22.2(16)	-2.5(12)	0.4(14)	0.9(13)
N1	18(2)	30.2(19)	20.2(18)	0.2(15)	5.1(16)	4.6(16)
N2	18(2)	30.8(19)	18.7(18)	0.8(15)	-1.1(15)	-2.9(16)
N3	35(2)	21.8(17)	18.0(18)	1.1(15)	4.1(17)	-8.2(16)
N4	19(2)	28.1(19)	15.8(17)	1.0(15)	-0.5(15)	0.7(15)
C22	26(3)	34(2)	25(2)	9(2)	-1(2)	-6(2)
C23	18(3)	43(3)	33(3)	9(2)	-4(2)	-4(2)
C8	21(2)	40(3)	25(2)	5(2)	5(2)	5(2)
C2	24(3)	29(2)	29(2)	-2(2)	0(2)	2(2)
C14	42(3)	24(2)	34(3)	-3(2)	-7(2)	-5(2)
C3	40(3)	42(3)	24(2)	-7(2)	-1(2)	-6(2)
C20	20(2)	39(2)	16(2)	0.2(19)	1.7(18)	-1(2)
C13	32(3)	22(2)	41(3)	-7(2)	-3(2)	2(2)
C9	24(3)	41(3)	19(2)	-3(2)	5.7(19)	0(2)
C1	24(2)	21(2)	17(2)	3.1(17)	0.6(18)	-1.8(18)
C16	25(3)	47(3)	32(3)	0(2)	4(2)	9(2)
C12	25(3)	19(2)	23(2)	4.3(17)	4.0(19)	0.3(18)
C26	29(3)	33(2)	21(2)	-1.1(19)	0(2)	5(2)
C10	29(3)	39(3)	21(2)	5(2)	5(2)	-10(2)
C15	20(3)	37(3)	32(3)	11(2)	2(2)	-3(2)
C21	17(2)	34(2)	15(2)	1.2(18)	0.2(18)	3.5(19)
C17	30(3)	30(2)	29(3)	-2(2)	4(2)	8(2)
C4	33(3)	49(3)	26(3)	4(2)	-3(2)	-7(2)
C18	24(3)	54(3)	46(3)	12(3)	-3(2)	-8(2)
C11	45(3)	27(2)	20(2)	1.6(19)	3(2)	-14(2)
C24	23(3)	53(3)	21(2)	13(2)	7(2)	10(2)
C6	25(3)	34(2)	24(2)	1(2)	1(2)	0(2)
C5	24(3)	47(3)	30(3)	12(2)	0(2)	-3(2)
C7	35(3)	92(5)	27(3)	-5(3)	-4(2)	-14(3)
C19	25(3)	36(2)	16(2)	7.5(19)	0.3(19)	0(2)
C25	37(3)	36(3)	23(2)	-3(2)	4(2)	12(2)

Atom	U_{11}	U_{22}	U_{33}	U_{23}	U_{13}	U_{12}
C27	28(3)	68(4)	31(3)	8(3)	3(2)	18(3)
Co2	19.5(3)	18.8(3)	16.7(3)	0.4(2)	-0.2(2)	-1.5(2)
S4	25.0(6)	20.3(5)	18.0(5)	1.8(4)	3.1(5)	-0.5(4)
S5	25.9(6)	20.1(5)	15.4(5)	2.9(4)	-1.1(4)	-2.2(4)
S6	19.8(6)	20.7(5)	23.5(5)	-1.2(4)	-0.7(5)	0.8(4)
O11	32.4(19)	20.8(14)	21.4(16)	5.1(12)	-0.7(14)	-4.3(13)
O8	26.1(18)	20.9(14)	20.8(16)	0.4(12)	1.9(13)	-1.4(13)
O9	34(2)	25.5(16)	30.7(18)	6.3(14)	-4.8(15)	1.0(14)
O13	20.1(17)	21.4(14)	33.1(18)	0.7(13)	-0.6(14)	-2.6(12)
O14	22.8(17)	26.9(15)	27.6(17)	-3.1(13)	2.4(14)	3.5(13)
O12	35.5(19)	25.3(15)	16.3(15)	1.1(12)	-1.3(14)	1.4(14)
O10	27.8(19)	32.8(17)	24.2(16)	-7.7(14)	10.1(14)	-5.1(14)
N6	24(2)	24.3(18)	20.1(19)	0.4(15)	3.2(16)	-4.0(15)
N5	26(2)	15.6(16)	22.8(19)	-2.2(14)	5.6(16)	-3.2(15)
N8	18(2)	24.4(18)	24.8(19)	1.1(15)	1.1(16)	2.5(15)
N7	29(2)	25.7(18)	15.8(18)	6.0(15)	1.7(16)	-0.2(16)
C47	22(3)	38(3)	22(2)	-3(2)	3(2)	-1(2)
C43	32(3)	35(3)	26(2)	2(2)	5(2)	-1(2)
C41	48(4)	62(4)	34(3)	23(3)	-17(3)	-15(3)
C51	23(3)	32(2)	26(2)	7(2)	7(2)	7(2)
C28	22(2)	22(2)	22(2)	-1.9(17)	7.2(19)	-0.2(18)
C48	16(2)	23(2)	21(2)	-3.3(17)	3.8(18)	0.5(17)
C42	31(3)	31(2)	41(3)	6(2)	-3(2)	-4(2)
C36	30(3)	29(2)	20(2)	-4.1(19)	4(2)	-3(2)
C29	29(3)	32(2)	27(2)	-1(2)	1(2)	2(2)
C35	28(3)	22(2)	28(2)	-6.7(19)	7(2)	-1.1(19)
C50	26(3)	36(3)	26(2)	-3(2)	-1(2)	-2(2)
C49	27(3)	25(2)	26(2)	-3.5(19)	4(2)	0.9(19)
C38	34(3)	33(2)	15(2)	3.4(18)	3(2)	3(2)
C31	25(3)	55(3)	28(3)	-17(2)	2(2)	5(2)
C53	26(3)	27(2)	24(2)	1.5(19)	4(2)	4.6(19)
C54	30(3)	45(3)	37(3)	15(2)	2(2)	9(2)
C40	34(3)	54(3)	33(3)	20(2)	-5(2)	-19(3)
C30	32(3)	47(3)	22(2)	-2(2)	2(2)	10(2)
C44	24(3)	29(2)	23(2)	2.8(19)	5(2)	3.3(19)
C37	32(3)	33(2)	22(2)	2(2)	5(2)	-5(2)
C32	26(3)	34(3)	56(3)	-14(3)	0(3)	-3(2)
C46	24(3)	30(2)	26(2)	-0.9(19)	7(2)	-1(2)
C39	28(3)	20(2)	20(2)	1.5(17)	-1.8(19)	3.1(18)
C34	35(3)	92(5)	46(3)	-25(3)	-11(3)	0(3)
C33	25(3)	24(2)	37(3)	-1(2)	2(2)	-1.7(19)
C52	24(3)	26(2)	32(3)	5(2)	4(2)	1.6(19)
C45	31(3)	46(3)	63(4)	12(3)	-8(3)	-8(3)
Co3	20.4(3)	24.9(3)	16.4(3)	1.5(2)	-0.3(2)	-0.1(2)
S7	19.8(6)	23.9(5)	19.9(5)	-1.0(4)	1.7(4)	0.5(4)
S8	32.2(7)	24.7(5)	15.2(5)	-0.5(4)	-1.6(5)	3.6(5)
S9	25.2(6)	21.1(5)	19.5(5)	-1.5(4)	-0.1(5)	-1.7(4)
O15	23.5(17)	24.8(15)	25.6(16)	0.3(13)	4.6(14)	-1.5(13)
O16	26.6(18)	33.0(17)	27.3(17)	-5.3(14)	2.3(14)	6.6(14)
O17	53(2)	30.7(17)	21.1(16)	-2.6(14)	-1.8(16)	12.8(16)
O18	35(2)	33.8(17)	14.9(15)	-1.0(13)	-2.4(14)	0.0(14)
O19	29.2(19)	28.7(16)	21.4(16)	3.2(13)	0.1(14)	-5.6(14)
O20	34(2)	25.9(16)	30.0(17)	-6.3(14)	-3.6(15)	-0.8(14)
N9	18(2)	28.9(19)	21.5(19)	-0.5(15)	2.3(16)	-0.9(16)
N11	29(2)	30.2(19)	13.1(17)	-3.9(15)	-0.3(16)	-0.7(17)
N12	26(2)	22.3(18)	23.8(19)	5.2(15)	0.2(17)	-0.8(16)
N10	22(2)	33(2)	22.3(19)	2.8(16)	3.1(16)	-3.0(17)

Atom	U_{11}	U_{22}	U_{33}	U_{23}	U_{13}	U_{12}
C62	21(3)	49(3)	27(3)	11(2)	3(2)	-1(2)
C78	26(3)	33(2)	24(2)	7(2)	8(2)	-4(2)
C77	30(3)	33(2)	24(2)	-6(2)	-2(2)	-5(2)
C76	32(3)	22(2)	32(3)	-4.1(19)	0(2)	2.9(19)
C63	24(3)	52(3)	30(3)	6(2)	5(2)	-9(2)
C64	49(4)	47(3)	19(2)	-1(2)	4(2)	-7(3)
C65	34(3)	31(2)	19(2)	0.9(19)	1(2)	-2(2)
C74	27(3)	27(2)	30(3)	6.2(19)	0(2)	-6(2)
C73	32(3)	36(3)	35(3)	13(2)	3(2)	-4(2)
C55	19(2)	30(2)	17(2)	1.3(18)	2.2(18)	1.6(18)
C56	19(2)	32(2)	27(2)	-1(2)	3(2)	0.9(19)
C57	19(3)	44(3)	30(3)	5(2)	1(2)	5(2)
C58	22(3)	43(3)	21(2)	-2(2)	3(2)	-7(2)
C59	27(3)	32(2)	28(2)	-6(2)	5(2)	-3(2)
C60	20(2)	34(2)	27(2)	2(2)	2(2)	0(2)
C61	25(3)	56(3)	40(3)	-7(3)	-6(2)	-9(2)
C75	24(3)	22(2)	23(2)	0.1(18)	5.5(19)	-0.8(18)
C80	23(3)	20(2)	32(3)	-2.2(19)	6(2)	-3.1(18)
C79	30(3)	25(2)	33(3)	5(2)	5(2)	0(2)
C81	30(3)	59(3)	38(3)	0(3)	-2(2)	7(3)
C66	28(3)	12.8(18)	24(2)	-1.3(17)	-4(2)	-7.2(17)
C67	37(3)	21(2)	24(2)	2.0(18)	1(2)	-1(2)
C68	29(3)	35(3)	40(3)	2(2)	14(2)	-5(2)
C69	34(3)	33(3)	34(3)	5(2)	-9(2)	-8(2)
C70	41(3)	23(2)	22(2)	3.2(18)	-6(2)	-8(2)
C71	38(3)	18(2)	20(2)	-0.4(17)	-1(2)	-1.6(19)
C72	35(3)	68(4)	53(4)	10(3)	-5(3)	-11(3)
Co4	19.4(3)	17.5(3)	17.0(3)	-0.6(2)	0.7(2)	-0.5(2)
S10	19.6(6)	20.5(5)	16.2(5)	0.3(4)	-0.3(4)	-0.8(4)
S11	20.3(6)	19.0(5)	20.3(5)	-0.6(4)	2.5(4)	-1.9(4)
S12	18.4(6)	21.2(5)	20.4(5)	-0.8(4)	1.7(4)	-1.8(4)
O21	19.8(16)	25.4(15)	15.5(14)	-0.7(12)	2.5(12)	-3.1(13)
O22	25.9(18)	23.8(15)	21.0(15)	1.5(12)	1.9(13)	-4.3(13)
O23	25.5(18)	22.0(15)	23.8(16)	1.9(12)	3.4(14)	-2.3(13)
O24	18.5(16)	24.3(15)	26.4(16)	-2.2(13)	3.0(13)	1.3(12)
O25	19.6(17)	27.5(15)	25.2(16)	-3.4(13)	0.6(13)	1.7(13)
O26	28.9(19)	23.2(15)	28.8(17)	3.2(13)	0.6(14)	-5.4(13)
N13	16.5(19)	28.3(18)	13.7(17)	-5.3(14)	1.6(15)	-0.2(15)
N15	22(2)	17.7(17)	23.5(19)	1.6(14)	2.3(16)	0.3(15)
N16	21(2)	23.2(17)	21.8(19)	-2.3(15)	7.1(16)	-2.2(15)
N14	23(2)	17.7(16)	19.4(18)	0.1(14)	0.3(16)	-0.2(15)
C89	29(3)	22(2)	17(2)	-1.8(17)	1.2(19)	3.3(19)
C90	40(3)	53(3)	24(3)	-10(2)	2(2)	4(3)
C91	59(4)	32(3)	39(3)	-1(2)	8(3)	12(3)
C92	31(3)	18(2)	22(2)	-2.8(17)	-1(2)	3.7(18)
C101	21(2)	28(2)	26(2)	-3.0(19)	6.0(19)	1.5(19)
C100	41(3)	50(3)	41(3)	-15(3)	17(3)	-10(3)
C82	21(2)	29(2)	10.4(19)	-1.6(17)	3.3(17)	0.9(18)
C83	25(3)	29(2)	16(2)	-1.4(18)	-0.1(19)	0.5(19)
C84	36(3)	30(2)	22(2)	-1.3(19)	5(2)	-9(2)
C85	24(3)	36(3)	20(2)	-9.7(19)	8(2)	-5(2)
C86	22(3)	40(3)	22(2)	-7(2)	-2(2)	3(2)
C87	25(3)	27(2)	21(2)	0.3(18)	3.1(19)	-2.1(19)
C88	25(3)	51(3)	41(3)	-15(3)	1(2)	-10(2)
C102	26(2)	16.6(19)	21(2)	-4.8(17)	0.7(19)	2.2(18)
C103	26(3)	33(2)	25(2)	-3(2)	6(2)	-3(2)
C104	19(3)	46(3)	37(3)	-12(2)	-4(2)	5(2)

Atom	U_{11}	U_{22}	U_{33}	U_{23}	U_{13}	U_{12}
C105	29(3)	42(3)	29(3)	-10(2)	-5(2)	13(2)
C106	39(3)	32(2)	22(2)	-2(2)	1(2)	9(2)
C107	21(2)	26(2)	27(2)	1.0(19)	3(2)	0.6(19)
C108	45(4)	78(4)	33(3)	-10(3)	-10(3)	22(3)
C93	27(3)	17.3(19)	17(2)	-5.0(16)	1.9(18)	0.4(18)
C94	24(3)	22(2)	26(2)	4.0(18)	4(2)	-1.1(18)
C95	26(3)	23(2)	30(3)	1.3(19)	7(2)	-4.5(19)
C96	23(2)	22(2)	25(2)	-7.3(18)	1.2(19)	5.3(18)
C97	32(3)	20(2)	23(2)	0.2(18)	-2(2)	4.8(19)
C98	31(3)	18(2)	22(2)	-0.7(17)	1(2)	-1.7(18)
C99	26(3)	34(3)	33(3)	-4(2)	0(2)	4(2)
O27	86(4)	67(3)	61(3)	0(2)	14(3)	3(3)
Sr1	19.6(2)	17.79(18)	15.40(19)	0.46(15)	1.16(16)	-0.66(15)
Sr2	19.9(2)	16.80(18)	14.92(19)	-0.37(15)	0.71(16)	0.08(15)

Table S14: Bond Lengths in Å for **CMW-03-086SRTS**.

Atom	Atom	Length/Å
Co1	O1	2.167(3)
Co1	N1	1.996(3)
Co1	N2	2.183(3)
Co1	N3	2.029(3)
Co1	N4	2.018(3)
S3	O6	1.460(3)
S3	O7	1.444(3)
S3	N4	1.573(4)
S3	C21	1.788(4)
S1	O2	1.449(3)
S1	O3	1.450(3)
S1	N1	1.571(4)
S1	C1	1.773(4)
S2	O4	1.448(3)
S2	O5	1.445(3)
S2	N3	1.557(4)
S2	C12	1.764(5)
O1	Sr1	2.560(3)
O5	Sr2	2.442(3)
O3	Sr1	2.448(3)
O6	Sr1	2.664(3)
N1	C8	1.468(5)
N2	C9	1.472(5)
N2	C10	1.480(5)
N2	C19	1.480(5)
N3	C11	1.487(5)
N4	C20	1.484(5)
C22	C23	1.392(6)
C22	C21	1.367(6)
C23	C24	1.374(7)
C8	C9	1.528(6)
C2	C3	1.395(6)
C2	C1	1.387(6)
C14	C13	1.381(6)
C14	C15	1.387(7)
C3	C4	1.383(7)
C20	C19	1.508(6)
C13	C12	1.387(6)

Atom	Atom	Length/Å
C1	C6	1.377(6)
C16	C15	1.385(7)
C16	C17	1.377(7)
C12	C17	1.384(6)
C26	C21	1.398(6)
C26	C25	1.379(6)
C10	C11	1.488(6)
C15	C18	1.501(6)
C4	C5	1.386(7)
C4	C7	1.506(6)
C24	C25	1.389(7)
C24	C27	1.509(6)
C6	C5	1.391(6)
Co2	O8	2.171(3)
Co2	N6	2.178(3)
Co2	N5	2.035(3)
Co2	N8	2.014(4)
Co2	N7	2.008(3)
S4	O9	1.445(3)
S4	O10	1.450(3)
S4	N5	1.564(4)
S4	C28	1.767(4)
S5	O11	1.444(3)
S5	O12	1.452(3)
S5	N7	1.568(4)
S5	C39	1.778(5)
S6	O13	1.444(3)
S6	O14	1.453(3)
S6	N8	1.575(4)
S6	C48	1.784(4)
O8	Sr2	2.555(3)
O14	Sr2	2.618(3)
O12	Sr2	2.456(3)
N6	C36	1.469(5)
N6	C37	1.485(5)
N6	C46	1.469(6)
N5	C35	1.481(5)
N8	C47	1.488(5)
N7	C38	1.476(5)

Atom	Atom	Length/Å
C47	C46	1.503(6)
C43	C42	1.372(6)
C43	C44	1.370(6)
C41	C42	1.387(7)
C41	C40	1.389(7)
C51	C50	1.383(6)
C51	C54	1.506(6)
C51	C52	1.381(6)
C28	C29	1.387(6)
C28	C33	1.398(6)
C48	C49	1.380(6)
C48	C53	1.387(6)
C42	C45	1.516(7)
C36	C35	1.521(6)
C29	C30	1.387(7)
C50	C49	1.397(6)
C38	C37	1.518(6)
C31	C30	1.374(7)
C31	C32	1.390(7)
C31	C34	1.511(7)
C53	C52	1.385(6)
C40	C39	1.384(6)
C44	C39	1.378(6)
C32	C33	1.379(6)
Co3	N9	1.942(4)
Co3	N11	1.954(3)
Co3	N12	1.948(4)
Co3	N10	2.106(4)
S7	O15	1.449(3)
S7	O16	1.443(3)
S7	N9	1.584(4)
S7	C55	1.780(4)
S8	O17	1.439(3)
S8	O18	1.452(3)
S8	N11	1.571(4)
S8	C66	1.766(5)
S9	O19	1.452(3)
S9	O20	1.450(3)
S9	N12	1.558(4)
S9	C75	1.773(5)
O15	Sr2[1]	2.668(3)
O20	Sr1	2.496(3)
N9	C62	1.478(5)
N11	C65	1.468(5)
N12	C74	1.496(5)
N10	C63	1.468(6)
N10	C64	1.496(6)
N10	C73	1.454(6)
C62	C63	1.499(6)
C78	C77	1.385(6)
C78	C79	1.394(6)
C78	C81	1.499(6)
C77	C76	1.373(6)
C76	C75	1.379(6)
C64	C65	1.501(6)
C74	C73	1.524(6)
C55	C56	1.374(6)

Atom	Atom	Length/Å
C55	C60	1.391(6)
C56	C57	1.384(6)
C57	C58	1.384(6)
C58	C59	1.393(6)
C58	C61	1.505(6)
C59	C60	1.386(6)
C75	C80	1.391(6)
C80	C79	1.377(6)
C66	C67	1.388(6)
C66	C71	1.398(6)
C67	C68	1.373(7)
C68	C69	1.399(7)
C69	C70	1.391(7)
C69	C72	1.506(7)
C70	C71	1.389(6)
Co4	N13	1.931(3)
Co4	N15	1.953(3)
Co4	N16	1.948(3)
Co4	N14	2.114(3)
S10	O21	1.464(3)
S10	O22	1.445(3)
S10	N13	1.567(3)
S10	C82	1.771(4)
S11	O23	1.452(3)
S11	O24	1.454(3)
S11	N15	1.555(4)
S11	C93	1.762(5)
S12	O25	1.459(3)
S12	O26	1.442(3)
S12	N16	1.579(3)
S12	C102	1.774(4)
O21	Sr1	2.669(3)
O23	Sr2	2.502(3)
O25	Sr1	2.471(3)
N13	C89	1.480(5)
N15	C92	1.481(5)
N16	C101	1.458(5)
N14	C90	1.461(6)
N14	C91	1.475(6)
N14	C100	1.468(6)
C89	C90	1.519(6)
C91	C92	1.498(7)
C101	C100	1.526(6)
C82	C83	1.389(6)
C82	C87	1.380(6)
C83	C84	1.385(6)
C84	C85	1.394(6)
C85	C86	1.381(6)
C85	C88	1.517(6)
C86	C87	1.395(6)
C102	C103	1.379(6)
C102	C107	1.396(6)
C103	C104	1.380(6)
C104	C105	1.405(7)
C105	C106	1.383(7)
C105	C108	1.498(6)
C106	C107	1.396(6)

Atom	Atom	Length/Å
C93	C94	1.385(6)
C93	C98	1.398(5)
C94	C95	1.382(6)
C95	C96	1.392(6)
C96	C97	1.381(6)
C96	C99	1.507(6)
C97	C98	1.384(6)

-------•

[1]+X,-1+Y,+Z

Table S15: Bond Angles in ° for **CMW-03-086SRTS**.

Atom	Atom	Atom	Angle/°
O1	Co1	N2	168.20(12)
N1	Co1	O1	109.10(12)
N1	Co1	N2	82.39(14)
N1	Co1	N3	111.56(15)
N1	Co1	N4	112.62(14)
N3	Co1	O1	92.39(12)
N3	Co1	N2	80.51(13)
N4	Co1	O1	96.05(12)
N4	Co1	N2	81.45(13)
N4	Co1	N3	129.07(14)
O6	S3	N4	108.86(18)
O6	S3	C21	107.05(19)
O7	S3	O6	115.43(17)
O7	S3	N4	113.58(18)
O7	S3	C21	104.83(19)
N4	S3	C21	106.43(19)
O2	S1	O3	116.61(18)
O2	S1	N1	113.08(19)
O2	S1	C1	105.59(19)
O3	S1	N1	106.81(18)
O3	S1	C1	105.60(19)
N1	S1	C1	108.68(19)
O4	S2	N3	109.38(17)
O4	S2	C12	104.44(19)
O5	S2	O4	114.13(19)
O5	S2	N3	112.99(19)
O5	S2	C12	105.19(19)
N3	S2	C12	110.2(2)
Co1	O1	Sr1	118.58(10)
S2	O5	Sr2	159.8(2)
S1	O3	Sr1	163.43(18)
S3	O6	Sr1	148.08(18)
S1	N1	Co1	129.7(2)
C8	N1	Co1	113.7(3)
C8	N1	S1	116.2(3)
C9	N2	Co1	105.2(3)
C9	N2	C10	112.4(4)
C9	N2	C19	113.1(3)
C10	N2	Co1	108.3(2)
C10	N2	C19	111.7(3)
C19	N2	Co1	105.5(3)
S2	N3	Co1	131.2(2)
C11	N3	Co1	113.4(3)
C11	N3	S2	114.5(3)
S3	N4	Co1	130.4(2)
C20	N4	Co1	114.9(3)
C20	N4	S3	111.7(3)
C21	C22	C23	119.6(4)
C24	C23	C22	121.5(5)
N1	C8	C9	107.3(4)
C1	C2	C3	119.2(4)
C13	C14	C15	121.8(4)
C4	C3	C2	121.4(5)
N4	C20	C19	108.5(3)
C14	C13	C12	119.9(4)
N2	C9	C8	110.5(3)
C2	C1	S1	119.0(3)
C6	C1	S1	120.8(3)
C6	C1	C2	120.2(4)
C17	C16	C15	121.8(4)
C13	C12	S2	119.7(3)
C17	C12	S2	120.9(3)
C17	C12	C13	118.9(4)
C25	C26	C21	119.3(4)
N2	C10	C11	111.2(4)
C14	C15	C18	121.2(5)
C16	C15	C14	117.2(4)
C16	C15	C18	121.7(4)
C22	C21	S3	120.5(3)
C22	C21	C26	120.0(4)
C26	C21	S3	119.5(3)
C16	C17	C12	120.2(4)
C3	C4	C5	118.3(4)
C3	C4	C7	120.3(5)
C5	C4	C7	121.4(5)
N3	C11	C10	107.7(3)
C23	C24	C25	118.1(4)
C23	C24	C27	121.9(5)
C25	C24	C27	120.0(5)
C1	C6	C5	119.8(4)
C4	C5	C6	121.1(5)
N2	C19	C20	110.7(3)
C26	C25	C24	121.4(4)
O8	Co2	N6	169.17(12)
N5	Co2	O8	92.68(12)
N5	Co2	N6	80.94(13)
N8	Co2	O8	94.83(12)
N8	Co2	N6	82.03(14)
N8	Co2	N5	125.64(14)
N7	Co2	O8	109.01(13)
N7	Co2	N6	81.73(14)
N7	Co2	N5	116.16(15)
N7	Co2	N8	111.76(14)

Atom	Atom	Atom	Angle/°
O9	S4	O10	115.48(18)
O9	S4	N5	112.48(19)
O9	S4	C28	104.22(19)
O10	S4	N5	109.78(18)
O10	S4	C28	104.68(19)
N5	S4	C28	109.6(2)
O11	S5	O12	116.33(17)
O11	S5	N7	112.99(18)
O11	S5	C39	105.74(19)
O12	S5	N7	107.30(18)
O12	S5	C39	105.0(2)
N7	S5	C39	109.01(19)
O13	S6	O14	115.29(18)
O13	S6	N8	112.63(19)
O13	S6	C48	104.33(19)
O14	S6	N8	109.49(19)
O14	S6	C48	107.57(19)
N8	S6	C48	106.96(18)
Co2	O8	Sr2	118.40(11)
S6	O14	Sr2	148.21(18)
S5	O12	Sr2	162.13(18)
C36	N6	Co2	107.9(3)
C36	N6	C37	111.8(3)
C37	N6	Co2	106.8(3)
C46	N6	Co2	104.9(3)
C46	N6	C36	111.9(3)
C46	N6	C37	112.9(3)
S4	N5	Co2	131.8(2)
C35	N5	Co2	113.8(3)
C35	N5	S4	113.5(3)
S6	N8	Co2	131.4(2)
C47	N8	Co2	114.2(3)
C47	N8	S6	112.5(3)
S5	N7	Co2	129.6(2)
C38	N7	Co2	113.9(3)
C38	N7	S5	115.9(3)
N8	C47	C46	108.3(4)
C44	C43	C42	122.8(4)
C42	C41	C40	120.6(5)
C50	C51	C54	120.9(4)
C52	C51	C50	118.4(4)
C52	C51	C54	120.6(4)
C29	C28	S4	119.1(3)
C29	C28	C33	120.2(4)
C33	C28	S4	120.5(3)
C49	C48	S6	118.6(3)
C49	C48	C53	120.1(4)
C53	C48	S6	121.3(3)
C43	C42	C41	117.7(5)
C43	C42	C45	121.5(5)
C41	C42	C45	120.8(5)
N6	C36	C35	111.0(3)
C30	C29	C28	119.0(4)
N5	C35	C36	107.1(3)
C51	C50	C49	121.0(4)
C48	C49	C50	119.5(4)
N7	C38	C37	108.0(3)

Atom	Atom	Atom	Angle/°
C30	C31	C32	117.7(5)
C30	C31	C34	121.8(5)
C32	C31	C34	120.5(5)
C52	C53	C48	119.4(4)
C39	C40	C41	120.0(5)
C31	C30	C29	122.1(5)
C43	C44	C39	119.2(4)
N6	C37	C38	110.0(4)
C33	C32	C31	122.2(5)
N6	C46	C47	111.6(4)
C40	C39	S5	119.7(4)
C44	C39	S5	120.5(3)
C44	C39	C40	119.7(4)
C32	C33	C28	118.7(4)
C51	C52	C53	121.5(4)
N9	Co3	N11	113.71(15)
N9	Co3	N12	124.13(15)
N9	Co3	N10	83.14(15)
N11	Co3	N10	84.54(14)
N12	Co3	N11	118.92(15)
N12	Co3	N10	84.39(14)
O15	S7	N9	106.70(18)
O15	S7	C55	108.31(19)
O16	S7	O15	116.30(18)
O16	S7	N9	113.60(19)
O16	S7	C55	105.8(2)
N9	S7	C55	105.52(19)
O17	S8	O18	116.80(18)
O17	S8	N11	113.3(2)
O17	S8	C66	106.9(2)
O18	S8	N11	106.34(18)
O18	S8	C66	106.7(2)
N11	S8	C66	106.26(19)
O19	S9	N12	107.45(18)
O19	S9	C75	105.82(19)
O20	S9	O19	115.83(18)
O20	S9	N12	113.89(19)
O20	S9	C75	104.69(19)
N12	S9	C75	108.6(2)
S7	O15	Sr2[1]	150.26(17)
S9	O20	Sr1	164.3(2)
S7	N9	Co3	125.6(2)
C62	N9	Co3	116.1(3)
C62	N9	S7	115.3(3)
S8	N11	Co3	128.0(2)
C65	N11	Co3	114.0(3)
C65	N11	S8	118.0(3)
S9	N12	Co3	129.2(2)
C74	N12	Co3	113.3(3)
C74	N12	S9	117.2(3)
C63	N10	Co3	106.0(3)
C63	N10	C64	110.9(4)
C64	N10	Co3	105.7(3)
C73	N10	Co3	106.2(3)
C73	N10	C63	114.2(4)
C73	N10	C64	113.1(4)
N9	C62	C63	107.0(4)

Atom	Atom	Atom	Angle/°
C77	C78	C79	117.2(4)
C77	C78	C81	122.4(4)
C79	C78	C81	120.4(4)
C76	C77	C78	121.5(4)
C77	C76	C75	120.6(4)
N10	C63	C62	112.4(4)
N10	C64	C65	111.6(4)
N11	C65	C64	109.2(4)
N12	C74	C73	106.5(3)
N10	C73	C74	111.7(4)
C56	C55	S7	121.2(3)
C56	C55	C60	120.6(4)
C60	C55	S7	118.1(3)
C55	C56	C57	119.6(4)
C56	C57	C58	121.6(4)
C57	C58	C59	117.6(4)
C57	C58	C61	121.9(5)
C59	C58	C61	120.5(4)
C60	C59	C58	121.8(4)
C59	C60	C55	118.7(4)
C76	C75	S9	119.7(3)
C76	C75	C80	119.3(4)
C80	C75	S9	121.0(3)
C79	C80	C75	119.3(4)
C80	C79	C78	122.0(4)
C67	C66	S8	121.1(3)
C67	C66	C71	120.2(4)
C71	C66	S8	118.5(4)
C68	C67	C66	119.5(4)
C67	C68	C69	121.5(5)
C68	C69	C72	121.6(5)
C70	C69	C68	118.5(5)
C70	C69	C72	119.9(5)
C71	C70	C69	120.7(4)
C70	C71	C66	119.5(4)
N13	Co4	N15	122.49(15)
N13	Co4	N16	116.75(15)
N13	Co4	N14	84.30(14)
N15	Co4	N14	84.18(13)
N16	Co4	N15	117.80(15)
N16	Co4	N14	84.33(14)
O21	S10	N13	105.75(17)
O21	S10	C82	108.48(18)
O22	S10	O21	116.18(17)
O22	S10	N13	114.07(18)
O22	S10	C82	106.20(18)
N13	S10	C82	105.57(19)
O23	S11	O24	114.78(17)
O23	S11	N15	113.56(18)
O23	S11	C93	106.30(18)
O24	S11	N15	107.19(18)
O24	S11	C93	105.99(18)
N15	S11	C93	108.63(19)
O25	S12	N16	105.87(18)
O25	S12	C102	105.32(19)
O26	S12	O25	117.47(18)
O26	S12	N16	112.78(18)
O26	S12	C102	106.44(19)
N16	S12	C102	108.45(18)
S10	O21	Sr1	149.47(16)
S11	O23	Sr2	154.12(18)
S12	O25	Sr1	173.32(19)
S10	N13	Co4	124.40(19)
C89	N13	Co4	115.2(3)
C89	N13	S10	118.0(3)
S11	N15	Co4	124.51(19)
C92	N15	Co4	113.7(3)
C92	N15	S11	119.2(3)
S12	N16	Co4	124.6(2)
C101	N16	Co4	115.0(3)
C101	N16	S12	119.9(3)
C90	N14	Co4	105.1(3)
C90	N14	C91	113.1(4)
C90	N14	C100	113.6(4)
C91	N14	Co4	105.9(3)
C100	N14	Co4	105.8(3)
C100	N14	C91	112.4(4)
N13	C89	C90	107.4(3)
N14	C90	C89	112.4(4)
N14	C91	C92	112.0(4)
N15	C92	C91	108.4(3)
N16	C101	C100	108.5(4)
N14	C100	C101	112.5(4)
C83	C82	S10	118.6(3)
C87	C82	S10	121.0(3)
C87	C82	C83	120.3(4)
C84	C83	C82	119.2(4)
C83	C84	C85	121.2(4)
C84	C85	C88	120.3(4)
C86	C85	C84	118.7(4)
C86	C85	C88	120.9(4)
C85	C86	C87	120.6(4)
C82	C87	C86	119.9(4)
C103	C102	S12	120.9(3)
C103	C102	C107	120.3(4)
C107	C102	S12	118.7(3)
C102	C103	C104	120.5(4)
C103	C104	C105	120.4(5)
C104	C105	C108	121.2(5)
C106	C105	C104	118.5(4)
C106	C105	C108	120.3(5)
C105	C106	C107	121.5(4)
C106	C107	C102	118.8(4)
C94	C93	S11	119.1(3)
C94	C93	C98	119.2(4)
C98	C93	S11	121.7(3)
C95	C94	C93	120.5(4)
C94	C95	C96	121.0(4)
C95	C96	C99	120.4(4)
C97	C96	C95	117.8(4)
C97	C96	C99	121.8(4)
C96	C97	C98	122.3(4)
C97	C98	C93	119.1(4)

--------•

[1]+X,-1+Y,+Z

Table S16: Hydrogen Fractional Atomic Coordinates (×10⁴) and Equivalent Isotropic Displacement Parameters (Å²×10³) for **CMW-03-086SRTS**. U_{eq} is defined as 1/3 of the trace of the orthogonalised U_{ij}.

Atom	x	y	z	U_{eq}
H22	1339	537	383	34
H23	724	1384	105	38
H8A	4081	242	1269	34
H8B	4162	1139	1529	34
H2	3586	893	2925	33
H14	4469	4453	3537	41
H3	4106	1275	3626	43
H20A	2437	1620	305	30
H20B	2815	908	383	30
H13	3765	4299	3069	38
H9A	3963	1356	636	33
H9B	3530	763	641	33
H16	4914	2400	2872	41
H26	1926	2448	1202	33
H10A	3761	2952	804	36
H10B	4018	2448	1279	36
H17	4205	2208	2427	35
H18A	5242	4078	3730	62
H18B	5460	3415	3367	62
H18C	5232	3116	3872	62
H11A	3706	3569	1647	37
H11B	3225	3430	1314	37
H6	4536	-599	2395	33
H5	5047	-223	3102	40
H7A	5033	1406	3863	78
H7B	5235	488	3893	78
H7C	4817	724	4214	78
H19A	3205	2091	210	31
H19B	2945	2623	612	31
H25	1318	3289	905	38
H27A	393	2751	-7	64
H27B	659	3527	259	64
H27C	345	2969	590	64
H47A	1120	5845	3762	33
H47B	888	6550	3388	33
H43	4121	6092	3665	37
H41	4077	5014	5058	59
H36A	2320	7427	4630	31
H36B	1843	7905	4589	31
H29	3353	7083	4078	35
H35A	1946	8399	3762	31
H35B	2416	8571	4111	31
H50	128	6407	1412	36
H49	602	5515	1934	31
H38A	2561	6102	4714	33
H38B	2326	5212	4747	33
H53	1266	7494	2594	31
H54A	-49	7780	1077	56
H54B	233	8558	1316	56
H54C	-175	8190	1609	56
H40	3334	4583	4809	49

Atom	x	y	z	U_{eq}
H30	4009	7324	4632	41
H44	3385	5689	3414	30
H37A	1618	5739	4450	35
H37B	1820	6356	4900	35
H32	4027	9687	4164	47
H46A	1341	7561	3787	32
H46B	1158	7037	4250	32
H34A	4406	9030	5129	88
H34B	4723	8992	4662	88
H34C	4622	8169	4974	88
H33	3378	9476	3599	35
H52	773	8368	2095	33
H45A	4871	5486	4399	71
H45B	4716	5886	4920	71
H45C	4708	6428	4401	71
H62A	3953	-3691	1114	39
H62B	4132	-3031	1552	39
H77	1117	-2843	245	35
H76	1719	-3033	872	35
H63A	3661	-2029	1205	42
H63B	3845	-2451	706	42
H64A	3448	-3695	404	46
H64B	3194	-3032	18	46
H65A	2496	-3530	151	34
H65B	2797	-4345	98	34
H74A	2999	-1316	1347	33
H74B	2506	-1186	1035	33
H73A	2651	-2146	409	41
H73B	3098	-1584	481	41
H56	4560	-4497	2606	31
H57	5073	-3748	3160	37
H59	4189	-1853	3136	34
H60	3681	-2575	2554	32
H61A	5165	-2593	3832	62
H61B	4855	-1788	3727	62
H61C	5249	-1983	3363	62
H80	1506	-764	1455	30
H79	897	-587	829	35
H81A	636	-1158	-194	64
H81B	288	-1343	229	64
H81C	464	-2082	-111	64
H67	1552	-4753	1262	33
H68	832	-4558	842	41
H70	1333	-4709	-558	35
H71	2058	-4945	-141	31
H72A	413	-4942	-316	79
H72B	573	-4034	-462	79
H72C	350	-4187	70	79
H89A	2487	1989	4700	27
H89B	2071	1348	4685	27
H90A	1734	2615	4756	47
H90B	2035	3028	4343	47
H91A	1275	3543	4046	52
H91B	1010	3010	3589	52
H92A	1439	3904	3167	28
H92B	1877	3764	3576	28
H10C	780	809	3833	29

Atom	x	y	z	U_{eq}
H10D	712	1637	3492	29
H10E	916	2123	4315	52
H10F	1291	1418	4434	52
H83	3065	2455	3738	28
H84	3721	3160	4055	35
H86	4098	1244	5000	34
H87	3437	533	4688	29
H88A	4655	2570	4526	59
H88B	4504	2571	5105	59
H88C	4359	3318	4718	59
H103	319	-192	2888	33
H104	-195	-79	2152	41
H106	804	803	1340	37
H107	1325	684	2081	30
H10G	-352	152	1240	79
H10H	66	192	891	79
H10I	-136	1025	1111	79
H94	920	2073	2632	28
H95	167	2149	2288	31
H97	456	4149	1455	30
H98	1211	4098	1802	28
H99A	-285	2727	1305	47
H99B	-316	3696	1418	47
H99C	-454	3043	1840	47
H1A	2847	1671	2555	26
H1B	2400	1677	2189	26
H8C	2684	6723	2842	26
H8D	2248(8)	6512(13)	2490(11)	26

4-3

EMORY UNIVERSITY | X-ray Crystallography Center

Submitted by: **Christian Wallen**
Emory University
Solved by: **John Bacsa**
Sample ID: **CMW-03-052**

Crystal Data and Experimental

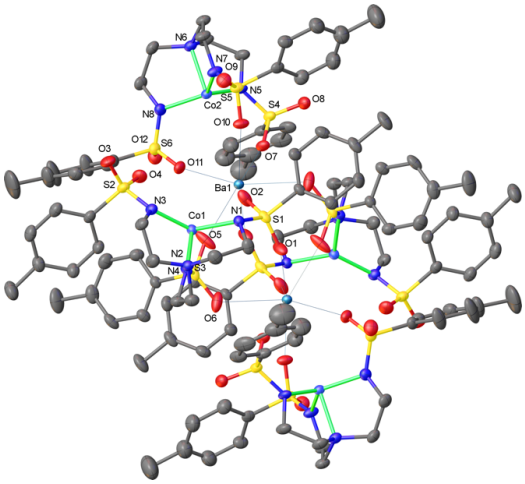

Experimental. Single violet prism-shaped crystals of (**CMW-03-052**) were recrystallised from a mixture of CH_2Cl_2 and diethyl ether by vapor diffusion. A suitable crystal (0.48×0.35×0.27) was selected and mounted on a loop with paratone oil on a Bruker APEX-II CCD diffractometer. The crystal was cooled to T = 100(2) K during data collection. The structure was solved with the **ShelXT** (Sheldrick, 2015) structure solution program using combined Patterson and dual-space recycling methods and by using **Olex2** (Dolomanov et al., 2009) as the graphical interface. The crystal structure was refined with version of **ShelXL** (Sheldrick, 2008) using Least Squares minimisation.

Crystal Data. $C_{112}H_{138}Ba_2Co_4N_{18}O_{24}S_{12}$, M_r = 3015.52, triclinic, P-1 (No. 2), a = 15.199(3) Å, b = 15.322(3) Å, c = 16.472(4) Å, α = 116.330(3)°, β = 93.430(3)°, γ = 102.116(3)°, V = 3309.8(12) Å^3, T = 100(2) K, Z = 1, Z' = 0.5, μ(MoK$_\alpha$) = 1.336, 60531 reflections measured, 20361 unique (R_{int} = 0.0387) which were used in all calculations. The final wR_2 was 0.1429 (all data) and R_1 was 0.0502 (I > 2σ(I)).

Compound	**CMW-03-052**
Formula	$C_{112}H_{138}Ba_2Co_4N_{18}O_{24}S_{12}$
$D_{calc.}$/ g cm^{-3}	1.513
μ/mm^{-1}	1.336
Formula Weight	3015.52
Colour	violet
Shape	prism
Max Size/mm	0.48
Mid Size/mm	0.35
Min Size/mm	0.27
T/K	100(2)
Crystal System	triclinic
Space Group	P-1
a/Å	15.199(3)
b/Å	15.322(3)
c/Å	16.472(4)
α/°	116.330(3)
β/°	93.430(3)
γ/°	102.116(3)
V/Å^3	3309.8(12)
Z	1
Z'	0.5
Θ_{min}/°	1.794
Θ_{max}/°	30.783
Measured Refl.	60531
Independent Refl.	20361
$I > 2\sigma(I)$	16303
R_{int}	0.0387
Parameters	846
Restraints	164
Largest Peak	2.478
Deepest Hole	-0.896
GooF	1.071
wR_2 (all data)	0.1429
wR_2	0.1293
R_1 (all data)	0.0680
R_1	0.0502
CCDC #	1434432

Structure Quality Indicators

Reflections:	d min	0.69	I/σ	15.4	Rint	3.87%	complete	98%
Refinement:	Shift	-0.030	Max Peak	2.5	Min Peak	-0.9	GooF	1.071

A violet prism-shaped crystal with dimensions 0.48×0.35×0.27 mm was mounted on a loop with paratone oil.X-ray diffraction data were collected using a Bruker APEX-II CCD diffractometer equipped with an Oxford Cryosystems low-temperature apparatus operating at T = 100(2) K.

Data were measured using ω scans with MoK$_\alpha$ radiation (fine-focus sealed tube, 45 kV, 35 mA). The total number of runs and images was based on the strategy calculation from the program **APEX2** (Bruker, 2014). The maximum resolution achieved was Θ = 30.783°.

Unit cell indexing was performed by using the **APEX2** (Bruker) software and refined using **SAINT** (Bruker, V8.34A, 2013) on 9976 reflections, 16% of the observed reflections. Data reduction, scaling and absorption corrections were performed using **SAINT** (Bruker, V8.34A, 2013) and **SADABS-2014/2** (Bruker, 2014) was used for absorption correction. wR_2(int) was 0.0844 before and 0.0456 after correction. The ratio of minimum to maximum transmission is 0.8376. The $\lambda/2$ correction factor is Not present. The software corrects for Lorentz polarisation. The final completeness is 99.6% out to 30.783° in Θ. The absorption coefficient (μ) of this material is 1.336 mm^{-1} and the minimum and maximum transmissions are 0.6249 and 0.7461.

The structure was solved in the space group P1 with the **ShelXT** (Sheldrick, 2015) structure solution program using combined Patterson and dual-space recycling methods. The space group P-1 (# 2) was determined by the **ShelXT** (Sheldrick, 2015) structure solution program. The crystal structure was refined by Least Squares using version of **ShelXL** (Sheldrick, 2008). All non-hydrogen atoms were refined anisotropically. Hydrogen atom positions were calculated geometrically and refined using the riding model.

The value of Z' is 0.5. This means that only half of the formula unit is present in the asymmetric unit, with the other half consisting of symmetry equivalent atoms.

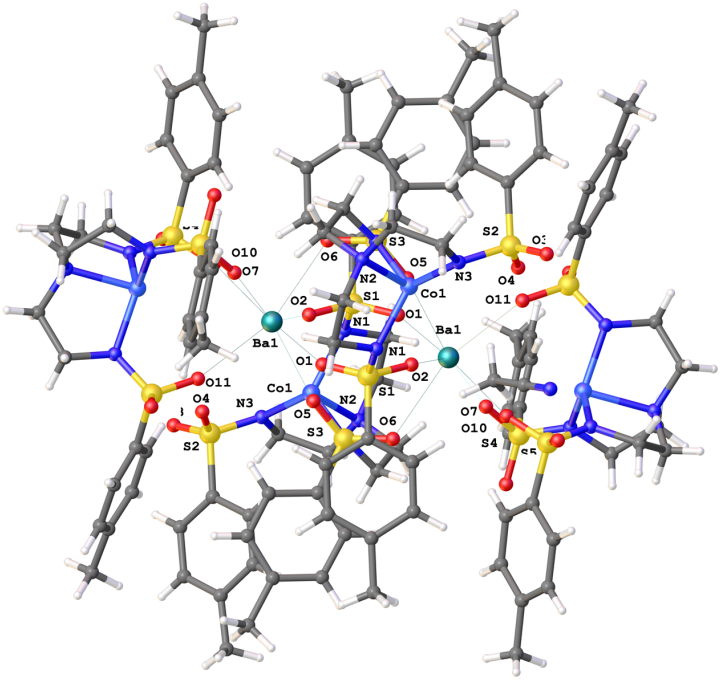

Figure S16:

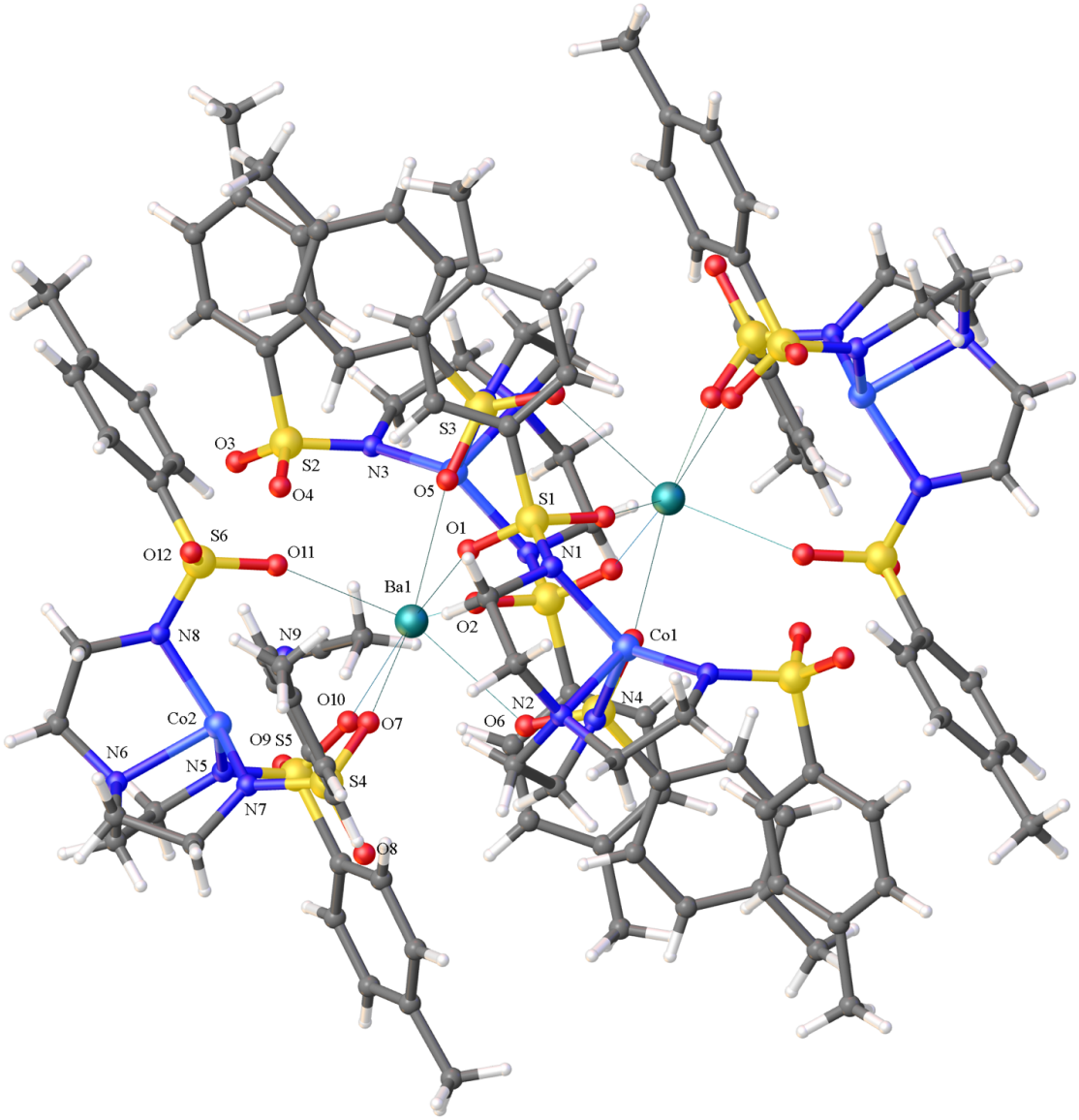
O3
S2
N3
S3
O4
O5
S1
O1
S6
O12
O11
N1
Ba1
O2
N8
N9
Co1
O10
N2
N4
Co2
O7
O6
N6
O9
S5
N5
S4
N7
O8

Figure S17:

Data Plots: Diffraction Data

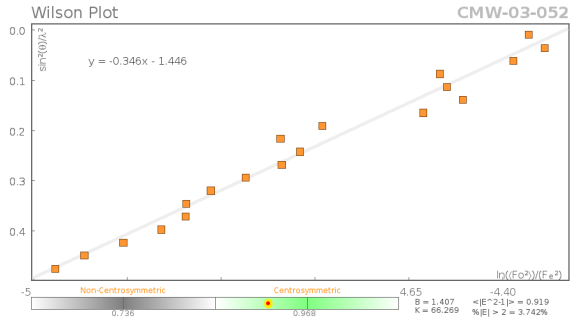

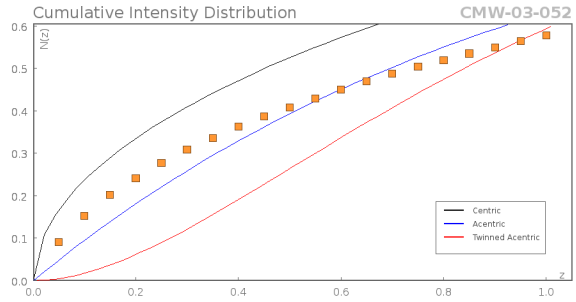

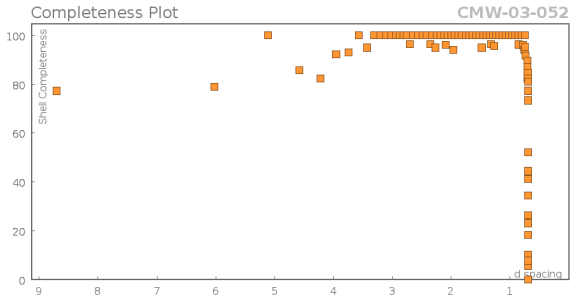

Data Plots: Refinement and Data

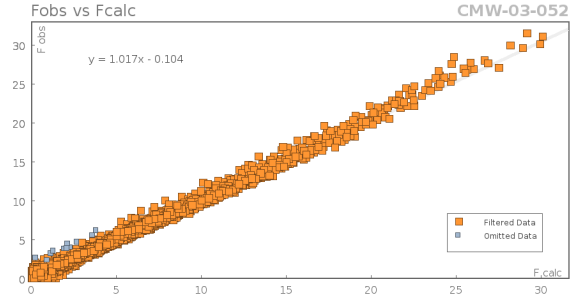

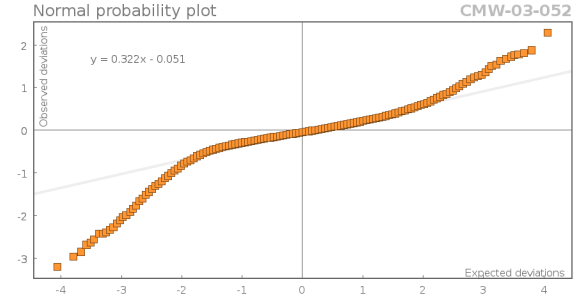

Reflection Statistics

Total reflections (after filtering)	60588	Unique reflections	20361
Completeness	0.984	Mean I/σ	15.43
hklsub>max</sub> collected	(21, 21, 22)	hklsub>min</sub> collected	(-21, -22, -23)
hkl_{max} used	(21, 19, 23)	hkl_{min} used	(-21, -22, 0)
Lim d_{max} collected	100.0	Lim d_{min} collected	0.36
d_{max} used	11.44	d_{min} used	0.69
Friedel pairs	18091	Friedel pairs merged	1
Inconsistent equivalents	0	R_{int}	0.0387
R_{sigma}	0.0452	Intensity transformed	0
Omitted reflections	0	Omitted by user (OMIT hkl)	57
Multiplicity	(20254, 14798, 2918, 496)	Maximum multiplicity	8
Removed systematic absences	0	Filtered off (Shel/OMIT)	0

Images of the Crystal on the Diffractometer

Table S17: Fractional Atomic Coordinates (×10⁴) and Equivalent Isotropic Displacement Parameters (Å²×10³) for **CMW-03-052**. U_{eq} is defined as 1/3 of the trace of the orthogonalised U_{ij}.

Atom	x	y	z	U_{eq}
Ba1	-562.3(2)	1178.1(2)	6383.4(2)	17.06(5)
Co1	2631.4(3)	2175.4(3)	6388.8(3)	17.94(9)
Co2	-1568.7(3)	2952.8(3)	8438.1(3)	17.82(9)
S1	1212.2(5)	1829.1(6)	4931.2(6)	22.28(16)
S2	3279.5(6)	3621.6(7)	8498.1(6)	24.98(17)
S3	1635.9(5)	-22.7(7)	6101.6(6)	23.87(17)
S4	-3168.2(5)	1294.4(6)	6911.5(6)	22.77(16)
S5	-631.8(6)	4139.0(6)	7484.2(6)	23.02(16)
S6	-677.6(6)	1674.4(7)	9019.0(6)	24.28(16)
O1	1085.9(19)	817(2)	4211(2)	37.5(7)
O2	816.4(19)	1957(2)	5753(2)	35.9(6)
O3	3685(2)	4685(2)	9090.5(19)	36.5(6)
O4	2302.8(18)	3246(2)	8419.9(19)	33.6(6)
O5	912.1(18)	471(3)	6323(3)	47.1(9)
O6	1427(2)	-960(2)	5239.6(19)	40.3(7)
O7	-2339.5(16)	1026.8(19)	6581.9(17)	26.6(5)
O8	-3792.0(18)	1393(2)	6283.6(18)	31.0(6)
O9	165.9(19)	4962(2)	7717(2)	32.0(6)
O10	-524.1(19)	3123.7(19)	6964.4(18)	28.8(5)
O11	-451.5(19)	1429(2)	8107.3(17)	29.2(5)
O12	-1332(2)	884(2)	9086(2)	35.9(6)
N1	2241.4(18)	2408(2)	5326.3(19)	20.5(5)
N2	3847.5(18)	2056(2)	5829.9(19)	21.2(5)
N3	3458.5(18)	3265(2)	7479.3(19)	22.0(5)
N4	2502.8(18)	772(2)	6136(2)	20.2(5)
N5	-2835.3(19)	2249(2)	7879(2)	24.0(6)
N6	-2112.2(19)	3903(2)	9507.0(19)	22.8(5)
N7	-1046(2)	4153(2)	8335(2)	26.3(6)
N8	-953(2)	2702(2)	9354(2)	25.7(6)
C1	2891(2)	2224(3)	4667(3)	30.8(8)
C2	3847(3)	2490(3)	5196(3)	32.0(8)
C3	4620(2)	2636(3)	6624(3)	31.9(8)
C4	4409(2)	3552(3)	7359(2)	27.2(7)
C5	3844(2)	2976(3)	8947(2)	24.2(6)
C6	3676(2)	1933(3)	8435(2)	27.4(7)
C7	4109(3)	1408(3)	8750(3)	30.9(8)
C8	4719(3)	1916(3)	9589(3)	33.6(8)
C9	4879(3)	2960(3)	10093(3)	32.2(8)
C10	4448(3)	3493(3)	9777(3)	30.7(8)
C11	5213(4)	1330(4)	9907(4)	50.4(12)
C12	3809(3)	964(3)	5362(3)	29.3(7)
C13	3321(2)	418(3)	5844(3)	26.2(7)
C14	1854(2)	-357(2)	6975(2)	20.7(6)
C15	2307(2)	-1094(3)	6832(3)	26.8(7)
C16	2535(3)	-1281(3)	7567(3)	33.4(8)

Atom	x	y	z	U_{eq}
C17	2301(3)	-752(4)	8420(3)	37.5(9)
C18	1825(3)	-36(3)	8530(3)	36.4(9)
C19	1608(3)	169(3)	7823(3)	29.7(7)
C20	2589(4)	-921(5)	9219(4)	60.2(16)
C21	635(2)	2411(3)	4437(2)	21.4(6)
C22	278(3)	3185(3)	5019(3)	27.8(7)
C23	-249(3)	3596(3)	4647(3)	31.4(8)
C24	-427(2)	3252(3)	3698(3)	31.4(8)
C25	-54(3)	2486(3)	3134(3)	32.3(8)
C26	471(3)	2058(3)	3494(3)	28.8(7)
C27	-1027(3)	3687(4)	3306(4)	43.9(11)
C28	-3768(2)	291(3)	7093(3)	28.4(7)
C29	-4663(2)	-213(3)	6670(3)	34.9(9)
C30	-5106(3)	-1027(4)	6812(4)	47.7(11)
C31	-4661(4)	-1310(4)	7375(4)	50.9(12)
C32	-3773(4)	-783(4)	7799(4)	53.7(12)
C33	-3320(3)	23(3)	7669(3)	40.6(9)
C34	-5129(5)	-2208(5)	7498(6)	77(2)
C35	-3502(2)	2756(3)	8370(3)	30.1(8)
C36	-3078(2)	3357(3)	9388(3)	29.1(7)
C37	-2037(3)	4842(3)	9420(3)	27.9(7)
C38	-1161(3)	5099(3)	9062(3)	28.0(7)
C46	-1545(3)	4084(3)	10358(2)	29.2(7)
C47	-1296(3)	3112(3)	10233(2)	28.9(7)
C48	346(3)	1905(3)	9741(2)	26.7(7)
C49	1167(3)	2421(3)	9646(3)	27.4(7)
C50	1970(3)	2641(4)	10229(3)	39.0(9)
C51	1956(3)	2358(5)	10918(4)	56.3(14)
C52	1141(4)	1820(6)	10997(4)	70(2)
C53	323(3)	1578(5)	10405(4)	51.7(13)
C54	2844(4)	2650(8)	11573(6)	96(3)
C39A	-1523(6)	4263(8)	6832(6)	23.3(14)
C40A	-2277(6)	3465(7)	6274(5)	35.2(16)
C41A	-2926(6)	3630(9)	5765(5)	49(2)
C42A	-2839(7)	4568(10)	5800(7)	54(3)
C43A	-2080(9)	5349(9)	6361(9)	46(2)
C44A	-1428(7)	5211(8)	6873(9)	30.8(18)
C45A	-3557(11)	4742(15)	5235(11)	85(5)
C39B	-1414(4)	4269(5)	6729(5)	23.1(12)
C40B	-2132(5)	3431(5)	6160(5)	34.4(14)
C41B	-2764(5)	3524(7)	5578(5)	49(2)
C42B	-2696(6)	4430(7)	5552(6)	53(2)
C43B	-1973(6)	5253(6)	6127(6)	45(2)
C44B	-1337(5)	5186(5)	6710(6)	29.7(15)
C45B	-3366(9)	4510(11)	4871(10)	84(5)
N9	3155(4)	6612(4)	8121(4)	72.5(15)
C55	2742(3)	5777(4)	7677(3)	45.6(10)
C57	2197(4)	4746(4)	7159(3)	46.1(11)

Table S18: Anisotropic Displacement Parameters (×10^4) **CMW-03-052**. The anisotropic displacement factor exponent takes the form: $-2\pi^2[h^2a^{*2} \times U_{11} + \ldots + 2hka^* \times b^* \times U_{12}]$

Atom	U_{11}	U_{22}	U_{33}	U_{23}	U_{13}	U_{12}
Ba1	18.10(9)	17.12(9)	16.30(9)	7.01(7)	4.07(6)	6.87(6)
Co1	17.02(18)	17.7(2)	19.5(2)	9.20(16)	2.58(15)	4.47(15)
Co2	19.67(19)	16.49(19)	16.80(19)	6.71(16)	4.96(15)	5.74(15)

Atom	U_{11}	U_{22}	U_{33}	U_{23}	U_{13}	U_{12}
S1	18.4(3)	23.6(4)	32.0(4)	19.0(3)	3.6(3)	6.1(3)
S2	27.0(4)	23.2(4)	21.1(4)	5.5(3)	6.1(3)	10.1(3)
S3	17.4(3)	27.6(4)	31.5(4)	20.7(4)	-2.0(3)	1.5(3)
S4	17.5(3)	21.3(4)	22.6(4)	3.5(3)	3.6(3)	7.0(3)
S5	31.3(4)	16.5(3)	22.9(4)	9.4(3)	10.5(3)	7.6(3)
S6	29.8(4)	26.3(4)	20.1(4)	13.1(3)	5.3(3)	8.3(3)
O1	33.6(14)	18.5(12)	49.8(17)	9.6(12)	-11.6(12)	5.7(10)
O2	29.0(13)	55.4(18)	46.4(17)	40.2(15)	14.1(12)	17.3(12)
O3	47.4(16)	22.4(13)	29.2(14)	1.7(11)	4.5(12)	13.2(12)
O4	25.9(12)	42.9(16)	33.2(14)	15.1(12)	11.4(11)	15.8(11)
O5	19.2(12)	59(2)	99(3)	65(2)	17.7(14)	17.0(13)
O6	46.1(16)	39.3(16)	26.0(13)	19.4(12)	-10.2(12)	-12.4(13)
O7	19.7(11)	26.6(12)	26.3(12)	4.8(10)	6.5(9)	8.4(9)
O8	26.6(12)	31.8(14)	27.9(13)	7.8(11)	0(1)	10(1)
O9	33.6(13)	27.7(13)	35.9(14)	18.2(12)	7.8(11)	2.2(11)
O10	42.9(15)	20.4(12)	29.8(13)	12.9(10)	18.5(11)	15.5(11)
O11	41.7(14)	31.4(13)	16.9(11)	11.3(10)	5.8(10)	14.2(11)
O12	38.2(15)	35.6(15)	36.4(15)	21.5(13)	5.2(12)	4.6(12)
N1	21.2(12)	20.6(13)	20.9(13)	10.5(11)	3.2(10)	6(1)
N2	20.2(12)	19.6(13)	22.0(13)	8.0(11)	4(1)	5.4(10)
N3	19.8(12)	20.6(13)	22.4(13)	7.5(11)	3.9(10)	4.5(10)
N4	17.7(11)	19.4(12)	27.1(14)	13.6(11)	3.6(10)	6(1)
N5	20.6(12)	21.0(13)	23.4(13)	2.3(11)	6.4(10)	9.1(10)
N6	23.5(13)	21.2(13)	20.8(13)	7.1(11)	7.4(10)	5.4(10)
N7	38.8(16)	16.8(13)	23.7(14)	8.7(11)	15.1(12)	7.6(11)
N8	30.8(14)	29.6(15)	21.4(13)	13.7(12)	7.5(11)	12.6(12)
C1	23.4(16)	45(2)	30.2(18)	24.4(17)	6.7(13)	6.5(15)
C2	27.1(17)	40(2)	36(2)	21.6(17)	12.3(15)	10.8(15)
C3	23.1(16)	32.6(19)	31.8(19)	8.7(15)	2.9(14)	5.9(14)
C4	22.7(15)	23.5(16)	25.7(16)	5.1(13)	3.0(12)	1.7(12)
C5	24.1(15)	26.4(16)	18.3(14)	7.6(13)	5.9(12)	5.0(12)
C6	27.6(16)	26.3(17)	23.1(16)	9.6(14)	-0.4(13)	3.1(13)
C7	31.8(18)	28.6(18)	30.5(18)	14.7(15)	-0.3(14)	4.0(14)
C8	30.1(18)	39(2)	35(2)	22.3(17)	0.9(15)	5.9(15)
C9	25.3(16)	38(2)	25.8(17)	13.5(16)	-0.8(13)	-1.7(14)
C10	28.4(17)	31.4(19)	23.9(17)	8.4(14)	3.9(13)	2.1(14)
C11	52(3)	49(3)	54(3)	31(2)	-10(2)	10(2)
C12	28.1(17)	27.6(18)	32.6(18)	12.9(15)	10.1(14)	9.3(14)
C13	28.0(16)	21.4(16)	29.0(17)	9.8(13)	10.2(13)	9.5(13)
C14	20.1(13)	22.3(15)	23.3(15)	14.1(12)	3.8(11)	4.7(11)
C15	25.3(15)	30.4(18)	33.7(18)	21.0(15)	10.2(13)	10.2(13)
C16	27.3(17)	41(2)	51(2)	36(2)	9.1(16)	14.3(15)
C17	32.0(19)	51(3)	38(2)	33(2)	5.3(16)	1.7(17)
C18	38(2)	43(2)	28.6(19)	17.4(17)	11.8(16)	7.9(17)
C19	33.7(18)	27.2(18)	30.7(18)	13.5(15)	11.3(14)	11.2(14)
C20	52(3)	95(5)	56(3)	61(3)	4(2)	7(3)
C21	19.7(13)	22.4(15)	27.9(16)	16.7(13)	4.0(12)	5.9(11)
C22	33.7(18)	29.2(18)	27.6(17)	17.3(15)	7.6(14)	12.4(14)
C23	33.8(18)	31.0(19)	40(2)	22.2(17)	12.0(16)	16.0(15)
C24	25.0(16)	36(2)	48(2)	32.6(18)	3.7(15)	6.4(14)
C25	38.0(19)	37(2)	28.0(18)	21.4(16)	2.1(15)	8.2(16)
C26	31.3(17)	30.3(18)	30.5(18)	18.9(15)	7.0(14)	8.8(14)
C27	38(2)	52(3)	62(3)	44(2)	1(2)	13.9(19)
C28	27.1(16)	18.4(15)	31.7(18)	4.6(13)	10.0(13)	5.0(12)
C29	20.6(15)	31.4(19)	45(2)	10.1(17)	11.2(15)	9.1(14)
C30	28.3(19)	37(2)	65(3)	13(2)	22.0(19)	4.1(16)
C31	53(3)	35(2)	64(3)	21(2)	31(2)	10.0(19)

Atom	U_{11}	U_{22}	U_{33}	U_{23}	U_{13}	U_{12}
C32	62(3)	40(2)	62(3)	28(2)	15(2)	8(2)
C33	40(2)	32(2)	45(2)	16.8(18)	3.2(18)	4.2(17)
C34	81(4)	56(4)	98(5)	42(4)	35(4)	4(3)
C35	23.7(16)	25.6(17)	32.5(18)	4.7(14)	8.7(13)	9.0(13)
C36	27.1(16)	25.2(17)	28.2(17)	5.8(14)	13.6(13)	6.4(13)
C37	33.3(18)	21.5(16)	25.8(17)	6.5(13)	10.3(14)	10.0(13)
C38	37.0(18)	16.5(15)	27.1(17)	6.3(13)	13.2(14)	7.0(13)
C46	33.8(18)	29.9(18)	18.6(15)	7.3(13)	6.5(13)	7.1(14)
C47	36.0(18)	32.5(19)	20.6(16)	14.2(14)	10.4(13)	8.4(15)
C48	31.6(17)	35.3(19)	19.8(15)	15.2(14)	7.5(13)	15.6(14)
C49	32.6(17)	24.6(16)	25.5(16)	10.3(14)	8.7(14)	11.1(14)
C50	35(2)	43(2)	38(2)	14.9(19)	6.8(17)	17.3(18)
C51	37(2)	101(5)	47(3)	43(3)	8(2)	32(3)
C52	51(3)	142(6)	67(4)	82(4)	19(3)	43(4)
C53	43(2)	94(4)	49(3)	56(3)	16(2)	24(3)
C54	47(3)	174(9)	89(5)	81(6)	-5(3)	35(4)
C39A	29(2)	24.6(18)	21(2)	12.8(17)	13(2)	8.9(17)
C40A	35(3)	34(2)	33(3)	14(2)	6(2)	4(2)
C41A	45(3)	54(3)	42(4)	20(3)	-2(3)	11(3)
C42A	55(4)	61(3)	51(5)	29(3)	5(4)	19(3)
C43A	55(3)	49(3)	47(5)	28(3)	10(3)	23(2)
C44A	38(3)	29(2)	34(4)	19(2)	15(3)	13.1(18)
C45A	82(7)	91(8)	87(10)	47(8)	-16(7)	26(5)
C39B	30(2)	23.8(17)	21(2)	13.3(16)	12.8(18)	8.2(16)
C40B	36(3)	33(2)	33(3)	15(2)	5(2)	5.6(19)
C41B	45(3)	54(3)	42(4)	19(3)	-2(3)	10(3)
C42B	54(4)	62(3)	49(5)	30(4)	3(4)	21(3)
C43B	55(3)	49(3)	47(5)	30(3)	11(3)	22(2)
C44B	38(2)	28(2)	33(3)	20(2)	15(2)	12.7(18)
C45B	81(7)	93(8)	85(9)	48(8)	-17(7)	29(5)
N9	72(3)	67(3)	68(3)	36(2)	-11(2)	-8(2)
C55	41(2)	60(2)	41(2)	28.9(18)	4.5(17)	12.6(17)
C57	54(2)	43(2)	41(2)	13.5(18)	0.4(19)	28.9(18)

Table S19: Bond Lengths in Å for **CMW-03-052**.

Atom	Atom	Length/Å
Ba1	O1[1]	2.677(3)
Ba1	O2	2.684(3)
Ba1	O5	2.675(3)
Ba1	O6[1]	2.755(3)
Ba1	O7	2.714(2)
Ba1	O10	2.683(3)
Ba1	O11	2.681(3)
Co1	N1	2.015(3)
Co1	N2	2.120(3)
Co1	N3	1.945(3)
Co1	N4	1.963(3)
Co2	N5	1.937(3)
Co2	N6	2.075(3)
Co2	N7	1.929(3)
Co2	N8	1.948(3)
S1	O1	1.437(3)
S1	O2	1.465(3)
S1	N1	1.562(3)
S1	C21	1.764(3)
S2	O3	1.443(3)
S2	O4	1.451(3)
S2	N3	1.579(3)
S2	C5	1.786(4)
S3	O5	1.438(3)
S3	O6	1.458(3)
S3	N4	1.575(3)
S3	C14	1.764(3)
S4	O7	1.466(2)
S4	O8	1.440(3)
S4	N5	1.568(3)
S4	C28	1.772(4)
S5	O9	1.443(3)
S5	O10	1.457(3)
S5	N7	1.564(3)
S5	C39A	1.772(4)
S5	C39B	1.772(4)
S6	O11	1.459(3)
S6	O12	1.447(3)
S6	N8	1.579(3)

Atom	Atom	Length/Å
S6	C48	1.770(4)
O1	Ba1[1]	2.677(3)
O6	Ba1[1]	2.755(3)
N1	C1	1.486(5)
N2	C2	1.467(5)
N2	C3	1.493(5)
N2	C12	1.485(5)
N3	C4	1.471(4)
N4	C13	1.482(4)
N5	C35	1.468(4)
N6	C36	1.482(4)
N6	C37	1.490(5)
N6	C46	1.482(5)
N7	C38	1.468(4)
N8	C47	1.479(5)
C1	C2	1.524(5)
C3	C4	1.506(5)
C5	C6	1.393(5)
C5	C10	1.386(5)
C6	C7	1.379(5)
C7	C8	1.403(5)
C8	C9	1.393(6)
C8	C11	1.516(6)
C9	C10	1.390(6)
C12	C13	1.510(5)
C14	C15	1.383(5)
C14	C19	1.390(5)
C15	C16	1.403(5)
C16	C17	1.389(6)
C17	C18	1.389(7)
C17	C20	1.507(6)
C18	C19	1.372(6)
C21	C22	1.394(5)
C21	C26	1.386(5)
C22	C23	1.382(5)
C23	C24	1.396(6)
C24	C25	1.392(6)
C24	C27	1.505(5)
C25	C26	1.388(5)
C28	C29	1.378(5)
C28	C33	1.386(6)
C29	C30	1.410(6)
C30	C31	1.383(8)
C31	C32	1.375(8)
C31	C34	1.515(7)
C32	C33	1.392(7)
C35	C36	1.525(5)
C37	C38	1.534(5)
C46	C47	1.542(6)
C48	C49	1.388(5)
C48	C53	1.391(5)
C49	C50	1.387(6)
C50	C51	1.384(7)
C51	C52	1.384(8)
C51	C54	1.527(7)
C52	C53	1.405(7)
C39A	C40A	1.393(6)
C39A	C44A	1.400(6)
C40A	C41A	1.391(7)
C41A	C42A	1.390(9)
C42A	C43A	1.388(8)
C42A	C45A	1.532(9)
C43A	C44A	1.373(7)
C39B	C40B	1.393(5)
C39B	C44B	1.400(6)
C40B	C41B	1.390(7)
C41B	C42B	1.390(9)
C42B	C43B	1.389(8)
C42B	C45B	1.532(9)
C43B	C44B	1.373(7)
N9	C55	1.159(7)
C55	C57	1.442(7)

-------•

[1]-X,-Y,1-Z

Table S20: Bond Angles in ° for **CMW-03-052**.

Atom	Atom	Atom	Angle/°
O1[1]	Ba1	O2	119.79(10)
O1[1]	Ba1	O6[1]	91.45(9)
O1[1]	Ba1	O7	82.36(9)
O1[1]	Ba1	O10	164.48(9)
O1[1]	Ba1	O11	88.07(9)
O2	Ba1	O6[1]	77.40(9)
O2	Ba1	O7	145.27(8)
O5	Ba1	O1[1]	70.39(9)
O5	Ba1	O2	64.18(9)
O5	Ba1	O6[1]	117.55(11)
O5	Ba1	O7	149.45(8)
O5	Ba1	O10	125.05(9)
O5	Ba1	O11	85.71(10)
O7	Ba1	O6[1]	75.53(9)
O10	Ba1	O2	72.96(9)
O10	Ba1	O6[1]	82.56(9)
O10	Ba1	O7	82.28(8)
O11	Ba1	O2	123.96(9)
O11	Ba1	O6[1]	155.04(10)
O11	Ba1	O7	79.69(8)
O11	Ba1	O10	91.38(8)
N1	Co1	N2	83.91(11)
N3	Co1	N1	120.23(12)
N3	Co1	N2	83.56(11)
N3	Co1	N4	119.42(12)
N4	Co1	N1	117.25(12)
N4	Co1	N2	84.93(11)
N5	Co2	N6	84.37(11)
N5	Co2	N8	120.72(14)

Atom	Atom	Atom	Angle/°
N7	Co2	N5	117.77(14)
N7	Co2	N6	84.55(12)
N7	Co2	N8	119.28(14)
N8	Co2	N6	86.13(12)
O1	S1	O2	117.56(19)
O1	S1	N1	112.79(16)
O1	S1	C21	105.16(17)
O2	S1	N1	103.41(16)
O2	S1	C21	105.11(16)
N1	S1	C21	112.79(15)
O3	S2	O4	117.41(18)
O3	S2	N3	112.90(17)
O3	S2	C5	105.97(17)
O4	S2	N3	105.63(16)
O4	S2	C5	108.00(17)
N3	S2	C5	106.36(16)
O5	S3	O6	115.9(2)
O5	S3	N4	107.39(16)
O5	S3	C14	106.31(18)
O6	S3	N4	111.80(17)
O6	S3	C14	105.71(17)
N4	S3	C14	109.52(15)
O7	S4	N5	105.95(15)
O7	S4	C28	106.12(17)
O8	S4	O7	115.85(16)
O8	S4	N5	114.80(16)
O8	S4	C28	106.37(18)
N5	S4	C28	107.13(17)
O9	S5	O10	116.50(17)
O9	S5	N7	113.85(17)
O9	S5	C39A	108.9(4)
O9	S5	C39B	104.1(3)
O10	S5	N7	105.64(15)
O10	S5	C39A	107.4(4)
O10	S5	C39B	105.0(3)
N7	S5	C39A	103.6(4)
N7	S5	C39B	111.5(3)
O11	S6	N8	105.56(16)
O11	S6	C48	106.59(16)
O12	S6	O11	115.94(17)
O12	S6	N8	114.62(18)
O12	S6	C48	105.72(18)
N8	S6	C48	107.94(17)
S1	O1	Ba1[1]	149.8(2)
S1	O2	Ba1	144.54(19)
S3	O5	Ba1	168.8(3)
S3	O6	Ba1[1]	123.17(18)
S4	O7	Ba1	161.06(15)
S5	O10	Ba1	163.40(15)
S6	O11	Ba1	160.14(17)
S1	N1	Co1	108.25(15)
C1	N1	Co1	112.1(2)
C1	N1	S1	117.4(2)
C2	N2	Co1	106.5(2)
C2	N2	C3	112.5(3)
C2	N2	C12	113.0(3)
C3	N2	Co1	106.4(2)

Atom	Atom	Atom	Angle/°
C12	N2	Co1	106.5(2)
C12	N2	C3	111.4(3)
S2	N3	Co1	124.99(16)
C4	N3	Co1	115.4(2)
C4	N3	S2	117.0(2)
S3	N4	Co1	128.94(16)
C13	N4	Co1	112.9(2)
C13	N4	S3	117.8(2)
S4	N5	Co2	124.99(16)
C35	N5	Co2	114.8(2)
C35	N5	S4	119.7(2)
C36	N6	Co2	106.6(2)
C36	N6	C37	111.8(3)
C36	N6	C46	113.0(3)
C37	N6	Co2	107.1(2)
C46	N6	Co2	105.1(2)
C46	N6	C37	112.6(3)
S5	N7	Co2	123.66(17)
C38	N7	Co2	115.6(2)
C38	N7	S5	120.3(2)
S6	N8	Co2	118.37(17)
C47	N8	Co2	112.1(2)
C47	N8	S6	118.7(2)
N1	C1	C2	108.6(3)
N2	C2	C1	111.5(3)
N2	C3	C4	111.3(3)
N3	C4	C3	108.5(3)
C6	C5	S2	118.4(3)
C10	C5	S2	121.4(3)
C10	C5	C6	120.2(4)
C7	C6	C5	120.2(3)
C6	C7	C8	120.5(4)
C7	C8	C11	119.6(4)
C9	C8	C7	118.6(4)
C9	C8	C11	121.8(4)
C10	C9	C8	121.2(3)
C5	C10	C9	119.4(4)
N2	C12	C13	111.8(3)
N4	C13	C12	110.5(3)
C15	C14	S3	120.4(3)
C15	C14	C19	120.7(3)
C19	C14	S3	118.8(3)
C14	C15	C16	118.7(4)
C17	C16	C15	121.0(4)
C16	C17	C18	118.6(4)
C16	C17	C20	120.6(5)
C18	C17	C20	120.8(5)
C19	C18	C17	121.3(4)
C18	C19	C14	119.7(4)
C22	C21	S1	117.8(3)
C26	C21	S1	121.4(3)
C26	C21	C22	120.6(3)
C23	C22	C21	119.4(3)
C22	C23	C24	121.1(4)
C23	C24	C27	120.2(4)
C25	C24	C23	118.3(3)
C25	C24	C27	121.5(4)

Atom	Atom	Atom	Angle/°
C26	C25	C24	121.4(4)
C21	C26	C25	119.1(4)
C29	C28	S4	120.7(3)
C29	C28	C33	120.7(4)
C33	C28	S4	118.6(3)
C28	C29	C30	118.8(4)
C31	C30	C29	121.0(4)
C30	C31	C34	120.8(5)
C32	C31	C30	118.8(5)
C32	C31	C34	120.3(6)
C31	C32	C33	121.3(5)
C28	C33	C32	119.3(4)
N5	C35	C36	107.4(3)
N6	C36	C35	110.5(3)
N6	C37	C38	110.7(3)
N7	C38	C37	107.8(3)
N6	C46	C47	110.5(3)
N8	C47	C46	107.1(3)
C49	C48	S6	119.7(3)
C49	C48	C53	120.3(4)
C53	C48	S6	120.0(3)
C50	C49	C48	120.4(4)
C51	C50	C49	120.2(4)
C50	C51	C52	119.4(4)
C50	C51	C54	118.8(5)
C52	C51	C54	121.8(5)
C51	C52	C53	121.2(5)
C48	C53	C52	118.4(5)
C40A	C39A	S5	123.2(6)
C40A	C39A	C44A	120.1(4)
C44A	C39A	S5	116.7(6)
C41A	C40A	C39A	118.9(5)
C42A	C41A	C40A	121.6(5)
C41A	C42A	C45A	121.2(6)
C43A	C42A	C41A	118.3(5)
C43A	C42A	C45A	120.5(6)
C44A	C43A	C42A	121.6(5)
C43A	C44A	C39A	119.6(4)
C40B	C39B	S5	118.0(4)
C40B	C39B	C44B	120.1(4)
C44B	C39B	S5	121.9(4)
C41B	C40B	C39B	118.9(5)
C42B	C41B	C40B	121.6(5)
C41B	C42B	C45B	121.2(6)
C43B	C42B	C41B	118.3(5)
C43B	C42B	C45B	120.5(6)
C44B	C43B	C42B	121.5(5)
C43B	C44B	C39B	119.6(4)
N9	C55	C57	177.0(6)

-------•

[1]-X,-Y,1-Z

Table S21: Hydrogen Fractional Atomic Coordinates (×10⁴) and Equivalent Isotropic Displacement Parameters (Å²×10³) for **CMW-03-052**. U_{eq} is defined as 1/3 of the trace of the orthogonalised U_{ij}.

Atom	x	y	z	U_{eq}
H1A	2881	2637	4361	37
H1B	2717	1521	4203	37
H2A	4252	2240	4764	38
H2B	4078	3219	5541	38
H3A	5167	2847	6411	38
H3B	4739	2204	6882	38
H4A	4821	3801	7933	33
H4B	4488	4084	7180	33
H6	3270	1589	7879	33
H7	3995	711	8403	37
H9	5281	3306	10652	39
H10	4564	4190	10118	37
H11A	4793	941	10113	76
H11B	5705	1792	10404	76
H11C	5453	885	9406	76
H12A	4426	886	5346	35
H12B	3495	661	4732	35
H13A	3139	-303	5432	31
H13B	3732	538	6379	31
H15	2457	-1458	6260	32
H16	2848	-1767	7482	40
H18	1650	311	9093	44
H19	1298	658	7912	36
H20A	2723	-1565	8992	90

Atom	x	y	z	U_{eq}
H20B	2103	-908	9567	90
H20C	3124	-398	9606	90
H22	392	3422	5652	33
H23	-489	4111	5034	38
H25	-159	2256	2501	39
H26	710	1542	3108	35
H27A	-1573	3703	3570	66
H27B	-1186	3276	2651	66
H27C	-705	4361	3446	66
H29	-4970	-19	6299	42
H30	-5707	-1378	6523	57
H32	-3470	-968	8180	64
H33	-2722	377	7967	49
H34A	-5775	-2274	7446	115
H34B	-4891	-2110	8094	115
H34C	-5018	-2811	7032	115
H35A	-4065	2263	8281	36
H35B	-3639	3205	8140	36
H36A	-3421	3836	9708	35
H36B	-3107	2901	9654	35
H37A	-2032	5397	10015	34
H37B	-2564	4750	8999	34
H38A	-1209	5562	8818	34
H38B	-639	5417	9558	34
H46A	-1878	4307	10865	35
H46B	-990	4614	10507	35
H47A	-829	3263	10739	35
H47B	-1829	2626	10218	35
H49	1179	2621	9188	33
H50	2519	2980	10156	47
H52	1135	1614	11450	85
H53	-220	1209	10457	62
H54A	3301	2401	11224	144
H54B	2740	2361	11981	144
H54C	3050	3372	11924	144
H40A	-2346	2832	6243	42
H41A	-3430	3099	5391	58
H43A	-2013	5981	6391	56
H44A	-925	5744	7245	37
H45A	-3951	4103	4788	128
H45B	-3257	5093	4928	128
H45C	-3912	5138	5637	128
H40B	-2187	2819	6169	41
H41B	-3245	2967	5196	59
H43B	-1919	5865	6118	54
H44B	-859	5746	7090	36
H45D	-3322	4057	4253	126
H45E	-3218	5189	4957	126
H45F	-3978	4333	4975	126
H57A	2197	4522	6515	69
H57B	1581	4706	7273	69
H57C	2449	4325	7344	69

4-4(OH$_2$)

EMORY UNIVERSITY | X-ray Crystallography Center

Submitted by: **Christian Wallen**
Emory University
Solved by: **John Bacsa**
Sample ID: **CMW-02-139aq**

Crystal Data and Experimental

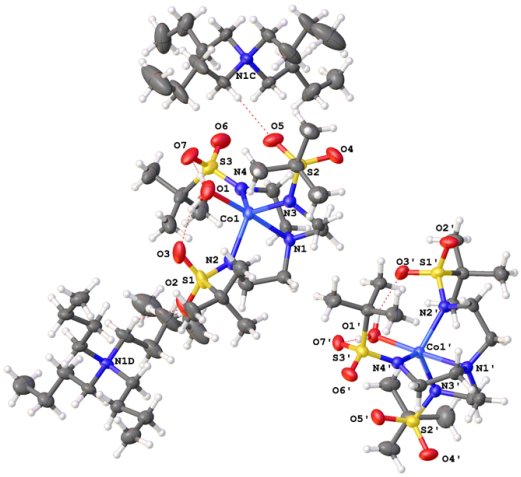

Experimental. Single violet needle-shaped crystals of (**CMW-02-139aq**) were recrystallised from --•by vapor diffusion. A suitable crystal (1.43×0.33×0.32 mm) was selected and mounted on a loop on a Bruker APEX-II CCD diffractometer. The crystal was cooled to T = 100(2) K during data collection. The structure was solved with the **ShelXT** (Sheldrick, 2015) structure solution program using combined Patterson and dual-space recycling methods and by using **Olex2** (Dolomanov et al., 2009) as the graphical interface. The crystal structure was refined with version 2013-4 of **ShelXL** (Sheldrick, 2008) using Least Squares minimisation.

Crystal Data. $C_{68}H_{154}Co_2N_{10}O_{14}S_6$, M_r = 1646.22, monoclinic, $P2_1/c$ (No. 14), a = 16.5036(15) Å, b = 25.928(2) Å, c = 22.811(2) Å, β = 106.650(2)°, $\alpha = \gamma = 90°$, V = 9351.7(14) Å^3, T = 100(2) K, Z = 4, Z' = 1, μ(MoK$_\alpha$) = 0.545, 52521 reflections measured, 21341 unique (R_{int} = 0.0607) which were used in all calculations. The final wR_2 was 0.1613 (all data) and R_1 was 0.0600 (I > 2σ(I)).

Compound	**CMW-02-139aq**
Formula	$C_{68}H_{154}Co_2N_{10}O_{14}S_6$
$D_{calc.}$/ g cm^{-3}	1.169
μ/mm^{-1}	0.545
Formula Weight	1645.22
Colour	violet
Shape	needle
Max Size/mm	1.43
Mid Size/mm	0.33
Min Size/mm	0.32
T/K	100(2)
Crystal System	monoclinic
Space Group	$P2_1/c$
a/Å	16.5036(15)
b/Å	25.928(2)
c/Å	22.811(2)
α/°	90
β/°	106.650(2)
γ/°	90
V/Å^3	9351.7(14)
Z	4
Z'	1
Θ_{min}/°	1.826
Θ_{max}/°	27.484
Measured Refl.	52521
Independent Refl.	21341
$I > 2\sigma(I)$	12581
R_{int}	0.0607
Parameters	952
Restraints	140
Largest Peak	1.171
Deepest Hole	-0.669
GooF	1.027
wR_2 (all data)	0.1613
wR_2	0.1361
R_1 (all data)	0.1153
R_1	0.0600
CCDC #	1344433

Structure Quality Indicators

Reflections:	d min 0.77	I/σ 7.8	Rint 6.07%	complete 100%
Refinement:	Shift 0.002	Max Peak 1.2	Min Peak -0.7	GooF 1.027

A violet needle-shaped crystal with dimensions 1.43×0.33×0.32 mm was mounted on a loop with paratone oil. X-ray diffraction data were collected using a Bruker APEX-II CCD diffractometer equipped with an Oxford Cryosystems low-temperature apparatus operating at T = 100(2) K.

Data were measured using ϕ and ω scans using MoK$_\alpha$ radiation (fine-focus sealed tube, 45 kV, 35 mA). The total number of runs and images was based on the strategy calculation from the program **APEX2** (Bruker, 2013). The maximum resolution achieved was Θ = 27.484.

Unit cell indexing was performed by using the **APEX2** (Bruker, 2013) software and refined using **SAINT** (Bruker, V8.34A, 2013) on 6548 reflections, 12% of the observed reflections. Data reduction, scaling and absorption corrections were performed using **SAINT** (Bruker, V8.34A, 2013) and **SADABS-2012/1** (Bruker, 2012) was used for absorption correction.wR_2(int) was 0.0753 before and 0.0483 after correction.The Ratio of minimum to maximum transmission is 0.8728.The $\lambda/2$ correction factor is 0.0015. The software corrects for Lorentz polarisation. The final completeness is 99.7% out to 27.484° in Θ. The absorption coefficient (μ) of this material is 0.545 mm-1 and the minimum and maximum transmissions are 0.6509 and 0.7458.

The structure was solved in the space group P1 with the **ShelXT** (Sheldrick, 2015) structure solution program using combined Patterson and dual-space recycling methods. The space group P2$_1$/c (# 14) was determined by the**ShelXT** (Sheldrick, 2015) structure solution program.The crystal structure was refined by Least Squares using version 2013-4 of **ShelXL** (Sheldrick, 2008). All non-hydrogen atoms were refined anisotropically. Hydrogen atom positions were calculated geometrically and refined using the riding model. There are two independent molecules in the asymmetric unit.

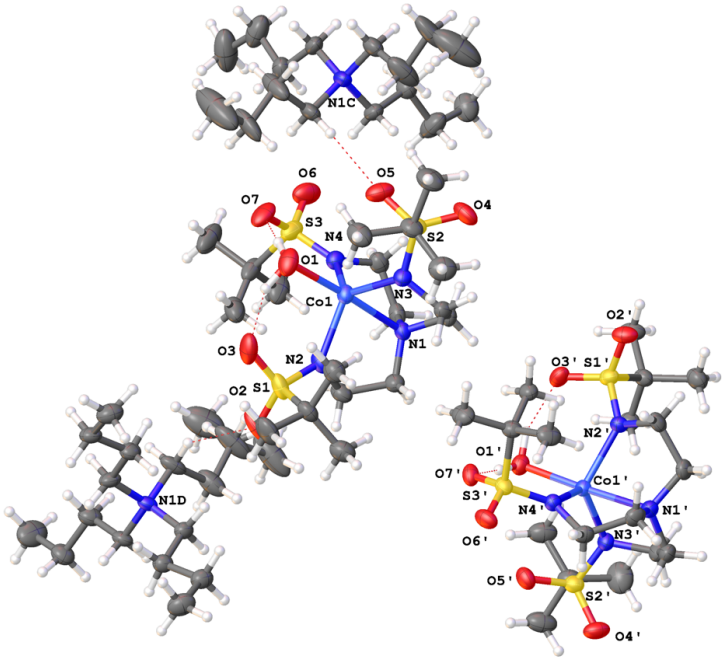

Figure S38:

Data Plots: Diffraction Data

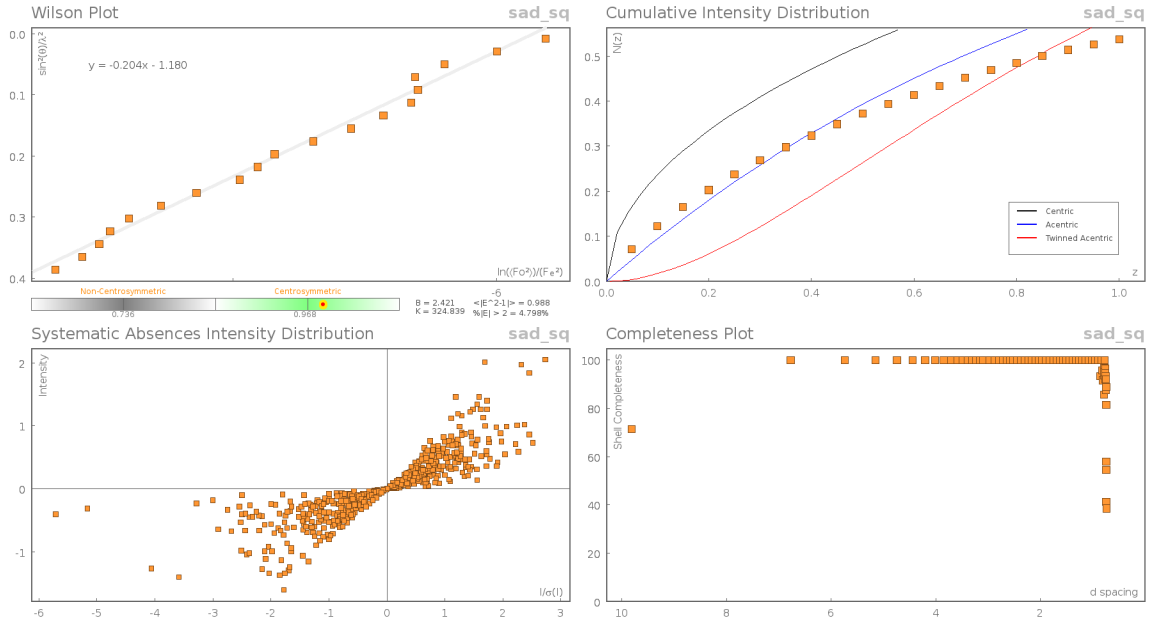

Data Plots: Refinement and Data

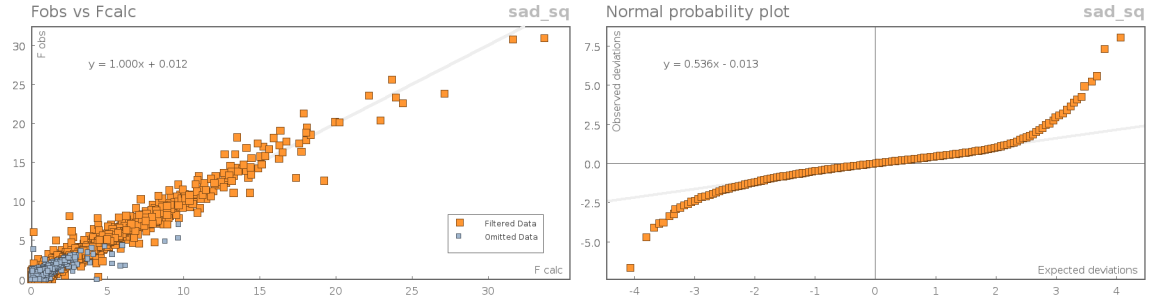

Reflection Statistics

Total reflections (after filtering)	53423	Unique reflections	21341
Completeness	0.995	Mean I/σ	7.76
hklsub>max</sub> collected	(22, 34, 30)	hklsub>min</sub> collected	(-22, -28, -15)
hkl_{max} used	(20, 33, 29)	hkl_{min} used	(-21, 0, 0)
Lim d_{max} collected	20.0	Lim d_{min} collected	0.77
d_{max} used	11.15	d_{min} used	0.77
Friedel pairs	6036	Friedel pairs merged	1
Inconsistent equivalents	0	R_{int}	0.0607
R_{sigma}	0.09	Intensity transformed	0
Omitted reflections	0	Omitted by user (OMIT hkl)	158
Multiplicity	(41686, 8320)	Maximum multiplicity	6
Removed systematic absences	744	Filtered off (Shel/OMIT)	4903

Images of the Crystal on the Diffractometer

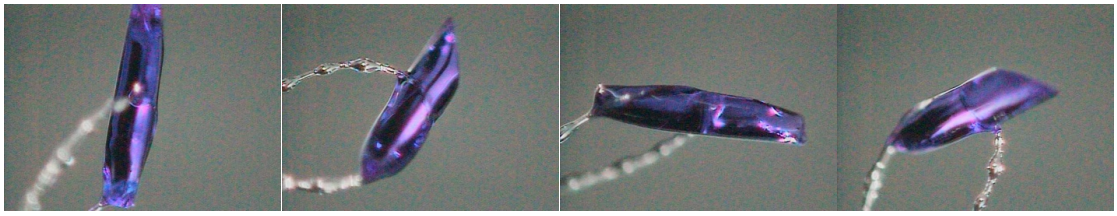

Table S87: Fractional Atomic Coordinates (×10⁴) and Equivalent Isotropic Displacement Parameters (Å²×10³) for **sad_sq**. U_{eq} is defined as 1/3 of the trace of the orthogonalised U_{ij}.

Atom	x	y	z	U_{eq}
C1	5661(2)	5141.0(13)	3051.1(17)	34.4(8)
C2	4900(2)	5472.9(14)	3030.7(17)	39.1(9)
C3	5952(2)	4246.2(13)	2849.7(15)	31.2(8)
C4	5517(2)	4196.8(14)	2167.5(16)	33.2(8)
C5	5532(2)	4466.5(14)	3766.2(15)	33.9(8)
C6	4905(2)	4042.8(14)	3796.9(17)	37.5(9)
C7	3826(2)	5774.2(14)	1454.8(17)	39.6(9)
C8	3164(3)	6138.9(17)	1046(2)	59.2(12)
C9	4707(3)	6015.8(15)	1614.3(19)	49.1(10)
C10	3818(2)	5257.1(14)	1137.5(17)	42.4(9)
C11	3960(2)	3502.1(14)	1007.6(16)	37.8(9)
C12	4606(3)	3763.0(16)	745.1(18)	52.4(11)
C13	3813(3)	2941.5(15)	779(2)	56.8(12)
C14	3129(3)	3797.8(16)	835.0(18)	49.7(10)
C15	3118(2)	4681.6(16)	4110.9(19)	47.8(11)
C16	2356(3)	4566(2)	4347(3)	77.5(17)
C17	2952(3)	5139.2(16)	3677(2)	58.4(12)
C18	3907(3)	4765.5(18)	4651.8(19)	58.4(12)
N1	5454.9(16)	4597.7(10)	3126.2(12)	28.1(6)
N2	4155.2(18)	5261.8(11)	2567.0(13)	35.3(7)
N3	4627.6(17)	4050.1(11)	2079.4(12)	30.5(6)
N4	4057.7(18)	4203.4(11)	3430.0(13)	34.2(7)
O1	2779.9(16)	4405.6(12)	2126.3(13)	50.7(7)
O2	3572(2)	6166.3(11)	2438.0(13)	65.9(9)
O3	2689.4(17)	5429.4(12)	1947.5(13)	56.7(8)
O4	5106.5(17)	3143.4(10)	1962.5(12)	50.9(7)
O5	3674.9(17)	3312.3(10)	2059.3(12)	51.3(7)
O6	3447.9(19)	3689.4(11)	4126.8(13)	58.4(8)
O7	2519.8(16)	4069.7(11)	3186.3(13)	54.0(8)
S1	3526.9(6)	5664.1(4)	2150.4(4)	43.3(3)
S2	4371.8(6)	3482.0(3)	1838.8(4)	35.1(2)
S3	3289.4(6)	4108.4(4)	3693.3(5)	42.7(2)
Co1	4090.9(3)	4478.1(2)	2604.0(2)	30.88(13)
C1'	281(2)	4694.3(13)	2010.8(18)	36.3(8)
C2'	-440(2)	4345.8(13)	2039.8(16)	33.9(8)
C3'	695(2)	5596.1(14)	2203.9(17)	36.9(9)
C4'	823(2)	5636.2(15)	2885.1(17)	37.6(9)
C5'	-455(2)	5361.9(14)	1293.1(16)	35.9(8)
C6'	-1138(2)	5759.8(13)	1261.6(16)	33.9(8)
C7'	-289(2)	3999.7(13)	3601.2(15)	31.7(8)
C8'	-628(2)	3605.6(14)	3972.4(17)	42.4(9)
C9'	469(2)	3773.4(14)	3428.7(18)	42.4(9)
C10'	-50(2)	4501.5(13)	3961.0(16)	35.4(8)
C11'	160(2)	6314.8(14)	4056.0(16)	37.5(9)
C12'	1045(3)	6085.0(19)	4313.1(19)	62.9(13)

Atom	x	y	z	U_{eq}
C13'	123(3)	6869.2(15)	4276.4(19)	55.0(12)
C14'	-502(3)	5981.9(15)	4226.0(18)	49.5(11)
C15'	-3096(2)	5038.6(13)	1003.1(14)	29.5(8)
C16'	-4053(2)	5111.1(15)	748.5(17)	41.8(9)
C17'	-2894(2)	4607.1(13)	1476.4(16)	33.2(8)
C18'	-2705(3)	4927.0(14)	489.6(16)	41.4(9)
N1'	-6.5(17)	5235.1(10)	1938.3(13)	31.1(7)
N2'	-814.5(17)	4547.2(10)	2514.7(12)	28.3(6)
N3'	3.0(16)	5768.7(10)	2989.9(13)	30.7(6)
N4'	-1671.2(16)	5591.2(10)	1645.1(12)	27.4(6)
O1'	-1872.0(15)	5388.1(10)	2951.1(11)	33.5(6)
O2'	-1318.8(16)	3641.4(9)	2585.9(11)	40.8(6)
O3'	-1810.2(14)	4354.1(9)	3111.0(11)	38.5(6)
O4'	520.2(17)	6684.2(10)	3096.1(12)	46.0(7)
O5'	-973.6(15)	6482.9(9)	3006.5(11)	39.9(6)
O6'	-2908.6(15)	6033.9(9)	907.4(11)	39.7(6)
O7'	-3030.5(14)	5688.0(9)	1884.4(10)	34.4(6)
S1'	-1132.0(5)	4133.1(3)	2902.2(4)	30.5(2)
S2'	-91.8(5)	6331.0(3)	3225.0(4)	32.2(2)
S3'	-2662.0(5)	5640.5(3)	1377.0(4)	29.11(19)
Co1'	-947.9(3)	5330.9(2)	2469.4(2)	25.66(11)
C1D	2639(2)	7880.9(12)	3283.2(15)	31.4(8)
C2D	2200(3)	7814.5(14)	3771.4(17)	42.0(9)
C3D	2188(3)	8314.4(14)	4116.3(17)	43.3(9)
C4D	1797(3)	8257.0(19)	4640(2)	69.8(14)
C5D	3173(2)	7513.4(13)	2461.9(16)	32.5(8)
C6D	2866(2)	7920.6(13)	1968.0(16)	34.1(8)
C7D	3375(2)	7891.3(15)	1505.3(16)	39.7(9)
C8D	2993(3)	8224.6(16)	941.9(18)	51.3(11)
C9D	1688(2)	7341.9(13)	2475.2(16)	34.6(8)
C10D	1572(2)	6961.0(14)	1948.5(17)	37.5(9)
C11D	669(2)	6970.5(14)	1530.0(16)	37.3(9)
C12D	564(3)	6662.3(16)	951.3(18)	49(1)
C13D	2896(3)	6933.5(13)	3240.8(17)	42.3(9)
C14D	3794(3)	6946.3(16)	3659.7(18)	57.2(12)
C15D	3997(4)	6460.4(18)	4033(2)	82.8(17)
C16D	3642(8)	6402(4)	4569(4)	98(4)
C16E	4881(5)	6424(4)	4469(4)	104(4)
N1D	2600.0(18)	7416.3(10)	2866.2(12)	29.5(6)
C1C	2825(2)	1923.3(14)	2668.9(18)	44.3(9)
C2C	3243(4)	2026.1(18)	2172(2)	80.0(17)
C3C	3229(4)	1509.7(18)	1811(3)	87.7(18)
C4C	3530(6)	1540(2)	1293(3)	138(3)
C5C	3617(2)	2575.9(14)	3431.1(18)	37.9(9)
C6C	4162(2)	2207.8(15)	3894.3(18)	43.0(9)
C7C	4977(3)	2457.3(19)	4236(2)	63.2(13)
C8C	5577(3)	2145.6(17)	4718.7(19)	57.4(12)
C9C	2257(2)	2187.4(15)	3486(2)	45.2(10)
C10C	2134(3)	2569.1(16)	3957(2)	56.7(11)
C11C	1663(3)	2315(2)	4365(2)	71.9(14)
C12C	1523(4)	2651(2)	4855(3)	99(2)
C13C	2315(2)	2839.6(14)	2692.5(19)	42.6(9)
C14C	1430(3)	2740.9(17)	2273(2)	76.6(16)
C15C	1109(3)	3228.1(18)	1894(2)	78.9(16)
C16C	313(5)	3197(3)	1432(3)	156(4)
N1C	2752.2(18)	2381.7(11)	3074.1(14)	36.7(7)

Table S18: Anisotropic Displacement Parameters (×10⁴) **sad_sq**. The anisotropic displacement factor exponent takes the form: $-2\pi^2[h^2a^{*2} \times U_{11} + \ldots + 2hka^* \times b^* \times U_{12}]$

Atom	U_{11}	U_{22}	U_{33}	U_{23}	U_{13}	U_{12}
C1	30.5(18)	30(2)	41(2)	-3.5(16)	7.5(16)	-2.8(16)
C2	43(2)	28(2)	44(2)	-3.8(16)	8.0(18)	1.9(17)
C3	23.3(17)	32(2)	40(2)	0.5(16)	10.5(15)	3.8(15)
C4	33.5(19)	28(2)	43(2)	1.1(16)	18.2(17)	1.1(15)
C5	29.0(18)	37(2)	33.2(19)	-3.2(16)	4.3(15)	10.0(16)
C6	41(2)	36(2)	38(2)	4.2(16)	14.5(17)	6.3(17)
C7	48(2)	27(2)	44(2)	3.5(17)	13.3(18)	10.3(17)
C8	72(3)	46(3)	60(3)	18(2)	19(2)	28(2)
C9	60(3)	36(2)	49(2)	1.4(19)	13(2)	1(2)
C10	44(2)	42(2)	39(2)	1.4(17)	8.2(18)	5.2(18)
C11	45(2)	30(2)	36(2)	-7.0(16)	7.2(17)	-1.6(17)
C12	67(3)	52(3)	39(2)	-8(2)	18(2)	-8(2)
C13	70(3)	38(2)	58(3)	-16(2)	13(2)	-3(2)
C14	53(3)	44(2)	43(2)	-6.5(19)	0(2)	3(2)
C15	33(2)	55(3)	62(3)	-31(2)	24(2)	-14.4(19)
C16	54(3)	94(4)	101(4)	-52(3)	48(3)	-25(3)
C17	40(2)	48(3)	82(3)	-23(2)	10(2)	5(2)
C18	48(3)	72(3)	56(3)	-31(2)	16(2)	-1(2)
N1	26.3(14)	27.3(16)	30.7(15)	-1.5(12)	8.1(12)	4.1(12)
N2	34.8(17)	29.9(17)	38.7(17)	0.4(13)	6.7(14)	10.8(13)
N3	28.8(15)	28.2(16)	34.4(15)	-4.0(13)	9.0(13)	-1.5(12)
N4	32.8(16)	30.9(17)	41.3(17)	-2.8(13)	14.6(14)	-0.7(13)
O1	30.4(14)	69(2)	50.0(17)	-16.8(16)	6.7(13)	-0.6(14)
O2	98(3)	48.3(19)	51.1(18)	-1.9(14)	21.8(17)	42.1(18)
O3	39.2(16)	76(2)	57.1(18)	20.7(15)	18.1(14)	25.6(15)
O4	56.9(18)	28.6(15)	60.3(18)	0.9(13)	5.9(15)	12.7(13)
O5	59.3(18)	46.4(17)	51.8(17)	-5.4(13)	21.6(15)	-22.2(14)
O6	76(2)	49.6(18)	65.5(19)	-10.1(15)	45.3(17)	-15.8(16)
O7	37.7(15)	66(2)	62.2(18)	-31.1(15)	19.9(14)	-24.6(14)
S1	46.0(6)	41.9(6)	43.3(5)	4.2(4)	14.6(5)	22.3(5)
S2	39.6(5)	26.3(5)	38.6(5)	-0.1(4)	9.7(4)	-1.9(4)
S3	41.2(5)	41.3(6)	52.4(6)	-15.5(5)	24.3(5)	-13.5(5)
Co1	24.9(2)	31.4(3)	35.7(3)	-4.6(2)	7.5(2)	1.4(2)
C1'	32.6(19)	34(2)	48(2)	-1.6(17)	21.6(17)	5.1(16)
C2'	38(2)	26.2(19)	40(2)	-2.5(16)	15.9(17)	8.0(16)
C3'	28.3(18)	33(2)	53(2)	1.6(17)	18.7(17)	-0.2(16)
C4'	24.2(18)	35(2)	52(2)	-4.7(17)	9.3(17)	-0.8(16)
C5'	37(2)	37(2)	39(2)	2.5(17)	20.0(17)	-4.3(17)
C6'	36(2)	30(2)	37(2)	5.5(15)	12.9(16)	-3.0(16)
C7'	30.8(18)	24.6(19)	36.2(19)	1.1(15)	4.1(15)	0.7(15)
C8'	53(2)	32(2)	39(2)	9.1(17)	7.5(18)	-8.1(18)
C9'	40(2)	34(2)	50(2)	2.1(18)	7.1(18)	6.2(17)
C10'	35(2)	32(2)	38(2)	-0.1(16)	8.4(16)	-2.9(16)
C11'	43(2)	33(2)	33.6(19)	-2.0(16)	7.0(17)	-6.7(17)
C12'	55(3)	81(4)	42(2)	-8(2)	-4(2)	7(2)
C13'	85(3)	38(2)	45(2)	-7.2(19)	24(2)	-13(2)
C14'	67(3)	42(2)	40(2)	-1.5(18)	17(2)	-14(2)
C15'	33.6(18)	26.5(19)	26.6(17)	-2.6(14)	5.8(15)	-3.5(15)
C16'	35(2)	38(2)	44(2)	-4.0(18)	-1.2(17)	-3.9(17)
C17'	28.6(18)	28(2)	41(2)	-2.2(16)	6.7(16)	-2.6(15)
C18'	57(2)	36(2)	34(2)	-10.4(17)	17.8(19)	-4.8(19)
N1'	27.9(15)	27.7(17)	40.1(16)	1.5(13)	13.6(13)	-1.0(12)
N2'	29.7(15)	22.4(15)	34.4(15)	1.3(12)	12.0(13)	-0.7(12)
N3'	23.8(14)	27.8(16)	40.4(16)	-2.1(13)	9.0(13)	0.1(12)

Atom	U_{11}	U_{22}	U_{33}	U_{23}	U_{13}	U_{12}
N4'	26.7(14)	25.2(15)	31.9(15)	1.3(12)	10.7(12)	0.5(12)
O1'	29.0(13)	38.6(16)	35.1(14)	-3.7(12)	12.5(11)	-0.2(11)
O2'	47.4(15)	29.6(14)	40.8(14)	-0.1(11)	5.3(12)	-11.5(12)
O3'	30.3(13)	41.5(15)	46.5(15)	13.8(12)	15.4(12)	-0.4(11)
O4'	55.0(17)	34.7(15)	52.8(16)	-2.1(12)	22.5(14)	-16.3(13)
O5'	37.0(14)	34.0(15)	45.4(15)	0.7(12)	6.6(12)	9.9(11)
O6'	41.4(15)	26.5(14)	43.6(15)	4.3(11)	0.3(12)	4.3(11)
O7'	26.8(12)	37.8(14)	37.7(13)	-10.8(11)	7.9(11)	4.3(11)
S1'	27.9(4)	27.1(5)	34.7(5)	3.7(4)	5.8(4)	-3.6(4)
S2'	33.2(5)	26.6(5)	35.9(5)	0.7(4)	8.5(4)	-1.9(4)
S3'	27.8(4)	24.7(5)	32.2(4)	-3.7(4)	4.3(4)	1.4(4)
Co1'	22.7(2)	23.9(2)	30.9(2)	-0.63(19)	8.43(19)	-0.04(18)
C1D	39(2)	17.6(18)	36.7(19)	-1.2(14)	9.3(16)	-1.7(15)
C2D	55(2)	29(2)	45(2)	-5.4(17)	18.8(19)	-4.9(18)
C3D	53(2)	33(2)	45(2)	-8.5(17)	15.1(19)	0.1(19)
C4D	88(4)	65(3)	68(3)	-31(3)	42(3)	-18(3)
C5D	33.7(19)	26.9(19)	40(2)	-0.2(15)	16.1(16)	-3.0(15)
C6D	38(2)	29(2)	37.0(19)	-1.1(15)	13.9(16)	-2.9(16)
C7D	44(2)	37(2)	42(2)	-4.4(17)	18.0(18)	-7.2(18)
C8D	57(3)	56(3)	42(2)	1(2)	17(2)	-15(2)
C9D	39(2)	27(2)	41(2)	-6.5(16)	16.8(17)	-12.1(16)
C10D	42(2)	27(2)	46(2)	-9.0(16)	17.5(18)	-6.3(17)
C11D	42(2)	26(2)	45(2)	-3.1(16)	15.3(18)	-9.4(16)
C12D	54(3)	46(3)	49(2)	-6(2)	18(2)	-16(2)
C13D	73(3)	19.4(18)	39(2)	2.9(15)	22.6(18)	5.0(17)
C14D	87(3)	38(2)	40(2)	-0.5(17)	7(2)	19(2)
C15D	156(5)	45(3)	45(2)	11(2)	25(3)	44(3)
C16D	167(11)	66(7)	56(5)	-7(5)	23(6)	2(7)
C16E	171(8)	81(7)	43(5)	0(5)	1(5)	70(6)
N1D	39.4(16)	16.9(14)	34.4(15)	-1.8(11)	14.1(13)	-2.0(12)
C1C	42(2)	26(2)	62(2)	2.6(17)	10.0(19)	6.6(16)
C2C	134(5)	43(3)	76(3)	18(2)	51(3)	32(3)
C3C	143(5)	46(3)	85(4)	9(3)	50(4)	47(3)
C4C	254(9)	62(4)	95(4)	3(3)	45(5)	37(5)
C5C	28.3(17)	30(2)	56(2)	4.1(17)	13.7(16)	-4.9(15)
C6C	38(2)	35(2)	55(2)	2.2(18)	12.3(18)	2.7(17)
C7C	37(2)	75(3)	73(3)	23(2)	10(2)	-9(2)
C8C	52(3)	64(3)	49(2)	-6(2)	4(2)	7(2)
C9C	28.8(19)	33(2)	79(3)	9.9(19)	22.9(19)	0.5(16)
C10C	49(2)	46(3)	84(3)	10(2)	34(2)	11(2)
C11C	42(2)	101(4)	77(3)	22(3)	24(2)	8(3)
C12C	89(4)	133(5)	91(4)	34(4)	50(3)	57(4)
C13C	41(2)	20.7(18)	62(2)	3.2(16)	9.8(18)	5.9(15)
C14C	59(3)	36(2)	103(4)	-17(2)	-27(3)	17(2)
C15C	82(3)	47(3)	84(3)	-15(2)	-14(3)	39(2)
C16C	151(6)	80(5)	166(6)	-46(4)	-69(5)	47(4)
N1C	30.8(15)	20.6(15)	59.2(19)	5.3(13)	13.7(14)	0.9(12)

Table S19: Bond Lengths in Å for **sad_sq**.

Atom	Atom	Length/Å
C1	C2	1.512(5)
C1	N1	1.471(4)
C2	N2	1.478(4)
C3	C4	1.521(5)
C3	N1	1.482(4)
C4	N3	1.473(4)
C5	C6	1.524(5)
C5	N1	1.469(4)
C6	N4	1.470(4)
C7	C8	1.541(5)
C7	C9	1.527(5)

Atom	Atom	Length/Å
C7	C10	1.522(5)
C7	S1	1.815(4)
C11	C12	1.522(5)
C11	C13	1.540(5)
C11	C14	1.522(5)
C11	S2	1.822(4)
C15	C16	1.531(5)
C15	C17	1.519(6)
C15	C18	1.532(6)
C15	S3	1.831(4)
N1	Co1	2.246(3)
N2	S1	1.582(3)
N2	Co1	2.038(3)
N3	S2	1.586(3)
N3	Co1	2.014(3)
N4	S3	1.570(3)
N4	Co1	2.030(3)
O1	Co1	2.134(3)
O2	S1	1.450(3)
O3	S1	1.459(3)
O4	S2	1.458(3)
O5	S2	1.449(3)
O6	S3	1.442(3)
O7	S3	1.456(3)
C1'	C2'	1.510(5)
C1'	N1'	1.474(4)
C2'	N2'	1.488(4)
C3'	C4'	1.511(5)
C3'	N1'	1.477(4)
C4'	N3'	1.481(4)
C5'	C6'	1.514(5)
C5'	N1'	1.483(4)
C6'	N4'	1.474(4)
C7'	C8'	1.531(5)
C7'	C9'	1.533(5)
C7'	C10'	1.529(5)
C7'	S1'	1.824(3)
C11'	C12'	1.531(5)
C11'	C13'	1.530(5)
C11'	C14'	1.527(5)
C11'	S2'	1.821(4)
C15'	C16'	1.530(5)
C15'	C17'	1.524(5)
C15'	C18'	1.519(5)
C15'	S3'	1.824(3)
N1'	Co1'	2.241(3)

Atom	Atom	Length/Å
N2'	S1'	1.573(3)
N2'	Co1'	2.043(3)
N3'	S2'	1.577(3)
N3'	Co1'	2.023(3)
N4'	S3'	1.578(3)
N4'	Co1'	2.032(3)
O1'	Co1'	2.125(2)
O2'	S1'	1.454(2)
O3'	S1'	1.454(2)
O4'	S2'	1.455(2)
O5'	S2'	1.451(2)
O6'	S3'	1.450(2)
O7'	S3'	1.459(2)
C1D	C2D	1.502(5)
C1D	N1D	1.525(4)
C2D	C3D	1.519(5)
C3D	C4D	1.519(5)
C5D	C6D	1.521(5)
C5D	N1D	1.519(4)
C6D	C7D	1.528(5)
C7D	C8D	1.527(5)
C9D	C10D	1.524(5)
C9D	N1D	1.526(4)
C10D	C11D	1.522(5)
C11D	C12D	1.510(5)
C13D	C14D	1.517(6)
C13D	N1D	1.516(4)
C14D	C15D	1.504(6)
C15D	C16D	1.508(2)
C15D	C16E	1.5144(14)
C1C	C2C	1.510(6)
C1C	N1C	1.531(5)
C2C	C3C	1.568(7)
C3C	C4C	1.410(8)
C5C	C6C	1.514(5)
C5C	N1C	1.513(4)
C6C	C7C	1.495(5)
C7C	C8C	1.491(6)
C9C	C10C	1.517(6)
C9C	N1C	1.499(4)
C10C	C11C	1.521(6)
C11C	C12C	1.488(7)
C13C	C14C	1.521(5)
C13C	N1C	1.526(4)
C14C	C15C	1.537(6)
C15C	C16C	1.432(7)

Table S20: Bond Angles in ° for **sad_sq**.

Atom	Atom	Atom	Angle/°
N1	C1	C2	109.3(3)
N2	C2	C1	108.9(3)
N1	C3	C4	109.3(3)
N3	C4	C3	108.7(3)

Atom	Atom	Atom	Angle/°
N1	C5	C6	110.3(3)
N4	C6	C5	108.5(3)
C8	C7	S1	107.6(3)
C9	C7	C8	110.7(3)
C9	C7	S1	109.6(3)

Atom	Atom	Atom	Angle/°
C10	C7	C8	110.2(3)
C10	C7	C9	110.7(3)
C10	C7	S1	108.0(3)
C12	C11	C13	110.3(3)
C12	C11	S2	109.1(3)
C13	C11	S2	107.5(3)
C14	C11	C12	110.8(3)
C14	C11	C13	110.2(3)
C14	C11	S2	108.9(3)
C16	C15	C18	109.8(4)
C16	C15	S3	106.8(3)
C17	C15	C16	111.7(4)
C17	C15	C18	111.5(3)
C17	C15	S3	108.7(3)
C18	C15	S3	108.2(3)
C1	N1	C3	111.4(3)
C1	N1	Co1	107.49(19)
C3	N1	Co1	106.37(19)
C5	N1	C1	112.4(3)
C5	N1	C3	112.3(3)
C5	N1	Co1	106.44(19)
C2	N2	S1	117.0(2)
C2	N2	Co1	112.5(2)
S1	N2	Co1	130.50(18)
C4	N3	S2	116.3(2)
C4	N3	Co1	111.5(2)
S2	N3	Co1	126.75(16)
C6	N4	S3	118.6(2)
C6	N4	Co1	110.7(2)
S3	N4	Co1	130.51(18)
N2	S1	C7	109.47(16)
O2	S1	C7	105.24(18)
O2	S1	N2	112.37(17)
O2	S1	O3	116.03(19)
O3	S1	C7	104.99(17)
O3	S1	N2	108.30(17)
N3	S2	C11	108.43(16)
O4	S2	C11	105.06(17)
O4	S2	N3	111.60(16)
O5	S2	C11	105.88(17)
O5	S2	N3	108.72(15)
O5	S2	O4	116.67(17)
N4	S3	C15	109.52(16)
O6	S3	C15	106.24(19)
O6	S3	N4	111.88(17)
O6	S3	O7	116.01(18)
O7	S3	C15	103.85(18)
O7	S3	N4	108.86(16)
N2	Co1	N1	80.10(11)
N2	Co1	O1	97.12(12)
N3	Co1	N1	81.18(10)
N3	Co1	N2	119.19(11)
N3	Co1	N4	119.46(11)
N3	Co1	O1	101.67(11)
N4	Co1	N1	81.12(11)
N4	Co1	N2	113.83(11)
N4	Co1	O1	98.63(12)

Atom	Atom	Atom	Angle/°
O1	Co1	N1	176.78(11)
N1'	C1'	C2'	110.0(3)
N2'	C2'	C1'	108.6(3)
N1'	C3'	C4'	109.1(3)
N3'	C4'	C3'	108.5(3)
N1'	C5'	C6'	110.6(3)
N4'	C6'	C5'	109.4(3)
C8'	C7'	C9'	109.9(3)
C8'	C7'	S1'	107.6(2)
C9'	C7'	S1'	108.8(2)
C10'	C7'	C8'	110.5(3)
C10'	C7'	C9'	111.1(3)
C10'	C7'	S1'	108.8(2)
C12'	C11'	S2'	108.4(3)
C13'	C11'	C12'	111.3(3)
C13'	C11'	S2'	107.6(3)
C14'	C11'	C12'	110.9(3)
C14'	C11'	C13'	110.5(3)
C14'	C11'	S2'	108.1(2)
C16'	C15'	S3'	107.3(2)
C17'	C15'	C16'	110.6(3)
C17'	C15'	S3'	108.7(2)
C18'	C15'	C16'	110.6(3)
C18'	C15'	C17'	110.6(3)
C18'	C15'	S3'	109.1(2)
C1'	N1'	C3'	111.5(3)
C1'	N1'	C5'	112.1(3)
C1'	N1'	Co1'	107.20(19)
C3'	N1'	C5'	112.1(3)
C3'	N1'	Co1'	107.0(2)
C5'	N1'	Co1'	106.6(2)
C2'	N2'	S1'	116.4(2)
C2'	N2'	Co1'	111.9(2)
S1'	N2'	Co1'	131.21(16)
C4'	N3'	S2'	117.0(2)
C4'	N3'	Co1'	111.5(2)
S2'	N3'	Co1'	125.64(15)
C6'	N4'	S3'	118.3(2)
C6'	N4'	Co1'	110.8(2)
S3'	N4'	Co1'	130.85(15)
N2'	S1'	C7'	109.12(15)
O2'	S1'	C7'	105.53(15)
O2'	S1'	N2'	112.16(15)
O3'	S1'	C7'	104.72(15)
O3'	S1'	N2'	109.08(14)
O3'	S1'	O2'	115.75(15)
N3'	S2'	C11'	108.52(16)
O4'	S2'	C11'	105.10(16)
O4'	S2'	N3'	111.78(15)
O5'	S2'	C11'	105.71(16)
O5'	S2'	N3'	108.76(15)
O5'	S2'	O4'	116.47(16)
N4'	S3'	C15'	109.65(15)
O6'	S3'	C15'	105.49(15)
O6'	S3'	N4'	112.55(15)
O6'	S3'	O7'	115.72(15)
O7'	S3'	C15'	104.25(14)

Atom	Atom	Atom	Angle/°
O7'	S3'	N4'	108.70(14)
N2'	Co1'	N1'	80.55(10)
N2'	Co1'	O1'	97.25(10)
N3'	Co1'	N1'	80.68(11)
N3'	Co1'	N2'	118.30(11)
N3'	Co1'	N4'	120.52(11)
N3'	Co1'	O1'	102.02(10)
N4'	Co1'	N1'	81.43(10)
N4'	Co1'	N2'	113.78(11)
N4'	Co1'	O1'	97.87(10)
O1'	Co1'	N1'	177.14(10)
C2D	C1D	N1D	115.4(3)
C1D	C2D	C3D	111.5(3)
C2D	C3D	C4D	113.3(3)
N1D	C5D	C6D	115.5(3)
C5D	C6D	C7D	110.1(3)
C8D	C7D	C6D	112.1(3)
C10D	C9D	N1D	115.0(3)
C11D	C10D	C9D	111.3(3)
C12D	C11D	C10D	112.8(3)
N1D	C13D	C14D	115.9(3)
C15D	C14D	C13D	110.9(4)
C14D	C15D	C16D	117.9(6)
C14D	C15D	C16E	116.1(6)

Atom	Atom	Atom	Angle/°
C1D	N1D	C9D	108.8(2)
C5D	N1D	C1D	109.0(2)
C5D	N1D	C9D	110.3(2)
C13D	N1D	C1D	110.6(3)
C13D	N1D	C5D	108.8(3)
C13D	N1D	C9D	109.3(3)
C2C	C1C	N1C	116.6(3)
C1C	C2C	C3C	107.6(4)
C4C	C3C	C2C	115.9(5)
N1C	C5C	C6C	116.5(3)
C7C	C6C	C5C	110.9(3)
C8C	C7C	C6C	117.3(4)
N1C	C9C	C10C	115.7(3)
C9C	C10C	C11C	110.2(4)
C12C	C11C	C10C	115.0(5)
C14C	C13C	N1C	116.1(3)
C13C	C14C	C15C	109.2(4)
C16C	C15C	C14C	117.6(5)
C5C	N1C	C1C	111.0(3)
C5C	N1C	C13C	105.5(3)
C9C	N1C	C1C	105.6(3)
C9C	N1C	C5C	112.0(3)
C9C	N1C	C13C	111.4(3)
C13C	N1C	C1C	111.5(3)

Table S21: Hydrogen Fractional Atomic Coordinates (×10⁴) and Equivalent Isotropic Displacement Parameters (Å²×10³) for **sad_sq**. U_{eq} is defined as 1/3 of the trace of the orthogonalised U_{ij}.

Atom	x	y	z	U_{eq}
H1C	2640(30)	4264(18)	2470(13)	84(12)
H1D	2590(30)	4764(6)	2090(20)	84(12)
H1A	5818	5183	2675	41
H1B	6137	5247	3390	41
H2A	4798	5475	3429	47
H2B	5003	5825	2926	47
H3A	5995	3910	3042	37
H3B	6518	4382	2915	37
H4A	5545	4523	1965	40
H4B	5799	3936	1991	40
H5A	5422	4770	3980	41
H5B	6103	4351	3967	41
H6A	5062	3723	3638	45
H6B	4909	3986	4218	45
H8A	2610	5992	977	89
H8B	3283	6184	661	89
H8C	3186	6467	1245	89
H9A	4706	6333	1831	74
H9B	4857	6084	1245	74
H9C	5110	5783	1867	74
H10A	4190	5022	1412	64
H10B	4005	5303	779	64
H10C	3254	5120	1021	64
H12A	4687	4113	887	79
H12B	4404	3760	306	79
H12C	5134	3581	876	79

Atom	x	y	z	U_{eq}
H13A	4341	2759	890	85
H13B	3582	2940	342	85
H13C	3425	2776	962	85
H14A	2725	3621	993	74
H14B	2917	3821	398	74
H14C	3221	4139	1006	74
H16A	1869	4498	4007	116
H16B	2246	4857	4571	116
H16C	2476	4269	4610	116
H17A	3449	5211	3553	88
H17B	2812	5436	3880	88
H17C	2490	5061	3323	88
H18A	4025	4458	4896	88
H18B	3811	5047	4897	88
H18C	4380	4844	4501	88
H1'C	-1970(30)	5038(6)	3044(19)	86(17)
H1'D	-2310(20)	5526(14)	2627(15)	78(16)
H1'A	744	4659	2383	44
H1'B	485	4595	1668	44
H2'A	-865	4338	1645	41
H2'B	-233	3997	2142	41
H3'A	563	5933	2016	44
H3'B	1209	5473	2126	44
H4'A	1029	5311	3081	45
H4'B	1239	5901	3058	45
H5'A	-708	5052	1080	43
H5'B	-55	5495	1092	43
H6'A	-881	6090	1406	41
H6'B	-1482	5801	841	41
H8'A	-1101	3750	4080	64
H8'B	-191	3519	4338	64
H8'C	-804	3300	3732	64
H9'A	293	3474	3177	64
H9'B	901	3679	3794	64
H9'C	689	4026	3207	64
H10H	127	4752	3713	53
H10I	404	4437	4325	53
H10J	-531	4631	4072	53
H12J	1054	5742	4158	94
H12K	1189	6074	4752	94
H12L	1448	6295	4191	94
H13F	539	7074	4163	83
H13G	237	6872	4713	83
H13H	-429	7010	4091	83
H14H	-1046	6144	4083	74
H14I	-354	5944	4663	74
H14J	-523	5648	4040	74
H16M	-4293	5166	1080	63
H16N	-4298	4808	525	63
H16O	-4168	5404	481	63
H17D	-2292	4559	1620	50
H17E	-3157	4293	1293	50
H17F	-3104	4697	1814	50
H18D	-2842	5201	194	62
H18E	-2923	4607	296	62
H18F	-2101	4903	654	62
H1DA	3228	7962	3479	38

Atom	x	y	z	U_{eq}
H1DB	2391	8174	3032	38
H2DA	2488	7550	4057	50
H2DB	1624	7700	3585	50
H3DA	1873	8571	3832	52
H3DB	2764	8439	4278	52
H4DA	2117	8012	4931	105
H4DB	1224	8138	4483	105
H4DC	1800	8585	4837	105
H5DA	3245	7191	2266	39
H5DB	3725	7616	2721	39
H6DA	2928	8260	2154	41
H6DB	2271	7866	1761	41
H7DA	3950	8004	1700	48
H7DB	3397	7536	1378	48
H8DA	2922	8571	1068	77
H8DB	2453	8087	718	77
H8DC	3363	8226	685	77
H9DA	1355	7225	2737	41
H9DB	1465	7674	2308	41
H10D	1959	7047	1714	45
H10E	1707	6616	2112	45
H11A	293	6833	1749	45
H11B	505	7325	1422	45
H12D	793	6323	1054	73
H12E	857	6831	698	73
H12F	-26	6637	734	73
H2	2846	6645	2962	51
H13D	2517	6868	3488	51
H14D	4186	6985	3416	69
H14E	3863	7241	3931	69
H15A	3913	6170	3754	99
H15B	3595	6426	4268	99
H15D	4331	6204	3936	99
H16D	3038	6369	4423	147
H16E	3786	6700	4828	147
H16F	3877	6100	4798	147
H16G	5287	6427	4240	157
H16H	4936	6110	4699	157
H16I	4981	6713	4744	157
H1CA	3139	1652	2930	53
H1CB	2261	1792	2478	53
H2CA	3821	2140	2350	96
H2CB	2939	2293	1898	96
H3CA	3565	1257	2090	105
H3CB	2652	1383	1681	105
H4CA	3161	1756	989	207
H4CB	3545	1201	1128	207
H4CC	4089	1684	1408	207
H5CA	3542	2888	3644	45
H5CB	3923	2669	3142	45
H6CA	3859	2101	4181	52
H6CB	4278	1903	3686	52
H7CA	5267	2561	3940	76
H7CB	4845	2769	4425	76
H8CA	6120	2311	4836	86
H8CB	5630	1807	4563	86
H8CC	5366	2118	5069	86

Atom	x	y	z	U_{eq}
H9CA	2540	1885	3699	54
H9CB	1704	2079	3234	54
H10F	1814	2864	3752	68
H10G	2680	2691	4206	68
H11C	1118	2197	4109	86
H11D	1979	2013	4553	86
H12G	1209	2464	5082	149
H12H	1211	2952	4675	149
H12I	2059	2753	5126	149
H13E	2283	3118	2969	51
H5	2667	2957	2444	51
H14F	1052	2653	2515	92
H14G	1441	2454	2003	92
H15C	1071	3502	2174	95
H15E	1533	3331	1697	95
H16J	374	2992	1097	234
H16K	129	3538	1289	234
H16L	-98	3041	1601	234

Table S22: Hydrogen Bond information for **sad_sq**.

D	H	A	d(D-H)/Å	d(H-A)/Å	d(D-A)/Å	D-H-A/deg
O1	H1D	O3	0.977(16)	1.771(16)	2.683(4)	154(4)
O1'	H1'C	O3'	0.957(16)	1.794(15)	2.704(3)	158(4)
O1'	H1'D	O7'	0.941(18)	1.82(2)	2.741(3)	165(4)
C1D	H1DB	O2'[1]	0.97	2.27	3.177(4)	155.1
C9D	H9DA	O4'	0.97	2.28	3.193(4)	157.4
C13D	H2	O2	0.97	2.29	3.118(5)	143.4

-------•

[1]-X,1/2+Y,1/2-Z

4-4

EMORY UNIVERSITY | X-ray Crystallography Center

Submitted by: **Christian Wallen**
Emory University
Solved by: **Thomas C. Pickel**
Sample ID: **CMW04BuCoBus**

Crystal Data and Experimental

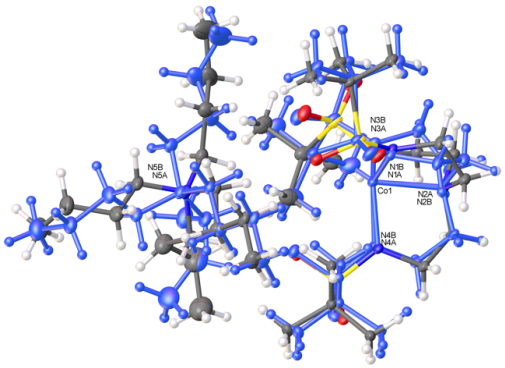

Experimental. Single violet prism-shaped crystals of (**cmw04bucobus**) were recrystallised from --•by vapor diffusion. A suitable crystal (0.57×0.48×0.24 mm) was selected and mounted on a loop with paratone oil on a Bruker APEX-II CCD diffractometer. The crystal was cooled to T = 100(2) K during data collection. The structure was solved with the **ShelXT** (Sheldrick, 2015) structure solution program using combined Patterson and dual-space recycling methods and by using **Olex2** (Dolomanov et al., 2009) as the graphical interface. The crystal structure was refined with version of **ShelXL** (Sheldrick, 2008) using Least Squares minimisation.

Crystal Data. $C_{34}H_{75}CoN_5O_6S_3$, M_r = 805.10, monoclinic, $P2_1/c$ (No. 14), a = 19.505(2) Å, b = 11.3473(14) Å, c = 19.833(2) Å, β = 99.185(2)°, $\alpha = \gamma = 90°$, V = 4333.3(9) Å^3, T = 100(2) K, Z = 4, Z' = 1, μ(MoK$_\alpha$) = 0.585, 51543 reflections measured, 11684 unique (R_{int} = 0.0614) which were used in all calculations. The final wR_2 was 0.2206 (all data) and R_1 was 0.0835 (I > 2σ(I)).

Compound	**cmw04bucobus**
Formula	$C_{34}H_{75}CoN_5O_6S_3$
$D_{calc.}$/ g cm^{-3}	1.234
μ/mm^{-1}	0.585
Formula Weight	805.10
Colour	violet
Shape	prism
Max Size/mm	0.57
Mid Size/mm	0.48
Min Size/mm	0.24
T/K	100(2)
Crystal System	monoclinic
Space Group	$P2_1/c$
a/Å	19.505(2)
b/Å	11.3473(14)
c/Å	19.833(2)
α/°	90
β/°	99.185(2)
γ/°	90
V/Å^3	4333.3(9)
Z	4
Z'	1
Θ_{min}/°	2.074
Θ_{max}/°	29.199
Measured Refl.	51543
Independent Refl.	11684
$I > 2\sigma(I)$	8299
R_{int}	0.0614
Parameters	848
Restraints	1142
Largest Peak	1.584
Deepest Hole	-1.143
GooF	1.080
wR_2 (all data)	0.2206
wR_2	0.1969
R_1 (all data)	0.1176
R_1	0.0835
CCDC #	1434434

Structure Quality Indicators

Reflections:	d min CIF	0.73	I/σ CIF	18.3	Rint CIF	6.14%	complete CIF	100%
Refinement:	Shift CIF	0.004	Max Peak CIF	1.6	Min Peak CIF	-1.1	GooF CIF	1.080

A violet prism-shaped crystal with dimensions 0.57×0.48×0.24 mm was mounted on a loop with paratone oil. X-ray diffraction data were collected using a Bruker APEX-II CCD diffractometer equipped with an Oxford Cryosystems low-temperature apparatus operating at T = 100(2) K.

Data were measured using ϕ and ω scans using MoK$_\alpha$ radiation (fine-focus sealed tube, 45 kV, 35 mA). The total number of runs and images was based on the strategy calculation from the program **APEX2** (Bruker, 2014). The maximum resolution achieved was Θ = 29.199°.

Unit cell indexing was performed by using the **APEX2** (Bruker, 2014) software and refined using **SAINT** (Bruker, V8.34A, 2013) on 9806 reflections, 19 percent of the observed reflections. Data reduction, scaling and absorption corrections were performed using **SAINT** (Bruker, V8.34A, 2013) and **SADABS-2014/5** (Bruker,2014) was used for absorption correction. wR_2(int) was 0.0821 before and 0.0579 after correction. The ratio of minimum to maximum transmission is 0.8248. The $\lambda/2$ correction factor is 0.00150. The software also corrects for Lorentz polarisation. The final completeness is 99.9% out to 29.199° in Θ. The absorption coefficient (μ) of this material is 0.585 and the minimum and maximum transmissions are 0.6151 and 0.7458. The structure was solved in the space group P1 with the **ShelXT** (Sheldrick, 2015) structure solution program using combined Patterson and dual-space recycling methods. The space group P2$_1$/c (# 14) was determined by **ShelXT** (Sheldrick, 2015) structure solution program.The crystal structure was refined by Least Squares using version 2014/7 of **ShelXL** (Sheldrick, 2008). All non-hydrogen atoms were refined anisotropically. Hydrogen atom positions were calculated geometrically and refined using the riding model.

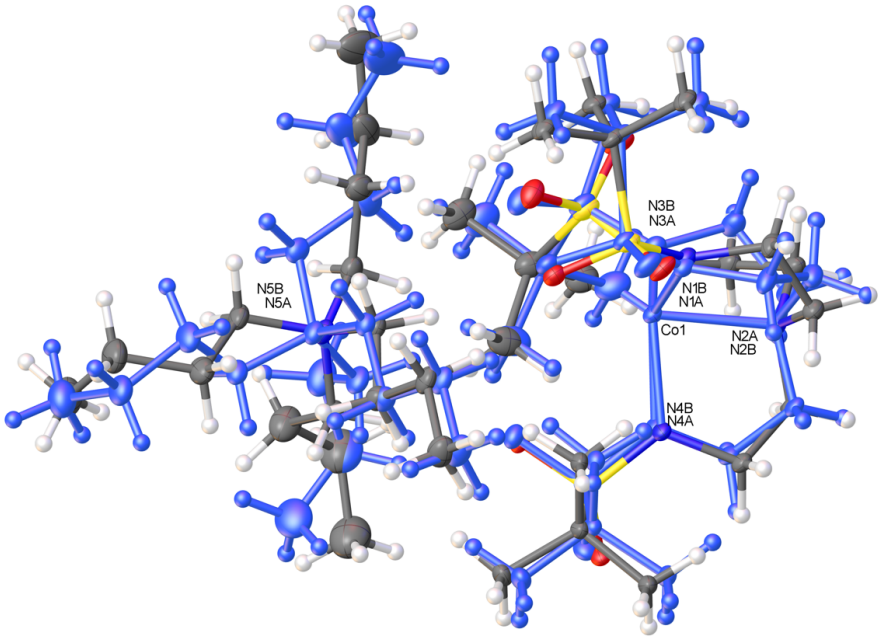

Figure S19: Plot of the asymmetric unit with the second disorder component shown in blue.

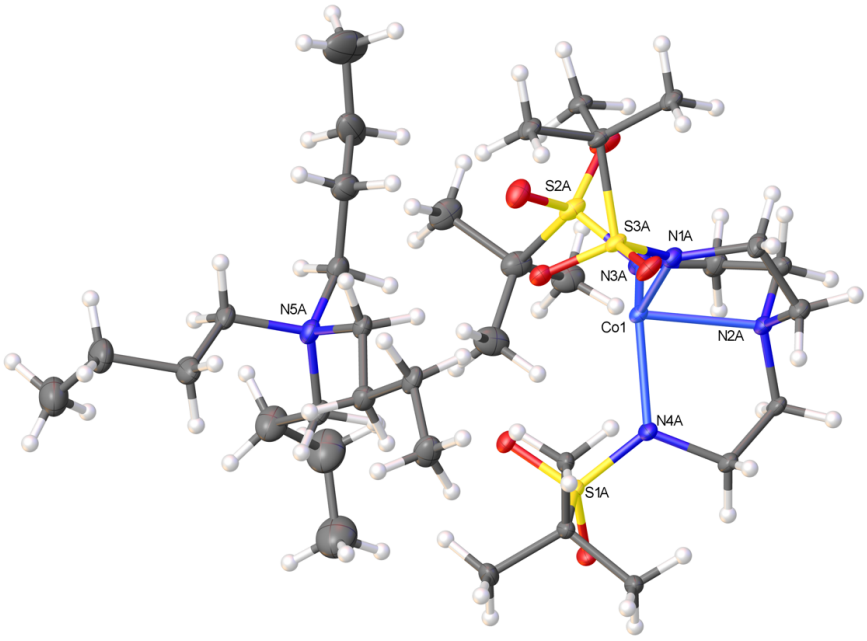

FigureS20: Plot of the asymmetric unit with the major disorder component shown only.

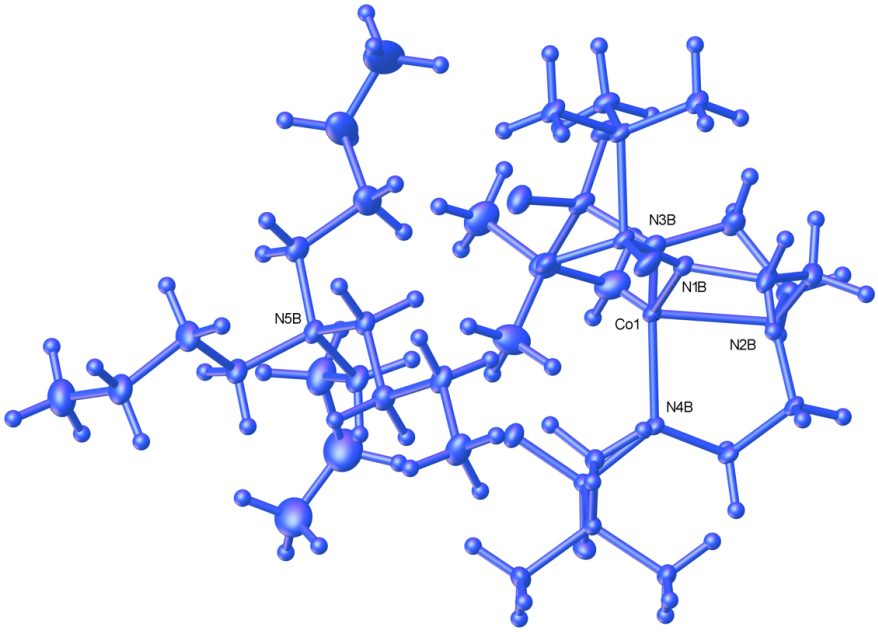

Figure S21: Plot of the asymmetric unit with the minor disorder component shown only.

There are two independent molecules in the asymmetric unit.

Data Plots: Diffraction Data

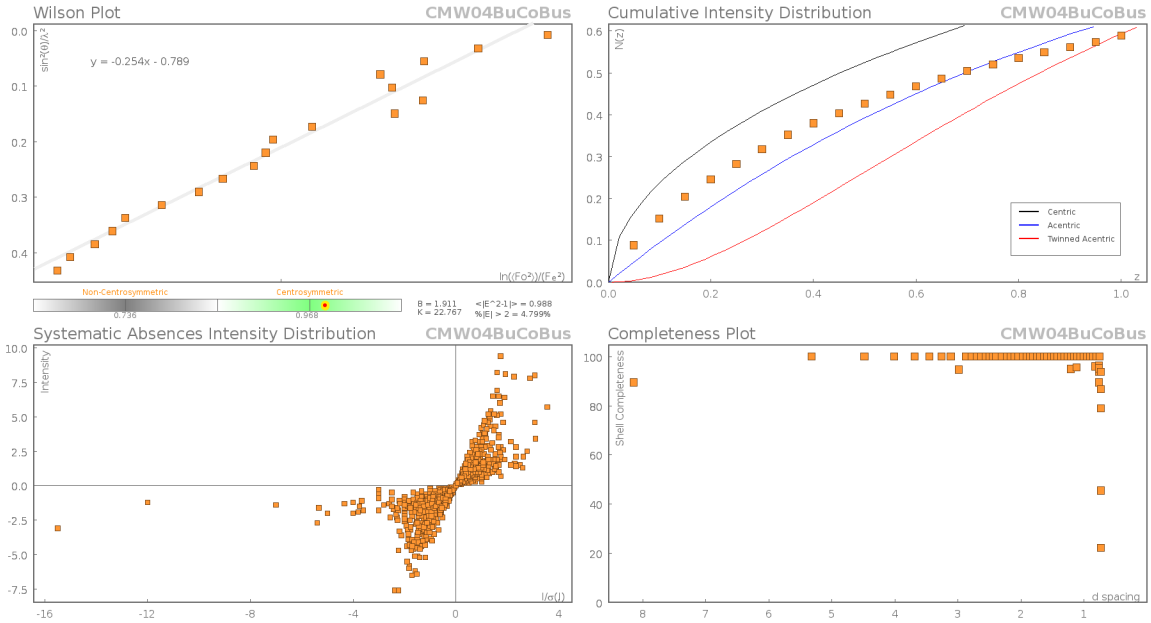

Data Plots: Refinement and Data

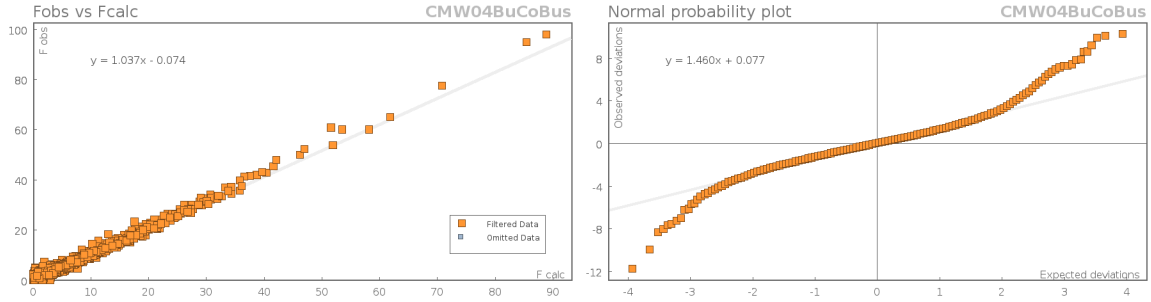

Reflection Statistics

Total reflections (after filtering)	52935	Unique reflections	11684
Completeness	0.995	Mean I/σ	12.23
hklsub>max</sub> collected	(24, 15, 27)	hklsub>min</sub> collected	(-26, -15, -27)
hkl_{max} used	(26, 15, 27)	hkl_{min} used	(-26, 0, 0)
Lim d_{max} collected	100.0	Lim d_{min} collected	0.36
d_{max} used	14.98	d_{min} used	0.73
Friedel pairs	13977	Friedel pairs merged	1
Inconsistent equivalents	0	R_{int}	0.0614
R_{sigma}	0.0547	Intensity transformed	0
Omitted reflections	0	Omitted by user (OMIT hkl)	0
Multiplicity	(22662, 12930, 1471)	Maximum multiplicity	12
Removed systematic absences	1392	Filtered off (Shel/OMIT)	0

Images of the Crystal on the Diffractometer

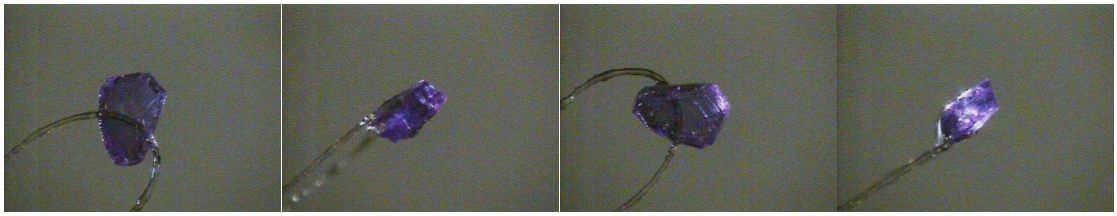

Table S93: Fractional Atomic Coordinates (×10⁴) and Equivalent Isotropic Displacement Parameters (Å²×10³) for **cmw04bucobus**. U_{eq} is defined as 1/3 of the trace of the orthogonalised U_{ij}.

Atom	x	y	z	U_{eq}
C1B	9408(3)	3687(6)	4595(3)	35.8(15)
C2B	9146(3)	2693(5)	4989(3)	34.9(13)
C3B	8039(3)	2114(5)	5367(3)	32.8(13)
C4B	7575(4)	1840(5)	4687(3)	40.3(15)
C5B	8730(3)	3741(5)	5930(2)	23.9(10)
C6B	8160(3)	4594(5)	6022(2)	24.9(11)
C7B	8428(3)	7551(4)	5446(3)	25.3(8)
C8B	8823(4)	7311(7)	4855(4)	27.1(17)
C9B	8142(4)	8808(5)	5410(5)	34.7(16)
C10B	8902(4)	7359(7)	6129(4)	29.3(15)
C11B	5902(3)	3361(7)	4296(4)	41.2(13)
C12B	5231(3)	3208(10)	3784(5)	56(2)
C13B	5995(4)	4625(8)	4536(6)	54.3(19)
C14B	5905(5)	2527(10)	4906(4)	53.3(19)
C15B	8858(4)	3991(6)	2763(2)	24.9(10)
C16B	8191(6)	3260(9)	2715(4)	31.5(18)
C17B	9497(6)	3206(9)	2844(4)	33.0(17)
C18B	8840(6)	4787(8)	2139(3)	32.9(17)
N1B	8810(2)	4209(5)	4147(2)	24.5(7)
N2B	8528(2)	3076(3)	5284.9(18)	24.6(6)
N3B	7307(2)	2958(4)	4390(2)	29.3(9)
N4B	7968(3)	5244(4)	5377(2)	23.8(8)
O1B	7293(3)	6769(5)	4707(3)	29.9(13)
O2B	7356(3)	6795(5)	5965(3)	32.9(14)
O3B	6651(3)	3897(6)	3367(3)	39.6(10)
O4B	6463(3)	1784(5)	3581(3)	40.6(11)
O5B	8311(4)	5730(5)	3357(3)	31.0(13)
O6B	9590(3)	5513(7)	3577(3)	36.4(14)
S1B	7692.5(19)	6555(2)	5375(2)	24.1(6)
S2B	6614.9(15)	2960(4)	3851.0(15)	31.4(3)
S3B	8911(2)	4965(3)	3501.6(15)	24.6(6)
C1A	9299(6)	3193(10)	4430(5)	32(2)
C2A	9274(4)	3122(10)	5184(4)	29.6(17)
C3A	8195(5)	1943(6)	5163(5)	32.3(18)
C4A	7406(5)	2100(10)	4996(5)	37.4(19)
C5A	8477(5)	3535(7)	6001(3)	23.9(10)
C6A	8551(6)	4856(7)	6014(4)	25.6(17)
C7A	8383(6)	7724(7)	5392(6)	25.3(8)
C8A	8752(9)	7489(16)	4783(8)	26(3)
C9A	7994(9)	8898(7)	5309(10)	34(3)
C10A	8906(7)	7732(13)	6054(8)	29(3)
C11A	5860(4)	3524(12)	4193(6)	41.9(17)
C12A	5287(5)	3550(20)	3565(8)	50(3)
C13A	6004(8)	4743(13)	4490(12)	52(3)
C14A	5659(8)	2678(18)	4733(8)	47(3)

Atom	x	y	z	U_{eq}
C15A	8862(8)	4156(11)	2734(4)	25.7(16)
C16A	8184(11)	3447(18)	2633(8)	28(3)
C17A	9488(12)	3358(18)	2739(8)	30(3)
C18A	8849(12)	5101(16)	2184(5)	30(3)
N1A	8776(4)	4051(9)	4116(3)	24.5(7)
N2A	8546(3)	3084(5)	5314(3)	24.6(6)
N3A	7264(3)	3079(7)	4517(5)	29.3(9)
N4A	8112(5)	5334(5)	5401(4)	23.8(8)
O1A	7250(6)	6685(9)	4806(6)	27(2)
O2A	7487(7)	6743(10)	6070(6)	30(2)
O3A	6759(6)	3759(14)	3366(5)	39.6(10)
O4A	6505(6)	1740(10)	3726(7)	40.6(11)
O5A	8383(8)	5795(10)	3457(6)	29(2)
O6A	9644(7)	5377(14)	3685(6)	33(2)
S1A	7745(4)	6573(5)	5428(4)	24.7(12)
S2A	6639(3)	2968(8)	3904(3)	31.4(3)
S3A	8938(5)	4935(7)	3548(3)	24.6(12)
Co1	7977.5(3)	4271.8(5)	4576.9(2)	20.73(14)
C25B	5785(7)	7943(9)	4189(5)	85(2)
C21B	8854(3)	8915(13)	3199(10)	33(3)
C29B	6240(5)	5503(9)	1777(7)	68(3)
C33B	6540(5)	11488(6)	1896(6)	46(2)
C23B	6703(4)	8007(8)	3440(3)	36.8(15)
C27B	6514(4)	7542(6)	2190(3)	34.0(13)
C31B	6574(4)	9615(6)	2582(3)	32.5(13)
C20B	8091(3)	9180(20)	3216(16)	34.5(17)
N5B	6859(2)	8391(5)	2741(2)	28.2(10)
C22B	9322(5)	9762(17)	3624(12)	46(4)
C24B	5940(4)	7755(9)	3463(4)	55.0(19)
C26B	5705(7)	9217(9)	4332(5)	76(3)
C28B	6735(5)	6268(7)	2264(6)	50(2)
C30B	6602(7)	4584(14)	1442(9)	101(4)
C32B	6724(5)	10176(6)	1936(4)	44.9(17)
C34B	5781(6)	11681(13)	1835(9)	63(3)
C19B	7642(3)	8329(7)	2743(4)	27.5(13)
C25A	5766(9)	7981(13)	4167(7)	86(2)
C21A	8800(4)	9090(20)	3108(16)	33(3)
C29A	6328(9)	5246(12)	1903(9)	62(3)
C33A	6292(5)	11018(8)	1711(5)	60(2)
C23A	6676(5)	8660(11)	3497(4)	36.7(17)
C27A	6571(5)	6958(7)	2685(4)	35.1(15)
C31A	6494(5)	9003(7)	2244(4)	33.0(16)
C20A	8038(5)	9220(30)	3190(20)	34.2(19)
N5A	6842(3)	8217(5)	2812(3)	29.8(13)
C22A	9248(7)	9960(30)	3535(19)	48(5)
C24A	5904(6)	8683(14)	3543(5)	60(2)
C26A	5884(12)	8720(20)	4795(5)	94(4)
C28A	6787(7)	6323(10)	2085(9)	46(2)
C30A	6437(11)	4699(19)	1253(10)	97(5)
C32A	6717(6)	10269(7)	2267(5)	43.0(19)
C34A	5636(10)	11440(30)	1915(13)	72(4)
C19A	7630(3)	8178(8)	2843(5)	28.3(16)

Table S24: Anisotropic Displacement Parameters (×10^4) **cmw04bucobus**. The anisotropic displacement factor exponent takes the form: $-2\pi^2[h^2a^{*2} \times U_{11} + \ldots + 2hka^* \times b^* \times U_{12}]$

Atom	U_{11}	U_{22}	U_{33}	U_{23}	U_{13}	U_{12}
C1B	32(2)	53(3)	22(2)	7(2)	2.2(18)	13(2)
C2B	40(2)	40(3)	24(2)	2(2)	4.4(19)	15(2)
C3B	46(2)	26(2)	24(2)	0.1(18)	-1.9(19)	0.7(19)
C4B	54(3)	29(2)	33(3)	-1(2)	-10(2)	-3(2)
C5B	30(2)	26.4(17)	13.9(14)	1.0(12)	-1.9(14)	0.9(15)
C6B	34(3)	27(2)	13.9(17)	0.5(15)	2.6(18)	1.9(19)
C7B	34.2(16)	21.5(16)	18.7(15)	-0.5(13)	-0.2(12)	6.7(14)
C8B	34(3)	24(3)	22(2)	1(2)	0(2)	5(3)
C9B	44(4)	24(2)	33(3)	-3(2)	-5(3)	10(2)
C10B	38(3)	27(4)	21(2)	0(2)	-2.7(19)	7(3)
C11B	35(2)	54(3)	36(2)	-8(2)	9.2(18)	-8.2(19)
C12B	35(3)	78(6)	53(4)	0(3)	5(3)	-14(3)
C13B	38(3)	61(3)	68(4)	-16(3)	20(3)	-8(3)
C14B	56(5)	67(4)	39(3)	-5(3)	15(3)	-10(4)
C15B	27(2)	33(2)	13.0(16)	-1.7(15)	-0.2(15)	-0.8(18)
C16B	34(2)	37(4)	22(3)	-6(3)	2(2)	-5(3)
C17B	36(3)	43(3)	19(3)	1(3)	2(2)	7(2)
C18B	38(3)	43(4)	16(2)	2(2)	1(2)	1(3)
N1B	25.0(12)	31.0(14)	16.9(10)	-0.2(10)	1.5(9)	3.1(11)
N2B	32.6(13)	24.1(12)	15.8(11)	-0.3(10)	-0.5(10)	4.4(10)
N3B	32.1(13)	28.8(14)	25.2(14)	-0.5(11)	-0.9(11)	-4.8(11)
N4B	31(2)	25.1(13)	14.3(12)	0.1(10)	2.3(12)	5.3(13)
O1B	30(2)	37(3)	22(2)	4.1(17)	0.4(17)	4.9(19)
O2B	42(3)	34(2)	25(2)	0.0(18)	11(2)	12(2)
O3B	35(2)	54(2)	29.0(13)	6.6(13)	4.0(14)	5.4(17)
O4B	43.9(19)	51.8(16)	24(3)	-8.6(16)	-0.9(16)	-9.4(14)
O5B	36(2)	33(2)	21(2)	-4.4(18)	-4.6(19)	2.7(18)
O6B	34(2)	49(3)	23(3)	-1(2)	-4.2(18)	-9(2)
S1B	29.9(10)	24.0(9)	18.4(11)	-1.5(7)	3.7(8)	6.8(8)
S2B	29.9(5)	42.9(6)	20.0(6)	-3.8(5)	-0.3(4)	-6.6(5)
S3B	25.9(10)	31.4(10)	15.0(9)	-1.7(7)	-0.9(7)	-1.1(8)
C1A	32(3)	44(4)	21(3)	4(3)	4(2)	11(3)
C2A	35(3)	33(4)	20(3)	1(3)	3(2)	5(2)
C3A	45(3)	27(3)	23(4)	-1(2)	0(3)	-2(2)
C4A	47(3)	31(3)	32(3)	3(3)	-3(3)	-4(2)
C5A	30(2)	26.4(17)	13.9(14)	1.0(12)	-1.9(14)	0.9(15)
C6A	33(4)	28(2)	15(3)	1(2)	0(3)	3(2)
C7A	34.2(16)	21.5(16)	18.7(15)	-0.5(13)	-0.2(12)	6.7(14)
C8A	34(4)	22(5)	19(4)	2(3)	-2(3)	6(4)
C9A	41(5)	23(3)	35(5)	-3(3)	-4(4)	9(3)
C10A	40(4)	24(6)	21(3)	-2(3)	-2(3)	10(4)
C11A	35(3)	54(3)	38(3)	-7(3)	8(2)	-6(2)
C12A	33(4)	73(7)	45(5)	-3(4)	7(3)	-8(4)
C13A	38(5)	59(4)	61(5)	-15(4)	15(4)	-5(3)
C14A	41(6)	61(5)	42(5)	-7(4)	13(4)	-6(4)
C15A	28(3)	34(3)	14(2)	-2(2)	0(2)	-1(2)
C16A	32(3)	34(5)	17(5)	-5(4)	3(3)	-1(4)
C17A	34(4)	40(5)	15(5)	0(4)	3(3)	4(4)
C18A	35(5)	39(5)	16(3)	1(3)	3(3)	1(4)
N1A	25.0(12)	31.0(14)	16.9(10)	-0.2(10)	1.5(9)	3.1(11)
N2A	32.6(13)	24.1(12)	15.8(11)	-0.3(10)	-0.5(10)	4.4(10)
N3A	32.1(13)	28.8(14)	25.2(14)	-0.5(11)	-0.9(11)	-4.8(11)
N4A	31(2)	25.1(13)	14.3(12)	0.1(10)	2.3(12)	5.3(13)
O1A	31(4)	31(4)	17(3)	3(3)	0(3)	5(3)
O2A	40(5)	33(4)	17(3)	0(3)	5(3)	12(3)
O3A	35(2)	54(2)	29.0(13)	6.6(13)	4.0(14)	5.4(17)
O4A	43.9(19)	51.8(16)	24(3)	-8.6(16)	-0.9(16)	-9.4(14)

Atom	U_{11}	U_{22}	U_{33}	U_{23}	U_{13}	U_{12}
O5A	31(3)	30(3)	23(3)	-3(2)	-2(2)	0(2)
O6A	32(3)	48(5)	17(4)	2(4)	-4(3)	-7(3)
S1A	33(2)	25.8(19)	14.0(19)	-0.7(14)	-0.6(15)	7.8(15)
S2A	29.9(5)	42.9(6)	20.0(6)	-3.8(5)	-0.3(4)	-6.6(5)
S3A	26.5(19)	32.2(19)	13.6(17)	-3.1(14)	-1.2(14)	-0.1(15)
Co1	24.3(3)	23.2(3)	14.0(2)	-0.44(18)	0.72(17)	1.5(2)
C25B	85(5)	106(5)	69(4)	17(3)	32(3)	12(4)
C21B	36(2)	36(5)	25(5)	11(4)	0(2)	-2(2)
C29B	50(4)	54(4)	90(6)	-20(4)	-19(4)	1(3)
C33B	57(5)	46(4)	35(5)	11(3)	5(3)	12(3)
C23B	41(3)	47(4)	23(2)	10(2)	5.8(18)	7(3)
C27B	26(3)	44(2)	30(2)	-1.2(19)	0(2)	2(2)
C31B	36(3)	39(2)	23(2)	4.8(18)	6(2)	10(2)
C20B	38(2)	31(3)	32(3)	1(3)	-1(2)	0(2)
N5B	29.2(19)	35(2)	19.9(19)	4.6(16)	2.2(15)	4.6(16)
C22B	46(4)	43(7)	45(6)	8(6)	-8(4)	-9(4)
C24B	42(3)	78(5)	47(3)	19(3)	13(2)	4(3)
C26B	89(7)	87(5)	58(5)	16(4)	31(5)	9(4)
C28B	41(3)	46(3)	59(5)	-8(3)	-8(3)	1(2)
C30B	55(7)	116(7)	115(8)	-60(7)	-36(6)	17(5)
C32B	56(4)	48(3)	33(3)	14(2)	13(3)	14(3)
C34B	61(5)	68(7)	60(6)	14(5)	10(4)	18(5)
C19B	29.7(19)	30(3)	22(3)	5(2)	1.8(16)	3.8(17)
C25A	85(5)	111(5)	70(4)	20(4)	31(4)	8(4)
C21A	37(3)	35(5)	24(6)	11(5)	-1(3)	-1(3)
C29A	44(4)	48(4)	84(6)	-15(4)	-19(4)	3(4)
C33A	76(5)	58(4)	45(4)	16(3)	2(3)	18(3)
C23A	45(3)	43(4)	22(2)	5(2)	4(2)	8(3)
C27A	31(3)	38(3)	33(3)	4(2)	-3(3)	1(2)
C31A	35(3)	42(3)	22(3)	6(2)	4(2)	11(2)
C20A	37(3)	31(3)	32(4)	1(3)	0(3)	0(3)
N5A	31(2)	35(2)	22(2)	5.1(19)	-0.2(18)	3.3(18)
C22A	47(5)	43(8)	49(8)	4(8)	-5(5)	-7(5)
C24A	49(3)	83(5)	49(4)	7(4)	15(3)	8(3)
C26A	98(9)	119(8)	68(5)	9(5)	26(5)	14(7)
C28A	40(3)	50(3)	45(5)	-9(3)	-2(3)	1(3)
C30A	50(8)	127(8)	104(7)	-56(7)	-21(6)	5(7)
C32A	58(4)	43(3)	29(4)	8(3)	9(4)	9(3)
C34A	74(6)	77(9)	64(7)	15(6)	7(5)	24(6)
C19A	32(2)	30(3)	22(3)	4(3)	-1(2)	3.8(19)

Table S25: Bond Lengths in Å for **cmw04bucobus**.

Atom	Atom	Length/Å
C1B	C2B	1.508(7)
C1B	N1B	1.474(6)
C2B	N2B	1.486(6)
C3B	C4B	1.532(7)
C3B	N2B	1.476(6)
C4B	N3B	1.459(7)
C5B	C6B	1.507(7)
C5B	N2B	1.484(5)
C6B	N4B	1.472(6)
C7B	C8B	1.526(6)
C7B	C9B	1.529(7)
C7B	C10B	1.530(6)
C7B	S1B	1.814(5)
C11B	C12B	1.534(8)
C11B	C13B	1.512(8)
C11B	C14B	1.535(9)
C11B	S2B	1.820(5)
C15B	C16B	1.533(6)
C15B	C17B	1.519(6)
C15B	C18B	1.528(6)
C15B	S3B	1.824(4)
N1B	S3B	1.579(4)
N1B	Co1	1.952(4)
N2B	Co1	2.118(4)
N3B	S2B	1.583(4)

Atom	Atom	Length/Å
N3B	Co1	1.978(4)
N4B	S1B	1.582(4)
N4B	Co1	1.934(4)
O1B	S1B	1.446(3)
O2B	S1B	1.456(3)
O3B	S2B	1.442(4)
O4B	S2B	1.450(4)
O5B	S3B	1.448(3)
O6B	S3B	1.449(4)
C1A	C2A	1.506(7)
C1A	N1A	1.473(6)
C2A	N2A	1.484(6)
C3A	C4A	1.531(7)
C3A	N2A	1.473(6)
C4A	N3A	1.459(7)
C5A	C6A	1.506(7)
C5A	N2A	1.481(5)
C6A	N4A	1.473(6)
C7A	C8A	1.526(6)
C7A	C9A	1.529(7)
C7A	C10A	1.530(6)
C7A	S1A	1.814(5)
C11A	C12A	1.534(8)
C11A	C13A	1.513(8)
C11A	C14A	1.535(9)
C11A	S2A	1.820(6)
C15A	C16A	1.533(6)
C15A	C17A	1.519(6)
C15A	C18A	1.528(6)
C15A	S3A	1.824(4)
N1A	S3A	1.579(4)
N1A	Co1	1.944(7)
N2A	Co1	2.160(5)
N3A	S2A	1.584(4)
N3A	Co1	1.932(7)
N4A	S1A	1.583(4)
N4A	Co1	2.013(6)
O1A	S1A	1.445(4)

Atom	Atom	Length/Å
O2A	S1A	1.456(4)
O3A	S2A	1.442(4)
O4A	S2A	1.450(4)
O5A	S3A	1.448(4)
O6A	S3A	1.450(4)
C25B	C24B	1.533(4)
C25B	C26B	1.486(7)
C21B	C20B	1.525(4)
C21B	C22B	1.491(6)
C29B	C28B	1.523(4)
C29B	C30B	1.475(6)
C33B	C32B	1.530(4)
C33B	C34B	1.482(7)
C23B	N5B	1.529(7)
C23B	C24B	1.525(9)
C27B	N5B	1.530(7)
C27B	C28B	1.508(10)
C31B	N5B	1.510(7)
C31B	C32B	1.501(8)
C20B	C19B	1.522(7)
N5B	C19B	1.529(6)
C25A	C24A	1.531(3)
C25A	C26A	1.486(6)
C21A	C20A	1.525(3)
C21A	C22A	1.490(6)
C29A	C28A	1.524(3)
C29A	C30A	1.477(6)
C33A	C32A	1.528(3)
C33A	C34A	1.482(6)
C23A	N5A	1.530(7)
C23A	C24A	1.525(9)
C27A	N5A	1.530(7)
C27A	C28A	1.508(10)
C31A	N5A	1.511(7)
C31A	C32A	1.500(8)
C20A	C19A	1.522(7)
N5A	C19A	1.529(6)

Table S26: Bond Angles in ° for **cmw04bucobus**.

Atom	Atom	Atom	Angle/°
N1B	C1B	C2B	108.2(4)
N2B	C2B	C1B	110.4(4)
N2B	C3B	C4B	110.8(4)
N3B	C4B	C3B	107.6(4)
N2B	C5B	C6B	109.4(3)
N4B	C6B	C5B	107.9(4)
C8B	C7B	C9B	110.9(4)
C8B	C7B	C10B	110.3(4)
C8B	C7B	S1B	108.6(3)
C9B	C7B	C10B	109.7(4)
C9B	C7B	S1B	107.5(3)
C10B	C7B	S1B	109.8(4)
C12B	C11B	C14B	110.3(6)

Atom	Atom	Atom	Angle/°
C12B	C11B	S2B	106.7(4)
C13B	C11B	C12B	111.3(6)
C13B	C11B	C14B	110.6(5)
C13B	C11B	S2B	109.1(4)
C14B	C11B	S2B	108.8(5)
C16B	C15B	S3B	108.5(3)
C17B	C15B	C16B	111.2(4)
C17B	C15B	C18B	110.2(4)
C17B	C15B	S3B	109.3(3)
C18B	C15B	C16B	111.1(4)
C18B	C15B	S3B	106.5(4)
C1B	N1B	S3B	121.2(3)
C1B	N1B	Co1	112.6(3)
S3B	N1B	Co1	123.7(2)

Atom	Atom	Atom	Angle/°
C2B	N2B	Co1	106.5(3)
C3B	N2B	C2B	113.9(4)
C3B	N2B	C5B	111.6(4)
C3B	N2B	Co1	106.2(3)
C5B	N2B	C2B	111.6(4)
C5B	N2B	Co1	106.4(3)
C4B	N3B	S2B	119.0(4)
C4B	N3B	Co1	113.4(3)
S2B	N3B	Co1	126.3(3)
C6B	N4B	S1B	120.8(3)
C6B	N4B	Co1	113.1(3)
S1B	N4B	Co1	125.6(2)
N4B	S1B	C7B	108.8(2)
O1B	S1B	C7B	105.7(2)
O1B	S1B	N4B	107.1(2)
O1B	S1B	O2B	117.3(3)
O2B	S1B	C7B	105.9(2)
O2B	S1B	N4B	111.7(2)
N3B	S2B	C11B	107.9(2)
O3B	S2B	C11B	105.1(3)
O3B	S2B	N3B	108.9(2)
O3B	S2B	O4B	117.5(2)
O4B	S2B	C11B	106.4(2)
O4B	S2B	N3B	110.5(2)
N1B	S3B	C15B	108.9(2)
O5B	S3B	C15B	105.3(2)
O5B	S3B	N1B	106.6(2)
O5B	S3B	O6B	117.3(3)
O6B	S3B	C15B	106.0(2)
O6B	S3B	N1B	112.3(2)
N1A	C1A	C2A	108.9(5)
N2A	C2A	C1A	111.0(4)
N2A	C3A	C4A	111.1(5)
N3A	C4A	C3A	108.1(5)
N2A	C5A	C6A	109.7(4)
N4A	C6A	C5A	108.1(4)
C8A	C7A	C9A	110.9(5)
C8A	C7A	C10A	110.3(4)
C8A	C7A	S1A	108.6(3)
C9A	C7A	C10A	109.8(5)
C9A	C7A	S1A	107.4(4)
C10A	C7A	S1A	109.8(4)
C12A	C11A	C14A	110.2(6)
C12A	C11A	S2A	106.8(5)
C13A	C11A	C12A	111.2(6)
C13A	C11A	C14A	110.6(5)
C13A	C11A	S2A	109.1(4)
C14A	C11A	S2A	108.8(5)
C16A	C15A	S3A	108.5(3)
C17A	C15A	C16A	111.3(5)
C17A	C15A	C18A	110.1(5)
C17A	C15A	S3A	109.3(3)
C18A	C15A	C16A	111.1(4)
C18A	C15A	S3A	106.4(4)
C1A	N1A	S3A	121.1(4)
C1A	N1A	Co1	116.1(4)
S3A	N1A	Co1	121.4(4)

Atom	Atom	Atom	Angle/°
C2A	N2A	Co1	105.4(4)
C3A	N2A	C2A	114.7(5)
C3A	N2A	C5A	112.5(4)
C3A	N2A	Co1	103.9(4)
C5A	N2A	C2A	112.3(4)
C5A	N2A	Co1	107.1(4)
C4A	N3A	S2A	118.9(4)
C4A	N3A	Co1	115.7(4)
S2A	N3A	Co1	124.2(4)
C6A	N4A	S1A	120.3(4)
C6A	N4A	Co1	115.7(3)
S1A	N4A	Co1	123.9(4)
N4A	S1A	C7A	108.7(3)
O1A	S1A	C7A	105.8(3)
O1A	S1A	N4A	107.1(3)
O1A	S1A	O2A	117.3(3)
O2A	S1A	C7A	105.9(3)
O2A	S1A	N4A	111.7(3)
N3A	S2A	C11A	108.0(3)
O3A	S2A	C11A	105.1(3)
O3A	S2A	N3A	108.9(3)
O3A	S2A	O4A	117.5(3)
O4A	S2A	C11A	106.4(3)
O4A	S2A	N3A	110.4(3)
N1A	S3A	C15A	109.1(3)
O5A	S3A	C15A	105.2(3)
O5A	S3A	N1A	106.6(3)
O5A	S3A	O6A	117.3(3)
O6A	S3A	C15A	106.0(3)
O6A	S3A	N1A	112.2(3)
N1B	Co1	N2B	84.08(16)
N1B	Co1	N3B	117.5(2)
N3B	Co1	N2B	83.77(16)
N4B	Co1	N1B	119.76(19)
N4B	Co1	N2B	83.79(15)
N4B	Co1	N3B	119.4(2)
N1A	Co1	N2A	82.8(2)
N1A	Co1	N4A	116.6(3)
N3A	Co1	N1A	120.3(4)
N3A	Co1	N2A	83.8(2)
N3A	Co1	N4A	117.9(4)
N4A	Co1	N2A	80.7(2)
C26B	C25B	C24B	110.9(5)
C22B	C21B	C20B	111.8(4)
C30B	C29B	C28B	112.9(5)
C34B	C33B	C32B	111.8(5)
C24B	C23B	N5B	114.6(5)
C28B	C27B	N5B	116.6(5)
C32B	C31B	N5B	116.9(4)
C19B	C20B	C21B	109.2(4)
C23B	N5B	C27B	109.9(5)
C31B	N5B	C23B	109.3(5)
C31B	N5B	C27B	109.0(3)
C31B	N5B	C19B	112.2(4)
C19B	N5B	C23B	109.1(4)
C19B	N5B	C27B	107.3(4)
C23B	C24B	C25B	110.0(6)

Atom	Atom	Atom	Angle/°
C27B	C28B	C29B	110.0(7)
C31B	C32B	C33B	112.4(6)
C20B	C19B	N5B	116.6(4)
C26A	C25A	C24A	111.1(5)
C22A	C21A	C20A	111.8(4)
C30A	C29A	C28A	112.5(5)
C34A	C33A	C32A	111.9(5)
C24A	C23A	N5A	114.3(5)
C28A	C27A	N5A	116.3(5)
C32A	C31A	N5A	116.7(4)
C19A	C20A	C21A	109.2(4)

Atom	Atom	Atom	Angle/°
C23A	N5A	C27A	109.6(5)
C31A	N5A	C23A	109.5(5)
C31A	N5A	C27A	109.0(4)
C31A	N5A	C19A	112.2(5)
C19A	N5A	C23A	109.1(4)
C19A	N5A	C27A	107.4(4)
C23A	C24A	C25A	110.1(6)
C27A	C28A	C29A	110.0(7)
C31A	C32A	C33A	112.9(6)
C20A	C19A	N5A	116.5(4)

Table S27: Hydrogen Fractional Atomic Coordinates (×10⁴) and Equivalent Isotropic Displacement Parameters (Å²×10³) for **cmw04bucobus**. U_{eq} is defined as 1/3 of the trace of the orthogonalised U_{ij}.

Atom	x	y	z	U_{eq}
H1BA	9639	4290	4914	43
H1BB	9750	3385	4318	43
H2BA	9020	2012	4682	42
H2BB	9517	2439	5361	42
H3BA	7747	2344	5710	39
H3BB	8303	1398	5536	39
H4BA	7846	1433	4375	48
H4BB	7186	1322	4763	48
H5BA	9167	4176	5915	29
H5BB	8809	3188	6321	29
H6BA	7753	4162	6136	30
H6BB	8324	5149	6399	30
H8BA	8500	7337	4423	41
H8BB	9039	6530	4912	41
H8BC	9184	7911	4851	41
H9BA	8529	9370	5451	52
H9BB	7878	8934	5785	52
H9BC	7838	8926	4973	52
H10A	9089	6556	6147	44
H10B	8635	7472	6503	44
H10C	9286	7926	6175	44
H12A	4831	3393	4007	83
H12B	5196	2392	3620	83
H12C	5237	3742	3396	83
H13A	5988	5145	4141	81
H13B	6441	4707	4840	81
H13C	5617	4842	4783	81
H14A	5517	2726	5145	80
H14B	6344	2610	5220	80
H14C	5854	1712	4742	80
H16A	8129	2793	2294	47
H16B	7793	3787	2711	47
H16C	8225	2731	3110	47
H17A	9511	2719	3254	50
H17B	9915	3696	2887	50
H17C	9475	2696	2442	50
H18A	8828	4301	1729	49
H18B	9255	5287	2198	49
H18C	8424	5285	2090	49

Atom	x	y	z	U_{eq}
H1AA	9767	3443	4355	39
H1AB	9201	2409	4217	39
H2AA	9522	2407	5375	36
H2AB	9511	3817	5416	36
H3AA	8308	1415	5563	39
H3AB	8366	1568	4771	39
H4AA	7188	1370	4789	45
H4AB	7213	2269	5418	45
H5AA	8840	3180	6347	29
H5AB	8018	3312	6113	29
H6AA	8401	5179	6431	31
H6AB	9042	5078	6016	31
H8AA	8428	7619	4358	39
H8AB	8918	6673	4799	39
H8AC	9148	8026	4800	39
H9AA	8324	9538	5274	51
H9AB	7763	9033	5707	51
H9AC	7645	8876	4895	51
H10D	9155	6979	6105	44
H10E	8660	7848	6443	44
H10F	9239	8375	6040	44
H12D	4849	3798	3705	75
H12E	5233	2767	3360	75
H12F	5414	4115	3231	75
H13D	6189	5243	4158	78
H13E	6344	4690	4910	78
H13F	5572	5086	4594	78
H14D	5251	2986	4906	71
H14E	6047	2606	5111	71
H14F	5550	1902	4527	71
H16D	8100	3121	2169	42
H16E	7798	3963	2699	42
H16F	8222	2802	2965	42
H17D	9499	2771	3104	45
H17E	9913	3831	2820	45
H17F	9455	2957	2298	45
H18D	8829	4723	1737	45
H18E	9271	5583	2281	45
H18F	8440	5604	2180	45
H25A	5353	7521	4243	102
H25B	6168	7612	4522	102
H21A	8961	8104	3368	39
H21B	8942	8954	2721	39
H29A	5905	5122	2034	81
H29B	5974	6011	1422	81
H33A	6778	11889	2312	56
H33B	6709	11841	1497	56
H23A	6976	7289	3583	44
H23B	6863	8634	3776	44
H27A	6005	7578	2181	41
H27B	6607	7828	1742	41
H31A	6064	9584	2561	39
H31B	6761	10136	2969	39
H20A	7992	9094	3687	41
H20B	7984	10001	3066	41
H22A	9228	10563	3448	69
H22B	9807	9558	3606	69

Atom	x	y	z	U_{eq}
H22C	9238	9723	4098	69
H24A	5829	6933	3318	66
H24B	5645	8287	3143	66
H26A	5533	9632	3905	113
H26B	6155	9545	4536	113
H26C	5373	9315	4650	113
H28A	6734	6006	2740	60
H28B	7213	6184	2161	60
H30A	6918	4956	1168	151
H30B	6260	4106	1145	151
H30C	6868	4079	1791	151
H32A	6455	9765	1540	54
H32B	7223	10081	1909	54
H34A	5536	11123	1504	95
H34B	5670	12489	1680	95
H34C	5636	11560	2281	95
H19A	7799	7517	2869	33
H19B	7729	8470	2271	33
H25C	5280	7695	4089	104
H25D	6076	7286	4230	104
H21C	8959	8282	3243	39
H21D	8847	9202	2623	39
H29C	6428	4658	2274	74
H29D	5835	5482	1869	74
H33C	6572	11706	1611	72
H33D	6184	10546	1287	72
H23C	6916	8148	3865	44
H23D	6866	9466	3577	44
H27C	6728	6488	3101	42
H27D	6057	6983	2618	42
H31C	6576	8664	1804	40
H31D	5987	8980	2247	40
H20C	7995	9242	3677	41
H20D	7850	9964	2973	41
H22D	9127	10758	3368	71
H22E	9736	9802	3506	71
H22F	9175	9892	4011	71
H24C	5636	8339	3124	72
H24D	5750	9509	3581	72
H26D	6317	9162	4810	141
H26E	5918	8207	5198	141
H26F	5495	9266	4790	141
H28C	7279	6074	2200	55
H28D	6747	6861	1687	55
H30D	6477	5316	916	146
H30E	6042	4187	1084	146
H30F	6865	4230	1328	146
H32C	7213	10310	2215	52
H32D	6673	10603	2719	52
H34D	5257	11359	1529	109
H34E	5686	12267	2053	109
H34F	5532	10964	2300	109
H19C	7806	7451	3088	34
H19D	7730	8115	2371	34

4-5^{Mg}

EMORY UNIVERSITY | X-ray Crystallography Center

Submitted by: **Christian Wallen**
Emory University
Solved by: **John Bacsa**
Sample ID: **MgCoBus**

Crystal Data and Experimental

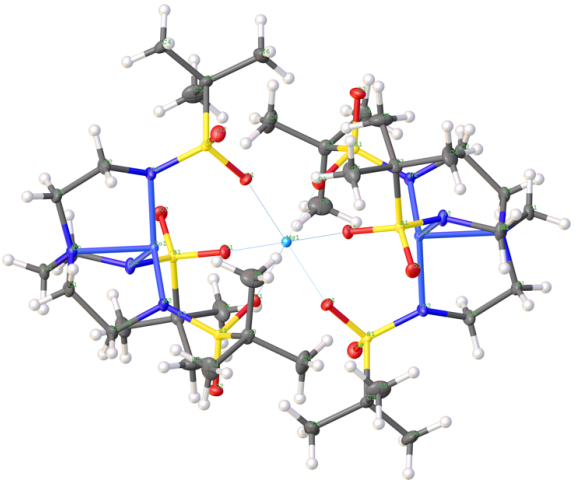

Experimental. Single violet prism-shaped crystals of (**MgCoBus**) were recrystallised from a mixture of CH_2Cl_2 and methanol by vapor diffusion. A suitable crystal (0.32×0.24×0.21) was selected and mounted on a MITIGEN holder with paratone oil on a Bruker APEX-II CCD diffractometer. The crystal was cooled to T = 100(2) K during data collection. The structure was solved with the **ShelXT** (Sheldrick, 2015) structure solution program using combined Patterson and dual-space recycling methods and by using **Olex2** (Dolomanov et al., 2009) as the graphical interface. The crystal structure was refined with version 2014/7 of **ShelXL** (Sheldrick, 2008) using Least Squares minimisation.

Crystal Data. $C_{36}H_{78}Co_2MgN_8O_{12}S_6$, M_r = 1149.59, trigonal, R-3 (No. 148), a = 12.684(2) Å, b = 12.684(2) Å, c = 27.867(6) Å, α = 90°, β = 90°, γ = 120°, V = 3882.7(16) Å^3, T = 100(2) K, Z = 3, Z' = 1/6, μ(MoK$_\alpha$) = 0.957, 39376 reflections measured, 7192 unique (R_{int} = 0.0362) which were used in all calculations. The final wR_2 was 0.0856 (all data) and R_1 was 0.0325 (I > 2σ(I)).

Compound	**MgCoBus**
Formula	$C_{36}H_{78}Co_2MgN_8O_{12}S_6$
$D_{calc.}$/ g cm^{-3}	1.475
μ/mm^{-1}	0.957
Formula Weight	1149.59
Colour	violet
Shape	prism
Max Size/mm	0.32
Mid Size/mm	0.24
Min Size/mm	0.21
T/K	100(2)
Crystal System	trigonal
Space Group	R-3
a/Å	12.684(2)
b/Å	12.684(2)
c/Å	27.867(6)
α/°	90
β/°	90
γ/°	120
V/Å^3	3882.7(16)
Z	3
Z'	1/6
Θ_{min}/°	2.361
Θ_{max}/°	45.276
Measured Refl.	39376
Independent Refl.	7192
Reflections Used	6105
R_{int}	0.0362
Parameters	115
Restraints	6
Largest Peak	1.467
Deepest Hole	-0.810
GooF	1.060
wR_2 (all data)	0.0856
wR_2	0.0797
R_1 (all data)	0.0418
R_1	0.0325
CCDC #	1434438

Structure Quality Indicators

Reflections:	d min	0.50	I/σ	24.5	Rint	3.62%	complete	99%
Refinement:	Shift	0.003	Max Peak	1.5	Min Peak	-0.8	GooF	1.060

A violet prism-shaped crystal with dimensions 0.32×0.24×0.21 mm was mounted on a MITIGEN holder with paratone oil.X-ray diffraction data were collected using a Bruker APEX-II CCD diffractometer equipped with an Oxford Cryosystems low-temperature apparatus operating at T = 100(2) K.

Data were measured using ϕ and ω scans and MoK$_\alpha$ radiation (fine-focus sealed tube, 45 kV, 35 mA). The total number of runs and images was based on the strategy calculation from the program **APEX2** (Bruker, 2014). The maximum resolution achieved was was Θ = 45.27°.

Unit cell indexing was performed by using the **APEX2** (Bruker, 2014) software and refined using **SAINT** (Bruker, V8.34A, 2013) on 9896 reflections, 25% of the observed reflections. Data reduction, scaling and absorption corrections were performed using **SAINT** (Bruker, V8.34A, 2013) and **SADABS-2014/5** (Bruker,2014/5) was used for absorption correction. wR_2(int) was 0.0848 before and 0.0460 after correction. The Ratio of minimum to maximum transmission is 0.8857. The $\lambda/2$ correction factor is 0.00150. This software which corrects for Lorentz polarisation. The final completeness is 99.4% out to 45.276° in Θ. The absorption coefficient (μ) of this material is 0.957 mm^{-1} and the minimum and maximum transmissions are 0.6633 and 0.7489.

The structure was solved in the space group P1 with the **ShelXT** (Sheldrick, 2015) structure solution program using combined Patterson and dual-space recycling methods. The space group R-3 (# 148) was determined by the **ShelXT** (Sheldrick, 2015) structure solution program. The crystal structure was refined by Least Squares using version 2014/7 of **ShelXL** (Sheldrick, 2008). All non-hydrogen atoms were refined anisotropically. Hydrogen atom positions were calculated geometrically and refined using the riding model. The value of Z' is 0.16667.

Data Plots: Diffraction Data

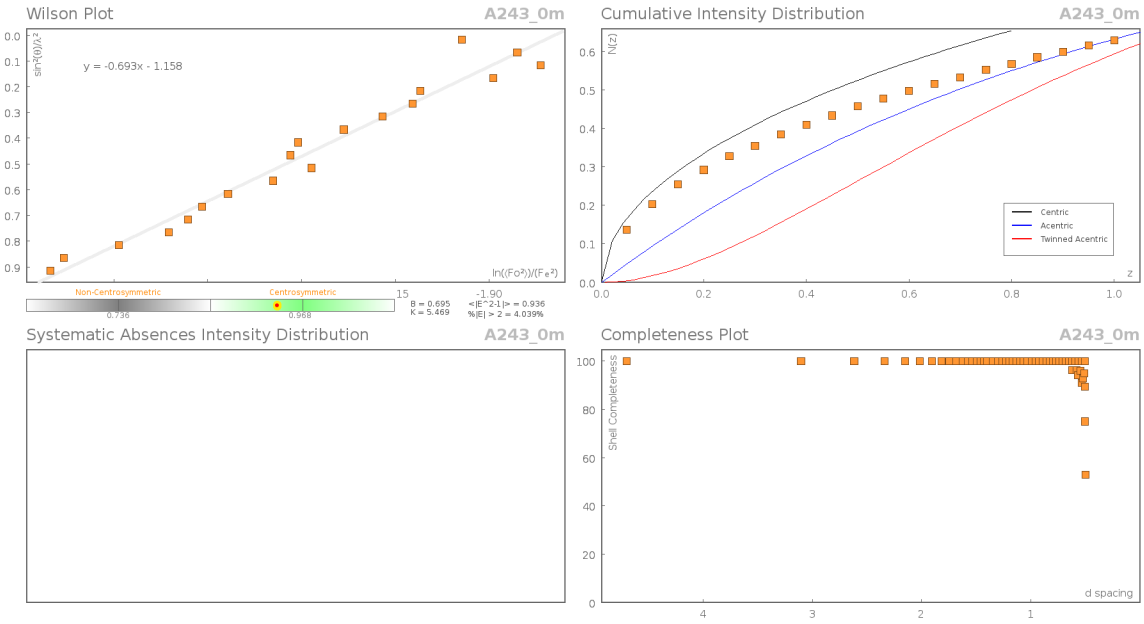

Data Plots: Refinement and Data

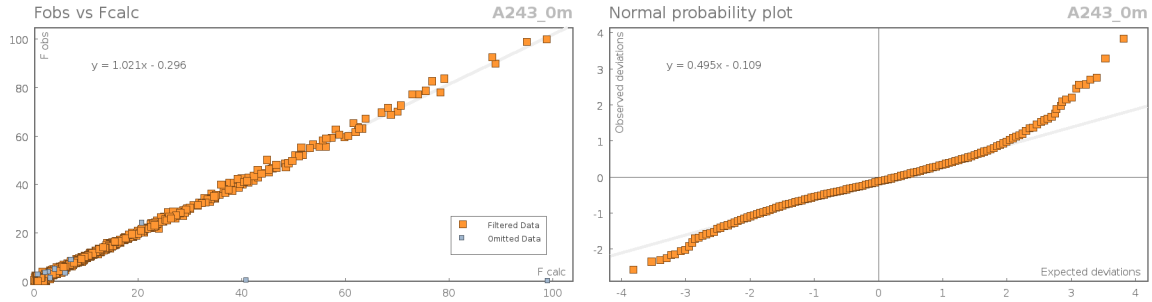

Reflection Statistics

Total reflections (after filtering)	39443	Unique reflections	7192
Completeness	0.994	Mean I/σ	24.51
hklsub>max</sub> collected	(25, 25, 48)	hklsub>min</sub> collected	(-24, -24, -54)
hkl_{max} used	(12, 25, 54)	hkl_{min} used	(-25, 0, 0)
Lim d_{max} collected	100.0	Lim d_{min} collected	0.36
d_{max} used	10.22	d_{min} used	0.5
Friedel pairs	5706	Friedel pairs merged	1
Inconsistent equivalents	0	R_{int}	0.0362
R_{sigma}	0.0271	Intensity transformed	0
Omitted reflections	0	Omitted by user (OMIT hkl)	67
Multiplicity	(11601, 7142, 2536, 1280, 166)	Maximum multiplicity	15
Removed systematic absences	0	Filtered off (Shel/OMIT)	0

Images of the Crystal on the Diffractometer

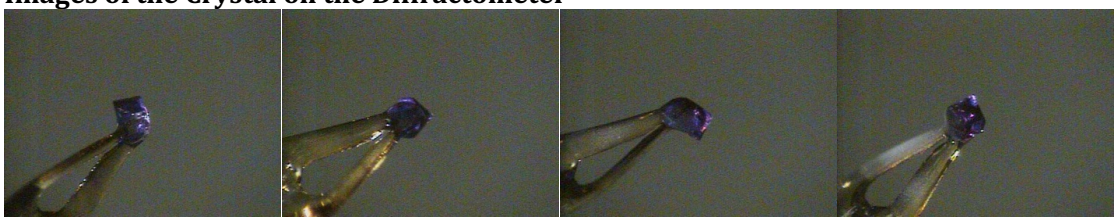

Table S28: Fractional Atomic Coordinates (×10⁴) and Equivalent Isotropic Displacement Parameters (Å²×10³) for **A243_0m**. U_{eq} is defined as 1/3 of the trace of the orthogonalised U_{ij}.

Atom	x	y	z	U_{eq}
Co1	10000	10000	3776.3(2)	7.76(3)
S1	7905.3(2)	10125.5(2)	4196.7(2)	8.52(3)
Mg1	10000	10000	5000	7.35(8)
O1	8670.3(4)	10104.4(5)	4588.3(2)	10.92(7)
O2	6675.2(5)	9104.6(5)	4182.2(2)	15.15(8)
N1	10000	10000	3020.3(3)	10.42(12)
N2	8656.8(5)	10319.6(6)	3723.6(2)	11.79(8)
C1	9115.9(6)	10383.2(7)	2878.7(2)	13.71(10)
C2	8086.2(6)	9942.6(8)	3246.8(2)	15.81(11)
C3	7791.7(6)	11483.1(6)	4298.8(3)	13.65(10)
C6	7130.4(10)	11343.4(10)	4773.6(3)	24.75(16)
C4	7069.4(10)	11600.5(9)	3883.3(3)	24.26(16)
C5	9081.2(9)	12566.6(8)	4322.4(4)	27.57(18)

Table S29: Anisotropic Displacement Parameters (×10⁴) **A243_0m**. The anisotropic displacement factor exponent

takes the form: $-2\pi^2[h^2a^{*2} \times U_{11} + \ldots + 2hka^* \times b^* \times U_{12}]$

Atom	U_{11}	U_{22}	U_{33}	U_{23}	U_{13}	U_{12}
Co1	8.37(4)	8.37(4)	6.55(5)	0	0	4.19(2)
S1	7.79(5)	10.11(5)	8.11(6)	0.16(4)	-0.82(4)	4.82(4)
Mg1	7.60(11)	7.60(11)	6.83(19)	0	0	3.80(6)
O1	11.43(16)	13.89(17)	9.47(17)	-0.03(13)	-2.53(12)	7.84(14)
O2	9.28(16)	15.26(19)	16.0(2)	0.50(15)	-1.88(14)	2.44(14)
N1	11.63(19)	11.63(19)	8.0(3)	0	0	5.82(9)
N2	11.34(18)	18.6(2)	7.75(18)	-1.17(15)	-0.86(14)	9.24(17)
C1	16.8(2)	18.9(3)	8.2(2)	1.01(18)	-1.02(17)	10.9(2)
C2	13.3(2)	25.9(3)	9.3(2)	-2.2(2)	-2.58(17)	10.6(2)
C3	17.3(2)	15.2(2)	13.1(2)	1.14(18)	0.23(18)	11.7(2)
C6	37.5(4)	33.5(4)	17.1(3)	1.6(3)	6.7(3)	28.1(4)
C4	35.1(4)	31.8(4)	19.5(3)	1.3(3)	-4.9(3)	27.0(4)
C5	25.2(4)	12.0(3)	42.9(5)	-1.0(3)	-2.6(3)	7.4(3)

Table S30: Bond Lengths in Å for **A243_0m**.

Atom	Atom	Length/Å
Co1	N1	2.1069(10)
Co1	N2[1]	1.9440(6)
Co1	N2	1.9440(7)
Co1	N2[2]	1.9440(7)
S1	O1	1.4694(5)
S1	O2	1.4465(6)
S1	N2	1.5725(6)
S1	C3	1.8208(7)
Mg1	O1[3]	2.0981(5)
Mg1	O1	2.0981(5)
Mg1	O1[4]	2.0981(5)
Mg1	O1[5]	2.0981(5)
Mg1	O1[1]	2.0981(5)
Mg1	O1[2]	2.0981(5)
N1	C1[1]	1.4814(8)
N1	C1[2]	1.4814(8)
N1	C1	1.4814(7)
N2	C2	1.4735(9)
C1	C2	1.5300(10)
C3	C6	1.5290(11)
C3	C4	1.5291(11)
C3	C5	1.5232(12)

--------•

[1]2-Y,1+X-Y,+Z; [2]1+Y-X,2-X,+Z; [3]2-X,2-Y,1-Z; [4]1-Y+X,+X,1-Z [5]+Y,1-X+Y,1-Z

Table S31: Bond Angles in ° for **A243_0m**.

Atom	Atom	Atom	Angle/°
N2	Co1	N1	85.662(17)
N2[1]	Co1	N1	85.662(17)
N2[2]	Co1	N1	85.662(17)
N2	Co1	N2[1]	119.433(5)
N2[1]	Co1	N2[2]	119.434(5)
N2	Co1	N2[2]	119.434(4)
O1	S1	N2	105.75(3)
O1	S1	C3	105.45(3)
O2	S1	O1	115.52(3)
O2	S1	N2	114.51(3)
O2	S1	C3	106.92(3)
N2	S1	C3	108.14(3)
O1[3]	Mg1	O1[2]	180.0
O1[4]	Mg1	O1[5]	92.95(2)
O1[3]	Mg1	O1[5]	92.95(2)
O1[5]	Mg1	O1[1]	180.0
O1[3]	Mg1	O1[1]	87.05(2)
O1[2]	Mg1	O1[1]	92.95(2)
O1[3]	Mg1	O1	87.05(2)
O1[3]	Mg1	O1[4]	92.95(2)
O1[4]	Mg1	O1	180.0
O1[2]	Mg1	O1	92.95(2)
O1[1]	Mg1	O1	92.95(2)
O1[4]	Mg1	O1[1]	87.05(2)
O1[2]	Mg1	O1[5]	87.05(2)
O1[5]	Mg1	O1	87.05(2)
O1[2]	Mg1	O1[4]	87.05(2)
S1	O1	Mg1	165.08(3)
C1[1]	N1	Co1	105.45(4)
C1	N1	Co1	105.45(4)
C1[2]	N1	Co1	105.45(4)
C1[2]	N1	C1	113.17(4)
C1[1]	N1	C1	113.18(4)
C1[2]	N1	C1[1]	113.18(4)
S1	N2	Co1	115.45(3)
C2	N2	Co1	109.88(4)
C2	N2	S1	122.97(5)
N1	C1	C2	110.45(6)

Atom	Atom	Atom	Angle/°
N2	C2	C1	107.16(6)
C6	C3	S1	108.90(5)
C6	C3	C4	110.24(7)
C4	C3	S1	107.96(5)
C5	C3	S1	107.64(5)
C5	C3	C6	110.27(8)
C5	C3	C4	111.73(7)

--------•

[1]1+Y-X,2-X,+Z; [2]2-Y,1+X-Y,+Z; [3]+Y,1-X+Y,1-Z; [4]2-X,2-Y,1-Z [5]1-Y+X,+X,1-Z

Table S32: Hydrogen Fractional Atomic Coordinates (×10⁴) and Equivalent Isotropic Displacement Parameters (Å²×10³) for **A243_0m**. U_{eq} is defined as 1/3 of the trace of the orthogonalised U_{ij}.

Atom	x	y	z	U_{eq}
H1A	8805(13)	10072(13)	2575(3)	20.4(16)
H1B	9532(13)	11230(7)	2853(5)	20.4(16)
H2A	7630(12)	9096(7)	3229(5)	20.4(16)
H2B	7599(11)	10276(12)	3169(5)	20.4(16)
H6A	7616	11299	5038	37
H6B	6335	10596	4766	37
H6C	7016	12045	4821	37
H4A	6290	10842	3851	36
H4B	7535	11760	3585	36
H4C	6921	12275	3947	36
H5A	9502	12634	4019	41
H5B	9523	12450	4586	41
H5C	9049	13313	4377	41

4-5^{Ca}

EMORY UNIVERSITY | X-ray Crystallography Center

Submitted by: **Christian Wallen**
Emory University
Solved by: **John Bacsa**
Sample ID: **CMW-03-020**

Crystal Data and Experimental

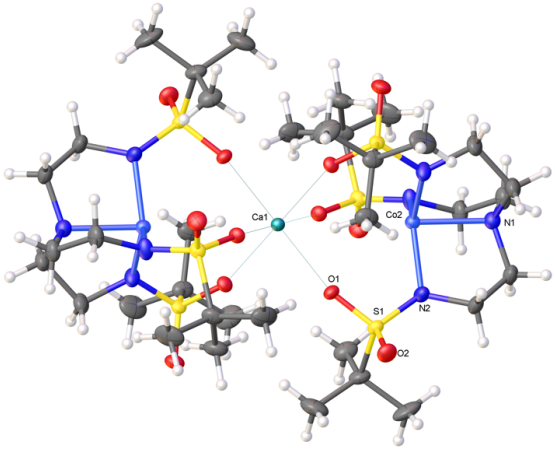

Experimental. Single violet prism-shaped crystals of (**CMW-03-020**) were recrystallised from a mixture of diethyl ether and CH_2Cl_2 by slow evaporation. A suitable crystal (0.41×0.18×0.11 mm) was selected and mounted on a loop with paratone oil on a Bruker APEX-II CCD diffractometer. The crystal was kept at T = 100(2) K during data collection. Using **Olex2** (Dolomanov et al., 2009), the structure was solved with the **ShelXT** (Sheldrick, 2015) structure solution program, using the Charge Flipping solution method. The model was refined with version 2013-4 of **ShelXL** (Sheldrick, 2008) using Least Squares minimisation.

Crystal Data. $C_{36}H_{78}CaCo_2N_8O_{12}S_6$, M_r = 1165.36, trigonal, R-3 (No. 148), a = 12.601(3) Å, b = 12.601(3) Å, c = 29.273(8) Å, α = 90°, β = 90°, γ = 120°, V = 4025(2) Å^3, T = 100(2) K, Z = 3, Z' = 0.16667, μ(MoK$_\alpha$) = 1.007, 17386 reflections measured, 4461 unique (R_{int} = 0.0389) which were used in all calculations. The final wR_2 was 0.1085 (all data) and R_1 was 0.0409 (I > 2(I)).

Compound	**CMW-03-020**
Formula	$C_{36}H_{78}CaCo_2N_8O_{12}S_6$
$D_{calc.}$/ g cm^{-3}	1.442
μ/mm^{-1}	1.007
Formula Weight	1165.36
Colour	violet
Shape	prism
Max Size/mm	0.41
Mid Size/mm	0.18
Min Size/mm	0.11
T/K	100(2)
Crystal System	trigonal
Space Group	R-3
a/Å	12.601(3)
b/Å	12.601(3)
c/Å	29.273(8)
α/°	90
β/°	90
γ/°	120
V/Å^3	4025(2)
Z	3
Z'	1/6
Θ_{min}/°	2.087
Θ_{max}/°	37.068
Measured Refl.	17386
Independent Refl.	4461
Reflections Used	3518
R_{int}	0.0389
Parameters	118
Restraints	45
Largest Peak	0.906
Deepest Hole	-0.604
GooF	1.032
wR_2 (all data)	0.1085
wR_2	0.0988
R_1 (all data)	0.0580
R_1	0.0409
CCDC #	1434436

Structure Quality Indicators

Reflections:	d min	0.59	I/σ	16.9	Rint	3.89%	complete 97%
Refinement:	Shift	-0.002	Max Peak	0.9	Min Peak	-0.6	GooF 1.032

A violet prism-shaped crystal with dimensions 0.41×0.18×0.11mm was mounted on a loop with paratone oil. Data were collected using a Bruker APEX-II CCD diffractometer equipped with an Oxford Cryosystems low-temperature apparatus operating at T = 100(2) K.

Data were measured using ϕ and ω scans with a narrow frame width with MoK_α radiation (fine-focus sealed tube, 45 kV, 35 mA). The total number of runs and images was based on the strategy calculation from the program **APEX2** (Bruker). The actually achieved resolution was Θ = 37.068°.

Cell parameters were retrieved using the **SAINT** (Bruker, V8.34A, 2013) software and refined using **SAINT** (Bruker, V8.34A, 2013) on 9971 reflections, 57% of the observed reflections. Data reduction was performed using the **SAINT** (Bruker, V8.34A, 2013) software which corrects for Lorentz polarisation. The final completeness is 99.70 out to 37.068 in Θ. The absorption coefficient (μ) of this material is 1.007 mm^{-1} and the minimum and maximum transmissions are 0.3299 and 0.4389.

The structure was solved in the space group R-3 (# 148) by Charge Flipping using the **ShelXT** (Sheldrick, 2015) structure solution program and refined by Least Squares using version 2013-4 of **ShelXL** (Sheldrick, 2008). All non-hydrogen atoms were refined anisotropically. The value of Z' is 1/6.

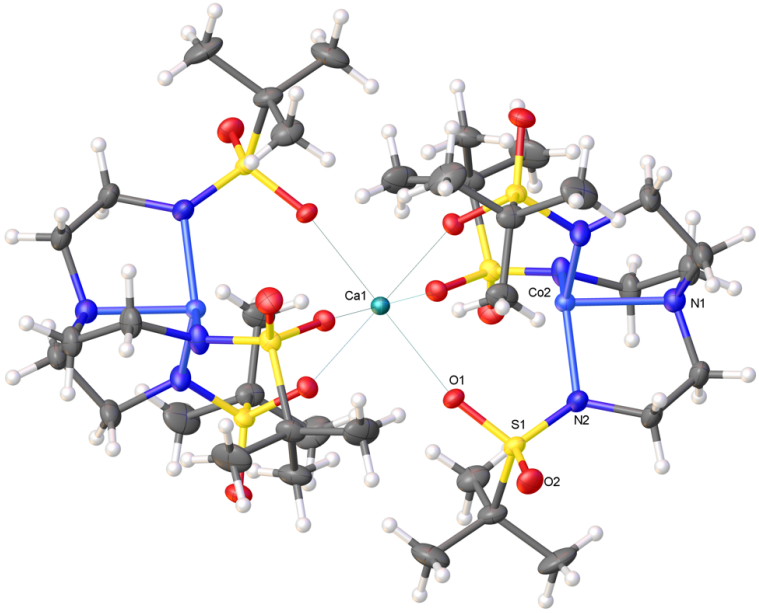

Figure S22: Plot of the dimeric Co^{2+} complex [$C_{36}H_{78}CaCo_2N_8O_{12}S_6$]. The molecule resides on a 3-fold rotation axis through the atoms Ca(1), Co(2) and N(1).

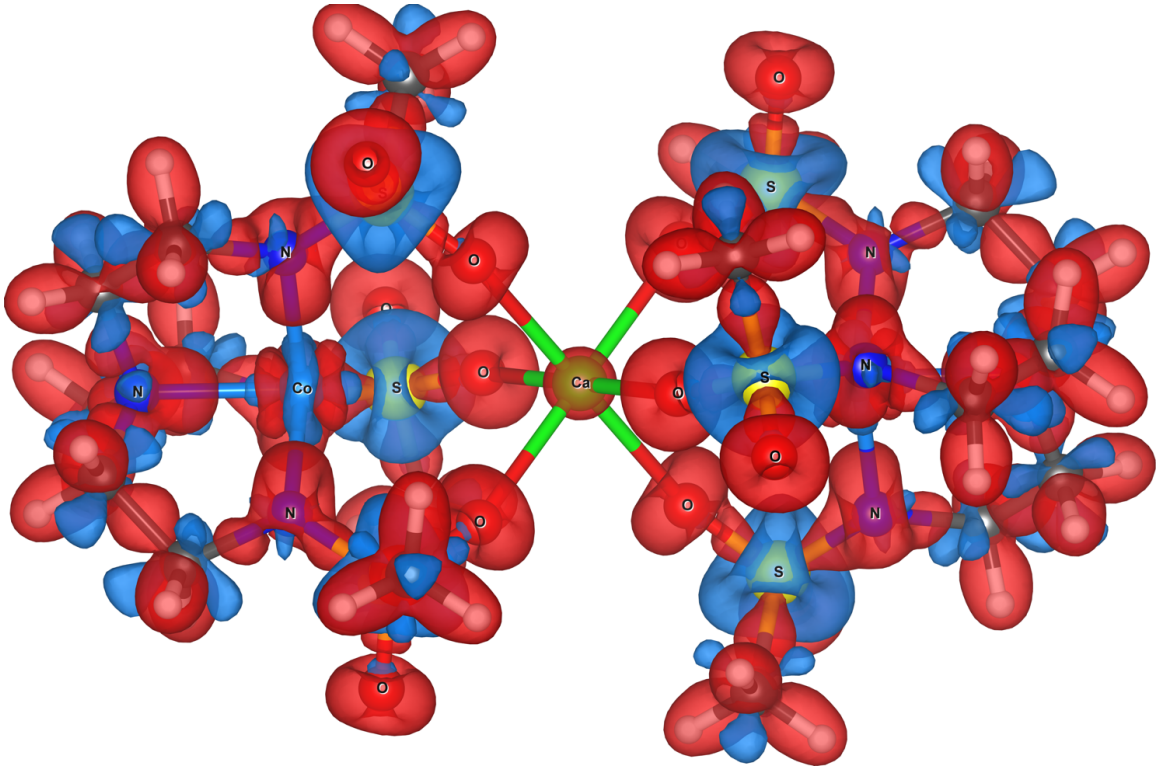

Figure S23: Positive and negative deformation density isosurfaces (0.01 e $Å^{-3}$) of the dimeric Co^{2+} complex $[C_{36}H_{78}CaCo_2N_8O_{12}S_6]$ from refinements with the predicted multipolar parameters. Charge concentrations are shown in red and depletions in blue. There are concentrations of charge corresponding to nitrogen and lone pair electrons. The density about Ca^{2+} is spherical and lobes of electron density from N to

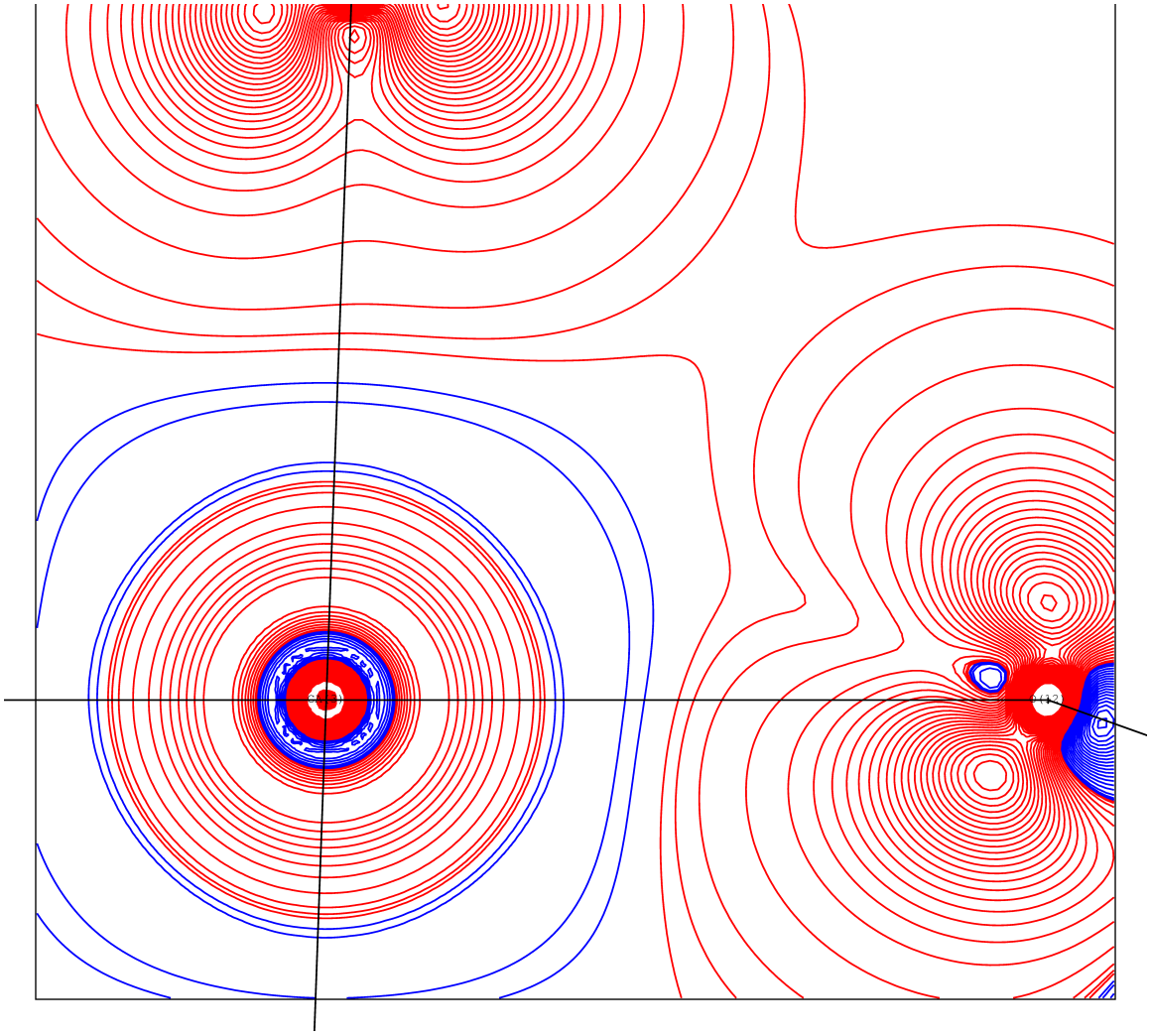

Figure S24: A deformation ED maps in the plane of the atoms Ca(1), O(1) and O(3) as calculated from the refinements with the theoretically predicted multipolar parameters. Red lines represent positive contours and blue lines negative contours. Contours are drawn at 0.1 e $Å^{-3}$ intervals.

Data Plots: Diffraction Data

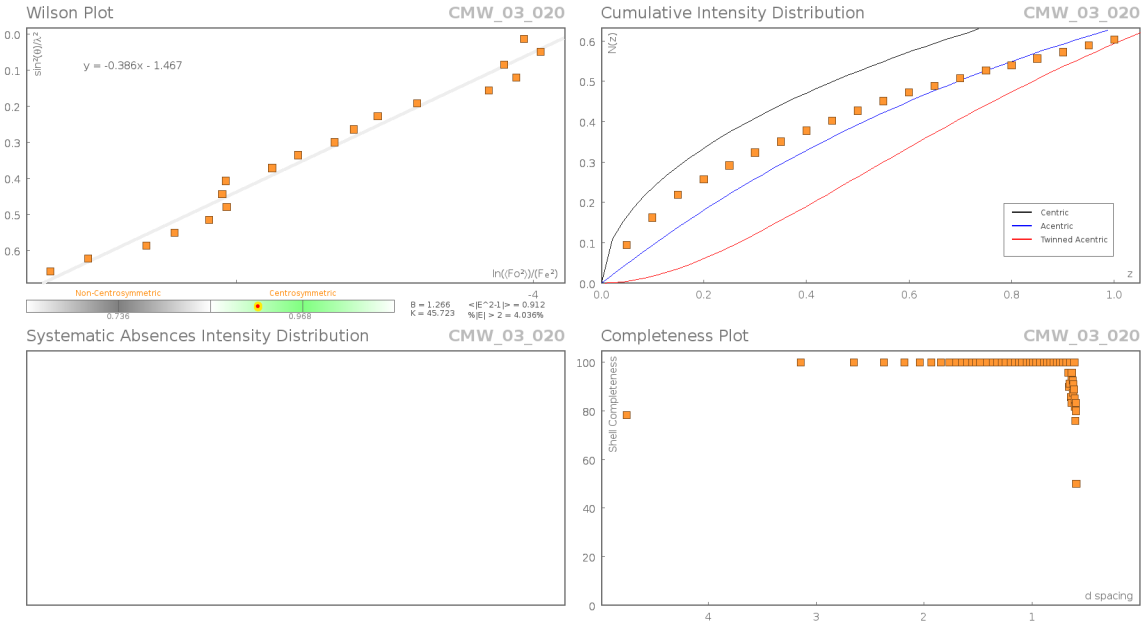

Data Plots: Refinement and Data

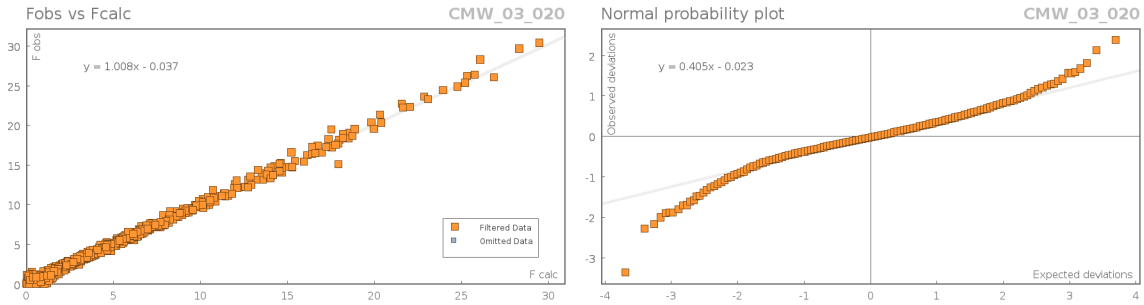

Reflection Statistics

Total reflections (after filtering)	17386	Unique reflections	4461
Completeness	0.972	Mean I/σ	16.87
hklsub>max</sub> collected	(17, 18, 49)	hklsub>min</sub> collected	(-21, -17, -44)
hkl_{max} used	(10, 21, 49)	hkl_{min} used	(-21, 0, 0)
Lim d_{max} collected	100.0	Lim d_{min} collected	0.36
d_{max} used	9.76	d_{min} used	0.59
Friedel pairs	3041	Friedel pairs merged	1
Inconsistent equivalents	0	R_{int}	0.0389
R_{sigma}	0.0407	Intensity transformed	0
Omitted reflections	0	Omitted by user (OMIT hkl)	0
Multiplicity	(9146, 3694, 284)	Maximum multiplicity	11
Removed systematic absences	0	Filtered off (Shel/OMIT)	0

Images of the Crystal on the Diffractometer

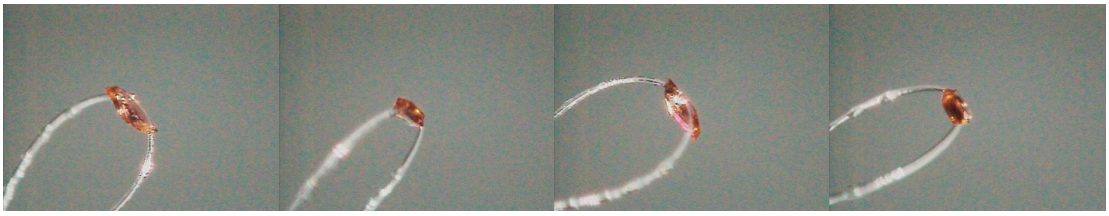

Table S33: Fractional Atomic Coordinates (×10⁴) and Equivalent Isotropic Displacement Parameters (Å²×10³) for **CMW_03_020**. U_{eq} is defined as 1/3 of the trace of the orthogonalised U_{ij}.

Atom	x	y	z	U_{eq}
C1	1273.4(18)	871(2)	2922.5(6)	26.6(4)
C2	1895(2)	1909.4(19)	3271.4(5)	27.5(4)
C1B	1073(4)	1229(3)	2982.7(18)	26.6(4)
C2B	2214(4)	1551(7)	3267.3(10)	27.5(4)
C3	3679.8(13)	1840.1(14)	4274.0(5)	25.0(3)
C4	4514.4(17)	2303.0(19)	3853.8(7)	43.0(4)
C5	3189.9(16)	474.9(16)	4344.4(6)	31.1(3)
C6	4349.3(17)	2558.7(19)	4701.6(7)	40.9(4)
N1	0	0	3072.1(6)	22.0(3)
N2	1676.0(11)	1322.6(12)	3735.1(3)	24.2(2)
O1	1561.3(8)	1499.2(9)	4557.4(3)	17.64(16)
O2	2890.9(10)	3381.5(9)	4120.4(3)	25.3(2)
S1	2394.8(3)	2078.0(3)	4168.6(2)	17.47(7)
Ca1	0	0	5000	13.52(10)
Co2	0	0	3787.8(2)	16.00(7)

Table S34: Anisotropic Displacement Parameters (×10⁴) **CMW_03_020**. The anisotropic displacement factor exponent takes the form: $-2\pi^2[h^2a^{*2} \times U_{11} + \ldots + 2hka^* \times b^* \times U_{12}]$

Atom	U_{11}	U_{22}	U_{33}	U_{23}	U_{13}	U_{12}
C1	28.2(9)	28.3(10)	17.2(6)	1.8(6)	3.4(5)	9.6(7)
C2	26.1(9)	29.6(10)	18.6(6)	3.2(6)	4.9(5)	7.7(7)
C1B	28.2(9)	28.3(10)	17.2(6)	1.8(6)	3.4(5)	9.6(7)
C2B	26.1(9)	29.6(10)	18.6(6)	3.2(6)	4.9(5)	7.7(7)
C3	16.2(6)	23.0(6)	34.8(6)	0.3(5)	5.2(5)	9.0(5)
C4	26.5(8)	40.6(10)	59.8(11)	12.8(8)	24.4(8)	15.3(8)
C5	27.3(7)	27.8(8)	43.7(8)	3.5(6)	8.3(6)	18.0(6)
C6	25.0(8)	42.3(10)	56.2(10)	-15.3(8)	-15.9(7)	17.6(8)
N1	22.9(6)	22.9(6)	20.1(7)	0	0	11.5(3)
N2	19.6(5)	25.1(6)	18.2(4)	-1.1(4)	2.1(3)	4.1(4)
O1	14.9(4)	18.6(4)	18.4(3)	2.7(3)	3.7(3)	7.6(3)
O2	26.9(5)	15.7(4)	29.1(4)	4.6(3)	2.9(4)	7.4(4)
S1	14.96(13)	14.96(14)	19.05(12)	0.88(9)	3.00(9)	4.91(11)
Ca1	12.99(15)	12.99(15)	14.57(19)	0	0	6.50(7)
Co2	15.35(10)	15.35(10)	17.31(12)	0	0	7.67(5)

Table S35: Bond Lengths in Å for **CMW_03_020**.

Atom	Atom	Length/Å
C1	C2	1.531(3)
C1	N1	1.4866(19)
C2	N2	1.5035(19)
C1B	C2B	1.531(3)
C1B	N1	1.483(3)

Atom	Atom	Length/Å
C2B	N2	1.491(3)
C3	C4	1.532(2)
C3	C5	1.523(2)
C3	C6	1.528(2)
C3	S1	1.8145(16)

Atom	Atom	Length/Å
N1	Co2	2.0949(19)
N2	S1	1.5731(12)
N2	Co2	1.9343(13)
O1	S1	1.4712(9)
O1	Ca1	2.3241(10)
O2	S1	1.4428(11)
Ca1	O1[1]	2.3240(10)
Ca1	O1[2]	2.3240(10)
Ca1	O1[3]	2.3240(10)
Ca1	O1[4]	2.3240(10)
Ca1	O1[5]	2.3240(10)
Ca1	Co2	3.5486(10)
Ca1	Co2[2]	3.5486(10)
Co2	N2[1]	1.9343(13)
Co2	N2[3]	1.9343(13)

-------•

[1]+Y-X,-X,+Z; [2]-X,-Y,1-Z; [3]-Y,+X-Y,+Z; [4]-Y+X,+X,1-Z; [5]+Y, X+Y,1-Z

Table S36: Bond Angles in ° for **CMW_03_020**.

Atom	Atom	Atom	Angle/°
N1	C1	C2	109.66(15)
N2	C2	C1	106.99(15)
N1	C1B	C2B	115.2(4)
N2	C2B	C1B	99.9(3)
C4	C3	S1	107.46(11)
C5	C3	C4	110.62(13)
C5	C3	C6	110.51(14)
C5	C3	S1	108.56(10)
C6	C3	C4	111.20(15)
C6	C3	S1	108.38(11)
C1	N1	Co2	107.14(9)
C1B	N1	Co2	100.2(2)
C2	N2	S1	121.46(11)
C2	N2	Co2	110.41(10)
C2B	N2	S1	123.7(2)
C2B	N2	Co2	115.8(2)
S1	N2	Co2	120.48(6)
S1	O1	Ca1	159.82(6)
N2	S1	C3	109.19(7)
O1	S1	C3	105.14(6)
O1	S1	N2	105.77(6)
O2	S1	C3	106.87(7)
O2	S1	N2	113.62(7)
O2	S1	O1	115.82(6)
O1[1]	Ca1	O1[2]	88.06(3)
O1[3]	Ca1	O1	91.94(3)
O1[3]	Ca1	O1[4]	88.06(3)
O1[5]	Ca1	O1[1]	88.06(3)
O1[1]	Ca1	O1	91.94(3)
O1[4]	Ca1	O1[2]	91.94(3)
O1[2]	Ca1	O1	180.00(3)
O1[5]	Ca1	O1[2]	91.94(3)
O1[4]	Ca1	O1[1]	180.0
O1[3]	Ca1	O1[1]	91.94(3)
O1[3]	Ca1	O1[2]	88.06(3)
O1[5]	Ca1	O1	88.06(3)
O1[5]	Ca1	O1[3]	180.0
O1[5]	Ca1	O1[4]	91.94(3)
O1[4]	Ca1	O1	88.06(3)
O1[5]	Ca1	Co2	123.88(2)
O1[2]	Ca1	Co2	123.88(2)
Co2	Ca1	Co2[2]	180.0
N1	Co2	Ca1	180.0
N2[1]	Co2	N1	85.43(3)
N2	Co2	N1	85.42(3)
N2[3]	Co2	N1	85.43(3)
N2	Co2	N2[3]	119.370(9)
N2	Co2	N2[1]	119.371(9)
N2[3]	Co2	N2[1]	119.371(9)
N2[3]	Co2	Ca1	94.57(3)
N2[1]	Co2	Ca1	94.57(3)
N2	Co2	Ca1	94.58(3)

-------•

[1]-Y,+X-Y,+Z; [2]-X,-Y,1-Z; [3]+Y-X,-X,+Z; [4]+Y,-X+Y,1-Z; [5] Y+X,+X,1-Z

Table S37: Hydrogen Fractional Atomic Coordinates (×10[4]) and Equivalent Isotropic Displacement Parameters (Å[2]×10[3]) for **CMW_03_020**. U_{eq} is defined as 1/3 of the trace of the orthogonalised U_{ij}.

Atom	x	y	z	U_{eq}
H1A	1259	1214	2620	32
H1B	1741	435	2894	32
H2B	2785	2402	3209	33
H2A	1542	2455	3256	33
H1BA	831	1853	3041	32
H1BB	1291	1279	2655	32
H2BA	2551	1009	3196	33
H2BB	2861	2417	3225	33

Atom	x	y	z	U_{eq}
H4A	4080	1794	3589	65
H4C	5256	2256	3911	65
H4B	4741	3155	3792	65
H5B	2710(20)	210(20)	4607(8)	47
H5A	2710(20)	20(20)	4099(9)	47
H6B	4601	3425	4660	61
H6A	5075	2480	4753	61
H6C	3801	2232	4966	61
H5C	3920(20)	370(20)	4381(8)	46(6)

4-5^{Sr}

EMORY UNIVERSITY | X-ray Crystallography Center

Submitted by: **Christian Wallen**
Emory University
Solved by: **John Bacsa**
Sample ID: **CMW-03-050**

Crystal Data and Experimental

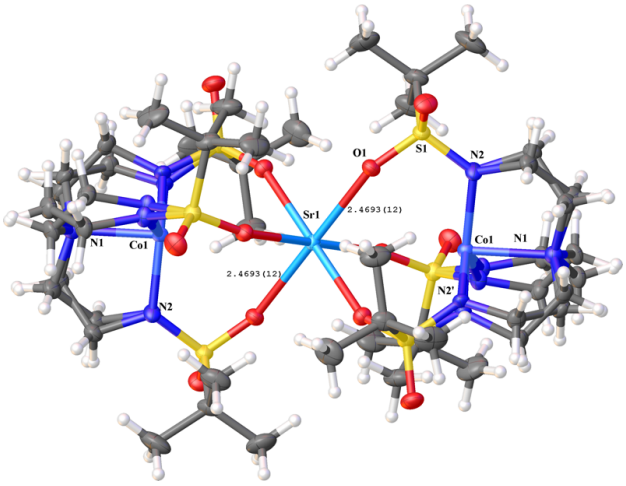

Experimental. Single violet prism-shaped crystals of (**CMW-03-050**) were recrystallised from a mixture of CH_2Cl_2, diethyl ether and methanol by vapor diffusion. A suitable crystal (0.36×0.29×0.20 mm) was selected and mounted on a loop with paratone oil on a Bruker APEX-II CCD diffractometer. The crystal was cooled to T = 100(2) K during data collection. The structure was solved with the **ShelXT** (Sheldrick, 2015) structure solution program using combined Patterson and dual-space recycling methods and by using **Olex2** (Dolomanov et al., 2009) as the graphical interface. The crystal structure was refined with version of **ShelXL** (Sheldrick, 2008) using Least Squares minimisation.

Crystal Data. $C_{36}H_{78}Co_2N_8O_{12}S_6Sr$, M_r = 1212.90, trigonal, R-3 (No. 148), a = 12.638(4) Å, b = 12.638(4) Å, c = 29.797(8) Å, α = 90°, β = 90°, γ = 120°, V = 4122(3) Å^3, T = 100(2) K, Z = 3, Z' = 1/6, μ(MoK$_\alpha$) = 1.850, 16290 reflections measured, 2798 unique (R_{int} = 0.0343) which were used in all calculations. The final wR_2 was 0.0937 (all data) and R_1 was 0.0363 (I > 2σ (I)).

Compound	**CMW-03-050**
Formula	$C_{36}H_{78}Co_2N_8O_{12}S_6Sr$
$D_{calc.}$/ g cm^{-3}	1.466
μ/mm^{-1}	1.850
Formula Weight	1212.90
Colour	violet
Shape	prism
Max Size/mm	0.36
Mid Size/mm	0.29
Min Size/mm	0.20
T/K	100(2)
Crystal System	trigonal
Space Group	R-3
a/Å	12.638(4)
b/Å	12.638(4)
c/Å	29.797(8)
α/°	90
β/°	90
γ/°	120
V/Å^3	4122(3)
Z	3
Z'	0.16667
Θ_{min}/°	1.982
Θ_{max}/°	30.513
Measured Refl.	16290
Independent Refl.	2798
$I > 2\sigma(I)$	2518
R_{int}	0.0343
Parameters	118
Restraints	3
Largest Peak	0.933
Deepest Hole	-0.441
GooF	1.066
wR_2 (all data)	0.0937
wR_2	0.0904
R_1 (all data)	0.0413
R_1	0.0363
CCDC #	1434439

Structure Quality Indicators

Reflections:	d min	0.70	I/σ	30.6	Rint	3.43%	complete 100%
Refinement:	Shift	0.000	Max Peak	0.9	Min Peak	-0.4	GooF 1.066

A violet prism-shaped crystal with dimensions 0.36×0.29×0.20 mm was mounted on a loop with paratone oil. X-ray diffraction data were collected using a Bruker APEX-II CCD diffractometer equipped with an Oxford Cryosystems low-temperature apparatus operating at T = 100(2) K.

Data were measured using ω scans using MoK$_\alpha$ radiation (fine-focus sealed tube, 45 kV, 35 mA). The total number of runs and images was based on the strategy calculation from the program **APEX2** (Bruker, 2014). The maximum resolution achieved was Θ = 30.513°.

Unit cell indexing was performed by using the **APEX2** (Bruker, 2014) software and refined using **SAINT** (Bruker, V8.34A, 2013) on 5438 reflections, 33% of the observed reflections. Data reduction, scaling and absorption corrections were performed using **SAINT** (Bruker, V8.34A, 2013) and **SADABS-2014/5** (Bruker, 2014) was used for absorption correction. wR_2(int) was 0.0685 before and 0.0489 after correction. The ratio of minimum to maximum transmission is 0.7793. The $\lambda/2$ correction factor is 0.00150. The software also corrects for Lorentz polarisation. The final completeness is 100.00 out to 30.513 in Θ. The absorption coefficient (μ) of this material is 1.850 and the minimum and maximum transmissions are 0.5814 and 0.7461.

The structure was solved in the space group P1 with the **ShelXT** (Sheldrick, 2015) structure solution program using combined Patterson and dual-space recycling methods. The space group R-3 (# 148) was determined by **ShelXT** (Sheldrick, 2015) structure solution program. The crystal structure was refined by Least Squares using version 2014/7 of **ShelXL** (Sheldrick, 2008). All non-hydrogen atoms were refined anisotropically. Hydrogen atom positions were calculated geometrically and refined using the riding model.

The value of Z' is 1/6.

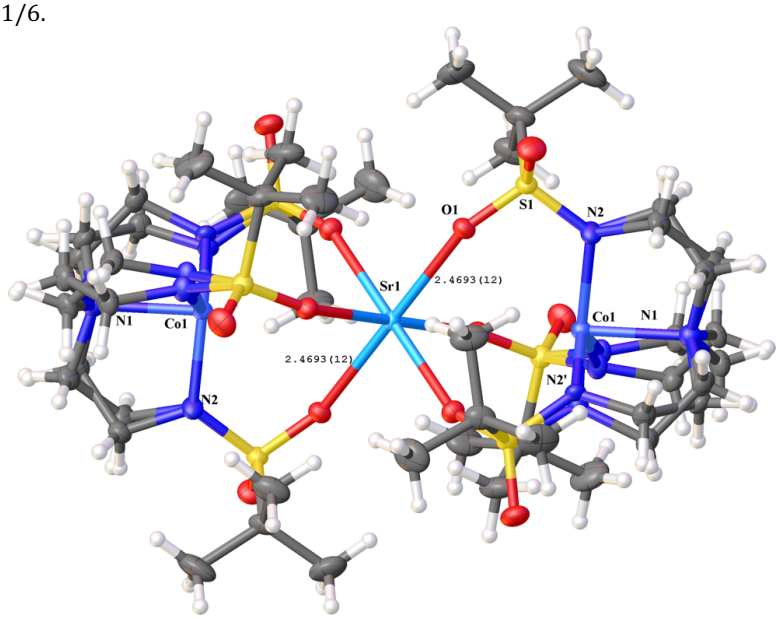

Figure S25:

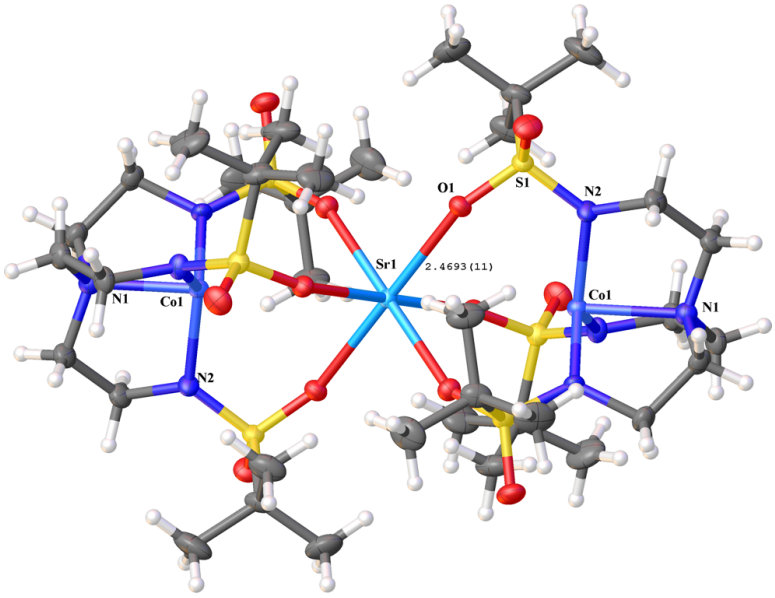

Figure S26:

Data Plots: Diffraction Data

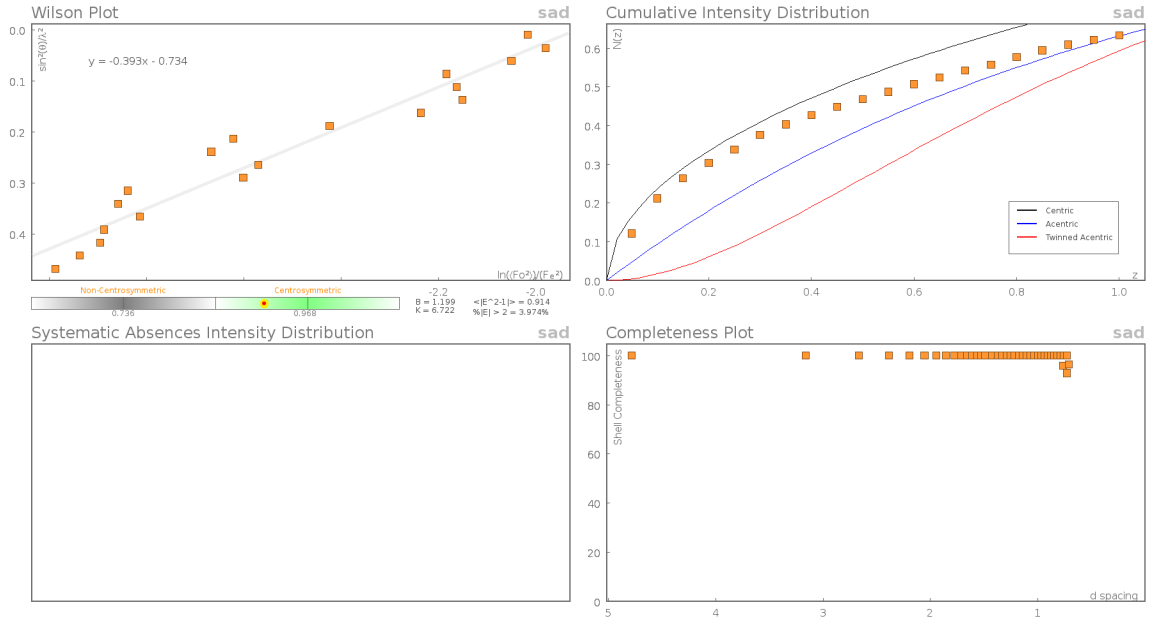

Data Plots: Refinement and Data

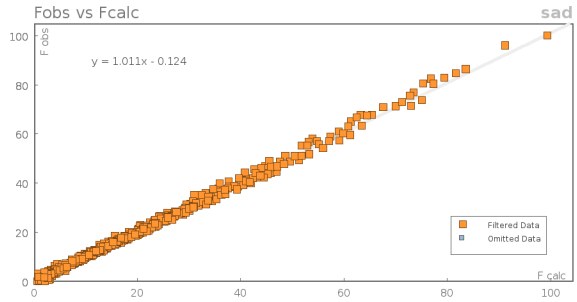

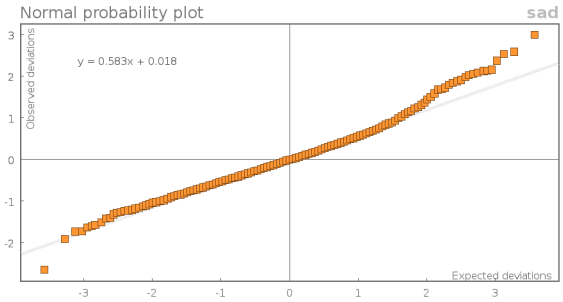

Reflection Statistics

Total reflections (after filtering)	16290	Unique reflections	2798
Completeness	0.999	Mean I/σ	30.63
hklsub>max</sub> collected	(17, 17, 42)	hklsub>min</sub> collected	(-18, -18, -42)
hkl_{max} used	(9, 18, 42)	hkl_{min} used	(-18, 0, 0)
Lim d_{max} collected	100.0	Lim d_{min} collected	0.36
d_{max} used	10.27	d_{min} used	0.7
Friedel pairs	5028	Friedel pairs merged	1
Inconsistent equivalents	0	R_{int}	0.0343
R_{sigma}	0.023	Intensity transformed	0
Omitted reflections	0	Omitted by user (OMIT hkl)	0
Multiplicity	(9327, 2816, 409, 26)	Maximum multiplicity	14
Removed systematic absences	0	Filtered off (Shel/OMIT)	0

Images of the Crystal on the Diffractometer

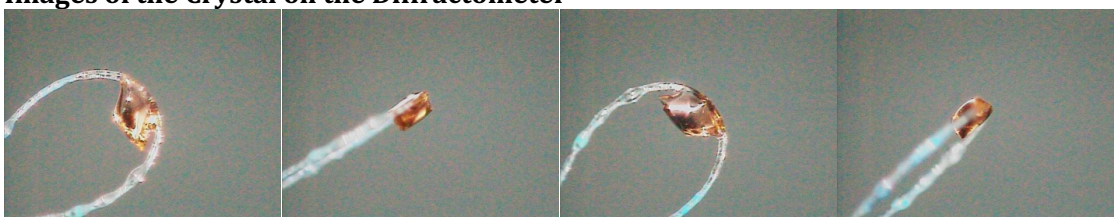

Table S108: Fractional Atomic Coordinates (×10⁴) and Equivalent Isotropic Displacement Parameters (Å²×10³) for **CMW-03-050**. U_{eq} is defined as 1/3 of the trace of the orthogonalised U_{ij}.

Atom	x	y	z	U_{eq}
C1	2932(4)	7540(3)	-403.6(12)	24.2(7)
C2	3377(4)	8594(3)	-68.9(10)	24.2(7)
N2	3053(7)	8057(6)	386.7(9)	18.9(12)
C1'	3440(5)	7857(5)	-368.4(16)	22.1(10)
C2'	2666(5)	8172(5)	-62.4(13)	22.3(12)
N2'	2801(11)	7835(9)	401.6(11)	18.9(12)
C3	1426.8(16)	8441.7(17)	921.2(7)	25.8(4)
C4	979(2)	8815(2)	506.3(9)	44.6(6)
C5	1481(2)	9191(2)	1330.9(9)	41.7(5)
C6	608.0(18)	7073.0(19)	1011.7(9)	35.2(5)
N1	3333	6667	-255.7(8)	19.5(5)
O1	3292.9(11)	8256.3(11)	1197.0(4)	18.8(2)
O2	3707.2(13)	10050.4(12)	735.6(5)	27.4(3)
S1	2965.5(4)	8746.4(3)	806.9(2)	17.51(10)
Co1	3333	6667	444.7(2)	14.58(10)

Atom	x	y	z	U_{eq}
Sr1	3333	6667	1667	14.27(10)

Table S39: Anisotropic Displacement Parameters (×10⁴) **CMW-03-050**. The anisotropic displacement factor exponent takes the form: $-2\pi^2[h^2a^{*2} \times U_{11} + \ldots + 2hka^* \times b^* \times U_{12}]$

Atom	U_{11}	U_{22}	U_{33}	U_{23}	U_{13}	U_{12}
C1	30.6(18)	24.2(13)	19.7(11)	5.9(9)	2.9(10)	15.2(12)
C2	30.6(18)	24.2(13)	19.7(11)	5.9(9)	2.9(10)	15.2(12)
N2	27(3)	13(2)	17.0(7)	2.3(7)	1.3(8)	10(3)
C1'	27(2)	18(2)	19(2)	6.5(16)	6.6(19)	9.8(19)
C2'	28(3)	25(2)	18.3(19)	2.3(15)	-0.3(16)	17(2)
N2'	27(3)	13(2)	17.0(7)	2.3(7)	1.3(8)	10(3)
C3	21.1(8)	23.0(8)	37.5(10)	-0.3(7)	-5.2(7)	14.1(7)
C4	38.6(12)	37.7(11)	63.4(16)	7.0(11)	-17.4(11)	23.5(10)
C5	34.0(11)	44.9(12)	55.8(14)	-11.7(11)	4.5(10)	26.9(10)
C6	19.1(8)	28.6(9)	54.9(14)	6.8(9)	-3.2(8)	9.6(7)
N1	19.0(6)	19.0(6)	20.6(12)	0	0	9.5(3)
O1	19.1(5)	20.1(5)	19.1(6)	2.0(4)	-1.0(4)	11.1(4)
O2	31.9(7)	17.0(6)	31.9(7)	5.4(5)	5.1(5)	11.3(5)
S1	21.37(19)	15.38(18)	18.43(19)	1.18(13)	-0.20(14)	11.18(15)
Co1	13.93(12)	13.93(12)	15.89(19)	0	0	6.97(6)
Sr1	14.74(12)	14.74(12)	13.33(17)	0	0	7.37(6)

Table S40: Bond Lengths in Å for **CMW-03-050**.

Atom	Atom	Length/Å
C1	C2	1.529(3)
C1	N1	1.493(4)
C2	N2	1.481(3)
N2	S1	1.561(4)
N2	Co1	1.965(6)
C1'	C2'	1.529(4)
C1'	N1	1.480(5)
C2'	N2'	1.481(3)
N2'	S1	1.609(7)
N2'	Co1	1.909(9)
C3	C4	1.529(3)
C3	C5	1.526(3)
C3	C6	1.532(3)
C3	S1	1.8158(19)
N1	C1[1]	1.493(4)
N1	C1[2]	1.493(4)
N1	C1'[1]	1.480(5)
N1	C1'[2]	1.480(5)
N1	Co1	2.087(3)
O1	S1	1.4706(12)
O1	Sr1[3]	2.4697(13)
O1	Sr1	2.4697(13)
O2	S1	1.4474(14)
Co1	N2[2]	1.965(6)
Co1	N2[1]	1.965(6)
Co1	N2'[2]	1.909(9)
Co1	N2'[1]	1.909(9)
Co1	Sr1[3]	3.6411(10)
Co1	Sr1	3.6411(10)
Sr1	O1[4]	2.4697(13)
Sr1	O1[5]	2.4697(13)
Sr1	O1[3]	2.4697(13)
Sr1	O1[2]	2.4697(13)
Sr1	Sr1[3]	0.0000

--------•

[1]+Y-X,1-X,+Z; [2]1-Y,1+X-Y,+Z; [3]2/3-X,4/3-Y,1/3-Z; [4]2/3 Y+X,1/3+X,1/3-Z; [5]-1/3+Y,1/3-X+Y,1/3-Z

Table S41: Bond Angles in ° for **CMW-03-050**.

Atom	Atom	Atom	Angle/°
N1	C1	C2	109.8(3)
N2	C2	C1	107.5(3)
C2	N2	S1	124.0(4)
C2	N2	Co1	111.0(3)
S1	N2	Co1	121.6(2)
N1	C1'	C2'	112.6(3)
N2'	C2'	C1'	107.6(3)
C2'	N2'	S1	119.2(5)
C2'	N2'	Co1	114.9(4)
S1	N2'	Co1	122.3(4)

Atom	Atom	Atom	Angle/°
C4	C3	C6	110.19(17)
C4	C3	S1	107.79(15)
C5	C3	C4	111.34(18)
C5	C3	C6	110.82(19)
C5	C3	S1	107.93(13)
C6	C3	S1	108.65(12)
C1	N1	C1[1]	111.67(15)
C1[2]	N1	C1[1]	111.67(15)
C1	N1	C1[2]	111.67(15)
C1[2]	N1	Co1	107.17(16)
C1	N1	Co1	107.17(16)
C1[1]	N1	Co1	107.17(16)
C1'	N1	C1'[1]	115.01(16)
C1'	N1	C1'[2]	115.01(16)
C1'[2]	N1	C1'[1]	115.01(16)
C1'[2]	N1	Co1	103.1(2)
C1'[1]	N1	Co1	103.1(2)
C1'	N1	Co1	103.1(2)
S1	O1	Sr1[3]	156.23(7)
S1	O1	Sr1	156.23(7)
Sr1[3]	O1	Sr1	0.0
N2	S1	C3	113.6(3)
N2'	S1	C3	104.3(4)
O1	S1	N2	106.6(2)
O1	S1	N2'	104.8(2)
O1	S1	C3	105.04(8)
O2	S1	N2	109.4(2)
O2	S1	N2'	118.9(3)
O2	S1	C3	106.51(8)
O2	S1	O1	115.93(8)
N2	Co1	N2[2]	119.23(2)
N2	Co1	N2[1]	119.24(2)
N2[2]	Co1	N2[1]	119.24(2)
N2	Co1	N1	84.96(8)
N2[2]	Co1	N1	84.96(8)
N2[1]	Co1	N1	84.96(8)
N2	Co1	Sr1[3]	95.04(8)
N2[1]	Co1	Sr1[3]	95.04(8)

Atom	Atom	Atom	Angle/°
N2[2]	Co1	Sr1[3]	95.04(8)
N2[1]	Co1	Sr1	95.04(8)
N2	Co1	Sr1	95.04(8)
N2[2]	Co1	Sr1	95.04(8)
N2'[2]	Co1	N2'[1]	119.55(2)
N2'	Co1	N2'[2]	119.55(2)
N2'	Co1	N2'[1]	119.55(2)
N2'[2]	Co1	N1	86.14(10)
N2'	Co1	N1	86.14(10)
N2'[1]	Co1	N1	86.14(10)
N2'[1]	Co1	Sr1[3]	93.86(10)
N2'[1]	Co1	Sr1	93.86(10)
N2'[2]	Co1	Sr1	93.86(10)
N2'[2]	Co1	Sr1[3]	93.86(10)
N2'	Co1	Sr1	93.86(10)
N2'	Co1	Sr1[3]	93.86(10)
N1	Co1	Sr1	180.0
N1	Co1	Sr1[3]	180.0
Sr1[3]	Co1	Sr1	0.0
O1[4]	Sr1	O1[5]	91.05(4)
O1[4]	Sr1	O1[3]	91.05(4)
O1[5]	Sr1	O1[2]	180.00(6)
O1	Sr1	O1[2]	91.05(4)
O1[5]	Sr1	O1	88.95(4)
O1[4]	Sr1	O1[2]	88.95(4)
O1[5]	Sr1	O1[3]	91.05(4)
O1[4]	Sr1	O1	88.95(4)
O1	Sr1	O1[3]	180.0
O1[3]	Sr1	O1[2]	88.95(4)
Sr1[3]	Sr1	O1[2]	0(10)
Sr1[3]	Sr1	O1	0(10)
Sr1[3]	Sr1	O1[3]	0(10)
Sr1[3]	Sr1	O1[4]	0(10)
Sr1[3]	Sr1	O1[5]	0(10)

-------•

[1]+Y-X,1-X,+Z; [2]1-Y,1+X-Y,+Z; [3]2/3-X,4/3-Y,1/3-Z; [4]2/3 Y+X,1/3+X,1/3-Z; [5]-1/3+Y,1/3-X+Y,1/3-Z

Table S42: Hydrogen Fractional Atomic Coordinates (×10[4]) and Equivalent Isotropic Displacement Parameters (Å[2]×10[3]) for **CMW-03-050**. U_{eq} is defined as 1/3 of the trace of the orthogonalised U_{ij}.

Atom	x	y	z	U_{eq}
H1A	2048	7120	-423	29
H1B	3263	7857	-699	29
H2A	4255	9123	-94	29
H2B	2989	9075	-129	29
H1'A	3187	7836	-677	27
H1'B	4290	8493	-344	27
H2'B	2944	9038	-80	27
H2'A	1816	7721	-154	27
H4A	200	8743	569	67
H4C	897	8289	260	67
H4B	1557	9645	429	67
H5A	2035	10041	1274	63

Atom	x	y	z	U_{eq}
H5C	1759	8934	1586	63
H5B	681	9070	1391	63
H6A	-223	6888	1046	53
H6B	871	6858	1282	53
H6C	663	6616	764	53

4-5^{Ba}

Submitted by: **Christian Wallen**
Emory University
Solved by: **John Bacsa**
Sample ID: **[Co2Ba] cluster**

Crystal Data and Experimental

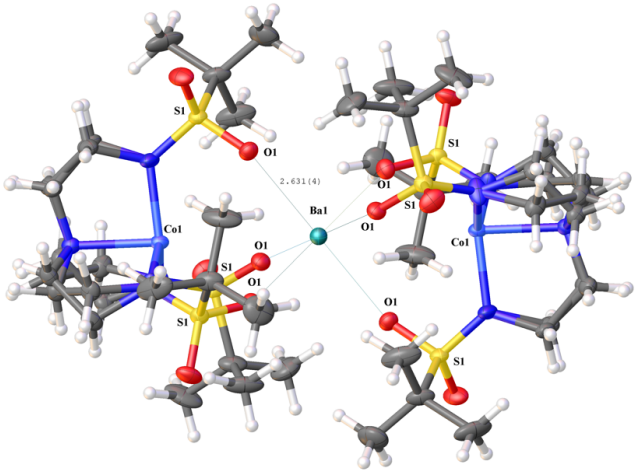

Experimental. Single violet prism-shaped crystals of (**CoBaCoBus**) were recrystallised from a mixture of CH_2Cl_2 and methanol by vapor diffusion. A suitable crystal (0.38×0.30×0.30) was selected and mounted on a loop with paratone oil on a Bruker APEX-II CCD diffractometer. The crystal was cooled to T = 100(2) K during data collection. The structure was solved with the **Superflip** (L. Palatinus & G. Chapuis, 2007) structure solution program using a charge flipping algorithm and by using **Olex2** (Dolomanov et al., 2009) as the graphical interface. The crystal structure was refined with version 2013-4 of **SHELXL** (Sheldrick, 2008) using Least Squares minimisation.

Crystal Data. $C_{36}H_{78}BaCo_2N_8O_{12}S_6$, M_r = 1262.62, trigonal, R-3 (No. 148), a = 12.6571(8) Å, b = 12.6571(8) Å, c = 30.388(2) Å, α = 90°, β = 90°, γ = 120°, V = 4216.0(6) Å^3, T = 100(2) K, Z = 3, Z' = 1/6, μ(MoK$_\alpha$) = 1.556, 36251 reflections measured, 5154 unique (R_{int} = 0.0276) which were used in all calculations. The final wR_2 was 0.1500 (all data) and R_1 was 0.0627 (I > 2(I)).

Compound	**CoBaCoBus**
Formula	$C_{36}H_{78}BaCo_2N_8O_{12}S_6$
$D_{calc.}$/ g cm^{-3}	1.492
μ/mm^{-1}	1.556
Formula Weight	1262.62
Colour	violet
Shape	prism
Max Size/mm	0.38
Mid Size/mm	0.30
Min Size/mm	0.30
T/K	100(2)
Crystal System	trigonal
Space Group	R-3
a/Å	12.6571(8)
b/Å	12.6571(8)
c/Å	30.388(2)
α/°	90
β/°	90
γ/°	120
V/Å^3	4216.0(6)
Z	3
Z'	1/6
Θ_{min}/°	2.011
Θ_{max}/°	38.564
Measured Refl.	36251
Independent Refl.	5154
$I > 2\sigma(I)$	4927
R_{int}	0.0276
Parameters	120
Restraints	0
Largest Peak	1.686
Deepest Hole	-1.346
GooF	1.357
wR_2 (all data)	0.1500
wR_2	0.1493
R_1 (all data)	0.0645
R_1	0.0627
CCDC #	1434435

Structure Quality Indicators

Reflections:	d min 0.57	I/σ 43.9	Rint 2.76%	complete 97%
Refinement:	Shift -0.002	Max Peak 1.7	Min Peak -1.4	GooF 1.357

A violet prism-shaped crystal with dimensions 0.38×0.30×0.30 mm was mounted on a loop with paratone oil. X-ray diffraction data were collected using a Bruker APEX-II CCD diffractometer equipped with an Oxford Cryosystems low-temperature apparatus operating at T = 100(2) K.

Data were measured using ω scans with MoK$_\alpha$ radiation (fine-focus sealed tube, 45 kV, 35 mA). The total number of runs and images was based on the strategy calculation from the program **APEX2** (Bruker). The maximum resolution achieved was Θ = 38.5°.

Unit cell indexing was performed by using the **APEX2** (Bruker) software and refined using **SAINT** (Bruker, V8.34A, 2013) on 9797 reflections, 27% of the observed reflections. Data reduction, scaling and absorption corrections were performed using **SAINT** (Bruker, V8.34A, 2013) and **SADABS-2014/2** (Bruker, 2014) was used for absorption correction.wR_2(int) was 0.0693 before and 0.0471 after correction.The Ratio of minimum to maximum transmission is 0.8416.The $\lambda/2$ correction factor is 0.00150. software which corrects for Lorentz polarisation. The final completeness is 98.5% out to 38.564 in Θ. The absorption coefficient (μ) of this material is 1.556 and the minimum and maximum transmissions are 0.6292 and 0.7476.

The structure was solved in the space group P1 with the **Superflip** (L. Palatinus & G. Chapuis, 2007) structure solution program using charge flipping methods. The space group R-3 (# 148) was determined by **Superflip** (L. Palatinus & G. Chapuis, 2007) structure solution program. The crystal structure was refined by Least Squares using version 2013-4 of **CoBaCoBusL** (Sheldrick, 2008). All non-hydrogen atoms were refined anisotropically. Hydrogen atom positions were calculated geometrically and refined using the riding model. The value of Z' is 1/6.

Data Plots: Diffraction Data

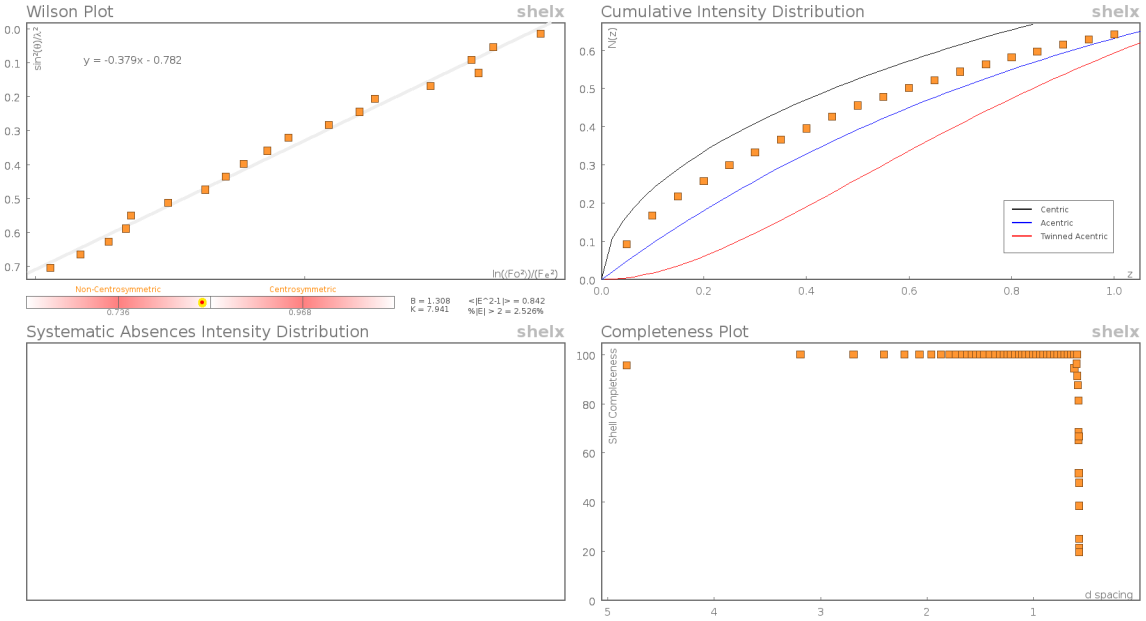

Data Plots: Refinement and Data

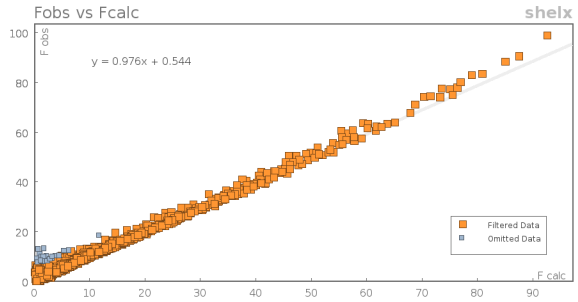

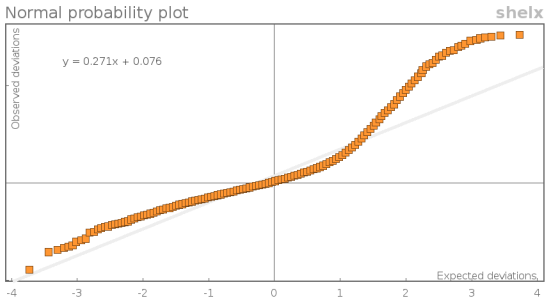

Reflection Statistics

Total reflections (after filtering)	36588	Unique reflections	5154
Completeness	0.97	Mean I/σ	43.9
hklsub>max</sub> collected	(21, 19, 51)	hklsub>min</sub> collected	(-20, -21, -52)
hkl_{max} used	(11, 22, 52)	hkl_{min} used	(-21, 0, 0)
Lim d_{max} collected	100.0	Lim d_{min} collected	0.36
d_{max} used	10.13	d_{min} used	0.57
Friedel pairs	8101	Friedel pairs merged	1
Inconsistent equivalents	0	R_{int}	0.0276
R_{sigma}	0.0187	Intensity transformed	0
Omitted reflections	0	Omitted by user (OMIT hkl)	337
Multiplicity	(10906, 5268, 4107, 540, 133)	Maximum multiplicity	22
Removed systematic absences	0	Filtered off (Shel/OMIT)	0

Images of the Crystal on the Diffractometer

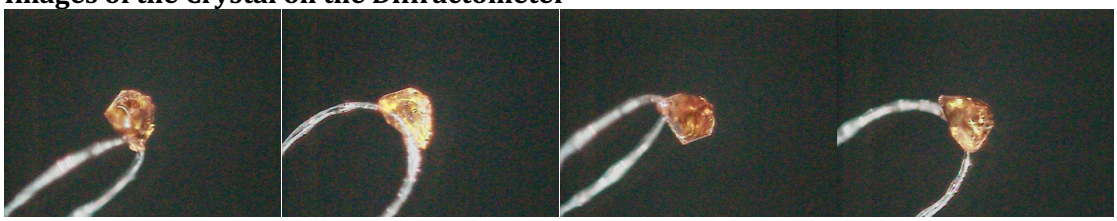

Table S113: Fractional Atomic Coordinates (×10⁴) and Equivalent Isotropic Displacement Parameters (Å²×10³) for **CoBaCoBus**. U_{eq} is defined as 1/3 of the trace of the orthogonalised U_{ij}.

Atom	x	y	z	U_{eq}
Ba1	10000	10000	5000	18.19(9)
Co1	10000	10000	6233.7(2)	15.98(12)
S1	7513.0(6)	7895.8(6)	5891.0(2)	18.66(13)
O2	6905(2)	6604(2)	5983.4(10)	29.8(5)
O1	8309(2)	8310(2)	5502.9(8)	22.1(4)
C6	5594(4)	7452(5)	5380.3(19)	46.1(11)
C4	6900(4)	9602(4)	5659(2)	49.7(14)
C5	5499(4)	7933(4)	6172(2)	51.0(14)
N1	10000	10000	6920.4(15)	19.0(7)
N2	8311(3)	8710(3)	6284.5(10)	30.7(6)
C3	6315(3)	8246(3)	5766.7(15)	30.2(7)
C1	10900(8)	9638(8)	7071(3)	24.2(14)
C2B	11458(6)	9288(6)	6729(2)	22(1)
C1B	11174(8)	10085(8)	7032(3)	22.1(12)
C2	11951(6)	10094(7)	6744(2)	26.2(12)

Table S44: Anisotropic Displacement Parameters (×10⁴) **CoBaCoBus**. The anisotropic displacement factor exponent takes the form: $-2\pi^2[h^2a^{*2} \times U_{11} + ... + 2hka^* \times b^* \times U_{12}]$

Atom	U_{11}	U_{22}	U_{33}	U_{23}	U_{13}	U_{12}
Ba1	18.25(11)	18.25(11)	18.07(16)	0	0	9.12(6)
Co1	13.00(15)	13.00(15)	21.9(3)	0	0	6.50(8)
S1	14.6(3)	15.2(3)	22.2(3)	0.2(2)	0.8(2)	4.5(2)
O2	25.6(11)	16.2(9)	40.0(14)	6.4(9)	-3.9(10)	4.7(8)
O1	19.5(9)	25.2(10)	22.3(9)	2.3(8)	3.1(7)	11.7(8)
C6	26.8(17)	52(3)	59(3)	0(2)	-13.3(18)	18.9(18)
C4	26.8(17)	28.0(17)	101(4)	15(2)	14(2)	18.8(15)
C5	25.2(17)	33(2)	86(4)	-3(2)	27(2)	8.6(15)
N1	17.2(10)	17.2(10)	22.6(18)	0	0	8.6(5)
N2	17.3(11)	31.7(14)	23.3(12)	-3.6(10)	3.6(9)	-2.7(10)
C3	15.5(11)	22.4(13)	52(2)	2.4(13)	4.8(12)	9(1)
C1	25(4)	29(4)	23(3)	-5(3)	-5(3)	16(3)
C2B	23(2)	26(3)	23(2)	2(2)	-1.2(19)	16(2)
C1B	20(3)	25(3)	23(3)	-3(3)	-4(2)	13(3)
C2	21(2)	34(3)	28(3)	-6(2)	-5(2)	17(2)

Table S45: Bond Lengths in Å for **CoBaCoBus**.

Atom	Atom	Length/Å
Ba1	Co1	3.7490(7)
Ba1	Co1[1]	3.7489(7)
Ba1	O1	2.629(2)
Ba1	O1[1]	2.629(2)
Ba1	O1[2]	2.629(2)
Ba1	O1[3]	2.629(2)
Ba1	O1[4]	2.629(2)
Ba1	O1[5]	2.629(2)
Co1	N1	2.087(5)
Co1	N2[5]	1.942(3)
Co1	N2[3]	1.942(3)
Co1	N2	1.942(3)
S1	O2	1.444(2)
S1	O1	1.467(2)
S1	N2	1.572(3)
S1	C3	1.820(4)
C6	C3	1.518(7)
C4	C3	1.527(5)
C5	C3	1.526(6)
N1	C1[5]	1.497(9)
N1	C1	1.497(9)
N1	C1[3]	1.497(9)
N1	C1B[5]	1.474(8)
N1	C1B[3]	1.474(8)
N1	C1B	1.474(8)
N2	C2B[3]	1.453(7)
N2	C2[3]	1.587(7)
C1	C2	1.524(12)
C2B	N2[5]	1.453(7)
C2B	C1B	1.535(11)
C2	N2[5]	1.587(7)

--------•

[1]2-X,2-Y,1-Z; [2]1-Y+X,+X,1-Z; [3]1+Y-X,2-X,+Z; [4]+Y,1-X+Y,1-Z
[5]2-Y,1+X-Y,+Z

Table S46: Bond Angles in ° for **CoBaCoBus**.

Atom	Atom	Atom	Angle/°
Co1[1]	Ba1	Co1	180.0
O1[2]	Ba1	Co1[1]	125.54(5)
O1[3]	Ba1	Co1[1]	125.54(5)
O1	Ba1	Co1[1]	125.54(5)
O1[1]	Ba1	Co1[1]	54.46(5)
O1[4]	Ba1	Co1	125.54(5)
O1[3]	Ba1	Co1	54.46(5)
O1[5]	Ba1	Co1	125.54(5)
O1[2]	Ba1	Co1	54.46(5)
O1[5]	Ba1	Co1[1]	54.46(5)
O1	Ba1	Co1	54.46(5)
O1[1]	Ba1	Co1	125.54(5)
O1[4]	Ba1	Co1[1]	54.46(5)
O1[4]	Ba1	O1[2]	180.00(8)
O1[3]	Ba1	O1[2]	89.61(8)
O1	Ba1	O1[5]	90.39(8)
O1[5]	Ba1	O1[2]	90.39(8)
O1	Ba1	O1[1]	180.00(10)
O1[5]	Ba1	O1[1]	89.61(8)
O1[5]	Ba1	O1[3]	180.0
O1[2]	Ba1	O1[1]	90.39(8)
O1	Ba1	O1[4]	90.39(8)
O1[3]	Ba1	O1[1]	90.39(8)
O1[5]	Ba1	O1[4]	89.61(8)

Atom	Atom	Atom	Angle/°
O1	Ba1	O1^{3}	89.61(8)
O1	Ba1	O1^{2}	89.61(8)
O1^{4}	Ba1	O1^{1}	89.61(8)
O1^{3}	Ba1	O1^{4}	90.39(8)
N1	Co1	Ba1	180.0
N2^{2}	Co1	Ba1	94.56(9)
N2	Co1	Ba1	94.56(9)
N2^{3}	Co1	Ba1	94.56(9)
N2^{3}	Co1	N1	85.44(9)
N2	Co1	N1	85.44(9)
N2^{2}	Co1	N1	85.44(9)
N2^{3}	Co1	N2	119.38(3)
N2^{2}	Co1	N2	119.38(3)
N2^{2}	Co1	N2^{3}	119.38(3)
O2	S1	O1	116.25(16)
O2	S1	N2	113.48(18)
O2	S1	C3	106.20(16)
O1	S1	N2	106.01(15)
O1	S1	C3	104.70(17)
N2	S1	C3	109.8(2)
S1	O1	Ba1	153.12(15)
C1	N1	Co1	107.8(4)
C1^{2}	N1	Co1	107.8(4)
C1^{3}	N1	Co1	107.8(4)
C1	N1	C1^{3}	111.1(4)
C1	N1	C1^{2}	111.1(4)
C1^{2}	N1	C1^{3}	111.1(4)
C1B	N1	Co1	103.3(4)
C1B^{2}	N1	Co1	103.3(4)
C1B^{3}	N1	Co1	103.3(4)
C1B^{2}	N1	C1B^{3}	114.9(3)
C1B	N1	C1B^{3}	114.9(3)
C1B	N1	C1B^{2}	114.9(3)
S1	N2	Co1	124.55(17)
S1	N2	C2^{2}	116.8(3)
C2B^{2}	N2	Co1	113.6(3)
C2B^{2}	N2	S1	121.8(3)
C2^{2}	N2	Co1	108.3(3)
C6	C3	S1	107.3(3)
C6	C3	C4	111.8(4)
C6	C3	C5	110.4(4)
C4	C3	S1	108.9(2)
C5	C3	S1	107.9(3)
C5	C3	C4	110.5(4)
N1	C1	C2	109.8(6)
N2^{3}	C2B	C1B	105.3(5)
N1	C1B	C2B	111.9(6)
C1	C2	N2^{3}	103.7(5)

-------•

^{1}2-X,2-Y,1-Z; ^{2}1+Y-X,2-X,+Z; ^{3}2-Y,1+X-Y,+Z; ^{4}1-Y+X,+X,1-Z ^{5}+Y,1-X+Y,1-Z

Table S47: Hydrogen Fractional Atomic Coordinates (×10^{4}) and Equivalent Isotropic Displacement Parameters (Å^{2}×10^{3}) for **CoBaCoBus**. U_{eq} is defined as 1/3 of the trace of the orthogonalised U_{ij}.

Atom	x	y	z	U_{eq}
H6A	6121	7681	5120	69
H6B	4899	7567	5320	69
H6C	5298	6593	5452	69
H4A	7404	10084	5908	75
H4B	6260	9807	5604	75
H4C	7411	9786	5396	75
H5A	5192	7079	6253	76
H5B	4811	8056	6106	76
H5C	5972	8462	6417	76
H1A	10494	8738	7095	29
H1B	11218	9991	7365	29
H2BA	12306	9467	6773	26
H2BB	10895	8412	6789	26
H1BA	11148	9826	7341	27
H1BB	11835	10945	7007	27
H2A	12491	9759	6813	31
H2B	12439	10996	6745	31

3-3^{P}(OH$_2$)

EMORY UNIVERSITY | X-ray Crystallography Center

Submitted by: **Christian Wallen**
Emory University
Solved by: **John Bacsa**
Sample ID: **CMW_01_053**

Crystal Data and Experimental

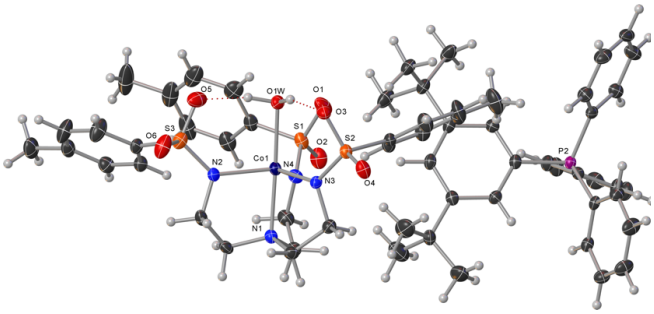

Experimental. Single clear light violet prism-shaped crystals of (**CMW_01_053**) were crystallised by vapor diffusion The crystal was chosen from the sample as supplied. A suitable crystal (0.37×0.32×0.22 mm^3) was selected and mounted on a loop with paratone oil on a Bruker APEX-II CCD diffractometer. The crystal was cooled to T = 100(2) K during data collection. The structure was solved with the **ShelXT-2014/4** (Sheldrick, 2015) structure solution program using the Charge Flipping solution method and by using **Olex2** (Dolomanov et al., 2009) as the graphical interface. The model was refined with version 2014/7 of ShelXL-2014/7 (Sheldrick, 2014) using Least Squares minimisation.

Crystal Data. $C_{59}H_{71}CoN_4O_{6.805}PS_3$, M_r = 1131.15, triclinic, P-1 (No. 2), a = 9.7734(8) Å, b = 15.3083(11) Å, c = 19.9544(15) Å, α = 75.0460(10)°, β = 86.6500(10)°, γ = 89.0230(10)°, V = 2879.4(4) Å^3, T = 100(2) K, Z = 2, Z' = 1, μ(MoK$_\alpha$) = 0.489 mm^{-1}, 29153 reflections measured, 15720 unique (R_{int} = 0.0625) which were used in all calculations. The final wR_2 was 0.1097 (all data) and R_1 was 0.0521 (I > 2σ(I)).

Compound	**CMW_01_053**
Formula	$C_{59}H_{71}CoN_4O_{6.805}PS_3$
$D_{calc.}$/ g cm^{-3}	1.305
μ/mm^{-1}	0.489
Formula Weight	1131.15
Colour	clear light violet
Shape	prism
Size/mm^3	0.37×0.32×0.22
T/K	100(2)
Crystal System	triclinic
Space Group	P-1
a/Å	9.7734(8)
b/Å	15.3083(11)
c/Å	19.9544(15)
α/°	75.0460(10)
β/°	86.6500(10)
γ/°	89.0230(10)
V/Å^3	2879.4(4)
Z	2
Z'	1
Wavelength/Å	0.71073
Radiation type	MoK$_\alpha$
Θ_{min}/°	1.058
Θ_{max}/°	29.573
Measured Refl.	29153
Independent Refl.	15720
Reflections with I > 2(I)	9512
R_{int}	0.0625
Parameters	692
Restraints	3
Largest Peak	0.600
Deepest Hole	-0.464
GooF	0.889
wR_2 (all data)	0.1097
wR_2	0.0991
R_1 (all data)	0.0913
R_1	0.0521

Structure Quality Indicators

Reflections:	d min (Mo) 0.72	I/σ 8.3	Rint 4.17%	complete 97%
Refinement:	Shift 0.004	Max Peak 0.6	Min Peak -0.6	GooF 0.885

A clear light violet prism-shaped crystal with dimensions 0.37×0.32×0.22 mm^3 was mounted on a loop with paratone oil. Data were collected using a Bruker APEX-II CCD diffractometer equipped with an Oxford Cryosystems low-temperature device, operating at T = 100(2) K.

Data were measured using ϕ and ω scans using MoK_α radiation (fine-focus sealed tube, 45 kV, 35 mA).The total number of runs and images was based on the strategy calculation from the program **APEX2** (Bruker). The maximum resolution that was achieved was Θ = 29.573°.

The diffraction patterns were indexed using **SAINT** (Bruker, V8.27A, 2012) and the unit cells were refined using **SAINT** (Bruker, V8.34A, 2013) on 5397 reflections, 19 % of the observed reflections. Data reduction, scaling and absorption corrections were performed using **SAINT** (Bruker, V8.34A, 2013) and **SADABS-2014/5** (Bruker, 2014) was used for absorption correction. The value of wR_2(int) was 0.0600 before and 0.0452 after correction. The ratio of minimum to maximum transmission is 0.7594. The $\lambda/2$ correction factor is Not present. The final completeness is 99.5% out to 29.573° in Θ. The absorption coefficient μ of this material is 0.489 mm^{-1} at this wavelength (λ = 0.71073 Å) and the minimum and maximum transmissions are 0.5667 and 0.7462.

The structure was solved and the space group P-1 (# 2) determined by the **ShelXT-2014/4** (Sheldrick, 2015) structure solution program using Charge Flipping and refined by Least Squares using version 2014/7 of **ShelXL-2014/7** (Sheldrick, 2014). All non-hydrogen atoms were refined anisotropically. Hydrogen atom positions were calculated geometrically and refined using the riding model.

_refine_special_details: ?

_exptl_absorpt_special_details: ?

There is a single molecule in the asymmetric unit, which is represented by the reported sum formula. In other words: Z is 2 and Z' is 1.

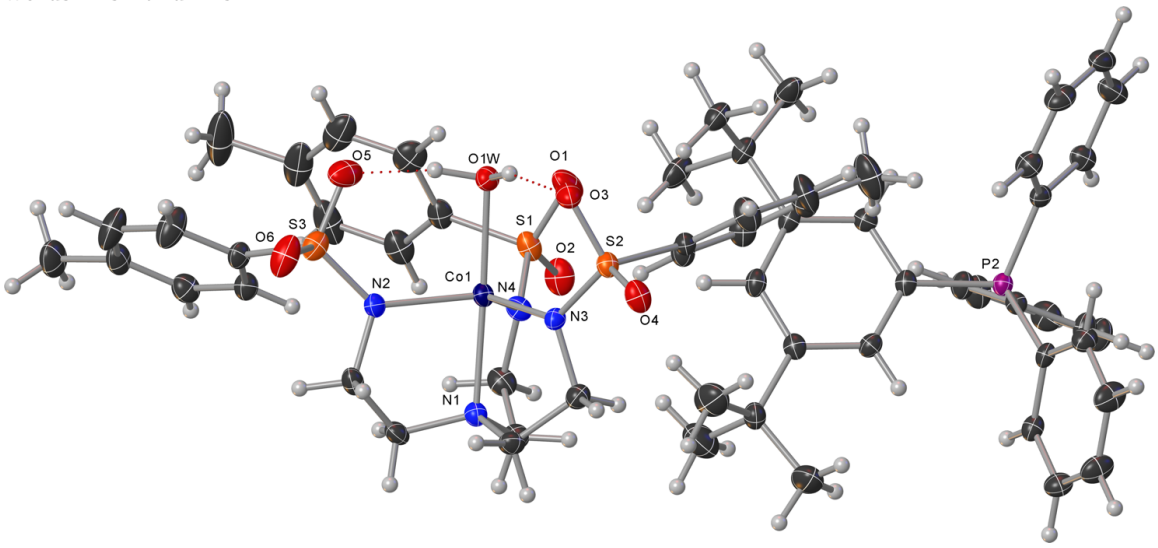

Figure 1: Plot of the asymmetric unit of $[Co^{II}(C_{27}\,H_{35}\,N_4\,O_6)(H_2O)_{0.8}]$. $[C_{32}\,H_{36}\,P]$

Data Plots: Diffraction Data

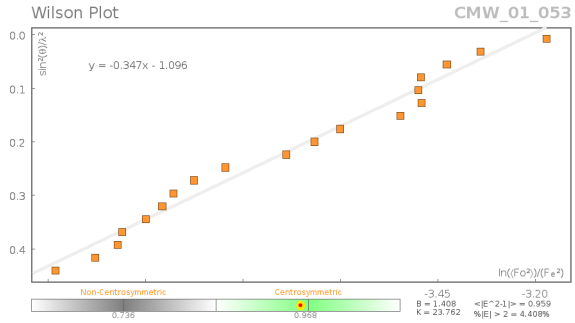

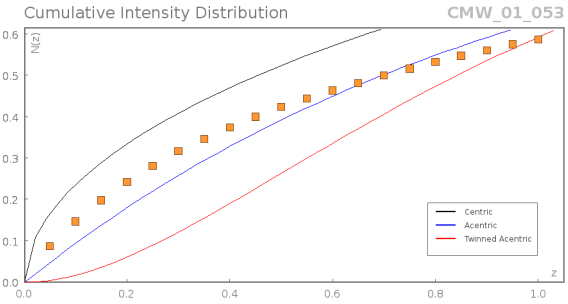

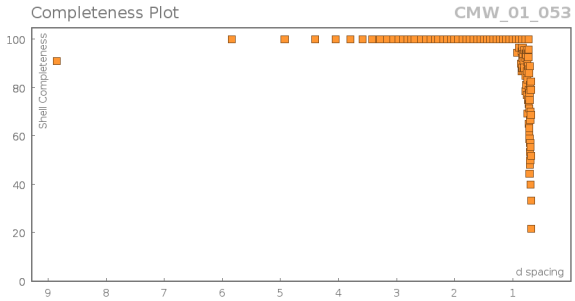

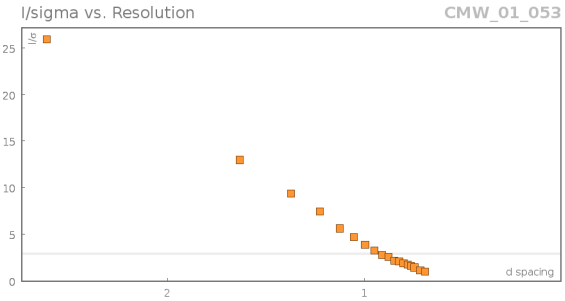

Data Plots: Refinement and Data

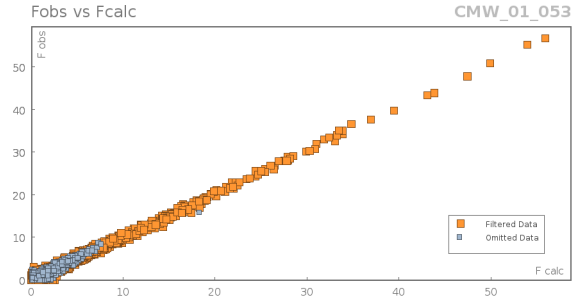

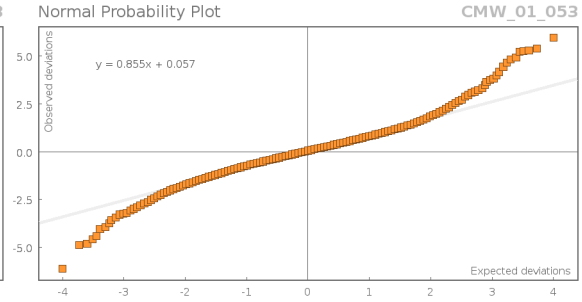

Reflection Statistics

Total reflections (after filtering)	29154	Unique reflections	15720
Completeness	0.972	Mean I/σ	6.22
hkl_{max} collected	(14, 13, 22)	hkl_{min} collected	(-13, -22, -27)
hkl_{max} used	(13, 21, 27)	hkl_{min} used	(-13, -20, 0)
Lim d_{max} collected	20.0	Lim d_{min} collected	0.72
d_{max} used	19.25	d_{min} used	0.72
Friedel pairs	6589	Friedel pairs merged	1
Inconsistent equivalents	40	R_{int}	0.0625
R_{sigma}	0.1168	Intensity transformed	0
Omitted reflections	0	Omitted by user (OMIT hkl)	1
Multiplicity	(17057, 6792, 263)	Maximum multiplicity	4
Removed systematic absences	0	Filtered off (Shel/OMIT)	2276

Images of the Crystal on the Diffractometer

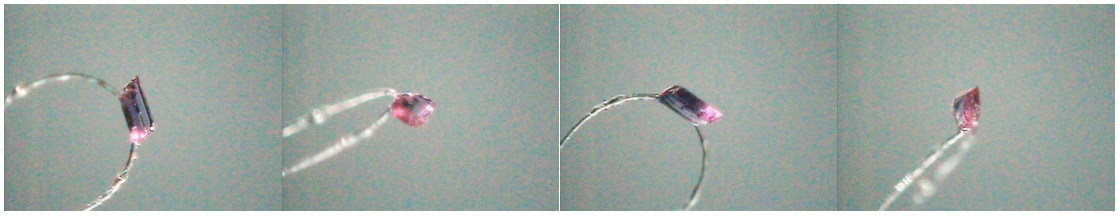

Table 1: Fractional Atomic Coordinates (×10⁴) and Equivalent Isotropic Displacement Parameters (Å²×10³) for **CMW_01_053**. U_{eq} is defined as 1/3 of the trace of the orthogonalised U_{ij}.

Atom	x	y	z	U_{eq}
Co1	9615.7(3)	3069.8(2)	1981.8(2)	17.30(8)
S2	10846.3(6)	2786.7(4)	3501.4(3)	19.30(14)
P1	5781.7(6)	8792.0(4)	3839.2(3)	16.48(14)
S1	6847.9(6)	4277.7(4)	1748.1(3)	24.37(15)
S3	9461.2(6)	1252.7(4)	1411.4(3)	25.24(15)
N3	11006.3(18)	3122.9(12)	2682.7(10)	17.2(4)
O6	10528.4(19)	574.6(12)	1514.7(10)	37.9(5)
O4	12135.8(16)	2718.3(11)	3833.9(9)	27.0(4)
O2	6401.9(18)	5201.3(12)	1453.3(10)	34.2(5)
O1	6448.0(17)	3878.2(12)	2463.3(9)	34.4(5)
O3	10023.1(17)	1966.1(11)	3676.3(8)	26.2(4)
N2	9997.9(19)	2239.1(13)	1354.4(10)	20.0(4)
O5	8304.5(18)	1065.6(12)	1913.7(9)	35.8(5)
N4	8466.9(19)	4187.9(13)	1637(1)	21.0(5)
N1	11160.7(19)	3880.1(12)	1274.3(10)	19.3(4)
O1W	8233(2)	2181.4(13)	2699.8(11)	20.9(7)
C28	4861(2)	8289.2(16)	4642.6(12)	18.7(5)
C14	9865(2)	3594.3(15)	3828.7(12)	18.7(5)
C34	4806(2)	9731.0(15)	3369.5(12)	16.6(5)
C40	5988(2)	7971.0(15)	3342.4(12)	18.0(5)
C44	7271(2)	7383.0(15)	2481.3(12)	19.2(5)
C55	8148(2)	9752.8(15)	3410.7(13)	20.0(5)
C54	7436(2)	9181.0(15)	3976.1(12)	17.2(5)
C42	4990(2)	6789.7(15)	2924.2(13)	19.4(5)
C41	4909(2)	7380.9(15)	3351.3(12)	19.2(5)
C21	8792(2)	1245.9(16)	602.7(13)	21.9(5)
C45	7156(2)	7965.6(15)	2912.1(12)	18.8(5)
C46	3823(2)	6130.2(16)	2926.0(13)	22.6(6)
C43	6180(2)	6801.9(15)	2501.2(12)	20.8(5)
C47	4299(3)	5167.8(15)	3290.9(13)	26.2(6)
C56	9482(2)	9997.6(16)	3469.8(13)	25.0(6)
C33	3702(2)	8700.5(17)	4864.4(13)	23.2(6)
C22	8329(2)	2021.0(17)	155.3(13)	23.6(6)
C2	11259(2)	2474.6(16)	900.9(13)	23.0(6)
C59	8056(2)	8867.3(16)	4602.7(13)	23.0(6)
C19	9014(2)	4198.6(16)	3411.7(13)	23.4(6)
C4	12431(2)	3827.4(17)	1658.3(12)	22.7(6)
C35	3890(2)	9621.1(16)	2890.2(13)	23.1(6)
C10	5004(3)	2515(3)	510(2)	50.2(9)
C3	12072(2)	3813.5(16)	2412.2(13)	22.6(6)
C24	7591(2)	1149.3(19)	-611.5(14)	29.2(6)
C25	8074(3)	380(2)	-159.6(16)	43.4(8)
C1	11354(2)	3495.4(16)	669.4(12)	22.6(6)
C29	5324(2)	7475.1(16)	5067.5(13)	25.9(6)
C50	8533(2)	7393.4(16)	1986.4(13)	23.7(6)

Atom	x	y	z	U_{eq}
C6	9083(2)	4791.5(17)	1004.2(13)	27.1(6)
C39	4864(2)	10553.0(16)	3545.2(13)	25.8(6)
C57	10099(3)	9679.1(17)	4093.7(14)	31.2(7)
C18	8191(2)	4775.3(17)	3696.5(14)	27.4(6)
C7	6094(2)	3612.2(18)	1262.3(13)	25.0(6)
C36	3026(3)	10324.5(17)	2596.7(13)	28.4(6)
C5	10614(2)	4812.0(16)	1083.6(13)	24.7(6)
C23	7743(2)	1963.9(18)	-446.5(14)	28.2(6)
C30	4644(3)	7100.2(17)	5697.9(14)	29.9(6)
C38	3996(3)	11252.4(17)	3252.5(14)	30.0(6)
C31	3499(3)	7512.3(18)	5914.1(13)	29.6(6)
C48	3490(3)	6175.3(17)	2177.9(14)	32.3(7)
C8	5822(3)	3969(2)	571.3(14)	32.9(7)
C20	7296(3)	5385(2)	4693.5(16)	48.8(9)
C15	9906(3)	3570.8(18)	4526.4(14)	30.4(6)
C58	9391(3)	9115.3(17)	4656.2(14)	31.9(7)
C49	2518(2)	6345.8(18)	3318.1(16)	36.5(7)
C17	8215(3)	4762.8(18)	4386.2(15)	31.5(7)
C37	3078(3)	11135.7(17)	2782.5(14)	28.7(6)
C16	9088(3)	4150.7(19)	4800.3(14)	36.7(7)
C32	3023(3)	8310.0(18)	5490.9(13)	29.8(6)
C9	5274(3)	3422(2)	197.0(17)	46.5(9)
C26	8677(3)	424.0(19)	437.0(16)	41.8(8)
C12	5827(2)	2708.0(19)	1571.2(16)	34.2(7)
C13	4429(3)	1914(3)	94(2)	80.4(14)
C27	6907(3)	1080(2)	-1254.7(14)	40.5(7)
C11	5292(3)	2170(2)	1193.5(19)	44.0(8)
C51	9212(3)	6461.2(19)	2139.5(16)	43.4(8)
C53	9608(3)	8079(2)	2045.3(16)	44.3(8)
C52	8085(3)	7640(2)	1237.1(15)	50.2(9)

Table 2: Anisotropic Displacement Parameters (×10^4) **CMW_01_053**. The anisotropic displacement factor exponent takes the form: $-2\pi^2[h^2a^{*2} \times U_{11} + \ldots + 2hka^* \times b^* \times U_{12}]$

Atom	U_{11}	U_{22}	U_{33}	U_{23}	U_{13}	U_{12}
Co1	19.56(16)	17.81(18)	14.70(18)	-4.19(14)	-3.11(13)	2.37(13)
S2	23.7(3)	18.6(3)	15.6(3)	-4.0(3)	-3.6(2)	2.9(2)
P1	18.4(3)	15.1(3)	16.3(3)	-4.6(3)	-2.4(2)	1.0(2)
S1	22.7(3)	31.1(4)	20.9(4)	-9.3(3)	-3.9(3)	7.2(3)
S3	29.7(3)	21.4(4)	24.2(4)	-3.1(3)	-11.2(3)	0.8(3)
N3	20.4(9)	15.1(10)	15.8(11)	-3.3(8)	-2.1(8)	-1.0(8)
O6	46.7(11)	24.3(11)	46.7(13)	-11.4(9)	-27.8(10)	11.7(9)
O4	28.4(9)	32.3(11)	21.3(10)	-7.9(8)	-7.8(8)	10.5(8)
O2	33.6(10)	32.6(11)	38.9(12)	-13.0(9)	-9.0(9)	15.8(9)
O1	28.6(10)	54.0(13)	20.9(11)	-10.5(9)	-0.9(8)	1.5(9)
O3	36.4(10)	19.0(9)	21.5(10)	-3.1(8)	2.7(8)	-1.9(8)
N2	22.1(10)	22.1(11)	17.0(11)	-7.0(9)	-1.3(8)	-1.4(8)
O5	39.4(11)	40.2(12)	22.7(11)	2.7(9)	-5.6(9)	-11.3(9)
N4	21.5(10)	22.9(11)	16.7(11)	-1.7(9)	-2.0(8)	3.0(8)
N1	23.1(10)	17.3(11)	16.8(11)	-3.3(9)	-2.2(8)	1.9(8)
O1W	23.6(11)	22.0(13)	16.9(13)	-3.9(9)	-3.3(9)	-0.5(9)
C28	20.5(11)	19.7(13)	16.4(13)	-4.8(10)	-2.3(10)	-3.6(10)
C14	20.5(11)	18.8(13)	17.5(13)	-6.2(10)	0(1)	-1(1)
C34	19.0(11)	14.8(12)	15.4(13)	-2.6(10)	-1.7(9)	3.3(9)
C40	21.5(11)	14.6(12)	18.2(13)	-4.2(10)	-5.1(10)	4.8(10)
C44	22.9(12)	16.3(12)	17.9(13)	-3.2(10)	-3.8(10)	5.7(10)

Atom	U_{11}	U_{22}	U_{33}	U_{23}	U_{13}	U_{12}
C55	24.5(12)	15.9(13)	20.2(14)	-4.3(10)	-7.1(10)	1.1(10)
C54	19.4(11)	14.7(12)	19.3(13)	-6.5(10)	-5.8(10)	1.0(9)
C42	21.7(11)	14.4(12)	23.0(14)	-5(1)	-8.9(10)	3.2(10)
C41	18.9(11)	17.8(13)	20.1(14)	-3.5(10)	-1.3(10)	2.7(10)
C21	22.9(12)	24.6(14)	20.1(14)	-8.0(11)	-6.8(10)	-1(1)
C45	19.4(11)	15.0(12)	21.9(14)	-3.8(10)	-4.4(10)	0.6(9)
C46	22.9(12)	17.9(13)	28.7(15)	-8.3(11)	-5.6(11)	-0.3(10)
C43	26.5(12)	16.7(13)	20.6(14)	-6.5(10)	-6.8(10)	4.1(10)
C47	31.5(14)	20.0(14)	27.3(15)	-4.7(11)	-9.2(12)	-3.7(11)
C56	26.3(13)	19.9(14)	26.2(15)	-0.8(11)	-1.5(11)	-2.7(10)
C33	21.4(12)	27.0(14)	21.0(14)	-5.1(11)	-3.8(10)	0.6(10)
C22	25.6(12)	23.3(14)	23.1(15)	-7.8(11)	-4.5(11)	1.8(11)
C2	21.4(12)	29.5(15)	20.9(14)	-11.7(11)	-2.1(10)	2.1(10)
C59	27.6(13)	20.4(13)	19.2(14)	-1.1(11)	-3.5(11)	-2.5(10)
C19	27.2(13)	24.6(14)	18.9(14)	-6.1(11)	-5.7(11)	1.7(11)
C4	18.8(11)	25.7(14)	23.0(14)	-5.1(11)	0.1(10)	-2.9(10)
C35	26.1(12)	20.7(14)	23.8(15)	-7.5(11)	-4.7(11)	2.6(10)
C10	17.9(13)	71(3)	81(3)	-54(2)	-9.6(16)	9.4(15)
C3	23.9(12)	21.3(14)	22.8(14)	-5.6(11)	-2.7(11)	-1.8(10)
C24	24.6(13)	42.4(18)	25.8(16)	-16.6(13)	-7.0(11)	-0.3(12)
C25	52.8(19)	32.6(18)	53(2)	-21.1(16)	-23.4(17)	1.6(14)
C1	22.5(12)	28.7(15)	16.2(13)	-5.9(11)	2(1)	-1.9(10)
C29	28.4(13)	20.0(14)	28.5(15)	-4.7(11)	-2.7(11)	0.7(11)
C50	27.0(13)	23.5(14)	22.8(15)	-10.1(11)	-0.7(11)	0.4(11)
C6	31.4(14)	24.1(14)	22.6(15)	-0.9(11)	-1.6(11)	6.5(11)
C39	29.2(13)	23.9(14)	27.4(15)	-10.7(12)	-10.1(11)	4.1(11)
C57	26.0(13)	31.2(16)	34.5(17)	-2.4(13)	-11.7(12)	-4.9(12)
C18	25.6(13)	28.8(15)	29.2(16)	-9.2(12)	-7.7(11)	6.6(11)
C7	17.7(11)	32.9(16)	27.3(15)	-12.9(12)	-4.6(11)	6.9(11)
C36	30.2(14)	32.1(16)	24.0(15)	-7.7(12)	-11.2(11)	7.7(12)
C5	30.8(13)	17.5(13)	23.4(15)	-1.4(11)	0.6(11)	0.6(11)
C23	28.8(13)	33.0(16)	22.1(15)	-5.3(12)	-4.3(11)	2.3(12)
C30	37.0(15)	20.6(14)	27.7(16)	3.0(12)	-5.1(12)	-4.8(12)
C38	35.0(14)	19.2(14)	38.3(17)	-11.6(12)	-6.0(13)	6.8(11)
C31	34.6(14)	36.3(17)	17.0(14)	-4.9(12)	2.0(11)	-16.0(12)
C48	36.9(15)	26.4(15)	34.9(17)	-6.3(13)	-16.4(13)	-6.5(12)
C8	25.6(13)	44.4(18)	31.0(17)	-13.2(14)	-7.4(12)	10.6(12)
C20	49.1(18)	63(2)	41(2)	-28.1(17)	-6.0(15)	26.0(17)
C15	35.9(15)	33.8(16)	21.6(15)	-6.7(12)	-7.3(12)	11.3(12)
C58	34.2(15)	33.1(16)	26.0(16)	-0.2(13)	-15.0(12)	-4.6(12)
C49	22.2(13)	36.0(17)	58(2)	-25.0(15)	0.3(13)	-5.6(12)
C17	29.0(14)	34.2(17)	34.8(17)	-16.3(13)	1.3(12)	6.0(12)
C37	28.0(13)	25.4(15)	29.8(16)	-2.5(12)	-3.3(12)	9.6(11)
C16	44.9(17)	47.7(19)	21.7(16)	-17.0(14)	-3.9(13)	12.6(14)
C32	23.9(13)	41.6(18)	23.1(15)	-7.3(13)	1.3(11)	-1.5(12)
C9	25.5(14)	85(3)	41(2)	-36.5(19)	-13.4(14)	20.3(16)
C26	55.6(19)	27.7(17)	45(2)	-10.8(14)	-26.0(16)	4.0(14)
C12	18.8(12)	38.7(18)	45.7(19)	-11.3(15)	-6.5(12)	5.3(12)
C13	31.4(17)	128(4)	123(4)	-105(3)	-9(2)	3(2)
C27	39.3(16)	56(2)	33.9(18)	-23.2(15)	-11.1(14)	-2.7(14)
C11	22.4(14)	44(2)	74(3)	-30.8(18)	-6.0(15)	4.2(13)
C51	32.3(15)	42.3(19)	58(2)	-19.7(16)	7.9(15)	4.3(14)
C53	38.8(16)	47(2)	50(2)	-21.6(16)	17.5(15)	-10.3(14)
C52	48.5(19)	68(2)	34.7(19)	-15.1(17)	5.4(15)	-3.3(17)

Table 3: Bond Lengths in Å for **CMW_01_053**.

Atom	Atom	Length/Å
Co1	N3	2.0235(19)
Co1	N2	2.0186(19)
Co1	N4	2.0201(18)
Co1	N1	2.1732(19)
Co1	O1W	2.135(2)
S2	N3	1.5804(19)
S2	O4	1.4480(16)
S2	O3	1.4568(17)
S2	C14	1.783(2)
P1	C28	1.786(2)
P1	C34	1.793(2)
P1	C40	1.793(2)
P1	C54	1.792(2)
S1	O2	1.4542(17)
S1	O1	1.4339(18)
S1	N4	1.5934(19)
S1	C7	1.772(3)
S3	O6	1.4441(17)
S3	N2	1.581(2)
S3	O5	1.4475(19)
S3	C21	1.779(2)
N3	C3	1.474(3)
N2	C2	1.478(3)
N4	C6	1.463(3)
N1	C4	1.487(3)
N1	C1	1.475(3)
N1	C5	1.478(3)
C28	C33	1.392(3)
C28	C29	1.399(3)
C14	C19	1.377(3)
C14	C15	1.386(3)
C34	C35	1.390(3)
C34	C39	1.394(3)
C40	C41	1.396(3)
C40	C45	1.390(3)
C44	C45	1.389(3)
C44	C43	1.393(3)
C44	C50	1.532(3)
C55	C54	1.394(3)
C55	C56	1.382(3)
C54	C59	1.389(3)
C42	C41	1.393(3)
C42	C46	1.535(3)
C42	C43	1.394(3)
C21	C22	1.375(3)
C21	C26	1.389(3)
C46	C47	1.543(3)
C46	C48	1.530(3)
C46	C49	1.533(3)
C56	C57	1.384(3)
C33	C32	1.375(3)
C22	C23	1.383(3)
C2	C1	1.514(3)
C59	C58	1.383(3)
C19	C18	1.390(3)
C4	C3	1.519(3)
C35	C36	1.385(3)

Atom	Atom	Length/Å
C10	C9	1.391(4)
C10	C13	1.523(4)
C10	C11	1.373(4)
C24	C25	1.380(4)
C24	C23	1.382(4)
C24	C27	1.509(3)
C25	C26	1.376(4)
C29	C30	1.377(3)
C50	C51	1.528(3)
C50	C53	1.528(4)
C50	C52	1.533(4)
C6	C5	1.515(3)
C39	C38	1.382(3)
C57	C58	1.383(4)
C18	C17	1.373(4)
C7	C8	1.386(3)
C7	C12	1.385(4)
C36	C37	1.387(3)
C30	C31	1.377(3)
C38	C37	1.380(3)
C31	C32	1.384(3)
C8	C9	1.389(4)
C20	C17	1.517(3)
C15	C16	1.379(3)
C17	C16	1.394(3)
C12	C11	1.379(4)

Table 4: Bond Angles in ° for **CMW_01_053**.

Atom	Atom	Atom	Angle/°
N3	Co1	N1	81.65(7)
N3	Co1	O1W	95.77(8)
N2	Co1	N3	118.20(7)
N2	Co1	N4	118.72(8)
N2	Co1	N1	81.47(8)
N2	Co1	O1W	95.98(8)
N4	Co1	N3	116.97(8)
N4	Co1	N1	82.04(7)
N4	Co1	O1W	103.07(8)
O1W	Co1	N1	174.89(7)
N3	S2	C14	109.11(10)
O4	S2	N3	113.48(10)
O4	S2	O3	115.45(10)
O4	S2	C14	105.10(11)
O3	S2	N3	107.62(10)
O3	S2	C14	105.64(10)
C28	P1	C34	108.57(10)
C28	P1	C40	108.92(11)
C28	P1	C54	111.56(11)
C40	P1	C34	109.31(11)
C54	P1	C34	109.23(11)
C54	P1	C40	109.22(11)
O2	S1	N4	110.81(11)
O2	S1	C7	105.95(11)
O1	S1	O2	117.05(11)
O1	S1	N4	109.03(10)
O1	S1	C7	106.45(12)
N4	S1	C7	106.97(11)
O6	S3	N2	113.66(11)
O6	S3	O5	115.40(12)
O6	S3	C21	105.05(11)
N2	S3	C21	107.92(11)
O5	S3	N2	108.71(11)
O5	S3	C21	105.47(11)
S2	N3	Co1	128.34(11)
C3	N3	Co1	113.42(14)
C3	N3	S2	114.86(16)
S3	N2	Co1	130.55(12)
C2	N2	Co1	113.32(15)
C2	N2	S3	113.44(15)
S1	N4	Co1	126.91(12)
C6	N4	Co1	112.08(14)
C6	N4	S1	115.33(15)
C4	N1	Co1	107.22(13)
C1	N1	Co1	107.31(14)
C1	N1	C4	112.13(18)
C1	N1	C5	112.23(18)
C5	N1	Co1	106.17(13)
C5	N1	C4	111.38(19)

Atom	Atom	Atom	Angle/°
C33	C28	P1	121.33(18)
C33	C28	C29	118.9(2)
C29	C28	P1	119.72(18)
C19	C14	S2	121.16(19)
C19	C14	C15	120.0(2)
C15	C14	S2	118.74(17)
C35	C34	P1	120.81(18)
C35	C34	C39	119.9(2)
C39	C34	P1	118.97(18)
C41	C40	P1	118.95(17)
C45	C40	P1	120.68(18)
C45	C40	C41	120.2(2)
C45	C44	C43	117.6(2)
C45	C44	C50	121.5(2)
C43	C44	C50	120.9(2)
C56	C55	C54	120.0(2)
C55	C54	P1	117.74(17)
C59	C54	P1	121.86(19)
C59	C54	C55	120.2(2)
C41	C42	C46	121.4(2)
C41	C42	C43	117.9(2)
C43	C42	C46	120.7(2)
C42	C41	C40	120.3(2)
C22	C21	S3	121.99(19)
C22	C21	C26	119.3(2)
C26	C21	S3	118.59(19)
C44	C45	C40	121.0(2)
C42	C46	C47	108.23(18)
C48	C46	C42	109.6(2)
C48	C46	C47	109.9(2)
C48	C46	C49	108.7(2)
C49	C46	C42	112.0(2)
C49	C46	C47	108.3(2)
C44	C43	C42	123.1(2)
C55	C56	C57	119.7(2)
C32	C33	C28	120.4(2)
C21	C22	C23	119.3(2)
N2	C2	C1	107.79(18)
C58	C59	C54	119.4(2)
C14	C19	C18	119.6(2)
N1	C4	C3	110.12(18)
C36	C35	C34	119.9(2)

Atom	Atom	Atom	Angle/°
C9	C10	C13	120.2(3)
C11	C10	C9	118.9(3)
C11	C10	C13	120.9(4)
N3	C3	C4	107.96(19)
C25	C24	C23	117.7(2)
C25	C24	C27	120.0(3)
C23	C24	C27	122.3(2)
C26	C25	C24	121.0(3)
N1	C1	C2	110.14(19)
C30	C29	C28	119.9(2)
C44	C50	C52	109.0(2)
C51	C50	C44	110.3(2)
C51	C50	C52	108.8(2)
C53	C50	C44	112.6(2)
C53	C50	C51	107.9(2)
C53	C50	C52	108.1(2)
N4	C6	C5	107.78(19)
C38	C39	C34	120.1(2)
C58	C57	C56	120.4(2)
C17	C18	C19	121.4(2)
C8	C7	S1	121.3(2)
C12	C7	S1	119.3(2)
C12	C7	C8	119.4(3)
C35	C36	C37	119.8(2)
N1	C5	C6	109.9(2)
C24	C23	C22	122.2(2)
C31	C30	C29	120.8(2)
C37	C38	C39	119.8(2)
C30	C31	C32	119.6(2)
C7	C8	C9	120.0(3)
C16	C15	C14	119.7(2)
C59	C58	C57	120.4(2)
C18	C17	C20	120.9(2)
C18	C17	C16	118.3(2)
C16	C17	C20	120.8(3)
C38	C37	C36	120.6(2)
C15	C16	C17	121.0(3)
C33	C32	C31	120.4(2)
C8	C9	C10	120.4(3)
C25	C26	C21	120.4(3)
C11	C12	C7	120.1(3)
C10	C11	C12	121.2(3)

Table 5: Torsion Angles in ° for **CMW_01_053**.

Atom	Atom	Atom	Atom	Angle/°
Co1	N3	C3	C4	-37.9(2)
Co1	N2	C2	C1	-38.0(2)
Co1	N4	C6	C5	-40.6(2)
Co1	N1	C4	C3	-36.7(2)
Co1	N1	C1	C2	-37.3(2)
Co1	N1	C5	C6	-37.8(2)
S2	N3	C3	C4	160.99(15)
S2	C14	C19	C18	175.44(19)

Atom	Atom	Atom	Atom	Angle/°
S2	C14	C15	C16	-175.9(2)
P1	C28	C33	C32	-178.8(2)
P1	C28	C29	C30	177.9(2)
P1	C34	C35	C36	172.06(19)
P1	C34	C39	C38	-172.0(2)
P1	C40	C41	C42	174.35(16)
P1	C40	C45	C44	-174.44(17)
P1	C54	C59	C58	173.12(19)
S1	N4	C6	C5	163.98(17)
S1	C7	C8	C9	177.77(19)
S1	C7	C12	C11	-177.40(19)
S3	N2	C2	C1	158.55(16)
S3	C21	C22	C23	-176.09(19)
S3	C21	C26	C25	175.3(2)
N3	S2	C14	C19	21.2(2)
N3	S2	C14	C15	-162.7(2)
O6	S3	N2	Co1	-115.01(15)
O6	S3	N2	C2	44.86(19)
O6	S3	C21	C22	-145.6(2)
O6	S3	C21	C26	37.5(2)
O4	S2	N3	Co1	165.33(11)
O4	S2	N3	C3	-36.97(18)
O4	S2	C14	C19	143.2(2)
O4	S2	C14	C15	-40.6(2)
O2	S1	N4	Co1	177.12(12)
O2	S1	N4	C6	-31.7(2)
O2	S1	C7	C8	29.9(2)
O2	S1	C7	C12	-152.88(19)
O1	S1	N4	Co1	46.91(17)
O1	S1	N4	C6	-161.96(18)
O1	S1	C7	C8	155.22(19)
O1	S1	C7	C12	-27.6(2)
O3	S2	N3	Co1	36.31(15)
O3	S2	N3	C3	-165.99(15)
O3	S2	C14	C19	-94.3(2)
O3	S2	C14	C15	81.9(2)
N2	S3	C21	C22	-24.1(2)
N2	S3	C21	C26	159.1(2)
N2	C2	C1	N1	49.7(2)
O5	S3	N2	Co1	14.99(17)
O5	S3	N2	C2	174.86(15)
O5	S3	C21	C22	92.0(2)
O5	S3	C21	C26	-84.9(2)
N4	S1	C7	C8	-88.3(2)
N4	S1	C7	C12	88.9(2)
N4	C6	C5	N1	52.5(3)
N1	C4	C3	N3	49.3(2)
C28	P1	C34	C35	-92.6(2)
C28	P1	C34	C39	80.4(2)
C28	P1	C40	C41	38.6(2)

Atom	Atom	Atom	Atom	Angle/°
C28	P1	C40	C45	-146.44(18)
C28	P1	C54	C55	-166.74(17)
C28	P1	C54	C59	18.9(2)
C28	C33	C32	C31	1.2(4)
C28	C29	C30	C31	0.7(4)
C14	S2	N3	Co1	-77.86(15)
C14	S2	N3	C3	79.84(17)
C14	C19	C18	C17	0.6(4)
C14	C15	C16	C17	0.0(4)
C34	P1	C28	C33	-9.2(2)
C34	P1	C28	C29	172.17(19)
C34	P1	C40	C41	-79.9(2)
C34	P1	C40	C45	95.08(19)
C34	P1	C54	C55	-46.7(2)
C34	P1	C54	C59	138.96(19)
C34	C35	C36	C37	0.0(4)
C34	C39	C38	C37	-0.4(4)
C40	P1	C28	C33	-128.1(2)
C40	P1	C28	C29	53.2(2)
C40	P1	C34	C35	26.1(2)
C40	P1	C34	C39	-160.91(19)
C40	P1	C54	C55	72.8(2)
C40	P1	C54	C59	-101.5(2)
C55	C54	C59	C58	-1.1(4)
C55	C56	C57	C58	0.2(4)
C54	P1	C28	C33	111.2(2)
C54	P1	C28	C29	-67.4(2)
C54	P1	C34	C35	145.53(19)
C54	P1	C34	C39	-41.5(2)
C54	P1	C40	C41	160.62(18)
C54	P1	C40	C45	-24.4(2)
C54	C55	C56	C57	-0.6(4)
C54	C59	C58	C57	0.7(4)
C41	C40	C45	C44	0.5(3)
C41	C42	C46	C47	-107.5(2)
C41	C42	C46	C48	132.6(2)
C41	C42	C46	C49	11.9(3)
C41	C42	C43	C44	-0.9(3)
C21	S3	N2	Co1	128.92(14)
C21	S3	N2	C2	-71.21(18)
C21	C22	C23	C24	0.8(4)
C45	C40	C41	C42	-0.7(3)
C45	C44	C43	C42	0.7(3)
C45	C44	C50	C51	122.1(2)
C45	C44	C50	C53	1.6(3)
C45	C44	C50	C52	-118.4(2)
C46	C42	C41	C40	179.7(2)
C46	C42	C43	C44	-179.7(2)
C43	C44	C45	C40	-0.5(3)
C43	C44	C50	C51	-59.6(3)
C43	C44	C50	C53	179.9(2)
C43	C44	C50	C52	59.9(3)
C43	C42	C41	C40	0.9(3)
C43	C42	C46	C47	71.3(3)

Atom	Atom	Atom	Atom	Angle/°
C43	C42	C46	C48	-48.7(3)
C43	C42	C46	C49	-169.4(2)
C56	C55	C54	P1	-173.43(18)
C56	C55	C54	C59	1.0(3)
C56	C57	C58	C59	-0.3(4)
C33	C28	C29	C30	-0.8(4)
C22	C21	C26	C25	-1.7(4)
C19	C14	C15	C16	0.4(4)
C19	C18	C17	C20	-179.1(3)
C19	C18	C17	C16	-0.2(4)
C4	N1	C1	C2	80.2(2)
C4	N1	C5	C6	-154.2(2)
C35	C34	C39	C38	1.1(4)
C35	C36	C37	C38	0.7(4)
C24	C25	C26	C21	1.0(5)
C25	C24	C23	C22	-1.4(4)
C1	N1	C4	C3	-154.3(2)
C1	N1	C5	C6	79.1(2)
C29	C28	C33	C32	-0.1(4)
C29	C30	C31	C32	0.4(4)
C50	C44	C45	C40	177.9(2)
C50	C44	C43	C42	-177.6(2)
C39	C34	C35	C36	-0.9(4)
C39	C38	C37	C36	-0.5(4)
C18	C17	C16	C15	-0.1(4)
C7	S1	N4	Co1	-67.83(17)
C7	S1	N4	C6	83.3(2)
C7	C8	C9	C10	-0.4(4)
C7	C12	C11	C10	-0.5(4)
C5	N1	C4	C3	79.0(2)
C5	N1	C1	C2	-153.58(19)
C23	C24	C25	C26	0.5(4)
C30	C31	C32	C33	-1.3(4)
C8	C7	C12	C11	-0.2(4)
C20	C17	C16	C15	178.7(3)
C15	C14	C19	C18	-0.7(4)
C9	C10	C11	C12	0.7(4)
C26	C21	C22	C23	0.8(4)
C12	C7	C8	C9	0.6(4)
C13	C10	C9	C8	-178.8(2)
C13	C10	C11	C12	179.2(2)
C27	C24	C25	C26	-178.7(3)
C27	C24	C23	C22	177.8(2)
C11	C10	C9	C8	-0.2(4)

Table 6: Hydrogen Fractional Atomic Coordinates (×10⁴) and Equivalent Isotropic Displacement Parameters (Å²×10³) for **CMW_01_053**. U_{eq} is defined as 1/3 of the trace of the orthogonalised U_{ij}.

Atom	x	y	z	U_{eq}
H1WA	8180(20)	1714(10)	2452(9)	25
H1WB	8790(20)	1940(12)	3091(7)	25
H55	7717	9974	2985	24

Atom	x	y	z	U_{eq}
H41	4116	7383	3650	23
H45	7888	8366	2913	23
H43	6250	6395	2213	25
H47A	5067	4990	3016	39
H47B	3539	4744	3335	39
H47C	4594	5158	3754	39
H56	9972	10383	3084	30
H33	3377	9254	4581	28
H22	8411	2589	258	28
H2A	11222	2223	492	28
H2B	12071	2220	1158	28
H59	7567	8486	4991	28
H19	8991	4221	2932	28
H4A	13020	4355	1439	27
H4B	12947	3273	1636	27
H35	3857	9064	2764	28
H3A	12895	3665	2687	27
H3B	11729	4414	2445	27
H25	7989	-188	-262	52
H1A	12262	3674	431	27
H1B	10643	3736	336	27
H29	6107	7181	4921	31
H6A	8693	5407	937	32
H6B	8896	4568	595	32
H39	5500	10633	3866	31
H57	11015	9849	4136	37
H18	7599	5187	3408	33
H36	2399	10252	2269	34
H5A	11074	5156	641	30
H5B	10800	5120	1448	30
H23	7436	2502	-756	34
H30	4969	6551	5987	36
H38	4030	11812	3374	36
H31	3040	7251	6351	36
H48A	3265	6800	1937	49
H48B	2706	5784	2181	49
H48C	4286	5971	1936	49
H8	6009	4587	353	39
H20A	7166	5955	4341	73
H20B	7723	5509	5092	73
H20C	6406	5095	4846	73
H15	10496	3157	4815	36
H58	9824	8897	5082	38
H49A	2703	6281	3806	55
H49B	1790	5926	3291	55
H49C	2228	6967	3108	55
H37	2477	11615	2585	34
H16	9119	4133	5279	44
H32	2222	8589	5634	36
H9	5082	3669	-276	56
H26	9017	-112	738	50
H12	6014	2458	2044	41
H13A	3477	1758	256	121
H13B	4977	1359	157	121
H13C	4463	2237	-400	121
H27A	7549	816	-1544	61
H27B	6633	1684	-1518	61

Atom	x	y	z	U_{eq}
H27C	6094	694	-1120	61
H11	5119	1549	1410	53
H51A	9456	6283	2626	65
H51B	10041	6485	1835	65
H51C	8573	6019	2056	65
H53A	9202	8686	1942	66
H53B	10384	8068	1714	66
H53C	9927	7924	2518	66
H52A	7470	7172	1175	75
H52B	8893	7683	916	75
H52C	7604	8223	1142	75

Table 7: Hydrogen Bond information for **CMW_01_053**.

D	H	A	d(D-H)/Å	d(H-A)/Å	d(D-A)/Å	D-H-A/deg
O1W	H1WA	O5	0.972(5)	1.639(7)	2.598(3)	168(2)
O1W	H1WB	O3	0.969(5)	1.733(9)	2.648(3)	156.2(18)

Table 8: Atomic Occupancies for all atoms that are not fully occupied in **CMW_01_053**.

Atom	Occupancy
O1W	0.804(5)

```
#==============================================================================
# PLATON/CHECK-( 70414) versus check.def version of 310314   for Entry: cmw_01_0
# Data: CMW_01_053.cif - Type: CIF              Bond Precision   C-C = 0.0037 A
# Refl: CMW_01_053.fcf - Type: LIST4                               Temp = 100 K
#                                              X-Ray         Nref/Npar =  22.7
# Cell   9.7734(8) 15.3083(11) 19.9544(15)    75.046(1)    86.650(1)   89.023(1)
# Wavelength 0.71073    Volume Reported     2879.4(4)   Calculated     2879.4(4)
# SpaceGroup from Symmetry P -1       Hall: -P 1                   triclinic
#                 Reported P -1             -P 1                   triclinic
# MoietyFormula C27 H35 Co N4 O6.80 S3, C32 H36 P
#      Reported C27 H35 Co N4 O6.8 S3, C32 H36 P
#    SumFormula C59 H71 Co N4 O6.80 P S3
#      Reported C59 H71 Co N4 O6.81 P S3
# Mr        =   1131.17[Calc],   1131.15[Rep]
# Dx,gcm-3  =     1.305[Calc],     1.305[Rep]
# Z         =         2[Calc],         2[Rep]
# Mu (mm-1) =     0.489[Calc],     0.489[Rep]
# F000      =    1194.9[Calc],    1195.0[Rep]  or F000' =   1196.92[Calc]
# Reported   T Limits: Tmin=0.567             Tmax=0.746  AbsCorr=MULTI-SCAN
# Calculated T Limits: Tmin=0.834 Tmin'=0.834  Tmax=0.898
# Reported   Hmax= 13, Kmax= 21, Lmax= 27, Nref=  15720        , Th(max)= 29.573
# Obs in FCF Hmax= 13, Kmax= 21, Lmax= 27, Nref=  15720[ 15720], Th(max)= 29.573
# Calculated Hmax= 13, Kmax= 21, Lmax= 27, Nref=  16178        , Ratio  =  0.972
# Reported   Rho(min) = -0.46, Rho(max) =  0.60 e/Ang**3 (From CIF)
# Calculated Rho(min) = -0.44, Rho(max) =  0.58 e/Ang**3 (From CIF+FCF data)
# w=1/[sigma**2(Fo**2)+(0.0331P)**2], P=(Fo**2+2*Fc**2)/3
# R= 0.0521(  9512), wR2= 0.1097( 15720), S = 0.890      (From CIF+FCF data)
# R= 0.0521(  9512), wR2= 0.1097( 15720), S = 0.890      (From FCF data only)
# R= 0.0521(  9512), wR2= 0.1097( 15720), S = 0.889, Npar=  692
#==============================================================================
For Documentation: http://http://www.platonsoft.nl/CIF-VALIDATION.pdf
#==============================================================================

#==============================================================================
>>> The Following Improvement and Query ALERTS were generated - (Acta-Mode) <<<
#==============================================================================
Format: alert-number_ALERT_alert-type_alert-level text
#=============================================================================
041_ALERT_1_C Calc. and Reported SumFormula    Strings  Differ     Please Check
068_ALERT_1_C Reported F000 Differs from Calcd (or Missing)...     Please Check
077_ALERT_4_C Unitcell contains non-integer number of atoms ..     Please Check
220_ALERT_2_C Large Non-Solvent  C     Ueq(max)/Ueq(min) Range        4.3 Ratio
222_ALERT_3_C Large Non-Solvent    H    Uiso(max)/Uiso(min) ..        4.8 Ratio
230_ALERT_2_C Hirshfeld Test Diff for    C50    --  C51     ..        6.5 su
230_ALERT_2_C Hirshfeld Test Diff for    C50    --  C53     ..        6.5 su
242_ALERT_2_C Low       Ueq as Compared to Neighbors for .....        C50 Check
601_ALERT_2_C Structure Contains Solvent Accessible VOIDS of .         42 Ang3
911_ALERT_3_C Missing # FCF Refl Between THmin & STh/L=  0.600         35 Why ?
#=============================================================================
002_ALERT_2_G Number of Distance or Angle Restraints on AtSite          3 Note
008_ALERT_5_G No _iucr_refine_reflections_details   in the CIF     Please Do !
042_ALERT_1_G Calc. and Reported MoietyFormula Strings  Differ     Please Check
154_ALERT_1_G The su's on the Cell Angles are Equal ..........    0.00100 Degree
301_ALERT_3_G Main Residue  Disorder ..... Percentage =          1 Note
380_ALERT_4_G Incorrectly? Oriented X(sp2)-Methyl Moiety .....        C27 Check
720_ALERT_4_G Number of Unusual/Non-Standard Labels ..........          2 Note
802_ALERT_4_G CIF Input Record(s) with more than 80 Characters          ! Info
860_ALERT_3_G Number of Least-Squares Restraints .............         3 Note
912_ALERT_4_G Missing # of FCF Reflections Above STh/L=  0.600        423 Note
#=============================================================================

ALERT_Level and ALERT_Type Summary
==================================
1 ALERT_Level_B = A Potentially Serious Problem - Consider Carefully
```

```
10 ALERT_Level_C = Check. Ensure it is Not caused by an Omission or Oversight
10 ALERT_Level_G = General Info/Check that it is not Something Unexpected

4 ALERT_Type_1 CIF Construction/Syntax Error, Inconsistent or Missing Data.
7 ALERT_Type_2 Indicator that the Structure Model may be Wrong or Deficient.
4 ALERT_Type_3 Indicator that the Structure Quality may be Low.
5 ALERT_Type_4 Improvement, Methodology, Query or Suggestion.
1 ALERT_Type_5 Informative Message, Check.
#==============================================================================

1 Missing  Experimental  Info Issue(s) (Out of  54 Tests) -   98 % Satisfied
0 Experimental  Data  Related Issue(s) (Out of  28 Tests) -  100 % Satisfied
10 Structural  Model   Related Issue(s) (Out of 117 Tests) -   91 % Satisfied
10 Unresolved or to be Checked Issue(s) (Out of 223 Tests) -   96 % Satisfied

#==============================================================================
```

5-1(OH$_2$)

EMORY UNIVERSITY | X-ray Crystallography Center

Submitted by: **Christian Wallen**
Emory University

Sample ID: **CMW04_055**

Crystal Data and Experimental

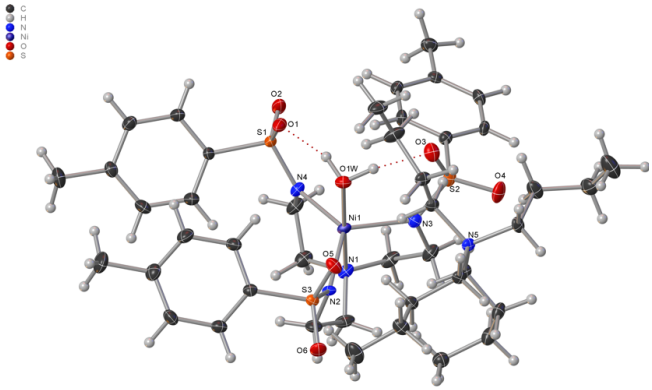

Experimental. Single green rect. prism-shaped crystals of (**CMW04_055**) were The crystal was chosen from the sample as supplied. A suitable crystal (0.50×0.40×0.33 mm^3) was selected and mounted on a loop with paratone oil on a Bruker APEX-II CCD diffractometer. The crystal was cooled to T = 100(2) K during data collection. The structure was solved with the **ShelXT** (Sheldrick, 2015) structure solution program using the Intrinsic Phasing solution method and by using **Olex2** (Dolomanov et al., 2009) as the graphical interface. The model was refined with version 2014/7 of **XL** (Sheldrick, 2008) using Least Squares minimisation.

Crystal Data. $C_{43}H_{71}N_5NiO_7S_3$, M_r = 924.93, monoclinic, $P2_1$ (No. 4), a = 14.5075(11) Å, b = 14.7787(11) Å, c = 22.0503(17) Å, β = 103.8550(10)°, α = γ = 90°, V = 4590.1(6) Å^3, T = 100(2) K, Z = 4, Z' = 2, μ(MoK$_\alpha$) = 0.613 mm^{-1}, 46116 reflections measured, 23424 unique (R_{int} = 0.0318) which were used in all calculations. The final wR_2 was 0.1100 (all data) and R_1 was 0.0438 (I > 2σ(I)).

Compound	**CMW04_055**
Formula	$C_{43}H_{71}N_5NiO_7S_3$
$D_{calc.}$/ g cm^{-3}	1.338
μ/mm^{-1}	0.613
Formula Weight	924.93
Colour	green
Shape	rect. prism
Size/mm^3	0.50×0.40×0.33
T/K	100(2)
Crystal System	monoclinic
Flack Parameter	0.464(9)
Hooft Parameter	0.470(4)
Space Group	$P2_1$
a/Å	14.5075(11)
b/Å	14.7787(11)
c/Å	22.0503(17)
α/°	90
β/°	103.8550(10)
γ/°	90
V/Å^3	4590.1(6)
Z	4
Z'	2
Wavelength/Å	0.710730
Radiation type	MoK$_\alpha$
Θ_{min}/°	1.528
Θ_{max}/°	29.129
Measured Refl.	46116
Independent Refl.	23424
Reflections with I > 2σ(I)	21423
R_{int}	0.0318
Parameters	1089
Restraints	7
Largest Peak	1.327
Deepest Hole	-0.336
GooF	1.053
wR_2 (all data)	0.1100
wR_2	0.1062
R_1 (all data)	0.0490
R_1	0.0438

Structure Quality Indicators

Reflections:	d min (Mo)	0.73	I/σ	14.9	Rint	3.18%	complete 95%
Refinement:	Shift	-0.001	Max Peak	1.3	Min Peak	-0.3	GooF 1.053

A green rect. prism-shaped crystal with dimensions 0.50×0.40×0.33 mm^3 was mounted on a loop with paratone oil. Data were collected using a Bruker APEX-II CCD diffractometer equipped with an Oxford Cryosystems low-temperature device, operating at T = 100(2) K.

Data were measured using ϕ and ω scans of 0.50° per frame for 20.00 s using MoK$_\alpha$ radiation (fine-focus sealed tube, 45 kV, 35 mA).The total number of runs and images was based on the strategy calculation from the program **APEX2** (Bruker). The maximum resolution that was achieved was Θ = 29.129°.

The diffraction patterns were indexed using **SAINT** (Bruker, V8.34A, 2013) and the unit cells were refined using **SAINT** (Bruker, V8.34A, 2013) on 9573 reflections, 21 % of the observed reflections. Data reduction, scaling and absorption corrections were performed using **SAINT** (Bruker, V8.34A, 2013) and **SADABS-2014/5** (Bruker,2014/5). wR_2(int) was 0.0827 before and 0.0482 after correction. The ratio of minimum to maximum transmission is 0.8951. The $\lambda/2$ correction factor is 0.00150. The final completeness is 99.9% out to 29.129° in Θ. The absorption coefficient μ of this material is 0.613 mm^{-1} at this wavelength (λ = 0.71073 Å) and the minimum and maximum transmissions are 0.6678 and 0.7461.

The structure was solved and the space group $P2_1$ (# 4) determined by the **ShelXT** (Sheldrick, 2015) structure solution program using Intrinsic Phasing and refined by Least Squares using version 2014/7 of **XL** (Sheldrick, 2008). All non-hydrogen atoms were refined anisotropically. Hydrogen atom positions, except those of the water molecules were calculated geometrically and refined using the riding model. The water molecule's hydrogen atoms were located from difference maps and refined with restraints.

_refine_special_details: Refined as a 2-component inversion twin.

The value of Z' is 2. This means that there are two independent molecules in the asymmetric unit.

The Flack parameter was refined to 0.464(9). Determination of absolute structure using Bayesian statistics on Bijvoet differences using the Olex2 results in 0.470(4). Note: The Flack parameter is used to determine chirality of the crystal studied, the value should be near 0, a value of 1 means that the stereochemistry is wrong and the model should be inverted. A value of 0.5 means that the crystal consists of a racemic mixture of the two enantiomers.

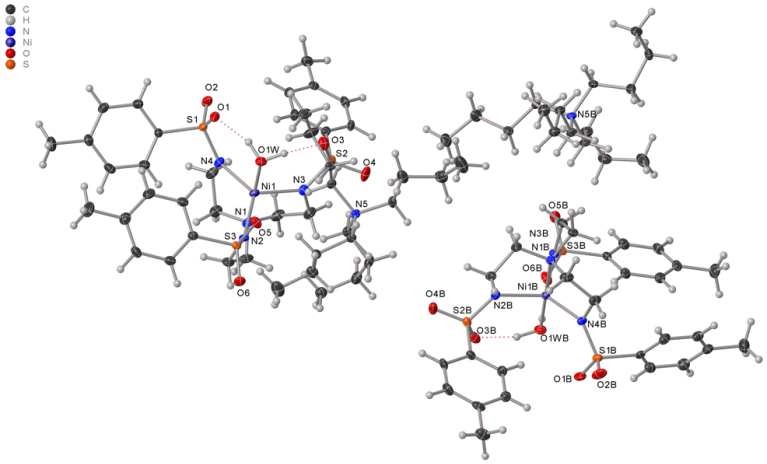

Figure 1: Plot of the asymmetric unit. There are two independent NiL(H_2O)-molecules (4 whole molecules) in the asymmetric unit.

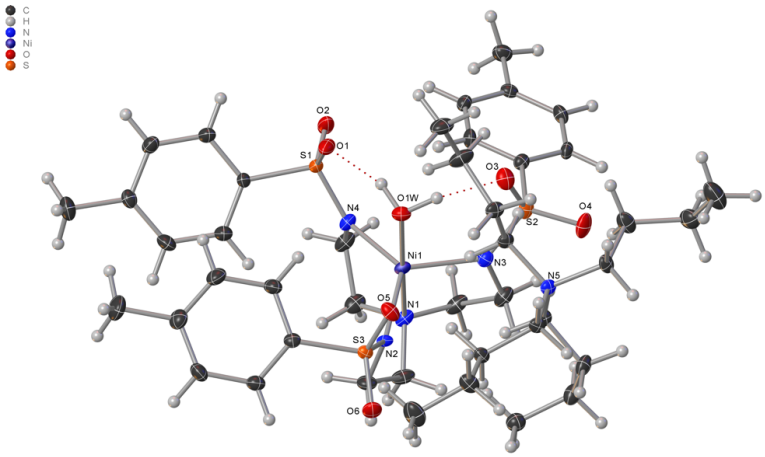

Figure 2: One of the two independent NiL(H_2O)-molecules (with its counterion) in the asymmetric unit.

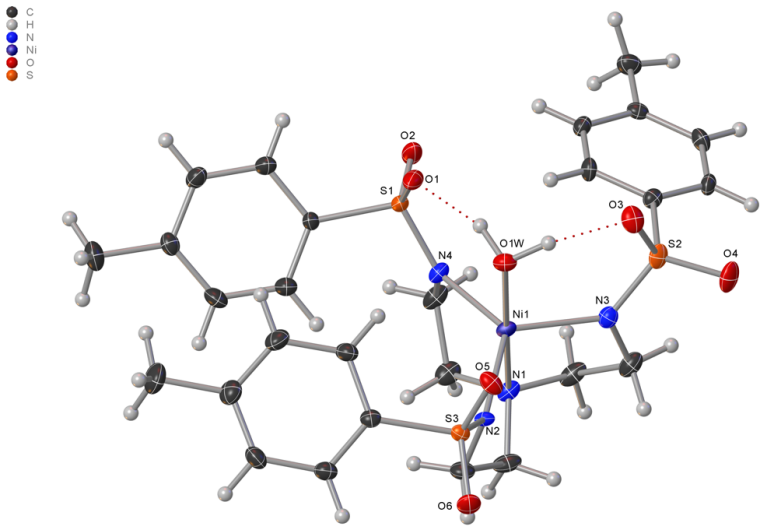

Figure 3: One of the two independent NiL(H_2O)-molecules (without its counterion) in the asymmetric unit.

Data Plots: Diffraction Data

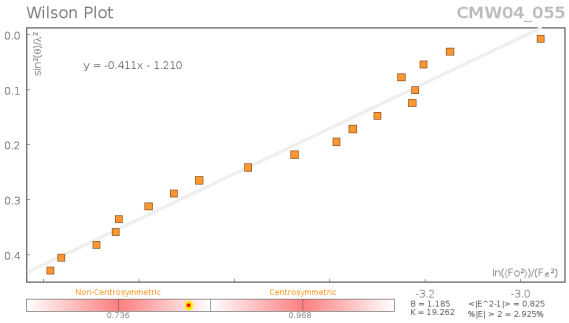

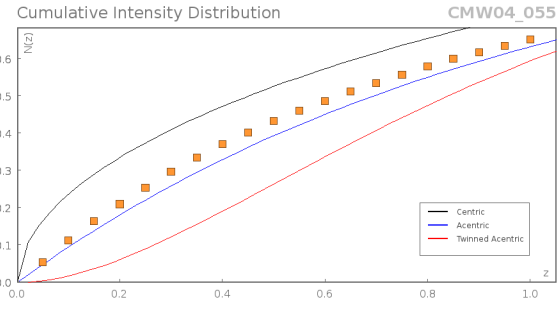

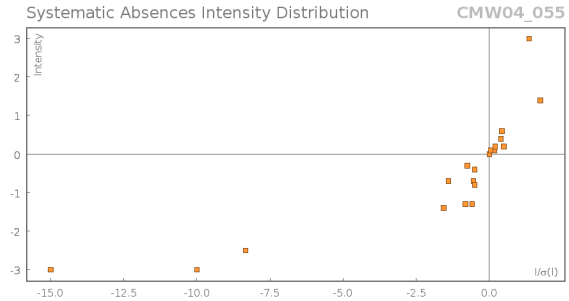

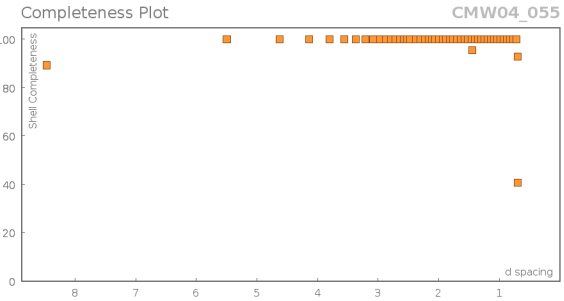

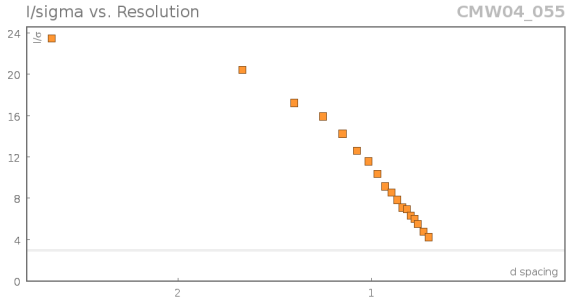

Data Plots: Refinement and Data

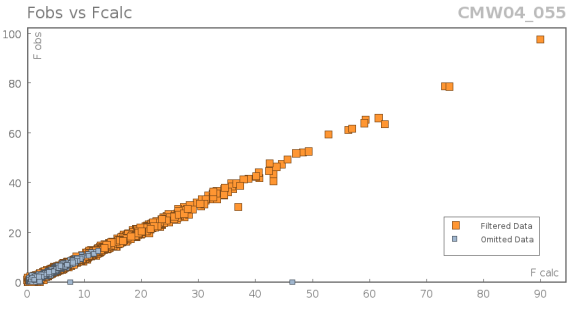

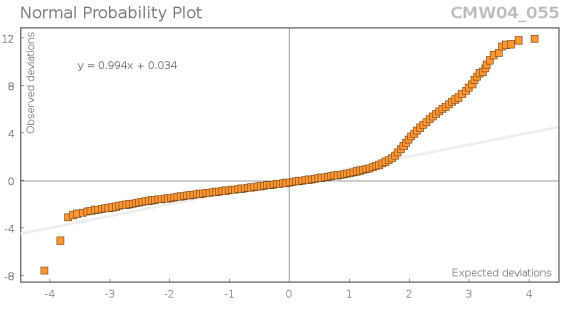

Reflection Statistics

Total reflections (after filtering)	46140	Unique reflections	23424
Completeness	0.948	Mean I/σ	14.88
hkl_{max} collected	(20, 21, 31)	hkl_{min} collected	(-20, -21, -31)
hkl_{max} used	(19, 20, 30)	hkl_{min} used	(-19, -20, 0)
Lim d_{max} collected	20.0	Lim d_{min} collected	0.73
d_{max} used	13.32	d_{min} used	0.73
Friedel pairs	14395	Friedel pairs merged	0

Inconsistent equivalents	2	R_{int}	0.0318
R_{sigma}	0.0489	Intensity transformed	0
Omitted reflections	0	Omitted by user (OMIT hkl)	3
Multiplicity	(31877, 8606, 475, 14)	Maximum multiplicity	6
Removed systematic absences	21	Filtered off (Shel/OMIT)	4430

Images of the Crystal on the Diffractometer

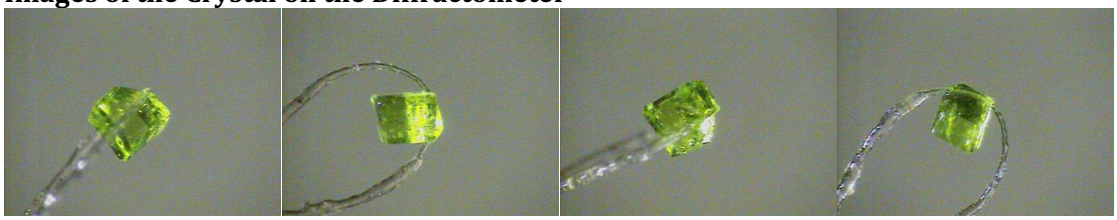

Table 1: Fractional Atomic Coordinates (×10⁴) and Equivalent Isotropic Displacement Parameters (Å²×10³) for **CMW04_055**. U_{eq} is defined as 1/3 of the trace of the orthogonalised U_{ij}.

Atom	x	y	z	U_{eq}
Ni1	3772.6(3)	2521.4(3)	98.2(2)	12.86(9)
Ni1B	1153.0(3)	3739.7(3)	4884.4(2)	12.43(9)
S3B	3374.6(5)	3846.5(6)	5719.2(4)	13.06(15)
S3	1572.5(5)	2166.6(6)	-679.4(4)	12.82(15)
S1	5407.6(6)	3036.7(6)	-694.2(4)	17.21(17)
S1B	-656.0(6)	3459.2(6)	5569.4(4)	18.16(17)
S2B	791.5(6)	2430.8(6)	3645.1(4)	17.73(17)
S2	4316.4(6)	3856.7(7)	1335.6(4)	18.30(17)
O6	763.4(17)	1611.3(18)	-635.8(12)	21.2(5)
O1W	3415.6(16)	3797.1(18)	-260.8(11)	18.2(5)
O6B	3335.1(18)	2865.5(17)	5708.2(12)	21.7(5)
O3	3975.2(19)	4564.2(18)	876.0(12)	22.2(6)
O2B	-1657.1(18)	3628(2)	5309.0(13)	30.1(7)
O5B	4272.6(17)	4236.8(19)	5668.9(12)	20.7(5)
O5	1464.5(17)	3129.4(17)	-621.0(12)	19.1(5)
O3B	1217.6(19)	1743.7(18)	4109.4(13)	23.5(6)
O1	4815.7(19)	3843.5(17)	-860.0(12)	23.9(6)
O4B	1052(2)	2369(2)	3050.4(13)	29.2(7)
O1B	-351(2)	2532.5(19)	5588.7(13)	27.1(6)
O4	4058.1(19)	3958(2)	1927.7(13)	27.2(6)
O1WB	1418.9(18)	2460.3(18)	5250.2(12)	20.6(5)
N5	1054.9(19)	4576.0(19)	805.9(13)	13.8(5)
N1	4237(2)	1259(2)	483.9(14)	16.7(6)
O2	6399.8(19)	3219(2)	-429.9(12)	28.7(6)
N3	4013(2)	2918(2)	1010.7(14)	17.1(6)
N3B	2504.8(19)	4235.0(19)	5221.1(13)	13.5(5)
N2	2516.0(19)	1858.2(19)	-203.7(13)	12.5(5)
N5B	5950(2)	6417.2(19)	5711.9(14)	14.2(5)
N4B	-4(2)	4039(2)	5233.2(14)	16.3(6)
N4	4937(2)	2401(2)	-282.1(13)	16.4(6)
N1B	913(2)	5036(2)	4512.1(13)	14.3(5)
C17	7562(2)	3939(2)	1752.0(17)	15.7(6)
C18	7006(2)	3864(2)	1141.3(16)	16.7(6)
C7B	-438(2)	3815(3)	6363.6(15)	15.1(6)
N2B	1007(2)	3387(2)	3961.6(14)	17.0(6)
C19	6031(2)	3847(3)	1019.5(15)	17.6(7)
C7	5363(2)	2472(2)	-1412.9(15)	14.6(6)
C32B	5978(2)	5704(2)	6214.8(16)	16.7(7)

Atom	x	y	z	U_{eq}
C41B	4700(2)	7296(2)	4896.4(17)	17.4(7)
C18B	-1949(3)	1951(3)	2753.6(18)	22.5(8)
C28B	6486(2)	6099(2)	5233.8(16)	14.6(6)
C41	1188(2)	5742(2)	-37.5(17)	17.9(7)
C31B	6449(3)	4190(3)	4037.5(19)	25.7(8)
C21	1730(2)	1969(2)	-1445.4(16)	14.6(6)
C37	-229(2)	3804(2)	-42.6(16)	15.4(6)
C24	2015(3)	1686(3)	-2639.7(18)	23.0(8)
C10B	-105(3)	4389(2)	7603.4(17)	18.5(7)
C8B	-700(3)	4692(2)	6503.8(17)	19.5(7)
C11	5822(2)	2440(3)	-2389.5(16)	20.5(7)
C14	5579(2)	3916(2)	1513.7(16)	15.6(6)
C17B	-2431(2)	2027(2)	3223.0(18)	19.7(7)
C40B	4909(2)	6578(2)	5408.6(16)	16.3(7)
C43B	3404(3)	7985(3)	4048.0(17)	22.3(7)
C42B	3654(2)	7257(3)	4549.2(17)	19.0(7)
C10	5229(3)	1693(2)	-2588.3(17)	18.2(7)
C12	5888(2)	2834(2)	-1814.2(17)	19.9(7)
C2B	660(3)	4154(3)	3539.5(17)	19.9(7)
C19B	-970(3)	2054(2)	2871.6(16)	19.6(7)
C38	-1264(2)	3883(3)	-401.2(18)	21.4(7)
C24B	2977(3)	4687(2)	7642.6(17)	20.0(7)
C21B	3224(2)	4177(2)	6468.7(15)	13.1(6)
C16	7098(3)	4013(2)	2236.4(17)	18.8(7)
C36	0(2)	4479(2)	494.9(16)	14.5(6)
C32	1499(2)	3668(2)	1034.0(16)	15.5(6)
C37B	6086(3)	7714(3)	6516.0(17)	22.8(8)
C15	6107(2)	3992(2)	2120.9(16)	16.7(7)
C29B	6070(2)	5299(2)	4834.6(16)	16.7(7)
C20	8626(3)	3938(3)	1876.7(19)	23.2(8)
C15B	-928(2)	2349(3)	3952.7(17)	19.0(7)
C42	1919(3)	6111(3)	-362(2)	26.6(8)
C9B	-525(2)	4968(2)	7119.6(17)	20.2(7)
C36B	6442(2)	7287(2)	5986.9(17)	16.7(7)
C12B	-17(2)	3234(2)	6841.9(17)	19.1(7)
C1	3397(3)	669(2)	433.2(18)	22.3(8)
C28	1120(2)	5241(2)	1343.4(16)	17.5(7)
C23B	3874(3)	4457(3)	7562.4(17)	21.3(7)
C4B	1602(2)	5644(2)	4931.9(17)	16.1(6)
C38B	6616(3)	8604(3)	6716.7(17)	22.9(8)
C3B	2583(2)	5213(2)	5098.6(16)	15.9(6)
C16B	-1910(2)	2233(2)	3823.3(17)	18.9(7)
C40	1606(2)	4923(2)	347.2(16)	14.9(6)
C8	4787(3)	1731(3)	-1597.6(18)	22.7(7)
C22	2417(3)	2472(3)	-1645.7(17)	20.3(7)
C6	5534(2)	1618(3)	-30.2(18)	21.3(7)
C30	2107(3)	5830(3)	2369.0(18)	28.3(8)
C13B	91(3)	4705(3)	8274.0(19)	29.4(9)
C5B	-77(2)	5294(3)	4510.0(18)	20.3(7)
C34B	6887(3)	4793(3)	7121.2(18)	24.2(8)
C33B	6959(3)	5408(3)	6572.9(17)	23.0(8)
C11B	150(3)	3528(2)	7459.0(17)	21.6(7)
C5	4894(3)	886(3)	123.1(19)	22.3(8)
C29	2117(3)	5473(3)	1714.4(18)	24.5(8)
C1B	1066(3)	5022(2)	3870.7(16)	18.1(7)
C20B	-3490(3)	1880(3)	3093(2)	28.0(8)
C33	1097(3)	3192(3)	1522.7(17)	21.1(7)

Atom	x	y	z	U_{eq}
C26	1185(2)	1339(2)	-1834.3(17)	19.4(7)
C14B	-459(2)	2254(2)	3474.9(16)	16.0(7)
C3	4216(3)	2128(3)	1434.2(18)	22.6(8)
C23	2541(3)	2332(3)	-2243.2(18)	24.2(8)
C25	1329(3)	1203(3)	-2430.2(17)	22.3(7)
C39	-1503(3)	3203(3)	-929(2)	32.9(10)
C27B	2840(3)	4964(3)	8274.0(19)	29.3(9)
C22B	3996(2)	4210(2)	6983.1(17)	19.0(7)
C39B	6440(3)	9311(3)	6205.8(19)	24.3(8)
C6B	-307(2)	4992(2)	5113.9(18)	19.9(7)
C35B	6574(4)	5296(3)	7641.8(19)	34.4(10)
C26B	2322(2)	4404(2)	6547.1(17)	17.6(7)
C25B	2208(3)	4655(2)	7127.2(17)	19.2(7)
C30B	6777(3)	5010(3)	4454.9(19)	23.6(8)
C34	1578(3)	2268(3)	1684.7(17)	21.9(8)
C35	1390(3)	1604(3)	1142.9(18)	22.4(8)
C43	1569(3)	6871(3)	-817(2)	27.9(9)
C13	5120(3)	1302(3)	-3233.9(19)	31.4(9)
C27	2165(4)	1535(4)	-3287(2)	38.8(11)
C2	2663(3)	873(2)	-168.8(18)	19.5(7)
C9	4728(3)	1342(3)	-2180.2(18)	25.5(8)
C4	4737(2)	1425(3)	1146.4(17)	21.7(7)
C31	1606(3)	6720(4)	2365(2)	40.6(11)

Table 3: Anisotropic Displacement Parameters ($\times 10^4$) **CMW04_055**. The anisotropic displacement factor exponent takes the form: $-2\pi^2[h^2a^{*2} \times U_{11} + \ldots + 2hka^* \times b^* \times U_{12}]$

Atom	U_{11}	U_{22}	U_{33}	U_{23}	U_{13}	U_{12}
Ni1	9.97(18)	13.9(2)	14.7(2)	3.79(17)	2.87(15)	-0.25(15)
Ni1B	12.91(19)	12.5(2)	11.46(19)	0.11(16)	2.11(15)	-3.06(15)
S3B	9.9(3)	13.0(4)	15.0(4)	-2.6(3)	0.5(3)	1.7(3)
S3	9.9(3)	12.4(3)	16.2(4)	-0.9(3)	3.1(3)	0.3(3)
S1	20.1(4)	18.3(4)	15.3(4)	-3.3(3)	8.3(3)	-7.6(3)
S1B	18.0(4)	18.9(4)	18.8(4)	-1.3(3)	6.8(3)	-7.5(3)
S2B	16.9(4)	19.1(4)	18.2(4)	-6.2(3)	6.0(3)	-3.5(3)
S2	14.3(4)	25.2(4)	16.6(4)	-0.6(4)	6.1(3)	5.7(3)
O6	12.9(11)	26.5(14)	25.0(13)	-1.7(11)	6.1(10)	-5.3(10)
O1W	17.1(11)	15.0(11)	22.1(12)	2.5(11)	4.2(9)	-1.7(10)
O6B	24.4(13)	15.5(12)	21.5(13)	-3.8(10)	-2(1)	6(1)
O3	21.9(13)	21.2(13)	22.4(14)	-0.8(11)	3.1(11)	8.9(10)
O2B	16.2(12)	47.2(19)	25.3(14)	6.2(13)	2(1)	-13.1(12)
O5B	10.4(11)	28.9(14)	22.2(13)	-5.4(11)	3(1)	-0.1(10)
O5	17.1(12)	14.5(12)	23.0(13)	-3.8(10)	-0.2(10)	4.1(9)
O3B	20.7(13)	16.6(12)	31.6(15)	-4.5(11)	3.4(11)	1.6(10)
O1	39.5(15)	12.5(11)	26.2(13)	-1.8(11)	20.1(12)	-3.3(11)
O4B	28.0(14)	39.0(17)	24.8(14)	-15.9(13)	14.4(12)	-11.9(12)
O1B	36.2(15)	21.7(13)	27.2(14)	0.4(12)	15.0(12)	-12.4(12)
O4	23.0(13)	41.7(18)	20.6(13)	-2.3(12)	12.6(11)	7.2(12)
O1WB	24.0(12)	16.9(12)	19.3(12)	4.5(11)	2.1(10)	-4.1(11)
N5	10.8(12)	14.5(13)	17.2(14)	0.3(11)	5.5(11)	2.3(10)
N1	12.5(13)	20.0(15)	18.2(15)	6.5(12)	4.8(11)	3.8(11)
O2	24.5(14)	43.8(18)	20.1(13)	-9.3(13)	9.9(11)	-17.1(13)
N3	16.4(14)	19.8(15)	15.0(14)	2.2(12)	3.6(11)	1.9(12)
N3B	10.7(12)	11.9(13)	16.8(14)	0.2(11)	1.1(11)	0.2(10)
N2	10.4(12)	11.7(12)	14.4(13)	3.1(11)	1.3(10)	-2.1(10)
N5B	12.7(12)	14.5(13)	15.9(14)	2.0(11)	4.0(11)	-4.2(10)

Atom	U_{11}	U_{22}	U_{33}	U_{23}	U_{13}	U_{12}
N4B	15.4(13)	16.1(14)	19.8(15)	-0.5(11)	8.7(11)	-2.7(10)
N4	15.1(13)	19.9(15)	15.5(14)	4.2(11)	6.1(11)	1.5(11)
N1B	14.9(13)	14.0(13)	14.2(14)	0.6(11)	3.7(11)	-0.8(11)
C17	16.2(15)	9.8(15)	20.6(16)	-0.1(12)	3.4(13)	-0.5(12)
C18	20.7(16)	15.5(16)	16.0(16)	0.7(13)	8.5(13)	0.7(13)
C7B	11.1(14)	18.0(16)	17.7(16)	1.2(14)	6.7(12)	-2.3(13)
N2B	19.0(14)	18.7(14)	14.2(14)	-0.2(12)	6.0(12)	-2.5(12)
C19	20.6(16)	21.4(17)	10.9(14)	-1.2(14)	4.1(13)	2.2(14)
C7	16.1(15)	14.4(15)	14.2(15)	-2.5(13)	5.6(12)	-1.5(13)
C32B	18.0(16)	15.7(16)	16.0(16)	5.7(13)	3.0(13)	-3.8(12)
C41B	18.0(16)	16.4(16)	18.9(17)	1.9(13)	6.7(13)	-3.0(13)
C18B	25.9(19)	19.5(18)	18.3(17)	-5.2(14)	-2.1(14)	-1.9(14)
C28B	13.7(15)	16.0(15)	16.0(15)	-0.8(13)	7.1(12)	-0.6(12)
C41	13.8(15)	16.8(17)	25.2(18)	0.9(14)	8.8(14)	2.8(12)
C31B	30(2)	19.1(18)	29(2)	-4.6(16)	9.7(17)	5.2(15)
C21	15.1(15)	11.4(15)	17.1(16)	3.1(12)	3.2(13)	1.7(12)
C37	11.6(14)	16.4(15)	18.6(16)	-3.0(14)	4.4(12)	-0.1(13)
C24	28.3(19)	23.3(19)	17.3(18)	5.1(15)	5.5(15)	2.0(15)
C10B	18.5(16)	19.7(17)	18.8(17)	3.4(14)	7.3(14)	-0.2(13)
C8B	20.1(17)	19.3(17)	21.4(17)	6.3(14)	9.6(14)	5.2(13)
C11	18.9(16)	25.7(18)	18.1(16)	1.4(14)	7.0(13)	-2.5(14)
C14	15.9(15)	14.6(16)	17.2(16)	1.0(13)	6.0(13)	2.8(12)
C17B	16.3(16)	10.8(15)	28.0(19)	0.5(14)	-2.5(14)	-0.3(12)
C40B	11.0(14)	20.8(17)	17.5(16)	1.9(13)	3.8(13)	-3.0(12)
C43B	22.3(18)	24.1(19)	19.0(17)	4.1(15)	1.9(14)	1.2(15)
C42B	16.7(16)	20.3(17)	19.8(17)	3.0(14)	3.6(13)	-2.7(13)
C10	20.8(17)	16.2(16)	17.0(17)	-2.8(13)	3.3(14)	3.1(13)
C12	19.9(17)	20.9(17)	19.5(17)	-0.6(13)	6.0(14)	-6.2(13)
C2B	24.0(18)	20.9(17)	13.9(16)	1.7(14)	2.8(14)	-7.5(14)
C19B	28.4(19)	16.3(16)	13.1(16)	-5.1(13)	2.9(14)	-2.4(14)
C38	14.5(15)	21.9(18)	26.2(19)	-3.5(15)	1.4(14)	2.1(14)
C24B	28.8(19)	14.1(16)	17.3(17)	-0.9(13)	5.7(15)	-0.6(14)
C21B	12.6(14)	11.7(14)	14.0(16)	-0.7(12)	1.2(12)	-0.2(12)
C16	20.9(17)	19.2(17)	13.8(16)	-4.1(13)	-0.9(13)	0.6(13)
C36	9.0(14)	15.9(15)	19.3(16)	-0.7(13)	4.8(12)	2.0(12)
C32	12.4(14)	15.6(16)	19.5(16)	-0.2(13)	5.8(12)	4.6(12)
C37B	30.6(19)	20.9(18)	18.9(17)	-3.5(14)	10.4(15)	-7.0(15)
C15	23.2(17)	16.1(16)	13.3(15)	-1.2(12)	8.9(13)	1.5(13)
C29B	19.0(16)	14.3(15)	16.6(16)	0.2(13)	3.8(13)	-2.1(13)
C20	18.9(17)	23.3(19)	28.1(19)	-3.4(15)	6.8(15)	-3.8(14)
C15B	18.4(16)	22.3(18)	16.0(16)	-2.3(13)	3.6(13)	-2.0(13)
C42	17.0(17)	31(2)	34(2)	11.9(17)	10.7(16)	0.6(15)
C9B	21.9(17)	15.4(16)	26.2(18)	2.7(14)	11.5(15)	2.1(13)
C36B	18.9(16)	14.3(16)	17.4(16)	-0.3(12)	5.7(13)	-5.7(12)
C12B	20.1(16)	13.9(16)	23.5(17)	0.9(13)	5.5(14)	2.7(13)
C1	20.0(17)	15.3(16)	33(2)	10.2(15)	8.9(15)	1.4(13)
C28	14.9(15)	18.8(16)	19.9(17)	-6.5(14)	6.5(13)	3.4(13)
C23B	21.3(17)	19.9(17)	18.8(17)	-3.5(14)	-2.4(14)	-2.5(14)
C4B	15.2(15)	12.8(15)	20.8(17)	-0.2(13)	5.3(13)	-1.4(12)
C38B	31.0(19)	22.0(19)	16.9(17)	-7.3(14)	7.9(15)	-3.6(15)
C3B	16.3(15)	11.5(15)	18.5(16)	-0.6(13)	1.7(13)	-1.4(12)
C16B	19.7(16)	18.6(17)	18.6(17)	0.8(14)	4.9(14)	0.2(13)
C40	11.4(14)	16.3(15)	18.4(16)	-0.1(13)	6.3(13)	1.2(12)
C8	26.8(19)	20.3(17)	22.5(18)	-1.9(15)	8.9(15)	-8.5(15)
C22	22.8(17)	17.5(16)	19.8(17)	0.2(14)	3.5(14)	-6.0(14)
C6	15.1(16)	29(2)	21.5(18)	9.7(15)	6.7(14)	5.9(14)
C30	27(2)	32(2)	22.5(19)	-1.5(16)	-0.2(16)	-7.5(16)

Atom	U_{11}	U_{22}	U_{33}	U_{23}	U_{13}	U_{12}
C13B	38(2)	29(2)	23(2)	-3.8(16)	9.9(17)	-0.2(17)
C5B	12.5(15)	18.5(16)	28.3(19)	6.6(15)	1.7(14)	1.0(13)
C34B	27.3(19)	18.9(17)	23.3(19)	6.7(14)	-0.3(15)	-3.6(14)
C33B	20.1(17)	25.1(19)	22.3(18)	5.5(15)	2.3(14)	-3.2(14)
C11B	22.9(17)	19.8(17)	21.3(17)	6.3(14)	3.3(14)	4.4(13)
C5	22.3(18)	18.8(17)	27(2)	7.6(15)	9.0(15)	8.0(14)
C29	15.8(16)	28(2)	28(2)	-9.4(16)	1.9(15)	1.0(14)
C1B	23.0(17)	15.4(15)	16.9(16)	4.3(13)	6.6(14)	-1.5(13)
C20B	18.6(18)	24.9(19)	38(2)	-1.1(17)	0.8(16)	-1.8(15)
C33	25.7(18)	22.3(18)	18.4(17)	3.1(14)	11.5(15)	7.6(14)
C26	18.3(16)	16.6(16)	23.4(18)	-0.4(14)	5.5(14)	-2.9(13)
C14B	15.7(15)	14.9(15)	16.8(16)	-3.7(13)	2.7(13)	-2.4(12)
C3	19.9(17)	29(2)	19.7(18)	8.3(16)	7.0(14)	4.3(15)
C23	29.8(19)	21.2(19)	24.2(19)	5.0(14)	11.7(16)	-2.8(15)
C25	26.6(18)	18.7(17)	20.6(17)	-5.5(14)	3.4(14)	-3.5(14)
C39	22(2)	40(3)	32(2)	-11(2)	-2.6(17)	0.6(18)
C27B	42(2)	30(2)	17.3(18)	1.0(16)	9.3(17)	0.9(18)
C22B	14.8(15)	19.4(16)	20.6(17)	-2.9(14)	-0.2(13)	1.0(13)
C39B	30(2)	15.5(17)	31(2)	-2.7(15)	13.0(17)	-5.3(14)
C6B	15.7(15)	17.7(16)	28.2(19)	3.4(14)	8.7(14)	1.9(13)
C35B	54(3)	25(2)	21.2(19)	-0.4(17)	2.3(19)	-8(2)
C26B	14.2(15)	19.0(17)	18.5(17)	-3.7(13)	1.5(13)	0.1(12)
C25B	19.5(17)	18.3(16)	20.5(17)	-0.5(14)	5.8(14)	1.1(13)
C30B	18.0(17)	23.4(18)	31(2)	-5.0(16)	8.9(15)	2.5(14)
C34	25.8(18)	22.0(18)	19.6(17)	4.7(14)	8.6(15)	7.8(14)
C35	22.3(18)	21.1(18)	24.1(19)	1.5(15)	6.2(15)	0.7(14)
C43	32(2)	18.0(18)	37(2)	6.4(16)	15.8(18)	-1.7(15)
C13	40(2)	33(2)	22(2)	-10.5(17)	9.4(18)	-2.1(19)
C27	56(3)	44(3)	20(2)	0.2(19)	16(2)	-6(2)
C2	22.1(17)	11.5(15)	24.9(18)	3.1(13)	5.4(15)	-1.2(13)
C9	33(2)	17.6(17)	25.6(19)	-6.0(15)	6.7(16)	-8.7(15)
C4	15.4(16)	27.0(18)	23.3(18)	13.4(15)	5.8(14)	7.1(14)
C31	32(2)	44(3)	42(3)	-21(2)	2(2)	0(2)

Table 4: Bond Lengths in Å for **CMW04_055**.

Atom	Atom	Length/Å
Ni1	O1W	2.062(3)
Ni1	N1	2.094(3)
Ni1	N3	2.044(3)
Ni1	N2	2.036(3)
Ni1	N4	2.066(3)
Ni1B	O1WB	2.056(3)
Ni1B	N3B	2.058(3)
Ni1B	N4B	2.055(3)
Ni1B	N1B	2.081(3)
Ni1B	N2B	2.062(3)
S3B	O6B	1.451(3)
S3B	O5B	1.453(3)
S3B	N3B	1.570(3)
S3B	C21B	1.786(3)
S3	O6	1.454(2)
S3	O5	1.441(3)
S3	N2	1.579(3)
S3	C21	1.782(3)
S1	O1	1.464(3)

Atom	Atom	Length/Å
S1	O2	1.443(3)
S1	N4	1.572(3)
S1	C7	1.778(3)
S1B	O2B	1.450(3)
S1B	O1B	1.437(3)
S1B	N4B	1.585(3)
S1B	C7B	1.783(3)
S2B	O3B	1.469(3)
S2B	O4B	1.452(3)
S2B	N2B	1.574(3)
S2B	C14B	1.782(3)
S2	O3	1.458(3)
S2	O4	1.450(3)
S2	N3	1.574(3)
S2	C14	1.782(3)
N5	C36	1.527(4)
N5	C32	1.521(4)
N5	C28	1.526(4)
N5	C40	1.521(4)
N1	C1	1.480(4)
N1	C5	1.487(4)
N1	C4	1.488(5)
N3	C3	1.481(5)
N3B	C3B	1.479(4)
N2	C2	1.471(4)
N5B	C32B	1.523(4)
N5B	C28B	1.526(4)
N5B	C40B	1.516(4)
N5B	C36B	1.524(4)
N4B	C6B	1.479(5)
N4	C6	1.471(4)
N1B	C4B	1.489(4)
N1B	C5B	1.486(4)
N1B	C1B	1.483(4)
C17	C18	1.399(5)
C17	C16	1.397(5)
C17	C20	1.502(5)
C18	C19	1.375(5)
C7B	C8B	1.406(5)
C7B	C12B	1.383(5)
N2B	C2B	1.477(5)
C19	C14	1.403(4)
C7	C12	1.404(4)
C7	C8	1.379(5)
C32B	C33B	1.517(5)
C41B	C40B	1.526(5)
C41B	C42B	1.527(5)
C18B	C17B	1.386(5)
C18B	C19B	1.389(5)
C28B	C29B	1.511(5)
C41	C42	1.515(5)
C41	C40	1.519(5)
C31B	C30B	1.527(5)
C21	C22	1.397(5)
C21	C26	1.380(5)
C37	C38	1.524(5)
C37	C36	1.524(5)

Atom	Atom	Length/Å
C24	C23	1.393(6)
C24	C25	1.390(5)
C24	C27	1.511(5)
C10B	C9B	1.389(5)
C10B	C13B	1.511(5)
C10B	C11B	1.383(5)
C8B	C9B	1.382(5)
C11	C10	1.403(5)
C11	C12	1.378(5)
C14	C15	1.379(5)
C17B	C16B	1.392(5)
C17B	C20B	1.508(5)
C43B	C42B	1.522(5)
C10	C13	1.509(5)
C10	C9	1.386(5)
C2B	C1B	1.522(5)
C19B	C14B	1.391(5)
C38	C39	1.515(6)
C24B	C23B	1.396(5)
C24B	C27B	1.509(5)
C24B	C25B	1.390(5)
C21B	C22B	1.391(5)
C21B	C26B	1.401(4)
C16	C15	1.398(5)
C32	C33	1.515(5)
C37B	C36B	1.522(5)
C37B	C38B	1.536(5)
C29B	C30B	1.531(5)
C15B	C16B	1.395(5)
C15B	C14B	1.391(5)
C42	C43	1.512(5)
C12B	C11B	1.393(5)
C1	C2	1.520(5)
C28	C29	1.521(5)
C23B	C22B	1.380(5)
C4B	C3B	1.522(5)
C38B	C39B	1.512(5)
C8	C9	1.391(5)
C22	C23	1.387(5)
C6	C5	1.516(5)
C30	C29	1.541(5)
C30	C31	1.502(6)
C5B	C6B	1.515(5)
C34B	C33B	1.536(5)
C34B	C35B	1.526(6)
C33	C34	1.536(5)
C26	C25	1.393(5)
C3	C4	1.511(5)
C26B	C25B	1.379(5)
C34	C35	1.519(5)

Table 5: Bond Angles in ° for **CMW04_055**.

Atom	Atom	Atom	Angle/°
O1W	Ni1	N1	175.85(10)
O1W	Ni1	N4	94.44(10)
N3	Ni1	O1W	94.78(11)
N3	Ni1	N1	83.89(12)
N3	Ni1	N4	117.46(12)
N2	Ni1	O1W	101.05(10)
N2	Ni1	N1	83.08(11)
N2	Ni1	N3	112.83(12)
N2	Ni1	N4	125.54(12)
N4	Ni1	N1	82.73(11)
O1WB	Ni1B	N3B	96.46(11)
O1WB	Ni1B	N1B	178.78(11)
O1WB	Ni1B	N2B	96.90(11)
N3B	Ni1B	N1B	82.51(11)
N3B	Ni1B	N2B	108.03(12)
N4B	Ni1B	O1WB	98.31(11)
N4B	Ni1B	N3B	125.58(12)
N4B	Ni1B	N1B	82.83(11)
N4B	Ni1B	N2B	121.58(12)
N2B	Ni1B	N1B	82.83(12)
O6B	S3B	O5B	115.33(16)
O6B	S3B	N3B	109.38(15)
O6B	S3B	C21B	106.00(16)
O5B	S3B	N3B	112.74(16)
O5B	S3B	C21B	105.82(15)
N3B	S3B	C21B	106.94(15)
O6	S3	N2	112.22(15)
O6	S3	C21	105.01(16)
O5	S3	O6	116.41(15)
O5	S3	N2	108.74(15)
O5	S3	C21	106.74(16)
N2	S3	C21	107.14(15)
O1	S1	N4	108.74(15)
O1	S1	C7	105.39(16)
O2	S1	O1	114.66(18)
O2	S1	N4	114.04(17)
O2	S1	C7	105.54(15)
N4	S1	C7	107.85(16)
O2B	S1B	N4B	112.02(17)
O2B	S1B	C7B	105.28(16)
O1B	S1B	O2B	116.57(18)
O1B	S1B	N4B	108.39(15)
O1B	S1B	C7B	105.73(17)
N4B	S1B	C7B	108.36(16)
O3B	S2B	N2B	107.82(16)
O3B	S2B	C14B	106.42(16)
O4B	S2B	O3B	115.40(18)
O4B	S2B	N2B	112.93(17)
O4B	S2B	C14B	105.83(16)
N2B	S2B	C14B	108.01(16)
O3	S2	N3	107.69(16)
O3	S2	C14	106.13(16)
O4	S2	O3	115.73(16)
O4	S2	N3	113.34(17)
O4	S2	C14	105.69(16)
N3	S2	C14	107.75(16)
C32	N5	C36	111.4(3)
C32	N5	C28	111.7(3)
C28	N5	C36	106.1(2)
C40	N5	C36	111.3(3)
C40	N5	C32	105.6(2)
C40	N5	C28	110.8(3)
C1	N1	Ni1	108.4(2)
C1	N1	C5	111.3(3)
C1	N1	C4	111.8(3)
C5	N1	Ni1	107.4(2)
C5	N1	C4	111.2(3)
C4	N1	Ni1	106.6(2)
S2	N3	Ni1	131.59(18)
C3	N3	Ni1	110.8(2)
C3	N3	S2	114.6(3)
S3B	N3B	Ni1B	131.24(17)
C3B	N3B	Ni1B	112.9(2)
C3B	N3B	S3B	113.7(2)
S3	N2	Ni1	130.09(16)
C2	N2	Ni1	110.6(2)
C2	N2	S3	114.3(2)
C32B	N5B	C28B	111.1(3)
C32B	N5B	C36B	111.4(3)
C40B	N5B	C32B	106.3(2)
C40B	N5B	C28B	111.2(3)
C40B	N5B	C36B	111.4(3)
C36B	N5B	C28B	105.5(2)
S1B	N4B	Ni1B	133.69(18)
C6B	N4B	Ni1B	111.9(2)
C6B	N4B	S1B	114.4(2)
S1	N4	Ni1	133.93(18)
C6	N4	Ni1	112.2(2)
C6	N4	S1	113.0(2)
C4B	N1B	Ni1B	106.6(2)
C5B	N1B	Ni1B	107.9(2)
C5B	N1B	C4B	110.6(3)
C1B	N1B	Ni1B	108.3(2)
C1B	N1B	C4B	111.7(3)
C1B	N1B	C5B	111.4(3)
C18	C17	C20	120.5(3)
C16	C17	C18	118.0(3)
C16	C17	C20	121.5(3)
C19	C18	C17	121.2(3)
C8B	C7B	S1B	119.6(3)
C12B	C7B	S1B	120.6(3)
C12B	C7B	C8B	119.8(3)
S2B	N2B	Ni1B	128.82(18)
C2B	N2B	Ni1B	111.5(2)
C2B	N2B	S2B	114.1(2)
C18	C19	C14	119.8(3)
C12	C7	S1	118.2(3)
C8	C7	S1	121.8(3)
C8	C7	C12	119.9(3)
C33B	C32B	N5B	115.9(3)
C40B	C41B	C42B	110.1(3)
C17B	C18B	C19B	121.9(3)
C29B	C28B	N5B	116.4(3)
C42	C41	C40	108.6(3)

Atom	Atom	Atom	Angle/°
C22	C21	S3	118.4(3)
C26	C21	S3	121.0(3)
C26	C21	C22	120.6(3)
C36	C37	C38	110.9(3)
C23	C24	C27	120.8(4)
C25	C24	C23	118.2(3)
C25	C24	C27	121.0(4)
C9B	C10B	C13B	120.4(3)
C11B	C10B	C9B	118.8(3)
C11B	C10B	C13B	120.8(3)
C9B	C8B	C7B	119.5(3)
C12	C11	C10	121.5(3)
C19	C14	S2	118.2(3)
C15	C14	S2	121.4(2)
C15	C14	C19	120.4(3)
C18B	C17B	C16B	118.1(3)
C18B	C17B	C20B	121.3(3)
C16B	C17B	C20B	120.5(4)
N5B	C40B	C41B	115.9(3)
C43B	C42B	C41B	111.9(3)
C11	C10	C13	120.9(3)
C9	C10	C11	117.9(3)
C9	C10	C13	121.1(4)
C11	C12	C7	119.4(3)
N2B	C2B	C1B	108.1(3)
C18B	C19B	C14B	119.3(3)
C39	C38	C37	111.3(3)
C23B	C24B	C27B	121.0(4)
C25B	C24B	C23B	118.6(3)
C25B	C24B	C27B	120.4(3)
C22B	C21B	S3B	120.7(3)
C22B	C21B	C26B	119.0(3)
C26B	C21B	S3B	120.3(3)
C17	C16	C15	121.4(3)
C37	C36	N5	114.8(2)
C33	C32	N5	116.1(3)
C36B	C37B	C38B	109.7(3)
C14	C15	C16	119.1(3)
C28B	C29B	C30B	108.1(3)
C14B	C15B	C16B	119.6(3)

Atom	Atom	Atom	Angle/°
C43	C42	C41	114.8(3)
C8B	C9B	C10B	121.1(3)
C37B	C36B	N5B	116.2(3)
C7B	C12B	C11B	119.5(3)
N1	C1	C2	110.0(3)
C29	C28	N5	115.9(3)
C22B	C23B	C24B	120.8(3)
N1B	C4B	C3B	110.3(3)
C39B	C38B	C37B	113.2(3)
N3B	C3B	C4B	110.2(3)
C17B	C16B	C15B	121.1(3)
C41	C40	N5	115.9(3)
C7	C8	C9	120.0(3)
C23	C22	C21	119.0(3)
N4	C6	C5	108.0(3)
C31	C30	C29	114.1(4)
N1B	C5B	C6B	109.7(3)
C35B	C34B	C33B	113.1(3)
C32B	C33B	C34B	110.4(3)
C10B	C11B	C12B	121.2(3)
N1	C5	C6	111.1(3)
C28	C29	C30	111.1(3)
N1B	C1B	C2B	109.9(3)
C32	C33	C34	110.4(3)
C21	C26	C25	119.4(3)
C19B	C14B	S2B	121.0(3)
C19B	C14B	C15B	120.0(3)
C15B	C14B	S2B	118.9(3)
N3	C3	C4	108.8(3)
C22	C23	C24	121.5(3)
C24	C25	C26	121.3(3)
C23B	C22B	C21B	120.5(3)
N4B	C6B	C5B	108.6(3)
C25B	C26B	C21B	120.1(3)
C26B	C25B	C24B	121.1(3)
C31B	C30B	C29B	113.5(3)
C35	C34	C33	113.9(3)
N2	C2	C1	107.7(3)
C10	C9	C8	121.3(3)
N1	C4	C3	110.5(3)

Table 6: Torsion Angles in ° for **CMW04_055**.

Atom	Atom	Atom	Atom	Angle/°
Ni1	N1	C1	C2	35.2(3)
Ni1	N1	C5	C6	40.2(3)
Ni1	N1	C4	C3	40.1(3)
Ni1	N3	C3	C4	33.2(3)
Ni1	N2	C2	C1	40.0(3)
Ni1	N4	C6	C5	31.5(4)
Ni1B	N3B	C3B	C4B	16.7(3)
Ni1B	N4B	C6B	C5B	30.9(3)
Ni1B	N1B	C4B	C3B	44.7(3)
Ni1B	N1B	C5B	C6B	41.4(3)

Atom	Atom	Atom	Atom	Angle/°
Ni1B	N1B	C1B	C2B	39.9(3)
Ni1B	N2B	C2B	C1B	33.6(3)
S3B	N3B	C3B	C4B	-148.4(2)
S3B	C21B	C22B	C23B	-179.4(3)
S3B	C21B	C26B	C25B	179.7(3)
S3	N2	C2	C1	-162.3(2)
S3	C21	C22	C23	-179.3(3)
S3	C21	C26	C25	180.0(3)
S1	N4	C6	C5	-157.5(3)
S1	C7	C12	C11	-176.3(3)
S1	C7	C8	C9	176.1(3)
S1B	N4B	C6B	C5B	-146.5(2)
S1B	C7B	C8B	C9B	-179.6(3)
S1B	C7B	C12B	C11B	179.8(3)
S2B	N2B	C2B	C1B	-170.2(2)
S2	N3	C3	C4	-129.6(3)
S2	C14	C15	C16	178.4(3)
O6	S3	N2	Ni1	-163.83(19)
O6	S3	N2	C2	43.8(3)
O6	S3	C21	C22	174.9(3)
O6	S3	C21	C26	-4.8(3)
O6B	S3B	N3B	Ni1B	30.6(3)
O6B	S3B	N3B	C3B	-167.7(2)
O6B	S3B	C21B	C22B	85.0(3)
O6B	S3B	C21B	C26B	-94.7(3)
O3	S2	N3	Ni1	27.9(3)
O3	S2	N3	C3	-173.8(2)
O3	S2	C14	C19	-55.9(3)
O3	S2	C14	C15	126.7(3)
O2B	S1B	N4B	Ni1B	-133.4(2)
O2B	S1B	N4B	C6B	43.2(3)
O2B	S1B	C7B	C8B	-53.4(3)
O2B	S1B	C7B	C12B	126.4(3)
O5B	S3B	N3B	Ni1B	160.35(19)
O5B	S3B	N3B	C3B	-38.0(3)
O5B	S3B	C21B	C22B	-37.9(3)
O5B	S3B	C21B	C26B	142.3(3)
O5	S3	N2	Ni1	-33.6(3)
O5	S3	N2	C2	174.0(2)
O5	S3	C21	C22	50.7(3)
O5	S3	C21	C26	-128.9(3)
O3B	S2B	N2B	Ni1B	-31.6(3)
O3B	S2B	N2B	C2B	177.2(2)
O3B	S2B	C14B	C19B	-120.1(3)
O3B	S2B	C14B	C15B	62.0(3)
O1	S1	N4	Ni1	-5.0(3)
O1	S1	N4	C6	-173.4(2)
O1	S1	C7	C12	75.1(3)
O1	S1	C7	C8	-101.0(3)
O4B	S2B	N2B	Ni1B	-160.3(2)
O4B	S2B	N2B	C2B	48.5(3)
O4B	S2B	C14B	C19B	3.1(4)
O4B	S2B	C14B	C15B	-174.7(3)
O1B	S1B	N4B	Ni1B	-3.4(3)
O1B	S1B	N4B	C6B	173.3(3)
O1B	S1B	C7B	C8B	-177.4(3)

Atom	Atom	Atom	Atom	Angle/°
O1B	S1B	C7B	C12B	2.4(3)
O4	S2	N3	Ni1	157.3(2)
O4	S2	N3	C3	-44.5(3)
O4	S2	C14	C19	-179.3(3)
O4	S2	C14	C15	3.3(3)
N5	C32	C33	C34	177.3(3)
N5	C28	C29	C30	-158.2(3)
N1	C1	C2	N2	-49.9(4)
O2	S1	N4	Ni1	124.3(2)
O2	S1	N4	C6	-44.1(3)
O2	S1	C7	C12	-46.6(3)
O2	S1	C7	C8	137.3(3)
N3	S2	C14	C19	59.2(3)
N3	S2	C14	C15	-118.2(3)
N3	C3	C4	N1	-49.3(4)
N3B	S3B	C21B	C22B	-158.4(3)
N3B	S3B	C21B	C26B	21.9(3)
N2	S3	C21	C22	-65.6(3)
N2	S3	C21	C26	114.7(3)
N5B	C32B	C33B	C34B	172.1(3)
N5B	C28B	C29B	C30B	-172.4(3)
N4B	S1B	C7B	C8B	66.6(3)
N4B	S1B	C7B	C12B	-113.6(3)
N4	S1	C7	C12	-168.9(3)
N4	S1	C7	C8	15.1(4)
N4	C6	C5	N1	-47.8(4)
N1B	C4B	C3B	N3B	-41.0(4)
N1B	C5B	C6B	N4B	-47.9(4)
C17	C18	C19	C14	0.8(6)
C17	C16	C15	C14	-1.5(5)
C18	C17	C16	C15	1.5(5)
C18	C19	C14	S2	-178.2(3)
C18	C19	C14	C15	-0.7(5)
C7B	S1B	N4B	Ni1B	110.9(2)
C7B	S1B	N4B	C6B	-72.5(3)
C7B	C8B	C9B	C10B	-0.8(5)
C7B	C12B	C11B	C10B	0.5(5)
N2B	S2B	C14B	C19B	124.3(3)
N2B	S2B	C14B	C15B	-53.6(3)
N2B	C2B	C1B	N1B	-48.7(4)
C19	C14	C15	C16	1.1(5)
C7	S1	N4	Ni1	-118.8(2)
C7	S1	N4	C6	72.8(3)
C7	C8	C9	C10	-0.9(6)
C32B	N5B	C28B	C29B	66.0(4)
C32B	N5B	C40B	C41B	178.3(3)
C32B	N5B	C36B	C37B	-55.1(4)
C18B	C17B	C16B	C15B	-0.9(5)
C18B	C19B	C14B	S2B	-177.8(3)
C18B	C19B	C14B	C15B	0.1(5)
C28B	N5B	C32B	C33B	57.1(4)
C28B	N5B	C40B	C41B	-60.7(4)
C28B	N5B	C36B	C37B	-175.8(3)
C28B	C29B	C30B	C31B	178.9(3)
C21	S3	N2	Ni1	81.4(2)
C21	S3	N2	C2	-71.0(3)
C21	C22	C23	C24	-1.8(6)

Atom	Atom	Atom	Atom	Angle/°
C21	C26	C25	C24	0.4(6)
C8B	C7B	C12B	C11B	-0.4(5)
C11	C10	C9	C8	1.7(6)
C14	S2	N3	Ni1	-86.2(2)
C14	S2	N3	C3	72.1(3)
C17B	C18B	C19B	C14B	-1.2(6)
C40B	N5B	C32B	C33B	178.2(3)
C40B	N5B	C28B	C29B	-52.2(4)
C40B	N5B	C36B	C37B	63.4(4)
C40B	C41B	C42B	C43B	178.0(3)
C42B	C41B	C40B	N5B	169.0(3)
C10	C11	C12	C7	1.0(6)
C12	C7	C8	C9	0.1(6)
C12	C11	C10	C13	176.4(4)
C12	C11	C10	C9	-1.8(6)
C19B	C18B	C17B	C16B	1.6(5)
C19B	C18B	C17B	C20B	-177.7(3)
C38	C37	C36	N5	-169.1(3)
C24B	C23B	C22B	C21B	-0.6(6)
C21B	S3B	N3B	Ni1B	-83.8(2)
C21B	S3B	N3B	C3B	77.9(3)
C21B	C26B	C25B	C24B	0.0(5)
C16	C17	C18	C19	-1.1(5)
C36	N5	C32	C33	-61.4(4)
C36	N5	C28	C29	-178.0(3)
C36	N5	C40	C41	48.2(4)
C36	C37	C38	C39	-179.0(3)
C32	N5	C36	C37	-55.6(4)
C32	N5	C28	C29	60.3(4)
C32	N5	C40	C41	169.3(3)
C32	C33	C34	C35	-64.1(4)
C20	C17	C18	C19	178.8(3)
C20	C17	C16	C15	-178.4(3)
C42	C41	C40	N5	168.3(3)
C9B	C10B	C11B	C12B	-0.6(5)
C36B	N5B	C32B	C33B	-60.2(4)
C36B	N5B	C28B	C29B	-173.2(3)
C36B	N5B	C40B	C41B	56.7(4)
C36B	C37B	C38B	C39B	63.2(4)
C12B	C7B	C8B	C9B	0.6(5)
C1	N1	C5	C6	158.7(3)
C1	N1	C4	C3	-78.1(4)
C28	N5	C36	C37	-177.4(3)
C28	N5	C32	C33	57.1(4)
C28	N5	C40	C41	-69.6(4)
C23B	C24B	C25B	C26B	-0.2(5)
C4B	N1B	C5B	C6B	-74.8(4)
C4B	N1B	C1B	C2B	157.1(3)
C38B	C37B	C36B	N5B	-177.1(3)
C16B	C15B	C14B	S2B	178.5(3)
C16B	C15B	C14B	C19B	0.6(5)
C40	N5	C36	C37	62.0(4)
C40	N5	C32	C33	177.6(3)
C40	N5	C28	C29	-57.1(4)
C40	C41	C42	C43	173.9(3)
C8	C7	C12	C11	-0.1(5)
C22	C21	C26	C25	0.3(5)

Atom	Atom	Atom	Atom	Angle/°
C13B	C10B	C9B	C8B	179.4(3)
C13B	C10B	C11B	C12B	-179.2(3)
C5B	N1B	C4B	C3B	161.8(3)
C5B	N1B	C1B	C2B	-78.7(4)
C11B	C10B	C9B	C8B	0.8(5)
C5	N1	C1	C2	-82.6(4)
C5	N1	C4	C3	156.9(3)
C1B	N1B	C4B	C3B	-73.4(3)
C1B	N1B	C5B	C6B	160.3(3)
C20B	C17B	C16B	C15B	178.4(3)
C26	C21	C22	C23	0.3(5)
C14B	S2B	N2B	Ni1B	83.0(2)
C14B	S2B	N2B	C2B	-68.2(3)
C14B	C15B	C16B	C17B	-0.2(5)
C23	C24	C25	C26	-1.8(6)
C25	C24	C23	C22	2.5(6)
C27B	C24B	C23B	C22B	-179.6(4)
C27B	C24B	C25B	C26B	180.0(3)
C22B	C21B	C26B	C25B	0.0(5)
C35B	C34B	C33B	C32B	-69.8(4)
C26B	C21B	C22B	C23B	0.4(5)
C25B	C24B	C23B	C22B	0.5(5)
C13	C10	C9	C8	-176.5(4)
C27	C24	C23	C22	-179.4(4)
C27	C24	C25	C26	-180.0(4)
C4	N1	C1	C2	152.4(3)
C4	N1	C5	C6	-76.0(4)
C31	C30	C29	C28	-65.7(5)

Table 7: Hydrogen Fractional Atomic Coordinates ($\times 10^4$) and Equivalent Isotropic Displacement Parameters ($Å^2 \times 10^3$) for **CMW04_055**. U_{eq} is defined as 1/3 of the trace of the orthogonalised U_{ij}.

Atom	x	y	z	U_{eq}
H1WA	3390(30)	4270(20)	38(16)	27
H1WB	3984(17)	3910(30)	-407(17)	27
H1WC	2082(10)	2380(30)	5466(15)	31
H1WD	1330(20)	2080(30)	4879(12)	31
H18	7307	3824	804	20
H19	5664	3788	602	21
H32C	5634	5943	6518	20
H32D	5629	5164	6016	20
H41C	5103	7191	4599	21
H41D	4850	7903	5084	21
H18B	-2297	1826	2339	27
H28C	6527	6613	4953	18
H28D	7142	5943	5460	18
H41A	605	5567	-351	22
H41B	1018	6212	237	22
H31D	5855	4335	3734	39
H31E	6345	3677	4295	39
H31F	6937	4031	3816	39
H37A	-105	3182	124	18
H37B	189	3918	-330	18
H8B	-995	5092	6178	23

Atom	x	y	z	U_{eq}
H11	6186	2679	-2657	25
H40C	4586	6756	5738	20
H40D	4626	5999	5229	20
H43D	3858	7964	3783	33
H43E	3432	8581	4246	33
H43F	2762	7879	3792	33
H42C	3513	6655	4353	23
H42D	3254	7337	4852	23
H12	6285	3345	-1690	24
H2BA	-42	4174	3437	24
H2BB	869	4085	3146	24
H19B	-653	1987	2544	24
H38A	-1681	3782	-112	26
H38B	-1384	4502	-574	26
H16	7463	4079	2653	23
H36A	-337	4291	815	17
H36B	-251	5079	336	17
H32A	1427	3261	669	19
H32B	2187	3761	1208	19
H37C	6191	7293	6875	27
H37D	5396	7832	6375	27
H15	5802	4028	2456	20
H29C	5456	5468	4551	20
H29D	5957	4793	5102	20
H20A	8838	3380	1712	35
H20B	8899	3973	2328	35
H20C	8835	4461	1671	35
H15B	-582	2492	4364	23
H42A	2472	6330	-40	32
H42B	2140	5609	-589	32
H9B	-695	5563	7213	24
H36C	7128	7159	6142	20
H36D	6375	7737	5646	20
H12B	158	2639	6750	23
H1A	3118	773	795	27
H1B	3592	26	437	27
H28A	799	5810	1172	21
H28B	763	4987	1635	21
H23B	4406	4471	7911	26
H4BA	1386	5760	5318	19
H4BB	1633	6231	4721	19
H38C	6417	8850	7083	28
H38D	7306	8478	6847	28
H3BA	2896	5298	4750	19
H3BB	2978	5510	5474	19
H16B	-2229	2296	4150	23
H40A	2257	5077	584	18
H40B	1659	4425	57	18
H8	4430	1485	-1327	27
H22	2794	2904	-1377	24
H6A	6014	1795	351	26
H6B	5869	1394	-342	26
H30A	1795	5376	2583	34
H30B	2771	5898	2615	34
H13D	450	5273	8319	44
H13E	461	4244	8547	44
H13F	-512	4803	8391	44

Atom	x	y	z	U_{eq}
H5BA	-523	5007	4151	24
H5BB	-152	5959	4466	24
H34C	6429	4301	6964	29
H34D	7514	4511	7295	29
H33C	7347	5947	6733	28
H33D	7278	5078	6290	28
H11B	443	3130	7787	26
H5A	4521	612	-269	27
H5B	5288	404	370	27
H29A	2394	5937	1487	29
H29B	2522	4926	1756	29
H1BA	1753	5059	3890	22
H1BB	751	5552	3634	22
H20D	-3753	1839	2641	42
H20E	-3784	2388	3262	42
H20F	-3620	1317	3292	42
H33A	405	3107	1363	25
H33B	1202	3570	1904	25
H26	717	1000	-1697	23
H3A	3615	1871	1496	27
H3B	4610	2316	1846	27
H23	2994	2686	-2385	29
H25	950	772	-2699	27
H39A	-1124	3331	-1233	49
H39B	-2179	3245	-1135	49
H39C	-1359	2591	-761	49
H27D	2565	4458	8459	44
H27E	2412	5485	8226	44
H27F	3455	5127	8548	44
H22B	4611	4060	6935	23
H39D	6755	9128	5878	37
H39E	6695	9894	6381	37
H39F	5756	9368	6027	37
H6BA	30	5379	5463	24
H6BB	-998	5045	5080	24
H35D	5903	5462	7499	52
H35E	6957	5844	7751	52
H35F	6659	4904	8010	52
H26B	1788	4385	6200	21
H25B	1593	4808	7175	23
H30C	6880	5524	4191	28
H30D	7393	4867	4746	28
H34A	2271	2360	1831	26
H34B	1351	1998	2034	26
H35A	1703	1818	822	34
H35B	705	1559	965	34
H35C	1642	1008	1292	34
H43A	1007	6670	-1130	42
H43B	2069	7042	-1025	42
H43C	1403	7394	-591	42
H13A	4573	1582	-3521	47
H13B	5020	647	-3221	47
H13C	5696	1423	-3379	47
H27A	1634	1799	-3597	58
H27B	2198	884	-3364	58
H27C	2759	1824	-3319	58
H2A	2891	660	-533	23

Atom	x	y	z	U_{eq}
H2B	2059	560	-170	23
H9	4336	826	-2301	31
H4A	5392	1637	1167	26
H4B	4778	854	1385	26
H31A	950	6663	2120	61
H31B	1934	7185	2178	61
H31C	1608	6893	2794	61

Table 8: Hydrogen Bond information for **CMW04_055**.

D	H	A	d(D-H)/Å	d(H-A)/Å	d(D-A)/Å	D-H-A/deg
O1W	H1WA	O3	0.970(7)	1.89(3)	2.693(4)	138(4)
O1W	H1WB	O1	0.969(7)	1.744(12)	2.676(3)	160(3)
O1WB	H1WC	O6B	0.973(7)	1.91(2)	2.786(4)	149(4)
O1WB	H1WD	O3B	0.975(7)	1.738(17)	2.680(4)	161(4)

```
#===============================================================================
# PLATON/CHECK-( 70414) versus check.def version of 310314   for Entry: cmw04_05
# Data: CMW04_055.cif - Type: CIF                Bond Precision   C-C = 0.0052 A
# Refl: CMW04_055.fcf - Type: LIST6                                 Temp = 100 K
#                                                X-Ray         Nref/Npar =  11.8
# Cell 14.5075(11) 14.7787(11) 22.0503(17)           90   103.855(1)          90
# Wavelength 0.71073    Volume Reported     4590.1(6)   Calculated     4590.1(6)
# SpaceGroup from Symmetry P 21       Hall: P 2yb               monoclinic
#                 Reported P 1 21 1         P 2yb               monoclinic
# MoietyFormula C27 H35 N4 Ni O7 S3, C16 H36 N
#      Reported C27 H35 N4 Ni O7 S3, C16 H36 N
#    SumFormula C43 H71 N5 Ni O7 S3
#      Reported C43 H71 N5 Ni O7 S3
# Mr        =    924.95[Calc],    924.93[Rep]
# Dx,gcm-3  =     1.339[Calc],     1.338[Rep]
# Z         =         4[Calc],         4[Rep]
# Mu (mm-1) =     0.613[Calc],     0.613[Rep]
# F000      =    1984.0[Calc],    1984.0[Rep]  or F000' =   1987.52[Calc]
# Reported   T Limits: Tmin=0.668              Tmax=0.746  AbsCorr=MULTI-SCAN
# Calculated T Limits: Tmin=0.745 Tmin'=0.736  Tmax=0.817
# Reported   Hmax= 19, Kmax= 20, Lmax= 30, Nref=  23424        , Th(max)= 29.129
# Obs in FCF Hmax= 19, Kmax= 20, Lmax= 30, Nref=  12804[ 12804], Th(max)= 29.129
# Calculated Hmax= 19, Kmax= 20, Lmax= 30, Nref=  24710[ 12809], Ratio=1.83/0.95
# Reported   Rho(min) = -0.34, Rho(max) =  1.33 e/Ang**3 (From CIF)
# w=1/[sigma**2(Fo**2)+(0.0641P)**2+  0.5903P], P=(Fo**2+2*Fc**2)/3
# R= 0.0399( 11983), wR2= 0.0883( 12804), S = 2.453      (From FCF data only)
# R= 0.0438( 21423), wR2= 0.1100( 23424), S = 1.053, Npar= 1089, Flack  0.464(9)
#===============================================================================
For Documentation: http://http://www.platonsoft.nl/CIF-VALIDATION.pdf
#===============================================================================

#===============================================================================
>>> The Following Improvement and Query ALERTS were generated - (Acta-Mode) <<<
#===============================================================================
Format: alert-number_ALERT_alert-type_alert-level text

#===============================================================================
094_ALERT_2_C Ratio of Maximum / Minimum Residual Density ....       3.95 Why ?
911_ALERT_3_C Missing # FCF Refl Between THmin & STh/L=  0.600          4 Why ?
914_ALERT_3_C No Bijvoet Pairs in FCF for Non-centro Structure     Please Check
921_ALERT_1_C R1  in the CIF and FCF Differ by ...............     0.0039 Check
#===============================================================================
002_ALERT_2_G Number of Distance or Angle Restraints on AtSite          6 Note
008_ALERT_5_G No _iucr_refine_reflections_details   in the CIF     Please Do !
033_ALERT_4_G Flack x Value Deviates > 2*sigma from Zero .....      0.464
720_ALERT_4_G Number of Unusual/Non-Standard Labels ..........         17 Note
802_ALERT_4_G CIF Input Record(s) with more than 80 Characters          ! Info
860_ALERT_3_G Number of Least-Squares Restraints .............          7 Note
910_ALERT_3_G Missing # of FCF Reflections Below Th(Min) .....          2 Why ?
961_ALERT_5_G Dataset Contains no Negative Intensities .......     Please Check
#===============================================================================

ALERT_Level and ALERT_Type Summary
==================================
2 ALERT_Level_A = Most Likely a Serious Problem - Resolve or Explain
2 ALERT_Level_B = A Potentially Serious Problem - Consider Carefully
4 ALERT_Level_C = Check. Ensure it is Not caused by an Omission or Oversight
8 ALERT_Level_G = General Info/Check that it is not Something Unexpected

4 ALERT_Type_1 CIF Construction/Syntax Error, Inconsistent or Missing Data.
2 ALERT_Type_2 Indicator that the Structure Model may be Wrong or Deficient.
5 ALERT_Type_3 Indicator that the Structure Quality may be Low.
3 ALERT_Type_4 Improvement, Methodology, Query or Suggestion.
2 ALERT_Type_5 Informative Message, Check.
```

```
#=============================================================================

1 Missing  Experimental  Info Issue(s) (Out of  54 Tests) -   98 % Satisfied
0 Experimental  Data  Related Issue(s) (Out of  28 Tests) -  100 % Satisfied
3 Structural  Model   Related Issue(s) (Out of 117 Tests) -   97 % Satisfied
11 Unresolved or to be Checked Issue(s) (Out of 223 Tests) -   95 % Satisfied

#=============================================================================
```

5-2(OH_2)

EMORY UNIVERSITY | X-ray Crystallography Center

Submitted by: **Christian Wallen**
Emory University
Solved by: **John Bacsa**
Sample ID: **BuCuTsAq**

Crystal Data and Experimental

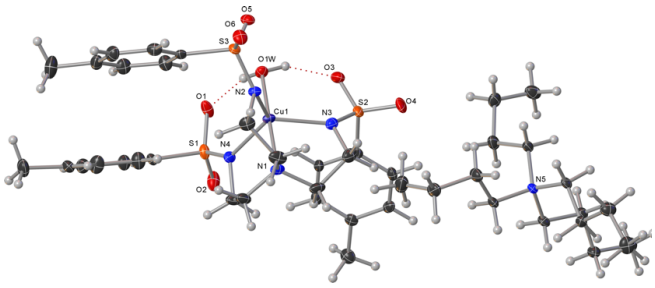

Experimental. Single green block-shaped crystals of (**BuCuTsAq**) were The crystal was chosen from the sample as supplied. A suitable crystal (0.60×0.50×0.40 mm³) was selected and mounted on a loop with paratone oil on a Bruker APEX-II CCD diffractometer. The crystal was cooled to T = 100(2) K during data collection. The structure was solved with the **ShelXT-2014/4** (Sheldrick, 2015) structure solution program using the Intrinsic Phasing solution method and by using **Olex2** (Dolomanov et al., 2009) as the graphical interface. The model was refined with version 2014/7 of **ShelXL-2014/7** (Sheldrick, 2014) using Least Squares minimisation.

Crystal Data. $C_{43}H_{71}CuN_5O_7S_3$, M_r = 929.76, monoclinic, $P2_1$ (No. 4), a = 14.542(4) Å, b = 14.743(4) Å, c = 22.114(5) Å, β = 104.116(4)°, $\alpha = \gamma = 90°$, V = 4597.8(19) Å³, T = 100(2) K, Z = 4, Z' = 2, μ(MoK$_\alpha$) = 0.665 mm^{-1}, 46223 reflections measured, 19781 unique (R_{int} = 0.0320) which were used in all calculations. The final wR_2 was 0.1116 (all data) and R_1 was 0.0425 (I > 2σ(I)).

Compound	**BuCuTsAq**
Formula	$C_{43}H_{71}CuN_5O_7S_3$
$D_{calc.}$/ g cm^{-3}	1.343
μ/mm^{-1}	0.665
Formula Weight	929.76
Colour	green
Shape	block
Size/mm³	0.60×0.50×0.40
T/K	100(2)
Crystal System	monoclinic
Flack Parameter	0.689(10)
Hooft Parameter	0.674(4)
Space Group	$P2_1$
a/Å	14.542(4)
b/Å	14.743(4)
c/Å	22.114(5)
α/°	90
β/°	104.116(4)
γ/°	90
V/Å³	4597.8(19)
Z	4
Z'	2
Wavelength/Å	0.710730
Radiation type	MoK$_\alpha$
Θ_{min}/°	1.444
Θ_{max}/°	27.483
Measured Refl.	46223
Independent Refl.	19781
Reflections with I > 2σ(I)	18092
R_{int}	0.0320
Parameters	1080
Restraints	1
Largest Peak	1.382
Deepest Hole	-0.414
GooF	1.054
wR_2 (all data)	0.1116
wR_2	0.1080
R_1 (all data)	0.0471
R_1	0.0425

Structure Quality Indicators

Reflections: d min (Mo) 0.77 | I/σ 16.5 | Rint 3.20% | complete 94%

Refinement: Shift -0.003 | Max Peak 1.4 | Min Peak -0.4 | GooF 1.054 | 0.685(4)

A green block-shaped crystal with dimensions 0.60×0.50×0.40 mm^3 was mounted on a loop paratone oil. Data were collected using a Bruker APEX-II CCD diffractometer equipped with an Oxford Cryosystems low-temperature device, operating at T = 100(2) K.

Data were measured using ϕ and ω scans of 0.50° per frame for 20.00 s using MoK_α radiation (fine-focus sealed tube, 45 kV, 35 mA).The total number of runs and images was based on the strategy calculation from the program **APEX2** (Bruker). The maximum resolution that was achieved was Θ = 27.483°.

The diffraction patterns were indexed using **SAINT** (Bruker, V8.34A, 2013) and the unit cells were refined using **SAINT** (Bruker, V8.34A, 2013) on 9777 reflections, 21 % of the observed reflections. Data reduction, scaling and absorption corrections were performed using **SAINT** (Bruker, V8.34A, 2013) and **SADABS-2014/5** (Bruker,2014/5). The wR_2(int) value was 0.0711 before and 0.0507 after correction. The ratio of minimum to maximum transmission is 0.8713.The $\lambda/2$ correction factor is 0.00150. The final completeness is 99.9% out to 27.483° in Θ. The absorption coefficient μ of this material is 0.665 mm^{-1} at this wavelength (λ = 0.71073 Å) and the minimum and maximum transmissions are 0.6501 and 0.7461.

The structure was solved and the space group $P2_1$ (# 4) determined by the ShelXT-2014/4 (Sheldrick, 2015) structure solution program using Intrinsic Phasing and refined by Least Squares using version 2014/7 of ShelXL-2014/7 (Sheldrick, 2014). All non-hydrogen atoms were refined anisotropically. Hydrogen atom positions, except those of the water molecules were calculated geometrically and refined using the riding model. The water molecules hydrogen atoms were located from difference maps and refined with restraints. The value of Z' is 2. This means that there are two independent molecules in the asymmetric unit.

The Flack parameter was refined to 0.685(4). Determination of absolute structure using Bayesian statistics on Bijvoet differences using the Olex2 results in 0.672(4). Note: The Flack parameter is used to determine chirality of the crystal studied, the value should be near 0, a value of 1 means that the stereochemistry is wrong and the model should be inverted. A value of 0.5 means that the crystal consists of a racemic mixture of the two enantiomers.

_refine_special_details: Refined as a 2-component inversion twin.

_exptl_absorpt_special_details: ?

The value of Z' is 2. This means that there are two independent molecules in the asymmetric unit.

The Flack parameter was refined to 0.689(10). Determination of absolute structure using Bayesian statistics on Bijvoet differences using the Olex2 results in 0.674(4). Note: The Flack parameter is used to determine chirality of the crystal studied, the value should be near 0, a value of 1 means that the stereochemistry is wrong and the model should be inverted. A value of 0.5 means that the crystal consists of a racemic mixture of the two enantiomers.

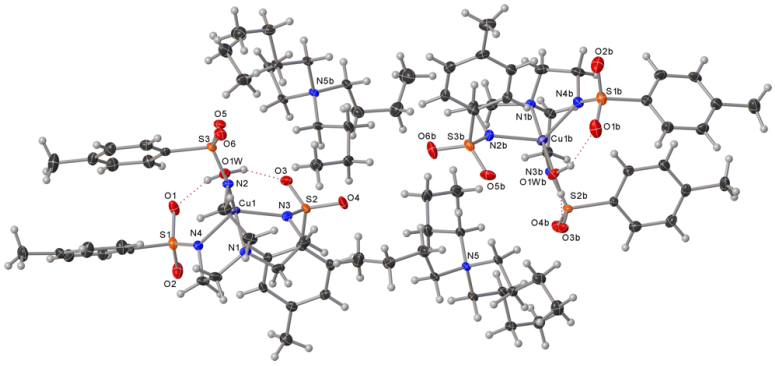

Figure 1: Plot of the asymmetric unit. There are two independent CuL(H_2O)-molecules (4 whole molecules) in the asymmetric unit.

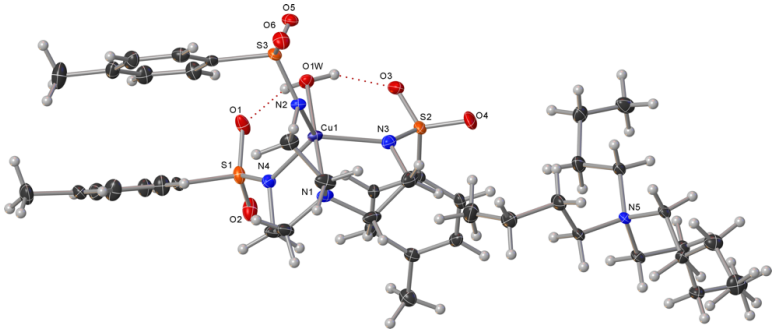

Figure 2: One of the two independent CuL(H_2O)-molecules (with its counterion) in the asymmetric unit.

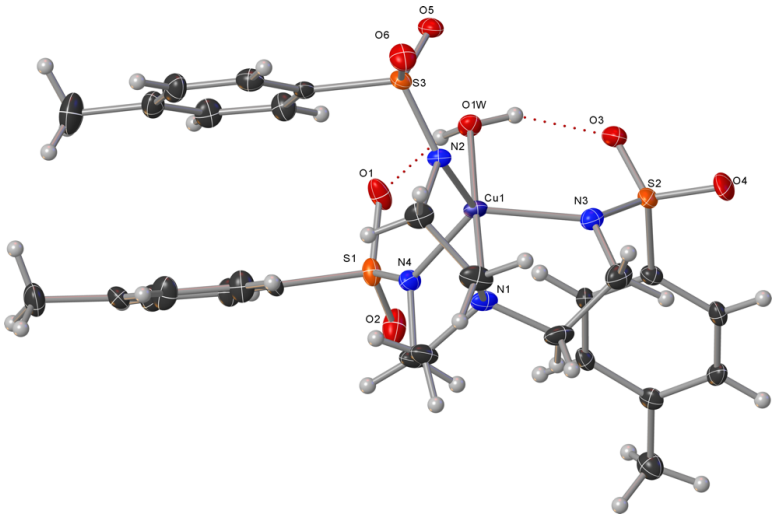

Figure 3: One of the two independent CuL(H_2O)-molecules (without its counterion) in the asymmetric unit.

Data Plots: Diffraction Data

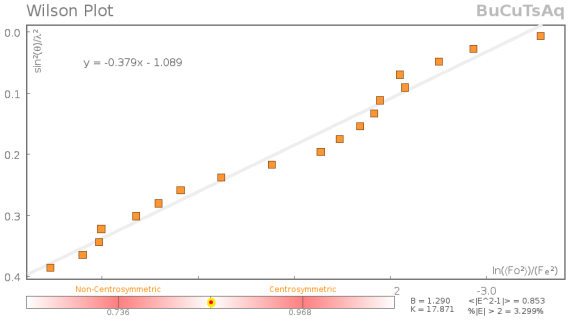

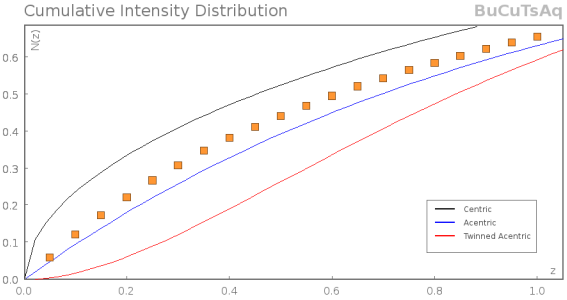

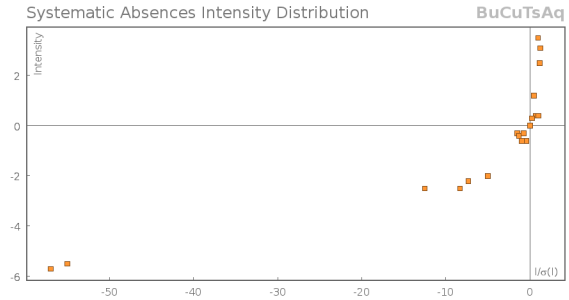

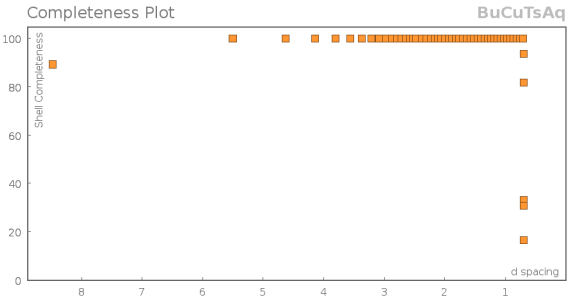

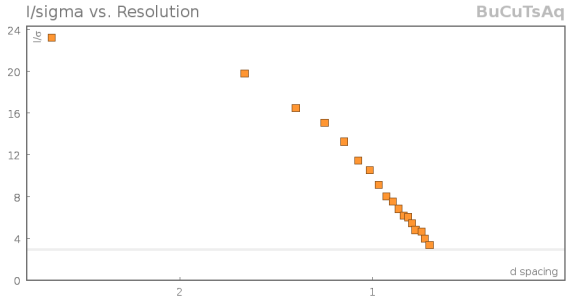

Data Plots: Refinement and Data

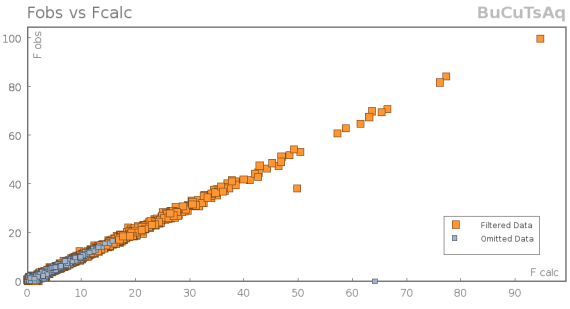

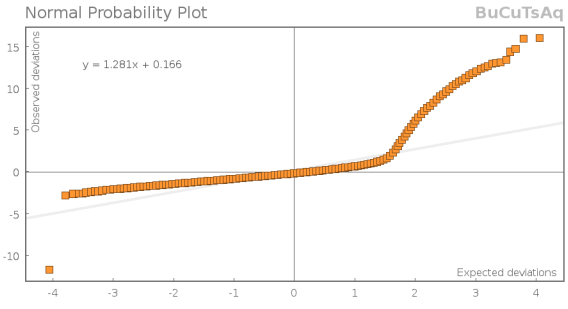

Reflection Statistics

Total reflections (after filtering)	46245	Unique reflections	19781
Completeness	0.939	Mean I/σ	16.5
hkl_{max} collected	(20, 20, 31)	hkl_{min} collected	(-17, -21, -31)
hkl_{max} used	(18, 18, 28)	hkl_{min} used	(-18, -19, 0)
Lim d_{max} collected	20.0	Lim d_{min} collected	0.77
d_{max} used	14.74	d_{min} used	0.77
Friedel pairs	14335	Friedel pairs merged	0

Inconsistent equivalents	0	R_{int}	0.032
R_{sigma}	0.0426	Intensity transformed	0
Omitted reflections	0	Omitted by user (OMIT hkl)	1
Multiplicity	(27494, 11373, 1969, 131)	Maximum multiplicity	6
Removed systematic absences	21	Filtered off (Shel/OMIT)	10426

Images of the Crystal on the Diffractometer

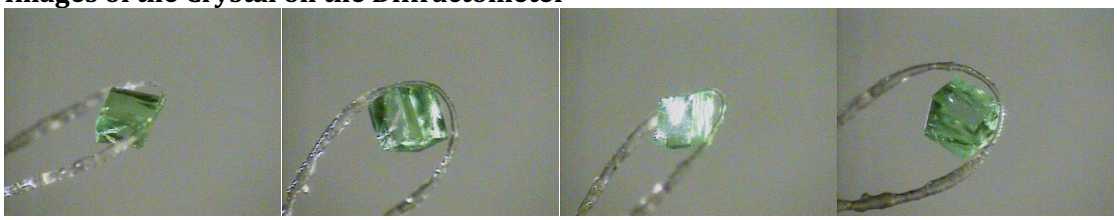

Table 1: Fractional Atomic Coordinates (×10⁴) and Equivalent Isotropic Displacement Parameters (Å²×10³) for **BuCuTsAq**. U_{eq} is defined as 1/3 of the trace of the orthogonalised U_{ij}.

Atom	x	y	z	U_{eq}
Cu1	1235.7(3)	6179.9(3)	4893.8(2)	14.55(11)
S3	3433.2(7)	5824.4(7)	5707.5(4)	14.28(19)
S2	662.1(7)	7531.9(8)	3641.6(4)	18.9(2)
S1	-397.3(7)	6717.0(7)	5690.5(4)	17.6(2)
O1W	1560.3(18)	7418(2)	5228.4(12)	17.4(6)
C7	-359(3)	6171(3)	6412.8(16)	15.3(7)
N3	974(2)	6594(3)	3961.5(15)	18.2(7)
O4	899(2)	7650(2)	3047.7(13)	28.8(8)
O3	1012(2)	8234(2)	4104.9(13)	23.6(7)
C14	-602(3)	7588(3)	3474.2(17)	15.8(8)
O5	3544.7(19)	6792(2)	5662.0(13)	19.8(6)
C21	3251(3)	5615(3)	6463.1(17)	14.8(8)
N2	2509(2)	5521(2)	5216.7(15)	13.9(6)
N1	776(2)	4954(2)	4523.8(15)	18.6(7)
C24	2958(3)	5327(3)	7650.3(19)	24.1(9)
N4	67(2)	6062(3)	5291.4(14)	17.5(7)
C10	-245(3)	5410(3)	7589.0(18)	19.8(9)
C11	-805(3)	6180(3)	7391.5(18)	22.9(8)
C18	-2011(3)	7519(3)	3857.9(16)	16.2(8)
C19	-1034(3)	7502(3)	3969.5(16)	18.6(8)
C3	760(3)	5792(3)	3549.7(19)	24.2(9)
O6	4245(2)	5265(2)	5673.8(13)	23.2(7)
C15	-1154(3)	7675(3)	2867.1(17)	17.1(8)
C16	-2134(3)	7690(3)	2764.3(18)	18.4(8)
C26	3807(3)	4994(3)	6861.8(19)	21.2(8)
C12	-872(3)	6565(3)	6810.4(17)	20.6(8)
C17	-2580(3)	7605(3)	3250.4(18)	16.1(8)
C22	2552(3)	6105(3)	6654.0(18)	22.4(8)
C23	2418(3)	5967(3)	7248.2(19)	24.3(9)
C1	1610(3)	4353(3)	4567(2)	25.1(9)
C2	2348(3)	4532(3)	5169(2)	22.1(9)
O2	-1387(2)	6922(2)	5426.8(13)	29.1(7)
C25	3645(3)	4855(3)	7453.3(18)	25.2(9)
C27	2784(4)	5168(4)	8289(2)	42.3(14)
C6	-530(3)	5279(3)	5031(2)	24.2(9)
C4	252(3)	5106(3)	3859.4(18)	23.8(9)
C13	-139(4)	5033(4)	8237(2)	31.2(11)
C9	224(3)	5027(3)	7179.6(19)	28.1(10)

Atom	x	y	z	U_{eq}
C20	-3644(3)	7594(3)	3136(2)	25.2(9)
C8	172(3)	5409(3)	6595.5(19)	25.0(9)
C5	123(3)	4563(3)	4883(2)	24.6(9)
Cu1B	3783.0(3)	7402.1(3)	127.2(2)	15.92(11)
S2B	1582.0(6)	7551.0(7)	-745.2(4)	13.65(19)
S3B	4235.5(7)	6085.8(8)	1390.2(5)	19.3(2)
S1B	5571.3(8)	7054.4(8)	-578.4(5)	21.0(2)
O1WB	3575(2)	6147(2)	-210.6(12)	18.3(6)
C7B	5410(3)	7434(3)	-1367.7(17)	17.2(8)
N2B	3989(2)	7035(3)	1069.3(15)	17.7(7)
O5B	3811(2)	5391(2)	926.2(15)	26.3(7)
O3B	1590(2)	6573(2)	-726.3(13)	21.9(6)
O6B	3996(2)	6011(3)	1984.4(14)	32.0(8)
N3B	2447(2)	7928(2)	-234.3(14)	13.5(6)
C14B	1766(3)	7864(3)	-1487.5(16)	13.7(7)
C21B	5484(3)	5928(3)	1544.1(17)	15.4(8)
N1B	4063(2)	8660(2)	482.8(14)	14.9(7)
O4B	688.0(19)	7979(2)	-715.0(13)	23.2(7)
C17B	2069(3)	8339(3)	-2649.9(18)	20.8(9)
C2B	4309(3)	7822(3)	1476.5(19)	21.5(9)
C12B	5004(3)	6865(3)	-1857.1(18)	22.0(8)
N4B	4956(2)	7664(2)	-249.2(15)	19.1(7)
C10B	5145(3)	8040(3)	-2592.8(19)	22.1(9)
C23B	6912(3)	5937(3)	1177.1(18)	19.4(9)
C26B	6017(3)	5699(3)	2137.0(17)	19.0(8)
C22B	5934(3)	6049(3)	1064.1(17)	20.0(9)
C18B	2824(3)	8293(3)	-2124.4(18)	22.1(8)
C1B	3897(3)	8672(3)	1122.3(17)	20.4(8)
C15B	1008(3)	7912(3)	-2007.9(18)	21.3(8)
O1B	5189(2)	6141(2)	-621.1(14)	30.8(7)
O2B	6578(2)	7137(3)	-301.5(14)	33.6(8)
C24B	7454(3)	5703(3)	1769.0(19)	19.0(8)
C19B	2681(3)	8049(3)	-1548.5(17)	18.5(8)
C9B	5551(3)	8605(3)	-2095.5(19)	22.5(9)
C5B	5068(3)	8880(3)	502.8(19)	23.7(9)
C3B	2408(3)	8914(3)	-122.8(17)	17.8(8)
C25B	6992(3)	5600(3)	2244.7(19)	22.0(9)
C4B	3405(3)	9298(3)	58.4(18)	17.0(8)
C13B	4983(4)	8380(4)	-3259(2)	30.9(11)
C20B	2242(4)	8595(4)	-3271.7(19)	29.8(11)
C8B	5695(3)	8306(3)	-1487.7(19)	22.9(9)
C27B	8516(3)	5565(3)	1883(2)	29.5(10)
C11B	4873(3)	7175(3)	-2469.3(19)	24.6(9)
C16B	1159(3)	8147(3)	-2585.2(18)	23.7(9)
C6B	5305(3)	8596(3)	-102(2)	22.8(9)
N5B	3940(2)	8228(2)	4207.0(14)	14.9(7)
N5	966(2)	5151(2)	720.1(14)	15.1(7)
C39B	4996(3)	8125(3)	4518.7(17)	15.9(8)
C36	-300(3)	6029(3)	-101.7(17)	17.8(8)
C41B	6267(3)	7517(4)	5405.3(19)	23.8(9)
C39	1457(3)	6029(3)	990.9(17)	16.6(8)
C40B	5224(2)	7443(3)	5046.9(17)	16.5(8)
C35B	3393(3)	8573(3)	4667.0(18)	15.5(8)
C35	-79(3)	5310(3)	409.5(18)	16.9(8)
C37	-1340(3)	5981(3)	-449.9(18)	20.6(9)
C28	1505(3)	4827(3)	249.0(17)	15.2(8)
C36B	3811(3)	9394(3)	5050.6(18)	18.2(8)

Atom	x	y	z	U_{eq}
C29	1082(3)	4028(3)	-153.7(17)	17.3(8)
C86B	3607(3)	5255(3)	3867(2)	24.5(9)
C32B	3490(3)	7322(3)	3974.6(17)	16.2(8)
C32	992(3)	4445(3)	1223.7(17)	17.0(8)
C42B	6513(3)	6831(4)	5928(2)	33.1(11)
C38	-1613(3)	6721(3)	-942.8(19)	25.2(10)
C38B	3438(3)	10526(3)	5830(2)	29.2(10)
C31	1470(3)	2901(3)	-938(2)	27.1(10)
C34B	3409(3)	5922(3)	3325.9(18)	23.0(9)
C28B	3875(3)	8899(3)	3667.9(18)	19.2(8)
C41	1618(3)	7357(3)	1704.3(17)	24.2(9)
C37B	3082(3)	9763(4)	5378(2)	29(1)
C42	1401(3)	8068(3)	1192(2)	27.3(10)
C40	1102(3)	6460(3)	1516.9(19)	24.8(10)
C30	1811(3)	3689(3)	-492(2)	25.3(9)
C33B	3888(3)	6845(3)	3483.7(18)	23.3(9)
C29B	2868(3)	9140(3)	3301(2)	25.1(9)
C30B	2860(3)	9482(4)	2646.5(19)	32.3(10)
C33	1972(3)	4148(3)	1589.2(19)	23.9(9)
C86	1558(4)	4001(4)	2635.5(19)	34.9(11)
C34	1894(3)	3521(3)	2129.3(19)	27.0(9)
O1	214(2)	7520(2)	5852.8(13)	23.2(6)
C31B	3374(4)	10369(4)	2631(2)	43.4(13)

Table 2: Anisotropic Displacement Parameters ($\times 10^4$) **BuCuTsAq**. The anisotropic displacement factor exponent takes the form: $-2\pi^2[h^2a^{*2} \times U_{11} + \ldots + 2hka^* \times b^* \times U_{12}]$

Atom	U_{11}	U_{22}	U_{33}	U_{23}	U_{13}	U_{12}
Cu1	11.7(2)	13.5(3)	18.1(2)	-4.83(18)	3.09(18)	-1.52(18)
S3	11.0(4)	14.6(5)	17.9(4)	1.4(3)	4.8(3)	0.0(3)
S2	14.5(5)	27.4(6)	15.6(4)	2.5(4)	5.3(3)	-5.3(4)
S1	18.6(5)	20.6(5)	15.7(4)	4.5(4)	8.2(4)	7.6(4)
O1W	20.1(14)	13.1(14)	18.4(12)	-2.2(12)	3.7(11)	-0.1(12)
C7	16.6(18)	16(2)	15.7(16)	2.3(16)	7.3(14)	-1.0(16)
N3	16.2(17)	21(2)	17.5(15)	-2.3(14)	4.1(13)	-0.6(14)
O4	23.7(16)	46(2)	20.2(14)	7.1(13)	11.6(12)	-6.8(14)
O3	21.7(15)	24.3(18)	22.8(14)	3.3(12)	1.7(12)	-7.9(13)
C14	14.7(18)	16(2)	18.3(17)	-1.4(15)	6.3(14)	-1.3(15)
O5	14.4(14)	19.6(16)	23.8(13)	3.0(12)	1.6(11)	-3.5(11)
C21	16.5(19)	12(2)	15.8(17)	-2.7(14)	3.4(15)	-4.5(15)
N2	11.3(15)	10.7(17)	19.0(15)	-2.0(12)	2.7(13)	1.3(12)
N1	17.0(17)	18.1(19)	21.8(16)	-9.4(14)	6.9(14)	-3.6(14)
C24	33(3)	22(2)	17.9(19)	-1.4(16)	7.2(18)	-3.5(19)
N4	15.2(16)	22(2)	16.5(14)	-2.1(13)	6.4(13)	-2.2(14)
C10	21(2)	20(2)	19.3(18)	2.3(16)	6.5(16)	-4.3(17)
C11	22(2)	26(2)	21.3(18)	-2.0(17)	7.8(16)	1.5(18)
C18	20.5(19)	15(2)	15.6(16)	0.1(15)	9.6(14)	-1.0(16)
C19	21(2)	22(2)	12.4(15)	2.4(16)	3.0(14)	-5.3(18)
C3	21(2)	31(3)	21.4(19)	-6.9(18)	7.7(17)	-0.4(19)
O6	15.0(14)	28.9(19)	27.0(14)	2.9(12)	7.6(12)	5.4(12)
C15	23(2)	15(2)	15.4(17)	2.9(14)	8.0(15)	0.1(15)
C16	21(2)	16(2)	15.7(16)	4.0(14)	-1.0(15)	-0.5(15)
C26	17.2(19)	19(2)	27.2(19)	-0.8(16)	4.3(16)	0.7(16)
C12	23(2)	21(2)	19.7(17)	-0.5(15)	9.2(16)	5.7(16)
C17	18.2(19)	8(2)	22.2(17)	1.5(14)	5.2(15)	1.4(15)
C22	22(2)	21(2)	24.0(19)	4.0(16)	6.6(16)	6.2(17)

Atom	U_{11}	U_{22}	U_{33}	U_{23}	U_{13}	U_{12}
C23	29(2)	20(2)	26(2)	-4.2(16)	10.1(17)	4.5(17)
C1	25(2)	16(2)	38(2)	-9.9(18)	13.1(19)	-0.1(17)
C2	25(2)	12(2)	29(2)	-3.0(16)	5.4(17)	3.7(16)
O2	24.4(16)	44(2)	20.6(13)	6.5(13)	9.2(12)	14.7(14)
C25	30(2)	21(2)	21.9(19)	5.1(17)	2.1(17)	2.6(18)
C27	55(4)	53(4)	20(2)	2(2)	12(2)	7(3)
C6	19(2)	29(3)	27(2)	-10.1(18)	10.5(17)	-10.1(18)
C4	19(2)	27(2)	25.4(19)	-12.6(17)	5.9(16)	-7.4(17)
C13	42(3)	31(3)	22(2)	8.6(19)	11(2)	0(2)
C9	40(3)	17(2)	26(2)	3.6(17)	6.3(19)	9.2(19)
C20	23(2)	25(3)	28(2)	5.5(18)	7.0(17)	2.8(18)
C8	30(2)	22(2)	25(2)	2.1(17)	10.3(17)	8.4(18)
C5	24(2)	24(2)	28(2)	-8.8(17)	11.4(18)	-10.8(18)
Cu1B	16.8(2)	12.8(3)	16.2(2)	-0.92(18)	0.11(18)	2.36(18)
S2B	10.1(4)	15.2(5)	15.1(4)	3.5(3)	2.0(3)	-0.5(4)
S3B	16.6(5)	21.6(6)	21.0(4)	8.7(4)	7.0(4)	2.9(4)
S1B	22.2(5)	22.4(6)	20.5(4)	5.1(4)	9.1(4)	7.4(4)
O1WB	22.5(14)	11.5(14)	17.0(12)	-3.3(11)	-2.4(11)	2.9(12)
C7B	12.2(18)	20(2)	20.0(17)	-1.0(17)	5.4(14)	4.5(17)
N2B	17.9(17)	20.5(19)	14.6(14)	0.9(14)	4.0(13)	2.8(14)
O5B	19.9(16)	17.1(17)	39.1(17)	6.2(13)	1.9(13)	-4.2(12)
O3B	23.8(16)	17.7(16)	21.1(13)	4.2(11)	-0.2(12)	-7.4(12)
O6B	33.4(18)	41(2)	27.6(15)	17.0(14)	18.2(14)	11.6(15)
N3B	13.8(16)	10.1(17)	16.5(14)	1.0(12)	3.8(12)	0.6(12)
C14B	16.0(19)	12.3(19)	12.7(16)	1.8(14)	3.3(14)	1.3(15)
C21B	14.4(18)	13(2)	18.3(17)	3.3(14)	3.1(15)	1.7(14)
N1B	16.2(16)	12.0(17)	16.8(14)	-0.9(12)	4.3(13)	-1.4(13)
O4B	9.6(13)	34.1(19)	25.9(14)	6.9(13)	4.3(11)	4.1(12)
C17B	32(2)	15(2)	15.3(17)	-0.4(15)	5.2(17)	0.4(17)
C2B	26(2)	22(2)	16.4(18)	-3.2(16)	3.8(17)	6.5(17)
C12B	25(2)	17(2)	23.3(18)	-1.5(15)	5.6(16)	-1.9(16)
N4B	19.4(17)	19(2)	20.6(15)	0.8(13)	7.3(13)	-0.6(13)
C10B	24(2)	21(2)	21.3(19)	-3.1(17)	6.8(17)	-0.9(17)
C23B	21(2)	19(2)	18.9(18)	-2.5(15)	5.9(16)	-0.8(16)
C26B	25(2)	16(2)	15.4(17)	4.6(15)	4.0(16)	3.0(16)
C22B	22(2)	22(2)	13.7(16)	2.2(16)	-0.3(15)	3.5(17)
C18B	21(2)	23(2)	22.9(19)	0.3(16)	8.0(16)	-2.0(17)
C1B	23(2)	15(2)	22.1(18)	-3.9(15)	4.0(16)	2.2(16)
C15B	20(2)	19(2)	23.6(19)	2.7(16)	1.2(16)	0.9(16)
O1B	47(2)	20.1(17)	31.4(15)	6.1(13)	20.8(15)	15.2(15)
O2B	21.1(16)	54(2)	25.4(14)	1.4(14)	4.8(12)	16.4(15)
C24B	16.9(19)	9(2)	27.7(19)	-3.6(15)	-1.5(16)	1.0(15)
C19B	15.3(19)	22(2)	16.9(17)	1.4(15)	0.8(15)	1.4(15)
C9B	23(2)	15(2)	33(2)	-4.7(16)	13.0(17)	-5.6(16)
C5B	17(2)	22(2)	30(2)	-8.2(17)	3.2(17)	-2.5(16)
C3B	19(2)	16(2)	17.8(17)	2.3(15)	3.8(15)	3.6(16)
C25B	27(2)	16(2)	19.1(18)	6.0(15)	-1.3(16)	-0.3(17)
C4B	18.0(19)	8.8(19)	25.4(18)	0.3(15)	8.0(15)	1.6(14)
C13B	43(3)	26(3)	27(2)	0.8(18)	13(2)	-1(2)
C20B	43(3)	29(3)	17.5(19)	2.1(18)	8.4(19)	-5(2)
C8B	20(2)	24(2)	25.1(19)	-8.5(17)	6.6(16)	-4.5(17)
C27B	18(2)	24(3)	41(2)	1(2)	-2.8(18)	4.7(18)
C11B	29(2)	19(2)	24.3(19)	-5.6(16)	3.1(17)	-4.4(17)
C16B	28(2)	22(2)	17.1(17)	3.0(16)	-2.7(16)	3.0(17)
C6B	17(2)	21(2)	32(2)	-2.4(17)	8.0(17)	-5.0(16)
N5B	11.5(15)	16.3(18)	18.7(15)	0.6(13)	7.0(12)	-1.8(13)
N5	13.6(16)	18.0(18)	14.4(14)	1.0(12)	5.0(12)	-4.3(13)

Atom	U_{11}	U_{22}	U_{33}	U_{23}	U_{13}	U_{12}
C39B	11.7(18)	17(2)	20.1(17)	-0.9(15)	6.2(15)	-1.1(15)
C36	18(2)	19(2)	17.5(17)	-0.3(15)	6.7(15)	-2.8(16)
C41B	17(2)	24(2)	28(2)	2.3(19)	2.7(16)	-0.9(18)
C39	19.3(19)	16(2)	15.5(16)	-0.6(14)	6.6(15)	-4.0(15)
C40B	10.3(18)	18(2)	23.0(17)	3.3(17)	6.3(14)	0.5(16)
C35B	12.3(18)	16(2)	20.4(17)	0.4(15)	8.5(15)	-0.7(15)
C35	13.0(19)	19(2)	20.5(18)	1.4(15)	8.3(15)	-1.9(15)
C37	16.4(19)	24(3)	21.0(18)	1.3(16)	3.9(15)	-3.6(16)
C28	13.2(18)	18(2)	16.4(16)	2.1(15)	7.0(14)	-0.5(15)
C36B	15.8(19)	16(2)	24.7(19)	1.8(15)	8.9(16)	-0.3(15)
C29	19(2)	17(2)	15.4(17)	-0.2(14)	4.2(15)	-3.7(16)
C86B	26(2)	23(2)	26(2)	-1.9(17)	9.3(18)	0.7(18)
C32B	14.6(18)	15(2)	19.2(17)	-1.7(15)	4.3(14)	-5.0(15)
C32	16.6(19)	19(2)	16.4(17)	3.7(15)	5.5(15)	-4.6(15)
C42B	27(2)	36(3)	32(2)	7(2)	-1(2)	-2(2)
C38	24(2)	30(3)	20.6(18)	5.2(18)	2.1(17)	0.2(19)
C38B	32(3)	25(3)	36(2)	-8.4(19)	19(2)	0.7(19)
C31	33(3)	22(2)	28(2)	-2.3(18)	12.6(19)	7.1(19)
C34B	28(2)	23(2)	18.9(18)	-7.2(16)	7.6(17)	-7.9(17)
C28B	19(2)	21(2)	19.8(18)	3.1(16)	7.0(15)	-5.3(16)
C41	32(2)	24(2)	18.0(17)	-5.8(17)	8.6(17)	-3.2(19)
C37B	18(2)	34(3)	37(2)	-12(2)	9.7(18)	-1.1(19)
C42	30(2)	23(3)	33(2)	-7.1(18)	14(2)	-6.3(19)
C40	32(2)	26(3)	19.3(18)	-3.5(16)	12.4(18)	-8.1(18)
C30	20(2)	26(3)	31(2)	-3.1(18)	8.7(18)	-0.2(18)
C33B	30(2)	22(2)	21.3(18)	-1.9(16)	13.2(17)	-7.2(18)
C29B	19(2)	27(3)	28(2)	6.5(18)	4.8(17)	0.3(17)
C30B	33(3)	36(3)	25(2)	2.0(19)	0.9(19)	4(2)
C33	23(2)	24(2)	23.2(19)	9.5(17)	3.1(16)	-2.3(17)
C86	51(3)	31(3)	22(2)	-0.7(18)	7(2)	-10(2)
C34	33(2)	21(2)	23.2(19)	7.9(17)	1.5(18)	-5.9(18)
O1	37.5(17)	11.7(15)	26.1(13)	3.2(12)	18.9(13)	3.4(13)
C31B	39(3)	46(4)	42(3)	16(2)	2(2)	-1(2)

Table 3: Bond Lengths in Å for **BuCuTsAq**.

Atom	Atom	Length/Å
Cu1	O1W	1.983(3)
Cu1	N3	2.094(3)
Cu1	N2	2.059(3)
Cu1	N1	2.028(4)
Cu1	N4	2.102(3)
S3	O5	1.443(3)
S3	C21	1.781(4)
S3	N2	1.572(3)
S3	O6	1.457(3)
S2	N3	1.569(4)
S2	O4	1.447(3)
S2	O3	1.458(3)
S2	C14	1.786(4)
S1	C7	1.778(4)
S1	N4	1.568(3)
S1	O2	1.447(3)
S1	O1	1.471(3)
C7	C12	1.409(5)
C7	C8	1.367(6)

Atom	Atom	Length/Å
N3	C3	1.478(6)
C14	C19	1.396(5)
C14	C15	1.392(5)
C21	C26	1.386(6)
C21	C22	1.393(6)
N2	C2	1.477(5)
N1	C1	1.487(5)
N1	C4	1.498(5)
N1	C5	1.494(5)
C24	C23	1.399(6)
C24	C25	1.373(6)
C24	C27	1.513(6)
N4	C6	1.475(5)
C10	C11	1.402(6)
C10	C13	1.509(5)
C10	C9	1.380(6)
C11	C12	1.386(5)
C18	C19	1.381(5)
C18	C17	1.401(5)
C3	C4	1.511(6)
C15	C16	1.388(6)
C16	C17	1.389(5)
C26	C25	1.399(6)
C17	C20	1.506(6)
C22	C23	1.390(6)
C1	C2	1.515(6)
C6	C5	1.508(6)
C9	C8	1.394(6)
Cu1B	O1WB	1.990(3)
Cu1B	N2B	2.102(3)
Cu1B	N3B	2.063(3)
Cu1B	N1B	2.017(3)
Cu1B	N4B	2.108(3)
S2B	O3B	1.443(3)
S2B	N3B	1.573(3)
S2B	C14B	1.787(4)
S2B	O4B	1.461(3)
S3B	N2B	1.570(4)
S3B	O5B	1.475(3)
S3B	O6B	1.443(3)
S3B	C21B	1.779(4)
S1B	C7B	1.793(4)
S1B	N4B	1.568(4)
S1B	O1B	1.451(4)
S1B	O2B	1.447(3)
C7B	C12B	1.383(6)
C7B	C8B	1.395(6)
N2B	C2B	1.473(6)
N3B	C3B	1.478(5)
C14B	C15B	1.388(5)
C14B	C19B	1.396(5)
C21B	C26B	1.392(5)
C21B	C22B	1.387(5)
N1B	C1B	1.492(5)
N1B	C5B	1.486(5)
N1B	C4B	1.498(5)
C17B	C18B	1.392(6)

Atom	Atom	Length/Å
C17B	C20B	1.505(5)
C17B	C16B	1.394(6)
C2B	C1B	1.522(6)
C12B	C11B	1.397(6)
N4B	C6B	1.472(6)
C10B	C9B	1.391(6)
C10B	C13B	1.519(6)
C10B	C11B	1.383(6)
C23B	C22B	1.392(6)
C23B	C24B	1.397(6)
C26B	C25B	1.387(6)
C18B	C19B	1.387(5)
C15B	C16B	1.391(6)
C24B	C25B	1.389(6)
C24B	C27B	1.516(6)
C9B	C8B	1.382(6)
C5B	C6B	1.519(6)
C3B	C4B	1.515(5)
N5B	C39B	1.530(5)
N5B	C35B	1.524(5)
N5B	C32B	1.522(5)
N5B	C28B	1.534(5)
N5	C39	1.528(5)
N5	C35	1.525(5)
N5	C28	1.525(5)
N5	C32	1.518(5)
C39B	C40B	1.516(5)
C36	C35	1.526(6)
C36	C37	1.523(5)
C41B	C40B	1.534(5)
C41B	C42B	1.512(6)
C39	C40	1.522(5)
C35B	C36B	1.517(6)
C37	C38	1.525(6)
C28	C29	1.514(6)
C36B	C37B	1.523(6)
C29	C30	1.522(6)
C86B	C34B	1.521(6)
C32B	C33B	1.522(5)
C32	C33	1.521(6)
C38B	C37B	1.510(6)
C31	C30	1.526(6)
C34B	C33B	1.529(6)
C28B	C29B	1.532(6)
C41	C42	1.520(6)
C41	C40	1.526(6)
C29B	C30B	1.529(6)
C30B	C31B	1.511(7)
C33	C34	1.535(5)
C86	C34	1.503(6)

Table 4: Bond Angles in ° for **BuCuTsAq**.

Atom	Atom	Atom	Angle/°
O1W	Cu1	N3	93.94(13)
O1W	Cu1	N2	101.12(12)
O1W	Cu1	N1	174.62(13)
O1W	Cu1	N4	93.62(13)
N3	Cu1	N4	117.67(13)
N2	Cu1	N3	114.28(13)
N2	Cu1	N4	124.50(13)
N1	Cu1	N3	84.22(14)
N1	Cu1	N2	84.23(14)
N1	Cu1	N4	82.80(14)
O5	S3	C21	106.35(18)
O5	S3	N2	108.97(18)
O5	S3	O6	116.72(18)
N2	S3	C21	107.51(18)
O6	S3	C21	104.95(18)
O6	S3	N2	111.76(18)
N3	S2	C14	107.67(19)
O4	S2	N3	114.1(2)
O4	S2	O3	115.68(19)
O4	S2	C14	105.48(18)
O3	S2	N3	107.22(18)
O3	S2	C14	106.14(19)
N4	S1	C7	107.66(19)
O2	S1	C7	105.50(18)
O2	S1	N4	115.14(18)
O2	S1	O1	114.4(2)
O1	S1	C7	105.08(18)
O1	S1	N4	108.38(17)
C12	C7	S1	117.9(3)
C8	C7	S1	122.0(3)
C8	C7	C12	120.1(4)
S2	N3	Cu1	131.6(2)
C3	N3	Cu1	109.5(3)
C3	N3	S2	115.6(3)
C19	C14	S2	118.1(3)
C15	C14	S2	121.8(3)
C15	C14	C19	120.0(4)
C26	C21	S3	120.9(3)
C26	C21	C22	120.3(4)
C22	C21	S3	118.7(3)
S3	N2	Cu1	130.5(2)
C2	N2	Cu1	109.1(3)
C2	N2	S3	115.1(3)
C1	N1	Cu1	108.8(3)
C1	N1	C4	111.3(3)
C1	N1	C5	110.5(4)
C4	N1	Cu1	107.5(3)
C5	N1	Cu1	108.6(2)
C5	N1	C4	110.0(3)
C23	C24	C27	120.1(4)
C25	C24	C23	118.7(4)
C25	C24	C27	121.2(4)
S1	N4	Cu1	133.4(2)
C6	N4	Cu1	111.1(2)
C6	N4	S1	114.1(3)
C11	C10	C13	120.7(4)
C9	C10	C11	118.0(4)
C9	C10	C13	121.3(4)
C12	C11	C10	121.6(4)
C19	C18	C17	120.9(3)
C18	C19	C14	119.9(3)
N3	C3	C4	108.0(3)
C16	C15	C14	119.2(3)
C15	C16	C17	121.7(4)
C21	C26	C25	119.1(4)
C11	C12	C7	118.8(4)
C18	C17	C20	120.2(4)
C16	C17	C18	118.2(4)
C16	C17	C20	121.6(4)
C23	C22	C21	119.5(4)
C22	C23	C24	120.8(4)
N1	C1	C2	110.1(3)
N2	C2	C1	107.5(3)
C24	C25	C26	121.6(4)
N4	C6	C5	106.9(3)
N1	C4	C3	110.9(3)
C10	C9	C8	121.2(4)
C7	C8	C9	120.3(4)
N1	C5	C6	111.1(4)
O1WB	Cu1B	N2B	95.99(13)
O1WB	Cu1B	N3B	99.27(12)
O1WB	Cu1B	N1B	177.14(13)
O1WB	Cu1B	N4B	94.92(13)
N2B	Cu1B	N4B	120.32(14)
N3B	Cu1B	N2B	111.98(13)
N3B	Cu1B	N4B	123.66(13)
N1B	Cu1B	N2B	83.36(14)
N1B	Cu1B	N3B	83.54(13)
N1B	Cu1B	N4B	83.05(14)
O3B	S2B	N3B	109.43(17)
O3B	S2B	C14B	106.43(18)
O3B	S2B	O4B	115.54(19)
N3B	S2B	C14B	107.18(18)
O4B	S2B	N3B	112.32(18)
O4B	S2B	C14B	105.36(17)
N2B	S3B	C21B	108.21(19)
O5B	S3B	N2B	107.09(18)
O5B	S3B	C21B	106.08(19)
O6B	S3B	N2B	113.6(2)
O6B	S3B	O5B	115.3(2)
O6B	S3B	C21B	106.10(19)
N4B	S1B	C7B	108.61(19)
O1B	S1B	C7B	105.6(2)
O1B	S1B	N4B	108.04(19)
O2B	S1B	C7B	105.32(18)
O2B	S1B	N4B	112.84(19)
O2B	S1B	O1B	115.9(2)
C12B	C7B	S1B	120.1(3)
C12B	C7B	C8B	120.0(4)
C8B	C7B	S1B	119.9(3)
S3B	N2B	Cu1B	129.7(2)
C2B	N2B	Cu1B	110.5(3)
C2B	N2B	S3B	115.0(3)
S2B	N3B	Cu1B	131.2(2)

Atom	Atom	Atom	Angle/°
C3B	N3B	Cu1B	112.1(2)
C3B	N3B	S2B	114.2(3)
C15B	C14B	S2B	120.5(3)
C15B	C14B	C19B	119.5(3)
C19B	C14B	S2B	119.9(3)
C26B	C21B	S3B	121.3(3)
C22B	C21B	S3B	119.1(3)
C22B	C21B	C26B	119.6(4)
C1B	N1B	Cu1B	108.4(2)
C1B	N1B	C4B	111.1(3)
C5B	N1B	Cu1B	108.4(2)
C5B	N1B	C1B	110.8(3)
C5B	N1B	C4B	110.9(3)
C4B	N1B	Cu1B	107.2(2)
C18B	C17B	C20B	120.1(4)
C18B	C17B	C16B	118.6(4)
C16B	C17B	C20B	121.3(4)
N2B	C2B	C1B	108.0(3)
C7B	C12B	C11B	119.4(4)
S1B	N4B	Cu1B	133.4(2)
C6B	N4B	Cu1B	110.6(3)
C6B	N4B	S1B	115.7(3)
C9B	C10B	C13B	120.3(4)
C11B	C10B	C9B	118.9(4)
C11B	C10B	C13B	120.8(4)
C22B	C23B	C24B	121.1(4)
C25B	C26B	C21B	119.9(4)
C21B	C22B	C23B	119.9(4)
C19B	C18B	C17B	121.0(4)
N1B	C1B	C2B	110.1(3)
C14B	C15B	C16B	120.2(4)
C23B	C24B	C27B	120.6(4)
C25B	C24B	C23B	118.0(4)
C25B	C24B	C27B	121.4(4)
C18B	C19B	C14B	120.0(4)
C8B	C9B	C10B	120.8(4)
N1B	C5B	C6B	110.2(3)
N3B	C3B	C4B	109.8(3)
C26B	C25B	C24B	121.5(4)
N1B	C4B	C3B	110.8(3)

Atom	Atom	Atom	Angle/°
C9B	C8B	C7B	119.9(4)
C10B	C11B	C12B	121.0(4)
C15B	C16B	C17B	120.7(4)
N4B	C6B	C5B	108.2(3)
C39B	N5B	C28B	106.2(3)
C35B	N5B	C39B	111.3(3)
C35B	N5B	C28B	111.1(3)
C32B	N5B	C39B	111.5(3)
C32B	N5B	C35B	105.5(3)
C32B	N5B	C28B	111.3(3)
C35	N5	C39	111.5(3)
C28	N5	C39	105.4(3)
C28	N5	C35	111.2(3)
C32	N5	C39	111.5(3)
C32	N5	C35	106.2(3)
C32	N5	C28	111.2(3)
C40B	C39B	N5B	114.8(3)
C37	C36	C35	110.2(3)
C42B	C41B	C40B	111.5(4)
C40	C39	N5	116.2(3)
C39B	C40B	C41B	110.7(3)
C36B	C35B	N5B	115.9(3)
N5	C35	C36	116.5(3)
C36	C37	C38	112.4(3)
C29	C28	N5	116.3(3)
C35B	C36B	C37B	108.7(3)
C28	C29	C30	108.2(3)
N5B	C32B	C33B	116.0(3)
N5	C32	C33	116.1(3)
C86B	C34B	C33B	114.0(3)
C29B	C28B	N5B	115.6(3)
C42	C41	C40	113.3(3)
C38B	C37B	C36B	114.5(4)
C39	C40	C41	109.5(3)
C29	C30	C31	114.3(4)
C32B	C33B	C34B	110.0(3)
C30B	C29B	C28B	111.3(3)
C31B	C30B	C29B	114.6(4)
C32	C33	C34	110.5(3)
C86	C34	C33	113.3(4)

Table 5: Torsion Angles in ° for **BuCuTsAq**.

Atom	Atom	Atom	Atom	Angle/°
Cu1	N3	C3	C4	32.9(4)
Cu1	N2	C2	C1	38.5(4)
Cu1	N1	C1	C2	36.6(4)
Cu1	N1	C4	C3	41.2(4)
Cu1	N1	C5	C6	41.4(4)
Cu1	N4	C6	C5	32.4(4)
S3	C21	C26	C25	179.5(3)
S3	C21	C22	C23	-178.4(3)
S3	N2	C2	C1	-164.2(3)
S2	N3	C3	C4	-129.2(3)

Atom	Atom	Atom	Atom	Angle/°
S2	C14	C19	C18	-178.4(3)
S2	C14	C15	C16	178.2(3)
S1	C7	C12	C11	-176.2(3)
S1	C7	C8	C9	176.6(4)
S1	N4	C6	C5	-158.9(3)
C7	S1	N4	Cu1	-120.7(3)
C7	S1	N4	C6	73.9(3)
N3	S2	C14	C19	58.4(4)
N3	S2	C14	C15	-118.9(4)
N3	C3	C4	N1	-49.6(5)
O4	S2	N3	Cu1	157.6(2)
O4	S2	N3	C3	-45.3(3)
O4	S2	C14	C19	-179.4(4)
O4	S2	C14	C15	3.3(4)
O3	S2	N3	Cu1	28.1(3)
O3	S2	N3	C3	-174.7(3)
O3	S2	C14	C19	-56.2(4)
O3	S2	C14	C15	126.5(4)
C14	S2	N3	Cu1	-85.7(3)
C14	S2	N3	C3	71.4(3)
C14	C15	C16	C17	-1.1(6)
O5	S3	C21	C26	-127.0(3)
O5	S3	C21	C22	51.5(4)
O5	S3	N2	Cu1	-34.0(3)
O5	S3	N2	C2	174.7(3)
C21	S3	N2	Cu1	80.8(3)
C21	S3	N2	C2	-70.5(3)
C21	C26	C25	C24	-0.8(7)
C21	C22	C23	C24	-1.6(7)
N2	S3	C21	C26	116.4(3)
N2	S3	C21	C22	-65.1(4)
N1	C1	C2	N2	-50.0(5)
N4	S1	C7	C12	-170.0(3)
N4	S1	C7	C8	12.2(4)
N4	C6	C5	N1	-48.7(4)
C10	C11	C12	C7	-0.3(6)
C10	C9	C8	C7	-0.8(7)
C11	C10	C9	C8	2.2(7)
C19	C14	C15	C16	1.0(6)
C19	C18	C17	C16	-1.1(6)
C19	C18	C17	C20	178.2(4)
O6	S3	C21	C26	-2.7(4)
O6	S3	C21	C22	175.8(3)
O6	S3	N2	Cu1	-164.5(2)
O6	S3	N2	C2	44.2(3)
C15	C14	C19	C18	-1.1(7)
C15	C16	C17	C18	1.1(6)
C15	C16	C17	C20	-178.2(4)
C26	C21	C22	C23	0.1(6)
C12	C7	C8	C9	-1.2(7)
C17	C18	C19	C14	1.1(7)
C22	C21	C26	C25	1.1(6)
C23	C24	C25	C26	-0.7(7)
C1	N1	C4	C3	-77.9(4)
C1	N1	C5	C6	160.7(3)
O2	S1	C7	C12	-46.5(4)
O2	S1	C7	C8	135.6(4)

Atom	Atom	Atom	Atom	Angle/°
O2	S1	N4	Cu1	122.0(3)
O2	S1	N4	C6	-43.4(4)
C25	C24	C23	C22	1.9(7)
C27	C24	C23	C22	-178.4(4)
C27	C24	C25	C26	179.6(5)
C4	N1	C1	C2	155.0(4)
C4	N1	C5	C6	-76.0(4)
C13	C10	C11	C12	176.6(4)
C13	C10	C9	C8	-176.0(4)
C9	C10	C11	C12	-1.6(6)
C8	C7	C12	C11	1.7(6)
C5	N1	C1	C2	-82.5(4)
C5	N1	C4	C3	159.3(4)
Cu1B	N2B	C2B	C1B	29.8(4)
Cu1B	N3B	C3B	C4B	16.0(4)
Cu1B	N1B	C1B	C2B	43.3(4)
Cu1B	N1B	C5B	C6B	44.2(4)
Cu1B	N1B	C4B	C3B	44.1(3)
Cu1B	N4B	C6B	C5B	27.9(4)
S2B	N3B	C3B	C4B	-148.1(3)
S2B	C14B	C15B	C16B	-179.3(3)
S2B	C14B	C19B	C18B	-179.9(3)
S3B	N2B	C2B	C1B	-172.2(3)
S3B	C21B	C26B	C25B	-178.6(3)
S3B	C21B	C22B	C23B	179.3(3)
S1B	C7B	C12B	C11B	179.3(3)
S1B	C7B	C8B	C9B	-178.6(3)
S1B	N4B	C6B	C5B	-146.0(3)
C7B	S1B	N4B	Cu1B	115.5(3)
C7B	S1B	N4B	C6B	-72.4(3)
C7B	C12B	C11B	C10B	0.1(7)
N2B	S3B	C21B	C26B	127.4(4)
N2B	S3B	C21B	C22B	-51.7(4)
N2B	C2B	C1B	N1B	-48.3(4)
O5B	S3B	N2B	Cu1B	-30.6(3)
O5B	S3B	N2B	C2B	176.5(3)
O5B	S3B	C21B	C26B	-118.0(4)
O5B	S3B	C21B	C22B	62.9(4)
O3B	S2B	N3B	Cu1B	31.4(3)
O3B	S2B	N3B	C3B	-168.4(3)
O3B	S2B	C14B	C15B	85.2(4)
O3B	S2B	C14B	C19B	-93.8(4)
O6B	S3B	N2B	Cu1B	-159.1(2)
O6B	S3B	N2B	C2B	48.0(4)
O6B	S3B	C21B	C26B	5.1(4)
O6B	S3B	C21B	C22B	-174.0(3)
N3B	S2B	C14B	C15B	-157.8(3)
N3B	S2B	C14B	C19B	23.2(4)
N3B	C3B	C4B	N1B	-39.6(4)
C14B	S2B	N3B	Cu1B	-83.6(3)
C14B	S2B	N3B	C3B	76.6(3)
C14B	C15B	C16B	C17B	-0.1(7)
C21B	S3B	N2B	Cu1B	83.4(3)
C21B	S3B	N2B	C2B	-69.5(3)
C21B	C26B	C25B	C24B	-1.5(7)
N1B	C5B	C6B	N4B	-47.6(5)
O4B	S2B	N3B	Cu1B	161.1(2)

Atom	Atom	Atom	Atom	Angle/°
O4B	S2B	N3B	C3B	-38.7(3)
O4B	S2B	C14B	C15B	-38.0(4)
O4B	S2B	C14B	C19B	143.0(3)
C17B	C18B	C19B	C14B	-1.4(6)
C12B	C7B	C8B	C9B	1.4(6)
N4B	S1B	C7B	C12B	-116.7(3)
N4B	S1B	C7B	C8B	63.3(4)
C10B	C9B	C8B	C7B	-1.5(6)
C23B	C24B	C25B	C26B	1.8(6)
C26B	C21B	C22B	C23B	0.2(6)
C22B	C21B	C26B	C25B	0.5(6)
C22B	C23B	C24B	C25B	-1.1(6)
C22B	C23B	C24B	C27B	178.7(4)
C18B	C17B	C16B	C15B	-0.2(7)
C1B	N1B	C5B	C6B	163.1(3)
C1B	N1B	C4B	C3B	-74.1(4)
C15B	C14B	C19B	C18B	1.1(6)
O1B	S1B	C7B	C12B	-1.0(4)
O1B	S1B	C7B	C8B	178.9(3)
O1B	S1B	N4B	Cu1B	1.4(3)
O1B	S1B	N4B	C6B	173.4(3)
O2B	S1B	C7B	C12B	122.2(3)
O2B	S1B	C7B	C8B	-57.9(4)
O2B	S1B	N4B	Cu1B	-128.1(3)
O2B	S1B	N4B	C6B	43.9(4)
C24B	C23B	C22B	C21B	0.1(7)
C19B	C14B	C15B	C16B	-0.3(6)
C9B	C10B	C11B	C12B	-0.2(7)
C5B	N1B	C1B	C2B	-75.6(4)
C5B	N1B	C4B	C3B	162.3(3)
C4B	N1B	C1B	C2B	160.8(3)
C4B	N1B	C5B	C6B	-73.2(4)
C13B	C10B	C9B	C8B	179.5(4)
C13B	C10B	C11B	C12B	-178.8(4)
C20B	C17B	C18B	C19B	-179.3(4)
C20B	C17B	C16B	C15B	-180.0(4)
C8B	C7B	C12B	C11B	-0.7(6)
C27B	C24B	C25B	C26B	-178.0(4)
C11B	C10B	C9B	C8B	0.9(6)
C16B	C17B	C18B	C19B	0.9(6)
N5B	C39B	C40B	C41B	-169.4(3)
N5B	C35B	C36B	C37B	168.2(4)
N5B	C32B	C33B	C34B	176.6(3)
N5B	C28B	C29B	C30B	-157.3(4)
N5	C39	C40	C41	-176.3(3)
N5	C28	C29	C30	-168.6(3)
N5	C32	C33	C34	173.4(3)
C39B	N5B	C35B	C36B	48.8(4)
C39B	N5B	C32B	C33B	-61.3(4)
C39B	N5B	C28B	C29B	-177.5(3)
C39	N5	C35	C36	55.8(4)
C39	N5	C28	C29	-172.1(3)
C39	N5	C32	C33	-60.4(4)
C35B	N5B	C39B	C40B	62.3(4)
C35B	N5B	C32B	C33B	177.8(3)
C35B	N5B	C28B	C29B	-56.4(4)
C35B	C36B	C37B	C38B	174.0(4)

Atom	Atom	Atom	Atom	Angle/°
C35	N5	C39	C40	63.9(4)
C35	N5	C28	C29	-51.2(4)
C35	N5	C32	C33	178.0(3)
C35	C36	C37	C38	176.8(4)
C37	C36	C35	N5	169.0(3)
C28	N5	C39	C40	-175.3(3)
C28	N5	C35	C36	-61.4(4)
C28	N5	C32	C33	56.9(4)
C28	C29	C30	C31	-177.8(4)
C86B	C34B	C33B	C32B	-64.5(5)
C32B	N5B	C39B	C40B	-55.2(4)
C32B	N5B	C35B	C36B	169.9(3)
C32B	N5B	C28B	C29B	60.8(4)
C32	N5	C39	C40	-54.6(4)
C32	N5	C35	C36	177.5(3)
C32	N5	C28	C29	66.9(4)
C32	C33	C34	C86	-68.8(5)
C42B	C41B	C40B	C39B	-179.1(4)
C28B	N5B	C39B	C40B	-176.7(3)
C28B	N5B	C35B	C36B	-69.3(4)
C28B	N5B	C32B	C33B	57.1(4)
C28B	C29B	C30B	C31B	-65.4(5)
C42	C41	C40	C39	65.0(5)
O1	S1	C7	C12	74.7(3)
O1	S1	C7	C8	-103.2(4)
O1	S1	N4	Cu1	-7.5(3)
O1	S1	N4	C6	-172.9(3)

Table 6 Hydrogen Fractional Atomic Coordinates (×10^4) and Equivalent Isotropic Displacement Parameters (Å^2×10^3) for **BuCuTsAq**. U_{eq} is defined as 1/3 of the trace of the orthogonalised U_{ij}.

Atom	x	y	z	U_{eq}
H1WA	1176	7589	5463	26
H1WB	1503	7811	4918	26
H11	-1146	6444	7663	27
H18	-2301	7471	4198	19
H19	-657	7432	4383	22
H3A	1354	5528	3484	29
H3B	354	5969	3139	29
H15	-864	7724	2527	21
H16	-2511	7760	2351	22
H26	4291	4667	6735	25
H12	-1256	7084	6683	25
H22	2171	6530	6380	27
H23	1953	6311	7383	29
H1A	1888	4465	4207	30
H1B	1407	3711	4553	30
H2A	2119	4311	5529	27
H2B	2945	4212	5166	27
H25	4020	4424	7725	30
H27A	2247	5539	8337	64
H27B	3352	5336	8610	64
H27C	2640	4526	8335	64
H6A	-1006	5458	4648	29

Atom	x	y	z	U_{eq}
H6B	-867	5045	5337	29
H4A	-396	5326	3845	29
H4B	198	4525	3629	29
H13A	436	5281	8515	47
H13B	-91	4371	8225	47
H13C	-693	5202	8391	47
H9	589	4493	7298	34
H20A	-3850	6999	3250	38
H20B	-3929	7711	2693	38
H20C	-3845	8065	3389	38
H8	507	5139	6323	30
H5A	501	4296	5276	29
H5B	-258	4073	4636	29
H1	3987	6021	-432	27
H2	2998	6096	-452	27
H2AB	5010	7853	1590	26
H2BB	4089	7766	1865	26
H12B	4816	6268	-1778	26
H23B	7215	6022	846	23
H26B	5713	5611	2467	23
H22B	5575	6207	659	24
H18B	3447	8431	-2161	26
H1AB	3207	8702	1094	24
H1BB	4198	9216	1349	24
H15B	385	7784	-1970	26
H19B	3205	8008	-1196	22
H9B	5732	9205	-2175	27
H5AB	5490	8559	857	28
H5BB	5173	9540	566	28
H3AB	2084	9028	215	21
H3BB	2042	9218	-505	21
H25B	7351	5458	2653	26
H4AB	3635	9403	-322	20
H4BB	3397	9888	271	20
H3	4679	8977	-3294	46
H4	4574	7953	-3542	46
H5	5594	8429	-3370	46
H6	2769	9028	-3209	45
H7	1669	8873	-3532	45
H10	2402	8050	-3479	45
H8B	5986	8692	-1152	28
H13	8643	4975	1716	44
H14	8806	5583	2333	44
H17	8787	6047	1675	44
H11B	4593	6785	-2806	30
H16B	637	8178	-2939	28
H6AB	4998	9012	-443	27
H6BB	5999	8619	-55	27
H39A	5330	7942	4198	19
H39B	5249	8724	4682	19
H36A	-156	6638	86	21
H36B	104	5931	-397	21
H41B	6678	7419	5114	29

Atom	x	y	z	U_{eq}
H41A	6391	8136	5580	29
H1C	2143	5904	1146	20
H1D	1385	6476	649	20
H40A	5096	6822	4876	20
H40B	4811	7553	5335	20
H35B	2741	8726	4432	19
H35A	3345	8073	4956	19
H1E	-404	5482	737	20
H1F	-356	4727	229	20
H37A	-1739	6039	-147	25
H37B	-1470	5380	-653	25
H28A	1556	5341	-29	18
H28B	2156	4663	479	18
H1G	3976	9865	4776	22
H1H	4396	9219	5363	22
H29A	496	4215	-460	21
H29B	920	3538	109	21
H86C	3335	4663	3721	37
H86A	3320	5478	4196	37
H86B	4293	5194	4032	37
H32A	2802	7420	3800	19
H32B	3559	6911	4337	19
H1I	644	3902	1027	20
H1J	647	4690	1522	20
H42A	6377	6219	5757	50
H42C	6134	6950	6230	50
H42B	7188	6880	6136	50
H38A	-1178	6706	-1219	38
H38B	-1573	7315	-738	38
H38C	-2263	6619	-1188	38
H1K	3602	11049	5603	44
H1L	4002	10324	6142	44
H1M	2943	10700	6039	44
H31A	921	3094	-1265	41
H31B	1289	2391	-707	41
H31C	1982	2712	-1128	41
H34A	2715	6016	3185	28
H34B	3626	5653	2975	28
H1N	4203	9466	3838	23
H1O	4221	8640	3375	23
H1P	1437	7598	2077	29
H1Q	2310	7243	1820	29
H1R	2525	9982	5058	35
H1S	2865	9261	5606	35
H1T	1673	7879	848	41
H1U	1677	8650	1358	41
H1V	712	8133	1039	41
H1W	1220	6046	1880	30
H1X	411	6569	1378	30
H30A	2386	3496	-178	30
H30B	1992	4199	-730	30
H33A	4581	6760	3643	28
H33B	3779	7223	3103	28

Atom	x	y	z	U_{eq}
H1Y	2459	8597	3268	30
H1Z	2606	9615	3528	30
H20	3153	9014	2432	39
H21	2193	9555	2409	39
H24	2355	4688	1756	29
H27	2297	3824	1308	29
H28	886	4158	2484	52
H29	1930	4556	2754	52
H2C	1639	3603	2999	52
H2D	1449	3022	1963	32
H2E	2523	3249	2311	32
H2F	3369	10521	2199	65
H2G	4030	10312	2877	65
H2H	3055	10850	2808	65

```
#==============================================================================
# PLATON/CHECK-( 70414) versus check.def version of 310314   for Entry: bucutsaq
# Data: BuCuTsAq.cif - Type: CIF                Bond Precision   C-C = 0.0060 A
# Refl: BuCuTsAq.fcf - Type: LIST4                                  Temp = 100 K
#                                               X-Ray         Nref/Npar =  10.1
# Cell   14.542(4)   14.743(4)   22.114(5)           90   104.116(4)          90
# Wavelength 0.71073    Volume Reported    4597.8(19)   Calculated       4598(2)
# SpaceGroup from Symmetry P 21       Hall: P 2yb               monoclinic
#                 Reported P 1 21 1         P 2yb               monoclinic
# MoietyFormula C27 H35 Cu N4 O7 S3, C16 H36 N
#      Reported C27 H35 Cu N4 O7 S3, C16 H36 N
#    SumFormula C43 H71 Cu N5 O7 S3
#      Reported C43 H71 Cu N5 O7 S3
# Mr        =    929.81[Calc],    929.76[Rep]
# Dx,gcm-3  =     1.343[Calc],     1.343[Rep]
# Z         =         4[Calc],         4[Rep]
# Mu (mm-1) =     0.665[Calc],     0.665[Rep]
# F000      =    1988.0[Calc],    1988.0[Rep]  or F000' =   1991.44[Calc]
# Reported   T Limits: Tmin=0.650              Tmax=0.746  AbsCorr=MULTI-SCAN
# Calculated T Limits: Tmin=0.678 Tmin'=0.664  Tmax=0.766
# Reported   Hmax= 18, Kmax= 19, Lmax= 28, Nref=  19781        , Th(max)= 27.483
# Obs in FCF Hmax= 18, Kmax= 19, Lmax= 28, Nref=  19781[ 10944], Th(max)= 27.483
# Calculated Hmax= 18, Kmax= 19, Lmax= 28, Nref=  21075[ 10949], Ratio=1.81/0.94
# Reported   Rho(min) = -0.41, Rho(max) =  1.38 e/Ang**3 (From CIF)
# w=1/[sigma**2(Fo**2)+(0.0703P)**2+  0.6544P], P=(Fo**2+2*Fc**2)/3
# R= 0.0425( 18094), wR2= 0.1116( 19781), S = 1.054      (From FCF data only)
# R= 0.0425( 18092), wR2= 0.1116( 19781), S = 1.054, Npar= 1080, Flack 0.689(10)
#==============================================================================
For Documentation: http://http://www.platonsoft.nl/CIF-VALIDATION.pdf
#==============================================================================

#==============================================================================
>>> The Following Improvement and Query ALERTS were generated - (Acta-Mode) <<<
#==============================================================================
Format: alert-number_ALERT_alert-type_alert-level text

094_ALERT_2_C Ratio of Maximum / Minimum Residual Density ....       3.34 Why ?
911_ALERT_3_C Missing # FCF Refl Between THmin & STh/L=  0.600          4 Why ?
#==============================================================================
007_ALERT_5_G Number of Unrefined Donor-H Atoms ..............          4 Why ?
008_ALERT_5_G No _iucr_refine_reflections_details   in the CIF     Please Do !
033_ALERT_4_G Flack x Value Deviates > 2*sigma from Zero .....      0.689
111_ALERT_2_G ADDSYM Detects (Pseudo) Centre of Symmetry .....         81 %Fit
113_ALERT_2_G ADDSYM Suggests Possible Pseudo/New Space group.      P21/n Check
720_ALERT_4_G Number of Unusual/Non-Standard Labels ..........         15 Note
794_ALERT_5_G Tentative Bond Valency for Cu1     (II)    .....       2.13 Note
794_ALERT_5_G Tentative Bond Valency for Cu1B    (II)    .....       2.12 Note
910_ALERT_3_G Missing # of FCF Reflections Below Th(Min) .....          1 Why ?
#==============================================================================

ALERT_Level and ALERT_Type Summary
==================================
2 ALERT_Level_C = Check. Ensure it is Not caused by an Omission or Oversight
9 ALERT_Level_G = General Info/Check that it is not Something Unexpected

3 ALERT_Type_2 Indicator that the Structure Model may be Wrong or Deficient.
2 ALERT_Type_3 Indicator that the Structure Quality may be Low.
2 ALERT_Type_4 Improvement, Methodology, Query or Suggestion.
4 ALERT_Type_5 Informative Message, Check.
#==============================================================================
```

```
1 Missing  Experimental  Info Issue(s) (Out of  54 Tests) -   98 % Satisfied
0 Experimental  Data  Related Issue(s) (Out of  28 Tests) -  100 % Satisfied
2 Structural  Model   Related Issue(s) (Out of 117 Tests) -   98 % Satisfied
7 Unresolved or to be Checked Issue(s) (Out of 223 Tests) -   97 % Satisfied

#===============================================================================
```

References

1. Bruker-AXS *APEX2. Version 2014.11-0*, Madison, WI, 2014.
2. Sheldrick, G., A short history of SHELX. *Acta Crystallographica Section A* **2008,** *64* (1), 112-122.
3. Dolomanov, O. V.; Bourhis, L. J.; Gildea, R. J.; Howard, J. A. K.; Puschmann, H., OLEX2: a complete structure solution, refinement and analysis program. *Journal of Applied Crystallography* **2009,** *42* (2), 339-341.
4. Bruker-AXS *SAINT-8.34A-2013 - Software for the Integration of CCD Detector System Bruker Analytical X-ray Systems*, Madison, WI, 2013.
5. Sheldrick, G., SHELXT - Integrated space-group and crystal-structure determination. *Acta Crystallographica Section A* **2015,** *71* (1), 3-8.
6. Palatinus, L.; Chapuis, G., SUPERFLIP - a computer program for the solution of crystal structures by charge flipping in arbitrary dimensions. *Journal of Applied Crystallography* **2007,** *40* (4), 786-790.